Explorations optiques multimodales et multiéchelles non invasives appliquées au revêtement cutanéomuqueux , étendues à l'appareil oculaire antérieur

Jean-Luc Perrot





UNIVERSITÉ JEAN MONNET – UNIVERSITÉ DE LYON
FACULTÉ DE MÉDECINE

ÉCOLE DOCTORALE SIS
FORMATION DOCTORALE BIOLOGIE ET PHYSIOLOGIE DE L'EXERCICE
Laboratoire SNA- EPIS (EA 4607)

Thèse présentée et soutenue publiquement
Par le Docteur Jean-Luc PERROT
09 /05/2017

EXPLORATIONS OPTIQUES MULTIMODALES ET MULTI-ÉCHELLES NON INVASIVES APPLIQUÉES AU REVÊTEMENT CUTANÉO-MUQUEUX, ÉTENDUES A L'APPAREIL OCULAIRE ANTÉRIEUR

Directeur de thèse : Professeur Frédéric CAMBAZARD

Mr le Professeur Frédéric Cambazard	Directeur de thèse
Mr le Professeur Frédéric Roche	Co-Directeur de thèse
Mme le Professeur Veronique Del Marmol	Rapporteur
Mr le Pr Michel D'Incan	Rapporteur
Mr le Professeur Philippe Gain	
Mr le Professeur Youcef Ouerdane	
Mr le Professeur Hassan Zahouani	
Mr le Professeur Frédéric Bérard	
Mme le Docteur Elisa Cinotti	Invitée
Mr le Professeur Jean Claude Barthelemy	Invité

REMERCIEMENTS

Je me permets de revendiquer des remerciements pour les membres du jury, plus libres qu'habituellement lors de ce genre d'exercice. C'est le privilège d'une thèse passée à un âge tardif et où mon activité professionnelle m'a permis de travailler en étroite collaboration, à certaines périodes de ma vie avec chacun des membres du jury, au cours d'expériences professionnelles riches et intenses. Tous d'une manière ou d'une autre, avez profondément influé sur mon travail de recherche et de clinique.

Mr le Professeur Frédéric Cambazard
Un soutient, une confiance sans faille depuis plus de 20 ans avec toute mon amitié.

Mr le Professeur Frédéric Roche
Au responsable de notre équipe de recherche qui a compris et accepté les cheminements complexes et parfois tortueux qui du psoriasis à l'imagerie permettront de mieux comprendre la dermatologie et d'enregistrer sans contact l'activité du SNA.

Mme le Professeur Véronique Del Marmol
Alors que nous étions émerveillés et rassasiés par ce monde que nous faisait découvrir la microscopie confocale, tu as de nouveau ouvert notre appétit de connaissances en nous emmenant vers l'OCT. Avec l'humour qui t'habite, tu nous diras que les belges ont toujours peur de mourir le ventre vide et que nous sommes grâce à toi devenus un peu belge.

Mr le Professeur Philippe Gain
Médecin, chercheur, capitaine d'industrie le tout porté à sa quintéscence : un modèle.

Mr le Professeur Youcef Ouerdane
Un soir il y a quelques années en me parlant amicalement des étoiles tu m'as fait découvrir des vibrations lumineuses de la peau que je n'avais jamais vues et ainsi m'ouvrir un champ de recherche et d'application dermatologique gigantesque qui est devenu un de mes rêves professionnels.

Mr le Professeur Hassan Zahouani
Tribologue, tu m'as éclairé un pan entier de ma discipline en me faisant comprendre l'intérêt de la métrologie en dermatologie. Mécanicien de la peau tu m'as fait découvrir le monde de la scientifique du cosmétique et tout cela avec amitié et humour.

Mme le Docteur Elisa Cinotti.
Ma sœur en dermatologie : La Magnifica ! Que dire de plus si ce n'est que Siena est quand même un peu loin de St Etienne.

Mr le Professeur Frédéric Bérard
C'est un immense honneur que le chercheur que tu es, ait bien voulu accepter de juger cette thèse. On a travaillé ensemble il y a bien des années, et malgré les ans ton amitié est toujours restée fidèle

Mr le Professeur Jean Claude Barthelemy
Tu as été mon tuteur en recherche et ce depuis bien longtemps. Plus récemment tu m'as fait découvrir le SNA et partager cette passion qui t'anime depuis des années. J'espère pouvoir dans les années à venir appliquer à la dermatologie tes idées et ainsi te rendre hommage, mais aussi me servir des méthodes d'imagerie moderne pour te permettre d'enregistrer différemment l'activité du SNA et augmenter les possibilités d'appliction des travaux de l'équipe.

Mr le Professeur Michel D'Incan
Le chercheur emminent que tu es, nous a fait retrouver la recherche en médecine nucléaire qui a ensuite pu être étendue à la microscopie confocale ex vivo.Tu perpétue la longue tradition d'amitié et de partenariat dermatologique Clermont St Etienne initiés par les Pr Pierre Souteyrand et Frédéric Cambazard sous les auspices du Pr Jean Thivolet

A ma Famille

A Sylvie
L'amour de ma vie sans qui ce travail ne serait probablement pas. A la mi-temps de notre vie, tu as même accepté cette nouvelle passion professionnelle chronophage.

A mes fils Alexandre et Guillaume
C'est vous ma fierté

A mes parents
Aux absents qui me manquent et aux présents que j'aime tant

A mes enseignants

A ceux et celles qui m'ont appris à lire, compter, réfléchir et travailler.
A ceux qui m'ont enseigné la médecine et la dermatologie en tout premier mon maitre Alain Claudy, à mes assistants, Bernard Rouchouse, Anna Mazuy,et Véronique Lévigne.
A tous ceux médecins et physiciens qui m'ont accompagné et tant appris moi qui croyait avoir rangé définitivement les mathématiques et la physique après mon bac

A mes collègues et amis

Vous êtes nombreux, très nombreux à m'avoir côtoyé, cette thèse est suffisamment épaisse pour ne par l'alourdir plus et vous connaissez l'affection que je vous porte aussi je resterai général

Mr le Docteur Bruno Labeille.
Mon frère en dermatologie. Tu ne m'auras causé qu'un désagrément ton départ trop tôt programmé du service. Mais tu sais que j'userai de toutes les ruses et artifices pour te garder un peu plus dans notre univers d'images improbables, quant à notre amitié….

Mr Le Pr Gilles Thuret
Gilles toi aussi tu aurais dû être membre de ce jury tant le chercheur que tu es y avait sa place de droit, mais les règles administratives sont là que tu connais bien comme responsable de la DRCI, mais nous avons tant à faire encore ensemble….

Mme le Docteur Catherine Douchet.
Notre juge de paix, toi qui confirme ou infirme nos visions et apporte de la couleur à nos articles illustrés sans cela que d'images en niveau de gris. Que n'as-tu été mise à contribution !!!!

Mr le Pr Hervé Decousus
Vous avez structuré la recherche clinique médicale stéphanoise, m'avez conseillé avec amitié et humour lors de mes première études cliniques, m'avez accueilli comme membre du

CCPPRB.Comme tant d'autres je vous dois tant et vous en suis profondément reconnaissant.

A tous les internes et assistants qui m'ont côtoyé alors que j'étais interne, CCA puis PH je ne puis les remercier individuellement mais tous à leur façon m'ont enrichi de leurs connaissances et de leur être.

Aux équipes soignantes, aux secrétaires, aux ARC qui m'ont accompagné tout au long de ma carrière et qui ont souvent souffert de ma suractivité.

A tous mes collègues plus particulièrement dermatologues, pathologistes, chirurgiens, médecins nucléaires, ophtalmologues, gynécologues et notamment le Dr Claude Soler et le Pr Olivier Tiffet sans qui le Réseau Ligérien du Mélanome, ma première grande aventure humaine et professionnelle, ne serait probablement pas, et plus récemment le Dr Thomas Alix qui s'était tant investi avant de nous quitter.
Mais aussi à ceux de RésoPso, de RésoVerneuil du GUS et du GICNI à vous tous encore merci de votre amitié et de votre soutient

A tous les chercheurs académiques ou industriels puisque cette classification est de mise même si dans les faits, la compétence et les liens d'amitié que j'ai pu établir avec vous n'y sont pas soumis.

A tous mes correspondants de l'industrie pharmaceutique causes ou non de mes multiples conflits d'intérêts (listés sur le site de l'HAS) et sans qui je n'aurai pu faire, mes présentations lors de congrès, acheter notre OCT, notre échographe, un de nos dermatoscope, ou payer des stages à l'étranger d'étudiants……Encore merci pour les échanges riches, intellectuellement et humain, que nous avons pu tisser aux cours de ces années.

A mes amis vous m'avez accompagné, et pour certain depuis le collège, qui ont partagé mes joies et m'ont aidé dans les moments difficiles de ma vie ils m'auront aidé à remplir mon rôle de médecin vous m avez permis d'avoir une vie affective et amicale riche.

Sommaire

A .INTRODUCTION ET JUSTIFICATION SCIENTIFIQUE DE LA RECHERCHE…….12
1 .Historique bref de l'imagerie en dermatologie 13
2. Historique bref de l'imagerie en dermatologie à St Etienne 15
3. Qu'espérer des outils d'imagerie en dermatologie 16
4. Un dialogue nécessaire avec les physiciens 17

B. RESPONSABILITES ET ACTIVITE HOSPITALIERE 20

C. ETUDE DOCT VCESL (projet ANR).....28

D. ETUDE INNOVATION EN IMAGERIE IN VIVO : MICROSCOPIE PAR COHERENCE OPTIQUE EN DERMATOLOGIE 70

E. DEMANDES D'ANR SOUMISES EN OCTOBRE 2016.....106

1. Molecular-contrast LC-OCT for enhanced skin cancer diagnosis
2. Système optique multimodal haute résolution et spectroscopique pour l'analyse de la peau appliqué aux tumeurs cutanées

F. LA DERMATOLOGIE AU JOUR LE JOUR : UNE ENTITE DE RECHERCHE A PART ENTIÈRE 118

1. Une approche synthétique des innovations au jour le jour : une continuité avec notre mission de soins…….119

2- Imagerie non invasive cancérologique cutanéo-muqueuse.....120
2.a identification des tumeurs ……..121
2. a 1. Cells of Langerhans cell histiocytosis and epidermal Langerhans cells differ under reflectance confocal microscopy : first observation
2. a 2. Solar lentigo diagnosed by reflectance confocal microscopy
2. a 3. Contribution of reflectance confocal microscopy to the diagnosis of fibroepithelioma of Pinkus
2. a 4. Contribution of reflectance confocal microscopy for the diagnosis of junctional naevus.
2. a 5. Yellow globules in balloon cell naevus.
2. a.6. Sensitivity of handheld reflectance confocal microscopy for the diagnosis of basal cell carcinoma: A series of 344 histologically proven lesions.
2. a 7. In vivo confocal microscopic substrate of grey colour in melanosis
2. a 8. Reflectance confocal microscopy features of acral lentiginous melanoma: a comparative study with acral nevi.
2. a 9. The role of reflectance confocal microscopy in the diagnosis of cutaneous melanoma metastasis

2. a 10. Reflectance confocal microscopy of Pigmented Bowen's disease: misleading dendritic cells.

2.b délimitation des marges des tumeurs et contrôle post opératoire.....156
2. b 1. Laser photodynamic treatment for in situ squamous cell carcinoma of the glans monitored by reflectance confocal microscopy
2. b 2. In vivo reflectance confocal microscopy to optimize the spaghetti technique for defining surgical margins of lentigo maligna.

3- Imagerie non invasive in vivo et processus infectieux cutanéo-muqueux et phanérien…….170

3.a Imagerie non invasive in vivo in vivo et processus infectieux cutanéo-muqueux et phanérien des parasites……171

3. a 1. Reflectance confocal microscopy for quantification of Sarcoptes scabiei I Norwegian scabies
3. a 2. Rapid diagnosis of scabies by manual confocal reflectance microscopy
3. a 4. On the feasibility of confocal microscopy for the diagnosis of scabies
3. a 5. Diagnosis of scabies by high-magnification dermoscopy: the "delta-wing jet" appearance of Sarcoptes scabiei
3. a 6. Inefficacy of alcohol-based hand rub on mites in a patient with hyperkeratotic scabies.
3. a 7. Tinea corporis diagnosed by reflectance confocal microscopy
3. a 8. Hair dermatophytosis diagnosed by reflectance confocal microscopy: six cases
3. a 9. Dermoscopy and confocal microscopy for in vivo detection and characterization of Dermanyssus gallinae mite.
3. a 10. Unusual reflectance confocal microscopy findings during the examination of perianal nevus: pinworms.
3. a 11. Videodermoscopy compared to reflectance confocal microscopy for the diagnosis of scabies.
3. a 12. Dermoscopy, confocal microscopy and optical coherence tomography for the diagnosis of bedbug infestation

3.b Imagerie non invasive in vivo et processus infectieux cutanéo-muqueux et phanérien des virus 218
3. b 1. First identification of the herpes simplex virus by skin-dedicated ex vivo fluorescence confocal microscopy during herpetic skin infections.
3. b 2. Role of in vivo and ex vivo confocal microscopy and of optical coherence tomography as aids in the diagnosis of molluscum contagiosum

3.c Imagerie non invasive in vivo et processus infectieux cutanéo-muqueux et phanérien des bactéries 218
The role of reflectance confocal microscopy in the diagnosis of secondary syphilis of the vulva and anus: A first case report

3.d articles de synthèse 222
3. d.1. Reflectance confocal microscopy in infectious diseases.
3. d 2. Reflectance confocal microscopy for cutaneous infections and infestations

4- Imagerie non invasive des phanères 243
Confocal microscopy for healthy and pathological nail.

5- imagerie non invasive cutanéo-muqueuse et de l'appareil oculaire 251
5.a imagerie non invasive de l'appareil oculaire..... 251
5. a 1. The role of in vivo confocal microscopy in the diagnosis of eyelid margin tumors: 47 cases
5 .a 1bi.s The role of in vivo confocal microscopy in the diagnosis of eyelid margin tumors: 47 cases: Reply from the authors
5. a 2. Handheld reflectance confocal microscopy for the diagnosis of conjunctival tumors
5.a 3. In vivo confocal microscopy of pine processionary caterpillar hair-induced keratitis.
5. a 4. Contribution of reflectance confocal microscopy in the diagnosis of eyelid dermal Nevus
5.a 5. In vivo confocal microscopy for eyelids and ocular surface: a new horizon for dermatologists.
5.a 6. In Vivo and Ex Vivo Confocal Microscopy for the Management of a Melanoma of the Eyelid Margin.
5.a 7. The role of reflectance confocal microscopy and optical coherence tomography in the diagnosis of epithelial-cystic conjunctival nevus
5.a 8. The role of reflectance confocal microscopy in the diagnosis of ocular-cutaneous erucism or dermatitis and keratitis induced by pine processionary caterpillar hairs

5.b imagerie des muqueuses 293
5.b 1. Reflectance confocal microscopy for the diagnosis of vulvar melanoma and melanosis: preliminary results
5.b 2. Anal melanosis diagnosed by reflectance confocal microscopy
5.b 3. The contribution of reflectance confocal microscopy in the diagnosis of Paget's disease of the breast
5.b 4. Reflectance confocal microscopy of mucosal pigmented macules: a review of 56 cases including 10 macular melanomas.
5.b 5. Reflectance confocal microscopy for the diagnosis of vulvar naevi: six cases

5 c articles de synthèse..... 326
5.c 1. Reflectance confocal microscopy for mucosal diseases
5.c 2. Confocal Microscopy for Special Sites and Special Uses

6- imagerie non invasive des maladies bulleuses.....344
6.1. The role of reflectance confocal microscopy and of optical coherence tomography in the diagnosis of pemphigus
6.2. Role of reflectance confocal microscopy and optical coherence tomography as aids in the diagnosis of pemphigoid gestationis

7- Elaboration d'outils pour améliorer au quotidien les instruments d'imagerie cutanéo-muqueux 350
7.1. Practical interest of in vivo reflectance confocal microscopy quantification of cutaneous vascular flow during iloprost treatment
7.2. The 'tissue press': a new device to flatten fresh tissue during ex vivo confocal microscopy examination. Skin

8- Spectrométrie Raman et Microscopie confocale ex vivo.....356
8.1- Spectrométrie Raman……...357

8.1.1. Optical diagnosis of a metabolic disease: cystinosis
8.1.2. Identification of a soft tissue filler by ex vivo confocal microscopy and Raman spectroscopy in a case of adverse reaction to the filler
8.1.3. Unintended changes in the composition of a drug commonly used in dermatology caused by its container
8.1.4. Characterization of coal tattoos by Raman spectroscopy
8.1.5. Characterization of cutaneous foreign bodies by Raman spectroscopy.

8.2-Microscopie confocale ex vivo…….382
8.2.1. Rapid characterization of human brain aspergillosis by confocal microscopy on a thick squash preparation.
8.2.2. A new diagnostic technique for mucormycosis
8.2.3. Ex vivo confocal microscopy imaging to identify tumor tissue on freshly removed brain sample.

9- Imagerie dermatologique de la répartition du tissu adipeux de l'obèse.....391
Non-irradiant Imaging of Fat Distribution: New Essential Tools for the Bariatric Surgery?

10-Varia.....393
10.1. In vivo reflectance confocal microscopy in dermatology: a proposal concerning French terminology
10.2. Quantification of capillary blood cell flow using reflectance confocal microscopy.
10.3. In vivo confocal microscopy for the diagnosis of lysosomal storage diseases
10.4. Role of dermoscopy and reflectance confocal microscopy as an aid in the diagnosis of exogenous ochronosis
10.5. The venous-arterial difference in CO2 should be interpreted with caution in case of respiratory alkalosis in healthy volunteer

G. PUBLICATIONS DE L'AUTEUR 424
1.1. Evolution de l'activité publicatoire après la these de médecine en 1991……..425
1.2. Publications soumises à comité de lecture (référencées dans la base PubMed)……..428
1.3. Participation à des congrès……..441

H.CONCLUSIONS ET PERSPECTIVES.....458
I. ANNEXES ET REFERENCES 463
J.TABLES ET FIGURES ET LISTES ET ABREVIATIONS 472
1.Tables et figures……..473
2.Listes et abréviations……..……..474

A. INTRODUCTION

JUSTIFICATION SCIENTIFIQUE DE LA RECHERCHE

1.Histoire brève de l'imagerie en dermatologie « un langage par l'image »

La dermatologie est une discipline médicale dont la spécificité première est liée à l'accès immédiat à son objet , la ou les lésions cutanées, par le simple examen clinique. Ceci a eu comme conséquence de stimuler très tôt, dans l'histoire de l'humanité, la curiosité et l'intérêt scientifique pour cette discipline . Ainsi, les maladies de la peau sont mentionnées dans toutes les civilisations antiques, et ce, aussi bien par des médecins que des artistes avec des représentations de dermatoses sous la forme de fresques, de dessins et de peintures sur tous types de supports mais aussi de sculptures et même de poésies. A titre d'exemple on peut rappeler que Syphilis était le nom d'un pâtre, d'un poëme de Fracastorius, qui après sa création au XVIéme siècle (1) a profondément marqué la dermatologie en désignant le nom de ce qui allait être la maladie princeps de notre discipline jusqu'à la découverte de la pénicilline. Toutefois cette facilité d'accès n'a pas été un élément stimulant quant à l'élaboration de nouvelles technologies permettant d'examiner la peau in vivo.
Ains,i la dermatologie de la fin du XIXème sciécle utilisait toujours la loupe comme moyen d'examen, in vivo, en complément de l'examen clinique de la peau. Et ce, lorsque dans le même temps les autres disciplines médicales étaient fécondées par les découvertes récentes de la physique moderne aux premier rang desquelles les radiations ionisantes.Celles-ci étaient mises en application au moyen de la radiologie (nouveau mot, nouvelle discipline,nouvelles possibilités) pour explorer les organes profonds. Seuls les moulages de cire, et la collection de la bibliothèque de l'Hôpital St Louis à Paris en sont un témoignage magnifique, puis l'utilisation de la photographie, ont marqué le passage d'une représentation « esthétique » de la peau à une approche plus physique au sens de la transcription (moulage de cire), puis de l'enregistrement (photographie) de la reflection de la lumière naturelle réfléchie par la peau, en l'occurrence, lésée. En effet les cires anatomiques qui étaient déjà largement pratiquées au XVIII^{ème} sciécle, avaient avant tout pour but de montrer l'anatomie de l'intérieur du corps sans se départir d'une composante artistique comme le montre par exemple les cires anatomiques de l'école vétérinaire de Maison Alfort réalisés par Honoré Fragonard cousin germain du peintre Jean-Honoré Fragonard, dont peut adminer des chefs-œuvres au musée du Louvre

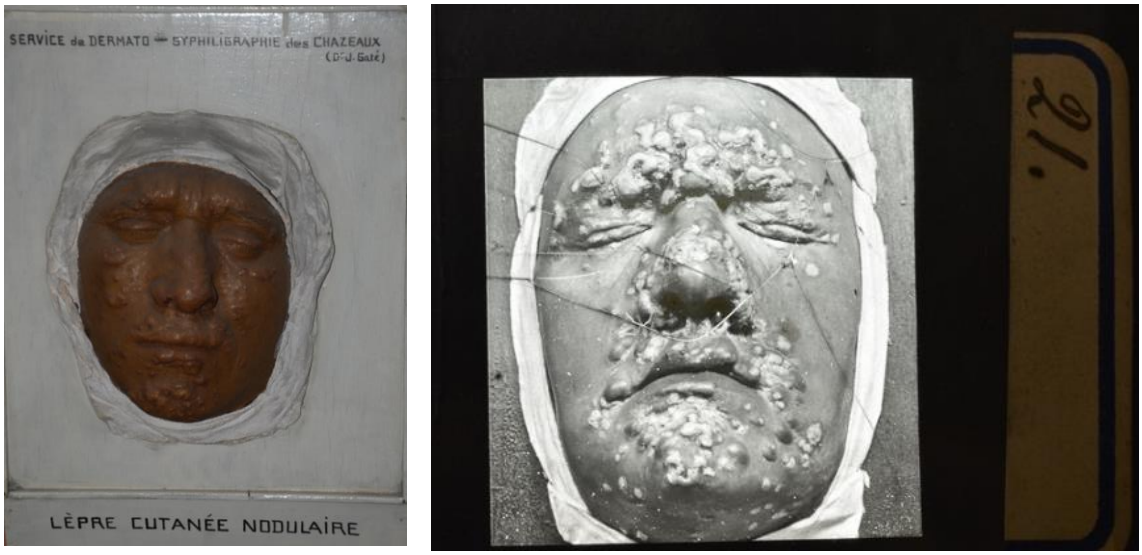

Figure 1 Moulage de lèpre nodulaire du visage (à droite) et Photographie sur plaque de verre (à gauche d'une cire anatomique datant de la fin du XIXéme sciècle collection du service de dermatologie du CHU de St Etienne ancienne collection du Pr Gaté

La caractérisation de la lumière ultra-violette, dite lumière de Wood, fût un premier apport de la « physique dure » pour explorer les caractéristiques, in vivo, de la peau. La découverte de ce spectre lumineux réalisé en 1903 attendra toutefois 1949 pour une première communication scientifique (2) concernant une application dermatologique : l'identification de dermatophytes . Dans le même temps la radiologie classique continuait de se dévelloper.
Ainsi la 2éme moitié du XXéme sciécle était marquée par les immenses progrès de l'imagerie radiologique moderne : échographie-scaner-IRM-scintigraphie. Or les applications dermatologiques de ces méthodes d'imagerie radiologique ne sont apparues que tardivement et essentiellement mises en application par des non dermatologues, des radiologues :scanner, IRM des tissus mous.Par ailleurs l'intérêt porté par les dermatologues à l'utilisation de l'échographie, méthode matériellement et économiquement la plus à leur portée, est restée très limitée quant à son application pratique. Probablement parce que la qualité des images (médiocre définition , absence de couleur , échelle de gris) n'étaient pas un élément très stimulant alors que l'immuno-histochimie et dans une moindre mesure la microscopie électronique focalisaient tous les regard de la recherche dermatologique.
Ainsi, la première franche innovation, ayant eu trait à l'équipement technique dermatologique dans le but d'améliorer la vision du dermatologue, in vivo, a été l'apparition du dermatoscope. Il s'agit d'un système optique en lumière visible avec ou sans contact permettant de magnifier l'image de la peau de 10 à 20 fois, dans la pratique courante. On peut considérer que cela a occasionné la première révolution technologique de l'imagerie dermatologique in vivo. Une recherche bibliographique a permis de retrouver plus de 3700 publications référencées dans PubMed début octobre 2016, après recherche avec le mot clés « dermatoscopy ».Toutefois, si la première publication faisant état de la dermatoscopie date de 1955 (3), la deuxième publication, et qui marque le début des travaux portant sur la dermoscopie, ne surviendra qu'en 1991(4), par une équipe qui créera une véritable école de dermatoscopie.
Dans le même temps des physologistes, des biologistes, plus que des dermatologues, à l'exception notable du Pr Agache de Besaçon, continuaient d'essayer de comprendre le fonctionnement de la peau normale au moyen de méthodes non invasives , in vivo. D'autre part, d'énormes efforts étaient réalisés à des fins de recherche fondamentale, et aussi il est vrai, dans un but commercia,l par l'industrie cosmétique. Cette dernière ayant fourni à de nombreux chercheurs les moyens d'explorer la peau in vivo et notamment de l'examiner au moyen de différents principes physiques pour obtenir de manière non invasive, des images in vivo de tous types.
En effet, il était difficile pour l'industrie cosmétique de justifier des explorations cutanées invasives, chez des sujets sains, dans le but de créer des produits à visée esthétique.Ces industriels ont donc été particulièrement attentifs à toutes les méthodes d'exploration et d'imagerie non invasive de la peau et encore aujourd'hui, les méthodes d'imageries les plus innovantes et souvent, malheureusement les plus onéreuses, sont utilisées en premier par l'industrie comestique. A titre d'exemple, si nous avons été les premiers, à St Etienne à utiliser la caméra de microscopie confocale in vivo, Vivascope 3000, dans un objectif médical , premier modèle réellement autonome pour pratiquer la microscopie confocale actuelle, il ne s'agissait que de la deuxiéme camera vendue, la premiére ayant été acquise par L'Oréal.

2.Historique bref de l'imagerie en dermatologie à St Etienne : « voir au delà des yeux »

Si l'histoire de l'imagerie au CHU de St-Etienne a débuté dans la droite ligne de l'imagerie dermatologique française on peut toutefois considérer que 2 étapes initiales ont marqué le dévellopement du service de dermatologie dans sa volonté de voir la peau « au-delà des yeux ».

- Le protocole d'étude thérapeutique CCPPRB sur l'identification du ganglion sentinelle des malades atteints de mélanome,initié en 1998 (5) et dont j'étais l'investigateur principal, nous a conduit à la collaboration avec une discipline à l'époque totalement étrangère à la dermatologie, à savoir la médecine nucléaire. Et il faut rendre hommage au Dr C Soler, Médecin Nucléaire, d'avoir été le premier initiateur m'ayant conduit à la prise en compte, de considérations de notions de physique pure, de manière consciente et réfléchie, dans ma reflexion scientifique dermatologique.
- La 2éme étape a été l'acquisition du 1er dermatoscope digital du service, le LUV325, en 1999, sur un financement pour parti donné par la ligue contre le cancer. Les images étaient extraordinaires pour l'époque et difficiles d'acquisition. Mais quelle différence de qualité avec les images actuelles…...

Toutefois l'élan était donné. Quatre autres dermatoscopes numériques succéderont à cette première machine, nous ont permettant d'acquérir une culture « d'imageur » en dermatologie, mais aussi d'accepter de ré-apprendre lors de l'acquisition de chaque nouvelle machine, des notions que l'on croyaient définitivement acquises. C'était aussi notre première éducation aux sauts technologiques. .

Il a fallu attendre l'issue de ces 2 étapes soit une longue maturation de 14 ans et notre première publication internationnale dans ce domaine (6), pour que l'activité d'imagerie du service deviennent une activité de recherche clinique à part entière. Si 14 ans de réflexion peuvent paraitre à la fois un clin d'œil aux 7 ans de reflexion de Billy Wilder (dont le titre anglais « Seven Year Itch » n'est pas sans être un rappel à la dermatologie) et surtout peut paraitre bien long, cela doit être mis en parallèle aux 43 ans qui ont séparé la découverte de la lumière de Wood, du premier article publié rapportant son utilité en dermatologie et les 36 ans séparant le 1er article ayant trait à la dermatoscopie et le 2éme confirmant son utilité en dermatologie.

Figure 2. 1er dermatoscope digital acquis par le service de dermatologie du CHU de St-Etienne utilisé pour la première fois par la nouvelle génération de dermatologues stéphanoises spécialisées en imagerie non invasive dermatologique

3. Qu'espérer des outils d'imagerie en dermatologie ? : « La peau est un organe semi transparent , la peau diaphane chantée par les poëtes ».

« Je suis l'enfant de l'air, un sylphe, moins qu'un rêve,
Fils du printemps qui naît, du matin qui se lève
L'hôte du clair foyer durant les nuits d'hiver,
L'esprit que la lumière à la rosée enlève,
Diaphane habitant de l'invisible éther »
V Hugo (7)

Cette transparence, partielle il est vrai, est l'explication physique de la couleur de la peau. A savoir essentiellement un mélange de brun noir et brun roux, apporté respectivement par l'eumélanine et la phaemélanine , le rouge vif et le rouge sombre apportés respectivement par l'hémoglobine oxygénée et l'hémoglobine non oxygénée, et le jaune vert de la bilirubine.La caractérisation des être humains en différentes « races » caractérisées par cette couleur de peau a été l'occasion d'écrire une lettre dans la revue française « La Presse Médicale » s'insurgeant contre ce concept issu du XVIIIéme sciécle, et que nous impose un certain environement nord américain, dans les études scientifiques et industrielles dermatologiques (8).
Cette transparence partielle offre de multiples possibiliter d'explorer la peau, encore faut-il utiliser les méthodes d'investigation adaptées.

Figure 3. La diaphane poudre de riz Sarah Bernhardt (Affiche J Cheret. Fond BNF Gallica)

4.Un dialogue nécessaire avec les physiciens : « comprendre le langage de l'autre pour éclairer la peau »

Les approches, que la physique moderne permet, quant à l'exploration in vivo de la peau sont multiples, volontiers complexes, et nécessitent une collaboration avec les physiciens pour tirer partie de toutes les possibilités qui s'offrent à nous.
En effet cette semi-transparence de la peau, si elle a initialement permis son exploration par la lumière visible, peut être utilisée selon d'autres modalités et selon différents procédés physiques, permettant de pratiquer de multiples techniques d'imagerie : OCT - microscopie confocale - microscopie bi-photonique - spectrométrie Raman - imagerie polarimétrique …..
Mais l'exploration par imagerie in vivo de la peau ne se limite pas à l'optique, l'échographie est un élément important de ce type d'approche qui permettant de visualiser différemment avec les photons l'anatomie de la peau .De plus certaines de ces techniques peuvent se coupler telle l'exploration photo-acoustique qui combine l'analyse l'enregistrement de l'onde mécanique induite par la modification spaciale d'une structure chimique secondaire, à la photoréaction entre cette strucure chimique et le faisceau laser qui l'illumine, et dont la longueur d'onde est spécifique de cette structure chimique. On peut ainsi par exemple, visualiser l'oxyhémoglobine et donc visualiser les vaisseaux la contenant dans la peau.
Par ailleurs, l'échographie de la peau conduit naturellement à l'étude des propriétés mécaniques de cette dernière, ce qui nous à fait envisager l'exploration de la peau non plus seulement sous son seul aspect optique , voir acoustique mais sous le prisme de différentes représentations en tant qu'object physique. Ainsi, par exemple, une collaboration avec la société Efiscience, qui développe un dispositif médical visant à traiter les ulcérations chroniques de la peau par l'utilisation de champs électriques nous a ammené à comprendre la peau comme une structure électrique.Toutefois ce travail initié récemment ne sera pas abordé dans cette thèse.
L'objet de ces différentes méthodes est d'appréhender les différentes caractéristiques, tant de la peau saine que pathologique, mais aussi d'évaluer l'effet de phénoménes physiologiques ou pathologiques interférant avec elle, notamment le vieillissement et plus particulièrement le vieillissement vasculaire en relation avec l'altération du Systène Nerveux Autonome ce qui a été l'objet de l'étude PeauPROOF sujet de la thèse de science du dr E Cinotti.
A cette imagerie d'échelle milimétrique à micrométrique, doit s'ajouter l'imagerie 3D, de parties du corps, ou du corps dans son ensemble. La peau étant, il ne faut pas l'oublier, le plus grand organe du corps.
Dans ce travail il sera donc question de dermatoscopie, de microscopie confocale in vivo et dans une bien moindre mesure ex vivo, d'OCT, et de spectrométrie :spectrométrie Raman et d'analyse multi-spectrale qui sont les 3 axes les plus dévellopés actuellement dans notre équipe et qui ont données lieux à 60 publications en imagerie (au 25 décembre 2016) référencées dans PubMed, et 2 dans Scopus .Mais aussi d'imagerie corporelle totale 3 D.
Cette combinaison de méthodes permettant l'exploration du revêtement cutanéo-muqueux dans sa totalité, étendue à l'appareil oculaire antérieur accessible à nos instruments, est le socle d'une analyse multi-échelle et multimodale que nous élaborons actuellement dans notre unité et dont nous rapportons dans cette thèse 5 ans d'activités exploratoires.

B. RESPONSABILITÉS ET ACTIVITÉ HOSPITALIÈRE

I) CURRICULUM VITAE

I.1) Cursus universitaire

- 1991 : Thèse de Médecine : Facteur Von Willebrand plasmatique et tumeurs endothéliales à propos de 21 cas (travail réalisé dans le Service de Dermatologie Pr Claudy Hôpital Nord).
- 1991 : nomination en tant que Chef de Clinique à la Faculté de Médecine J. Lisfranc (ST ETIENNE).
- 1997 : Chargé d'enseignement auprès de la Faculté de Médecine J. Lisfranc (ST ETIENNE).

I.2) Diplômes universitaires

- 1991 : validation du DES de Dermatologie Vénérologie.
- 1983 Certificat d'Informatique Médicale dans le cadre de la Biologie Humaine : Faculté de Médecine J. Lisfranc (Pr Healy) :
- 1991 : Maitrise de Biologie Humaine d'Hématologie : (Pr Guyotat, Pr Brizard, Faculté de Médecine J. Lisfranc (ST ETIENNE).
- 2013 : DESC de cancérologie

.

I.3) Titres et fonctions hospitalo-universitaires

- 1981 : major au concours de 1ére année de médecine Faculté de Médecine J. Lisfranc (ST ETIENNE).
- 1986 : reçu au concours de l'Internat inter-régions Nord-Ouest (Nantes), inter-régions Est (Nancy-Metz) et inter-régions Rhône-Alpes (Lyon). Choix filière Médecine Spécialisée inter-régions Rhône-Alpes sous-division ST ETIENNE.
- 1990 : major du concours interne Médaille d'Or CHU de ST ETIENNE.
- 1991 : nomination en tant qu'Assistant des Hôpitaux de ST ETIENNE (Service de Dermatologie).
- 1994 : validation du concours de Praticien Hospitalier
- 1995 : nomination en tant que Praticien Hospitalier dans le Service de Dermatologie du CHU de ST ETIENNE (Pr F. CAMBAZARD)

I.4) Activités administratives et responsabilités collectives

Membre du CCPPRB CHU de Saint Etienne 1997à 2001
Expert après du CPRV St Etienne pour les enquêtes nationales de pharmacovigilance :

Neuriplège : comité technique 26/10/95 et commission nationale 01/02/96
Immunostimulants (Biostim, Ribomunil, IRS19….) : Comité technique 12/05/99 commission nationale 21/09/99
Membre fondateur du **Réseau Ligérien du Mélanome** en 1999 association Loi 1901 dont je suis secrétaire générale. Initiation du registre des tumeurs malignes du département de la Loire : Mélanome, Carcinome baso-cellulaire, Carcinome épidermoïde.
Membre du comité plaies et cicatrisation du CHU de St Etienne

I.5) Sociétés savantes

- Membre de la Société Française de Dermatologie et de Vénéréologie (SFD).
- Membre fondateur du GICNI (Groupe d'Imagerie Cutanée Non Invasive) groupe thématique de la SFD
- Président du GICNI (Groupe d'Imagerie Non Invasive) depuis décembre 2015)
- Membre de l'ICWG (International Confocal World Group)
- Président du comité de choix des FMC, Ateliers et Forum pour les Journées Dermatologiques de Paris 2015-2016-2017
- Membre de RésoPso : Réseau Ville Hôpital Universitaire et libéral regroupant plus de 200 dermatologues spécialisés dans la prise en charge du psoriasis
- Membre fondateur de RésoVerneuil : Réseau Ville Hôpital Universitaire et libéral regroupant plus de 120 dermatologues, gynécologues, proctologues chirurgiens, infectiologues, spécialisés dans la prise en charge de la maladie de Verneuil

Initiation de l'Etude Epiver qui consiste en la mise en place d'une étude épidémiologique française concernant 1000 malades affectés par la maladie de Verneuil
- Membre du GUS : Groupe Urticaire de la SFD pour la prise en charge de l'urticaire chronique

I.6) Participation à ouvrage ou livres

Encyclopédie médicochirgical 827-A-10 7p Perrot JL et Misery L : dermatoses liées à Malassezia furfur

I.7) Relecteur de revues scientifiques

- Annales de Dermatologie
- JEADV (Journal of European Academy of Dermatology)
- European Journal of dermatology
- Prescrire

I.8) Activité de conseil scientifique en tant que dermatologue

1.8.1 Société Kamax :
Start up issue de l'unité CNRS Limoge qui développe un système d'imagerie polarimétrique ex vivo. Conseils pour l'application à la dermatologie du système

1.8.2 Société Newtone :
Société de métrologie dermatologique. Conseils pour le développement et l'application à la dermatologie d'une caméra d'analyse multi-spectral Spectra-cam
1.8.3 Société SamanTree :
Start up Suisse qui développe un microscope confocal ex vivo. Conseils pour l'application à la dermatologie.
1.8.4 Société EikoSim :
Start up issue de l'Ecole Normale Supérieure de Cachan qui développe un logiciel permettant de déterminer à partir d'une image d'une structures 3 D les forces de tensions exercées. Conseils pour l'application à la dermatologie du système.
1.8.5 Société LightEcho :
Dispositif issu d'une start up issue de l'école Polytechnique à type de microscope in vivo photo acoustique Conseils pour l'application à la dermatologie du système.
1.8.6 Société efiscience :
Start up rhône-alpine développant des dispositifs médicaux innovant pour la prise en charge des plaies. Conseils pour l'application à la dermatologie des systèmes.
1.8.7 Société Biovotec :
Start up norvégienne développant un dispositif médical à base d'œuf innovant pour la prise en charge des plaies. Conseils pour l'application à la dermatologie du dispositif médical
1.8.8 Société DAMAE :
Start up Française issue de l'Institut Supérieur Optique de Palaiseau, développant un dispositif médical d'imagerie OCT HD. Conseil pour l'application à la dermatologie.

II. ACTIVITE DE SOINS

II.1) Emploi du temps hebdomadaire

- Trois 1/2 journées de consultation médicale et d'imagerie
- 1/2 journée de consultation de microscopie confocale Dermato-ophtalmologique
- 1/2 journée de consultation de microscopie confocale Gynéco-dermatologique mensuelle
- Repérages des marges d'exérèse en microscopie confocale : les jeudis matin de 8h à 9h00
- 1/2 journée de consultation chirurgicale dermatologique
- Deux 1/2 journées consacrées à la visite des malades hospitalisés dans le service

II.2) Consultation et hospitalisation

- Consultation
  80 à 90 patients vus en consultation par semaine.
  Délais de rendez-vous à 5 mois.
  2989 malades vus personnellement en consultations diverses en 2015
- Hospitalisation
  Participation à la rédaction et signature de 661 comptes rendus d'hospitalisation en 2015

- Bon réseau avec les médecins du CHU, mais aussi et surtout, les médecins de ville notamment au sein du Réseau Ligérien du Mélanome créé en 1999

II.3) Réunion de Concertation Pluridisciplinaire RCP

- Une par semaine de cancérologie (jeudi après-midi)

III. ACTIVITE D'ENSEIGNEMENT

III.1) Enseignement des étudiants de médecine et internes

- **A/ service de dermatologie**
- Enseignement au lit du malade pour les externes et les internes
- Coaching pour les publications des internes
- **B/ service d'ophtalmologie**
- Enseignement au lit du malade pour les internes
- Coaching pour les publications des internes

III.3) EPU, Séminaire, FMC pour l'année 2016

Depuis de nombreuses années j'ai été amené à participer à de nombreuses réunions : EPU, FMC, Séminaire. Par esprit de concision je ne rapporterai que les principales réunions pour lesquelles j'ai été sollicité comme orateur mais pas ma participation à des board d'experts auprès de l'industrie pharmaceutique pour l'année 2016

- EPU mensuel pour les dermatologues du réseau ligérien et d'ailleurs depuis 1991.En tant que co-animateur (**10 réunions** mensuelles, les vendredis toute la matinée)
- SFIIC (Société Française d'Imagerie et d'Ingénierie Cutanée) **Mars** Paris
- Lausanne, Suisse FMC des dermatologues libéraux romands **Juin**
- Journée de l'académie des sciences à l'Université de St Etienne **Juin**
- Biomedical imaging applied to dermatology organisé par le Le2i - UMR CNRS 6306 Univ. Bourgogne Franche-Comté, LE2I Lab. **Septembre** Dijon
- MINALOGIC « Technologies du numérique pour la médecine personnalisée » Grenoble **novembre**
- Soirée Automne **Novembre** / Maison de la Recherche (Paris) « Prise en charge de la maladie de Verneuil en 2016 »
- JDP 2016 **décembre** :
    - Atelier de microscopie confocale : Formation niveau 1
    - FMC : Nos plus beaux Cas
    - FMC : Quand la microscopie confocale éclaire la dermatoscopie
    - Forum : Le lentigo malin en 2016

IV. ACTIVITE DE RECHERCHE

IV.1) Travaux personnels

- **Mémoire** : traitement informatique d'une phrase logique permettant de caractériser un sous-ensemble au sein d'une population donnée.
- **Mémoire** : Variant Normandie de la maladie de Von Willebrand à propos d'un cas.

IV.2) Investigateur principal – coordinateur

1/ Étude mono centrique avec CHU promoteur :

- Projet : « Détection du ganglion sentinelle du mélanome par lymphoscintgraphie » 1996
- Projet: « Scintigraphie au sestamMibi ».1997
- Projet Erysipèle et TVP 1993
- Projet OCT Galaxy 2016

2/ Étude multicentrique observationnellle de cohortes (travail en cours) :
- EpiVer (Etude Epidémiologique de la maladie de Verneuil : 100 centres investigateurs du groupe RésoVerneuil
- Epidémiologie du Mélanome dans le département de la Loire de 2004 à 2015
- Epidémiologie du carcinome baso cellulaire dans le département de la Loire de 2005 à 2015
- Epidémiologie du carcinome épidermoîde de la peau dans le département de la Loire de 2005 à 2015

IV.3) Encadrement de travaux de recherche

- M2 : encadrement des travaux de M2 de Mme Alexia Brehon
- Thèse de médecine : encadrement des travaux de Mme C Couzan

IV.4) CCPPRB

- Membre du CCPPRB (Comité Consultatif pour la Protection des Personnes et la Recherche Biomédicale) du CHU de Saint Etienne de 1991 à 2001

IV.4) Prix de recherche

- Prix Bioderma JDP 2009 pour le meilleur poster d' « Angio-dermatologie /Cicatrisation »

C/ Projet DOCT-VCSEL

Portable Optical Coherence Tomography with MEMS-VCSEL swept-sources for skin analysis

ANR 2015 / Défi sociétal « Vie, Santé et Bien-Etre »
Axe 13 « Technologies pour la santé »

Dr Jean-Luc Perrot
Responsable scientifique médical du projet

(*Scientific leader partner 4 (UHSE), Medical specifications, medical expert, clinical trial responsible)*

Il s'agit d'un projet visant à créer un nouvel OCT moins cher qu'un microscope confocal et ou un OCT HD, soit aux environs 15 000€, alors qu'un microscope confocal in vivo coûte actuellement plus de 80 000 € et qu'un OCT HD coûte environ 90 000€, mais aussi un dispositif plus simple d'apprentissage en s'aidant pour l'interprétation des images de l'apport de l'intelligence artificielle.
Ceci permettra :
- de définir ce que les anatomopathologistes appellent le signe de la silhouette, à savoir visualiser la forme de la tumeur et ses rapports avec les structures cutanées adjacentes
- d'avoir une définition optique suffisante pour pouvoir compléter le diagnostic évoqué par l'examen clinique et la dermatoscopie réalisés préalablement
- de pouvoir aider l'analyse des images OCT ainsi obtenues par l'intelligence artificielle.

DOCT-VCSEL
Portable Optical Coherence Tomography with MEMS-VCSEL swept-sources for skin analysis

ANR 2015 / Défi sociétal « Vie, Santé et Bien-Etre »
Axe 13 « Technologies pour la santé »

Sommaire

ABSTRACT 1

TABLEAU RECAPITULATIF DES PERSONNES IMPLIQUEES DANS LE PROJET 2

EVOLUTIONS EVENTUELLES DE LA PROPOSITION DETAILLEE PAR RAPPORT A LA PRE-PROPOSITION 3

1. CONTEXT AND PROJECT OBJECTIVES 3

1.1. CONTEXT, MOTIVATIONS 3
1.2. PROJECT OBJECTIVES AND TECHNOLOGICAL CHALLENGES 6
1.3. PROJECT POSITIONING (NATIONAL AND INTERNATIONAL) 9

2. SCIENTIFIC AND TECHNICAL PROGRAM, PROJECT ORGANIZATION 12

2.1. PROJECT ORGANIZATION 12
2.2. DESCRIPTION BY TASK 13
2.3. TASKS SCHEDULE, DELIVERABLES AND MILESTONES 22
2.4. QUALIFICATION AND CONTRIBUTION OF EACH PARTNER 22
2.5. SCIENTIFIC JUSTIFICATION OF REQUESTED RESOURCES 26

3. RESULTS EXPLOITATION AND DISSEMINATION STRATEGY, GLOBAL IMPACT . 27

REFERENCES 29

Abstract

Invasive biopsy is still today the reference diagnostic technique of a lot of skin pathologies (inflammation, tumors). Nevertheless, several situations of diagnosis should be kept as conservative as possible. Consequently, non-invasive imaging methods (ultrasounds, computed tomography, magnetic resonance imaging) have been developed for clinical use. In particular, existing optical coherence tomography (OCT) systems can perform non-invasive 3D optical biopsies of skin, improving patient's quality of life. Nevertheless, these bulk systems are expensive (100 k€), essentially only affordable at the hospital and hence not sufficiently employed by physicians or dermatologists as an early diagnosis tool. MEMS-VCSEL technology offers a novel combination of high compactness, high speed, record coherence length, and flexibility for wavelength-tuned OCT systems. The use of optically pumped MEMS-VCSELs sources for SS-OCT at 1.3 µm for ophthalmology was first demonstrated in 2011 but since that time, the threshold towards the use of low-cost electrically-pumped devices is still not crossed. DOCT-VCSEL project aims at demonstrating a portable SS-OCT imaging system based on novel electrically-pumped MEMS-VCSEL light-source technology operating at 850 nm and taking advantage of polymers and semiconductors -based collective micro-nanotechnologies. These new compact and low cost sources can be arranged in arrays and will be completing an adapted architecture of array-type active Mirau interferometers developed within the European collaborative project VIAMOS (2012 -2015). Thanks to this combination, we will develop a miniature (< 20 cm^3), low cost SS-OCT imager (15 k€) providing cross-sectional 3-D tomograms with a depth greater than 0.5 mm, axial and transverse resolutions of 6 µm (corresponding to a laser tunability of 35 nm) and imaging field of 8x8 mm^2, enabling doctors to perform painless and earlier detection of skin pathologies, including intra-operatively for the delimitation of gesture. For this purpose, DOCT-VCSEL brings together an experienced consortium made of 2 research institutes (LAAS/Toulouse and FEMTO ST/Besançon) and 1 medical group (Service de Dermatologie CHU de St Etienne). Partner's expertise includes MEMS, MOEMS, VCSELs, OCT microscopy and dermatology. A unique team of transverse expertise is thus gathered in DOCT-VCSEL to design and demonstrate a miniature solution for in vivo 3D skin imaging to further address the early diagnosis of cutaneous pathologies that will potentially benefit millions of people worldwide. To validate the technical and functional performances of DOCT-VCSEL microsystem, translational trials will be performed at the CHUSE in the department of Dermatology by the end of the project. For an easy and rapid analysis, a specific imaging processing tool will be developed with the help of the company Pixience specialized in skin measurements tools.

Tableau récapitulatif des personnes impliquées dans le projet

Partner	Name	First name	Current position	Involvement (P.M.)	Role and Contribution in the project (4 lines max)
LAAS CNRS (Partner 1)	*BARDINAL-DELAGNES*	*Véronique*	*DR2 CNRS*	*20*	*Project coordinator Scientific leader partner 1 (LAAS) Design, technology and characterization of MEMS-VCSEL*
LAAS CNRS	*CAMPS*	*Thierry*	*Professor PR1*	*12*	*Design and characterization of thermal and electro-actuation polymer MEMS*
LAAS CNRS	*DOUCET*	*Jean-Baptiste*	*IE2 CNRS*	*10*	*MEMS and VCSEL technology Polymer chemistry*
LAAS CNRS	*ARNOULT*	*Alexandre*	*IR1 CNRS*	*5*	*VCSEL epitaxial growth*
LAAS CNRS	*DARAN*	*Emmanuelle*	*IR1 CNRS*	*5*	*Nanotechnology for MEMS and Mirror fabrication*
LAAS CNRS	*TEMPLE-BOYER*	*Pierre*	*DR2 CNRS*	*3*	*Dielectric mirror fabrication and characterization*
LAAS CNRS	*ROUSSET*	*Bernard*	*IRHC CNRS*	*2*	*Dielectric mirror fabrication*
LAAS CNRS	***Not yet recruited***		*PhD student (paid by ANR)*	*36*	*MEMS-VCSEL design, growth and technology and system integration*
FEMTO-ST (Partner 2)	*GORECKI*	*Christophe*	*DR1 CNRS*	*11*	*Scientific leader partner 2 participation to the design & specifications, microsystem integration , dissemination and exploitation, risk analysis*
FEMTO-ST	*PASSILLY*	*Nicolas*	*CR1 CNRS*	*15*	*Mirrors design & OCT microsystem design*

					microsystem integration, dissemination
FEMTO-ST	*FROEHLY*	*Luc*	*CR1 CNRS*	*9*	*OCT and Metrology specifications, development of OCT bench*
FEMTO-ST	*Hong FU*	*Chen*	*PhD student*	*10*	*Metrology specifications, development of OCT bench*
FEMTO-ST	*DE LABACHELERIE*	*Michel*	*DR1 CNRS*	*6.5*	*Participation to the design*
FEMTO-ST	***Not yet recruited***		*Contractual researcher paid by ANR*	*18*	*Participation to optical design, packaging & assembling, participation to tests of microsystem*
CHU St Etienne (Partner 3)	*PERROT*	*Jean Luc*	*MD*	*9*	*Scientific leader partner 4 (UHSE) Medical specifications, medical expert, clinical trial responsible*
CHUSE	*Labeille*	*Bruno*	*MD*	*4*	*Medical specifications, medical expert*
CHUSE	*Garcin*	*Arnaud*	*Clinical Research Engineer*	9	*UHSE coordination and clinical trial management*
CHUSE	*Douchet*	*Catherine*	*MD*	*3*	*Anatomo-pathology expert Pathological Anatomy and Cytology Department*
CHUSE	*Cambazard*	*Frédéric*	*MD PhD*	*9*	*Histological/new images correspondence*
CHUSE	***Not yet recruited***	*-*	*Research engineer paid by ANR*	*12*	*Data acquisition and transformation*

Evolutions éventuelles de la proposition détaillée par rapport à la pré-proposition

Compared to the short proposal, no significant change has to be mentioned in project organization. As announced, DOCT-VCSEL consortium is a PRC project with 3 academic

partners. Nevertheless, it is worth noting that in 2014, this proposal was a PRCE project including an industrial partner, PIXIENCE, a French SME in charge of the development of imaging tasks. Our project was evaluated as “an ambitious and very innovative project” by ANR 2014 TecSan committee, which encouraged us to submit it again with a reduction of requested resources. Moreover, PIXIENCE’s contribution was evaluated to be “less innovative” than the other ones. We have then decided to modify the type of partnership and to convert the project into a PRC one (academic). PIXIENCE company is now a sub-contractor of CHUSE and will ensure a part of image processing tasks. Image interpretation and comparison to other types of images (histology and images from bulky equipments) will be insured by CHUSE, thanks to the recent recruitment of a new permanent INSERM engineer and to the acquisition and/or to the renting of bulky OCT equipment. This way, the requested resources have been significantly decreased (from ~850k€ to ~663k€), as asked, while scientific innovation of the project is fully preserved. As a potential end-user of the results, Pixience still fully supports DOCT-VCSEL project (cf. Letter at the end of this document). Moreover, the “Pôle de Compétitivité Cancer-Bio-Santé” which, in principle, only supports PRCE projects, has decided to maintain its agreement to the project despite it is now a PRC.

1. Context and project objectives

1.1. Context, Motivations

The target: OCT for early detection of skin pathologies

Invasive biopsy is still today the reference diagnostic technique of a lot of **skin pathologies** (inflammation, tumors). Nevertheless, several situations of diagnosis should be kept as conservative as possible. Consequently, non-invasive imaging methods (ultrasounds, computed tomography, magnetic resonance imaging) have been developed for clinical use [1][2][3]. However, the resolutions of these techniques are on the order of 100-200 µm, what is not sufficient to resolve the skin morphology usually investigated in the frame of histopathology (5-10 µm resolution). Confocal microscopy allows reaching almost this size in details visualization, but is not depth enough in its exploration (maximum of 250µm under the skin surface). Other issues involved with these techniques are low contrast, high costs, and in some cases intrusiveness of radiations. One of powerful solutions is the **non-invasive OCT** that can generate micron-resolution 3D images of tissues and thus provide a kind of **“optical biopsy”** of skin. Based on the principle of white-light interferometry and developed initially in 1991 for in-vivo imaging of the human eye (Fujimoto’s group, Ref [4][5]), OCT was investigated by a large number of groups worldwide. With regards to penetration depth and resolution, OCT is a perfect trade-off between ultrasound and confocal microscopy (Fig. 1).

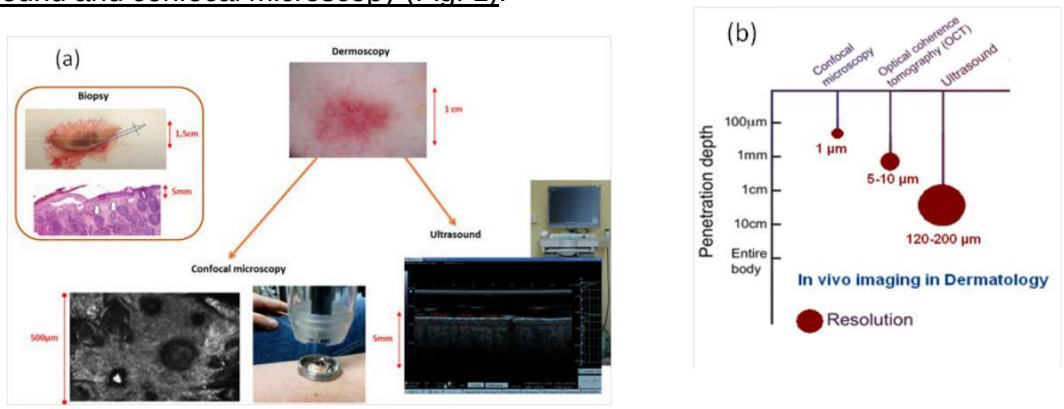

Fig.1 (a) Existing techniques for dermatology (b) Comparison of OCT resolution and imaging depths to those of alternative techniques; the length represents imaging depth and the "sphere" size represents resolution.

OCT uses non-ionizing radiation at biologically safe levels, allowing long exposure times. Its level of complexity is closer to ultrasounds than to CT or MRI (magnetic resonance imaging), allowing the realization of low-cost portable scanners. The point-scanning nature of usual OCT technology

allows it today to be implemented in fibre optics, which makes endoscopic and catheter-based imaging possible. OCT technique has already become established as a standard technique for biological tissue imaging, with numerous commercial instruments on the market and a rapid extension of applications of OCT to various medical areas (cardiology, dentistry, pulmonary, dermatology). However, the conventional OCT microscopes are bulky, performing micro-scale measurements from the macro word. Existing solutions are strongly dominated by fiber optics interferometers, combined often with massive scanners and bulk optical components. These building blocks are assembled by conventional technologies, making it expensive. For economic reasons, OCT microscopes, with clinical use agreement, are then only accessible in hospitals and clinics. Figure 2 shows respectively Michelson Diagnostics and Agfa microscopes which are used currently in dermatology. These OCT systems are commercially available with EC homologation for clinical use. Corresponding performances and technical characteristics are listed in Table 1. AGFA system is very fast (320 000 A-scan per second) and leads to high quality measurements (3µm axial and lateral resolutions). However, dermatologists need a system with a larger field of view (5 x 5 mm^2) such as Michelson system. The two current devices are then complementary tools. An ideal OCT tool should show a large view (8 x 8 mm^2 with lower resolution) and make possible a switch and focus with high resolution on the area of interest, in order to obtain a cellular view. These choices could allow us to cover a large field of targeted pathologies. Moreover, existing device's volume is around 3000 cm^3 and the units cost around 100 k€. The consequence is that compactness and low-cost are not within reach of their conventional approach. With the recent developments of VCSEL technology combined with MEMS and micro-optical technologies, significant advance in miniaturization of OCT systems can be expected, making OCT imaging suitable for Point Of Care (POC) applications

Table 1:

Society	AGFA, Germany	Michelson, UK
Product	SkinTell®	VivoSight®
Type of OCT system	High Resolution Optical Coherence Tomography	Multi Beam Optical Coherence Tomography
Scan depth (mm)	0.520	2
Lateral resolution (µm)	3.5	7.5
Axial resolution (µm)	3	5
Wavelength (nm)	1305	1300
Field Of View (mm^2)	1.8 x 1.5	5 x 5
Acqui + reconstruct (min)	1	1
Gel needed?	YES (possibility to add also a drop of glycerin to improve the quality of the image)	NO
Artefact	NO (the skin stay flat)	YES: there is a little curved deformation of the surface of the skin, due to the probe application

a) b)

Fig. 2: (a), Skintell® Agfa (image from Agfa booklet) and (b) Vivosight®, Michelson Diagnostics OCT Table 1: Comparison of Agfa (left) and Michelson (right) OCT bulky systems technical parameters.

Towards miniaturized SS-OCT systems

There are two major categories of OCT instruments: time-domain OCT (TD-OCT) and spectral-domain OCT (SD-OCT) . This last (SD-OCT), provides advantages in sensitivity (which can reach 120 dB), and allows faster signal acquisition. A variant of OCT, called “Swept-Source” (SS-OCT), combines the advantages of standard TD-OCT and SD-OCT. **SS-OCT** detection uses a laser light source whose emission sweeps back and forth across a wide range of wavelengths and enables orders of magnitude faster imaging speeds compared to original TD-OCT. Recent maturity of MEMS and laser diodes technologies starts to be useful in miniaturization of SS-OCT systems**.** Some MEMS-swept sources have been recently reported for OCT imaging [6][7] Among them, VCSELs are of great interest owing to their very short cavity length (~1 µm). Among these new compact sources, **VCSELs** (for Vertical-Cavity Surface-Emitting Lasers) [8] are the best candidates owing to their true single longitudinal mode emission in continuous-wave operation without any mode hopping, combined to a Gaussian beam, a low power consumption (mW) thanks to their short cavity (~1 µm), and a long coherence length (>10 mm). Furthermore, these laser diodes can be easily arranged in arrays and fabrication of electrically-pumped (non tunable) 850nm devices is already mature and low cost (few euros)(fig 3)

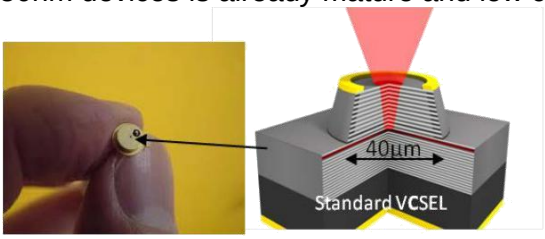

Fig. 3: Schematic view of a standard (non tunable one) electrically-pumped 850nm VCSEL source after mounting on a TO can.

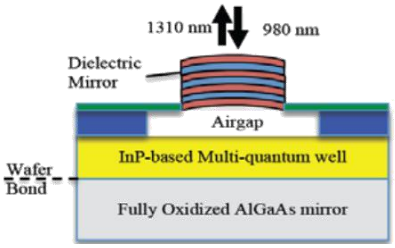

Fig. 4: Schematic view of a 1.3µm spectrally tunable MEMS-VCSEL (optical pumping) [7]. (Praev. Res. Thorlabs). A bulk fibered coupling system is necessary.

Moreover, a wide spectral tunability can be obtained in specific VCSELs called “**MEMS-VCSELs**” [9], where a movable micro-mirror is used above a half -VCSEL structure (Fig. 4). When changing the vertical position of the micro-mirror, the optical length of the cavity changes, leading to a

variation of the laser emission wavelength [8]. However, these devices are not yet commercially available and up to now, research mainly focuses on their application to optical communications. Nevertheless, a first SS-OCT system using an optically-pumped MEMS-VCSEL was reported at the end of 2011 by the MIT, Praevium Research, and Thorlabs [7]. The MEMS-VCSEL device proposed by Praevium Research et al. emits at 1.3 µm (and more recently at 1.06 µm) on a broad range (>100 nm). Thanks to this first breakthrough, this consortium was able to perform 3D imaging of anterior eye segment at record depths (>6 mm). This impressive technology recently enabled new imaging modes including pulsatile Doppler blood flow imaging, high speed-endoscopic imaging and wide-field retinal imaging. However, this technology did not have sufficient potential for miniaturization due to optical pumping. In a recent conference (2015), the same consortium reported the first electrically-injected MEMS-VCSEL at 1050nm suitable for OCT ophthalmologic imaging [13]. This is a significant breakthrough since electrical injection avoids optical pumping and associated hardware. **However, this device is not emitting at 850nm and it is not integrated in a truly low-cost portable SS-OCT prototype so far**. It still has to be coupled to an optical fibre with a strong reduction of the output power (~100µW) and thus to an optical amplifier. Moreover, high swept-frequencies are required for the MEMS prototypes proposed by Praevium (>300 kHz) because their principle is based, as for many OCT systems, on raster scanning of a single detection point. As a result, high speed electrostatic actuation is needed to allow a reasonable inspection time, implying important voltages for MEMS driving.

OCT for skin imaging at short wavelength (850 nm) using an active array-type Mirau interferometer (VIAMOS project)

FEMTO-ST is currently developing in collaboration with CHUSE and other European partners an active array-type Mirau interferometer for SS-OCT imaging [14]. This is in the frame of European collaborative project VIAMOS (FP7 ICT program, 2012-2015) applied for early detection of skin cancer and operating at 850 nm [15]. Figure 5 illustrates the principle of VIAMOS microsystem and shows three tested building blocks before the assembly of complete microsystem. Here, a doublet of microlens arrays and a wafer of movable reference mirrors are vertically integrated to build the active Mirau interferometer. Here, the incident light beam from a deported broadband light source is frequency swept by a mobile membrane of a piezo-electrically actuated tunable Fabry-Perot interferometer (FPI), creating a swept-source. The light is then collected by microlenses and directed towards the skin sample. For each single-channel interferometer, the collected light passes through a planar beam-splitter that reflects half of it back to a moving reference mirror while the rest of light is transmitted towards the sample to be measured. The beams reflected by the sample and by the reference mirror interfere, generating a “spectral” interferogram directed by the microlens towards a high speed camera after reflection on a cube beam-splitter. The array of Mirau reference mirrors is integrated on top of an electrostatic vertical actuator used to generate the phase shifting schema what enables a rapid measurement of the amplitudes and phases. The FPI acts as a narrow-band transmission filter for active wavelength selection. Table 2 shows the expected specifications.

The building blocks of VIAMOS microsystem are now assembled by multi-wafer bonding and the complete, experimentally validated prototype will be installed in June 2015 at CHUSE.

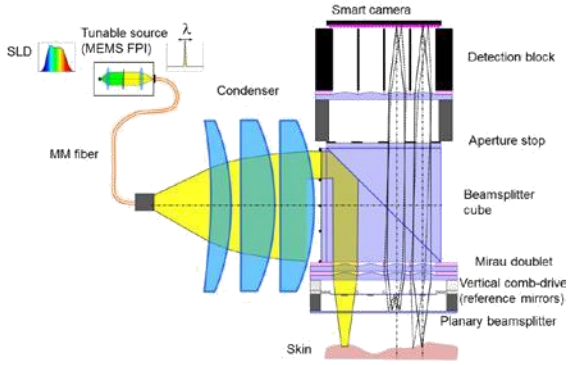

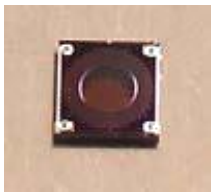

FPI chip aperture 1.5 mm and doublet of 4x4 glass micro lenses (8x8 mm^2) of Mirau interferometer.

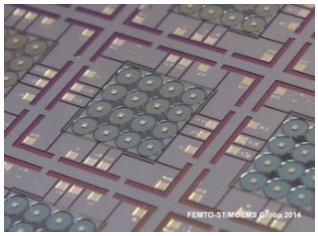

Mirau MEMS actuator carrying the glass platform with reference mirrors ((8x8 mm^2)

Fig. 5: VIAMOS project: principle of array-type OCT system (left) and components of active Mirau interferometers (right). The source stage is not integrated in this configuration.

.

Light source: SLED	bandwidth: 50 nm, 50 mW per channel
Laser center wavelength	850 nm
Fabry-Perot interferometer resolution	1.2 nm ,will be improved by DOCT-VCSEL
Optical resolution (in tissue)	~5 µm lateral, ~5 µm axial
Total penetration depth	500 µm
Surface scanned (4x4 single-channel Mirau interferometers)	8x8 mm^2
Sensitivity	75-85 dB
Volume of full system (source not included)	< 20 cm^3

Table 2 VIAMOS specifications of OCT microsystem

In the frame of VIAMOS, it has not been possible to consider advanced and miniaturized light sources. Consequently, FEMTO's choice was to use a broadband source (SLED) filtered by a piezoelectric FPI in order to build the swept-source. However, this source is not sufficiently miniaturized, thus deported from the handheld device. In addition, the optical power is limited since one source is split between all the different channels of the Mirau interferometer. Finally, resolution of the piezoelectric FPI (barely>1 nm) does not allow recording a large depth per sweep. In these conditions, the development of a compact electrically-pumped 850 nm highly coherent tunable sources that can be arranged in arrays will significantly upgrade the performances of the OCT microsystem: scanned depth per sweep, depth penetration, and improved potential of miniaturization, lowering the power consumption and reducing again the cost of OCT microsystem

1.2. Project objectives and technological challenges

DOCT-VCSEL project will aim at demonstrating a new type of electrically-injected 850 nm MEMS-VCSEL swept-source that can be directly integrated in a highly miniaturized and low-cost full-field SS-OCT system for non-invasive detection of skin pathologies. Thanks to the combination of MOEMS and electrically-injected VCSELs technologies that are more mature for 850 nm than at 1.06 or 1.3µm, this will lead to a portable instrument for dermatology, operating at low power consumption and adapted for parallel inspection, and suitable for 3D reconstructions of skin with lateral and axial resolutions as low as 6 µm and a penetration depth of 0.5 mm. More precisely, DOCT-VCSEL scientific and technological objectives are the following:

(1) Demonstration of a low consumption tunable 850 nm MEMS-VCSEL

Our technological approach will be based on an electro-thermal polymer MEMS instead of a classical dielectric electrostatic one (Fig.6-left). Indeed, the exploitation of an original parallel OCT architecture (fig. 6-right and next paragraph) will drastically reduce the requirements on the MEMS swept frequency, which will be in the range of few tens of Hz (instead of hundreds of kHz).This will also reduce the MEMS actuation power and lead to a **simpler, low cost and small footprint fabrication**. **LAAS** recently developed this kind of MOEMS (carrying a microlens) for the dynamic focusing of 850 nm standard VCSELs [16][17]. Thanks to SU-8 polymer thermal properties, a large vertical shift is obtained in our MEMS-VCSEL, and thus a sufficient spectral tuning is achievable with a significant reduction of the operation temperature (100°C compared to 300°C reported before [17]) and of MEMS resulting power consumption. A **better reliability** of the MEMS is also expected, as well as a shorter time response

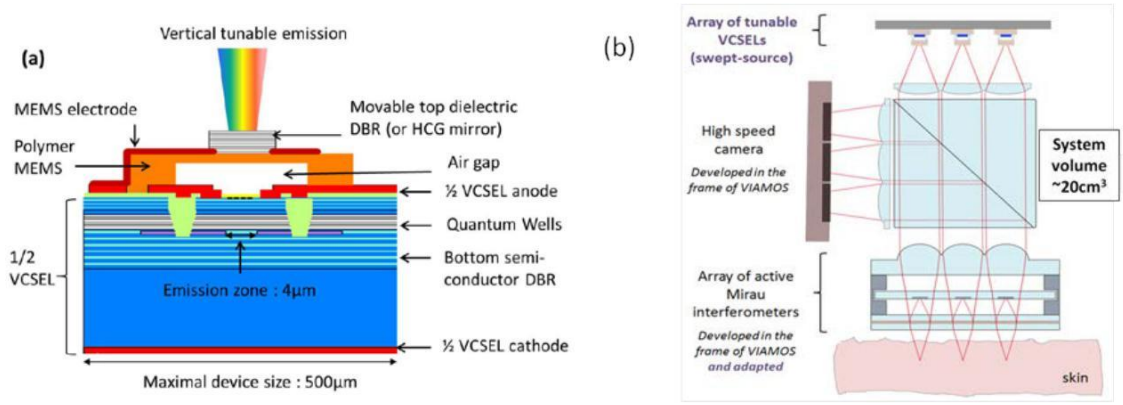

Fig. 6: a) Description of the electrically-pumped polymer-based MEMS-VCSEL (maximal footprint: 500 µm) b) Complete OCT µ-system including 850 nm MEMS- VCSEL arrays and a parallel treatment (~20 cm^3).

In SD -OCT systems, axial resolution is directly related to the spectral range used to illuminate the sample, i.e. wider the spectral range, better the axial resolution. In the case of SS-OCT (which is a particular case of the SD-OCT), it means a larger tunable range of the swept source allows a better resolution. The maximal tunable range of MEMS-VCSELs mainly depends on the FSR (Free Spectral Range) of the laser micro-cavity. FSR is much lower at shorter wavelengths (λ=760 and 850 nm) than at λ= 1.55 µm due to a scaling factor. It is mainly fixed by the bandwidth of the DBR mirrors. The main limitation comes from the bottom semiconductor mirror with a stop-band limited to ~70 nm. This mirror has indeed to include ternary alloys (typically $Al_{15\%}Ga_{85\%}As$ and $Al_{90\%}Ga_{10\%}$ As) instead of binary ones (GaAs/AlAs) to avoid optical absorption below the GaAs band gap edge (870nm) and allow the selective oxidation of a single Al-rich layer for electrical confinement in the device. As a result, the refractive index contrast in the DBR is low and the resulting lasing span (corresponding to the correspondence of high

reflectivity and high quantum well emission zones) is finally limited to ~18 nm@850 nm. A red-shift of the aimed central mirror wavelength can help to slightly enlarge this span up to 25 nm@865 nm. The first part of the project will therefore explore a classical DBR approach for the mirrors in order to target a spectral tuning range of ~20 nm at a central wavelength of ~860 nm (low risk, expected corresponding OCT resolution: 12µm). The laser polarization will be stabilized by means of a standard etching of a micro-scale pattern on the cap layer of the half-VCSEL structure. As for the top DBR to be deposited on the SU -8 MEMS, it will be composed of a dielectric (SiN_x/SiO_2) multilayer fabricated by ICP-PECVD at low temperature (<100°C), for which we recently obtained a top DBR reflectivity high enough for laser emission at low current (~1mA) (Fig.8b).

In the second part of DOCT-VCSEL project, we will extend the spectral range of our source to ~35nm (for an OCT resolution of ~6 µm) by optimizing the bottom DBR design and/or by exploiting a novel type of SWG-HCG (Sub-Wavelength/High-Contrast-Grating) mirror (higher risk). This kind of nanostructure grating combines many advantages compared to a conventional vertical DBR such as a better control of the reflectivity level, a wider bandwidth, a higher compactness and an intrinsic polarization stabilization thanks to 1D grating geometry. This approach is more suited to electrical injection in 850nm devices than the one of Praevium, which is based on oxidized mirrors and only

applicable at longer wavelengths (λ>1µm). Only one demonstration of tunable MEMS-VCSEL including a HCG mirror was reported at 850 nm [18]. Its fabrication is complex because of narrow tolerances and requires the use of electronic lithography to generate a nano-pattern transferred afterwards in GaAs. In DOCT-VCSEL, we will evaluate the feasibility of HCG mirrors fabricated by Nano-Imprint Lithography (NIL) in the semiconductor layers or in a thin polymer layer followed by a low temperature conformal deposition of a high index layer [20]. NIL is a collective fabrication technique compatible with large production and will be a key technological step to meet the requirements of a highly tunable and low-cost SS-OCT prototype.

(2) Source validation and integration in a parallel and miniaturized low-cost SS-OCT system

Simultaneously to swept-source fabrication and validation, we will design and implement a parallel OCT architecture for the inspection of hundreds of thousands points simultaneously. It is based on full-field imaging (8x8mm²) and on a technology of active array-type Mirau interferometer [14] . The microsystem is being made in the frame of the European project VIAMOS in which the resolution of the MEMS FPI (>1 nm) does not allow a large depth per sweep. The **ultimate miniaturization** brought by the insertion of the **MEMS- VCSELs** developed within DOCT-VCSEL project will thus significantly upgrade the performances of scanned depth per sweep and depth penetration while increasing the potential of miniaturization, lowering the power consumption and reducing the cost of complete OCT system. To this end, a new prototype will be jointly designed to take into account the specificities of MEMS-VCSELs sources arrays requiring the modified optical design (Fig. 7b) and to experimentally validate the complete chain of OCT microsystem with swept-source VCSEL. A summary of the needs and specifications of our prototype can be found in Table 3.

Table 3: Summary of the specifications and their consequences onto the MEMS-VCSEL source

Needs	Answers	Consequences for DOCT-VCSEL project

low cost	Full-field imaging > combining: CCD detector and “less demanding“ source (power/speed)		**VCSEL:** GaAs technology, polymer MEMS arrays **MOEMS interferometer:** Arrays
Handheld system	MEMS and VCSELs technologies		**VCSEL:** Electrical injection, monolithic **MOEMS interferometer:** Multi-wafer bonding
B-scan acquisition time <2s	SD-OCT, full-field imaging, high speed CCD imager.		**VCSEL:** Tuning speed ~10 Hz => MEMS-VCSEL: thermal actuation
Resolution similar or better than histopathology	Axial resolution 12 µm 6 µm	Sweep range: 20 nm 35 nm	**VCSEL:** =>with standard DBRs =>with HCG grating and /or optimized DBR
Imaging depth: reach dermo /epidermal junction	High coherence length => Spectral resolution <0.5 nm Source Power >1 mW/channel		**VCSEL:**Short cavity single mode linewidth =10MHz; coherence length>10 mm > 1 mW power, target: 2 mW

Success of this new medical equipment is not only linked to its intrinsic performances but also to the much lower cost than the existing systems on the market . The lower cost will ensure access to more users and then a more efficient early diagnosis. The low-cost asset is achieved thanks to the combination of MEMS and VCSELs technologies that lead to a significant reduction of the cost because of the collective fabrication. Similarly, and as mentioned earlier, choice of a matrix of full-field systems (based on a camera) significantly releases the constraints onto the sweep frequencies and the optical power of the source, and thus one again its cost. This is also why the wavelength is chosen to be λ=850 nm, so that the quantum efficiency of the detector remains acceptable. Although depth penetration into tissues might be lower at λ=850 nm than at λ=1.3 µm, higher resolution is expected at this wavelength [21], as well as the possibility to build a matrix of sources that, added to the full field architecture allows to reduce the required power. We will also develop accurate and user-friendly software for OCT signal processing since it is a crucial issue to demonstrate the interest of our approach. This will be done with the help of PIXIENCE company, as a sub-contractor of CHUSE.

(3) Pre-clinical tests, clinical tests and preliminary translational trials

Technical validation and testing of our OCT µsystem as well as the translational trials will be performed in CHUSE hospital and applied to in vivo models of cutaneous pathologies. After the verification of its specifications the inspection system is applied to ex vivo skin samples delivered by medical Partner CHUSE (for instance from abdominiplasties), experimental demonstration of principles of OCT detection will be made in semi-integrated version based on the use of commercially available high-performance swept- source technology. Then the tests will be performed with selected low-cost MEMS VCSELs Swept sources. Both results and performances of the inspection station will be evaluated and its applicability in industrial validation will be assessed. In order to experiment the technical performances (sensitivity, accuracy, reliability, reproducibility and usability), translational trials will be performed with some in vivo tests on human, for whom a surgery should be conducted for an excision specifically those for a malignant doubtful lesion. A comparison of the new system imaging will be made with the existing OCT systems. Image processing strategy will take into account initially reference images from commercial OCT imager (Vivosight®, Michelson Diagnostics), recently obtained by CHUSE from regional grants, or that will be rent for the project (Skintell®, AGFA) and later compared with images from the DOCT-VCSEL prototype. OCT images will be compared to histology images to find correspondences between OCT and this gold standard for the morphological evaluation of skin (Fig.7a). Furthermore, DOCT-VCSEL prototype will combine the following characteristics: adjustment of probe size, probe repositioning as well as correspondence between the 2 imaging planes (sagittal and transversal) (fig.7b). Automation of malignant, inflammatory or abnormal cells or tissues detection will be targeted. The objective is to propose to doctors the nearest landmark as the one they are used to. Main problem for dermatologists is indeed to **interpret images**.

Coherent OCT images are often affected by speckle noise and the contrast of images is decreased by diffusion in skin. This can make pattern recognition very difficult but surprisingly, it can also turn out to be very useful to identify the observed micro-structures [22]. In particular, **analyzing and filtering the speckle information** will allow the development of segmentation algorithm to recognize and separate skin structures [23].The last step will aim at giving reliable measurements of depth, volume, uniformity, and vascular network for the follow- up of skin lesions. CHUSE will contract with PIXIENCE company to perform the technical tasks of the development of algorithm, on the basis of acquired images at dermatology department.

a) 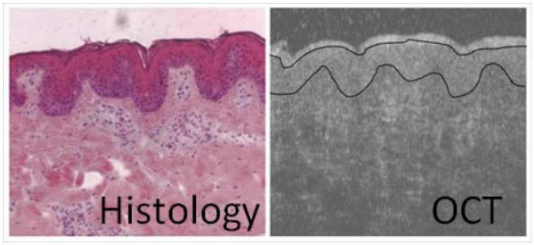

b) 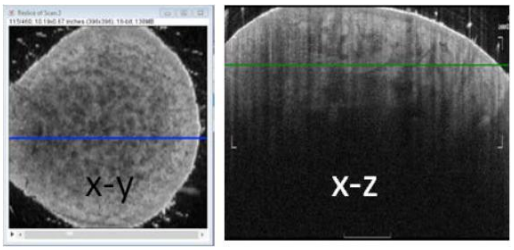

Fig. 7: a) Correspondence between histology (left) and OCT (right) images of skin. (b) Processed 3D image stack from by Michelson Diagnosis OCT: top-view in xy-plane (left) and slice along xz-plane (right).

The in vivo models of skin pathologies could be recruited in the current active list of patients from the Department of Dermatology of the University Hospital (CHUSE) through the Clinical Investigation Center. Accordingly to french regulations, the preparation of successful trials will include design of the study protocol, submission to regulatory institution and to local Ethical Committees and procedure of volunteer patients recruitment. Procedure: pigmented lesions with clinical suspicion of melanoma, nevi lesions, suspected BCCs and normal regions will be studied. All the imaging examination will be reproduced by using existing and new OCT µsystem. The usability of the new system will be assessed by open-labelled questionnaires and satisfaction scale among medical operators who have to use it. Finally, technical calibration, validation and testing of OCT microsystem will be performed during translational trials performed at CHUSE, applied to *in vivo* models of cutaneous pathologies (non-cancerous and cancerous skin lesions).

1.3. Project positioning (national and international)

Electrically-pumped tunable MEMS-VCSELs: state of the art and preliminary results

Electrically-pumped MEMS-VCSELs have been studied for more than 10 years for optical interconnects applications. Good tuning performances, in particular at 1.55 µm, have been reported by several groups, although no commercialized devices are available so far. One can cite for example the pioneering works from C. J. Hasnain's group in Berkeley, USA [19] and the achievements of the recent European project SUBtune that aimed at fabricating high speed tunable lasers for optical links. This latter consortium is now considered as the world leader in the field of electrically-driven MEMS-VCSELs, with record tuning ranges (102 nm) [25]. The general approach for tunable MEMS-VCSELs fabrication consists in associating a movable micro-mirror (top Bragg reflector deposited on a cantilever or on a membrane) above a half-VCSEL structure, including the bottom distributed Bragg reflector (DBR) and the active quantum-well region, to form an air gap in the cavity (see fig.5). When changing the vertical position of the micro-mirror, the optical length of the cavity changes, leading to a variation of the laser emission wavelength. The mirror displacement can be either driven by thermal actuation (current flow) or by electrostatic actuation (voltage) of the suspended membrane. Main significant results obtained on electrically-driven devices are reported in Table 4. They mainly differ by the materials used for the membrane

and the top DBR fabrication. An important voltage or power can be required to tune the VCSEL wavelength depending on the membrane/mirror dimension and thickness.

Table 4: Recent results on **electrically-pumped** tunable MEMS-VCSELs reported at long and short wavelengths

λ(nm)	Membrane material	Actuation	Tuning range (nm)	Swept frequency	I/V/P tuning	Ref, group, year
Long wavelengths						
1550	DBR on a micro-machined SOI MEMS	Electrostatic	55	500 kHz	150 V	[24] Tokyo Tech, 2009
1550	dielectric DBR membrane	Thermal	102	215 Hz	43 mW	[25] Amman group, SUBTune project, 2011
1550	dielectric DBR membrane	Electrostatic	74	215 kHz	130 V	[26]Amman group SUBTune project,2012
1550	HCG InP membrane polarization control	Electrostatic	26.3	-	8.5 V	[27]Chang-Hasnain group 2012
1060	HCG GaAs membrane	Electrostatic	24	-	30 V	[28] Ansbaek DTU Danemark2013
1050	Dielectric DBR membrane	Electrostatic	58	400KHz	48V	[13] John, Praevium / MIT/Thorlabs, 2015
Short wavelengths						
850	AlAs/AlGaAs HCG membrane /polarization	Electrostatic	18	3 MHz	15 V	[18] Chang-Hasnain's group, 2008
760	dielectric DBR membrane	Electrostatic	6	1MHz	20 V	[30]Goddard group, Urbana Champaign 2008
850	dielectric DBR membrane	Thermal	18/24	400 Hz	10 mA	[31][32]Larsson group, SUBTune project, 2012
850	AlGaAs/GaAs cantilever	Electrostatic + thermal	36	-	20.8V	[33]Nakahama Koyama Group Tokyo Tech, 2013

DOCT-VCSEL project will rely on an electro-thermal polymer MEMS (SU-8 based), instead of a dielectric one, in order to lower the power actuation (Fig. 8). **LAAS** recently demonstrated this type of MOEMS for the active focusing of 850 nm standard non tunable VCSELs [16][17] with displacements of the membrane as high as **8 µm with only 42 mW** applied (corresponding to an applied thermal gradient of 100°C). These characteristics have to be compared to the ones reported in [25] at 1.55 µm or in references [32][33] at 850 nm, in the frame of the recent European project SUBTune: 1µm@43 mW (corresponding to a thermal gradient of ~300°C). Consequently, we expect a significant reduction of the operation temperature in our MEMS compared to these "all-dielectric" approaches.

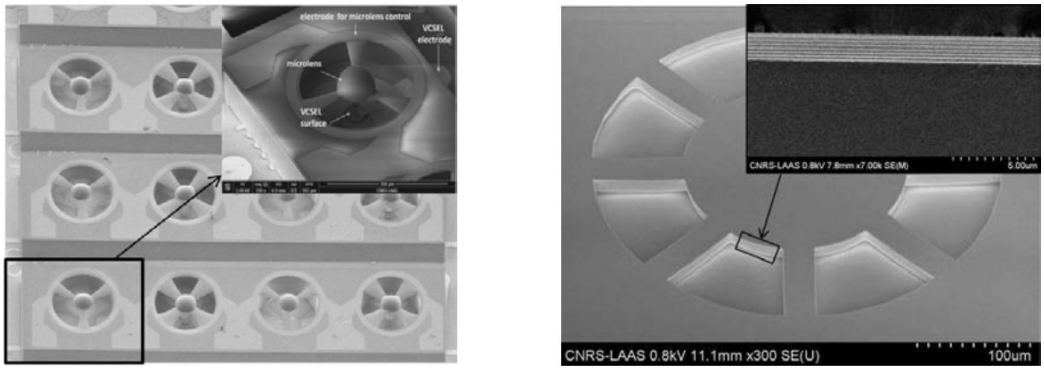

a) b)

Fig 8: Preliminary results: a) SEM (Scanning Electron Microscope) top view image of SU -8 MOEMS with polymer microlens integrated on standard VCSELs arrays (non tunable) (inset: zoom on a single MOEMS) (LAAS, 2013) / b) SEM image of a SU-8 membrane with a top dielectric DBR recently fabricated at LAAS. DBR deposition was optimized to reach a high reflectivity (>99%) necessary for a MEMS-VCSEL laser emission at low current injection (inset: zoom on DBR's cross-section) (LAAS, 2015).

Swept frequency of tunable VCSEL is also a critical parameter for optical interconnects applications and this explains why electrostatic actuation is often preferred in this field. High swept-frequencies are also required for the prototypes proposed by Praevium and Thorlabs for SS-OCT (frequency>300 kHz) because their principle is based, as for many OCT systems, on raster scanning of a single detection point and slower swept-frequencies could not allow reasonable inspection time. This is not the case for DOCT-VCSEL that will capitalize on the VIAMOS results where a parallel architecture is implemented. In DOCT-VCSEL project, a different type of OCT imaging scheme, based on full-field imaging will be exploited. This architecture allows inspection of hundreds of thousands points simultaneously, reducing significantly the requirements on swept frequency, which will be in the range of few tenth of Hz. Despite this lower constraint, both electro-thermal (low risk) and electrostatic (high risk) will be explored in order to determine the best approach for our technology. Finally, it is worth noting that development of such arrays of 850 nm MEMS-VCSELs with specifications that have not been yet achieved by any other previously demonstrated OCT light-source technology will also have an impact in other application fields (spectroscopy, optical communications). Finally, it is also worth noting that we are also exploring with FOTON and Telecom Bretagne a prospective "MEMS-free" approach based on the monolithical insertion of an electro-optic polymer (containing liquid crystals) in a VCSEL for 1.55 µm emission. Up to now, these devices operate under optical pumping. This approach is nevertheless complementary to MEMS technology.

OCT MEMS-based systems for dermatology: state of the art and preliminary results

In the bio-medical field, Praevium Research, Thorlabs and MIT reported in 2011 the first SS-OCT system using a MEMS-VCSEL emitting at 1.3 µm opening a new application field for these devices. They put a strong effort on Dethe extension of the tuning range and the tuning speed. This team recently developed an electrically-driven device emitting at 1.06 µm [13] but up-to now, it did not tried to work at 850 nm, as it mainly focuses on ophthalmic applications. To our knowledge, no other group is involved in a project on electrically-driven 850 nm MEMS-VCSELs for OCT analysis. **FEMTO-ST** has already a strong experience in the technology of microoptical components and microoptical scanners. In particular, a microlens scanner has been proposed based on the combination of 2D comb-drive table [37] with 1-D vertical parallel-plate scanner, both carrying glass microlenses. In parallel, the partner FEMTO developed a fabrication method

of molded microlenses in polymers [38] or in reflow glass from silicon molds [39]. This technology using the wet etching of silicon is well suited for achieving high fill-factor arrays of refractive microlenses that can be monolithically integrated on top of MEMS actuators – this is the specific need of DOCT-VCSEL for Mirau interferometer. The basic technology of passive array-type Mirau interferometer has been developed by FEMTO in the frame of collaborative project SMARTIEHS (2008-2011). Finally, the researchers from IMTEK (Freiburg, Germany) and FEMTO-ST demonstrated a tunable microlens scanner for OCT [40]. The microsystem strongly concerning DOCT-VCSEL is the active version of Mirau interferometer, carried-out by VIAMOS project. Today, this project is at the stage of delivery of individual components (see Fig. 8), the assembly of different blocks starting at the end of 2014, while the complete microsystem will be operational in May 2015. VIAMOS architecture will be adapted to include an array of MEMS-VCSELs. This adaptation includes a new design of the illumination block and operates minor modifications of actuator carrying the reference mirrors of active Mirau interferometer. The resulting DOCT-VCSEL OCT microsystem, having a volume around 20 cm^3, will complete the family portable OCT microsystem for early diagnosis of skin cancer. Thus, we address the following issues: instrument 150 x smaller than standard OCT systems, 10 x cheaper, batch-fabricated, multifunctional, performing parallel inspection and offering high resolution 3D reconstructions of skin. Today, the conventional OCT microscopes are bulky, making it expensive. For economic reasons, OCT microscopes are then only accessible in hospitals and clinics. By maintaining the similar performances to bulk OCT systems, DOCT-VCSEL approach will offer a particular potential for earlier recognition and screening of cutaneous pathologies. **The unit price of DOCT-VCSEL OCT microsystem will target the range of 15 k€ thanks to the low cost technologies including MEMS and VCSELs.** Moreover, low-cost and portable OCT allows doctors to view 3D reconstructions of the skin and offers more resolution than dermoscopy techniques could provide, offering a valuable diagnostic tool which is accessible out of the hospital. Whereas dermoscopy is limited to the detection of lesions based on the visualisation of morphological changes without resolving axial information (in depth), portable OCT offers the potential of detecting the very earliest changes at the micrometer-scale of skin tissue, identifying microscopic features and enabling cross-sectional imaging with high spatial resolution and in real-time. The imaging depth of 0.5-0.6 mm should be enough to reach the dermis/epidermis junction in most of the human body zones. Thus, DOCT-VCSEL technology will promote the technological refinements, contributing in portability and accessibility of OCT imagers. To conclude, DOCT-VCSEL is a cooperative project (PRC) matching perfectly the challenges and the thematic areas addressed by ANR Societal Challenge n°4:"Vie, Santé et Bien- Être". The project goals aim the objectives of Axis 13:"Technologies pour la Santé" and received the agreement from "Pôle de Compétitivité Cancer-Bio-Santé" in 2013 and 2014.

2. Scientific and technical program, project organization

2.1. Project organization

The research program of DOCT-VCSEL is planned over a period of 48 months and the corresponding organization is described in Fig. 9.

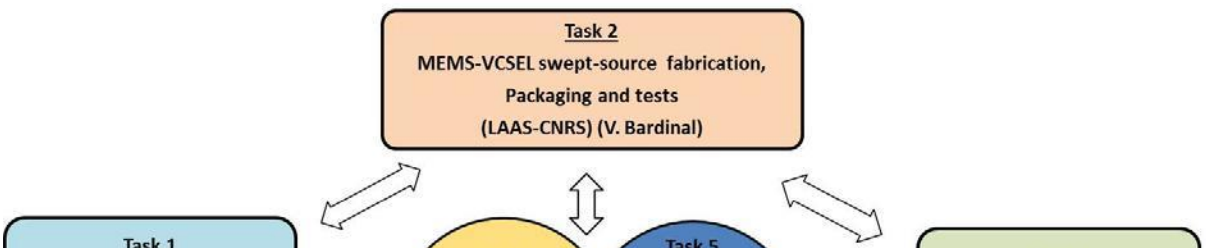

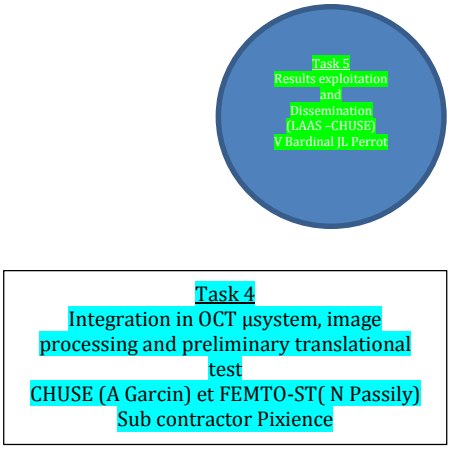

Fig. 9: DOCT-VCSEL project organization

LAAS will coordinate the project (Task 0). SS-OCT micro-system and MEMS-VCSELs will be designed by all partners taking into account dermatologic specifications (Task 1: Design and SS-OCT system specifications, image processing strategy). Images interpretation strategy will be investigated by CHUSE and its subcontractor using first existing images from TD-OCT commercial bulky systems and secondly from our prototype. Simultaneously, the swept-sources arrays will be fabricated at LAAS in interaction with FEMTO-ST taking advantage of their respective facilities and know-how in MOEMS and photonics fields (Task 2: MEMS-VCSEL swept-source fabrication). The sources will be then validated by FEMTO in a bulk OCT test configuration and acquired images will be interpreted by CHUSE (Task 3: Validation of the swept-source and image interpretation in bulk OCT configuration). Finally, the swept-sources arrays will be assembled in a fully integrated OCT microsystem at FEMTO (Task 4: Integration in SS-OCT microsystem, image processing and clinical proof of concept). System validation will be performed through series of translational trials in screening of different infectious and cancerous lesions made at the CHUSE hospital on the basis of processed images. Finally, LAAS and CHUSE will be in charge of the dissemination of the technical results from the project (Task 5: Results dissemination and exploitation), in interaction with potential industrial end-users.

2.2. Description by task

Task 0: Coordination and management (LAAS)

Task number	0	Start date: M0			End date: M48		
Task	Coordination and management / Task Leader : V. Bardinal (LAAS)						
Partners involved	LAAS	FEMTO	UHB				

Task T0, driven by LAAS, is aimed at managing the rest of the work tasks and is driven by LAAS. It will concern conduction of daily management actions and organization, preparation and organization of proposal meetings and supervision of project results. The day-to-day management of the project proposal will be done by an Advisory Board (AB responsible for the overall execution of the proposal and including the task leaders and the Coordinator. The responsibilities of this board cover all aspects of the technical management, such as the progress monitoring with the treatment of any potential deviations from the work plan and to estimate the impact of such deviations on project running and deliverables, dissemination and exploitation of research results, managing and guidelines for reporting, communication with ANR, CNRS, as well as administrative and financial tasks. The meetings of AB will be organised at least twice a year.

T0.1 Conduction of daily management actions and organization of Advisory Board (M0->M48)

Includes all daily administration tasks and make the interface contacts with the administration. This contains the dissemination of information of general relevance to partners, the respect of time scales, monitoring the progress of technical working groups, remedial actions when necessary and prevents any conflict of tasks. Governance of consortium: general project progress including both administrative, technical management as well as monitoring of proposal progress.

T0.2 Preparation and organisation of proposal meetings (M0->M48)

We will initialize and prepare regular general project meetings at least twice a year including project meetings as well technical task meetings in Toulouse and in Besançon. There will be different categories of meetings: kick-off meeting, annual meetings, mid-term meeting, final meeting and other technical task meetings.

T0.3 Supervision of project results (M0->M48)

This task concerns the supervision of project progress on the basis of deliverables and reports, according to the proposed planning. In case of a corrective action being needed, update of work plan and schedule will be done.

Deliverables:
D0.1: Minutes of kick-off meeting (M6)
D0.2: Minutes of annual meeting and annual report (M12)
D0.3: Minutes of intermediate meetings and annual report (M24)
D0.4: Minutes of intermediate meetings and annual report (M36)
D0.5: Final report (M48)
Milestones M0.1: Consortium agreement (M3)

- **Task 1: Design of SS-OCT system /image processing strategy (FEMTO-ST)**

Task number	1	Start date: M0			End date: M18		
Task	Design of SS-OCT µ-system and image processing strategy Task Leader: N. Passilly (FEMTO-ST)						
Partners involved	FEMTO	LAAS	UHB				

Task 1, driven by FEMTO, will permit the design and specifications of OCT microsystem with emphasis to the technology of tunable MEMS-VCSEL source taking into account input from all

partners. The design parameters will be selected according to the system specifications and technological constraints which will be used latter by the tasks T2-T3. At this level, important aspects of the optical design concerning the spatial resolution of the system, the field of view and imaging magnification will be fixed.

T1.1: OCT µ-system design and assembling specifications (M0->M6)

The parameters of OCT microsystem design have to be determined by examining the biomedical application requirements as well as the instrumental characteristics of selected array-type Mirau -interferometer and MEMS-VCSEL as well as camera requirements. The overall functional specifications of the OCT microsystem will be worked out in close cooperation between Partners LAAS and FEMTO. Other Partners will be consulted to ensure that all the constraints posed by different technologies in the assembling process of building blocks, the requirements of system integration and metrology specifications to be obtained by laboratory prototype in qualifying environment for hospital tests are respected. A study on possible implementation plans of overall integration technology will be performed and based on this analysis; an agreement on interfacing specifications will be concluded. All interfaces between the different building blocks have to be determined. Furthermore the biomedical application cases will be selected in this task: the design and assembling of the system will be done in accordance –or as close as possible (function of technical constraints) -with medical expectations and needs. The device will be then adapted to practical use, and better accepted and adopted by the medical community. The functional specifications of the OCT microsystem and a preliminary system concept will be given (deliverable D11).

T1.2 : MEMS-VCSEL source design (M0->M12)

The MEMS-VCSEL source will be designed taking into account system specifications defined in T1.1 and described by deliverable D12. LAAS optical modelling tools will be used to optimize the epitaxial structure and to calculate quantum wells emission and polarization-resolved microcavity reflectivity spectra. The best operation wavelength will be chosen in the range 850-865 nm. As for MEMS displacement, a recent model developed by LAAS using COMSOL Multiphysics™ tool will be used. In a first step, the epitaxial structure will be close to the one of a standard VCSEL in order to rapidly obtain a 20 nm tuning range corresponding to a ~12 µm resolution (first generation, low risk). In a second step, the bandwidth of the bottom and top mirrors as well as the GaAs quantum wells emission spectrum will be optimized to increase the tuning range up to 35 nm (second generation, higher risk). For this latter case, a FDTD modelling tool will be used by FEMTO to design the SWG mirror.

T1.3: Image processing strategy (M0->M18)

Starting from the begin of the project, image processing strategy task includes four main objectives: implementation of a dedicated software designed for experiments using SS-OCT imaging, identification of surface parameters using automatically processed dermoscopy images, computing of sub-epidermal data produced by SS-OCT and processed with speckle modeling and comparative presentation of data: TD-OCT, SS-OCT versus dermoscopy and histology. In order to perform this task, the work will consist firstly in acquiring database imaging with existing OCT imagers: after authorization of this clinical study by ethical committee, in vivo images will be taken before a biopsy, and then ex-vivo on the removed part of the skin; this step will be realized in accordance with the usual plan and section well known and used in anatomopathology. Classical histology treatment and analysis will be then realized on the excision piece, but also different colorations/handling could be tested: the aim is to try to identify correspondences between the views obtained in histology and in OCT. We will have then to reveal the possible congruencies of chemical affinities for the skin structures (colour on histology), and optical properties of these same structure as they will appear on the OCT images.

The numerical comparison of the 2 kinds of images will be facilitated by the existing scanner available in the anatomo-pathology department of medical partner CHUSE (Hamamatsu NanoZoomer 2.0 HT): indeed this device allows digitalizing the histological slides. For this task,

a collaboration will be necessary between the medical partner CHUSE and subcontractor Pixience and, at all stages of the process: acquisition of *in vivo* and *ex vivo* imagingsince the beginning of the project with existing agreed OCT (Michelson Diagnostics available in CHUSE, Agfa by renting); interpretation of images with the dermatologists and anatomy-pathologists experts, in order to design correspondence results between each techniques and tools for interpretation help. The work on the algorithm will start early, and will be then adapted progressively to the prototype, depending on its state of readiness.

-Image filtering and segmentation: OCT images are strongly affected by speckle phenomena. It can degrade the quality of automatic image analysis but surprisingly, it can also turn out to be very useful to identify the observed micro structures. Better interpretation of OCT images by providing automatic segmentation and classification algorithms will then be targeted. As a further work, malignant lesions may be segmented using 3D techniques so as to give reliable measurements of depth, volume, uniformity, and vascular network.

-Sub-epidermal data processing: Expectations regarding the depth and volume parameters will be discussed with the clinical team to ensure the developments properly fit their needs. Starting from the currently available OCT software mock-up, PIXIENCE will design a program with dermoscopy and OCT support to be used in clinical trials. This way, dermatologists should be able to record both dermoscopic and OCT images in a single environment. Corresponding deliverable is D1.3.

T1.4: Product Risk analysis (M0->M36)

The Medical ISO13485 methodology requires a Product Risk Analysis of the new OCT µsystem. The aim of this Risk Analysis is twice: (1) prevention of technical risks and (2) anticipation of environmental risks including practical misuses by doctors.. The proposed OCT microsystem involves substantial experimental risks that might obscure their potential for highly significant outcomes. Different types of technical risks will be identified from each task. The presence of those risks justifies the intensive benchmarking and the goal of building intermediate proof-of-concept demonstrators. In consequence, a well-structured risk management process is needed during all the project to ensure that all significant risks to the success of DOCT-VCSEL project should be taken into account.. To hear the user's voice as well as the development partner's is crucial to understand the constraints and the needs from the beginning. Specification and a Functional Analysis will describe what we (scientific partners and medical users) expect from the Medical Device and split it in building blocks. We remind that the objective is to achieve a platform that supports wafer-scale/massive parallel testing, adjustable field of views, selectable areas of interest, high resolution measurements and appropriate penetration depth of skin tissues for all selected detection modes of OCT. The corresponding deliverable is D1.4.

Deliverables
D1.1: Technical and interface specification for individual building blocks and assembling (M6)
D1.2: Design completed for MEMS-VCSEL source (M12)
D1.3: Testing strategy and technical specifications for image processing (M18)
D1.4: Implementation of Risk Analysis (M36)
Milestones
M1.1: Agreement on general development principle including OCT microsystem and MEMS-VCSEL reached (M12)
M1.2: Design completed with updated specifications and risk analysis (M18, updated M36)

Technical risks analysis for T1.1 and T2.2: Simulations may reveal that operational performances of MEMS-VCSEL as well as tolerances on optical alignment of Mirau arrays with MEMS-VCSEL are as not high as expected so that the proposed specifications have to be reconsidered. Actions will be taken to evaluate all these parameters during the modelling and if problems are detected

to do a rapid iteration so as to integrate the new data. The new system parameters will be discussed with technology partners and medical end-users.

- Task 2: MEMS-VCSEL swept source fabrication (LAAS)

Task number	**2**	**Start date: M0**		**End date: M36**		
Task	**MEMS-VCSEL swept source fabrication** **Task Leader: V. Bardinal (LAAS)**					
Partners involved	**LAAS**	**FEMTO**				

Task 2, driven by LAAS, aims the implementation of 850 nm polymer MEMS-VCSEL swept-source arrays and their fabrication and optimization in collaboration with FEMTO according to T1. This task includes four sub-tasks: half-cavity fabrication (growth and technology), polymer MEMS design and fabrication, top mirror technology and finally, fabrication and packaging of MEMS-VCSEL arrays with aimed tuning ranges of 20 nm (for 12 µm resolution at milestone M.24) and 35 nm (for 6 µm resolution at milestone M.36).

T 2.1:Half-cavity fabrication (M0->M12)

LAAS will fabricate GaAs-based half-VCSEL structures including the laser active zone (deliverable D2.1) by Molecular Beam Epitaxy (MBE) in collaboration with LAAS TEAM technical service. We will use our epitaxial equipment dedicated to optoelectronic devices growth (Riber 412). It insures a high growth uniformity and a precise control of carbon and silicon doping profiles in (Ga,Al)As semiconductor alloys. In case of technical problem with our growth equipment and as a backup, it could be possible to ask an external company (IQE Ltd) to grow our designed epilayers. The grown structures will be processed to achieve an electrical injection using successive fabrication steps (surface micro-relief and mesa etchings, oxide confinement, anti-reflection coating deposition, anode and cathode depositions and device passivation) that are already established at LAAS.

T2.2: Polymer MOEMS design and fabrication (M0->M18)

LAAS will adapt the existing MOEMS fabrication method developed for VCSEL beam focusing to significantly reduce the air gap between the VCSEL and the membrane (~3 µm instead of 100 µm). This will lead to new issues to solve for our SU-8 double exposure technology, such as the precise control of the air gap and the risk of membrane sticking on the half-device surface. In case this method would not be directly transposable, an alternative method based on a sacrificial layer etching will be used to avoid these problems. This will also help to control the membrane curvature radius and to form a plano-concave cavity allowing larger gaps. We also test the new method we recently developed for the collective assembling of SU-8 patterns on III-V wafers using our NIL equipment. After this step, thermally-actuated polymer MEMS (low risk) will be fabricated on glass substrates and their electro-mechanical performances will be optimized in terms of power (< 10mW) and voltage (< 5V) actuation. Secondly, electrostatic actuation will be investigated with a similar technology and a modified geometry (higher risk, D2.2) and voltage actuation will be specifically optimized (< 20V) in collaboration with FEMTO. The test devices fabricated on glass substrates will be characterized using a set-up suited for MEMS characterization and available at LAAS. Final choice for MEMS technology and actuation type will be fixed at month 12.

T2.3: MEMS top mirror technology (M0->M36)

Dielectric multilayer mirrors composed of (SiN_x/SiO_2) periods will be fabricated at LAAS and at FEMTO by ICP-PECVD deposition at low temperature (<100 °C). The compatibility of DBR deposition on a thick SU-8 layer was recently demonstrated by LAAS (Fig.8 b). Precise control of the layer thicknesses (better than 2%) will be the critical point of the process that we will improve

to meet device requirements. In particular, we will optimize the deposition conditions and implement an optical *in situ* control in the deposition chamber. The final choice for top mirror deposition method will be fixed at month 18. In the most prospective part of the project, polymer-based HCG mirrors will be jointly designed by FEMTO-ST and LAAS to extend the spectral range up to 35 nm. We will also explore a collective approach based on a nano-imprint step to define nano-stripes in a thin polymer layer deposited on the SU-8 membrane. These patterns will be then recovered by a high index layer (TiO_2) deposited by Atomic Layer Deposition (ALD) at low temperature [36] The aim is to find a robust design that can be easily integrated on our MEMS with a low temperature process and large fabrication tolerances. Final choice for SWG mirror design and technology will be fixed at month 30.

T2.4: MEMS-VCSEL fabrication, tests and packaging (M12->M36)

Two complete fabrication runs of MEMS-VCSELs (see description in Fig.a) will be performed to provide single devices as well as 4x4 arrays to our partners with specifications in agreement with requirements defined by T1.3 and taking into account experimental results from T2.1, T2.2 and T3.3. Before device dicing and mounting, collective tests will be realized under probes to measure the laser electro-optics characteristics (L-I-V curves, beam divergence, modal behavior) and spectral tuning range under actuation. The devices will be mounted in dedicated packages with FEMTO-ST.

Deliverables **D2.1:** Half-VCSEL devices (growth and process) (M12) **D2.2:** Polymer MEMS including top DBR mirrors on glass substrates (M18) **D2.3:** Polymer MEMS-VCSEL sources mounted on dedicated package, tuning range ~20 nm (M24) **D2.4:** Polymer MEMS-VCSEL sources mounted on dedicated package, range > 20 nm (M30) **D2.5:** Report on MEMS-VCSEL technology (M36) **Milestones** **M2.1**: Agreement on MEMS technology (M12) **M2.2**: Agreement on top standard DBR technology (M18) **M2.3**: Agreement on device technology for extended tuning range (M30)

Technical risks analysis for Task 2: If epitaxial growth does not match specifications, commercial epi-layers can be provided from our design by a company (IQE Ltd). This company is identified as a potential actor for a future industrial transfer. If SU8 double exposure fabrication method not directly transposable for tunable MEMS-VCSEL fabrication with short air gap, an alternative method based on a sacrificial layer etching will be developed. In case of unsatisfactory results and as a backup, DBR deposition step could be also performed with (SiO_2/TiO_2) by sputtering. In case SWH mirror fabrication (higher risk) is not possible using NIL on a polymer suspended membrane, we will use e-beam lithography. With the suitable technologies available at LAAS, chances of success are nevertheless important and no significant delay is expected for delivery of sources for Tasks 3 and 4.

- **Task 3: Swept-source validation & image processing in a bulk SS-OCT configuration (FEMTO-ST)**

Task number	3	Start date: M6			End date: M42
Task	Swept-source validation in bulk SS-OCT configuration & image processing / Task Leader : C. Gorecki (FEMTO-ST)				
Partners involved	FEMTO	CHUSE	LAAS		

This task is devoted to the demonstration of our MEMS-VCSEL sources capability to be used as a swept-source for SS-OCT. Optical and electrical characterizations will be first led at LAAS to precisely measure VCSEL emission characteristics (beam quality, emitted power) and MEMS tuning performances (range, driving power, speed). Preliminary imaging tests will be then performed using an experimental bulk OCT set-up at FEMTO and corresponding images of reference samples will be treated by our subcontractor (Pixience) that will be in charge of the development of a software module for image processing.

T3.1 Swept-sources characterization (M6->M42)

The two successive generations of fabricated sources (classical mirror and SWG mirror) will be finely characterized at LAAS. Optoelectronic properties of MEMS-VCSEL emission (emitted power, beam properties, modal behavior, driving power and static tuning range) will be first checked after mounting and packaging steps. A comparison with modeling results obtained in T1.2 will be made to make possible device optimization. In particular, the impact of SWG mirror insertion on the tuning range and on polarization stabilization will be studied. MEMS dynamic behavior under a sinusoidal drive at high frequencies will be also investigated although this feature is not critical in our configuration. Nevertheless, the determination of the maximal operation frequency will help us to position our source with regards to the state-of-the -art. Finally, long term reliability of our sources will be also investigated through ageing tests led in collaboration with Elemca Company (sub-contracting). The corresponding deliverable is D3.1.

T3.2 Swept-source validation in bulk SS-OCT configuration (M18->M42)

First imaging experiments using MEMS-VCSEL arrays will be performed thank to the use of a SS-OCT bench set-up, developed at FEMTO. It is a one-channel OCT system composed from bulk optics that performs as close as possible to the wafer based solution to test out the individual components of OCT microsystem and evaluate the optical performance. This will help to get a first demonstration of SS-OCT imaging mode with 850nm VCSELs at mid-term of the project. The optical bench will be completed and modified (in particular the illumination optics) to include the array-type VCSEL source. Cross -sectional and 3D tomograms will be measured on a set of transparent samples with evaluation of optical performances (resolution, depth of penetration), validating OCT operation with DOCT-VCSEL light source. These results obtained with DOCT-VCSEL source will be compared with that obtained with a commercial swept-source source. This evaluation prepares the operational phase of system integration and will deliver information on the optical performances of our miniature swept-source in terms of accuracy of the measurement, spatial resolution, the wavelength, bandwidth, and power of the light source. The corresponding deliverable is D3.2.

T3.3 Processing of images acquired from bulk SS-OCT (M24->M42)

The objective for the dermatologist will be to accurately detect skin cancer on the basis of the examination of the morphology of tissues and correlate with the results of histopathology which is today the current gold standard. DOCT-VCSEL microsystem will have to answer the following key points: (i) vertical layers in depth is preferred like histological view ("sagittal plane"); (ii) depth: imaging on the epidermis, until dermal-epidermal junction (ideally> 500 µm) (iii) importance of lateral precision (control of the margins)-area of exploration would be ideally 5 to 8 mm width; (iv) resolution must authorize the identification of the edge of the lesion, which corresponds to an optical resolution within an range between 5 µm and 10 µm; and (v) image processing techniques will permit the evaluation of the skin with reconstruction matching anatomopathology exams (color, morphology, etc..) and quantification (example: number of inflammatory cells, asymmetry of collagen fibers…). DOCT-VCSEL device will deliver 3D images of size 8x8 mm^2 and view in both the vertical and horizontal plane at the same time.

Deliverables
D3.1: Report on VCSEL sources characteristics (M42)
D3.2: Report on bulk SS-OCT tests (M42)
D3.3: Report on image processing from bulk SS-OCT tests (M42)
Milestones
M3.1: Updated specifications of SS-source from on-bench experiments (M42)
M3.2: Updated specifications of image processing software from on-bench experiments (M42)

Technical risks analysis for Task 3: The success of this task is mainly related to devices deliveries from Task 2 (MEMS-VCSEL), as the bulk SS-OCT bench will be available from VIAMOS before M18. Nevertheless, image processing can start on reference samples with a commercial source in case of delay in MEMS-VCSEL fabrication.

- **Task 4: Integration in OCT microsystem and preliminary translational tests (CHUSE & FEMTO-ST)**

Task number	**4**	**Start date: M13**		**End date: M48**	
Task	**Integration in OCT µ-system and preliminary translational tests** **Task Leaders : T. Lihoreau (CHUSE) and N. Passilly (FEMTO-ST)**				
Partners involved	**CHUSE**	**FEMTO**	**LAAS**		

Task 4 includes the construction of complete prototype of OCT µsystem including the array-type Mirau interferometer and MEMS-VCSEL sources. This task is coordinated by CHUSE and includes two parts: (i) integration of complete prototype of OCT microsystem including the array-type Mirau interferometer and MEMS-VCSEL source; and (ii) translational trials performed in hospital CHUSE applied to in vivo models of cutaneous pathologies. This task includes the construction of a complete prototype of OCT microsystem including the array-type Mirau interferometer and MEMS-VCSEL source. This work is justified by deliverable D4.2 (MEMS-VCSEL source assembled with OCT system and qualified), where the assembly and qualification of the Mirau interferometer is reported by the deliverable D3.1 (adapted Mirau interferometer wafers manufactured and qualified). The results of the development of a complete software module for image processing are given by the deliverable D3.3. Finally, the experimental validation and testing of OCT microsystem as well as the translationnal trials performed in hospital, applied to in vivo models of cutaneous pathologies, are reported by deliverable D3.4.

T4.1 Mirau interferometer assembly (M6->M24)

The first part aims to build the complete prototype of OCT microsystem including the array-type Mirau interferometer and MEMS-VCSEL source. The collaborative project VIAMOS developed an “N-bonding process”, in which n-layers of substrates (3<n<18) made from different materials can be sequentially stacked and bonded by use of multilayer wafer bonding techniques. In this process the different wafers are joined together by using sequential anodic bonding steps. The “N-bonding process” will be adapted to the needs of DOCT-VCSEL proposal where we will replace a unique point light source tuned by FPI by 5x5 arrays of tunable VCSELs. MEMS-VCSEL array will be flip-chipped to the input of Mirau interferometers through a specific imaging optics and a discrete beam splitter. The first step will be to build a platform that supports wafer-scale testing, variable field of views, selectable areas of interest and high resolution of OCT µsystem including:

- optical system: accuracy of the measurement, spatial resolution, the wavelength, bandwidth, control of aberrations (geometrical and chromatic) and power of the light source
- MEMS z-scanner: axial range of scanning, axial accuracy of z motion, resonance frequencies
- MEMS-VCSEL source well aligned on the Mirau interferometer input.

Here, the strong collaboration of Partners FEMTO and LAAS is required. Functional specifications obtained from task 1 will be implemented within at the OCT system body. A functional prototype based on the specifications and the design gained from Task 1 will be respected, based on key elements are the sub-modules from the other work packages. The inspection system includes the following modules:

Modules	Designed in	Constructed in
MEMS-VCSEL	Task 1	Task 2
Illumination	Task 1	Task 4
Mirau interferometer	Adapted from VIAMOS in Task1	Task 4
Camera	VIAMOS	VIAMOS
Control and processing unit	Adapted from VIAMOS in Task 1	Task 4
Stitching system	VIAMOS	VIAMOS

The system design parameters of the platform have to be determined by examining the application requirements as well as the characteristics of selected modules of OCT µ-system. The objective is to reach a platform that supports wafer-scale/parallel testing, variable field of views, selectable areas of interest and high resolution for all selected testing techniques. The overall functional specifications of the inspection system will be worked out in cooperation between LAAS and FEMTO. This sub-task will define the modalities and constraints of integration within a complete inspection platform of following specifications optical system, mechanical system and software user interfaces. In particular the interfaces between the different components of the different work packages have to be determined. The functional specifications of DOCT-VCSEL inspection system will be the deliverable of this task.

T4.2 Source integration in OCT system (M12->M36)

EU project VIAMOS relied on a unique SLED source, split between all the different channels of the MEMS interferometer. In DOCT-VCSEL, the strategy is to parallelize the source as well, towards the realization of a matrix of tunable VCSELs, arranged according to the interferometer pitch. This approach allows a more compact and cheaper beam shaping together with a deeper imaging depth. Consequently, the Task 4.1 includes optical design using Zemax software and fabrication of micro-optical components for beam-shaping and integration of the source matrix into the interferometer. Here, the strong collaboration of Partners FEMTO and LAAS is required.

T4.3 Image processing from OCT microsystem prototype (M24->M48)

This part consists in the development of a complete software module for image processing. Preliminary characterizations will be made, based on the evaluation of the 3D cartography: optimization of z-scanning, resonance frequency evaluation and parallelism of single-channels. A calibration procedure for the integrated Mirau interferometer associated with MEMS-VCSEL and numerical procedures for 2D measurements and measurements of 3D topography by stacking of focal planes will be developed. Anatomo-pathology analysis is considered as gold standard and reference for the image interpretation of our project: the image processing from scan of the histologic exams should be integrated with the image obtained from the new system to perform a net distinction between malignant and non-malignant tissue. This integration will be realized by the Clinical Investigation Center, with the Anatomo-pathology department and the Dermatology Department with with the bulk OCT system (M24 to M30) and finally adapted with the prototype (specifications and planning from M30 to M36; this will lead to clinical tests with the new system from M36 to M48).

T4.4 Pre-clinical and clinical tests (M36->M48)

This task is aiming at performing the technical validation and testing of OCT µsystem as well as the translationnal trials performed in hospital, applied to in vivo models of cutaneous pathologies.

-*In vitro* functional tests and optimisation of OCT microsystem

The medical end-user CHUSE will deliver, for testing, human skin equivalent (i.e skin from pig) to allow an appropriate evaluation of the technical performances of OCT µ-system. Thanks to several iterations (internal reproducibility), the performance of the inspection system (as well as the algorithm developed in collaboration with Pixience) will be optimised and the limits will be identified. In particular, the interaction of the illumination, Mirau and FPI wafers, and the imaging wafer with the smart pixel camera will be investigated. The complete positioning system undergoes a thorough functional test. The software of the inspection system and the user interface will also be tested.

-Application tests and validation of preliminary tests

After the verification of its specifications the inspection system is applied to *ex* vivo skin samples delivered by medical Partner CHUSE (for instance from abdominal plastic surgery). Experimental demonstration of principles of OCT detection will be made in semi-integrated version based on the use of commercially available high-performance swept-source technology. Then the tests will be performed with selected low -cost MEMS VCSELs Swept sources. Both results and performances of the inspection station will be evaluated and its applicability in industrial validation will be assessed.

-Translational trials *in vivo* from patients with cutaneous pathologies

In order to experiment the technical performances (sensitivity, accuracy, reliability, reproducibility and usability), translational trials will be performed with some in vivo tests on human, for whom a surgery should be conducted for an excision specifically those for a malignant doubtful lesion. A comparison of the new system imaging will be made with the existing OCT systems. The *in vivo* models of skin pathologies could be recruited in the current active list of patients from the Department of Dermatology of the University Hospital (CHUSE) through the Clinical Investigation Center. Accordingly to French regulations, the preparation of successful trials will include design of the study protocol, submission to regulatory institution and to local Ethical Committees and procedure of volunteer patients recruitment. Procedure: pigmented lesions with clinical suspicion of melanoma, nevi lesions, suspected BCCs and normal regions will be studied. All the imaging examination will be reproduced by using existing and new OCT µsystem. The usability of the new system will be assessed by open-labelled questionnaires and satisfaction scale among medical operators who have to use it.

Deliverables

D4.1: Adapted Mirau interferometer wafers manufactured and qualified (M24) **D4.2:** MEMS-VCSEL source assembled with OCT system and qualified (M36) **D3.3:** Software and description of the image processing algorithm (M36)
D4.4: Clinical tests results analysis and report (M48)
Milestones:
M4.1: Delivery of OCT µ-system for preclinical tests (M36)
M4.2: Experimental proof-of-principle of OCT µ-system validated by clinical tests (M48)

Technical risks analysis for Task 4: Despite the numerous challenging points addressed in this final integration task, risks are pretty narrow, as most of them will have been already demonstrated individually with partners' preliminary results or from results obtained in Tasks 1, 2 and 3.

- **Task 5: Dissemination and results exploitation (LAAS and CHUSE)**

Task number	**5**	**Start date: M12**		**End date: M48**			
Task	**Dissemination and results exploitation** **Task Leader: V. Bardinal (LAAS) and L. Pazart (CHUSE)**						
Partners involved	**LAAS**	**CHUSE**	**FEMTO**				

The aim of Task 5, driven by LAAS, consists in the preparation of the overall strategy for the dissemination of the project results and implementation of future exploitation. It includes dissemination of results via publications and conferences (Deliverable D5.1), clear understanding of possible primary and secondary markets for partial as well as overall project results (deliverable D5.2) aiming at their future industrial exploitation, and development of an exploitation plan of the project results (Milestone M5.1). This task shall also define the strategy and the supports to disseminate the results of DOCT-VCSEL project to different publics (academic experts, industrial experts, students, etc.). The aim will be to identify and prepare as many market areas as possible for products, services and processes that can derive from the direct and indirect results of the project.

T5.1 Communication through conferences and publication (M12->M48)

In order to reinforce the dissemination the consortium will actively participate in national and internationally organized events such as workshops and conferences. The consortium will submit papers acknowledging ANR for financial support. In short term, the consortium members will engage
themselves to participate to the relevant conferences in the fields concerned by DOCT-VCSEL technologies. List of dissemination vehicles is given in the Table below. Furthermore, the DOCT-VCSEL project results will be disseminated to the European industry through cooperation of Partners with microscopy manufacturers, microoptics, MOEMS and VCSELs european suppliers (Philips Ulm Photonics, Oclaro,.) and biomedical companies. Accordingly these communication channels will be used also for the dissemination.

Conferences to be attended	Refereed journals
IEEE MEMS/Transducers/ Euro-sensors/ Photonics	Optics Express, Applied Physics Letters, IEEE PTL
IEEE/LEOS conferences on VCSEL, MOEMS	Optics Letters, Applied Optics, Sensors and Actuators
SPIE Photonics West, SPIE Photonics Europe	J. of Micromechanics and Microengineering
Congrès annuels : Asso. of Dermatologic Oncology, European Academy of Dermatology and Venerology, American Academy of Dermatology, Dermatology, International Society for Biophysics and imaging of the Skin, Recherche en Dermatologie, Journées Dermatologiques de Paris	J. of Microsyst.Technol., IEEE Trans. on Medical Imaging J. of Eur. Acad. of Dermatology and Venereology, J. of Eur. Acad. of Dermatology and Venereology, European J. of Dermatology, Skin Research Technology
European Conf on Smart System Integration, European Conf. On Biomedical Optics, VCSEL Day European workshop	Biomed Optics, Biomed Optics Express, J. of Clinical Oncology,
Exhibitions to be attended: Biotechnica, Biomedical, Transducer's, SPIE Photonics Europe	**Communication with European plateforme** EPOSS, Photonics 21,COWIN

T5.2 Market analysis (M24->M48)

This task will produce information sets, including papers, databases and contact references in the field of dermatology systems, as a "map" to which all DOCT-VCSEL developments should be referred to. This activity will include comprehensive bibliographic surveys of concerned markets. The task will be led in interaction with potential end-users (such as PIXIENCE) and shall identify not only the applications, but also the actors in the complete product/service chain from the knowledge source to the potential end users. Distribution of flyers will be given and SWOT analysis will be presented for DOCT-VCSEL technologies. The marketing analysis will be important for the exploitation of DOCT-VCSEL results and will have 3 objectives: to collect market trends and regulation for consolidation of the DOCT-VCSEL vision, to diffuse the awareness of the DOCT-VCSEL technology in the dermatology community to prepare the future commercialisation phase and to attract additional OEM manufacturers which will be the future users of our miniature OCT head. Research methodology will include: market information obtained through secondary research on company websites and articles; market size of the segments calculated using the bottom-up approach and market incomes of key players determined by primary and secondary research, including study of annual reports of company and interviews with key opinion leaders, CEOs, directors, and managers.

T5.3 Results dissemination and exploitation (M36->M48)

Exploitation roadmap: a clear exploitation/commercialization roadmap will be elaborated based on the identification and description of the different exploitable results from the project, as defined by the consortium Partners. Estimations will be derived in a quantitative manner of the economic impact the exploitation will have on the individual industrial beneficiaries.

Development of the exploitation plan: The initial exploitation objectives of the partners will be expanded and business lines will be identified in order to transfer the project results to the commercial field. Production costs for the DOCT-VCSEL microsystem will be analysed and possible manufacturing partners identified. A continuous dialogue with various potential manufacturers will be maintained throughout the project to closely follow the requirements and time line of introduction of the proposed products. The consortium will contribute to detailed technical and market analyses. Property generated in the DOCT-VCSEL project will be protected through patent applications where applicable, in accordance to the consortium agreement.

Deliverables
D5.1: DOCT-VCSEL flyer updated (M12, updated in M24)
D5.2: Market analysis and SWOT analysis (M36)
D5.3: Exploitation plan (M48)

Milestones
M5.1: DOCT-VCSEL exploitation plan integrating market analysis (M48)

2.3. Tasks schedule, deliverables and milestones

DOCT-VCSEL duration is 48 months and corresponding **task schedule** is shown in Fig.10 below.

TASK / months	0-6	7-12	13-18	19-24	25-30	31-36	37-42	43-48
T0 Coordination	D0.1	D0.2		D0.3		D0.4		D0.5
Milestones	*M0.1*							
T1 Design and specifications of OCT µ-system, image processing strategy								
T1.1 OCT µ-system design and assembling specifications	D1.1							
T1.2 MEMS-VCSEL source design		D1.2						
T1.3 Image processing (existing OCT) & strategy			D1.3					
T1.4 Risk analysis						D1.4		
Milestones		*M1.1*	*M1.2*			*M1.2*		
T 2 MEMS-VCSEL swept source fabrication								
T2.1 Half-cavity fabrication		D2.1						
T2.2 Polymer MEMS design and fabrication			D2.2					
T2.3 MEMS top mirror technology			D2.2					
T2.4 MEMS-VCSEL fabrication, tests and packaging				D2.3	D2.4	D2.5		
Milestones		*M2.1*	*M2.2*			*M2.3*		
T3 Swept-source validation & image processing in a bulk SS-OCT configuration								
T3.1. Swept-source characterization							D3.1	
T3.2 Swept-source validation in bulk SS-OCT configuration							D3.2	
T3.3 Image processing from bulk SS-OCT configuration							D3.3	
Milestones						*M3.1*	*M3.2*	
T4 Integration in OCT microsystem and preliminary translational tests								
T4.1 Mirau interferometer assembly				D4.1				
T4.2 Source integration in OCT microsystem						D4.2		
T4.3 Image processing from OCT microsystem						D4.3		
T4.4 Pre-clinical and clinical tests								D4.4
Milestones						*M4.1*		*M4.2*
T5 Dissemination and results exploitation								
T5.1 Conferences/ publications			D5.1	D5.1				
T5.2 Market analysis						D5.2		
T5.3 Results dissemination and exploitation								D5.3
Milestones								*M5.1*

Fig. 10: DOCT-VCSEL Gantt chart: tasks, deliverables and milestones.

2.4.Qualification and contribution of each partner

DOCT-VCSEL objectives, according its challenging aspect, can only be achieved in an efficient manner by a concerted effort among a consortium of 3 Partners, having a leading position in the fields of VCSEL and MEMS technologies (LAAS-CNRS, http://www.laas.fr/), MEMS/MOEMS technologies, microscopy and OCT metrology (FEMTO-ST, (http://www.femto-st.fr/), OCT imaging and dermato-oncology (CHUSE, Besancon University Hospital, JL http://www.chu-st-etienne.fr.fr/).

➢ **LAAS-CNRS (Scientific leader: V. Bardinal, DR CNRS)** will coordinate the project and be in charge of Tasks 0 and 2. V. Bardinal and co-workers have long track records on 850nm VCSEL technology and photonic integration in the frame of several European projects (FP5 Optonanogen, FP6 FunFACS) and ANR projects. MICA (MICrosystems Analysis) group concerned by DOCT–VCSEL aims at integrating VCSELs in optical µ-systems by combining MEMS and micro-optics technologies for bio-sensing [41][43][16][17]. LAAS is a member of Carnot Institute and belongs to RTB national network of technological platforms; it is equipped with a 1500m² 100/1000 class clean-room (epitaxy, micro-nanotechnologies) and with characterization and design platforms.

➢ **FEMTO-ST (Scientific leader: C. Gorecki, DR CNRS)** will be in charge of Task 1 (N. Passilly) and Task 3 (C. Gorecki) and Task 4 (N.Passilly). FEMTO-ST is affiliated to the CNRS (UMR), UFC, ENSMM and UTBM, having 7 research departments and the technological platforms of RTB: 850-m² class 100/1000 clean room.
Two Departments participate in DOCT-VCSEL project: Micro- and Nano Sciences and Systems (MN2S) and Optics. MN2S scope covers micro and nano, phononics, microoptics/MOEMS, MEMS and microfluidics, material science and micro/nano-scale instrumentation. The team concerned by DOCT-VCSEL is the MOEMS group headed by C. Gorecki, leader or partners in several FP7 projects (MAC-TFC, VIAMOS, SMARTIEHS) and national projects (DWST-DIS, ISIMAC) [11][37][37][39]. L. Froehly's activity in OCT is directly concerned here.

• **CHUSE (Scientific leader: JL Perrot MD)** will be in charge of Task 4 in strong interaction with FEMTO-ST. The Department of Dermatology will be implied and define the medical specifications, and constitute the iconographic data collection of pathological cases. The Department of Dermatology role will be to define the specifications and risk analysis for the aimed microsystem, to define the development steps towards clinical tests, to manage the pre-clinical trials with *ex vivo* study on biological sample and finally to perform *in vivo* "optical biopsies" study. The Histology Laboratory will be also involved and carry out the necessary histological tests during the pre-clinical phase and for the tests of new devices. For the images processing and data interpretation readable for a clinician, CHUSE will contract with PIXIENCE which is a SME directly involved in this matter for dermatologists.
•

• **Qualification of project coordinator (V. Bardinal)**: The project coordinator will be **Dr. Véronique Bardinal**, permanent researcher (DR2) at CNRS (French National Center for Scientific Research) in LAAS laboratory (Toulouse, France) since 1997. She received her Applied Physics Engineer degree from INSA Toulouse in 1992 and her PhD in optoelectronics in 1995. In 1996-1997 she was a postdoctoral scientist at EPFL, Switzerland, and joined the Photonics group at LAAS-CNRS in 1997 as a permanent CNRS researcher. Throughout her research experiences, mainly focused on 850nm VCSEL design, growth and technology and on polymer micro-optics, she was involved in 3 European projects and many national granted projects (CNRS, ANR, Midi-Pyrénées region) as well as in international collaborations (LIA CNRS with South Korea, NSC-CNRS with NCKU Taiwan). She has authored and co-authored 44 peer-review papers, more than 30 contributions in international conferences and 1 patent. In 2011, she organized the 4th European workshop VCSEL Day in Toulouse, bringing together the largest European groups in this field. In 2012, she joined MICA team to develop optical microsystems based on VCSELs in the framework of LAAS'research topic on "Micro and Nano Technologies for biology". She is co-head of MICA team since October 2012. Her coordination role is justified by her strong experience on VCSELs sources that are the key elements of the project.

Significant recent publications

1. B Reig *et al*. "Fabrication of polymer-based optical microsystem arrays suited for the active focusing of vertical laser diodes "J. Micromech. Microeng. **22** 065006 (2012). (Cover issue).
2. D. Barat *et al*. "Photo-chemical study and optical properties of microtips self- written on vertical laser diodes using NIR photo-polymerization" Opt. Express, **20**, 22922-22933 (2012)
3. D. Barat *et al*,"Microlens self-writing on vertical laser diodes by Near Infra-Red photo-polymerization", Microelectronics Eng. Vol 111, 204–209, (2013)
4. B.Reig *et al* "Study of SU-8 reliability in wet thermal ambient for application to polymer microoptics on VCSELs", Japanese Journal of Applied Physics, Vol.53, 8S2, 14045. (2014)
5. V. Bardinal *et al*, "Advances in Polymer-Based Optical MEMS Fabrication for VCSEL Beam Shaping, (Invited paper) IEEE Selected Topics in Quantum Electronics, vol.21,.4, pp.1,8, (2015)

Pr. Thierry Camps is Professor in Electronics at University Paul Sabatier, Toulouse and permanent researcher in N2IS group (Nano-Systems Engineering and Integration) at LAAS-

CNRS since 1993. He received his PhD thesis on GaAs power HBTs in 1991 and his HDR in 2000. His research scope covers design and fabrication of MEMS based on thermo-mechanical. He also exploits his skills in GaAs devices technology for the realization and the optimization of electrically-injected VCSEL with MICA Team. He is currently exploring several complementary approaches for integrating micro-optical elements and electro-thermal actuators in polymers MOEMS for VCSELs beam shaping.

Significant recent publications

1. T. Camps et al. "Development of polysilicon devices for microfluidic thermal instrumentation", Sens. Actuat. A: Phys., 189, 67-73 (2012).
2. B. Reig et al. "Fabrication of polymer-based optical microsystems arrays suited for the active focusing
of vertical laser diodes", J. Micromech. Microeng., 22, 065006 (2012).
3. D. Barat *et al*,"Microlens self-writing on vertical laser diodes by Near Infra-Red photo-polymerization", Microelectronics Eng. Vol 111, 204–209, (2013)
4. B.Reig *et al* "Study of SU-8 reliability in wet thermal ambient for application to polymer microoptics on VCSELs", Japanese Journal of Applied Physics, Vol.53, 8S2, 14045. (2014)
5. V. Bardinal *et al*, "Advances in Polymer-Based Optical MEMS Fabrication for VCSEL Beam
Shaping, (Invited paper) IEEE Selected Topics in Quantum Electronics, vol.21,.4, pp.1,8, (2015)

Partner 2 (FEMTO-ST)

The following permanent staff of FEMTO/UFC will work on DOCT-VCSEL: **Christophe Gorecki** is a Director of Research CNRS (DR1 CNRS) at FEMTO-ST. He received the Ph.D. in Optics at the University of Besançon in 1983 and joined Laboratoire d'Optique P.M. Duffieux (LOPMD) as a CNRS Scientist. His research interests included optical inspection and micro-measurements, applications of image processing techniques in optical metrology and Optical Pattern Recognition methods. From 1995 to 1998 he joined the University of Tokyo where he was involved in research and development of Optical MEMS. Back to LOPMD he conducts research in novel MOEMS architectures for micro and nanosensors as well as development of metrology methods for characterization of MOEMS/MEMS. He has more than 150 technical papers and 3 book chapters. He is a Fellow of the SPIE and member of SPIE Board of Directors. He is the President of the French-Swiss Collégium SMYLE (FEMTO-ST and EPFL/Lausanne). He has supervised many national projects and several European projects. From 2007 to 2009, Dr. Gorecki was a member and expert of Disciplinary Committee of French ANR and received the prize of European Optical Society (2012).

Significant recent publications

1. S. Bargiel et al., "Towards micro-assembly of hybrid MOEMS components on a reconfigurable silicon free-space micro-optical bench", J. Micromech. Microeng. 20, 045012 (2010).
2. J. Albero et al., "Micromachined array-type Mirau interferometer for parallel inspection of MEMS", J. Micromech. Microeng. 21, 065005 (2011).
3. M. Baranski et al., "A simple method for quality evaluation of micro-optical components based on 3D IPSF measurement", Optics Express 22(11), 13202-12212, (2014).
4. H. Ottevaere et al., "Plastic light coupler for absorbance detection in silicon microfluidic channels", Microfluidics and Nanofluidics, 2014, 1-10, (2014).
5. M. Baranski et al.,"Wafer-level Fabrication of Micro Cube-typed Beam-splitters by Saw-dicing of Glass Substrate », Photonics Technology Letters 26(1), 100 – 103, (2014).

Dr. Nicolas Passilly is Chargé de Recherche (CR1 CNRS) and is member of the department MN2S of FEMTO-ST. He received his M. Sc. Degree in Physics in 2002 and his PhD degree in

2005 from the University of Caen, France. In the framework of his PhD studies, he worked on diffractive optics used to improve the performances of solid state lasers at the CIRIL laboratory in Caen. At the beginning of 2006, he has joined for 2 and half years the wave optical engineering group (led by Prof. J. Turunen) at the University of Joensuu, Finland, where he focused on nano-structured diffractive optics and form-birefringent elements as well as some replication of diffractive optical elements. During his stay in Finland, he was involved in the Network of Excellence on Micro-optics (NEMO) as a representative person of the University of Joensuu. Since September 2008, he has been working in Dep. MN2S as a CNRS scientist. He has authored or co-authored 34 peer-reviewed articles, 22 proceedings papers and filled 1 patent.

Significant recent publications

1. J. Albero et al., "Micromachined array-type Mirau interferometer for parallel inspection of MEMS", J. Micromech. Microeng., 21, 065005 (2011).
2. E. Cagniot et al., "Transverse super-resolution technique involving rectified Laguerre Gaussian LGp0 beams", JOSA A, 28, 1709-1715 (2011).
3. D. Naidoo et al. « Transverse mode selection in a monolithic microchip laser », Optics Commun., 284, 5475-5479 (2011).
4. R. K. Chutani et al. « Thermal management of fully LTCC packaged Cs vapor cell for MEMS atomic clock", Sens. Act. A, 174, 58-68 (2012).
5. M. Baranski, et al.,Wafer-level Fabrication of Micro Cube-typed Beam-splitters by Saw-dicing of Glass Substrate », Photonics Technology Letters 26(1), 100 – 103, (2014).

Dr. Luc Froehly is Chargé de Recherche at CNRS (CR1 CNRS). He received his PhD in Saint Etienne France at Laboratoire TSI in the field of metrology of gradient index. In 2000, he shared his time between a short postdoctoral Internship at the Department of Electronics of the Glasgow University and in the TSI laboratory in St Etienne. From 2001 to 2004 he was a project leader at EPFL, in the Institute of Applied Optics (Faculty of Microtechnics) where he focused on Optical Coherence Tomography. Since November 2004 he joined FEMTO-ST as a full time researcher (CR CNRS) to continue his research in biophotonics. He is currently developing OCT systems and participating also to works on spatial and temporal pulse shaping for laser ablation. He is author or co-author of 26 publications or communications.

Signifiant recent publications

1. I. Kaminer et al., "Accelerating Beyond the Horizon"; Optics & Photonics News, 23, 12, 26-26, (2012).
2. A. Mathis et al., "Direct machining of curved trenches in silicon with femtosecond accelerating beams",
J. of the EOS - Rapid publications, (2013).
3. A. Mathis et al.,"Arbitrary nonparaxial accelerating periodic beams and spherical shaping of light," Opt. Lett. 38, 2218-2220, (2013)
4. M. Guillerm et al., "Ultrafast turbidity compensation in the optical therapeutic window by three-wave mixing phase conjugation", J. of Optics 15, 5, 055204, (2013)
5. L Froehly et al., "Spatio-temporal structure of femtosecond Bessel beams from spatial light modulators",
J. Opt. Soc. Am. A31, 4, 90-793, (2014).

Partner 3 (CHUSE)

Jean Luc Perrot is an M.D. He is member of Inserm EA **4607 –** Système Nerveux Autonome, Epidémiologie, Physiologie, Ingénierie, Santé » at University Hospital of St Etienne, a clinical

research center dedicated to develop innovative technologies.
He is a member of skin imaging groups: International Confocal World Group…, president for the "Groupe d'Imagerie Non Invasive" of the French Dermatology Society.
He has published more than 120 papers in peer-review international journals (more than 45 papers about skin imaging).

Significant recent publications:

1. Cinotti E, Perrot JL, Labeille B, Campolmi N, Thuret G, Naigeon N, Bourlet T, Pillet S, Cambazard F. First identification of the herpes simplex virus by skin-dedicated ex vivo fluorescence confocal microscopy during herpetic skininfections. Clin Exp Dermatol. 2015 Jun ; 40(4):421-5.
2. Cinotti E, Jaffelin C, Charriere V, Bajard P, Labeille B, Witkowski A, Cambazard F, Perrot JL. Sensitivity of handheld reflectance confocal microscopy for the diagnosis of basal cell carcinoma: A series of 344 histologically proven lesions. J Am Acad Dermatol. 2015 Aug;73(2):319-20
3. Cinotti E, Perrot JL, Labeille B, Campolmi N, Espinasse M, Grivet D, Thuret G, Gain P, Douchet C, Andrea C, Haouas M, Cambazard F. Handheld reflectance confocal microscopy for the diagnosis of conjunctival tumors. Am J Ophthalmol. 2015 Feb ;159(2): 324-33.
4. Cinotti E, Perrot JL, Campolmi N, Labeille B, Espinasse M, Grivet D, Thuret G, Gain P, Douchet C, Forest F, Haouas M, Cambazard F. The role of in vivo confocal microscopy in the diagnosis of eyelid margin tumors: 47 cases. J Am Acad Dermatol. 2014 Nov;71(5):912-918
5. Cinotti E, Perrot JL, Labeille B, Espinasse M, Ouerdane Y, Boukenter A, Thuret G, Gain P, Campolmi N, Douchet C, Cambazard F. Optical diagnosis of metabolic disease: cystinosis. J Biomed Opt. 2013 Apr;18(4)

Frederic Cambazard is a MD and Ph.D. He is the leader of the dermatological team of the Hospital of St-Etienne. He is member of Inserm EA 4607 at the Hospital of St-Etienne. He has published more than 260 papers in peer-review international journals (more than 45 papers about skin imaging).
He has managed more than 110 protocols studies for the last 10 years

1.Cinotti E, Couzan C, Perrot JL, Habougit C, Labeille B, Cambazard F, Moscarella E, Kyrgidis A, Argenziano G, Pellacani G, Longo C. In vivo confocal microscopic substrate of grey colour in melanosis. J Eur Acad Dermatol Venereol. 2015 Dec;29(12):2458-62.
2. Cinotti E, Couzan C, Perrot JL, Labeille B, Bahadoran P, Puig S, Wantz M, Vicente-Villa A, Habougit C, Butori C, Cambazard F. Reflectance confocal microscopy for the diagnosis of vulvar naevi: six cases. J Eur Acad Dermatol Venereol. 2016 Jan;30(1):30-5.
3. Cinotti E, Fouilloux B, Perrot JL, Labeille B, Douchet C, Cambazard F. Confocal microscopy for healthy and pathological nail. J Eur Acad Dermatol Venereol. 2014 Jul;28(7):853-8.
4. Champin J, Perrot JL, Cinotti E, Labeille B, Douchet C, Parrau G, Cambazard F, Seguin P, Alix T. In vivo reflectance confocal microscopy to optimize the spaghetti technique for defining surgical margins of lentigo maligna. Dermatol Surg. 2014 Mar;40(3):247-56.
5. Cinotti E, Perrot JL, Labeille B, Raberin H, Flori P, Cambazard F. Hair dermatophytosis diagnosed by reflectance confocal microscopy: six cases. J Eur Acad Dermatol Venereol. 2015 Nov;29(11):2257-9.

Arnaud Garcin is a clinical research project manager in the Unité de Recherche Clinique, de l'Innovation et Pharmacologie (URCIP) du CHU de Saint-Etienne, France. He is member of Inserm EA 4607. He manages the clinical protocols as regards the regulatory aspects,

organization and quality. He is involved in several publications :

1. Kassir R, Barthelemy JC, Roche F, Blanc P, Zufferey P, Galusca B, Perrot JL, Garcin A, Charier D, Tiffet O. Bariatric surgery associated with percutaneous auricular vagal stimulation: A new prospective treatment on weight loss. Int J Surg. 2015 Jun;18:55-6
2. Avet J, Pichot V, Barthélémy JC, Laurent B, Garcin A, Roche F, Celle S. Leukoaraiosis and ambulatory blood pressure load in a healthy elderly cohort study: the PROOF study. Int J Cardiol. 2014 Mar 1;172(1):59-63.
3. Chouchou F, Pichot V, Pépin JL, Tamisier R, Celle S, Maudoux D, Garcin A, Lévy P, Barthélémy JC, Roche F; PROOF Study Group. Sympathetic overactivity due to sleep fragmentation is associated with elevated diurnal systolic blood pressure in healthy elderly subjects: the PROOF-SYNAPSE study. Eur Heart J. 2013 Jul;34(28):2122-31.
4. Degache F, Sforza E, Dauphinot V, Celle S, Garcin A, Collet P, Pichot V, Barthélémy JC, Roche F; PROOF Study Group. Relation of central fat mass to obstructive sleep apnea in the elderly. Sleep. 2013 Apr 1;36(4):501-7.
5. Delavenne X, Ollier E, Basset T, Bertoletti L, Accassat S, Garcin A, Laporte S, Zufferey P, Mismetti P. A semi-mechanistic absorption model to evaluate drug-drug interaction with dabigatran: application with clarithromycin. Br J Clin Pharmacol. 2013 Jul;76(1):107-13

3.1. Scientific justification of requested resources

The total amount solicited from ANR for our project (48 months) is ~**663k€** for a total cost of ~**2100 k€**. The distribution of requested resources by partner is detailed below:

•Partner 1 : LAAS (aide demandée frais de gestion inclus: 324.39 k€)

Equipment: 54k€: An adaptation of LAAS ICP-PECVD equipment (Oxford) will be purchased to make possible the installation of an optical *in situ* control based on laser reflectometry for the precise control of MEMS multilayer mirror fabrication (T2.3) (**50k€**). A plan apo NIR-treated microscope objective and a spectrum sensor will be purchased to adapt our optical test bench for tunable devices characterization under probes (T2.4) (**4k€**).

Staff: (103.92k€): a PhD student recruited for 36 months will be dedicated to MEMS-VCSEL design, technology and characterizations (**97.24 k€).** Two Master student's internships will be recruited during the 4-year project (6 months gratifications x2: **6.6k€**).

Operating costs: 154 k€

-*Fabrication* costs: **105 k€** A strong technological effort on new optoelectronic microdevices fabrication technology will be made all along the 48 months project. The technological fabrication center (RENATECH platform) at LAAS operates with internally affected costs for the processing steps realized in the clean room. Costs for individual processing steps have been evaluated and are charged to the concerned research project. They include gas and material consumptions and other costs of maintenance for equipment and infrastructure. They concern: epitaxy calibrations and growth of 20 VCSEL wafers (20x50h) (T2) **(38k€)**; masks fabrication (2x9 levels) and technological fabrication steps for each wafer (T3/T4**)**: photolithography, etchings, oxidations, top and bottom metallization, passivation, MEMS complete fabrication and final mirror deposition and delimitation **(43k€)**; structural characterizations (SEM, FIB, confocal microscopy) (**6k€)**; wafer dicing, chip mounting and bonding on dedicated packages (**10k€);** Micro/nanotechnology studies for top and bottom mirror optimization and validation (epitaxial growths and electronic beam/ nano-imprint NIL)(**8 k€)** (T2.3)

-*Other operating costs:* **49 k**€: Participation costs for electro-thermo-mechanical characterizations of devices in LAAS characterization platform (T2.2) (**6k€)**; Participation costs to annual design software licenses (COMSOL and ZEMAX -EE) for electro-thermo-mechanical and optical

modeling (T1.2): **6k€;** Coordination costs (T0 and T5.3) and publication fees in international journals (T5.1): **4k€**; Travels costs **16k€** : for 7 project meetings for 3 persons (T0), for 3 stays of the PhD student at FEMTO-ST (3x1 week) (T3) and for results dissemination in international conferences and workshops (T4.1)**;** Sub-contracting : **6k€** for reliability mechanical tests (T2.2) and **11k€** for market analysis (T5)

.

•**Partner 2 : FEMTO-ST (aide demandée frais de gestion inclus : 202,18 k€)**

Equipment: (47 k€) : Most of the equipments related to DOCT-VCSEL are aimed for building-up a macroscopic experiment in order to test the different micro-optical components and eventually to be used as a reference. This experiment will require optical components (lenses, mirrors, beam splitters) and optomechanics (standard mounts and mounts XY, Z, θ): 13k€; 3-axis motorized translation stage + motor controllers and power suppliers: travel: 12mm; incremental movement: 0.5µm, repeatability: 1.5 µm. (9k€); Camera CMOS with power supply: megapixel resolution, frame rate at least 150fps, grey level at least 10bit, possibility of logarithmic response curve (4k€), frame grabber for camera LabView compatible (2k€) + Cable Camera Link;Computer (1k€), oscilloscope (12k€) and generic optical and electronic components from Thorlabs (6k€).

Staff (90 k€): a contractual researcher (3-5 years of experience) recruited for 18 months will be dedicated to the DOCT-VCSEL project during the phase of DOCT-VCSEL source characterization and of system integration. This person will focus on assembling and packaging the OCT system and will be in charge of the different tests required to validate the system as an OCT one (mostly T3.1, T3.2, T4.1 and T4.2).

Operating costs: 57.4 k€:

-*Prestations de service externe **(15 k€)**:* Fraunhofer ENAS subcontracting for multi-wafer assembly (T3.2): (**7.5k€**) High speed CCD detector from CSEM (developed in the frame of VIAMOS): (**7.5 k€**)

-*Missions **(13 k€)**:* Travels for task and project meetings : (each 6 months : 7 meetings from which 4 hosted in Toulouse : 2 days - 500€ /trip : 4 x 0.5k€ x 3 persons : **6 k€**) ; international conferences to present the scientific advances: 5 days : 2350€/person with registration: 3 conferences: (**7k€**)

-*Autres dépenses de charge externe **(13 k€)**:* Clean room supplies (wafers, consumables): (**10k€**) ; Publications fees in Journal such as Optics Express, Biomed Opt. Express : (**3k€**)

- *Dépenses externes **(16.4 k€):*** Expenses for use of clean rooms at MIMENTO platform: (500 hours x 45€ per hour)

•**Partner 3 : CHUSE (aide demandée frais de gestion inclus : 137.525k€)**

Equipment (20k€) : Equipment fees concern a renting of a commercially OCT System EC homologated for clinical use from the beginning of the project (AGFA Skintell® system plus handy step dispenser); Michelson Diagnostics Vivosight® being recently acquired by CHUSE. These complementary set-ups are necessary for the project, in order to acquire OCT images for task T1.3 since the beginning of the project then to compare the performance of our new integrated product with the existing reference in the research field (Tasks T4.3 and T4.4). At the moment, OCT for dermatology is still a research topic and clinicians cannot directly interpret images produced by OCT. Therefore, image processing strategy is a challenge and needs to be developed to lead to comprehensive information to the clinician using our new product.

Staff (45k€): A research engineer (12h.m) will be enrolled with a part-time contract, for the realization of tasks 1.3 and 4.4. The main mission of his work will be to acquire the images with the existing and new devices, then collaborating with PIXIENCE to guide the orientations of the algorithm and to perform the test-retest of images processing before the interpretation with dermatologists.

Operating costs (22.26k€): realization of clinical study (promotion expenses, insurance relative to the realization of the clinical trial on patients, quality control, data management, statistical analysis 12k€); missions (travels for task and project meetings, conferences, publications 5k€), management costs (5.26k€).

External sub-contracting (49.5k€):

Pixience society will be sub-contracted by CHUSE with 2 deliverables: 1) feasibility work on an algorithm of identification of the specific pathologies pattern that will be defined during this phase, based on existing OCT and available images (31.5k€) 2) adaptation to MEMS-OCT prototype (18k€).

4. Results exploitation and dissemination strategy, global impact

The target: noninvasive exploration of skin lesions

Non-invasive skin imaging methods respond to several situations requiring to be as conservative as possible like children, lesions on the face, people who makes hypertrophic scar or keloids, population screening. Thus, the delimitation of the lesion is crucial to guide the surgical gesture, before the intervention and intraoperatively in order to remove all the lesional tissue and only this one. This last objective is particularly important for the two main types of skin cancer: the malignant melanoma skin cancer (MSC) and non-melanoma skin cancer (NMSC). MSCs are responsible for the majority (90%) of deaths related to skin cancer. An estimated number of 69000 new cases of melanoma were diagnosed in 2008 in the EU (27 countries) with, e.g., 6000 new cases each year only in France. Most of the time, MSC growths horizontally beneath the epidermis during a prolonged initial phase but has not yet invaded the underlying dermis. This horizontal growth phase may provide lead time for early detection, affordable to an OCT exploration. MSC is more easily cured if treated before the onset of the vertical growth phase with its metastatic potential[3]**.** Today, conventional OCT microscopes are bulky, performing micro-scale measurements from the macro world. Existing solutions are strongly dominated by optical fiber interferometers. By maintaining similar performances compared to bulk OCT systems, DOCT-VCSEL approach will offer a particular potential for point- of-care and earlier recognition and screening of cutaneous pathologies. DOCT-VCSEL's approach is a breakthrough in OCT microscopy offering a portable (150 x smaller) and cheaper (x10) OCT system. **Social impact of DOCT-VCSEL** concerns the improvement of the Quality of Life and Environment focusing mainly on the healthcare sector. DOCT-VCSEL technology will lead to **better diagnostic tools, to better treatment and quality of life for patients** by simultaneously reducing costs of public healthcare systems, providing quasi real-time high resolution 3D cartography of cutaneous lesions. Whereas dermoscopy is limited to surface detection of lesions (based on the visualization of morphological changes without resolving axial information in depth), low cost and portable OCT offers the potential of detecting the very earliest changes at the micro-scale of skin tissue, identifying microscopic features and enabling cross-sectional imaging with high spatial resolution and in real-time. The imaging depth of 0.5mm should be enough to reach dermis/epidermis junction in most of the human body zones and our technology will contribute in portability and accessibility of OCT imagers.

OCT market for dermatology

The global OCT market is in constant growth, with revenues expected to reach $800 million by 2012 [46]. Historically, in the 1990's the field of OCT was studied by a relatively small set of research groups around the world with a limited number of start-ups, so that the field was dominated by academic researchers. Today, there is a tremendous amount of both commercial and research activity. On the commercial side there are about 50 companies selling and developing OCT systems or subsystems. Some of these companies are big (e.g. St. Jude or Zeiss Meditec) and some are new seedling start-ups of small size. This situation is synthesized in Table 5. The global market for OCT systems is growing at an annual rate of 34% and OCT's first commercial application – the ophthalmology - will continue to dominate through 2013. New applications and products are emerging in areas such as cardiology, dentistry and dermatology, this last sector of market concerning DOCT-VCSEL proposal. The OCT has been introduced in dermatology in 1997 and now is routinely employed in clinical diagnosis and treatment of skin related disorders [47][48]. Operating with high resolution and of simple use, OCT is a powerful tool compared to other morphological techniques used for dermatology. The total market for dermatology diagnostic devices was estimated to be $175 million in 2010. The growth of this market concerns strongly the OCT systems because some OCT scanners for dermatological

purposes are already available on a commercial basis (e.g. AGFA, Michelson Diagnostics, IMALUX, Bioptigen, Thorlabs, Lltech). We think that DOCT-VCSEL technology will provide dermatologists (4000 in France, 60000 in Europe) new and very useful information about what occurs below skin surface of patients subjected to cutaneous pathologies.

Table 5: OCT system manufacturers

Company	***Application***
Carl Zeiss Meditec, Heidelberg Engineering, OPKO, Optopol, Optovue, Bioptigen, Thorlabs	Ophtalmology (dominant: SD & SS-OCT)
Glucolight	Blood-glucose measurements (LCI OCT)
Lightlab Imaging	Cardiology (FD-OCT)
Lantis Laser	Dentistry (SD-OCT)
AGFA, ISIS Optronics, Michelson Diagnostics, Lightlab Imaging, Lltech, Imalux, Thorlabs	Dermatology (TD-OCT, SD-OCT, LCI OCT)
Tomophase	Pulmonary (LCI OCT)
Imalux	Urology (SS & SD-OCT)
Heliotis, Santec	General research (LCI OCT)
Optiphase, Thorlabs	OEM engines (dominant: SD & SS-OCT)
Novacam Technologies	Multifunctional (TD& LCI OCT)

Dissemination and exploitation of results (see also Task 5 in section 2.2) / Intellectual property

The partners will sign a Consortium Agreement wherein the access rights and conditions of protection of knowledge are defined. This agreement will also define the conditions under which the publication and use of the knowledge acquired during the project can be undertaken. The project will contribute to increase the level of knowledge and skills available to the French industry and academia in this technology field, all this representing a significant advantage towards the foreign competition. For LAAS, an important outcome of the project will be to improve the visibility in tunable MEMS-VCSEL technology at the international level. FEMTO prototype being developed by the European project VIAMOS (ending at the beginning of DOCT-VCSEL) belongs entirely to FEMTO. Moreover, the architecture will be amended for DOCT-VCSEL as we will go far beyond in system miniaturization. There is therefore no conflict of interest between the two projects.

Intellectual Property: Each Party retains full and total ownership of its Own Knowledge. New Knowledge belongs to the Party having created it alone and any resulting new patents shall only be registered in the name, and at the expense, of said Party and at its sole initiative. In the event that New Knowledge were to be created by the staff of two or several Parties in an in dissociable way, this New Knowledge, hereinafter referred to as the “Joint New Knowledge”, shall be jointly owned by these Parties, hereinafter referred to as the “Co-Owner Parties”, proportionally to their intellectual, human, material and financial contributions, unless said Parties were to contractually agree to the related property rights being transferred to one of them. Any and all Joint New Knowledge consisting of a new patent, software or other knowledge protected by an intellectual property right, shall be subject to rules of co-ownership, that shall be drawn-up between the Co-Owner Parties as soon as necessary and, in all cases, prior to any and all industrial and/or commercial u

References

[1] AW Kopf et al., Arch. Dermatol., 1975.
[2] SQ Wang et al., Clin. Dermatol. 2004.
[3] P. Guitera-Rovel et al., Ann Dermatol Venereol 135, 828-834, 2008.
[4] D. Huang et al., Science 254, 1178–81, 199.
[5] J. Fujimoto et al., Biomedical Optical Imaging, Oxford University Press, 2009.
[6] K. Totsuka et al., Proc. SPIE 7554, 75542Q, 75542Q-5 (2010).

[7] V. Jayaraman et al., CLEO 2011 - Laser Applications to Photonic Applications, PDPB2, 2011.
[8] K. Iga, et al ; Japanese Journal of Applied Physics Vol.47 N°1 pp1-10 (2008).
[9] Wu et al.. Electronics Letters 31(19), pp.1671, 199.
[10] I . Grulkowski et al., Biomed Opt Express 3(11), 2733-51, 2012.
[11] V. Jayaraman et al., A.; Electronics Letters 48(14), 867-869, 2012.
[12] V. Jayaraman et al.; Electronics Letters 48(21), 1331-1333, 2012.
[13] DD. John et al, *Lightwave Technology, Journal of* , vol.PP, no.99, pp.1,1, 2015
[14] J. Albero et al., J. of Micromechanics and Microengineering 21, 065005, 2011.
[15] www.viamos.eu/
[16] B Reig et al. J. Micromech. Microeng. 22 065006 (2012), JMM select and June cover issue.
[17] B. Reig.et al., IEEE Sensors 2012, 1-4, 28-31 Oct. 2012, Taipei, Taïwan.
[18] B. Kögel et al., A. Quantum Electronics, IEEE Journal 48(2), 144-152, 2012.
[19] Michael C.et al., Nature Photonics 2, 180-184, 2008.
[20] T. Saastamoinen et al., Adv. Opt. Techn. 1, 181–185, 2012.
[21] A. Aneesh et al Proc. SPIE 7554, , 75540V (2010).
[22] A. Mcheik, C. Tauber, H. Batatia, J. George and J.M. Lagarde (2008) Thesis.
[23] G.Josse, et al, Skin Research and Technology, Volume 17, Issue 3, pages 314–319, 2011.
[24] T. Yano et al., IEEE J. Sel. Topics Quantum Electron. 15(3), 528–534, 2009.
[25] C. Gierl et al., Opt. Express 19, 17336-17343, 2011.
[26] C. Gierl et al.; Proc. SPIE 8276, Vertical-Cavity Surface-Emitting Lasers XVI, 82760P, 2012.
[27] Y. Rao et al., IEEE Semiconductor Laser Conference (ISLC), 40, 2012.
[28] Ansbaek, T et al , *Photonics Technology Letters, IEEE* , vol.25, no.4, pp.365,367, 2013
[29] M. C. Y. Huang et al., IEEE J. Sel. Topics Quantum Electron. 11(2), 374-380, 2007.
[30] G. Cole et al., Opt. Express 16, 16093-16103, 2008.
[31] Kögel B. et al., Electronics Letters 47(13), 764-765, 2011.
[32] Kögel B. et al., A. Quantum Electronics, IEEE Journal 48(2), 144-152, 2012.
[33] M. Nakahama et al, MOC'13 conference, october 27-30, Tokyo, Japan.
[34] B Reig et al., J. Micromech. Microeng. 22, 065006, 2012.
[35] B. Reig.et al., IEEE Sensors 2012, 1-4, 28-31 Oct. 2012, Taipei.
[36] V. Bardinal et al., IEEE PTL 22(21), 1592-1594, Nov. 2010.
[37] K. Laszczyk et al., Sensors and Actuators A 163, 255-265, 2010.
[38] R. Won, Micro-optics one-stop shop, Nature Photonics 5, 9-10, 2011.
[39] J. Albero et al., Opt. Express 17, 6283-6292, 2009.
[40] R. Carrasco et al., Proc. SPIE 5836, 657-666, 2005.
[41] Khaled Aljasem et al 2008 J. Opt. A: Pure Appl. Opt. 10 044012.
[42] T. Camps et al., Electronic Letters 41(3), 129-131, 2005.
[43] L.M. Lechuga et al. Sensors and Actuators B 118(1−2), 2−10, 2006.
[44] D. Penso-Assathiany et al., J Am Acad Dermatol. 68, 185-6 (2013).
[45] F. Grange et al., Arch Dermatol. 17, 1-7 (2012)
[46] G. Smolka, Optical Coherence Tomograph: Technology, Markets, 2008, Penn Well, Corp.
[47] J. Welzel et al., J Am Acad Dermatol. 37, 958—63, 1997.
[48] T. Gambichler et al., Arch Dermatol Res 303, 457–473, 201

D/ Innovation en imagerie in vivo : Microscopie par Cohérence Optique en Dermato-oncologie

Dr Jean-Luc Perrot
Investigateur principal et coordonnateur

D. Innovation en imagerie in vivo : Microscopie par Cohérence Optique en Dermato-oncologie

Il s'agit d'un projet visant à qualifier un nouveau prototype d'OCT haute définition .C'est une travail avec la société DAMAE, startup de l'institut supérieur d'Optique de Palaiseau. Cette collaboration est due au souhait de la société DAMAE de travailler avec une équipe ayant l'expérience de l'OCT HD et de l'imagerie microscopique dermatologique au sens large et à notre souhait de participer au développement d'un outil performant permettant au dermatologue d'assurer une médecine de qualité en permettant des diagnostic précis et non invasifs à une époque où de plus en plus de traitement médicaux non invasif sont mis à notre disposition pour traiter certains cancers cutanés.
En effet faire des biopsies chirurgicales pour initier ou surveiller des traitements médicaux dont le but est d'éviter un geste invasif est totalement illogique. D'autre part permettre d'apporter un choix dans les techniques d'imagerie non invasive de la peau aux dermatologues nous parait plus que légitime.
Enfin de participer une fois de plus au développement d'une technologie française nous a paru être un objectif stimulant.

Innovation en imagerie in vivo : Microscopie par Cohérence Optique en Dermato-oncologie

N° de la recherche : xxxx

Investigateur-coordonnateur :

Dr Jean-Luc PERROT
Service de Dermatologie
CHU de St-Etienne
Avenue Albert Raimond
42055 St-Etienne Cedex 02
Tel : 04 77 12 75 40
Fax : 04 77 12 05 49
Mail : jeanluc.Perrot@univ-st-etienne.fr

Investigateurs associés :
Service de Dermatologie, CHU Saint-Etienne :
Dr Bruno LABEILLE
Pr Frédéric CAMBAZARD

Equipes impliquées dans le projet :
Service d'Ophtalmologiste, CHU Saint-Etienne :
Pr Gilles THURET

Service d'Anatomopathologie, CHU Saint-Etienne :
Pr Michel PEOC'H
Dr Jean Marc DUMOLLARD
Dr Fabien FOREST

Expérimentateurs :

- CHU de Saint-Étienne : TBD ?
- DAMAE Medical : Mme Anaïs BARUT - M. David SIRET - Mme Dahbia AGHER - M. Olivier LEVECQ - M. Hicham AZIMANI

Promoteur :
CHU de Saint Etienne,
42055 SAINT-ETIENNE Cedex 2

Représentant du promoteur :
Mme Aurélie CHANNET
Direction des Affaires Médicales et de la Recherche
Bât 31 - Hôpital Bellevue, CHU de Saint-Étienne
42055 SAINT-ETIENNE Cedex 2

CPP Sud-Est 1
Direction des Affaires Médicales et de la Recherche
Bât 31 - Hôpital Bellevue, CHU de Saint-Étienne
42055 SAINT-ETIENNE Cedex 2

PAGE DE SIGNATURE DU PROTOCOLE

Titre de l'étude :

Innovation en imagerie in vivo : Microscopie par Cohérence Optique en Dermato-oncologie

Version du protocole et date : Version 1.7 du 10/10/2015

N° interne :

Représentant du promoteur

Mme Aurélie CHANNET
Direction des Affaires Médicales
et de la Recherche
Bât 31 - Hôpital Bellevue
CHU de Saint-Étienne
42055 SAINT-ETIENNE Cedex
2.

Date : …./…../2015
Signature

Investigateur coordonnateur

Dr Jean-Luc PERROT
Service de Dermatologie
Hôpital Nord
CHU de Saint-Étienne
42055 SAINT-ETIENNE Cedex
2

Date : …./…../2015
Signature

Résumé de l'étude

Title	***In vivo* imaging innovation : Optical Coherence Microscopy in dermato-oncology**
Collaborators (organisme financeur)	CHU Saint Etienne
Brief summary (10-12 lignes)	The present study aims at evaluating the interest of an innovative non invasive, imaging technology, for the real time, in vivo diagnosis of skin cancer. • The primary objective is to consolidate and validate an image interpretation classification of GALAXY images on cutaneous cancerous lesions • The secondary objective is to evaluate the performance of the device for the characterisation of cutaneous cancerous lesions based on this newly defined classification.
Conditions (primary disease or condition being studied)	Skin cancer (melanoma, basal cell carcinoma, squamous cell carcinoma)
Primary purpose	Diagnostic
Intervention model	Single groupe
Study classification	Safety/Efficacy
Number of arm(s)	1
Intervention	Imaging device
Device name	Galaxy (Damae medical, Paris, France)
Intervention description (max 1 000 characters)	The imaging procedure with Galaxy is performed by placing the tip of the microscope directly in slight contact with the skin of the patient, without need for a specific preparation. Images or videos sequences of the microscopic architecture of the tissue are then obtained in real time and can be interpreted by the physician.
Other Intervention (if applicable)	Device
Other intervention name	Na

Other intervention description (max 1 000 characters)	na
Medical Device administe ed, evaluated	Galaxy (Damae medical, Paris, France)
Primary outcome	Diagnostic performance of GALAXY for the characterization of cutaneous cancerous skin lesions (accuracy, sensitivity, specificity, positive predictive value, negative predictive value)
Time point(s) at which primary outcome measure is assessed	Once enrollment is finalized
Secondary outcome measure	Comprehensive and validated classification of GALAXY images, for the characterization of cutaneous cancerous skin lesions.
Time point(s) at which Secondary outcome measure is assessed	Once enrollment is finalized and images classification is validated
Inclusion criteria	• Male, female, Aged > 18 • Patient affiliated or eligible to the french social insurance • Willing and able to comply with study procedures and provide written informed consent to participate in the study. • Patient presenting with a cutaneous lesion suspicious for melanoma, BCC, SCC, requiring a surgical excision.
Exclusion criteria	• Allergy or intolerance to immersion oil (used for microscopy) • If female, pregnant or breast-feeding • patient unable to stand still for 20 seconds • Skin lesions located near patient eyes (<3 cm)
Keywords (3 à 5)	Optical biopsy, skin cancer, diagnostic performance

SOMMAIRE

JUSTIFICATION SCIENTIFIQUE ET DESCRIPTION GÉNÉRALE DE LA RECHERCHE 78
I.1. Description du dispositif médical Galaxy de DAMAE Medical 78
2. Justification scientifique de la recherche 78
I.1.1. Définition du cadre général de la recherche 78
I.1.1.1. Méthode traditionnelle de diagnostic en dermato-oncologie : la biopsie 78
I.1.1.2. État de l'art des techniques d'imagerie microscopique non-invasive utilisées en dermato-oncologie 78
I.1.1.3. Solution apportée par le dispositif Galaxy : la Microscopie par Cohérence Optique 79
I.1.2. Description des pathologies cutanées à étudier lors de la recherche 79
2.2.1. Le mélanome 79
2.2.2. Le carcinome basocellulaire 80
I.1.3. Présentation des dispositifs commerciaux existants sur le marché de la dermato-oncologie 80
I.1.4. Description et justification de la recherche 80
I.1.1.1. Hypothèses de la recherche : positionnement de la technologie Galaxy. 81
I.1.1.2. Description du plan expérimental de la recherche 81
I.1.5. Perspectives de la recherche 81
I. OBJECTIFS DE LA RECHERCHE 81
I.1. Objectif principal 82
I.2. Objectifs secondaires 82
II. CONCEPTION DE LA RECHERCHE 82
I.1. Critères d'évaluation 82
I.1.1. Critère d'évaluation principal 82
I.1.2. Critères d'évaluation secondaires 82
I.2. Méthodologie de la recherche 82
I.1.1. Design de l'étude 82
I.1.2. Examen de référence 83
I.3. Mesures prises pour réduire et éviter les biais 83
I.1.1. Diagnostic « dermatologique » standardisé 83
I.4. Déroulement et durée prévue de participation des personnes 83
I.5. Description des règles d'arrêt définitif ou temporaire 84
III. SELECTION ET EXCLUSION DES PERSONNES DE LA RECHERCHE 84
I.1. Population étudiée 84
I.2. Critères d'inclusion 85
I.2. Critères de non-inclusion 85
I.3. Procédure d'arrêt prématuré de la recherche ou d'exclusion pour une personne de la recherche et procédure de suivi de la personne 85
IV. TRAITEMENT UTILISE CHEZ LES PERSONNES QUI SE PRETENT A LA RECHERCHE AUTRE QUE LE DISPOSITIF MEDICAL FAISANT L'OBJET DE LA RECHERCHE 85
I.1. Description du ou des traitements nécessaires à la réalisation de la recherche. 85
I.2. Procédures de comptabilité - Méthodes de suivi de l'observance 85
I.3. Maintien de l'insu et procédures de levée de l'insu 85
I.4. Conditions de stockage des médicaments expérimentaux 85
I.5. Médicaments et traitements autorisés et interdits dans le cadre du protocole, y compris les médicaments de secours 85

V. EVALUATION DE LA PERFORMANCE 85
I.1. Description des paramètres d'évaluation des performances 85
I.2. Méthodes et calendrier prévus pour mesurer, recueillir et analyser les paramètres d'évaluation de la performance 86
A compléter **Erreur ! Signet non défini.**

VI. EVALUATION DE LA SECURITE 86
I.1. Description des paramètres d'évaluation de la sécurité 86
I.2. Méthodes et calendrier prévus pour mesurer, recueillir et analyser les paramètres d'évaluation de la sécurité 86
I.3. Procédures mises en place en vue de l'enregistrement et de la notification des événements indésirables 86
I.1.1. Définition 86
I.1.2. Déclaration de l'investigateur au promoteur 86
I.1.3. Déclaration du promoteur au CPP et aux autorités de santé 87
I.4. Modalités et durée du suivi des personnes suite à la survenue d'événements indésirables 87

VII. ANALYSE STATISTIQUE 87
I.1. Description des méthodes statistiques prévues, y compris du calendrier des analyses intermédiaires prévues 87
I.2. Nombre prévu de personnes à inclure dans la recherche, et nombre prévu de personnes dans chaque lieu de recherche avec sa justification statistique 88
I.3. Degré de signification statistique 88
I.4. Méthode de prise en compte des données manquantes, inutilisées ou non valides 88
I.5. Gestion des modifications apportées au plan d'analyse de la stratégie initiale 88
I.6. Choix des personnes à inclure dans les analyses 88

VIII. DROIT D'ACCES AUX DONNEES ET DOCUMENTS SOURCES 88
I.1. Droit d'accès aux données 89
I.2. Description des variables recueillies 89
I.3. Identification des données sources 89

IX. CONTRÔLE ET ASSURANCE QUALITE 89

X. FAISABILITE ET CALENDRIER DE L'ETUDE 90

XI. ORGANISATION DE L'ETUDE 90

XII. CONSIDERATIONS ETHIQUES 90
I.1. Déclaration indiquant que la recherche sera conduite conformément au protocole, aux bonnes pratiques et aux dispositions législatives et réglementaires en vigueur 90
I.2. Protection des personnes 91
I.3. Assurance 91
I.4. Rapport Bénéfice/Risque 91

XIII. TRAITEMENT DES DONNEES ET CONSERVATION DES DOCUMENTS ET DES DONNEES RELATIVES A LA RECHERCHE 91
I.1. Circuit des données 91
I.2. Modalités de traitement, vérification et validation des données (data management) 92
I.3. Archivage des documents de l'essai 92

XIV. PROPRIETES DES DONNEES - PUBLICATIONS DES RESULTATS 92
XV. Références bibliographiques 92
XVI. ANNEXES 94

I. JUSTIFICATION SCIENTIFIQUE ET DESCRIPTION GÉNÉRALE DE LA RECHERCHE

I.1. Description du dispositif médical Galaxy de DAMAE Medical

Galaxy est un dispositif médical se basant sur une nouvelle technique d'imagerie appelée **Microscopie par Cohérence Optique,** développé par la société DAMAE Medical. Cette technologie permet d'imager à haute-résolution (cellulaire) les microstructures internes de tous types de tissus biologiques *in vivo* ou *ex vivo*, sur une profondeur de pénétration de 800 µm, ce qui permet d'explorer l'épiderme, la jonction dermo-épidermique et le derme moyen voir en et de façon totalement non-invasive (directement au contact du tissu, sans prélèvement). A la différence des microscopes par cohérence optique usuel ce dispositif utilise un principe physique qui lui est propre permettant d'atteindre une profondeur d'exploration utile supérieure à celle de la microscopie confocale

Le dispositif médical Galaxy se présente sous la forme d'un microscope orientable :

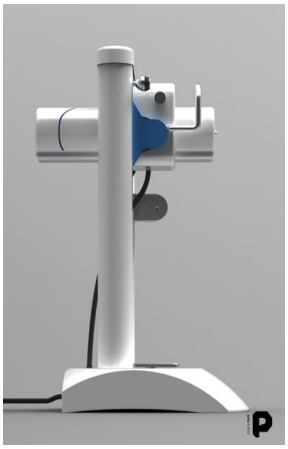

- En configuration verticale, il est utilisé pour étudier des échantillons biologiques (*ex vivo*) *Figure A*.

- En configuration horizontale, il permet de faire des coupes tomographiques *in vivo* sur un patient qui se présente devant la tête de mesure, afin d'étudier les lésions sans avoir recours à la biopsie : *Figure B*.

Annexe 1 : Tableau récapitulatif des caractéristiques techniques du dispositif médical Galaxy.

Annexe 2 : Notice d'utilisation du dispositif médical Galaxy

2. Justification scientifique de la recherche

I.1.1. Définition du cadre général de la recherche

I.1.1.1. Méthode traditionnelle de diagnostic en dermato-oncologie : la biopsie

Le diagnostic formel d'un cancer requiert l'examen de la lésion suspecte au moyen d'un examen histologique qui est aujourd'hui considéré comme le Gold Standard. Pour améliorer la pertinence clinique du diagnostic en onco-dermatologie, s'est développée la dermoscopie et plus récemment la microscopie confocale. Ces méthodes ont déjà permis de réduire le nombre de biopsies/exérèses inutiles tout en permettant de diagnostiquer des tumeurs malignes cliniquement non suspectes et d'améliorer la capacité de nouvelles thérapeutiques en onco-dermatologie (Imiquimod, Ingénol Mébutate, photothérapie dynamique). Ces nouvelles modalités de traitement permettent la prise en charge de tumeurs malignes cutanées, de manière non vulnérante. L'émergence de méthodes permettant d'établir un diagnostic et un suivi non invasif parait dès lors légitime.

I.1.1.2. État de l'art des techniques d'imagerie microscopique non-invasive utilisées en dermato-oncologie

Il existe 2 type dispositifs commercialisés actuellement à la disposition des dermatologues

La Microscopie Confocale (MC) : introduite à partir de 1980, elle permet de sélectionner la lumière ne provenant que de la zone correspondant au « point focal ». Par un système de balayage du point focal, on peut reconstituer *in vivo* des sections optiques horizontales, et donc parallèles à la surface de la peau, de haute résolution (1-2µm) et ainsi étudier des phénomènes cellulaires dynamiques et avec marqueur. Il s'agit de la technique de référence pour le diagnostic en routine des cancers en dermatologie. Sa profondeur de pénétration est **cependant limitée à ≈150µm**, ce qui ne permet pas d'étudier certaines pathologies cutanées plus profondes, par exemple.

La Tomographie par Cohérence Optique (OCT) : basée sur l'interférométrie en lumière faiblement cohérente, l'OCT a été mise au point dans les années 1990 et permet de visualiser en temps réel et sans marqueur l'intérieur des tissus (jusqu'à 2-3mm) mais avec une **résolution spatiale limitée** à plusieurs micromètres (≈20µm). Par un système de balayage, l'OCT permet de reconstituer des sections optiques verticales. L'impact majeur de l'OCT s'est révélé en ophtalmologie, pour l'étude des pathologies de la rétine, mais **le manque de spécificité** des images d'OCT, dans un milieu aussi diffusant que la peau, ne permet pas d'étudier précisément les pathologies cutanées.

I.1.1.3. Solution apportée par le dispositif Galaxy : la Microscopie par Cohérence Optique

La technologie novatrice développée par la société DAMAE Medical est appelée **Microscopie par Cohérence Optique**. Basée à la fois sur l'interférométrie en lumière faiblement cohérente et sur la microscopie optique, la force de l'innovation consiste à combiner la qualité d'imagerie, en termes de résolution, accessible avec les techniques de microscopie utilisées en *ex vivo* sur des tissus prélevés ; avec la capacité d'imager des phénomènes dynamiques sur les tissus vivants, de façon non-invasive.

Cette solution permet une visualisation *in vivo* à une résolution cellulaire (1-2µm), avec une pénétration jusque dans le derme (environ 800µm) – soit 5 fois plus que la MC – ce qui élargit très fortement le champ des pathologies cutanées détectables. Enfin, la technologie propose une visualisation **en sections verticales** à travers les différentes couches de la peau, représentant une manière plus logique d'imager les tissus pour les anatomopathologistes, habitués à interpréter des images de coupes histologiques orientées verticalement.

I.1.2. Description des pathologies cutanées à étudier lors de la recherche

Nous nous proposons d'étudier via la présente étude; les cancers de la peau les plus fréquents en termes de prévalence (+ de 95% de tous les cancers cutanés).

- Les mélanomes, (MSC : Melanoma Skin Cancer) qui se développent à partir des mélanocytes. On parle par convention de tumeurs noires ou mélanocytaires
- Les cancers non-mélanocytaires (NMSC : Non-Melanoma Skin Cancer) les plus fréquents. Il s'agit pour l'essentiel des **carcinomes basocellulaires** et les **carcinomes épidermoïdes**, qui se développent à partir de la prolifération des cellules appelées kératinocytes.

2.2.1. Le mélanome

Le mélanome est un problème de santé publique en France car son incidence est en constante augmentation, sa morbidité est importante et sa capacité à métastaser met en jeu le pronostic vital du patient. L'incidence du mélanome en France en 2012 était de 11 176 cas annuels soit au 9e rang de tous les cancers tous sexes confondus et au 6e rang chez la femme (BEH 2012, INCa 2013). Chez l'homme comme chez la femme, le taux d'incidence du mélanome cutané a augmenté de manière notable entre 1980 et 2012 passant de 2,5 à 10,8 pour 100000 hommes et de 4,0 à 11,0 pour 100000 femmes et cette tendance à l'augmentation se poursuit actuellement.

2.2.2. Le carcinome basocellulaire

Le carcinome basocellulaire (CBC) est le cancer de la peau le plus fréquent : il représente environ 70 % de l'ensemble des cancers cutanés. En 2010, plus de 65 200 patients ont été traités et pris en charge dans les établissements de santé publics et privés français pour un carcinome de la peau (PMSI MCO 2010). Selon les données du registre du Doubs entre 1983 et 2002, l'incidence a été multipliée par 2,3 chez l'homme et par 2 chez la femme (Grange et al, 2008).

2.2.3. le carcinome epidermoide

Le carcinome épidermoïde cutané (CE), également appelé carcinome spinocellulaire, vient au deuxième rang des cancers de la peau par ordre de fréquence, après le carcinome basocellulaire. Dans un pays comme les Etats-Unis, on estime à 450000 le nombre de nouveaux cas de CE par an.

Ce type de cancer de la peau se développe à partir des cellules de la couche épineuse de l'épiderme, qui est la couche superficielle de la peau. Les CE peuvent atteindre toutes les parties du corps, mais ils sont plus fréquents sur les zones de peau exposées au soleil, comme le visage, les oreilles, la lèvre inférieure, le cuir chevelu chauve, le cou, le dos des mains, les bras et les jambes. Souvent, ces zones de peau révèlent des signes de dommages du soleil, comme la présence de rides, de taches brunes ou d'une perte d'élasticité

I.1.3. Présentation des dispositifs commerciaux existants sur le marché de la dermato-oncologie

Basés sur les technologies de MC et d'OCT, trois dispositifs sont présents sur le marché et cherchent à remplacer la biopsie standard.

Il s'agit d'une part du dispositif **Vivascope** (MC), développé par la société américaine Caliber I.D, qui permettrait de passer de 8% à 40% de biopsies positives pour le mélanome. Mais est d'une efficacité limitée en cas de mélanome achromique (un piège majeur de l'onco-dermatologie). Sa pénétration dermique limitée au derme papillaire ne permet pas d'évaluer les CBC et carcinome épidermoïdes dans leur totalité.

Deux entreprises commercialisent des dispositifs basés sur l'OCT:

- La première est la société suédoise Michelson Diagnostics, qui commercialise le **Vivosight** en Australie, au Brésil et dans 5 pays européens.
- La deuxième société est la société belge Agfa Healthcare qui commercialise le **Skintell**, marqué CE mais non disponible commercialement aux USA et au Canada.

Ces dispositifs souffrent d'un manque d'adoption de la part des dermatologues, en raison du manque de preuves cliniques et médico-économiques. La technique est encore très peu connue et adoptée des praticiens. Les différentes recherches cliniques menées avec ces dispositifs ont porté sur l'évaluation de la performance diagnostique pour la caractérisation des lésions non mélanocytaires. En revanche, il existe peu de données disponibles quant à la performance diagnostique de ces dispositifs pour la caractérisation du mélanome. De fait, l'évaluation proposée ici, portera en partie sur l'évaluation de cette pathologie.
L'équipe du service de dermatologie du CJU de St Etienne à la pratique de ces 3 dispositifs (possède le visvascope et le Skintell) et a utilisé durant 6 mois le Vivosight.

Annexe 3 : complément d'informations sur les technologies concurrentes.

I.1.4.

I.1.5. Description et justification de la recherche

I.1.1.1. Hypothèses de la recherche : positionnement de la technologie Galaxy.

La comparaison initiale des images obtenues avec le dispositif Galaxy, à celles des coupes histologiques standards, confirme la possibilité d'établir des corrélations histologiques afin d'établir un diagnostic clinique en temps réel. Toute la recherche de ce projet est orientée vers cet objectif.

Les performances techniques d'imagerie à atteindre par la technologie développée par DAMAE Medical se déclinent en deux spécifications techniques principales :

Résolution micrométrique et spécificité : la qualité des images doit s'approcher au maximum du micron de résolution, de façon à permettre une visualisation cellulaire des structures de la peau.
En effet, le mélanome est une lésion mélanique qui nécessite une étude cytologique (c'est-à-dire une étude des cellules) pour être diagnostiqué avec certitude. De plus, ayant une plus forte concentration en mélanine, les cellules mélanocytaires sont mises en évidence sur les images optiques par des structures très brillantes, car elles réfléchissent plus la lumière. Les images doivent donc avoir un contraste suffisamment bon pour détecter ces structures plus brillantes significatives.

Profondeur de pénétration dermique : la grande profondeur de pénétration est l'un des avantages concurrentiels les plus fondamentaux de la technologie. De l'ordre de 800µm, elle permet de visualiser les couches internes de la peau telles que la partie profonde du derme, et donc de donner accès à un champ bien plus large de pathologies détectables, telles que le mélanome infiltrant ou les carcinomes, et par ailleurs d'évaluer le caractère infiltrant ou non de la lésion, paramètre indispensable à la formulation d'un diagnostic complet et crucial dans le choix de la prise en charge thérapeutique.

I.1.1.2. Description du plan expérimental de la recherche

L'étude se déroulera en deux parties:

1**. Collecte prospective des données**

- des images Galaxy de tumeurs suspectes d'être des mélanomes, CBC et carcinomes épidermoïdes
- des données cliniques associées

2. Analyse de ces images pour :

- la définition et validation des critères d'interprétation pour chacune des pathologies étudiées,
- puis l'évaluation rétrospective de la performance diagnostique

I.1.5. Perspectives de la recherche

Cette étude mono-centrique permettra de fournir une évaluation préliminaire de la performance diagnostique de la technologie Galaxy, pour la caractérisation des 3 principaux cancers cutanés. Cette étude vise à valider l'intérêt clinique de cette technologie pour la caractérisation de ces lésions et à obtenir les données nécessaires à la mise en place d'études cliniques futures, de plus grande ampleur, visant à valider prospectivement la précision diagnostique de cette technologie, ainsi que son impact thérapeutique.

II. OBJECTIFS DE LA RECHERCHE

II.1 Objectif principal

L'objectif principal de cette étude est d'évaluer les performances diagnostiques globales de Galaxy pour la caractérisation de lésions cutanées de différentes natures (mélanomes, carcinomes basocellulaires et carcinomes épidermoides)

II.2. Objectifs secondaires

Les objectifs secondaires de cette étude sont :
- de **définir des critères d'interprétation diagnostiques** à partir des images obtenues avec le dispositif Galaxy, en identifiant des corrélations avec les images histologiques standards correspondantes, obtenues sur tumeurs opérées car suspectes d'être des mélanomes, carcinomes basocellulaires et carcinomes épidermoides.
- d'évaluer la courbe d'apprentissage associée à l'utilisation de cette technologie.

III. CONCEPTION DE LA RECHERCHE

III.1. Critères d'évaluation

III.1.1. Critère d'évaluation principal

Le critère d'évaluation principal de la recherche porte sur:
- la définition de critères d'interprétation des images Galaxy obtenues pour la caractérisation de lésions cutanées de mélanomes, carcinomes basocellulaires et carcinomes épidermoides.

III.1.2. Critères d'évaluation secondaires

Les critères d'évaluation secondaires portent sur:
II. L'évaluation de la sensibilité (Se), la spécificité (Sp), la valeur prédictive positive, la valeur prédictive négative et l'aire sous la courbe, l'accord inter-observateur, l'accord intra-observateur
- L'évaluation de la courbe d'apprentissage "clinique" mesurée par la comparaison entre la performance diagnostique des investigateurs pré et post formation à l'interprétation des images.

III.2. Méthodologie de la recherche

III.1.1. Design de l'étude

L'étude Galaxy est une étude prospective, monocentrique, française visant à évaluer l'intérêt d'une nouvelle méthode d'aide au diagnostic pour la caractérisation de lésions cutanées.

L'étude se déroulera comme suit:

1. **Collecte prospective des images Galaxy,** des données cliniques et prélèvement histologiques associés au cours de procédures diagnostiques en dermatologie. Pour chaque patient, une double imagerie sera effectuée avec Galaxy sur la lésion et/ou pathologie ; et sur la zone adjacente dite « saine ».

2. **Définition et validation des critères d'interprétation** pour chacune des pathologies étudiées. Pour chaque cas, les séquences Galaxy seront revues par 3 investigateurs et anatomopathologistes. Ils disposeront pour chaque cas des données suivantes : histoire clinique

du patient, informations relatives à la procédure, résultats de cytologie, histologie, ou marqueurs tumoraux si disponibles, séquences Galaxy et, pour certains cas, lames anatomopathologiques. Cette revue permettra de formuler des critères d'interprétation susceptibles de caractériser les lésions et pouvant être corrélés de manière histologique aux structures observées sur ce type de lésions.

3. **Evaluation de la performance diagnostique**. Cette évaluation rétrospective sera réalisée en aveugle par des investigateurs, non impliqués dans la définition des critères d'interprétation.
Cette revue sera précédée d'une présentation des critères d'interprétation des images GALAXY.
Le diagnostic final de chaque cas aura préalablement été établi par histologie.

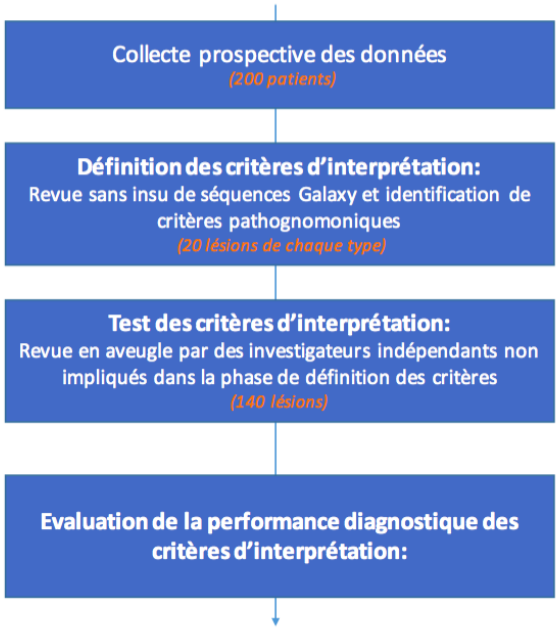

Fig 1 : study flow

III.2.2. Examen de référence

Le gold-standard diagnostic sera l'analyse histologique du prélèvement réalisé sur chacune des lésions étudiées.

III.3. Mesures prises pour réduire et éviter les biais

Diagnostic « dermatologique » standardisé

Pour chacune des pathologies analysées, une grille de lecture des images de Galaxy sera établie d'après la littérature et la grille de lecture des anatomopathologistes.

III.4. Déroulement et durée prévue de participation des personnes

III.4.1. Déroulement pour un patient consultant en dermatologie :

- ***Le recrutement*** sera réalisé dans le service de dermatologie du CHU de Saint-Etienne.
- ***L'inclusion*** sera réalisée pour tout patient consécutif répondant aux critères d'inclusion/exclusion.

Aucun traitement ou suivi supplémentaire à la pratique habituelle ne sera nécessaire.

Visite de sélection : consultation auprès du dermatologiste.
Présentation du protocole aux patients correspondants aux critères d'inclusion (lors de la consultation pré-chirurgicale) et remise des deux exemplaires du formulaire de consentement, avec délai de réflexion d'une semaine et l'image Galaxy réalisée le même jour).

- Réalisation de photographies couleur des lésions : macro-photographie soit avec l'appareil macro photographique et au dermoscope dermatologique (et si besoin en microscopie confocale in vivo) selon les procédures standard du service. Ces examens sont de pratique habituelle.

Visite d'inclusion : convocation pour l'imagerie Galaxy.
Une journée dédiée, examens réalisés par les investigateurs ou l'un des internes en dermatologie.

- Récupération du formulaire de consentement signé (un exemplaire pour le patient et un exemplaire pour l'investigateur).
- Réalisation de l'image Galaxy en dermatologie (environ 5 minutes).

III.4.2. Description de la procédure Galaxy et collecte des données.

L'examen se déroule après le dépôt d'une goutte d'huile d'immersion sur la zone de peau à imager.
L'examen dure de 1 à 5 minutes. Il s'agit d'un examen indolore, de surface, qui n'exerce qu'une pression très limitée sur la zone à explorer et sur quelques millimètres carrés.
Les images et films collectés au cours de l'étude seront conservés après la fin de l'étude de manière anonyme dans le réseau informatique du CHU. Pour chaque patient, un dossier anonymisé sera créé et les images, films, désignés par un numéro y seront stockées.

III.5. Description des règles d'arrêt définitif ou temporaire

a/ Arrêt de participation d'une personne à la recherche
- Retrait volontaire
- Allergie ou intolérance

b/ Arrêt d'une partie ou de la totalité de la recherche
Si les inclusions n'ont pas commencé au bout d'un an, l'étude sera arrêtée. Si le taux d'inclusion paraît insuffisant et non justifié, le promoteur pourra décider de l'arrêt de l'étude.

IV. SELECTION ET EXCLUSION DES PERSONNES DE LA RECHERCHE

IV.1. Population étudiée

La population étudiée sera composée de plusieurs groupes de patients. Les patients seront inclus de façon consécutive pendant 6 mois.
La population cible sera issue des patients du service de dermatologie (consultation et hospitalisation) du CHU de Saint-Étienne pour les groupes de lésions et/ou pathologies suivantes
- Mélanome : superficiel, nodulaire voire lentigo malin jusqu'à mélanose de Dubreuilh,
- Carcinome basocellulaire,
- Carcinome épidermoïde,

IV.2. Critères d'inclusion

- Patient majeur
- Sujet affilié à (ou ayant droit à) un régime de sécurité sociale
- Ayant signé le formulaire de consentement de participation

II. Tout patient des services de dermatologie du CHU de Saint-Etienne, consultant ou hospitalisé et pour lequel doit être procédée l'exérèse d'une lésion suspecte de correspondre à un:

- Mélanome
- Carcinome baso-cellulaire,
- Carcinome épidermoïde

IV.3. Critères de non-inclusion

- Allergie ou intolérance connue à l'huile d'immersion
- Femme enceinte ou allaitant
- Impossibilité de rester immobile 20 secondes le temps de l'examen
- Lésions oculaires et lésions situées à < 3cm de l'œil du patient

IV.4. Procédure d'arrêt prématuré de la recherche ou d'exclusion pour une personne de la recherche et procédure de suivi de la personne

- Survenue d'un événement indésirable grave (EIG)

V. TRAITEMENT UTILISE CHEZ LES PERSONNES QUI SE PRETENT A LA RECHERCHE AUTRE QUE LE DISPOSITIF MEDICAL FAISANT L'OBJET DE LA RECHERCHE

V.1. Description du ou des traitements nécessaires à la réalisation de la recherche.

Non applicable

V.2. Procédures de comptabilité - Méthodes de suivi de l'observance

Un tableau de comptabilité Excel sera réalisé pour le suivi global des patients.

V.3. Maintien de l'insu et procédures de levée de l'insu

Non applicable

V.4. Conditions de stockage des médicaments expérimentaux

Non applicable

V.5. Médicaments et traitements autorisés et interdits dans le cadre du protocole, y compris les médicaments de secours

Aucun médicament n'est interdit dans le cadre du protocole.

VI. EVALUATION DE LA PERFORMANCE

VI.1. Description des paramètres d'évaluation des performances

L'évaluation de la performance sera mesurée par les paramètres suivants :

- Précision diagnostique
- Sensibilité
- Spécificité

- Valeur prédictive positive
- Valeur prédictive négative

VI.2. Méthodes et calendrier prévus pour mesurer, recueillir et analyser les paramètres d'évaluation de la performance

Le jour de l'inclusion

VII. EVALUATION DE LA SECURITE

XIV.1. Description des paramètres d'évaluation de la sécurité

La réalisation d'observation de lésions cornéennes avec Galaxy n'est pas prévue dans ce protocole. Une exposition accidentelle pourrait néanmoins se produire dans l'axe visuel. L'expérimentateur prendra donc soin de ne pas exposer les yeux du patient ou les siens dans l'axe de mesure.

XIV.2. Méthodes et calendrier prévus pour mesurer, recueillir et analyser les paramètres d'évaluation de la sécurité

- Examen clinique avant et après l'examen d'imagerie.
- En cas de suspicion de photo-traumatisme : examen du fond d'œil, rétino-photo couleur et tomographie par cohérence optique (OCT).
- Surveillance clinique standard

XIV.3. Procédures mises en place en vue de l'enregistrement et de la notification des événements indésirables

VI.1.1. Définition

Un effet/événement indésirable est une manifestation nocive survenant chez une personne qui se prête à la recherche biomédicale que cette manifestation soit liée ou non à la recherche ou au produit sur lequel porte la recherche.
Un effet/événement indésirable grave est un effet/événement indésirable qui :
- Entraîne la mort,
- Met en danger la vie de la personne qui se prête à la recherche,
- Nécessite une hospitalisation ou la prolongation de l'hospitalisation,
- Provoque une incapacité ou un handicap important ou durable,

II. Se traduit par une anomalie ou une malformation congénitale.

Tout effet/événement indésirable grave (EIG) figurant dans le paragraphe VIII de ce protocole sera considéré comme étant un événement attendu (EIGA). A l'inverse, tout EIG non mentionné dans ce paragraphe est considéré comme un EIG inattendu (EIGI).

VI.1.2. Déclaration de l'investigateur au promoteur

L'investigateur devra déclarer au promoteur :
- Tout EIG inattendu dès qu'il en a connaissance et,
- Tout EIG attendu dans un délai de 8 jours après qu'il en a eu connaissance.
- Que cet EIG soit ou non lié au produit/technique expérimental/étude.

Dans les 2 cas, l'investigateur complétera puis faxera au promoteur le bordereau spécifique de déclaration d'EIG figurant dans les cahiers d'observation. A réception du bordereau d'EIG, un ARC de l'URCIP documentera cet événement et le transmettra aux membres du comité de

validation des EIG du promoteur (constitué d'un médecin et d'un pharmacien de l'URCIP). Ce comité jugera du caractère attendu ou inattendu et de l'imputabilité de cet EIG par rapport au produit/technique expérimental/étude. Tous les EIGI pour lesquels le comité de validation des EIG n'aura pu totalement écarter un quelconque lien avec le produit/technique expérimental/étude seront déclarés à l'ANSM par le promoteur.

VI.1.3. Déclaration du promoteur au CPP et aux autorités de santé

Dès qu'il aura eu connaissance de la survenue d'un EIGI susceptible d'être lié à l'étude, le promoteur effectuera une déclaration à l'ANSM et au CPP :

- Dans un délai de 7 jours ouvrés pour tout décès ou événement mettant en jeu le pronostic vital,
- Dans un délai de 15 jours ouvrés pour tout autre type d'EIG

En cas de déclaration initiale incomplète d'un EIGI, le promoteur adressera, dès réception d'informations complémentaires, un rapport de suivi référencé et numéroté de cet EIGI.

S'il survient des EIG dans cette étude, le promoteur transmettra au CPP et à l'ANSM :

- Tous les 6 mois, un listing (accompagné d'une synthèse) de ces EIGI
- Chaque année, dans les 60 jours suivant la date anniversaire de la 1ère inclusion, un rapport annuel de sécurité

La survenue et la déclaration des EIG attendus et inattendus seront systématiquement vérifiées lors des visites de monitoring.

En cas de survenue d'un fait nouveau (par exemple nouvelle donnée de sécurité), le promoteur adressera une déclaration de ce fait nouveau et des éventuelles mesures prises, dès qu'il en a connaissance, au CPP et à l'ANSM. Si le promoteur a connaissance d'informations complémentaires pertinentes concernant ce fait nouveau, il adressera un rapport de suivi, à l'ANSM et au CPP.

XIV.4. Modalités et durée du suivi des personnes suite à la survenue d'événements indésirables

Les patients ayant présenté un EIG « dermatologique » seront suivi dans le service de dermatologie du CHU jusqu'à la résolution de l'événement ou jusqu'à la fin de la recherche.

Les patients ayant présenté un EIG « général » seront suivi par le service d'urgence qui les aura pris en charge selon les modalités habituelles, jusqu'à la résolution de l'événement ou jusqu'à la fin de la recherche.

XV. ANALYSE STATISTIQUE

VIII.1. Description des méthodes statistiques prévues, y compris du calendrier des analyses intermédiaires prévues

- Une description de la population des patients inclus sera effectuée grâce aux statistiques suivantes :

- Variables quantitatives : nombres de données disponibles, moyenne, écart-type, médiane, minimum et maximum,
- Variables qualitatives : fréquences absolue et relative (exprimée en %).

La performance diagnostique sera évaluée via les paramètres suivants:
• Calcul de la sensibilité = (nombre de vrais positifs)/ (nombre de vrais positifs+ nombre de faux négatifs)
• Calcul de la spécificité = (nombre de vrais négatifs)/ (nombre de vrais négatifs + nombre de faux positifs)
• VPP = (nombre de vrais positifs)/ (nombre de vrais positifs + nombre de faux positifs)
• VPN = (nombre de vrais négatifs)/ (nombre de vrais négatifs + nombre de faux négatifs)

- Aucune analyse intermédiaire n'est prévue.

- Autres critères :
- Pourcentage de cas non analysables par catégories de pathologie et en fonction de l'expérience de l'expérimentateur,
- Sensibilité et spécificité en fonction de l'expérience de l'investigateur
- Accords intra et interobservateur
- courbe d'apprentissage
- Qualité des images (score à 3 niveaux) :

VIII.2. Nombre prévu de personnes à inclure dans la recherche, et nombre prévu de personnes dans chaque lieu de recherche avec sa justification statistique

Nous jugeons que Galaxy aura un intérêt dans le diagnostic des pathologies dermatologiques si sa sensibilité est de 80%. Nous souhaitons avoir une précision absolue de 5%. Le nombre de sujets nécessaires est celui pour avoir un intervalle de confiance à 95% de la Sensibilité entre 60,25 et 79,75.
Le calcul de n donne un nombre de patients positifs pour le gold-standard de 81.
Compte tenu d'un nombre d'erreur diagnostic clinique attendu assez important (20%) en raison de l'inclusion de certaines pathologies bénignes, nous inclurons 200 patients.

VIII.3. Degré de signification statistique

$$P < 0,05$$

VIII.4. Méthode de prise en compte des données manquantes, inutilisées ou non valides

Aucune imputation des valeurs manquantes n'est prévue.

VIII.5. Gestion des modifications apportées au plan d'analyse de la stratégie initiale

Le plan d'analyse statistique comprend une analyse descriptive qui sera possible dans tous les cas.

VIII.6. Choix des personnes à inclure dans les analyses

Toutes les personnes pour lesquelles un diagnostic de référence aura pu être établi et pour lesquelles les images Galaxy sont exploitables.

XVI. DROIT D'ACCES AUX DONNEES ET DOCUMENTS SOURCES

IX.1. Droit d'accès aux données

Les personnes participantes à cette recherche seront informées de leur droit d'accès et de rectification aux données les concernant ainsi que des modalités d'application de ce droit via la notice d'information de l'étude. Le promoteur (par l'intermédiaire de l'ARC ou des investigateurs) s'engage à répondre à toute demande d'accès aux données dans un délai de 2 mois maximum. Par ailleurs, seule le personnel habilité par le promoteur (investigateurs, ARC, TEC) et les représentants des autorités de santé pourront avoir accès à ces informations.

IX.2. Description des variables recueillies

Les données de l'étude seront recueillies directement dans les cahiers d'observation et CRF, au fur et à mesure des visites de l'étude. Ces données seront validées par l'investigateur qui signera (manuellement ou électroniquement) les cahiers d'observation.

Les informations recueillies dans le cadre de cette étude sont les suivantes :

- Données démographiques
- Antécédents médicaux
- informations sur l'examen clinique
- informations sur l'examen dermoscopique si réalisé
- informations sur l'examen par le dispositif Galaxy
- informations sur le prélèvement histologique effectué
- potentiel événement indésirable survenu au cours de la recherche
- diagnostic final

Les données manquantes devront être justifiées (par exemple dans un tableau des violations de protocole). Toute correction apportée dans le CRF devra être traçable (barrée, datée et paraphée par le correcteur sur un CRF « papier », via l'audit trial » sur un e-CRF).

IX.3. Identification des données sources

Les données des patients inclus dans l'étude seront colligées sur un CRF papier : 2 premières lettres du nom, première lettre du prénom, sexe, âge, n° d'inclusion attribué de façon chronologique, date de réalisation, ensemble des résultats qualitative ou quantitative notées dans le CRF. Ces données anonymisées, issues de la lecture des images de MCIV, seront colligées dans un fichier informatique spécifique.

Les documents sources seront constitués par l'ensemble des informations et résultats d'examens figurant dans le dossier médical des personnes participants à cette recherche. Les informations suivantes devront figurer dans le dossier médical :

- titre de l'étude,
- date d'information et d'inclusion du patient dans l'étude (signature du consentement),
- les différentes visites du patient dans le cadre du protocole,
- la survenue des complications (Evénements Indésirables Graves).

L'investigateur s'engage à donner un accès direct à l'ensemble de ces documents aux personnes mandatées par le promoteur.

XVII. CONTRÔLE ET ASSURANCE QUALITE

Le contrôle de qualité sera réalisé par l'Attaché de Recherche Clinique (ARC) de l'URCIP. Le promoteur ayant classé cette étude en niveau de monitoring minimal, ce qui signifie que l'ARC réalisera 1 visite de mise en place, le nombre de visites de monitoring (contrôle critères d'inclusion/non inclusion, critères d'évaluation, randomisation, EIG, présence des consentements signés) et une visite de fermeture dans le centre. Ces visites seront réalisées selon les

procédures opératoires standards du promoteur et donneront lieu à la rédaction de comptes-rendus de visites.

XVIII. FAISABILITE ET CALENDRIER DE L'ETUDE

Cette étude s'appuie sur les technologies innovantes utilisées dans le service de dermatologie du CHU de Saint-Etienne et dont la preuve de concept de l'utilisation

Les capacités de recrutement des patients présentant les différentes pathologies ciblées ne poseront pas de problèmes. Plus de 35 000 consultants franchissent la porte du service de dermatologie du CHU de St-Etienne, et plus de 13 000 celle du service de dermatologie.

Nous prévoyons d'inclure les patients vus en dermatologie.
Chaque semaine, un interne de dermatologie occupe un poste dédié en partie à la recherche clinique et sera chargé d'organiser le recrutement.
Deux autres internes du service de dermatologie (en Master 2 recherche) lui prêteront main forte.
Le service d'anatomie-pathologique est rompu à l'analyse des prélèvements dermatologique.

Durée de l'étude : 6 mois
Date prévisionnelle de début des inclusions : Avril 2016
Date prévisionnelle de fin des inclusions : Septembre 2016
Date prévisionnelle de fin de la période de suivi : Septembre2016
Date prévisionnelle d'analyse et validation des données : Q4 2016
Date prévisionnelle de rapport final : Q4 2016

XIX. ORGANISATION DE L'ETUDE

Investigateur principal :
Dr Jean Luc PERROT

Co-investigateurs :
Dr Jean Luc PERROT
Dr Bruno LABEILLE

Services concernés par la recherche :
Service de dermatologie, CHU de Saint-Etienne
Service d'Ophtalmologie
Laboratoire d'Anatomopathologie

Responsable de la mesure des critères d'évaluation :
Pr Gilles THURET

Personne chargé de la saisie des données :

Responsable de l'analyse statistique :
Pr Gilles THURET

XX. CONSIDERATIONS ETHIQUES

XIII.1. Déclaration indiquant que la recherche sera conduite conformément au protocole, aux bonnes pratiques et aux dispositions législatives et réglementaires en vigueur

Le protocole est en conformité avec les principes d'éthique établis par la 18ème Assemblée Médicale Mondiale (Helsinki 1964) et par les amendements établis lors des 29ème (Tokyo 1975), 35ème (Venise 1983), 41ème (Hong Kong 1989), 48ème (Somerset West 1996) et révisée lors

de la 52ème Assemblées Médicales Mondiales (Edinburg 2000) et qu'il sera conduit en conformité avec les recommandations ICH de Bonnes Pratiques Cliniques.

XIII.2. Protection des personnes

Ce protocole relève du cadre réglementaire de la Loi du 09 août 2004 du fait de la réalisation d'une imagerie supplémentaire. Le protocole sera soumis à l'avis du Comité de Protection des Personnes (CPP) Sud-Est I et de l'ASNM avant de débuter les inclusions. Une notice d'information sera explicitée et remise aux patients et leur consentement écrit obtenu.

XIII.3. Assurance

Le promoteur de l'étude, a contracté une police d'assurance en responsabilité civile sous le numéro 144.942.

XIII.4. Rapport Bénéfice/Risque

Bénéfices

Le bénéfice futur de l'étude est d'améliorer la performance diagnostique de certains diagnostics en dermatologie, comme celui des cancers cutanés, en limitant l'exérèse aux lésions le nécessitant et en limitant les délais associés au diagnostic anatomopathologique

Risques

Les risques identifiés sont ceux liés à l'utilisation du laser. Les mesures suivantes ont été prises afin de les mitiger :

- la limitation de la durée d'exposition (60 secondes maximum),
- les lasers ne seront par ailleurs allumés uniquement lorsque l'objectif sera parfaitement positionné en face de la zone à analyser, puis éteint immédiatement avant que l'objectif ne soit retiré de sa position : cette procédure reconnue minimise le risque de croiser l'axe optique du patient et du personnel.
- Pour les lésions situées sur le visage, les patients présentant des lésions situées à moisn de 3 cm des yeux seront exclus de la recherche. Pour les autres, le port de lunettes de protection, communément utilisées pour le traitement au laser, seront utilisées.

Ces deux risques seront signalés dans la notice d'utilisation et explicité aux patients lors de la visite d'inclusion. En cas de survenue, ils seront immédiatement pris en charge par l'équipe de dermatologie.

XXI. TRAITEMENT DES DONNEES ET CONSERVATION DES DOCUMENTS ET DES DONNEES RELATIVES A LA RECHERCHE

XIV.1. Circuit des données

Lors de leur recueil, les informations concernant les patients participant à cette étude seront anonymisées (identification par le monogramme et le n° d'inclusion) selon les recommandations établit par la CNIL dans la déclaration de conformité enregistrée sous le n°1167710 pour le CHU de Saint-Étienne.

La saisie des données sera réalisée, sous la responsabilité de l'investigateur, par un membre de son équipe (TEC, infirmière,…) sur un fichier Access ou Excel, hébergé sur le réseau du CHU, dans le domaine réservé au service concerné. Ce fichier sera protégé par un mot de passe d'au moins 8 caractères alpha-numériques. L'investigateur principal/coordonnateur s'engage à assurer la sauvegarde des données sur le réseau du CHU. Il est fortement conseillé de faire valider la grille de saisie préalablement par la personne en charge de l'analyse statistique.

XIV.2. Modalités de traitement, vérification et validation des données (data management)

Aucun contrôle des données n'est prévu au moment de la saisie. Le data-management sera réalisé avant l'analyse statistique de façon succincte et automatique pour les contrôles de bornes relatives (données à vérifier) et absolues (données aberrantes) et les données manquantes. Des demandes de correction seront établies par variable (avec la liste des patients).

En fonction du cahier des charges, une validation des données sera éventuellement réalisée pour l'analyse statistique, et des demandes de correction seront émises à l'investigateur ou à l'ARC de l'étude, qui s'engage à compéter et corriger les données en conséquence.

XIV.3. Archivage des documents de l'essai

A la fin de la recherche, l'ensemble des documents (différentes versions du protocole, cahiers d'observation, classeur investigateur, consentements, correspondances,…) figurant sur support papier seront archivés puis conservés, dans chaque centre, et chez le promoteur, durant 10 ans.

Une fois le rapport final de la recherche réalisé ou publié et, au maximum dans un délai de 5 ans après la fin de la recherche, les données figurant sur support informatique seront archivées sur CD/disque dur/clé USB et conservés pendant 15 ans dans une armoire fermée à clé du service concerné.

XXII. PROPRIETES DES DONNEES - PUBLICATIONS DES RESULTATS

Les données seront la propriété du promoteur. DAMAE Medical aura la possibilité d'avoir accès à ces données sous la responsabilité de l'investigateur coordonnateur.

L'étude devra donner lieu à une publication dans les meilleurs délais après la fin de l'étude, sous la responsabilité des investigateurs.

Le CHU de Saint-Etienne sera cité en tant que promoteur de l'étude.

XXIII. REFERENCES BIBLIOGRAPHIQUES

1. Gambichler T1, Jaedicke V, Terras S. Optical coherence tomography in dermatology: technical and clinical aspects. Arch Dermatol Res. 2011 Sep;303(7):457-73.
2. García-Hernández A, Roldán-Marín R, Iglesias-Garcia P, Malvehy J. In Vivo Noninvasive Imaging of Healthy Lower Lip Mucosa: A Correlation Study between High-Definition Optical Coherence Tomography, Reflectance Confocal Microscopy, and Histology. Dermatol Res Pract. 2013;2013:205256.
3. Alawi S. A., Kuck M., Wahrlich, C., Batz S., McKenzie G., Fluhr J. W., Lademann J. and Ulrich M. Optical coherence tomography for presurgical margin assessment of non-melanoma skin cancer – a practical approach. Experimental Dermatology. 2013 22: 547–551.

4. Kuck M., Strese H., Alawi S. A., Meinke M. C., Fluhr J. W., Burbach G. J., Krah M., Sterry W. and Lademann J. Evaluation of optical coherence tomography as a non-invasive diagnostic tool in cutaneous wound healing. Skin Research and Technology. 2014 20: 1–7.
5. Banzhaf CA, Themstrup L, Ring HC, Mogensen M, Jemec GB. Optical coherence tomography imaging of non-melanoma skin cancer undergoing imiquimod therapy. Skin Res Technol. 2014 May;20(2):170-6.
6. Hamed NS, Khachemoune A. Microcystic adnexal carcinoma: A focused review and updates. Journal of Dermatology & Dermatologic Surgery 04/2015; 33.
7. Ring H.C., Mogensen M., Hussain A.A., Steadman N., Banzhaf C., Themstrup L. and Jemec G.B. Imaging of collagen deposition disorders using optical coherence tomography. Journal of the European Academy of Dermatology and Venereology. 2015 29: 890–898.
8. Alawi S. A., Batz S., Röwert-Huber J., Fluhr J. W., Lademann J. and Ulrich M. Correlation of optical coherence tomography and histology in microcystic adnexal carcinoma: a case report. Skin Research and Technology, 2015 21: 15–17.
9. Wahrlich C., Alawi S.A., Batz S., Fluhr J.W., Lademann J. and Ulrich M. Assessment of a scoring system for Basal Cell Carcinoma with multi-beam optical coherence tomography. Journal of the European Academy of Dermatology and Venereology, 2015 29: 1562–1569.
10. Ulrich M, von Braunmuehl T, Kurzen H, Dirschka T,Kellner C, Sattler E, Berking C, Welzel J , Reinhold U. The sensitivity and specificity of optical coherence tomography for the assisted diagnosis of nonpigmented basal cell carcinoma: an observational study. Br J Dermatol. 2015 Aug;173(2):428-35.

XXIV. ANNEXES

Annexe 1: Tableau récapitulatif des caractéristiques techniques du dispositif médical Galaxy.

données techniques	OCT Galaxy
Dimensions	310 x 360 x 700 mm
Poids	20 kg
Manipulation	Microscope
Orientation	Verticale /Horizontale
T° de fonctionnement	[10-40]°C
T° de stockage	[0-50]°C
Alimentation	230V, [50-60] Hz, 3A
Format des images	IMG, JPEG
Logiciel	GalaxySoft
Écran d'affichage	1920x1080 px - VGA
Type de section	Verticale
Résolution axiale	2 µm
Résolution latérale	2 µm
Champ (FOV) axial	3 mm
Champ (FOV) latéral	1,5 mm
Pénétration optique	800 µm
Fréquence d'acquisition	5 Hz
Source	Laser Supercontinuum
Longueur d'onde centrale	800 nm
Puissance de sortie	40 mW

Annexe 2 : Notice d’utilisation du dispositif médical

1. **Identification du fabricant du dispositif médical Galaxy : Damae Medical, Paris, France**

2. **Destination prévue et exigences environnementales d’installation du dispositif médical**
Le dispositif médical sera installé sur une table dans la salle de consultation du Dr. Jean-Luc Perrot, investigateur-coordinateur de l’étude, ou dans la salle du service de dermatologie dédiée aux tests d’imagerie non-invasive. De manière générale, le dispositif sera utilisé et stocké dans une salle du service, dans des conditions de température, de pression et d’humidité liées à son utilisation normale.

3. **Instructions de démarrage et d’utilisation du dispositif médical**
Afin de démarrer l’appareil, brancher l’alimentation du dispositif sur une prise secteur (230V, 50Hz). Le mettre sous tension en actionnant le premier interrupteur situé sur le bloc d’alimentation. L’allumer en actionnant le deuxième interrupteur situé en façade du dispositif médical.

Choisir l’orientation (verticale ou horizontale) du bloc optique en fonction de l’objet biologique à étudier. Pour l’analyse d’une lésion sur un patient assis ou debout face à l’appareil, le basculer en position horizontale. Pour cela, commencer par positionner le bloc en position haute verticale en déverrouillant la poignée de serrage située en haut à gauche de l’appareil, comme illustré ci-après :

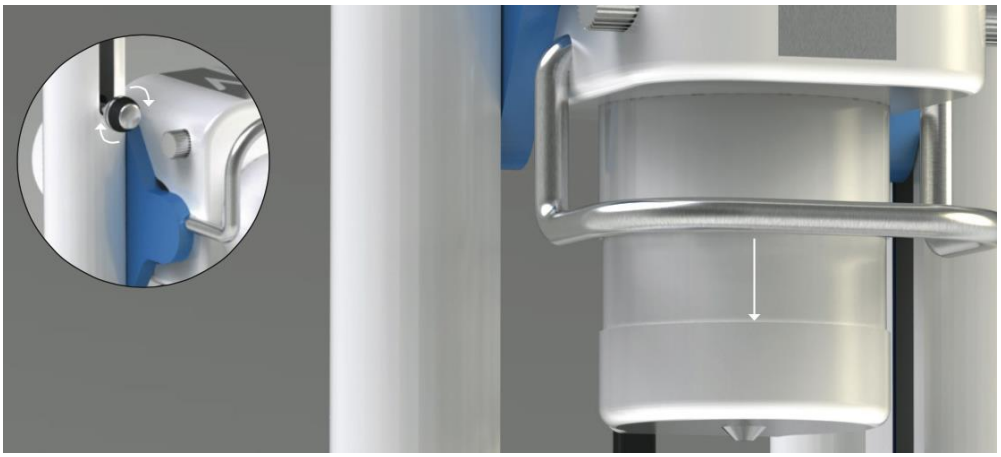

Une fois en position haute, déverrouiller la tirette de bascule manuelle située sur le côté droit de l’appareil, comme illustré ci-après :

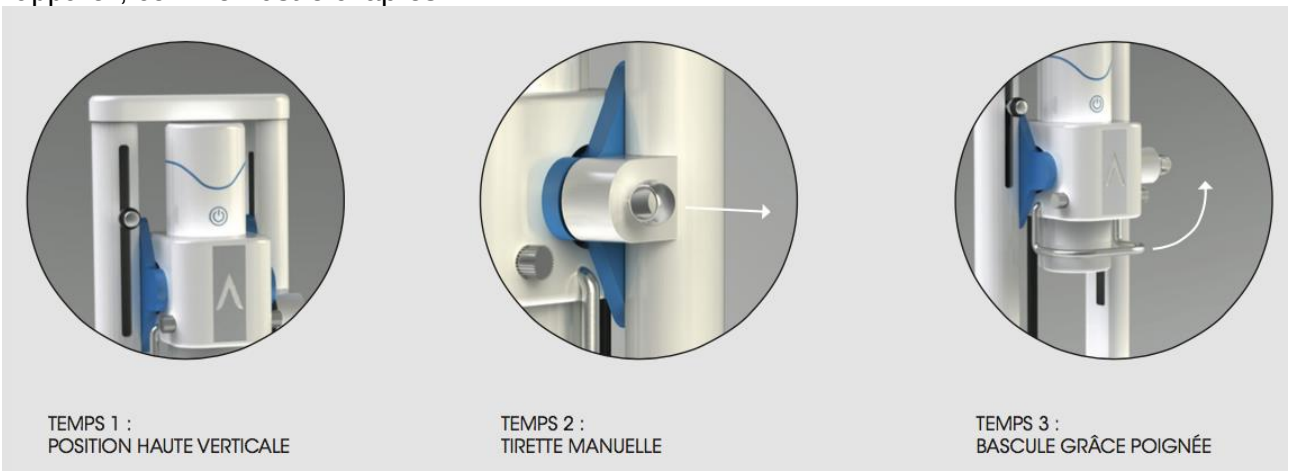

Ajuster la hauteur du bloc optique en fonction de la localisation de la lésion et de la position du patient en déverrouillant à nouveau la poignée de serrage.

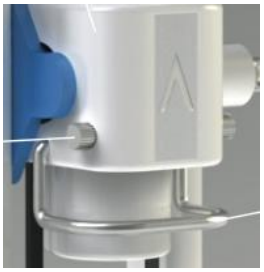

Afin d'effectuer la mesure, une huile d'immersion est préalablement appliquée sur la zone de peau à imager. Ce liquide permet d'assurer la continuité des indices optiques traversés par la lumière.
L'extrémité de la tête de mesure est constituée d'une fine lame de verre qu'il faut venir positionner au contact de la lésion. Pour cela, utiliser les molettes de réglage fin situées sur le bloc optique, et illustrées ci-contre.

Ce point de contact avec le patient devra être nettoyé entre chaque nouveau patient selon **la procédure de nettoyage** définie dans **la notice d'utilisation du dispositif (Annexe 1)**.
A la fin de l'utilisation, remettre le cache de protection de la tête de mesure.

4. **Contre-indications, avertissements et risques possibles :**
Avant toute utilisation, le processus d'installation du dispositif médical comme décrit dans la notice aura été mis en œuvre.
La tête de mesure devra être nettoyée avant chaque utilisation pour éviter toute contamination du patient comme du personnel.
L'expérimentateur prendra soin de ne pas placer l'œil du patient ou le sien dans l'axe de mesure pour éviter de recevoir un rayonnement lumineux involontaire dans les yeux.

5. **Formation et expérience nécessaires à l'utilisation du dispositif médical**
La formation à l'utilisation du dispositif médical est rapide et intuitive, Galaxy requiert peu d'expérience pour correctement maîtriser son utilisation.

6. **Description et justification des modalités d'utilisation de Galaxy de DAMAE Medical**
Le dispositif Galaxy est piloté par son logiciel GalaxySoft, qui permet l'authentification de l'expérimentateur, l'identification du patient et de la lésion à étudier, de lancer la mesure, d'enregistrer, de sélectionner et de sauvegarder les images d'intérêt, et de gérer la base de données patient.
Une fois le dispositif installé et mis en place, lancer le logiciel sur l'ordinateur. Afin de réaliser une analyse, suivre la procédure décrite ci-après :

1. Une première fenêtre d'authentification apparaît : identifier le centre d'investigation et rentrer le mot de passe commun au service, préalablement délivré par DAMAE Medical.
2. L'expérimentateur doit ensuite s'identifier en se sélectionnant dans la liste des utilisateurs déjà enregistrés ou en rentrant son prénom et son nom si c'est la première fois.
3. Rentrer toutes les informations sur le patient dont on veut étudier une lésion ou le choisir dans la liste des patients déjà enregistrés si une de ses lésions a déjà été étudiée.
4. Rentrer toutes les informations de description de l'anomalie à étudier ou la sélectionner dans la liste des anomalies déjà enregistrées si celle-ci a déjà fait l'objet d'une analyse.
5. La fenêtre d'acquisition s'ouvre alors :

a. Ajuster la molette de réglage fin du dispositif pour bien centrer l'image tomographique sur l'écran de visualisation. L'image s'actualise 5 fois par seconde pour assurer une visualisation confortable de la lésion et pour suivre en temps réel les déplacements du tissu sous l'appareil.
b. Les paramètres de configuration de l'acquisition se situent à gauche de l'écran.
c. Les actions de lancement de la mesure et d'enregistrement d'images et de vidéos se situent au-dessus de l'image tomographique.
d. L'image macroscopique de visualisation de la zone de mesure se situe en haut à gauche de l'écran.

e. Les différentes acquisitions successives viennent s'afficher en miniature à droite de l'écran. En plaçant le curseur de la souris dessus, ces miniatures s'agrandissent pour permettre à l'expérimentateur de re-visualiser ses précédentes acquisitions.
f. Cliquer sur « Terminer l'acquisition » lorsque les images enregistrées sont suffisantes pour l'analyse.
6. La fenêtre suivante présente toutes les acquisitions et permet à l'expérimentateur de sélectionner celles qui l'intéressent pour son diagnostic.
7. Les images sélectionnées seront copiées dans un rapport d'analyse généré automatiquement, sur lequel l'expérimentateur pourra ajouter les images d'histologie et les images prises avec les dispositifs concurrents, pour comparaison. Il pourra également ajouter des sur les images.

Les images, les données du patient et les rapports d'analyse sont enregistrés par défaut sur le disque dur de l'ordinateur du dispositif. L'expérimentateur pourra les copier sur le serveur de l'hôpital si nécessaire.

Annexe 3 : Revue des produits concurrents mis sur le marché

VivaScope; VivaScope 1500; VivaScope 3000; VivaScope System : Le système VivaScope® produit des images de haute résolution de la peau en utilisant la microscopie confocale à balayage laser. La principale caractéristique de la microscopie confocale est la capacité de produire des images de mise au point de « sectionnement optique ». Le système est capable d'accomplir des images, l'affichage, stocker, récupérer, importation et l'exportation dans confocale in vivo et des images en couleur macroscopiques en utilisant le logiciel d'exploitation et de soutien VivaScan® matériel PC. Les images sont enregistrées et stockées en utilisant des algorithmes de compression d'image sans perte standard. Les images sont communiquées aux autres appareils via la fonctionnalité standard DICOM qui est intégré dans le logiciel d'exploitation VivaScan®. Le système VivaScope® est composé de quatre principaux composants fonctionnels : un imageur, un écran, un PC et un panier. Un système VivaScope® aura soit une tête VivaScope® de bras monté d'imagerie ou d'un VivaScope® tête d'imagerie portable, ou les deux, et, éventuellement, un VivaCam® couleur tête d'imagerie macroscopique.

VivoSight™ Topical OCT system : est un système d'imagerie optique, une tomographie par cohérence (OCT) qui fournit aux cliniciens un outil unique, non-invasif pour diagnostiquer une variété de pathologies de la peau. VivoSight utilise la lumière pour fournir des images en continu et précis de la sous-surface de la peau qui peut être facilement interprété par un clinicien pour faciliter le diagnostic et le traitement des conseils. Les dermatologues peuvent utiliser VivoSight ™ pour visualiser le sous-sol de la peau, et peuvent utiliser cette vue d'aider dans leur évaluation d'un patient. Un VivoSight ™ balayage OCT est totalement non invasif et indolore pour le patient et l'utilisation de routine du système peut facilement être intégré dans les processus cliniques. Le VivoSight ™ topique PTOM système est indiqué pour une utilisation dans les deux dimensions en coupe transversale, l'imagerie en temps réel des tissus externes du corps humain. Cette utilisation indiquée permet l'imagerie de la microstructure des tissus, y compris la peau, afin d'aider les cliniciens formés et compétents dans leur évaluation des conditions cliniques du patient. VivoSight a la marque CE en Europe et TGA-jeu réglementaire en Australie pour une utilisation dans le diagnostic des cancers de la peau non-mélanome (CNSM). Compte tenu de la résolution et de l'image de qualité d'image sans précédent, VivoSight a de nombreuses applications cliniques potentielles au-delà du foyer initial en dermatologie. VivoSight est actuellement vendu en Allemagne, où les analyses sont remboursées pour les patients ayant une assurance de soins de santé privé. D'autres études cliniques sont actuellement menées dans les centres de premier plan dans les Etats-Unis, où VivoSight a actuellement au nombre de 510 (k) de la clairance K093520. La loi fédérale américaine limite la vente de cet appareil par ou sur l'ordre d'un médecin. Le système topique octobre VivoSight ™ n’est pas actuellement autorisé à la vente au Canada.

Agfa HealthCare’s SKINTELL : est un moyen non invasif pour visualiser la morphologie de la peau, potentiellement sans biopsie, et de mesurer les dimensions dans les couches de la peau, fournissant des informations auparavant uniquement disponibles par biopsie. Rayonnement infrarouge (1300 nm), avec une profondeur de 1 mm de pénétration.

Annexe 5: Formulaire de consentement éclairé

Formulaire d'information et de Consentement Eclairé

Ce formulaire d'information sera signé en trois exemplaires :

- un exemplaire sera remis au patient,
- un exemplaire sera conservé par l'investigateur
-

INFORMATIONS ET RECOMMANDATIONS CONCERNANT L'ESSAI

Innovation en imagerie in vivo : Microscopie par Cohérence Optique en Dermato-oncologie

Protocole Numéro : xxx

Numéro d'enregistrement ANSM : xxx

PROMOTEUR Chu de Saint-Etienne.

INVESTIGATEUR PRINCIPAL

Xxx

N° de téléphone

Madame, Monsieur,

Votre médecin vous propose de participer à un essai clinique. Votre participation à cet essai doit être entièrement volontaire. Prenez le temps de lire cette fiche d'information et discutez-en avec votre médecin et vos proches, si vous le souhaitez. N'hésitez pas à poser des questions à votre médecin si vous souhaitez obtenir davantage d'informations quant à cet essai clinique. Si vous acceptez de participer, vous demeurez libre de revenir sur votre accord à tout moment, sans avoir à le justifier. Cette décision serait alors sans conséquences sur les relations que vous avez avec votre médecin et avec l'équipe soignante, ou sur la qualité des soins que vous recevrez. Cette fiche d'information et de consentement patient décrit les procédures concernées par cet essai, les risques éventuels et les bénéfices possibles de votre participation à celui-ci, ainsi que les précautions prises pour assurer la confidentialité de vos données.

Si vous décidez de participer à cet essai, il vous sera demandé de signer ce document.

BUT DE L'ETUDE

Le but de cet essai est d'évaluer l'intérêt et l'efficacité d'une nouvelle méthode de diagnostic, appelée Microscopie confocale.

Ce nouveau dispositif médical ne dispose pas encore du marquage CE, mais a été testé sur X patients. Ce nouveau dispositif permet d'obtenir des images très précises des structures internes de la peau, de manière immédiate et sans prélèvement, en le plaçant directement au contact de la peau.

EN QUOI CONSISTE CET ESSAI ?

Il vous a été proposé de participer à cette étude, en raison de la présence d'une lésion cutanée identifiée sur votre peau. Votre médecin souhaite évaluer plus précisément la nature de cette lésion et vous a recommandé une biopsie ou exérèse (prélèvement d'une lésion, dont le tissu sera analysé de la même façon qu'une biopsie). Quelque soit votre décision de participer ou non à cette étude, ce prélèvement sera effectué. Si vous décidez de participer à cet essai, un examen complémentaire de la lésion sera réalisé à l'aide du nouveau dispositif testé, préalablement au prélèvement. Cet examen se déroulera en placant le microscope directement au contact de la peau. Cela ne dure que quelques minutes (entre 3 et 5) , est sans douleur, et ne nécessite pas de prélèvement supplémentaire.

PRECAUTIONS ET CONTRAINTES PARTICULIERES LIEES A LA REALISATION DE L'ETUDE

- Vous devez vous engager à ne pas participer à une autre étude sans bénéfice individuel direct pendant la durée de la présente étude.
- Si vous consultez votre Médecin traitant durant la période de l'essai, nous vous demandons de lui signaler votre participation à cette étude.

RISQUES ET BENEFICES

- **Risques**

Pas d'autres risques que ceux associés la biopsie ou l'exérèse habituellement réalisée dans le cadre du diagnostic des lésions cutanées

- **Bénéfices**

Si vous acceptez de participer à cet essai, il est possible qu'il y ait des bénéfices pour vous. Nous espérons que les informations collectées grâce à cette procédure permettront d'améliorer le diagnostic de certaines lésions cutanées et d'en optimiser la prise en charge. Par ailleurs, nous espérons également que les informations obtenues dans cet essai bénéficierons aux futurs patients atteints de ces mêmes lésions.

NOMBRE DE PATIENTS

Environ 200 patients seront inclus dans cet essai. Tous seront recrutés au CHU de Saint-Etienne.

INFORMATIONS CONFIDENTIELLES VOUS CONCERNANT :

Dans le cadre de la recherche biomédicale à laquelle le Dr. xxx vous propose de participer, un traitement de vos données personnelles va être mis en œuvre pour permettre d'analyser les résultats de la recherche au regard de l'objectif qui vous a été présenté.

A cette fin, les données médicales vous concernant pourront être transmises au Promoteur de la recherche ou aux personnes ou sociétés agissant pour son compte, en France ou à l'étranger. Ces données seront anonymisées et identifiées par un numéro de code et/ou vos initiales ou les

trois premières lettres de votre nom. Ces données pourront également, dans des conditions assurant leur confidentialité, être transmises aux autorités de santé françaises ou étrangères.

Conformément aux dispositions de loi relative à l'informatique aux fichiers et aux libertés, vous disposez d'un droit d'accès et de rectification. Vous disposez également d'un droit d'opposition à la transmission des données couvertes par le secret professionnel susceptibles d'être utilisées dans le cadre de cette recherche et d'être traitées.

Vous pouvez également accéder directement ou par l'intermédiaire d'un médecin de votre choix à l'ensemble de vos données médicales en application des dispositions de l'article L 1111-7 du Code de la Santé Publique.
Ces droits s'exercent auprès du médecin qui vous suit dans le cadre de la recherche et qui connaît votre identité.

INFORMATION AU TERME DE L'ETUDE:

Vous avez le droit d'être informé des résultats globaux de la recherche une fois que celle-ci sera achevée, conformément à la loi 2004-806 du 9 août 2004 relative à la politique de santé publique.

Ce formulaire d'information sera signé en trois exemplaires :

-un exemplaire sera remis au patient,

-un exemplaire sera conservé par l'investigateur

-

CONSENTEMENT

Innovation en imagerie in vivo : Microscopie par Cohérence Optique en Dermato-oncologie

Protocole Numéro : xxxx

Par le présent consentement, j'atteste que :

1. J'ai reçu une explication détaillée sur la nature, les buts, la méthodologie, les modalités pratiques et la durée de cet essai et ce qu'il est attendu de ma part. Le médecin investigateur ou l'un de ses collaborateurs m'a expliqué les possibles effets indésirables sur ma santé et mon bien-être. J'ai reçu une réponse satisfaisante à toutes les questions que j'ai pu poser librement à propos de l'étude.

2. Je suis parfaitement conscient(e) que l'essai auquel je participerai est purement expérimental et que je ne peux en attendre aucun bénéfice direct pour ma santé.

3. J'accepte de respecter fidèlement les consignes du protocole et de coopérer avec l'équipe médicale du centre _____. A cet effet, je signalerai immédiatement à un membre de l'équipe médicale du centre _____si je ressens un quelconque trouble prévu, imprévu ou inhabituel.

4. J'accepte de participer librement à cet essai. Je sais que je peux interrompre à tout moment cette participation sans encourir de responsabilité, en fournissant cependant les éléments de ma décision, ceci dans mon propre intérêt.

J'ai également été informé(e) que l'essai pourrait être interrompu à tout moment sur décision de l'investigateur ou du promoteur.

Si le médecin estime que mon état de santé nécessite des examens complémentaires, du fait d'effets secondaires, j'accepterai de les subir.

Si je ne respectais pas pendant toute la durée de l'essai les termes du protocole dont j'ai été informé(e), ma participation serait immédiatement suspendue.

5. Mon consentement ne dégage pas les organisateurs de cette étude de leurs responsabilités. Je conserve tous mes droits légaux.

6. J'accepte la transmission des données me concernant, dans des conditions assurant leur confidentialité, aux autorités de santé françaises ou étrangères,

7. J'accepte que les données enregistrées à l'occasion de cet essai puissent faire l'objet d'un traitement informatisé par le promoteur ou par les personnes ou sociétés agissant pour son compte, en France ou à l'étranger. J'ai bien noté que, conformément aux dispositions de la loi relative à l'informatique aux fichiers et aux libertés, je dispose d'un droit d'accès et de rectification. Je dispose également d'un droit d'opposition à la transmission des données couvertes par le secret professionnel susceptibles d'être utilisées dans le cadre de la présente recherche et d'être traitées.

J'accepte que, pour le besoin de l'étude, le Promoteur et/ou des Autorités de Santé en collaboration avec le médecin puissent accéder directement aux documents médicaux me concernant, pour vérifier les procédures cliniques et/ou les données, sans violation de la confidentialité.

8. Toute nouvelle information importante concernant le produit étudié, qui pourrait modifier mon consentement à participer à l'essai, me sera communiquée.

9. Je m'engage à ne pas communiquer, dans les limites fixées par les dispositions du code de la santé publique, les informations, connaissances, documents, données quels qu'en soient la forme, la nature et le support, notamment, le contenu et déroulement de cette étude, les activités, méthodes, savoir-faire, modèles, procédures, secrets scientifiques, techniques et commerciaux, dénominations du centre _____.

Je m'engage à ne pas user (ni publier, ni divulguer) de quelque façon que ce soit, les activités et toute autre information possédées ou détenues par le centre _____, l'objet, le déroulement, et les résultats de cette étude, dans les limites fixées par le code de la santé publique .

La présente obligation de confidentialité subsistera, nonobstant l'expiration de cette étude pour quelle que cause que ce soit, tant que les informations relatives ne seront pas tombées dans le domaine public.

10. Je m'engage à ne pas divulguer à un tiers les renseignements confidentiels qui m'ont été communiqués sur le produit, ni les résultats ou effets constatés sur moi-même ou sur les autres, consécutifs à l'administration du produit.
Afin que les réactions rapportées restent aussi indépendantes que possible les unes des autres, je ne discuterai pas d'un effet indésirable éventuel avec les autres participants à l'étude

11. J'ai été informé(e) que le protocole de cet essai a été soumis à l'avis du Comité de

Protection des Personnes (C.P.P.) de Sud Est France 1, qui a donné un avis favorable en date du dd/mm/yyyy.

12. J'ai été informé(e) que le protocole de cet essai a été soumis à l'ANSM (Agence Nationale de Sécurité du Médicament), qui a donné une autorisation en date du dd/mm/yyyy.

13. J'ai été informé(e) que cet essai est couvert par le contrat d'assurance responsabilité civile de xxx souscrit auprès de la compagnie XXX me couvrant en cas d'accident conformément à la loi 2004-806 du 9 août 2004 relative à la politique de santé publique.

14. Je certifie être affilié(e) à un régime de Sécurité Sociale. Je certifie également ne pas être privé(e) de liberté par une décision judiciaire ou administrative et ne pas être placé(e) sous un régime de protection légale.

15. Si j'ai des questions à propos de l'essai, la survenue d'un préjudice dû à l'étude ou sur mes droits en tant que Patient, je n'hésiterai pas à contacter l'investigateur, le Dr _____. Tel _____.

16. Je confirme qu'un exemplaire de ce document m'a été remis. Je signe ce formulaire de consentement en ayant reçu, lu et parfaitement compris les informations et recommandations concernant l'essai

17. Le médecin investigateur ou son représentant confirme avoir pleinement expliqué au patient nommé ci-après la nature, les procédures, ainsi que les risques éventuels liés à cette étude. Il confirme que le patient a reçu la fiche d'information, en a pris connaissance et a accepté librement de participer à l'étude.

NOM - PRENOM DU PATIENT	***NOM DU MEDECIN INVESTIGATEUR***
Date :	***Date*** *:*
Signature*:*	***Signature*** *:*

E. Demandes d’ANR soumises en octobre 2016

1.Molecular-contrast LC-OCT for enhanced skin cancer diagnosis

Il s'agit d'un projet qui poursuit la collaboration initiée il y a 18 mois avec l'institut supérieur d'optique de Palaiseau visant à intégrer dans un appareil d'OCT in vivo (le successeur à l'appareil décrit dans l'étude du chapitre précédent (chapitre C) un spectromètre Raman afin de pouvoir caractériser chimiquement de manière optique les structures vues en OCT. Ce projet est en accord avec l'objectif prioritaire du CHU de St-Etienne et confié au service de dermatologie à savoir l'intégration d'un spectromètre Raman dans un dispositif d'imagerie microscopique de la peau

Ce projet s'intègre dans l'AAPG ANR 2017 Défi 4 PRCE

Molecular-contrast LC-OCT for enhanced skin cancer diagnosis

Context, positioning and objectives

Skin cancer is the most common form of all human cancers. Recent studies show the number of skin cancer cases growing at an alarming rate. In addition to causing illness and death, skin cancer is a huge economic burden. Early detection seems to be the most promising way to reduce morbidity and mortality. The standard of care procedure consists in a clinical and dermoscopic evaluation of skin lesions followed by biopsies. Nearly 60% of all skin biopsies result in benign diagnoses [1]. Given this challenge, improved diagnostic modalities have been developed to provide earlier, more accurate detection of suspicious lesions, decreasing the false positive rates of dermoscopy and unnecessary biopsies. Non-invasive imaging techniques, including **Confocal Microscopy** (CM) and **Optical Coherence Tomography** (OCT) are increasingly being used in dermatology. These techniques are attractive because they enable real-time, in vivo imaging of suspicious lesions. CM provides the highest spatial resolution (~ 1 µm) enabling cellular-level resolution imaging. Unfortunately, the penetration in the depth of skin tissue is limited to the most superficial skin layers (~ 200 µm), while most lesions develop underneath. Moreover, the CM images are en face tomographic views - whereas histology images are vertically oriented sections - which makes their interpretation difficult. OCT utilizes reflected light to produce vertically oriented tomographic images of tissue at a higher resolution than ultrasound imaging, with a penetration of ~ 1 mm. The spatial resolution of OCT, between 3 and 15 µm depending on the OCT device, is however not high enough for cellular-level imaging. The main commercially available CM and OCT devices for dermatology are presented in appendix.

A. Dubois (coordinator of the project) has invented an imaging technique (patented), termed **Line-field Confocal Optical Coherence Tomography (LC-OCT).** Combining confocal microscopy and OCT, LC-OCT merges the advantages of both technologies, i.e. a high spatial resolution (~ 1 µm, isotropic) and a penetration of ~ 1 mm in skin tissue. The images correspond to vertically oriented sections and are produced in real-time (15 Hz). Compared to all other non-invasive imaging technologies, LC-OCT provides images that are the closest to histological images. The technique is based on line illumination and detection using a broadband spatially coherent light source and a line-scan camera in a two-beam interference microscope. It has been developed by the startup company **DAMAE Medical** (partner 2 of this project), leading to OCTAV®, a prototype device for research applications. Images of skin lesions generated by OCTAV® have been positively - even enthusiastically - received by opinion leader dermatologists met in France, Germany, USA and Australia. A portable version of the technology (OLIV®) is currently in development.

The image contrast in LC-OCT (as in OCT) arises from variations in the tissue refractive index. In most cases, there is little change in the refractive index in distinct areas of soft tissues. In order to target specific molecules or receptors, providing detailed information on the local biochemistry at high spatial resolution, “molecular-imaging” approaches based on fluorescence emission and Raman scattering have been implemented in CM. Several studies have reported the relevance of **fluorescence imaging / spectroscopy** and **Raman spectroscopy (RS)** for in vivo detection of cancers in various organs including skin [2-8].

Since it relies on coherent detection of photons, OCT inherently lacks the incoherent functional molecular imaging capability of CM. A few attempts to couple OCT with fluorescence imaging and Raman spectroscopy have been reported [9-11]. Because LC-OCT is the combination of CM and OCT, it can operate in CM mode, thus enabling a straightforward implementation of fluorescence imaging and Raman spectroscopy. The implementation of these two modalities in LC-OCT is the core of this project. They will operate with LC-OCT almost simultaneously using the same microscope objective. Furthermore, the development of two other spectroscopic extensions of LC-OCT are also proposed to provide spectroscopic-based contrasts to the conventional morphological images generated by LC-OCT.

Fluorescence / LC-OCT. The CM imaging modality of LC-OCT will be adapted to operate in fluorescence mode (imaging and spectroscopy) by using dichroic optical components and additional laser source(s)

emitting at appropriate wavelengths for the fluorescence excitation. The axial resolution of the fluorescence images (determined by the depth of field of the microscope objective) and the accessible depth in tissue will be lower compared to LC-OCT images. Nevertheless, high-resolution morphological information provided by LC-OCT will benefit from molecular specific contrasts (at 5-50 µm axial resolution and moderate depth) given by fluorescence that will be superimposed using color encoding. Exogenous fluorophores will be tested for in vivo skin imaging such as Fluorescein, Methylene blue, Patent blue and Fluorocoxib A [4,5]. Autofluorescence of skin tissues due to the presence of endogenous fluorophores such as collagen, elastin, keratin and flavin will also be investigated for image contrast enhancement (despite low specificity). Moreover, non-linear (2-photon) fluorescence excitation (for higher penetration in tissue) will be compared to linear excitation using a Ti-Sapphire femtosecond laser available in our laboratory (LCF).

Raman / LC-OCT. The LC-OCT setup will be modified to incorporate a Raman confocal microscope**.** The very weak nature of spontaneous Raman scattering requires detection times of a few seconds typically [9], limiting the technique to point measurements. LC-OCT will provide high-resolution morphological overview images to define suspicious regions, which will be afterwards characterized in more detail on a molecular level by means of Raman spectroscopy. Compared to Raman CM alone, LC-OCT will provide images with significantly improved axial resolution in vertically-oriented view and increased imaging depth (compared to CM). Although the Raman measurements will be performed with a relatively weak axial resolution (5-50 µm, depending on the microscope objective employed), they should be useful for better identification of suspicious skin regions detected by LC-OCT and for their transverse localization.

Spectroscopic LC-OCT. Spectroscopic measurement methods will be implemented in LC-OCT to enhance image contrast and facilitate the characterization of the tissue, through its spectroscopic properties or functional state. One approach will consist in acquiring images in different bands (centered at 600, 850 and 1300nm typically), simultaneously, using the supercontinuum laser source of LC-OCT and several line-scan cameras. Another approach will consist in processing the interferometric LC-OCT signal using windowed Fourier transform analysis. These methods will enable the differentiation of biological structures through their wavelength-dependent scattering properties and their absorption spectra. The results may be enhanced by using exogenous absorption or scattering based contrast agents. Both spectroscopic approaches have already been validated in conventional OCT [12, 13] and by A. Dubois in full-field OCT (not applicable to in vivo imaging) [14, 15].

Organization of the project and means implemented

The project will be carried out by a consortium of 3 members: The Charles Fabry Laboratory (LCF), the company DAMAE Medical and the University Hospital (CHU) of St-Étienne. LCF and DAMAE Medical have already been working in close collaboration for 3 years for the development of the LC-OCT technology. A collaboration between DAMAE Medical and St-Etienne Hospital started 1 year ago for testing a LC-OCT prototype on excised human skin samples. Clinical trials on human patients for skin cancer characterization using LC-OCT will start in November 2016 in St-Etienne hospital.

- **Arnaud Dubois** at **LCF** (Institute of Optics, Palaiseau) will be the **scientific coordinator** of the project. He will bring the benefits of leading-edge research in the field of OCT, carried out over 20 years. He has published over 100 research articles and has edited in 2016 the first review book on FF-OCT. A. Dubois is the inventor of LC-OCT (patent WO2015092019A1, 2013, exclusively licensed to DAMAE Medical).

- **DAMAE Medical** is a French startup founded in Sept. 2014 by Arnaud Dubois and 2 entrepreneurs: Anaïs Barut (CEO, HEC Paris) and David Siret (CTO, Institut d'Optique Graduate School). DAMAE develops state-of-the-art optical imaging devices for medical applications. The company aims at bringing those innovations to the medical imaging market, by paving the way for technical and industrial developments, clinical validation and market-regulatory approvals. 12 people are currently working at DAMAE.

- The **dermatology department of St-Étienne CHU** (J.L. Perrot, B. Labeille, E. Cinotti) has acquired a strong experience in skin imaging. It is the only French dermatology department, and one of the rare in Europe, to perform *in vivo* and *ex vivo* clinical examinations using confocal microscopy, OCT and Raman spectroscopy. The department has more than 50 publications in this field. It is involved in collaborations with European (Italy, Spain) and Australian (Sydney) research teams.

- 3 external collaborators (not financed by ANR) will be involved in the project as expert in Raman Microscopy (A. Tfayli & A. Baillet-Guffroy, Lab. Chimie Analytique, Faculté de Pharmacie U-PSud / M. Manfait, Université de Reims) and in Fluorescence Imaging (S. Lévèque-Fort & S. Lécart, Centre de Photonique Biomédicale, U-PSud).

The duration of the project is **36 months**. A total budget of approximately **300 k€** is envisaged.

Impact and outcomes of the project

Early non-invasive detection of all types of skin cancer – melanoma and non-melanoma cancers (NMSC) – is not achieved with today's performance-limited methods (dermoscopy, ultrasound, CM, OCT, IRM).

Whereas melanoma diagnosis requires cellular resolution imaging, NMSC evaluation needs an access to the tumor depth. Additionally, the complex, pathological mechanisms of disease progression requires a comprehensive analysis of the molecular composition of the lesion.

By combining CM and OCT, LC-OCT bridges the gap between cellular resolution and depth of imaging. The addition of fluorescence and spectroscopic measurements to the morphological information provided by LC-OCT gives the ability to perform disease classification based on the molecular composition of skin lesions, and thus incrementally improve the diagnostic accuracy of the technique. The information provided by the analysis if the molecular signature of the lesion represents an objective tool that is not based on a visual method, thus overpassing the limitations associated with individual interpretation. **Combining high spatial resolution (1 μm, isotropic), deep penetration (~ 1 mm) and molecular contrast in a single device would revolutionize skin cancer diagnosis**. This is the aim of the present project. The objective is to deliver unmatched diagnostic performances with an accuracy > 90% at a competitive cost (< 120k€).

Based on this objective and health-economic estimations, the project is expected to **significantly improve skin cancer management** and hold the promise of **reducing lifetime healthcare costs**.

- With the developed technology, medical doctors will gain an objective aid that can help them detect malignant skin cancer at an earlier stage, which leads to more skin cancer being detected in time.
- At the same time, the instrument can help exclude benign lesions and thereby reduce the number of unnecessary operations. In France about 200,000 nevi (moles) are surgically removed every year, of which 60% could have been avoided, at a cost of more than 142€ per procedure. With the help of our technology, healthcare in France could reduce these operations by more than 50%, which can potentially lead to reduced costs for removing suspected lesions of approximately 14€ million per year.
- In Europe, there is also a considerable shortage of pathologists, who analyze removed lesions. With fewer operations, the wait will accordingly be shorter, which means less worry and more effective care processes, which benefits the patients. Of course, earlier detection of malignant lesions also means that the chance to cure the cancer increases considerably.

All partners will undertake the dissemination of the project outcomes. A communication campaign including the technology-related scientific publications during and after the project will be implemented in anticipation of the short-term marketing of the innovation. Additionally, the clinical evidence will be made stronger with the implementation of an international multicentric clinical trial at leading centers, starting at the end of the project. The technology itself will be reported in international journals serving

the biomedical optics community such as "Biomedical Optics Express" (OSA) and "J. Biomedical Optics" (SPIE). The work will be presented at international conferences including BiOS Photonics west (SPIE) - the largest Biomedical Optics & Photonics international Conference (San Francisco, annually) - and OSA Biomedical Optics (BIOMED, Florida). Clinical results will be disseminated in medical publications such as "J. of Investigative Dermatology", "J. Am. Acad. Dermatol.", "Br. J. Dermatol.", etc. Presentations will be made to the medical community in special events such as "Journées dermatologiques de Paris" and "European Academy of Dermatology".

The LC-OCT technology is **protected by a patent** (filed in Dec. 2013 and extended (PCT) in Dec. 2014) owned by the CNRS. DAMAE Medical benefits from an exclusive license ensuring the full exploitation of the patent for all types of domains, in every country and with no limitation of time. The contract also allows full sub-licensing rights. The future results obtained during this project will be protected through **further patents**. The ownership of the knowledge created during the project will be the property of the partner generating that foreground. Where the partners have jointly carried out project tasks generating foreground, they will have joint in proportion to their respective share of the work undertaken. Where the respective share cannot be ascertained, they will have equal joint ownership of the new knowledge.

2. Système optique multimodal haute résolution et spectroscopique pour l'analyse de la peau appliquée aux tumeurs cutanées

Il s'agit d'un projet s'intègre dans le cadre d'une collaboration initiée il Ya 18 mois avec le CEA-LETI de Grenoble concernant différents domaines de l'imagerie dermatologique à des stades de maturités divers, dont un en collaboration avec un industriel de la dermato-cosmétique, confidentiel et particulièrement ambitieux tant sur le plan industriel que scientifique. Ce projet soumis à l'ANR porte sur l'intérêt d'un système d'analyse multi spectrale haute définition pour l'identification des tumeurs cutanées et de caractériser leur localisation uniquement superficielle (épidermique) ou invasive (dermique et plus) pour déterminer le traitement les plus appropriés et éviter si possible un geste chirurgical.

Ce projet s'intègre dans l'AAPG ANR 2017 Défi 4 PRCE

Système optique multimodal haute résolution et spectroscopique pour l'analyse de la peau appliquée aux tumeurs cutanées
High resolution and spectroscopic multimodal optical system for skin and tumors characterization

Contexte, positionnement et objectif(s) de la proposition

L'observation et la compréhension des mécanismes impliqués dans l'état physiologique ou pathologique de la peau sont essentielles pour le diagnostic de ses pathologies. Les paramètres physiologiques fournis par différentes techniques de mesures in vivo permettent, par leur combinaison, un diagnostic d'un état cutané donné. Dans le domaine précis des cancers cutanés (mélanomes, carcinomes baso- et spinocellulaires …), il est par exemple possible d'évaluer une lésion à partir d'un examen clinique, d'une analyse dermoscopique, de techniques d'échographie ou de tomographie à cohérence optique (OCT), d'une approche de microscopie confocale ou d'une analyse de ses capacités diélectriques. **L'approche par analyses multimodales reste essentielle** pour qualifier de la manière la plus fiable possible l'ensemble des caractéristiques du tissu cutané. En revanche, l'accessibilité à un ensemble de caractéristiques pertinentes reste une problématique fondamentale pour les chercheurs et les médecins dermatologues. Actuellement, pour préciser les diagnostics douteux en dermatoscopie sans réaliser de geste vulnérant (biopsie) le recours à des technologies évoluées d'investigation est extrêmement onéreux (80 000€ OCT-160 000€ microscopie confocale in vivo) et nécessite de plus une expertise avancée du dermatologue. Ainsi moins de 12 centres en France, surtout des plateformes de recherche, pratiquent l'une ou l'autre technique et seuls quelques experts sont formés à leur utilisation. **Les dermatologues restent en attente à la fois d'une amélioration de la préconisation de diagnostic et d'une simplification technique de leur pratique quotidienne avec des coûts d'instruments leur ouvrant l'accès à ces technologies.**

La présente proposition vise à répondre à ces deux problématiques en associant une **vision épimicroscopique 2D HD et 3D**, comme celle fournie par le dermoscope C-Cube de Pixience, à une **signature multi-spectrale** de lésions cutanées à différentes profondeurs afin d'évaluer leur nature, leur malignité potentielle et, le cas échéant leur stade de développement. Le CEA-LETI développe une approche d'analyse optique multi spectrale quantitative de la composition et de la structure de la peau dans l'épiderme et le derme. Cette approche par DRS (Diffuse Reflectance Spectroscopy) a montré ses potentialités pour des applications cliniques (détection précoce de la réaction d'hypersensibilité retardée, mesure non invasive de l'anémie, ….), pour des applications en cosmétique (rosacée, objectivation de l'éclat du teint). Pour gagner en spécificité de la signature spectrale, il est proposé dans ce projet d'enrichir cette approche DRS par une approche DRS multi échelle fournissant une analyse multi-profondeurs des évolutions de composition et de structure de la peau, tout en restant sur un coût d'instrument compatible avec la pratique en cabinet de dermatologie.
Ce couplage de la DRS multi-profondeurs à la dermatoscopie 2D HD et 3D permettra d'évaluer l'épaisseur de la tumeur en mesurant la profondeur à laquelle un signal de tissus non tumoraux apparait, d'affirmer le caractère superficiel ou non de la tumeur (CBC, Mélanome, CE), et in fine de choisir dans certains cas des traitements médicaux non invasifs pour le patient et moins couteux pour les organismes de santé. Ce nouveau système permettra aussi d'établir un thesaurus des différents spectres tumoraux, d'identifier le spectre de la tumeur cible pour le comparer à une banque de spectres existant (carcinome baso cellulaire, carcinome épidermoïde, mélanome, nævus …), de construire un algorithme permettant d'établir un diagnostic en combinant les données de la DRS multi-profondeurs et de la dermoscopie. Une tumeur pourra être formellement diagnostiquée et son site surveillé de manière non invasive après un traitement médical.

Une **première étape** (18 mois) du projet visera à étendre la technologie multi spectrale DRS du CEA-LETI au domaine spécifique de l'analyse multi-profondeurs des lésions cutanées. Dans ce cadre il s'agira de concevoir, en fonction de la morphologie moyenne des lésions, un prototype de sonde (conception de la chaîne optique et géométrie de sonde, protocole d'acquisition, algorithmie d'analyse) fournissant une information multi-profondeurs et adaptée à une utilisation en milieu médical.

Une **seconde étape** (6 mois) visera alors à mettre en œuvre ce dispositif médical en environnement clinique au CHU de Saint-Etienne pour construire une base de données représentative sur une large gamme de lésions. Outre les modalités de dermoscopie 2D HD et 3D, et DRS, seront également utilisés les systèmes d'imagerie et de diagnostic existants et présents au sein du CHU (examen clinique, OCT, échographie, microscopie confocale, anatomopathologie).
Dans **une troisième étape** (12 mois), Pixience développera des algorithmes d'analyse et de combinaison des informations issues des trois modalités (C-Cube 2D, C-Cube 3D et DRS) pour fournir des marqueurs de caractérisation des lésions.

Les **principaux risques** identifiés inhérents à ce dossier sont associés à la démonstration du bénéfice clinique apporté par la technologie. Outre l'aspect pathologique d'une lésion, les caractéristiques mêmes de la peau d'un sujet (épaisseur des stratums, teneur en collagène, mélanine, élastine …) peuvent induire des différences entre signaux. Compte tenu de la grande variabilité des individus, il pourra être nécessaire d'avoir recours à des cohortes cliniques importantes. La potentialité d'intégration de la sonde DRS au sein d'un dispositif de dermoscopie constitue également un verrou technique important qu'il sera néanmoins possible de résoudre en adoptant la solution de 2 sondes indépendantes associées à une même structure logicielle. Le coût de l'ensemble dermoscope + DRS devra permettre d'assurer, à terme, un développement commercial privilégié vers les cabinets médicaux libéraux. Un risque inhérent aux essais de certification électromagnétique du dispositif et à l'analyse de risques patients réalisés, est clairement identifié et l'ensemble du développement devra prendre en compte cette contrainte pour mener l'étude clinique.

Organisation du projet et moyens mis en œuvre

Pixience est une TPE SAS dont l'activité s'articule majoritairement autour de la conception et la commercialisation de dispositifs médicaux. Spécifiquement dédiée aux domaines de la dermatologie et de la dermocosmétique cette activité vise à contribuer à l'amélioration technique de ces deux secteurs d'activité. Pixience commercialise aujourd'hui notamment le dermoscope C-Cube visant à aider le praticien dans sa pratique quotidienne de détection du mélanome. Reposant sur les dernières technologies existantes, il permet le suivi et l'aide au diagnostic des lésions cutanées. Alexandre Delalleau, Directeur Général et Directeur R&D de **Pixience coordonnera le projet**.
L'équipe de JL Perrot du CHU de Saint-Etienne est une équipe Clinique de référence dans le domaine de la dermatologie et tout particulièrement des lésions cutanées. JL Perrot est président du groupe « Imagerie cutanée non invasive » de la Société française de dermatologie, auteur de 56 Publications référencées PubMed ayant trait à l'imagerie dermatologique microscopique non invasive (microscopie confocale, OCT ou Raman) participe au développement de 2 OCT. Cette expertise clinique permettra d'orienter les développements pour fournir les paramètres cliniques de caractérisation pertinents, assurera l'évaluation sur patients et mènera à terme les validations cliniques qui démontreront les performances de la nouvelle approche développée.
Depuis 2010, le **Laboratoire LISA du CEA-LETI** a développé une expertise en développement de techniques d'imagerie optique par spectrométrie pour caractériser les tissus biologiques à partir de leurs propriétés optiques intrinsèques d'absorption et de diffusion. La caractéristique d'absorption fournit des informations sur la concentration des différents composants des tissus (eau, différents types d'hémoglobines, lipides, …). La diffusion fournit, quant à elle, des informations sur la structure des tissus. Jean-Marc Dinten, responsable du laboratoire cordonnera l'action du CEA-Leti.

Le coût environné du projet pour **Pixience** est de l'ordre de 375k€ (frais de personnel (hardware, suivi étude clinique, informatique, électronique, qualité), achats, missions) soit une aide demandée de l'ordre de **170k€**. En fonction de la charge ponctuelle associée aux développements R&D de Pixience, une ressource complémentaire pourra être intégrée afin d'apporter son aide sur les développements en cours.

Le CHU de Saint-Etienne est en cours d'acquisition des instruments qui permettront de caractériser les lésions (en particulier, un échographe HD pour évaluer l'épaisseur in vivo de la tumeur, un scanner à lames pour accéder à l'imagerie histologique). Pour l'étude il sera nécessaire de disposer d'un biostatisticien, de temps d'ARC pour saisir et faire évoluer la base des données cliniques Ces ressources nécessiteront un budget de 128k€ soit une aide demandée de **57.6k€.**
Le **CEA-LETI** prévoit pour le développement de l'approche DRS, la participation aux évaluations cliniques des compétences et des ressources en instrumentation optique, en développement de la méthode logicielle associée et en expérimentation. Ces ressources sont évaluées à environ 3ha, soit environ 575 k€. Il faudra également prévoir environ 30k€ d'achats de composants pour construire les dispositifs de mise au point de l'approche et d'évaluation clinique. Soit un budget d'environ 600k€ et une aide demandée de **300k€.**

Impact et retombées du projet

La thématique de ce projet s'inscrit parfaitement dans les axes 2017 définis par l'ANR à travers la thématique DEFI 4 – Vie, Santé et Bien-être. Aujourd'hui, les pathologies cutanées cancéreuses, dont près de **80% des exérèses sont réalisées à tort**, présentent un coût sociétal important. Selon le rapport 2012 de la HAS, 486 879 actes d'exérèses ont été réalisés impliquant une dépense nette de 15 millions d'euros. Le seul coût de prise en charge du mélanome (représentant 20% des cancers cutanés) est estimé à 254 millions d'euros (2008)**. Les enjeux économiques et de santé sont donc conséquents** si l'on cumule la prise en charge de l'ensemble des cancers cutanés. Au-delà, **les conséquences d'une exérèse pour un patient peuvent être très importantes** (localisation et marges chirurgicales). Le recours à des technologies améliorant la sensibilité et la spécificité de détection apparaît ainsi fondamental pour diminuer le nombre d'exérèses inutiles.
La problématique d'investissement des cabinets médicaux de dermatologues constitue également une donnée importante. Cette profession souffrant d'actes peu valorisés présente des moyens d'équipement faibles en comparaison d'autres disciplines. En conséquence, le recours à des technologies plus onéreuses que la simple vidéo-dermoscopie est exclu au sein des cabinets libéraux à quelques rares exceptions près. Le dermatologue libéral, généralement seul, éprouve le besoin de recourir à des technologies simples, fiables et raisonnablement onéreuses afin de l'aider dans son quotidien.
Finalement, la diminution drastique du nombre de dermatologues en France, présentant une **chute anticipée de 50% dans les 20 prochaines années**, a pour conséquence directe de créer de nombreux **déserts médicaux**. Les régions ainsi isolées n'ont qu'un accès restreint à l'expertise dermatologique et le coût de déplacement d'un patient, qu'il soit à la charge de ce dernier ou à la charge du système de santé, est conséquent et pourrait être réduit dans des proportions importantes avec la présence de technologie d'aide au diagnostic disponibles au sein des cabinets de médecins généralistes. Dans ce cadre il s'agit alors, en lieu et place des 3 500 dermatologues du territoire, de bénéficier de l'appui de première intention de près de 90 000 médecins généralistes. **Le développement du système bimodal issu de ce projet fournira un outil simple jouant un rôle de conseil dermatologique plus pertinent quant à l'adressage des malades au dermatologue**. Le rôle de ces examens de première intention est clairement défini dans la convention médicale des médecins généralistes et a récemment été revalorisé. Un tel exercice pourrait également être intégré au sein des nouvelles ouvertures offertes par la télésanté en France comme à l'international.

Une extension de ce projet pourrait également être valorisée pour le suivi et le traitement des plaies. A travers la mesure de la teneur en oxygène dans le derme il est possible de constituer des indicateurs pronostics de survenues d'escarres (11.4%), plaies diabétiques (10.7%) et autres plaies chroniques (ulcères, purpuras séniles …), d'en définir le stade de développement et le traitement adapté. Avec une durée de cicatrisation moyenne de 211 jours, escarres et ulcères

représentent actuellement 245000 patients pris en charge à domicile pour un coût de 965M€ en 2011 au seul titre des soins de ville.

La stratégie de valorisation de ce projet consiste en conséquence à faire bénéficier des développements réalisés aux dermatologues libéraux et hospitaliers. Des Dermatologues référents sont d'ores et déjà identifiés afin de réaliser les premières publications nécessaires à assurer l'adhésion de l'ensemble de la profession à l'utilisation de la technologie. Après une année de commercialisation et de remontées clients un produit plus spécifique et dédié à une distribution a plus grande échelle sera conçu. Ce dernier sera destiné, avec un objectif de prix plus drastique, aux cabinets de médecine générale et solutions de de télésanté. En parallèle de ce dernier développement, la problématique de suivi des plaies pourra être envisagée ainsi que le conseil diététique en pharmacie. Ces autres développements nécessiteront un nouvel investissement, mais bénéficieront du recul pris sur la technologie. En termes de protection intellectuelle, les résultats seront protégés par des dépôts de brevet en cas d'inventivité avérée. Des Communications et publications scientifiques, notamment concernant les résultats de l'étude clinique, pourront être réalisées à l'initiative des différents partenaires du projet.

F. LA DERMATOLOGIE AU JOUR LE JOUR : UNE ENTITÉ DE RECHERCHE À PART ENTIÈRE

1-Une approche synthétique des innovations au jour le jour : une continuité avec notre mission de soins.

L'intérêt premier des méthodes d'explorations non invasives de la peau est de caractériser les tumeurs cutanées en procédant à une sorte de « biopsie optique ». Ainsi, peuvent être éviter des prises en charges chirurgicales inutiles au malade et ses corrolaires (inquiétude du résultat, douleur dûe au geste, cicatrice, coût pour la société) mais aussi, d'identifier des lésions débutantes dont on peut espérer une prise en charge moins mutilante que si le diagnostic avait été plus tardif.
La collaboration avec l'anatomopathologiste devient quasiment fusionnelle, la microscopie confocale et l'OCT faisant un pont entre le clinicien et le pathologiste. Par ailleurs la responsabilité du dermatologue s'est accrue du nombre des tumeurs pour lesquelles les biopsies optiques ont conduit à l'absence de réalisation de biopsie ou exérèse. Ceci revient à donner au dermatologue une nouvelle responsabilité qu'endossait préalablement le pathologiste qui signait le compte rendu anatomopathologique des biopsies et ou d'exérèses maintenant non réalisées du fait des méthodes d'imagerie dermatologiques modernes mises en œuvre par le dermatologue. Il nous parait que ces nouvelles techniques d'imagerie sont des outils de haute valorisation de l'acte diagnostic dermatologique.
L'autre utilité de la MCIV est la possibilité in vivo d'identifier les marges d'exérèse de la tumeur et ainsi de guider la main du chirurgien pour lui permettre de réaliser une exérèse carcinologique sans pour autant provoquer une perte de tissus excessive.
Les travaux présentés sont, en ce qui concerne les articles publiés en langue anglaise des travaux originaux, certains étant même des premières médicales (application de la microscopie confocale à la technique du spaghetti (9)) . Inversement les travaux en langue française sont pour la plupart des articles didactiques destinés à faire connaitre à des dermatologues ne lisant pas les revues internationales et non spécialistes de l'imagerie, ces nouvelles méthodes d'imagerie non invasive et de leur faire acquérir une culture de microscopie confocale notamment .
Nous rapporterons des travaux portant sur l'identification non invasives des tumeurs et l'identification des marges chirurgicales,l'intégration de la microscopie confocal ex vivo ou de la spectrométrie Raman à une prise en charge de nos patient et une activité de caractérisation des parasites particulièrement fournie et toujours en dévellopement.
L'ensemble de ces travaux est le fruit d'un travail totalement intégré au sein de la pratique clinique quotidienne du service ce qui explique en partie son caractère protéiforme mais aussi sa richesse.

2- Imagerie non invasive cancérologique cutanéo-muqueuse.

L'imagerie dermatologique non invasive s'est, initialement, principalement intéressée à l'identification des tumeurs cutanées et plus particulièrement les mélanomes et carcinomes baso-cellulaires.

Lorsque nous avons acquis à St Etienne nos 2 premières caméras de microscopie confocale une grosse partie du travail de pionnier en MCIV avait été réalisé, et plus particulièrement par les équipes italiennes de Modena et Reggio Emilia. Le champ d'investigation potentiel n'en demeurait pas moins vaste. Nos travaux ont porté :
- sur l'identification des tumeurs rares (histiocytose langhershansienne)
- sur la description des potentialités de la toute nouvelle caméra Vivascope 3000 jamais validée dans ces indications. En effet, nous avons été le premier acquéreur, non industriel, de cette caméra au monde à l'utiliser en pratique clinique. Tous les travaux antérieurs en MCIV avaient été réalisés avec la caméra Vivascope 1500 qui permet d'acquérir une image sous la forme d'une mosaïque d'images. Or cette nouvelle caméra Vivascope 3000 nécessitait d'élaborer mentalement l'image de la mosaïque que proposait l'ancienne caméra, ce qui n'avait jamais été mis en application pour l'évaluation in vivo des tumeurs en MCIV, mais surtou,t nous offrait la possibilité de travailler beaucoup plus vite et surtout d'examiner des sites jamais explorés jusqu'alors.

Ceci nous a conduits d'une part à être la première équipe à présenter des images de microscopie confocale des muqueuses en l'occurrence la vulve (d'autres travaux suivront en collaboration avec des équipes françaises puis espagnoles et italiennes),et d'autre part à être la première équipe à présenter l'utilité de la microscopie confocale pour l'aide à la délimitation des marges d'exérèse chirurgicale.Ces travaux ont été complétés par la mise en place d'un projet de recherche ayant bénéficié d'une bourse de la part du laboratoire Roche pour évaluer l'apport respectif de la microscopie confocale in vivo et de la dermoscopie à propos de 200 tumeurs en double insu regroupant les confocalistes et dermoscopistes ayant le plus publiés dans ces domaines. Ce travail piloté par St Etienne était en soit une reconnaissance de notre activité en MCIV et dermatoscopie par nos pairs. L'article qui en a résulté est actuellement soumis à publication et ne sera pas de ce fait cité parmi la série des articles qui sont présentés par la suite. Enfin un investissement important a été réalisé pour la diffusion de la microscopie confocale dans le cadre d'articles didactiques dans les annales de dermatologie vénéréologie, revue de la société française de dermatologie pour faire connaitre à tous les dermatologue l'existence et surtout les possibilités de cette technique, jusqu'à peu, encore confinée à quelques CHU.

2. a identification des tumeurs

2.a 1 Cells of Langerhans cell histiocytosis and epidermal Langerhans cells differ under reflectance confocal microscopy: first observation

2.a 3 Contribution of reflectance confocal microscopy to the diagnosis of fibroepithelioma of Pinkus

2.a 4 Contribution of reflectance confocal microscopy for the diagnosis of junctional naevus

2.a 5 Cinotti E, Perrot JL, Labeille B, Douchet C, Thuret G, Cambazard F. Yellow globules in balloon cell naevus

2.a 6 Sensitivity of handheld reflectance confocal microscopy for the diagnosis of basal cell carcinoma: A series of 344 histologically proven lesions

2.a 7 In vivo confocal microscopic substrate of grey colour in melanosis

2. a 8 Reflectance confocal microscopy features of acral lentiginous melanoma: a comparative study with acral nevi.

2. a 9 The role of reflectance confocal microscopy in the diagnosis of cutaneous melanoma metastasis

2.a 10 Reflectance confocal microscopy of Pigmented Bowen's disease: misleading dendritic cells.

Skin Research and Technology 2013; 0: 1–3
Printed in Singapore · All rights reserved
doi: 10.1111/srt.12114

Published by John Wiley & Sons Ltd
Skin Research and Technology

Letter to the Editor

Cells of Langerhans cell histiocytosis and epidermal Langerhans cells differ under reflectance confocal microscopy: first observation

E. Cinotti[1], B. Labeille[1], J. L. Perrot[1], C. Douchet[2] and F. Cambazard[1]

[1]Department of Dermatology, University Hospital of Saint-Etienne, Saint Etienne Cedex 2, France and [2]Department of Pathology, University Hospital of Saint-Etienne, Saint Etienne Cedex 2, France

LANGERHANS CELL histiocytosis (LCH) is a rare disease characterized by an accumulation of Langerhans cells (LCs) in the early stage of maturation in skin and other tissues (1). The relation between LCH cells and normal LCs is currently uncertain (2). We present for the first time the *in vivo* reflectance confocal microscopy (RCM) features of an adult LCH and compare *in vivo* RCM features of LCH cells with reactive epidermal LCs present in the same skin lesions.

An 86-year-old man referred to our department for a pruritic eruption persisting for one year. The clinical examination revealed multiple red-brownish scaly papules on the trunk suggestive of LCH of Letterer-Siwe type (Fig. 1a, b). *In vivo* RCM (VivaScope 1500 and 3000) examination showed clusters of large, medium reflective, polygonal cells, a few with short dendrites, in the lower epidermis and in the dermis, surrounded by numerous high reflective cells with long dendrites in the epidermis (Fig. 1c, d). Histological examination revealed a proliferation of large cells with an either oval or reniform nucleus in the dermis and focally in the epidermis. Anti-CD1a (Fig. 1e, f) and anti-fascine antibodies strongly marked these cells, confirming the diagnosis of LCH, and also stained the epidermal dendritic cells visible under *in vivo* RCM showing that they were LCs.

In vivo RCM is an emerging technique that allows *in vivo* non-invasive high-resolution histomorphological skin analysis. The main *in vivo* RCM characteristic of the LCH was the presence of a proliferation of monomorphous medium reflective, polygonal, large cells in the dermis, sometimes with short dendrites. These cells were also focally invading the epidermis, thus determining an obscuration of the dermo-epidermal junction. Curiously enough, in the epidermis they were surrounded by numerous bright dendritic cells. Anti-CD1a and anti-fascine antibodies immunostainings showed that epidermal dendritic cells were LCs but did not allow a distinction from LCH cells. However, we assumed that these dendritic cells were inflammatory reactive LCs and not LCH cells since they had a different morphology (they presented long dendrites and were not organized in clusters) and had higher reflectance under *in vivo* RCM. We hypothesize that the higher reflectance of reactive LCs compared to LCH cells may depend on the higher amount of organelles of the endosomal/lysosomal system at later stages of maturation and activation.

LCs are antigen-presenting cells for T lymphocytes and play an important role in the immune surveillance of epidermis. Usually they account for approximately 2% (3) of the epidermal cells, but can be increased in number in various cutaneous tumors (4), and in mucosa (5). We hypothesize that in our case they were increased in response to the LCH proliferation since they were located around LCH cell clusters.

In conclusion, although histological examination remains the gold standard for diagnosis of histiocytosis, *in vivo* RCM can support the

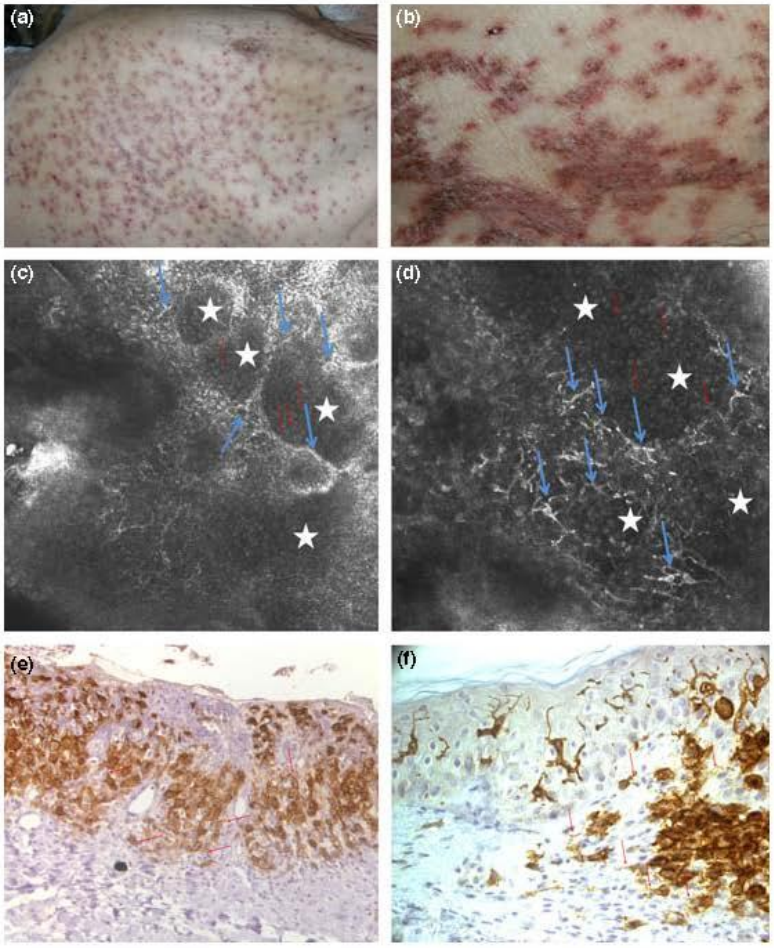

Fig. 1. (a, b) Clinical aspect of the Langerhans cell histiocytosis (LCH): multiple red-brownish scaly papules, sometimes coalescent, localized on the trunk. (c, d) In vivo reflectance in vivo confocal microscopy (RCM) of the LCH shows large, medium reflective, polygonal cells (stars), some with short dendrites (red arrows) in the lower epidermis and in the upper dermis, surrounded by numerous high reflective dendritic cells in the epidermis (blue arrows). (e, f) The histological aspect of the LCH reveals a proliferation of large mononuclear cells in the papillary dermis, immediately beneath the epidermis, and focally in the epidermis, as well as dendritic cells in the epidermidis. Both cell populations stain for CD1a (e, 20×, f, 40×).

clinical suspicion of LCH, showing a proliferation of medium reflective polygonal cells in the upper dermis and epidermis.

Characteristically, numerous dendritic cells can also be present around LCH cells. *In vivo* RCM can distinguish cells of LCH from epidermal LCs, being the first population less reflective, without or with just few short dendrites. Further studies are needed to validate our data and to evaluate the usefulness of *in vivo* RCM for LCH either in adults or in the more frequent pediatric forms.

Conflict of interest

The authors declare not to have any conflicts of interest.

References

1. Laman JD, Leenen PJM, Annels NE et al. Langerhans-cell histiocytosis "insight into DC biology". Trend Immunol 2003; 24: 190–196.
2. De Graaf JH, Tamminga RY, Kamps WA et al. Expression of cellular adhesion molecules in Langerhans cell histiocytosis and normal Langerhans cells. Am J Pathol 1995; 147: 1161–1171.

3. Bauer J, Bahmer FA, Wörl J et al. A strikingly constant ratio exists between Langerhans cells and other epidermal cells in human skin. A stereologic study using the optical dissector method and the confocal laser scanning microscope. J Invest Dermatol 2001; 116: 313 318.
4. Segura S, Puig S, Carrera C et al. Dendritic cells in pigmented basal cell carcinoma: a relevant finding by reflectance-mode confocal microscopy. Arch Dermatol 2007; 143: 883 886.
5. Cinotti E, Perrot JL, Labeille B et al. Reflectance confocal microscopy for the diagnosis of vulvar melanoma and melanosis: preliminary results. Dermatol Surg 2012; 38: 1962 1967.

Address:
Elisa Cinotti
University Hospital of Saint Etienne
42055 Saint Etienne Cedex 2
France
Tel: +33 (0) 4 77 82 84 21
Fax: +33 (0) 4 77 82 84 0
e-mail: elisacinotti@gmail.com

2.a 2 Solar lentigo diagnosed by reflectance confocal microscopy

Annales de dermatologie et de vénéréologie (2014) 141, 71—73

ELSEVIER MASSON

Disponible en ligne sur ScienceDirect www.sciencedirect.com

Elsevier Masson France EM|consulte www.em-consulte.com

FICHE THÉMATIQUE / MICROSCOPIE CONFOCALE PAR RÉFLECTANCE

Lentigo actinique diagnostiqué par microscopie confocale

Solar lentigo diagnosed by reflectance confocal microscopy

E. Cinotti[a], J.-L. Perrot[a], B. Labeille[a,*], C. Douchet[b], F. Cambazard[a], au nom du groupe imagerie cutanée non invasive de la Société française de dermatologie

[a] *Service de dermatologie, hôpital universitaire de Saint-Étienne, 42055 Saint-Étienne cedex 2, France*
[b] *Service d'anatomatologie, hôpital universitaire de Saint-Étienne, 42055 Saint-Étienne cedex 2, France*

Reçu le 19 août 2013 ; accepté le 4 octobre 2013
Disponible sur Internet le 9 novembre 2013

Formation médicale continue

Observation

Un patient de 55 ans était adressé pour un examen annuel de ses naevus. Nous avons observé une héliodermie avec de nombreux lentigos actiniques du haut du dos. Parmi ces lésions se démarquait une macule hyper-pigmentée de 1 cm de diamètre (Fig. 1), qui avait rapidement augmenté de taille selon la femme du patient. L'examen dermoscopique (Fig. 2) montrait une lésion avec une forme irrégulière, des bords nets, et un fin réseau brun clair avec hyperpigmentation focale. Ces aspects étaient compatibles avec un lentigo actinique.

Microscopie confocale par réflectance

Un examen en microscopie confocale (MC) (Vivascope 3000®; Lucid Inc, Rochester, NY, États-Unis, distribué en France par Mavig, Munich) était réalisé pour confirmer le diagnostic de lentigo actinique. Il mettait en évidence dans l'épiderme un patron en nid d'abeille régulier avec des zones focales de kératinocytes hyper-reflétants (Fig. 3), et au niveau de la jonction dermo-épidermique, il montrait des papilles bien délimitées (papilles marginées) par des crêtes épidermiques étirées et denses (cord-like rete ridges), avec une bordure de kératinocytes hyper-reflétants (Fig. 4). Ces aspects ont permis de confirmer le diagnostic de lentigo actinique. Un examen histologique a été réalisé à des fins iconographiques (Fig. 5).

Commentaires

Les lentigos actiniques sont des lésions acquises caractérisées par une hyperplasie et une hyperpigmentation des kératinocytes, qui apparaissent cliniquement comme des macules brun clair ou brun foncé de forme et taille variables. Ils se situent sur les zones photo-exposées et ils sont souvent multiples. Sur peau héliodermique, le diagnostic différentiel avec le mélanome de Dubreuilh et la kératose actinique pigmentée peut être difficile.

L'examen en MC permet facilement de confirmer le diagnostic de lentigo actinique en montrant un épiderme normal avec une hyperpigmentation des kératinocytes

* Auteur correspondant.
Adresse e-mail : bruno.labeille@chu-st-etienne.fr (B. Labeille).

0151-9638/$ — see front matter
http://dx.doi.org/10.1016/j.annder.2013.10.028

Figure 1. Aspect clinique.

principalement basaux [1,2]. En particulier, la MC permet d'apprécier la taille et la forme des kératinocytes qui apparaissent monomorphes dans le lentigo actinique. En MC, les kératinocytes non pigmentés sont caractérisés par une partie centrale hypo-reflétante et une membrane externe hyper-reflétante (patron de l'épiderme normal, en nid d'abeille), tandis que les kératinocytes pigmentés apparaissent comme des corps arrondis hyper-reflétants. Dans le lentigo actinique, on trouve un patron en nid d'abeille dans la partie superficielle de l'épiderme (Fig. 3) et des kératinocytes hyper-reflétants dans la couche basale de l'épiderme (Fig. 4) et focalement dans les assises suprabasales (Fig. 3). La vision de la MC étant horizontale, les kératinocytes hyper-pigmentés de la couche basale de l'épiderme apparaissent en anneaux hyper-reflétants autour des papilles dermiques au niveau de la jonction dermo-épidermique (Fig. 4). De plus, dans le lentigo actinique, on trouve souvent à l'examen histologique des crêtes épidermiques étirées et fines (Fig. 5), et cet aspect correspond en MC à des structures étirées et tassées l'une contre l'autre (Fig. 4), hyper-reflétantes (car hyper-pigmentées), autour des papilles dermiques.

Le diagnostic différentiel avec le mélanome, et en particulier avec le mélanome de Dubreuilh, est fait par l'absence de grosses cellules pagétoïdes hyper-reflétantes correspondant aux mélanocytes tumoraux et par la bonne délimitation des papilles dermiques. Le diagnostic différentiel avec la kératose actinique pigmentée est fait par la régularité des kératinocytes épidermiques.

En conclusion, la MC est une technique non invasive qui peut aider à confirmer le diagnostic de lentigo actinique et éliminer la possibilité d'un mélanome ou d'une kératose actinique pigmentée.

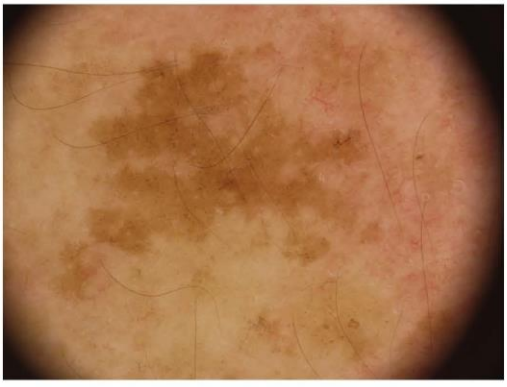

Figure 2. L'examen dermatoscopique montre une lésion avec une forme irrégulière, des bords nettement délimités, et un fin réseau brun clair régulier avec une hyperpigmentation focale.

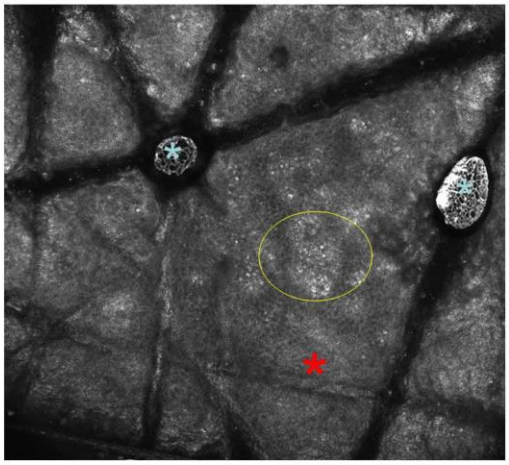

Figure 3. L'examen en microscopie confocale de l'épiderme montre un pattern en nid d'abeille régulier (astérisque rouge) et une hyperpigmentation focale des kératinocytes (cercle jaune). Des artéfacts sont présents dans l'image (astérisque bleu), correspondant à l'huile d'interface.

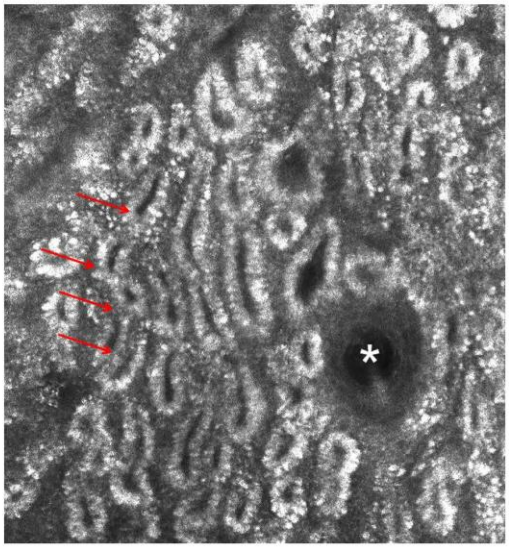

Figure 4. L'examen en microscopie confocale de la jonction dermo-épidermique montre des crêtes épidermiques (flèche rouge) étirées et denses (cord-like rete ridges), composées par des kératinocytes hyper-reflétants, autour des papilles dermiques bien délimitées. Dans cette image, un follicule pileux (astérisque blanc) est aussi présent.

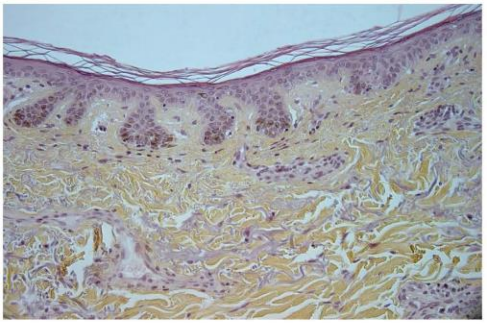

Figure 5. L'examen histologique montre une hyperpigmentation des kératinocytes basaux et des crêtes épidermiques allongées.

Déclaration d'intérêts

Les auteurs déclarent ne pas avoir de conflits d'intérêts en relation avec cet article.

Références

[1] Pollefliet C, Corstjens H, González S, Hellemans L, Declercq L, Yarosh D. Morphological characterization of solar lentigines by in vivo reflectance confocal microscopy: a longitudinal approach. Int J Cosmet Sci 2013;35:149—55.

[2] Langley RG, Burton E, Walsh N, Propperova I, Murray SJ. In vivo confocal scanning laser microscopy of benign lentigines: comparison to conventional histology and in vivo characteristics of lentigo maligna. J Am Acad Dermatol 2006;55:88—97.

2.a 3 Contribution of reflectance confocal microscopy to the diagnosis of fibroepithelioma of Pinkus

Annales de dermatologie et de vénéréologie (2014) 141, 643—645

ELSEVIER MASSON

Disponible en ligne sur ScienceDirect www.sciencedirect.com

Elsevier Masson France EM|consulte www.em-consulte.com

FICHE THÉMATIQUE / *Microscopie confocale par réflectance*

Apport de la microscopie confocale par réflectance dans le carcinome basocellulaire de type Pinkus

Contribution of reflectance confocal microscopy to the diagnosis of fibroepithelioma of Pinkus

J.L. Perrot[a], B. Labeille[a], C. Douchet[b], F. Cambazard[a], E. Cinotti[a,*], au nom du Groupe imagerie cutanée non invasive de la Société française de dermatologie

[a] *Service de dermatologie, hôpital universitaire de Saint-Étienne, 42055 Saint-Étienne cedex 2, France*
[b] *Service d'anatomopathologie, hôpital universitaire de Saint-Étienne, 42055 Saint-Étienne cedex 2, France*

Reçu le 3 avril 2014 ; accepté le 9 juillet 2014
Disponible sur Internet le 10 septembre 2014

Formation médicale continue

Observation

Une patiente de 97 ans était hospitalisée dans notre service pour la prise en charge d'un ulcère veineux de jambe. L'examen dermatologique montrait une tumeur rose pâle inter-mammaire de 18 mm de diamètre de grand axe, associée à une profusion de kératoses séborrhéiques (Fig. 1a). La lésion asymptomatique n'était connue ni de la patiente ni de son entourage. L'examen dermoscopique (Fig. 1b) montrait une structure centrale rosée homogène avec en périphérie des structures brunâtres en forme de feuille d'érable, des petites érosions et des fins vaisseaux linéaires.

Microscopie confocale par réflectance

Un examen en microscopie confocale (MC) (Vivascope 3000®; Caliber, Rochester, NY, États-Unis, distribué en France par Mavig, Munique) était réalisé pour orienter le diagnostic de façon non invasive compte tenu de la topographie et de l'âge de la patiente. L'épiderme présentait un patron en nid d'abeille régulier, sans cellule anormale. Il était constaté des projections tumorales appendues à l'épiderme, constituées de cellules à disposition palissadique, et anastomosées entre elles autour de

* Auteur correspondant.
Adresse e-mail : elisacinotti@gmail.com (E. Cinotti).

http://dx.doi.org/10.1016/j.annder.2014.07.008

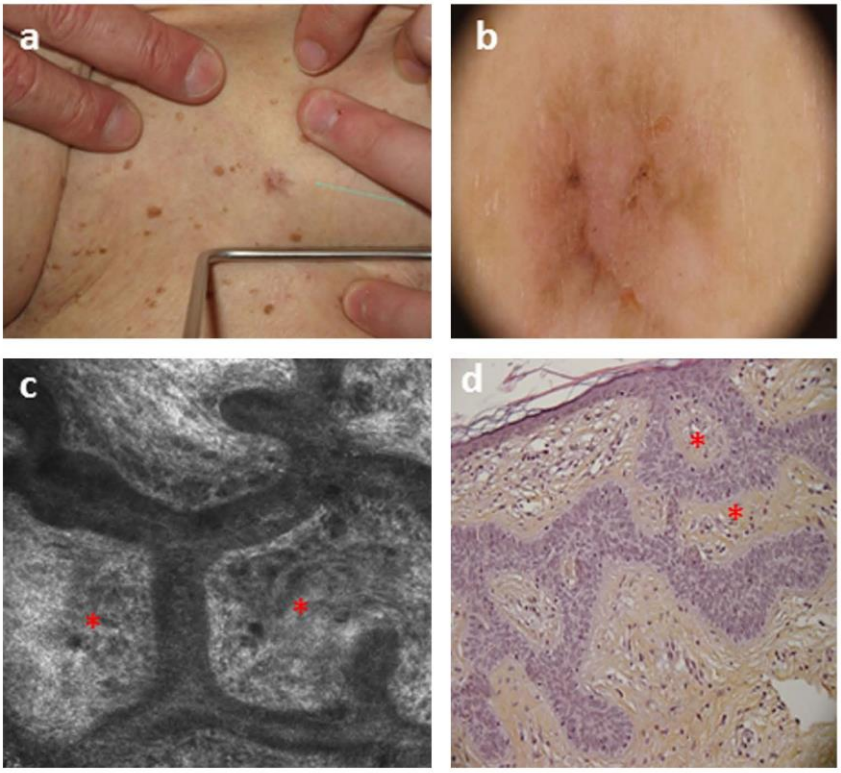

Figure 1. Aspect clinique (a), en dermatoscopie (b), en microscopie confocale (MC) (c) et en histologie (d) de la tumeur de la patiente n° 1. La MC et l'examen histologique (coloration hematoxyline-éosine-safran, × 10) montrent des boyaux trabéculaires formés de cellules à disposition palissadique autour de travées fibreuses (étoile rouge).

travées fibreuses formant un aspect en dentelle (Fig. 1c). Ces aspects tout à fait évocateurs d'un carcinome basocellulaire de type Pinkus étaient confirmés histologiquement dans un second temps (Fig. 1d).

Commentaires

Le carcinome basocellulaire de type Pinkus est une forme rare de carcinome basocellulaire représentant 1 % des carcinomes basocellulaires diagnostiqués par les dermatologues du réseau ligérien du mélanome dans le département de la Loire entre le 1er janvier 2005 et le 31 décembre 2012 [1]. Le diagnostic précis de ce type de tumeur est difficilement posé par le dermatologue tant sur l'aspect clinique qu'après examen en dermatoscopie [2].

Le carcinome basocellulaire de type Pinkus est caractérisé en MC comme en histologie par la présence de travées tumorales constituées de cellules à disposition

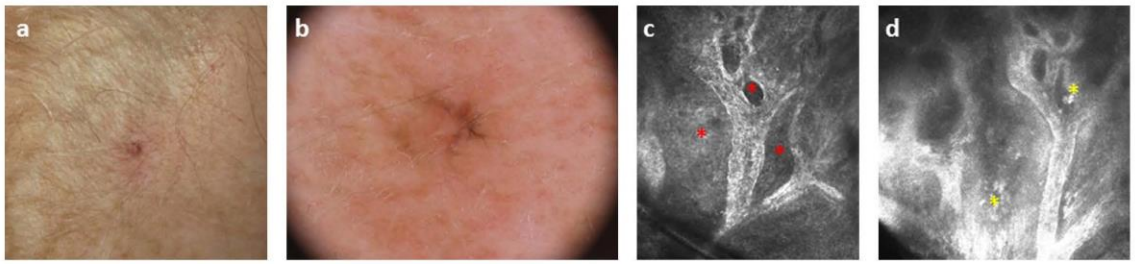

Figure 2. Aspect clinique (a), en dermatoscopie (b) et en microscopie confocale (c, d) de la tumeur du patient n° 2. La dermatoscopie montre une structure rosée homogène avec présence de structures en forme de feuille d'érable périphérique. L'examen en microscopie confocale montre des travées tumorales anastomosées entourant des structures fibreuses (étoile rouge), et cellules hyper-reflétantes correspondant à des mélanophages plus en profondeur (étoile jaune).

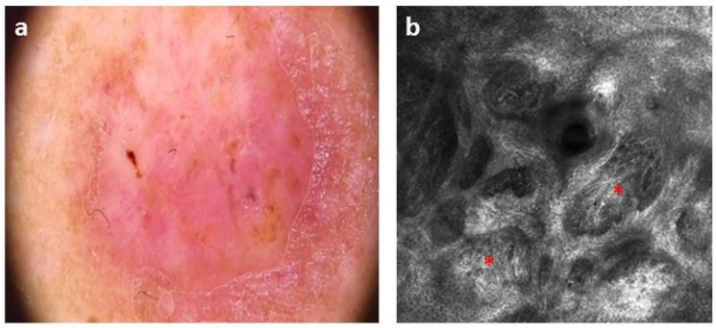

Figure 3. Aspect en dermatoscopie (a) et en microscopie confocale (b) de la tumeur du patient n° 3. La dermatoscopie montre une structure rosée avec petites érosions centrales, des points marron et un patron vasculaire avec des vaisseaux linéaires et en points. L'examen en microscopie confocale montre des travées tumorales anastomosées entourant des structures fibreuses (étoile rouge).

palissadique, anastomosées entre elles et isolant des structures fibreuses plus ou moins arrondies (Fig. 1c, d) [2,3]. En MC, on trouve un aspect évocateur de carcinome basocellulaire (boyaux appendus à l'épiderme constitués de cellules tumorales à disposition palissadique) et de plus, une architecture en dentelle correspondant au signe de la silhouette employé en anatomopathologie pour évoquer ce sous-type de tumeur.

La présente observation avait été présentée sous forme de communication affichée aux JDP 2011 [4], tandis que la première description dans la littérature date d'avril 2012 [3]. Nous avons par la suite identifié deux autres tumeurs de Pinkus sur les mêmes critères de MC : patient n° 2 (Fig. 2) et patient n° 3 (Fig. 3) ayant les mêmes caractéristiques avec par ailleurs mise en évidence de cellules hyper-reflétantes grossièrement triangulaires dermiques, correspondant à des mélanophages [5] (Fig. 2d).

En conclusion, la MC est une technique non invasive qui peut permettre le diagnostic précis d'un sous-type rare de carcinome basocellulaire dont le diagnostic est habituellement posé par l'anatomopathologiste. Cette observation est caractéristique du pont que la MC établit entre l'examen dermatologique et anatomopathologique.

Déclaration d'intérêts

Les auteurs déclarent ne pas avoir de conflits d'intérêts en relation avec cet article.

Références

[1] Perrot JL, Labeille B, Biron AC, Cinotti E, Adegbidi H, Trombert B, et al. Aspects épidémiologique de 12 091 carcinomes basocellulaires consécutifs pris en charge de 2005 à 2011 dans le département de la Loire. Ann Dermatol Venereol 2012;139 hors—série 6:B246.
[2] Reggiani C, Zalaudek I, Piana S, Longo C, Argenziano G, Lallas A, et al. Fibroepithelioma of Pinkus: case reports and review of the literature. Dermatology 2013;226:207—11.
[3] Longo C, Soyer HP, Pepe P, Casari A, Wurm EM, Guitera P, et al. In vivo confocal microscopic pattern of fibroepithelioma of pinkus. Arch Dermatol 2012;148:556.
[4] Perrot JL, Labeille B, Douchet C, Cambazard F. Diagnostic en microscopie confocale d'un carcinome basocellulaire de type Pinkus. Ann Dermatol Venereol 2011;138P:A209—10.
[5] Kanitakis J, Bahadoran P, Braun R, Debarbieux S, Labeille B, Perrot JL, et al. In vivo reflectance confocal microscopy in dermatology: a proposal concerning French terminology. Ann Dermatol Venereol 2013;140:678—86.

2.a 4 Contribution of reflectance confocal microscopy for the diagnosis of junctional naevus.

Annales de dermatologie et de v n r ologie (2015) 142, 595—597

Disponible en ligne sur ScienceDirect www.sciencedirect.com

Elsevier Masson France EM|consulte www.em-consulte.com

FICHE TH MATIQUE / IMAGERIE EN DERMATOLOGIE

Apport de la microscopie confocale par r flectance dans le diagnostic de nævus jonctionnel

Contribution of reflectance confocal microscopy for the diagnosis of junctional naevus

E. Cinotti[a,*], B. Labeille[a], C. Habougit[b], C. Douchet[b], F. Cambazard[a], J.L. Perrot[a], Groupe imagerie cutan e non invasive de la Soci t française de dermatologie

[a] *Service de dermatologie, h pital universitaire de Saint- tienne, 42055 Saint- tienne cedex 2, France*
[b] *Service d'anatomopathologie, h pital universitaire de Saint- tienne, 42055 Saint- tienne cedex 2, France*

Reçu le 26 janvier 2015 ; accept le 17 mars 2015
Disponible sur Internet le 28 avril 2015

Formation médicale continue

Observation

Une patiente de 43 ans se pr sentait pour une l sion pigment e ayant augment de taille depuis quelques mois (Fig. 1a). Ses ant c dents taient une leuc mie aigu lympho de trait e par allogreffe. Le conditionnement de greffe avait consist en une irradiation corporelle totale en 1998. Son tat g n ral tait excellent. Un examen en dermatoscopie trouvait un r seau irr gulier asym trique et une zone d'allure r gressive (Fig. 1b).

Microscopie confocale par r flectance

Un examen en microscopie confocale (MC) (Vivascope 3000®; Caliber Inc, Rochester, NY, tats-Unis, distribu en France par Mavig, Munich) tait r alis pour orienter le diagnostic. Nous constations la pr sence d'un piderme avec patron pavimenteux [1] sans pr sence de cellule pag to de (Fig. 2a), des cavit s sombres la jonction dermo- pidermique (JDE) correspondant l'ouverture des

* Auteur correspondant.
Adresse e-mail : elisa.cinotti@gmail.com (E. Cinotti).

http://dx.doi.org/10.1016/j.annder.2015.03.023

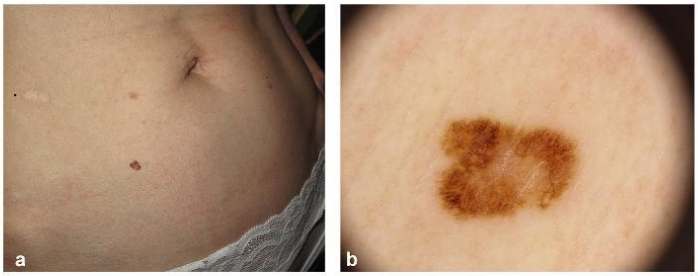

Figure 1. Aspect clinique (a) et dermoscopique (b). La dermatoscopie (b) montre une l sion asym trique avec patron en r seau irr gulier et une zone d'allure r gressive paracentral.

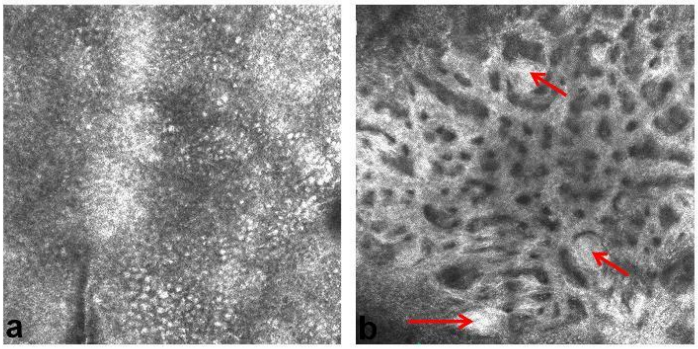

Figure 2. Examen en microscopie confocale par r flectance : a : piderme avec patron pavimenteux r gulier sans pr sence de cellule pag to de ; b : la jonction dermo- pidermique, il est possible d'observer des paississements des cr tes pidermiques et des th ques m lanocytaires (fl che rouge) avec protrusion dans les papilles dermiques.

papilles dermiques et des paississements des cr tes pidermiques form s de cellules rondes hyper-refl tantes, homog nes, avec un aspect protrusif dans les papilles dermiques (Fig. 2b). Nous ne retrouvions pas de cellule atypique (de grosse taille et de forme irr guli re) la JDE et dans le derme superficiel (Fig. 2b).

L'examen histologique tait r alis la demande de la patiente qui tait tr s inqui te. Il montrait la pr sence de th ques m lanocytaires r guli res la JDE (Fig. 3) sans pr - sence de cellule pag to de ni de prolif ration m lanocytaire atypique la JDE et dans le derme, confortant le diagnostic de nævus jonctionnel.

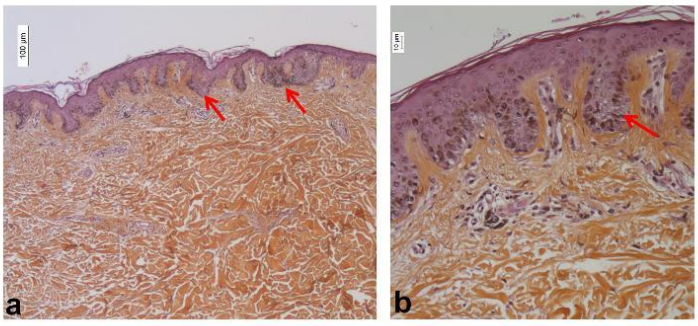

Figure 3. a et b. L'examen histologique (hematoxyline- osine) montre la pr sence de th ques m lanocytaires (fl che rouge) r guli res la jonction dermo- pidermique.

Commentaires

Un examen en MC in vivo a t r alis compte tenu de l'augmentation de taille r cente de la l sion, de l'aspect non rassurant en dermatoscopie et des ant c dents h matologiques de la patiente. Il a permis de visualiser un piderme normal avec un patron pavimenteux, caract ris par des espaces hyper-refl tants arrondis, de taille et de forme homog ne, correspondant aux k ratinocytes. On trouvait des th ques m lanocytaires la JDE, visibles sous forme d' paississement des cr tes pidermiques et des structures protrusives intra-papillaires (Fig. 2b).

Les cellules m lanocytaires du nævus se pr sentaient comme des cellules hyper-refl tantes, rondes, homog nes [2]. Le diagnostic de m lanome pouvait tre limin devant l'absence de cellule pag to de intra- pidermique, de cellule hyper-refl tante anormale (de grande taille) dans l' piderme, la JDE et dans le derme [2].

D claration d'int r ts

Les auteurs d clarent ne pas avoir de conflits d'int r ts en relation avec cet article.

R f rences

[1] Kanitakis J, Bahadoran P, Braun R, Debarbieux S, Labeille B, Perrot JL, et al. La microscopie confocale par r flectance in vivo en dermatologie : proposition de terminologie en langue française. Ann Dermatol Venereol 2013;140:678—86.

[2] Pellacani G, Scope A, Farnetani F, Casaretta G, Zalaudek I, Moscarella E, et al. Towards an in vivo morphologic classification of melanocytic nevi. J Eur Acad Dermatol Venereol 2014;28:864—72.

2.a 5 Cinotti E, Perrot JL, Labeille B, Douchet C, Thuret G, Cambazard F. Yellow globules in balloon cell naevus.

Australasian Journal of Dermatology

Australasian Journal of Dermatology (2013) **54**, 268–270 doi: 10.1111/ajd.12006

DERMOSCOPY

Yellow globules in balloon cell naevus

Elisa Cinotti,[1] Jean Luc Perrot,[1] Bruno Labeille,[1] Catherine Douchet,[2] Gilles Thuret[3] and Frédéric Cambazard[1]

Departments of [1]Dermatology, [2]Pathology and [3]Ophthalmology, Hôpital Nord, Saint Etienne Cedex 2, France

The balloon cell naevus is a rare variant of melanocytic naevus in which most of the cell population is composed of clear, swollen cells.[1] The dermatoscopic clue is the presence of white globules.[2,3] We present the first case characterised by yellow globules and describe the correlation with the reflectance confocal microscopy (RCM) and the histological aspect.

An 8-year-old child presented with a yellowish-brown congenital papule on her right cheek (Fig. 1). Dermatoscopy demonstrated aggregates of yellowish globules, distributed throughout the lesion background with structureless brown areas and peripheral linear vessels (Fig. 2). RCM (VivaScope 3000, Lucid, MAVIG, Munich, Germany) revealed roundish, moderately refractive large cells with a hyporefractive central part, grouped in well-defined clusters in the superficial dermis (Fig. 3). An excisional biopsy was performed because of the unusual dermatoscopic aspect and because the parents of the child were very anxious and wanted to remove the lesion for cosmetic reasons. The histological examination showed a dermal melanocytic naevus with confluent nests and sheets of large clear cells with a foamy cytoplasm (balloon-cell changes) (Fig. 4a), which were positive for S100 protein and MelanA (Fig. 4b) immunostaining.

The balloon cell naevus is characterised by balloon cells that are formed by the progressive vacuolisation of melanocytes because of the enlargement and disintegration of melanosomes.[1] These cells are therefore less pigmented than typical melanocytes and this may result in a clinical and dermatoscopic yellowish appearance.

To date, the dermatoscopic aspect of a balloon cell naevus has been reported in only three cases[2,3] and white globules have been identified as a clue for the diagnosis. We suggest that either yellow globules (as observed in our case) or white globules (as reported in previous cases) found at dermatoscopy may correspond to balloon cell clusters. The difference in colour (white or yellow) may depend on the grade of melanosome degeneration. A brown pigmentation was also present in our patient's lesion and in the previous reported case, and corresponds to the component of the naevus with normally pigmented melanocytes.

The yellow globules observed in balloon cell naevus should be differentiated from those corresponding to sebaceous glands, as seen in sebaceous hyperplasia.[2] In this case the yellowish globular structures have ill-defined borders and cluster together, presenting a popcorn-like appearance.[2] Yellow globules can also correspond to aggregates of sebocytes, as seen in some tumours with sebaceous differentiation such as naevus sebaceous, sebaceous adenoma and keratoacanthoma.[4,5] These lesions are often characterised by a central crater and elongated radial crown vessels[4] that are not present in balloon cell naevi.

Juvenile xanthogranuloma (JXG) should also be considered in the differential diagnosis of yellow globules, especially in children. Moreover, in JXG we can distinguish

Figure 1 Clinical image of the yellow-brown naevus on the right cheek.

Abbreviations:

JXG	Juvenile xanthogranuloma
RCM	reflectance confocal microscopy

Correspondence: Miss Elisa Cinotti, Hôpital Nord Saint-Etienne, 42055 Saint Etienne Cedex 2, France. Email: elisacinotti@gmail.com

Elisa Cinotti, MD. Jean Luc Perrot, MD. Bruno Labeille, MD. Catherine Douchet, MD. Gilles Thuret, PhD. Frédéric Cambazard, PhD.

Conflict of interest: none

Submitted 17 September 2012; accepted 2 October 2012.

pigmented areas and peripheral vessels,[6] as observed in our patient. However, in JXG the yellow globules are less well defined because they correspond to the sheet-like proliferation of histiocytic cells and not to circumscribed nests of cells, and the pigmented areas are usually sparse. An additional characteristic in JXG is the possible presence of white linear streaks, corresponding to fibrosis at histology,[6] which has never been described in balloon cell naevus.

The RCM aspect of balloon cell naevus has been reported in one patient[9] and the authors stated that RCM features did not differ from RCM findings of naevi with dermoscopically identified brown aggregated globules. However, in our patient and in the one already reported, the cells are larger than in conventional naevi and present a central, roundish and large hyporefractive part, corresponding to a big nucleus, and a moderately refractive surrounding part due to the absence of melanin in the vacuolated cytoplasm. Therefore, nests of moderately refractive and large cells with large hyporefractive nuclei may be suggestive of balloon cells.

In conclusion, we suggest that yellow or white globules associated with a brown pigmentation at dermatoscopy and an RCM showing clusters of large cells with large hyporefractive nuclei and moderately refractive cytoplasm could be indicative of a balloon cell naevus. Moreover, balloon cell naevi should be included in the differential diagnosis of yellow lesions.

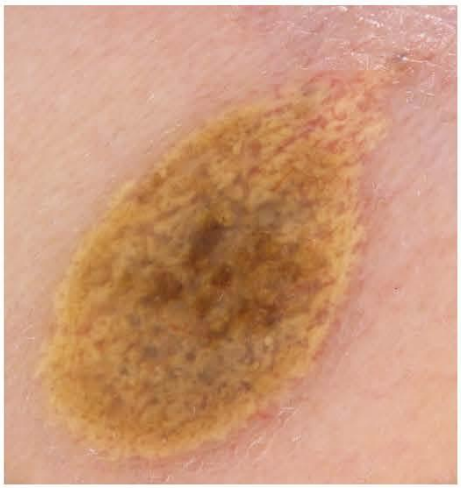

Figure 2 Dermatoscopy reveals a symmetrical lesion with yellow globules and overlapping structureless brown areas (20×).

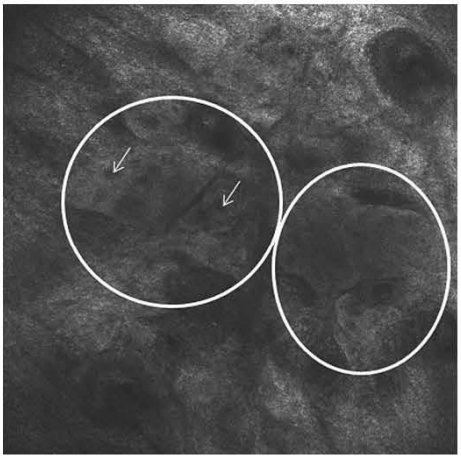

Figure 3 Reflectance confocal microscopy reveals roundish, moderately refractive large cells with hyporefractive central nuclei (arrows), grouped in well-defined clusters (circles) with polycyclic margins in the dermis.

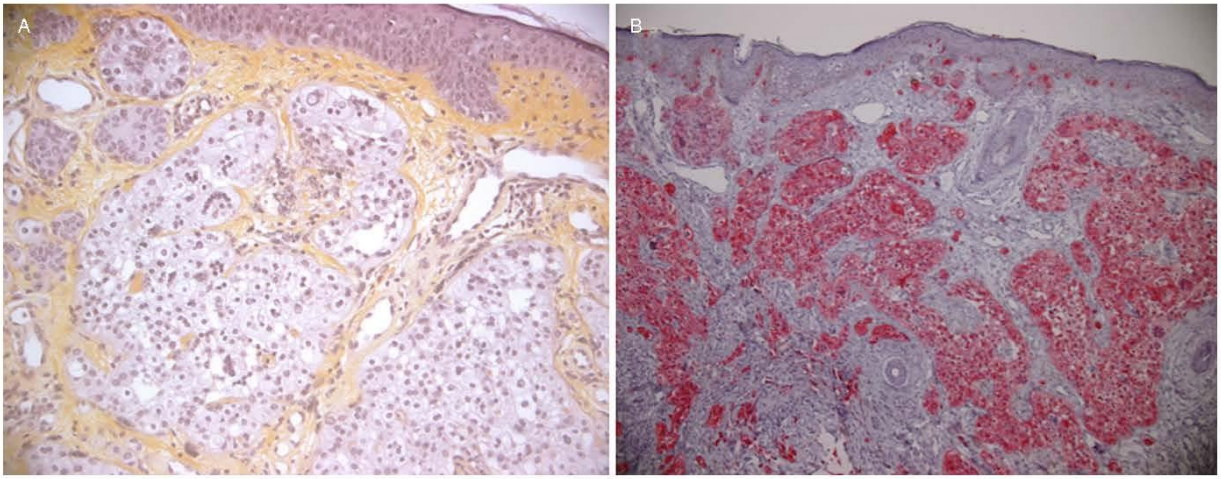

Figure 4 Histopathological examination shows a compound naevus characterised by large cells with a clear, foamy or vacuolated cytoplasm and a central basophilic nucleus, some multinucleated (balloon cell changes). These cells are arranged in nests and sheets in the superficial and deep dermis (a) (HE stain ×20). (b) Clear cells are positive for MelanA immunostaining (MelanA, ×10).

REFERENCES

1. Martinez-Casimiro L, Sánchez Carazo JL, Alegre V. Balloon cell naevus. *J. Eur. Acad. Dermatol. Venereol.* 2009; **23**: 236–7.
2. Jaimes N, Scope A, Welzel J *et al.* White globules in melanocytic neoplasms: *in vivo* and *ex vivo* characteristics. *Dermatol. Surg.* 2012; **38**: 128–32.
3. Jaimes N, Braun RP, Stolz W *et al.* White globules correlate with balloon cell nevi nests. *J. Am. Acad. Dermatol.* 2011; **65**: e119–e20.
4. Kim NH, Zell DS, Kolm I *et al.* The dermoscopic differential diagnosis of yellow lobular like structures. *Arch. Dermatol.* 2008; **144**: 962.
5. Moscarella E, Argenziano G, Longo C *et al.* Clinical, dermoscopic and reflectance confocal microscopy features of sebaceous neoplasms in Muir-Torre syndrome. *J. Eur. Acad. Dermatol. Venereol.* 2012; doi: 10.1111/j.1468-3083.2012.04539.x.
6. Song M, Kim SH, Jung DS *et al.* Structural correlations between dermoscopic and histopathological features of juvenile xanthogranuloma. *J. Eur. Acad. Dermatol. Venereol.* 2011; **25**: 259–63.

2.a 6 Sensitivity of handheld reflectance confocal microscopy for the diagnosis of basal cell carcinoma: A series of 344 histologically proven lesions.

80.5% and 64.1%, respectively.[2] The confocalist in our study is, in fact, the same trained confocalist in this previous study that had a reported specificity of 64.1%. This suggests that our confocalist's diagnostic capabilities, as indicated by increased specificity, improved overtime with further experience with using RCM.

Also, based on the histopathology results of the 119 lesions, our calculated benign-to-malignant ratio was 2.13:1 (81 benign lesions biopsied, 38 malignant lesions). Studies on the use of dermoscopy in practice report a reduction in the benign-to-malignant ratio of excised melanocytic lesions from 18:1 to 4:1 with it's use.[3] This suggests that RCM may dramatically reduce the biopsy rate of benign lesions beyond clinical and dermoscopic examination. Ultimately, these results should encourage more dermatologists to pursue training in RCM and integrate its use in daily clinical practice.

Danielle Giambrone, BS,[a] Mahin Alamgir, MD,[b] Aisha Masud, BS,[c] Tara Bronsnick, MD,[a] and Babar Rao, MD[a,b]

Rutgers Robert Wood Johnson Medical School, New Brunswick, NJ,[a] Maimonides Medical Center, Brooklyn, NY,[b] and Cornell University, Ithaca, NY[c]

Funding sources: None.

Conflict of interests: Dr Rao is a consultant for CaliberID. Ms Giambrone, Dr Bronsnick, Ms Masud, and Dr Alamgir have no conflicts to declare.

IRB status: Rutgers, reapproved on Nov 7, 2014, entitled "Confocal Microscopy of Suspicious Lesions."

New York and New Jersey, Quorum IRB, re-approved Dec 14, 2014 entitled "In Vivo Confocal Microscopy of Suspicious Lesions."

Correspondence to: Danielle Giambrone, BS, 1 World's Fair Drive, Suite 2400, Somerset, NJ 08873-1344

E-mail: Daniellegiam10@gmail.com

REFERENCES

1. Ahlgrimm-Siess V, Hofmann-Wellenhof R, Cao T. Reflectance confocal microscopy in the daily practice. *Semin Cutan Med Surg.* 2009;28:180-189.
2. Rao BK, Mateus R, Wassef C, et al. In vivo confocal microscopy in clinical practice: comparison of bedside diagnostic accuracy of a trained physician and distant diagnosis of an expert reader. *J Am Acad Dermatol.* 2013;69:295-300.
3. Terushkin V, Warycha M, Levy M, et al. Analysis of the benign to malignant ratio of lesions biopsied by a general dermatologist before and after adoption of dermoscopy. *Arch Dermatol.* 2010; 146:343-344.

http://dx.doi.org/10.1016/j.jaad.2015.03.052

Sensitivity of handheld reflectance confocal microscopy for the diagnosis of basal cell carcinoma: A series of 344 histologically proven lesions

To the Editor: Most studies about the sensitivity of reflectance confocal microscopy (RCM) for the diagnosis of the basal cell carcinoma (BCC) are based on the retrospective analysis of the RCM images acquired by the traditional wide-probe (TWP)-RCM. We evaluated the sensitivity of handheld (HH)-RCM for the diagnosis of BCC in clinical practice. All histologically confirmed BCCs excised at the University Hospital of Saint-Etienne, France, that underwent a HH-RCM (VivaScope 3000; MAVIG GmbH, München, Germany) examination between 2011 and 2014 were included. RCM examination was dedicated to cases from which a biopsy specimen was obtained because they were equivocal at dermoscopy. BCCs of the eyelid margin were excluded.[1] HH-RCM diagnosis was retrospectively searched in the patient's clinical records.

The diagnosis of BCC was established in the presence of tumor islands of tightly packed cells with or without peripheral palisading of elongated cells, or if ≥2 of the following criteria were present: dark silhouette with peripheral thickened collagen bundles, dark peritumoral clefts, linear or convoluted dilated blood vessels, and polarized elongated cells in the epidermis (streaming).[2-4] All examinations were carried out by 3 dermatologists experienced with dermoscopy and who began reading RCM images in 2010.

Our study revealed excellent sensitivity of HH-RCM for the diagnosis of BCC in a series of 344 lesions (Table I). Interestingly, the sensitivity of 87.5% reported in 2011 suggests that BCC is easy to recognize with RCM even for dermatologists with little experience. A learning curve was noticed from 2011 to 2013/2014. Most misdiagnosed BCCs were not completely negative for BCC at RCM, but had equivocal images where it was difficult to affirm with certainty the presence of tumor islands and dark silhouettes.

No statistically significant difference in the sensitivity for different histologic subtypes and body sites was found for 2013 and 2014 (Table II; chi-squared test; $P > .05$).

The sensitivity in the last 2 years was similar to previous study data reported in the literature,[2-5] ranging from 93% to 100%. However, these studies cannot be directly compared with ours because all but 1 of these studies[5] were based on retrospective analysis of RCM images and not on the diagnoses performed at the patient's bedside. Moreover, they evaluated smaller series (39,[5] 45,[4] 52,[2] and 83[3]

Table I. Reflectance confocal microscopy sensitivity for basal cell carcinoma

	Year				
Number of BCCs	2011	2012	2013	2014	Total
Diagnosed by histopathology	280	196	281	232	989
Examined under RCM	88	84	76	96	344
Correctely diagnosed by RCM	77	76	72	90	315
Incorrectly diagnosed by RCM, n (%)					
Uncertain diagnosis of BCC	7 (8)	4 (4.8)	4 (5.3)	5 (5.2)	20 (5.8)
No elements of BCC	4 (4.5)	4 (4.8)	0	1 (1)	9 (2.6)
RCM sensitivity (%)	87.5	90.5	94.7	93.8	91.6*

BCC, Basal cell carcinoma; *RCM*, reflectance confocal microscopy.
*Mean RCM sensitivity.

Table II. Reflectance confocal microscopy sensitivity for basal cell carcinoma stratified by histologic subtype and localization

BCC features	No. of BCCs, n (%)	RCM sensitivity (%)	Confidence interval
Histologic subtype			
Nodular	76 (44.2)	94.7	89.6-99.7
Infiltrative	40 (23.2)	90.0	80.7-99.3
Superficial	56 (32.6)	96.4	>91.6
Location			
Trunk	39 (22.7)	97.4	>92.5
Face	119 (69.2)	93.3	88.8-97.8
Neck	4 (2.3)	100.0	—
Inferior limb	4 (2.3)	100.0	—
Upper limb	3 (1.7)	100.0	—
Scalp	2 (1.2)	100.0	—
Vulva	1 (0.6)	0.0	—

BCC, Basal cell carcinoma; *RCM*, reflectance confocal microscopy.

BCCs, respectively) and used different diagnostic criteria and different criteria threshold for BCC. HH-RCM was found to have a slightly lower sensitivity than TWP-RCM.[4] This could be related to the fact that HH-RCM acquires smaller images (1 mm in diameter vs 8 mm in diameter) and is more often used on the face, where hair follicles and dermal collagen architecture are more prominent and can mask tumor islands. In our experience, to help differentiate a hair follicle from a BCC tumor island we can move to the surface of the skin during RCM examination and check for the presence of a follicle orifice in its correspondence. Despite the drawback of the slightly reduced BCC detection rate, HH-RCM is handy, and its image acquisition is faster than TWP-RCM, making it more suitable for the clinical practice.

Elisa Cinotti, MD,[a] Cécile Jaffelin, MD,[a] Victoria Charriere, MD,[b] Pierre Bajard, MD,[b] Bruno Labeille, MD,[a] Alexander Witkowski, MD,[c] Frédéric Cambazard, PhD,[a] and Jean-Luc Perrot, MD[a]

Departments of Dermatology[a] and Pharmacology,[b] University Hospital of Saint-Etienne, Saint-Etienne, France, and the Department of Dermatology,[c] University Hospital of Modena and Reggio Emilia, Modena, Italy

Supported by a medical educational grant from F. Hoffmann-La Roche

Conflicts of interest: None declared.

Correspondence to: Elisa Cinotti, MD, Hôpital Nord, 42055 Saint Etienne Cedex 2, France

E-mail: elisacinotti@gmail.com

REFERENCES

1. Cinotti E, Perrot JL, Campolmi N, et al. The role of in vivo confocal microscopy in the diagnosis of eyelid margin tumors: 47 cases. *J Am Acad Dermatol*. 2014;71:912-918.e2.
2. Guitera P, Menzies SW, Longo C, et al. In vivo confocal microscopy for diagnosis of melanoma and basal cell carcinoma using a two-step method: analysis of 710 consecutive clinically equivocal cases. *J Invest Dermatol*. 2012;132:2386-2394.
3. Nori S, Rius-Díaz F, Cuevas J, et al. Sensitivity and specificity of reflectance-mode confocal microscopy for in vivo diagnosis of basal cell carcinoma: a multicenter study. *J Am Acad Dermatol*. 2004;51:923-930.
4. Castro RP, Stephens A, Fraga-Braghiroli NA, et al. Accuracy of in vivo confocal microscopy for diagnosis of basal cell carcinoma: a comparative study between handheld and wide-probe confocal imaging. *J Eur Acad Dermatol Venereol*. October 22, 2014. http://dx.doi.org/10.1111/jdv.12780 [Epub ahead of print].
5. Pellacani G, Pepe P, Casari A, Longo C. Reflectance confocal microscopy as a second-level examination in skin oncology improves diagnostic accuracy and saves unnecessary excisions: a longitudinal prospective study. *Br J Dermatol*. 2014;171:1044-1051.

http://dx.doi.org/10.1016/j.jaad.2015.04.048

2.a 7 In vivo confocal microscopic substrate of grey colour in melanosis

Background

Melanosis is the most common cause of mucosal pigmentation and can be clinically difficult to differentiate from early melanoma (MM). Dermoscopy can help in the distinction between melanosis and MM, but in some instances, melanoses may exhibit overlapping features with MM such as the presence of grey colour.

Objective

We sought to evaluate whether reflectance confocal microscopy (RCM) can help to better understand the dermoscopic features of melanoses in order to assist clinicians in their diagnosis.

Methods

All melanoses diagnosed between June 2011 and December 2014 in the Departments of Dermatology of the University of Saint-Etienne (France) and of Modena and Reggio Emilia (Italy), for which dermoscopic and RCM images were available, were included. Twenty-two lesions were biopsied to confirm the clinical diagnosis, whereas the others did not present any change at a follow-up of at least 6 months. The correlation between dermoscopic and RCM features were evaluated by the Spearman's rho correlation coefficient.

Results

55 melanoses were studied: 31 of the oral mucosa and 24 of the genital mucosa. 49% (n = 27) of melanoses exhibited a grey colour under dermoscopy. The grey colour correlated with the presence of melanophages under RCM (q = 0.424, P = 0.002).

Conclusion

Our findings highlight that the presence of the grey colour on dermoscopy, considered as an alerting fea- ture, is common in melanoses and it is related to the presence of melanin-laden inflammatory cells in the papillary dermis on RCM. When it is present as a 'pure' feature not associated to other colours than brown or to atypical dermoscopical structures, it could be related to the diagnosis of melanosis.

DOI: 10.1111/jdv.13394 JEADV

ORIGINAL ARTICLE

In vivo confocal microscopic substrate of grey colour in melanosis

E. Cinotti,[1,*] C. Couzan,[1] J.L. Perrot,[1] C. Habougit,[2] B. Labeille,[1] F. Cambazard,[1] E. Moscarella,[3] A. Kyrgidis,[3] G. Argenziano,[3] G. Pellacani,[4] C. Longo[3]

[1]Department of Dermatology, University Hospital of Saint Etienne, Saint Etienne, France
[2]Department of Pathology, University Hospital of Saint Etienne, Saint Etienne, France
[3]Skin Cancer Unit, Arcispedale S. Maria Nuova-IRCCS, Reggio Emilia, Italy
[4]Department of Dermatology, University of Modena and Reggio Emilia, Modena, Italy
*Correspondence: E. Cinotti. E-mail: elisacinotti@gmail.com

Abstract

Background Melanosis is the most common cause of mucosal pigmentation and can be clinically difficult to differentiate from early melanoma (MM). Dermoscopy can help in the distinction between melanosis and MM, but in some instances, melanoses may exhibit overlapping features with MM such as the presence of grey colour.

Objective We sought to evaluate whether reflectance confocal microscopy (RCM) can help to better understand the dermoscopic features of melanoses in order to assist clinicians in their diagnosis.

Methods All melanoses diagnosed between June 2011 and December 2014 in the Departments of Dermatology of the University of Saint-Etienne (France) and of Modena and Reggio Emilia (Italy), for which dermoscopic and RCM images were available, were included. Twenty-two lesions were biopsied to confirm the clinical diagnosis, whereas the others did not present any change at a follow-up of at least 6 months. The correlation between dermoscopic and RCM features were evaluated by the Spearman's rho correlation coefficient.

Results 55 melanoses were studied: 31 of the oral mucosa and 24 of the genital mucosa. 49% (n = 27) of melanoses exhibited a grey colour under dermoscopy. The grey colour correlated with the presence of melanophages under RCM (ρ = 0.424, P = 0.002).

Conclusion Our findings highlight that the presence of the grey colour on dermoscopy, considered as an alerting feature, is common in melanoses and it is related to the presence of melanin-laden inflammatory cells in the papillary dermis on RCM. When it is present as a 'pure' feature not associated to other colours than brown or to atypical dermoscopical structures, it could be related to the diagnosis of melanosis.

Received: 3 June 2015; Accepted: 27 July 2015

Conflict of interest

The authors declare no conflicts of interest to disclose.

Funding sources

Dr Cinotti was supported by the grant 'bourse d'aide à la mobilité' from the College des Enseignants de Dermatologie de France CEDEF.

Introduction

Melanosis, also called melanotic macule and mucosal-pigmented macule, is a benign pigmentation of the mucosa, corresponding to hyperpigmentation of basal keratinocytes with possible slight proliferation of melanocytes at the epithelial-chorion junction (ECJ). It is the most common cause of mucosal pigmentation and can be clinically difficult to differentiate from early melanoma (MM), especially when occurring on genitalia.[1,3] In fact, in this special body site, melanosis can reveal worrisome clinical features, as multiple, asymmetric macules or patches with variable colour and irregular and poorly demarcated borders.[3] To further complicate the matter, early mucosal MM can present as brown macule thus simulating a benign pigmentation which can lead to a misdiagnosis.[4]

A correct differential diagnosis between melanosis and MM is crucial to avoid unnecessary biopsies of the mucosa which is a sensitive tissue, and to avoid a delay in the diagnosis of mucosal MM. In fact, mucosal MM is often diagnosed too late with related poor prognosis, whereas its early identification and intervention could improve patient outcomes.[3]

Dermoscopy can help in the distinction between melanosis and MM, but in some instances, melanoses may exhibit overlapping features with MM such as the presence of grey colour associated to structureless pattern. Reflectance confocal microscopy (RCM) is a new non-invasive imaging technique that has recently shown its usefulness for the distinction between melanosis and MM.[4,5] In our study, we sought to evaluate whether RCM can help to disclose some dermoscopic features of melanoses that may assist clinicians to improve their diagnosis.

Materials and methods

All 55 flat-pigmented macules of the mucosa diagnosed as melanoses in the Departments of Dermatology of the University of Saint-Etienne (France) and of Modena and Reggio Emilia (Italy) and with available dermoscopic (FotoFinder Systems GmbH, Germany, combined with Canon PowerShot G10 camera, Canon New York, NY, USA, and Dermlite Photo®, 3gen, San Juan Capistrano, CA USA combined with Canon PowerShot G15 camera) and RCM images (Vivascope 1500® or 3000®, MAVIG Gmbh, Munich, Germany) were included between June 2011 and December 2014. Twenty-two lesions were biopsied to confirm the clinical diagnosis, whereas the others did not present any change at a follow-up of at least 6 months.

Clinical characteristics including patient age and gender and melanosis body site were recorded. Dermoscopic and RCM features were retrospectively evaluated. Three dermatologists (C.L., G.A., E.M.) jointly reviewed all digital dermoscopic images whereas RCM images were evaluated by one investigator (E.C.) in blind for dermoscopic images.

Colours (brown, grey, red, blue, white, black, purple) and patterns (parallel lines, reticular lines, curved lines, circles, structureless, globules, dots) previously described by Blum *et al.*[6] were assessed for each dermoscopic image. It should be noticed that some patterns assume different names according to different studies: parallel lines are elsewhere called 'finger-print',[7] circles 'ring-like'[2,7,8] pattern and structureless pattern 'homogeneous pigmentation'.[7,8]

RCM images were evaluated for the shape of the dermal papillae (ringed or draped pattern or both),[5] for the presence of suprabasal pigmentation (absent, focal or homogeneous) and of melanophages (absent or present in the papillary dermis) and dendritic cells (absent, rare in the basal layer, abundant in the basal layer, present in both the basal and the supra-basal layers). All histopathological sections were reviewed in light of the RCM results.

Absolute and relative frequencies of dermoscopic and RCM features were calculated. The correlation between (i) dermoscopic features and different body sites, (ii) RCM features and different body sites and (iii) dermoscopic pattern and RCM features were evaluated by the Spearman's correlation coefficient (ρ). We used univariate logistic regression to quantify associations that reached significance. A P-value less than 0.05 was considered statistically significant.

Results

Descriptive statistics

Fifty-five melanoses were included from 14 (25.5%) men and 41 (74.5%) women. The mean age of the patients was 42.5 (standard deviation: 12.5) years. Thirty-one lesions were located in the oral mucosa and 24 in the genital mucosa. Two lesions were located in the gum, five in the upper lip, 24 in the lower lip, seven in the glans, two in the prepuce, 15 in the vulva (13 in the labia minora and two in the medial part of labia majora).

Dermoscopic features Dermoscopic features are reported in Table 1. Parallel lines were found in 43% ($n = 24$) of patients, reticular lines in 9% ($n = 5$), curved lines in 36% ($n = 20$), circles in 22% ($n = 12$), structureless pattern in 24% ($n = 13$), globules in 9% ($n = 5$) and dots in 3% ($n = 2$). Concerning the number of different dermoscopic pattern: in 63% ($n = 35$) cases only one dermoscopic pattern, in 27% ($n = 15$) two dermoscopic patterns and in 9% ($n = 5$) three dermoscopic patterns were present.

In 89% ($n = 49$) of melanoses the brown colour, in 49% ($n = 27$) the grey colour and in 7% ($n = 4$) the red colour were present. Blue, white, black and purple colours were never observed. In 55% ($n = 29$) of lesions only one colour was present, in 45% ($n = 25$) two colours. 11% ($n = 6$) lesions were only grey. No more than two colours were present simultaneously in a given lesion.

Reflectance confocal microscopy features RCM features are reported in Table 2. Melanophages were present in 56% ($n = 31$) of lesions. A ringed pattern was present in 78%

Table 1 Dermoscopic features of melanoses

Localization	Reticular lines	Parallel lines	Curved lines	Circles	Structureless	Globules	Dots	Brown	Grey	Red
Oral mucosa (n – 31)	3	12	13	3	10	2	1	27	16	1
Male genital mucosa (n – 9)	2	4	2	0	0	3	1	9	1	2
Female genital mucosa (n – 15)	0	8	5	9	3	0	0	13	10	1
Total (n – 55)	5	24	20	12	13	5	2	49	27	4

Table 2 Reflectance confocal microscopy features of melanoses

Localization	Ringed papillae	Drapped papillae	Ringed and drapped papillae	Suprabasal pigmentation	Melanophages	Basal dendritic cells	Suprabasal dendritic cells
Oral mucosa (n – 31)	25	6	2	5	22	7	5
Male genital mucosa (n – 9)	6	3	0	2	0	4	0
Female genital mucosa (n – 15)	12	3	0	2	9	4	0
Total (n – 55)	43	12	2	9	31	15	5

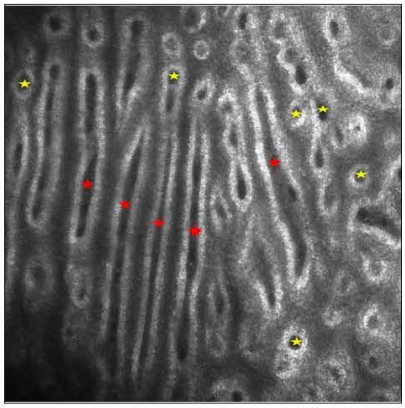

Figure 1 Reflectance confocal microscopy aspect of a melanosis showing a combination of both a ringed (yellow stars) and a draped (red stars) pattern.

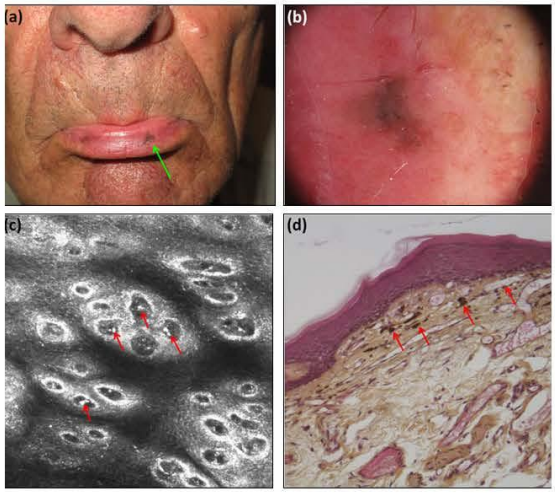

Figure 2 Clinical (a), dermoscopical (b), reflectance confocal microscopy (RCM) (c) and histological (d) aspect of a grey melanosis of the lower lip (green arrow). Dermoscopy (b) showed a structureless brown and grey pigmentation. RCM (c) showed a ringed pattern with hyper-reflective melanophages (red arrows) inside the papillae. The histological examination (d) confirmed the presence of melanophages (red arrows) in the papillary dermis (hematoxilin and eosin, ×20).

(n = 43), a draped pattern in 18% (n = 10), a combination of both a ringed and a draped pattern in 4% (n = 2) (Fig. 1).

Suprabasal pigmentation was found in 16% (n = 9) of cases: focal in 4% (n = 2) and homogeneous in 13% (n = 7). Dendritic cells were found in 36% (n = 20) of cases. They were in the basal layer in 27% (rare in 14%, n = 8, and abundant in 13%, n = 7) and in the basal and suprabasal layers in 9% (n = 5).

Histological features All 16 biopsied grey melanoses showed melanophages. In five grey lesions melanophages were present under histological examination but not upon RCM.

Analytical statistics

Circles were associated with the female genital mucosa and in particular with the medial surface of the labium minor (ρ = 0.411, P = 0.002), whereas they were uncommon in the oral mucosa and absent in the male genital mucosa. Parallel lines were associated with the presence of curved lines (ρ = 0.402, P = 0.002) and inversely correlated with the structureless pattern (ρ = −0.490, P = 0.0009).

Concerning the correlation between dermoscopy and RCM features, grey colour correlated with the presence of melanophages (ρ = 0.424, P = 0.002). More specifically, the odds of detecting melanophages are at least sixfold higher when the dermoscopic image exhibits grey colour (OR = 6.30, 95% Confidence Interval: 1.91 20.74, P = 0.002) (Fig. 2). In addition, grey colour was associated with the presence of circles (ρ = 0.362, P = 0.007).

Discussion

Few studies evaluated dermoscopic features of melanosis[1,2,6 8] and two of them are dedicated to vulvar lesions.[2,8] They highlight that a brown colour and a structureless,[1,2,6] or circle,[2,6,7] or parallel[1,2,6,7] pattern are the most common features of melanosis

and can be used for their non-invasive diagnosis.[1,2,8] However, melanoses may sometimes exhibit a grey, blue, white or black colour[1,2,6,8] or a mixed pattern that are more frequently found in MM.[7] Moreover, the structureless pattern observed in melanoses is also common in mucosal MM.[6,7]

In our study, nearly half of the lesions presented with a grey colour in addition to a brown one and this aspect would have been considered suspicious of MM according to the first model of Blum *et al.*[6] Nearly a quarter of the lesions exhibited a structureless pattern and four lesions had both a structureless pattern and a grey colour that increase the suspicion for MM diagnosis.[6] Notably, the structureless pattern was mainly found on the oral mucosa and also in the four grey cases. The other grey cases mainly had parallel lines and/or curved lines and/or or circles that are rarely associated with MM.[6] In particular, quite all lesions with circles were grey and this pattern was mainly found in the female genital mucosa.

Moreover, around one-third of melanoses had more than one dermoscopic pattern, rendering more challenging the differential diagnosis with MM. However, most of these cases only had two patterns and those that had three patterns were characterized by the presence of parallel lines and curved lines and circles, that are less common in MM.[6] Interestingly, parallel lines were associated with the presence of curved lines, probably related to a similar anatomical substrate (elongated papillae, more or less separated among them, giving coupled or single lines).

Curiously there were no cases with blue, white, black or purple pigmentation and, as already reported,[8] none of the melanoses had more than two colours. It should be noticed that, when considering the colours of a mucosal lesion, we should not consider the overlapped structures of the normal mucosa such as the vessels and the glands that form red and white structures and are also present in the surrounding tissue.

As expected in pigmented lesions, RCM showed hyper-reflective keratinocytes at the ECJ in all cases. These keratinocytes rimmed the dermal papillae that were mainly roundish (ringed pattern) and sometimes elongated (draped pattern). In few lesions of the oral mucosa the two patterns coexisted.

As already pointed out in previous studies,[4,5] dendritic cells were a possible finding in the epithelium of more than a third of cases. They were of small in size and mainly confined in the basal layer of the epithelium around the dermal papillae, rendering possible a differential diagnosis with malignant melanocytes that are preferentially located in the suprabasal layer (pagetoid scattering). Only in the oral mucosa dendritic cells were found in the suprabasal layers in a small number of cases. In a large part of these cases with dendritic cells in the epithelium, melanophages were also seen, confirming the presence of inflammation.

No association was found between any particular RCM feature and any specific body site. Moreover, we could not demonstrate any correlation between a particular dermoscopic pattern and the shape of the dermal papillae, the presence of a suprabasal pigmentation or the presence of the dendritic cells in the epithelium under RCM. Interestingly, melanophages highly correlated with the presence of grey colour on dermoscopy. This aspect underlines that RCM could be used in case of grey mucosal lesions in order to look for the presence of melanophages that could justify the worrisome grey colour of some benign mucosal lesions. In the absence of RCM that can demonstrate the presence of melanophages, our study highlighted that grey melanoses usually do not present additional features evocative of MM under dermoscopy, such as the presence of more than two colours and multiple patterns, especially the structureless pattern, reticular lines and dots that are more common in MM.[6] The possible presence of melanophages in melanoses is well-known[9] and in our study all biopsied grey lesions showed melanophages on histological examination. In few lesions melanophages were present under histological examination but not upon RCM. This could be possibly related to the RCM image sampling that partially explored the lesions. Our study has the limitation that only melanosis was included in the study population and thus, the presence of grey colour was not assessed in MMs. Moreover, another limitation of the current study is the small sample size, despite the cooperation of three tertiary referral centres with experience in both RCM and dermoscopy. For that, we cannot reject the hypothesis that other dermoscopic features are also correlated with RCM features in melanoses, but our study was not adequately powered to detect them.

In conclusion, our study confirmed that melanoses usually have less than two colours and few dermoscopical patterns (rarely more than two patterns, and in case of three patterns parallel and curved lines and circles were present in our series). Moreover, our findings highlighted that the presence of grey colour on dermoscopy, considered as an alerting feature for MM, could be related to the presence of melanin-laden inflammatory cells in the superficial dermis on RCM and thus, when it is present as a 'pure' feature not associated to other colours than brown or to atypical dermoscopical structures, is related to the diagnosis of melanosis. This could help clinicians to differentiate melanosis from early MM although larger prospective studies are warranted to demonstrate this finding in the clinical setting.

References

1 Mannone F, De Giorgi V, Cattaneo A, Massi D, De Magnis A, Carli P. Dermoscopic features of mucosal melanosis. *Dermatol Surg* 2004; **30**: 1118 1123.

2 Ferrari A, Buccini P, Covello R *et al.* The ringlike pattern in vulvar melanosis: a new dermoscopic clue for diagnosis. *Arch Dermatol* 2008; **144**: 1030 1034.

3 Murzaku EC, Penn LA, Hale CS, Pomeranz MK, Polsky D. Vulvar nevi, melanosis, and melanoma: an epidemiologic, clinical, and histopathologic review. *J Am Acad Dermatol* 2014; **71**: 1241 1249.

4 Debarbieux S, Perrot JL, Erfan N *et al.* Reflectance confocal microscopy of mucosal pigmented macules: a review of 56 cases including 10 macular melanoma. *Br J Dermatol* 2014; **70**: 1276 1284.

5 Cinotti E, Perrot JL, Labeille B, Adegbidi H, Cambazard F. Reflectance confocal microscopy for the diagnosis of vulvar melanoma and melanosis: preliminary results. *Dermatol Surg* 2012; **38**: 1962 1967.
6 Blum A, Simionescu O, Argenziano G *et al.* Dermoscopy of pigmented lesions of the mucosa and the mucocutaneous junction: results of a multicenter study by the International Dermoscopy Society (IDS). *Arch Dermatol* 2011; **147**: 1181 1187.
7 Lin J, Koga H, Takata M, Saida T. Dermoscopy of pigmented lesions on mucocutaneous junction and mucous membrane. *Br J Dermatol* 2009; **161**: 1255 1261.
8 Ronger-Savle S, Julien V, Duru G, Raudrant D, Dalle S, Thomas L. Features of pigmented vulval lesions on dermoscopy. *Br J Dermatol* 2011; **164**: 54 61.
9 Calonje E, Neill S. Disease of the genital skin. In: McKee PH, Calonje E, Granter S, eds. Pathology of the Skin With Clinical Correlation, 3rd edn. Elsevier, China, 2005: 511.

2. a 8 Reflectance confocal microscopy features of acral lentiginous melanoma: a comparative study with acral nevi.

Background

Acral lentiginous melanoma (ALM) can be difficult to differentiate from acral nevus. Reflectance confocal microscopy (RCM) is widely used for the diagnosis of melanocytic tumours, but the RCM features of ALM and acral nevus have not been described yet.

Objective

To determine the RCM features of ALM and acral nevus, and their correlation with clinical and histological characteristics.

Methods Retrospective study of 17 cases of ALM and 26 acral nevi.

Results

Pagetoid cells were present in all ALMs with a visible epidermis and in three nevi. A proliferation of atypical melanocytes at the dermal–epidermal junction (DEJ) and/or in the dermis was visible in nine ALMs but not in nevi. The histopathological examination of initial skin biopsies was unable to diagnose ALM in four cases, differing from RCM that could identify malignant tumour cells by exploring the whole lesions.

Conclusion

Reflectance confocal microscopy can help in the differentiation of ALM and acral nevus, and to guide the biopsy.

DOI: 10.1111/jdv.13399 JEADV

SHORT REPORT

Reflectance confocal microscopy features of acral lentiginous melanoma: a comparative study with acral nevi

E. Cinotti,[1,*,†] S. Debarbieux,[2,†] J.L. Perrot,[1] B. Labeille,[1] E. Long-Mira,[3] C. Habougit,[4] C. Douchet,[4] L. Depaepe,[5] H. Hammami-Ghorbel,[3] J.P. Lacour,[3] L. Thomas,[2] F. Cambazard,[1] P. Bahadoran,[3,6] on behalf of the Groupe Imagerie Cutanée Non Invasive de la Société Française de Dermatologie

[1]Dermatology Department, CHU of Saint-Etienne, Saint Etienne, France
[2]Dermatology Department, Hospices Civils of Lyon, Lyon, France
[3]Pathology Department, LPCE, CHU of Nice, Nice, France
[4]Pathology Department, CHU of Saint-Etienne, Saint-Etienne, France
[5]Pathology Department, Hospices Civils of Lyon, Lyon, France
[6]Centre de Recherche Clinique, INSERM U 1065 Equipe 1 CHU of Nice, Nice, France
*Correspondence: E. Cinotti. E-mail: elisacinotti@gmail.com

Abstract

Background Acral lentiginous melanoma (ALM) can be difficult to differentiate from acral nevus. Reflectance confocal microscopy (RCM) is widely used for the diagnosis of melanocytic tumours, but the RCM features of ALM and acral nevus have not been described yet.

Objective To determine the RCM features of ALM and acral nevus, and their correlation with clinical and histological characteristics.

Methods Retrospective study of 17 cases of ALM and 26 acral nevi.

Results Pagetoid cells were present in all ALMs with a visible epidermis and in three nevi. A proliferation of atypical melanocytes at the dermal–epidermal junction (DEJ) and/or in the dermis was visible in nine ALMs but not in nevi. The histopathological examination of initial skin biopsies was unable to diagnose ALM in four cases, differing from RCM that could identify malignant tumour cells by exploring the whole lesions.

Conclusion Reflectance confocal microscopy can help in the differentiation of ALM and acral nevus, and to guide the biopsy.

Received: 1 May 2015; Accepted: 5 August 2015

Conflicts of interest

None declared.

Funding source

None.

Introduction

The diagnosis of Acral Lentiginous Melanoma (ALM) is often delayed.[1,2] Histopathology can also be of difficult interpretation due to partial biopsies or incipient tumours with scant malignant cells.

Reflectance confocal microscopy (RCM) is a non-invasive *in vivo* imaging technique that enables dermatologists to examine cutaneous lesions down to a cellular resolution. RCM features of special body site melanomas such as lentigo maligna[3–5] and mucosal melanoma[6–8] have been extensively reported, but RCM features of ALM have been described only in one case report.[9] Here, we compared RCM features of ALMs and acral nevi in a case series.

Materials and methods

Reflectance confocal microscopy images of 17 ALMs and 26 acral nevi from consecutive patients (13 women, four men, mean age 72.2 years, range 54 88 years for melanoma; 19 women, seven men, mean age 38.5 years, range 13 70 years for nevi) were retrospectively studied. All ALMs and 12 acral nevi were histologically confirmed. The excised nevi presented with dermoscopic and/or clinical atypical features; all other nevi did not present any changes at a follow-up of at least 1 year. Five melanomas were *in situ*, 12 invasive, nine of the latter ulcerated.

†These authors contributed equally.

Clinical, dermoscopic and RCM features were evaluated by three dermatologists. Five ALMs were located on the hands and 12 on the feet. Nine ALMs were nodules or plaques, and eight were flat lesions. Six ALMs were hypomelanotic. Dermoscopy showed an involvement of the ridges in all pigmented ALMs (parallel ridge pattern in five, structureless pigmentation encompassing ridges and furrows in six). In hypomelanotic ALMs, atypical vessels were seen in three cases and milky-red areas in two; two lesions were too bloody and crusty for dermoscopy.

All nevi presented as brown macules; two had a raised central part; two had a greyish part; one had a bluish area. Dermoscopy identified atypical features in nine cases and found a pigmentation of the ridges in seven.

Reflectance confocal microscopy imaging was performed using Vivascope 1500® or the hand-held Vivascope 3000® camera (Caliber, New York, NY, USA) in nail fold and in nodular and ulcerated lesions. A skin scraping was performed in three ALMs in order to reduce stratum corneum thickness.

First, normal acral skin was evaluated. Concerning the tumours, the epidermis was evaluated identifying three possible patterns: (i) honeycombed pattern, formed by 10 20 μm polygonal keratinocytes with dark nuclei and bright membranes, (ii) irregular honeycomb pattern, in case of focal alteration of the normal architecture of the epidermis and (iii) disarranged pattern, characterized by complete disarray of the normal architecture. The presence, density, shape, pleomorphism and localization (around acrosyringia or not) of pagetoid cells (typically large hyper-reflective cells within the epidermis) were evaluated. The presence of granular dust-like hyper-reflective particles in the epidermis, and of junctional and/or dermal melanocytic nests or proliferations of atypical cells was also assessed.

The chi-squared test corrected for continuity (Yates value) was used to analyse RCM features of nevi and ALM. A *P*-value less than 0.01 was considered statistically significant.

Results

In normal acral skin, RCM showed a hyper-reflective inhomogeneous upper layer (stratum corneum) and, lower in the epidermis, parallel bands of honeycomb pattern (ridges) alternating to dark areas (furrows) (Fig. 1).

Reflectance confocal microscopy allowed to image up to the superficial dermis in 21 nevi. In ALMs, the epidermis was well recognizable in 14 cases (three cases had a severe epidermis consumption), the DEJ in four (seven cases had a DEJ disrupted by the tumour cell proliferation) and the dermis in nine (mainly in advanced ulcerated ALM characterized by a consumption of the epidermis).

Lesions of the fingers allowed a deeper imaging in relation to the thinner epidermis. Concerning the epidermis, ALMs had an irregular honeycomb (*in situ* ALM) or a disarranged (invasive ALM) pattern, whereas all nevi showed a honeycomb pattern.

We found a difference in pagetoid cell frequency in ALM and nevi ($P < 0.0001$). Infiltration of the epidermis by numerous single or grouped melanocytes characterized all ALMs with a visible epidermis (Figs 2 and 3). In ALMs, pagetoid cells were roundish (15 cases) and/or dendritic (seven cases) and/or triangular (three cases). They were pleomorphic in shape in seven cases and in size in seven additional cases, and they were located around acrosyringia (Figs 2 and 3) in nine.

Pagetoid cells were found in three nevi (dendritic in two cases and roundish and dendritic in one; around acrosyringia in one). Small dendritic hyper-reflective cells in the epidermis corre-

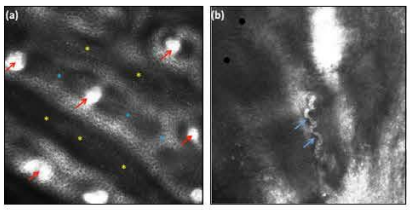

Figure 1 *In vivo* reflectance confocal microscopy (RCM) aspect of the normal epidermis from acral skin of palm and sole. Ridges appear as broad parallel bands with a regular honeycomb pattern (a, blue asterisk), and furrows as parallel dark areas disrupting the honeycomb pattern (a, yellow asterisk). Acrosyringia appear as bright roundish circles plugged in lines in the centre of the honeycomb pattern (a, red arrow) or as hyper-reflective coiled structures (b, blue arrow) when the image plan is not exactly horizontal. Hair follicles are absent.

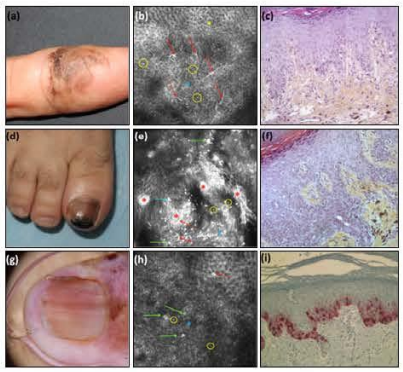

Figure 2 Clinical (a, d, g), *in vivo* reflectance confocal microscopy (RCM) (b, e, h) and histological (c, f, i; haematoxylin and eosin stain, 20 ×) aspect of three *in situ* acral lentiginous melanomas. RCM shows an irregular honeycomb (b, yellow asterisk) and a disarranged pattern (b, e, h blue asterisk) of the epidermis, dendritic (red arrow), roundish (green arrow) and triangular (blue arrow) pagetoid cells, and granular dust-like hyper-reflective particles (yellow circles) in the epidermis. Acrosyringia are indicated by red asterisks.

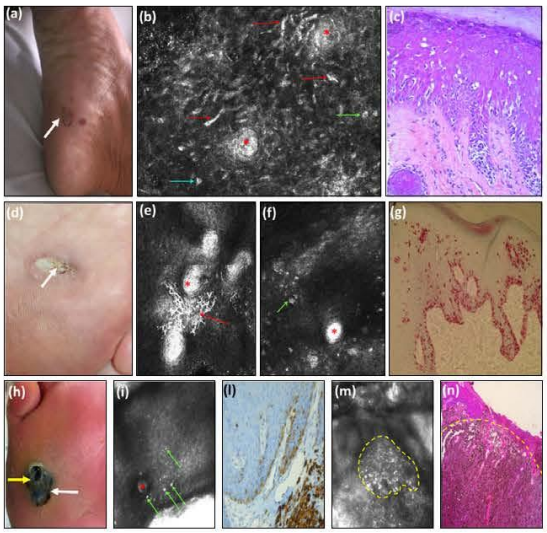

Figure 3 Clinical (a, d, h), *in vivo* reflectance confocal microscopy (RCM) (b, e, f, i, m) and histological (c, 20× and n, 10×, hematoxylin and eosin stain; g and l, 20× melanA stain) aspect of three invasive non-ulcerated (first two cases) and ulcerated (third case) acral lentiginous melanomas. Dendritic (red arrow), roundish (green arrow) and triangular (blue arrow) pagetoid cells are visible in the epidermis, and especially around acrosyringia (red asterisk). For the first and second tumour, RCM images of the epidermis are available (b, e, f) (from the part of the tumour, indicated by the white arrow on the clinical images a and d). For the third tumour, RCM images of both the epidermis (i) (from the peripheral part of the tumour, indicated by the white arrow on the clinical image h) and the dermis (M) (from the central part of the tumour, indicated by the yellow arrow on the clinical image h) are available. A proliferation of roundish cells (yellow dotted line) is visible in the dermis under a thin epidermis destroyed by the tumour proliferation (M).

sponding to Langerhans cells were found in other three nevi. Granular dust-like hyper-reflective particles in the epidermis were more frequently found in ALMs (all ALMs and seven nevi; $P < 0.0001$).

A proliferation of atypical melanocytes was visible at the DEJ and in the dermis in four and nine ALMs respectively (Fig. 3). Atypical cells in the dermis were large, mainly roundish, and sometimes dendritic or triangular. In five cases, they were pleomorphic in size and shape. They were mainly in sheets and in only one case, arranged in nests. In the centre of the ulcerated tumours, tumour cells were difficult to identify because of the presence of blood cells and skin debris.

In nevi, we found regular melanocytic nests at the DEJ in 14 cases and in the superficial dermis in nine (Fig. 4). In one nevus, with a blue nevus component, homogeneous dendritic melanocytes were visible in the dermis. In seven nevi, it was not possible to identify any melanocytic proliferation and five of

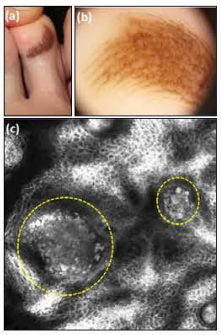

Figure 4 *In vivo* reflectance confocal microscopy of an acral nevus. Nests of homogeneous melanocytes (red circles) are visible inside dermal papillae.

these lesions corresponded to the cases where RCM could not reach the DEJ.

Interestingly, RCM was reassuring in five out of nine nevi suspicious at dermoscopy. For the other four cases: RCM found pagetoid cells in two lesions and was unable to detect any melanocytic proliferation in two.

In three *in situ* ALMs and in one invasive non-ulcerated ALM, the initial histopathology on skin biopsies diagnosed benign lesions and RCM findings incited to perform new biopsies.

Discussion

The clinical and histological diagnosis of ALM may be very difficult, especially in the early phase of growth. Dermoscopy may be useful for the diagnosis.[1] However, *in situ*, amelanotic, nodular or ulcerated lesions can lack specific dermoscopic criteria. In one *in situ* ALM, the only dermoscopic sign of melanoma was the ridge pigmentation in a small area, and in two ulcerated ALMs only crusts and blood were visible at the surface. Moreover, in nine nevi, dermoscopy was suspicious.

Palms and soles are rarely studied by RCM because of the increased thickness of the epidermis that hampers the visualization of deeper layers. However, early ALM is characterized by a lentiginous spread[10] and the epidermal thickness of acral areas is variable.

We found that pagetoid cells were the predominant clue for suspecting ALM by RCM. The pagetoid spread of melanocytes also determined a disarrangement of the normal honeycomb pattern of the epidermis, feature that was not found in nevi. Pagetoid melanocytosis is a major RCM criteria of melanoma,[11 13] especially when there is marked cell density, polymorphism and widespread cell distribution as in our study. Noteworthy in cases with a thick stratum corneum, a skin scraping allowed us to identify pagetoid cells in the epidermis that was previously not visible. However, this procedure did not allow RCM to reach the DEJ.

It should be noticed that a proliferation of solitary arranged melanocytes can also be detected within the epidermis of MANIACs (melanocytic acral nevus with intraepidermal ascent),[14] as confirmed by our study. However, pagetoid cells in these cases were monomorphous.

A characteristic feature of some ALMs was the infiltration of sweat duct structures by atypical bright cells, that corresponds to a melanocytic extension along adnexal structures in histology.[10] Nevi show more rarely a melanocytic proliferation around sweet duct structures and in these cases, melanocytes are mainly organized in nests.[15] In our series of nevi, we found a case with pagetoid cells and six cases with junctional regular nests around acrosyringia.

Another peculiar feature of ALM in our series was the higher presence of granular dust-like hyper-reflective particles in the epidermis compared to nevi, possibly corresponding to free pigment. Free pigment is randomly distributed in ALMs and tends to be arranged in columns in the furrows in nevi.[15] In our series, we could not identify a different distribution. Therefore, the exact signification of granular dust-like particles remains to be demonstrated.

In all ALMs with a visible dermis, sheets and/or nests of large atypical cells were seen, whereas these features were never found in nevi.

Since ALMs are often difficult to excise due to the localization, biopsies are often performed before surgical excision. In our series, four ALMs were initially diagnosed as benign lesions on skin biopsies. These findings confirm the interest of RCM to guide biopsies in large lesions as reported for lentigo maligna[3,4] and pigmented mucosal lesions.[7]

Based on this case series, we suggest that RCM can provide sufficient arguments to suspect ALM and perform a surgical excision.

However, ALM diagnosis cannot be excluded in the absence of RCM signs because early ALM can present only subtle atypia such as slight proliferation of atypical melanocytes at the DEJ that may not be identified under RCM.

Acknowledgements

Dr Bruno Fouilloux, from the Dermatology Department of the University Hospital of Saint-Etienne, France, for referral of a patient.

References

1 Phan A, Touzet S, Dalle S, Ronger-Savlé S, Balme B, Thomas L. Acral lentiginous melanoma: histopathological prognostic features of 121 cases. *Br J Dermatol* 2007; **157**: 311 318.
2 Soon SL, Solomon AR, Papadopoulos D, Murray DR, McAlpine B, Washington CV. Acral lentiginous melanoma mimicking benign disease: the Emory experience. *J Am Acad Dermatol* 2003; **48**: 183 188.
3 Guitera P, Pellacani G, Crotty KA *et al.* The impact of in vivo reflectance confocal microscopy on the diagnostic accuracy of lentigo maligna and equivocal pigmented and nonpigmented macules of the face. *J Invest Dermatol* 2010; **130**: 2080 2091.
4 Champin J, Perrot J-L, Cinotti E *et al.* In vivo reflectance confocal microscopy to optimize the spaghetti technique for defining surgical margins of lentigo maligna. *Dermatol Surg* 2014; **40**: 247 256.
5 Ahlgrimm-Siess V, Massone C, Scope A *et al.* Reflectance confocal microscopy of facial lentigo maligna and lentigo maligna melanoma: a preliminary study. *Br J Dermatol* 2009; **161**: 1307 1316.
6 Cinotti E, Perrot JL, Labeille B, Adegbidi H, Cambazard F. Reflectance confocal microscopy for the diagnosis of vulvar melanoma and melanosis: preliminary results. *Dermatol Surg* 2012; **38**: 1962 1967.
7 Debarbieux S, Perrot JL, Erfan N *et al.* Reflectance confocal microscopy of mucosal pigmented macules: a review of 56 cases including 10 macular melanoma. *Br J Dermatol* 2013; **170**: 1276 1284.
8 Cinotti E, Perrot JL, Campolmi N *et al.* The role of in vivo confocal microscopy in the diagnosis of eyelid margin tumors: 47 cases. *J Am Acad Dermatol* 2014; **71**: 912 918.
9 Kolm I, Kamarashev J, Kerl K *et al.* Acral melanoma with network pattern: a dermoscopy-reflectance confocal microscopy and histopathology correlation. *Dermatol Surg* 2010; **36**: 701 703.
10 Phan A, Touzet S, Dalle S, Ronger-Savlé S, Balme B, Thomas L. Acral lentiginous melanoma: histopathological prognostic features of 121 cases. *Br J Dermatol* 2007; **157**: 311 318.
11 Pellacani G, Cesinaro AM, Seidenari S. Reflectance-mode confocal microscopy of pigmented skin lesions improvement in melanoma diagnostic specificity. *J Am Acad Dermatol* 2005; **53**: 979 985.
12 Pellacani G, Guitera P, Longo C, Avramidis M, Seidenari S, Menzies S. The impact of in vivo reflectance confocal microscopy for the diagnostic accuracy of melanoma and equivocal melanocytic lesions. *J Invest Dermatol* 2007; **127**: 2759 2765.
13 Segura S, Puig S, Carrera C, Palou J, Malvehy J. Development of a two-step method for the diagnosis of melanoma by reflectance confocal microscopy. *J Am Acad Dermatol* 2009; **61**: 216 229. 20.
14 LeBoit PE. A diagnosis for maniacs. *Am J Dermatopathol* 2000; **22**: 556 558.
15 Saida T, Koga H, Goto Y, Uhara H. Characteristic distribution of melanin columns in the cornified layer of acquired acral nevus: an important clue for histopathologic differentiation from early acral melanoma. *Am J Dermatopathol* 2011; **33**: 468 473.

2. a 9 The role of reflectance confocal microscopy in the diagnosis of cutaneous melanoma metastasis

Annales de dermatologie et de v n r ologie (2016) 143, 863—865

Disponible en ligne sur ScienceDirect www.sciencedirect.com

Elsevier Masson France EM|consulte www.em-consulte.com

Formation médicale continue

FICHE TH MATIQUE / MICROSCOPIE CONFONCALE PAR R FLECTANCE

Apport de la microscopie confocale par r flectance dans le diagnostic de m tastase cutan e de m lanome

The role of reflectance confocal microscopy in the diagnosis of cutaneous melanoma metastasis

J.-L. Perrot[a], B. Labeille[a], C. Habougit[b], C. Douchet[b], L. Tognetti[c], F. Cambazard[a], E. Cinotti[a,*], groupe d'imagerie cutan e non invasive (ICNI) de la Soci t française de dermatologie

[a] *Service de dermatologie, h pital universitaire de Saint- tienne, 42055 Saint- tienne cedex 2, France*
[b] *Service d'anatomopathologie, h pital universitaire de Saint- tienne, 42055 Saint- tienne cedex 2, France*
[c] *Service de dermatologie, h pital universitaire de Siena, AOUS « Le Scotte », 16, viale Bracci, 53100 Siena, Italie*

Reçu le 25 mars 2016 ; accept le 3 mai 2016
Disponible sur Internet le 11 juillet 2016

Observation

Une femme de 88 ans tait examin e dans le cadre de la surveillance semestrielle d'un m lanome de la jambe gauche de niveau de Clark 4 et d'indice de Breslow 0,8 mm op r deux ans plus t t. Nous constations la pr sence d'une micropapule brun tre de 3 mm de diam tre de la jambe gauche non r f renc e jusqu'alors dans le dossier m dical (Fig. 1a). Un examen en dermatoscopie montrait un patron mixte associant une partie homog ne ryth mateuse et brun clair et un r seau brun plus fonc sur une partie p riph rique (Fig. 1b).

Microscopie confocale par r flectance

Un examen en microscopie confocale (MC) (Vivascope 3000® ; Caliber Inc, Rochester, NY, tats-Unis, distribu en France par Mavig, Munich) tait r alis pour orienter le diagnostic. Nous constations la pr sence d'un piderme type de nid d'abeille r gulier sans pr sence de cellule pag to de (Fig. 2a). Des nombreuses cellules atypiques refl tantes (de grosse taille et de forme irr guli re) taient pr sentes dans le derme superficiel alors que la jonction dermo pidermique n' tait plus identifiable pr cis ment (Fig. 2b). L'examen histologique montrait (Fig. 2c) une l sion constitu e de cellules m lanocytaires pigment es sans gradient de maturation s' tendant sur toute la hauteur du derme. La coloration M lan A montrait une positivit de ces

* Auteur correspondant.
Adresse e-mail : elisacinotti@gmail.com (E. Cinotti).

http://dx.doi.org/10.1016/j.annder.2016.05.004

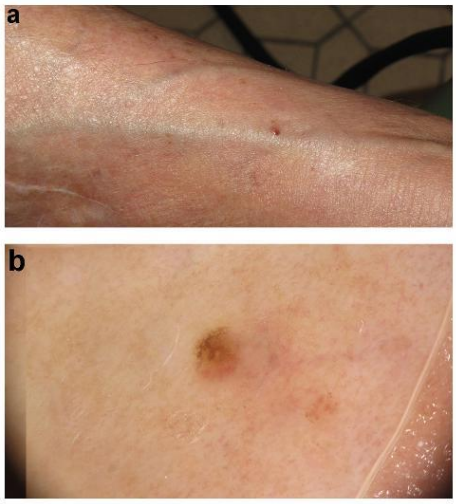

Figure 1. L'examen clinique (a) et dermoscopique (b).

cellules tumorales (Fig. 2d). Il s'agissait d'une m tastase de m lanome.

Commentaires

Un examen en MC in vivo a t r alis , compte tenu de la possible apparition r cente de la l sion malgr un aspect non inqui tant l'examen clinique. Il a permis de visualiser sous un piderme normal des cellules refl tantes tr s anormales de par leur aspect morphologique (grandes cellules avec une anisocytose marqu e) et aussi de par une distribution architecturale anormale en nappe h t rog ne associ e une perte de la visualisation de la jonction dermo pidermique. Le diagnostic de tumeur maligne m lanocytaire a pu tre pos . Devant la pr sence de cellules anormales (de grande taille, rondes et dendritiques) dans le derme et leur absence dans l' piderme, nous avons voqu un m lanome dermique ou, ce qui tait plus probable dans le contexte pr sent, une m tastase de m lanome intradermique.

Les m tastases cutan es de m lanome n'ont pas de caract res sp cifiques en dermoscopie mais elles pr sentent une fr quence plus lev e du patron homog ne, du patron vasculaire (vaisseaux polymorphes, en pointill s, lin aires irr guliers, en tire-bouchon et aire rouge laiteuse), du patron globulaire et du halo p riph rique pigment qui peuvent tre trouv s avec une fr quence variable dans d'autres l sions cutan es b nignes et malignes [1]. De

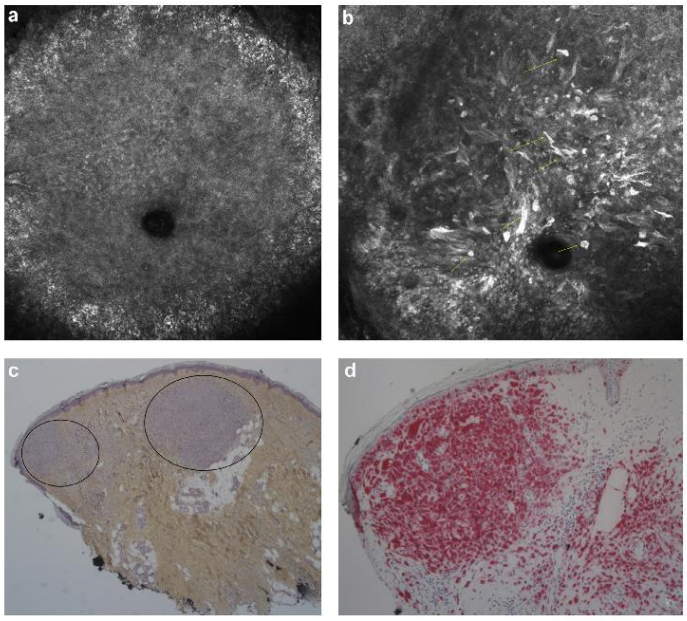

Figure 2. L'examen en microscopie confocale par r flectance montre un piderme type de nid d'abeille normal (a) et des grandes cellules refl tantes (fl ches) rondes et dendritiques dans le derme superficiel (b). L'examen histologique avec coloration h matoxyline-osine (grossissement × 2,5) montre des cellules m lanocytaires pigment es, sans gradient de maturation, s' tendant sur toute la hauteur du derme (c : cercles). La coloration par immunohistochimie M lan A (×10) montre une positivit des cellules tumorales (d).

mani re int ressante notre l sion pr sentait un patron homog ne en correspondance de la masse tumorale dermique et une partie avec r seau p riph rique en correspondance d'une zone o la prolif ration m lanocytaire dermique atteignait la jonction dermo pidermique. Dans la litt rature, un seul cas de m tastase cutan e de m lanome a t d crit en MC [2]. l'instar de notre observation, cette m tastase pr sentait des nids de m lanocytes atypiques dans le derme. De plus, il tait possible d'observer une invasion de l' piderme par les m lanocytes tumoraux, aspect constat moins fr quemment dans les m tastases de m lanomes [2].

D claration de liens d'int r ts

Les auteurs d clarent ne pas avoir de liens d'int r ts.

R f rences

[1] Rubegni P, Lamberti A, Mandato F, Perotti R, Fimiani M. Dermoscopic patterns of cutaneous melanoma metastases. Int J Dermatol 2014;53:404—12.
[2] Moscarella E, Zalaudek I, Agozzino M, Vega H, Cota C, Catrical C, et al. Reflectance confocal microscopy for the evaluation of solitary red nodules. Dermatology 2012;224:295—300.

2.a 10 Reflectance confocal microscopy of Pigmented Bowen's disease: misleading dendritic cells.

Skin Research and Technology 2016; 0: 1–3
Printed in Singapore · All rights reserved
doi: 10.1111/srt.12304

Published by John Wiley & Sons Ltd
Skin Research and Technology

Letter to the Editor

Reflectance confocal microscopy of Pigmented Bowen's disease: misleading dendritic cells

S. Debarbieux[1], J. L. Perrot[2], E. Cinotti[2], B. Labeille[2], J. Fontaine[3], C. Douchet[4], B. Balme[3] and L. Thomas[1]

[1]*Dermatology Department, Centre Hospitalier Lyon Sud, Pierre-Bénite, France,*
[2]*Dermatology Department, Hôpital Nord, Saint Etienne, France,*
[3]*Pathology Department, Centre Hospitalier Lyon Sud, Pierre-Bénite, France and* [4]*Pathology Department, Hôpital Nord, Saint Etienne, France*

REFLECTANCE CONFOCAL microscopy (RCM)'s use is increasing in dermatology for non-invasive diagnosis of skin neoplasias. The presence of intraepidermal pagetoid bright cells is a feature usually suggestive of melanoma, though it must be kept in mind that morphological aspect of Langerhans cells (LC) with RCM can be similar to melanocytes (1).

We report herein three cases of Bowen's disease which were falsely diagnosed melanomas with RCM because of a high density of hyper-reflective dendritic intraepithelial cells.

Case 1: a phototype IV, 44-year-old nurse was referred for a 4-mm pigmented macule of the eyelid margin that she had noticed 2 years previously. RCM (VivaScope® 3000; Caliber Inc., New York, NY, USA) revealed numerous fusiform and stellate hyper-reflective cells within the epithelium and occasional ones around the papillae at the epithelium–chorion junction. The whole lesion was excised and histopathological examination showed a typical Bowen's disease (Fig. 1).

Case 2: a phototype IV, 37-year-old man was referred for a dermoscopically atypical pigmented macule of the sole of the left foot evolving from 1 year. RCM (VivaScope® 3000) revealed numerous intraepidermal stellate hyper-reflective cells. Histopathological examination was typical for a Bowen's disease (Fig. 1).

Case 3: a phototype III, 56-year-old, woman was referred for skin examination after onset of brain metastasis of unknown origin. A clinically and dermoscopically atypical pigmented lesion of the gluteal fold was found. RCM (VivaScope® 3000) revealed intraepithelial atypical hyper-reflective dendritic cells. Histopathology was typical for a Bowen's disease.

The first RCM descriptions of actinic keratoses, Bowen's diseases, and spinous cell carcinomas outlined the cytological atypia of the keratinocytes and the architectural disorganization of the epidermis, which are the histopathological and RCM hallmarks of such non-melanocytic neoplasias (2). Recently, Moscarella et al. reported their experience of dermoscopy and RCM of pigmented actinic keratosis and highlighted that intraepidermal dendritic cells, which can be a confounding feature, were found in 12 out of their 17 cases (3). The surprisingly high number of actinic keratoses exhibiting intraepidermal dendritic cells in Moscarella et al.'s study is associated with a peculiar subset of actinic keratoses clinically characterized by pigmentation (3). The authors assume that these dendritic cells correspond to intraepidermal LC rather than melanocytes, as the latter are limited to the basal layer on immunohistochemistry sections. They also make the assumption that there might be a melanosome transfer to LC that could explain their brightness with RCM. The similarity between dendritic melanocytes and LC under RCM is indeed well known and was first reported a few years ago by Hashemi et al. (1).

Our small series highlights that the density of intraepithelial hyper-reflective cells can, at least

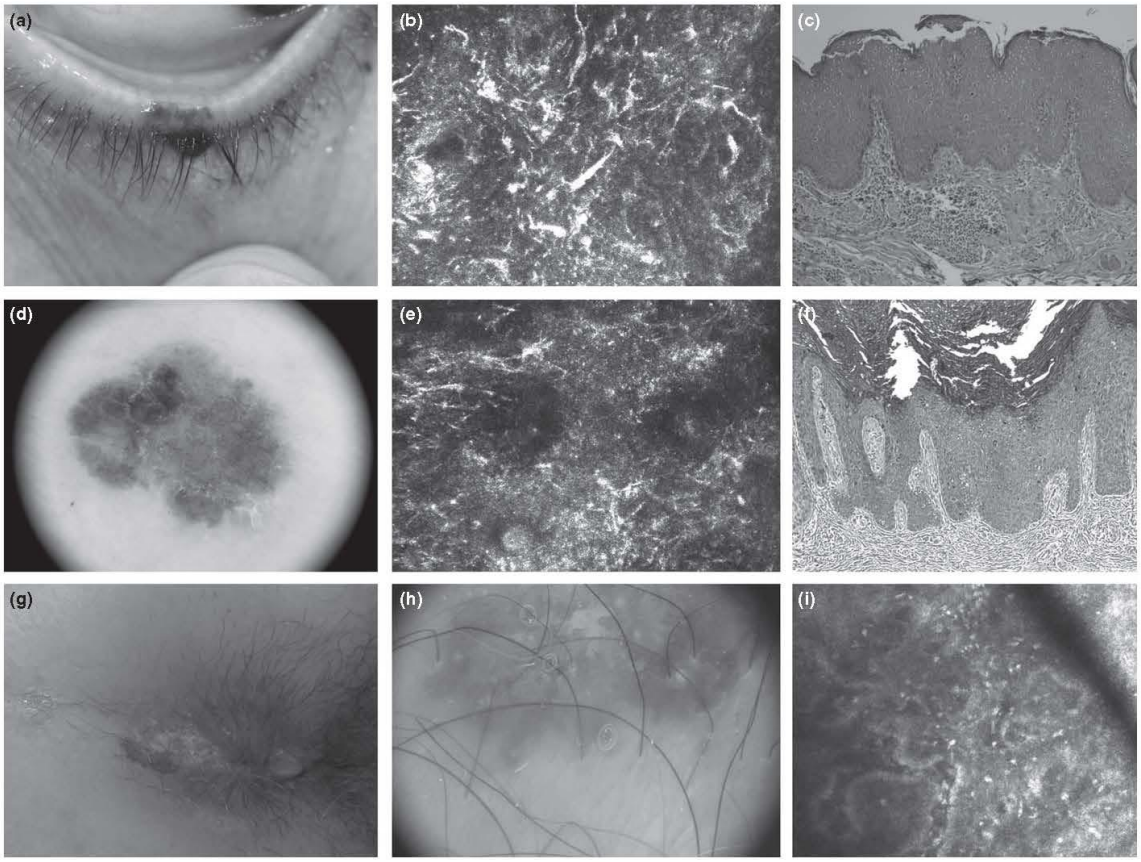

Fig. 1. (a–c) Case 1: Pigmented Bowen's disease of the eyelid margin. (a) Clinical aspect. (b) Reflectance confocal microscopy showing numerous hyper-reflective intraepithelial cells. (c) Histopathology (HES ×4). (d–f) Case 2: Pigmented Bowen's disease of the left foot. (d) Dermoscopy showing a multicomponent pattern. (e) Reflectance confocal microscopy. (f) Histopathology (HES ×10). (g–i) Case 3: Pigmented Bowen's disease of the gluteal fold. (h) Dermoscopy showing dotted vessels, milky red areas and pigmentation with a blue-white structureless area. (i) Reflectance confocal microscopy showing numerous hyper-reflective intraepithelial cells (blue arrows).

occasionally, be quite high in Bowen's disease. This aspect could lead without this knowledge to falsely conclude to a melanoma despite the absence of roundish pagetoid cells. Indeed, these lesions were clinically challenging because of their pigmentation and their clearly atypical dermoscopical features (in two cases). Our clinical data are consistent with Moscarella et al.'s clinical assumption that dendritic cells are found in pigmented lesions (1). However, Cinotti et al. previously reported a case of non-pigmented Bowen's disease of the glans penis treated with photodynamic therapy (4) with abundant dendritic cells. The exact nature of these hyper-reflective cells remains to be clearly elucidated. Such misleading lesions need to be kept in mind in order to avoid worrying patients and excessive surgical treatment.

Conflict of interest

None declared.

References

1. Hashem P, Pulitzer MP, Scope A, Kovalyshyn I, Halpern AC, Marghoob AA. Langerhans cells and melanocytes share similar morphologic features under in vivo reflectance confocal microscopy: a challenge for melanoma diagnosis. J Am Acad Dermatol 2012; 66: 452 462.
2. Ulrich M, Kanitakis J, González S, Lange-Asschenfeldt S, Stockfleth E,

Roewert-Huber J. Evaluation of Bowen disease by in vivo reflectance confocal microscopy. Br J Dermatol 2012; 166: 451 453.
3. Moscarella E, Rabinovitz H, Zalaudek I et al. Dermoscopy and reflectance confocal microscopy of pigmented actinic keratoses: a morphological study. J Eur Acad Dermatol Venereol 2015; 29: 307 314.
4. Cinotti E, Perrot JL, Labeille B, Douchet C, Mottet N, Cambazard F. Laser photodynamic treatment for in situ squamous cell carcinoma of the glans monitored by reflectance confocal microscopy. Australas J Dermatol 2014; 55: 72 74.

Address:
Sébastien Debarbieux
Service de Dermatologie
Centre Hospitalier Lyon Sud
Chemin du Grand Revoyet
69495 Pierre Benite Cedex
France
Tel: +33 4 78 86 16 08
Fax: +33 4 78 86 41 97
e-mail: sebastien.debarbieux@chu-lyon.fr

2.b délimitation des marges des tumeurs et contrôle post opératoire

2.b 1 Laser photodynamic treatment for in situ squamous cell carcinoma of the glans monitored by reflectance confocal microscopy

While mutilating surgery can be avoided with non- surgical treatment of *in situ* squamous cell carcinoma (SCC) of the penis, such as photodynamic therapy (PDT), this procedure is not followed by histological evaluation to verify the total removal of the lesion, leading to possible recurrence. We present the first case of *in situ* penile SCC treated with laser PDT, where the efficacy of the treatment was monitored by reflectance confocal microscopy (RCM) using a hand- held camera. In the future RCM may be regarded as a complementary technique to assess the efficacy of non-surgical treatment of mucous membrane cancers.

Australasian Journal of Dermatology

Australasian Journal of Dermatology (2013) ••, ••–•• doi: 10.1111/ajd.12052

BRIEF REPORT

Laser photodynamic treatment for *in situ* squamous cell carcinoma of the glans monitored by reflectance confocal microscopy

Elisa Cinotti,[1] Jean Luc Perrot,[1] Bruno Labeille,[1] Catherine Douchet,[2] Nicolas Mottet[3] and Frédéric Cambazard[1]

Departments of [1]Dermatology, [2]Pathology and [3]Urology, University Hôpital of Saint Etienne, Saint Etienne, France

ABSTRACT

While mutilating surgery can be avoided with non-surgical treatment of *in situ* squamous cell carcinoma (SCC) of the penis, such as photodynamic therapy (PDT), this procedure is not followed by histological evaluation to verify the total removal of the lesion, leading to possible recurrence. We present the first case of *in situ* penile SCC treated with laser PDT, where the efficacy of the treatment was monitored by reflectance confocal microscopy (RCM) using a handheld camera. In the future RCM may be regarded as a complementary technique to assess the efficacy of non-surgical treatment of mucous membrane cancers.

Key words: confocal microscopy, glans, *in situ* squamous cell carcinoma, laser, methyl aminolevulinate, mucosal cancer, penis, photodynamic therapy.

INTRODUCTION

International guidelines recommend a penis preserving strategy for treating *in situ* squamous cell carcinoma (SCC) with local excision, Mohs micrographic surgery, laser vaporisation, photodynamic therapy (PDT), topical fluorouracil or imiquimod.[1] Although conservative treatment improves quality of life, local recurrence rates are higher than with ablative surgery and therefore a histological assessment of tumoral margins is recommended.[1] We present the first case of an *in situ* glans SCC treated with two sessions of laser PDT, where the efficacy of the treatment was monitored by a handheld camera coupled with reflectance confocal microscopy (RCM).

CASE REPORT

A 65-year old man presented with a 2×1.5 cm shiny erythematous eroded plaque on his penis (Fig. 1), which had been developing over several months, suggestive of an *in situ* SCC. RCM showed a disarranged pattern of the epithelium (Fig. 2a) with many hyper-refractive dendritic cells compatible with Langerhans cells (Fig. 2a,b). Post-biopsy

Figure 1 Erythematous shiny eroded plaques on the penis.

Abbreviations:

PDT	photodynamic therapy
RCM	reflectance confocal microscopy
SCC	squamous cell carcinoma

Correspondence: Dr Elisa Cinotti, University Hospital of Saint Etienne, 42055 Saint Etienne Cedex 2, France. Email: elisacinotti@gmail.com

All authors contributed in drafting the manuscript.

Elisa Cinotti, MD. Jean Luc Perrot, MD. Bruno Labeille, MD. Catherine Douchet, MD. Nicolas Mottet, PhD. Frédéric Cambazard, PhD.

Conflict of interest: none

Submitted 6 December 2012; accepted 13 March 2013.

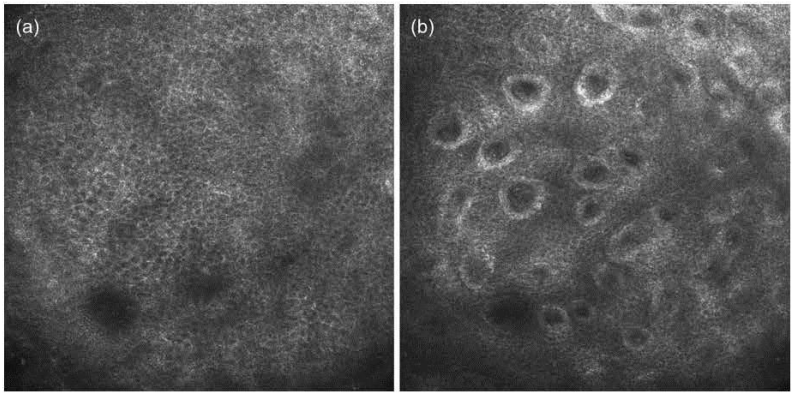

Figure 4 Reflectance confocal microscopy image of the glans 5 months after the second photodynamic therapy session, showing a normal mucosa showing (a) spinous cell layer; (b) epithelium–chorion junction.

tion, edged papillae with a roundish shape rimmed by bright monomorphous cells and the possible presence of scattered bright dendritic cells around the chorion papillae. The RCM-generated image of the SCC was comparable to that of cutaneous SCC with a disarranged pattern of the whole epithelium (Fig. 2c).

In our patient, thanks to handheld camera RCM we were able to establish a clinical diagnosis prior to biopsy and to monitor the efficacy of PDT to decide when to stop treatment. After two sessions of PDT, RCM showed a normal mucosa, confirming that the tumour was in remission. We also found that mucous membrane SCC regression was supported by the disappearance of dendritic cells, which have a role in the immune response against tumour cells and are easily detected with RCM. Scattered dendritic cells can be shown by RCM[7] in normal mucosa, but in our case of SCC we found in the tumour area numerous dendritic cells, which disappeared after PDT treatment with complete tumoural regression. In conclusion, we present the first *in situ* penile SCC treated with laser PDT and the first case monitored by RCM. Methyl-aminolevulinate laser PDT combined with RCM provides a non-mutilating treatment of this carcinoma with the ability to monitor the outcome with a non-invasive examination comparable to routine histology. In future RCM may be regarded as a complementary technique for PDT for assessing treatment efficacy.

REFERENCES

1. Pizzocaro G, Algaba F, Horenblas S *et al.* EAU penile cancer guidelines 2009. *Eur. Urol.* 2010; **57**: 1002–12.
2. Fai D, Romano I, Cassano N *et al.* Methyl-aminolevulinate photodynamic therapy for the treatment of erythroplasia of Queyrat in 23 patients. *J. Dermatolog. Treat.* 2012; **23**: 330–2.
3. Axcrona K, Brennhovd B, Alfsen GC *et al.* Photodynamic therapy with methyl aminolevulinate for atypial carcinoma *in situ* of the penis. *Scand. J. Urol. Nephrol.* 2007; **41**: 507–10.
4. Feldmeyer L, Krausz-Enderlin V, Töndury B *et al.* Methylaminolaevulinic acid photodynamic therapy in the treatment of erythroplasia of Queyrat. *Dermatology* 2011; **223**: 52–6.
5. Paoli J, Ternesten Bratel A, Löwhagen G-B *et al.* Penile intraepithelial neoplasia: results of photodynamic therapy. *Acta Derm. Venereol.* 2006; **86**: 418–21.
6. Feldman AS, McDougal WS. Long-term outcome of excisional organ sparing surgery for carcinoma of the penis. *J. Urol.* 2011; **186**: 1303–7.
7. Lee MR, Ryman W. Erythroplasia of Queyrat treated with topical methyl aminolevulinate photodynamic therapy. *Australas. J. Dermatol.* 2005; **46**: 196–8.
8. Stables GI, Stringer MR, Robinson DJ *et al.* Erythroplasia of Queyrat treated by topical aminolaevulinic acid photodynamic therapy. *Br. J. Dermatol.* 1999; **140**: 514–7.
9. Venturini M, Sala R, Gonzàlez S *et al.* Reflectance confocal microscopy allows *in vivo* real-time noninvasive assessment of the outcome of methyl aminolaevulinate photodynamic therapy of basal cell carcinoma. *Br. J. Dermatol.* 2013; **168**: 99–105.
10. Cinotti E, Perrot JL, Labeille B *et al.* Reflectance confocal microscopy for the diagnosis of vulvar melanoma and melanosis: preliminary results. *Dermatol. Surg.* 2012; **38**: 1962–7.

2.b 2 In vivo reflectance confocal microscopy to optimize the spaghetti technique for defining surgical margins of lentigo maligna.

Background

Lentigo maligna (LM) is a therapeutic challenge for surgeons because of its location in aesthetic areas and the difficultly in determining margins.

Objective

To investigate a new procedure combining the “spaghetti” technique described by Gaudy- Marqueste and colleagues in 2011 with in vivo reflectance confocal microscopy (RCM) to define the margins of LM more accurately and allow strict histologic control.

Method and material

Thirty-three consecutive patients with LM of the head underwent a RCM- guided delineation of the margins followed by the “spaghetti” technique.

Results

The excision of the first “spaghetti” in a tumor-free area was obtained in 28 of 33 patients. In the other five cases, persistence of LM foci was found in <5% of the length of spaghetti. The average number of pieces of “spaghetti” was 1.2 (range 1–3). Definitive histologic examination of the lesion showed a minimum average margin of 2.7 mm. Follow-up in 27 patients after an average of 10 months (range 4–25 months) did not show any recurrence.

Conclusion

This procedure allows accurate definition of the surgical margins of LM, with a low rate of multiple excisions, sparing tissue in functional and aesthetic areas. These results should be confirmed on the basis of a larger series with longer follow-up.

In Vivo Reflectance Confocal Microscopy to Optimize the Spaghetti Technique for Defining Surgical Margins of Lentigo Maligna

Julie Champin, MD,*† Jean-Luc Perrot, MD,‡ Elisa Cinotti, MD,‡ Bruno Labeille, MD,‡ Catherine Douchet, MD,§ Grégory Parrau, MD,* Frédéric Cambazard, MD,†‡ Pierre Seguin, MD,*† and Thomas Alix, MD*†¶

BACKGROUND Lentigo maligna (LM) is a therapeutic challenge for surgeons because of its location in aesthetic areas and the difficultly in determining margins.

OBJECTIVE To investigate a new procedure combining the "spaghetti" technique described by Gaudy-Marqueste and colleagues in 2011 with in vivo reflectance confocal microscopy (RCM) to define the margins of LM more accurately and allow strict histologic control.

METHODS AND MATERIALS Thirty-three consecutive patients with LM of the head underwent a RCM-guided delineation of the margins followed by the "spaghetti" technique.

RESULTS The excision of the first "spaghetti" in a tumor-free area was obtained in 28 of 33 patients. In the other five cases, persistence of LM foci was found in <5% of the length of spaghetti. The average number of pieces of "spaghetti" was 1.2 (range 1 3). Definitive histologic examination of the lesion showed a minimum average margin of 2.7 mm. Follow-up in 27 patients after an average of 10 months (range 4 25 months) did not show any recurrence.

CONCLUSION This procedure allows accurate definition of the surgical margins of LM, with a low rate of multiple excisions, sparing tissue in functional and aesthetic areas. These results should be confirmed on the basis of a larger series with longer follow-up.

The authors have indicated no significant interest with commercial supporters.

Lentigo maligna (LM) is a type of melanoma occurring on the sun-exposed skin of elderly people, usually on the face and neck. It presents a therapeutic challenge for surgeons because it is usually large and located in aesthetic areas, and determining its margins is difficult, leading to a high frequency of local recurrence.[1–3]

Outlining the peripheral margins is challenging because LM is characterized by horizontal growth and can extend beyond its clinically visible margins because of the superficial spreading of isolated malignant melanocytes[3] (Figure 1A). Moreover, because it develops on photodamaged skin, clear demarcation with respect to neighboring solar lentigo can be difficult to see[4] (Figure 1B). Consequently, surgeons are often forced to choose between sufficiently wide margins to prevent recurrence and minimal margins to preserve functional and aesthetic areas of face and neck. They also need to employ an effective and simple technique in a population that is often elderly.

Department of Maxillofacial and Plastic Surgery, University Hospital of Saint Étienne, Saint-Étienne, France; †Faculty of Medicine, University of Saint-Étienne, Saint-Étienne, France; ‡Department of Dermatology, University Hospital of Saint Étienne, Saint-Étienne, France; §Department of Pathology, University Hospital of Saint Étienne, Saint-Étienne, France; ¶CREATIS CNRS UMR 5220, INSERM U1044, University of Lyon 1, INSA, Lyon, France

ISSN: 1076-0512 • Dermatol Surg 2014;40:247–256 • DOI: 10.1111/dsu.12432

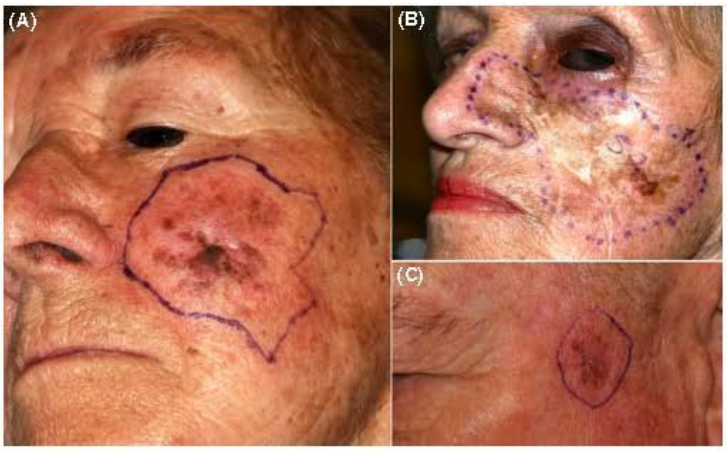

Figure 1. In vivo reflectance confocal microscopy margins of lentigo maligna (LM; blue outline) can extend more than 1 cm beyond the clinically visible margins (A) and are particularly useful in cases of severe sun-damaged skin with actinic lentigo overlapping the LM area (B) and in cases of subtle pigmentation, like in LM recurrences (C).

Mohs micrographic surgery (MMS) and staged excision are the reference techniques employed to accurately delineate the surgical margins of LM, but they are expensive, involve a long learning curve,[5] and are used by only a small number of teams. Gaudy-Marqueste and colleagues[6] recently described an alternative technique, the "spaghetti" technique, which consists of analyzing the entire tumor marginal area, excised in a band.

In vivo reflectance confocal microscopy (RCM) is also effective in improving the definition of surgical margins in melanoma,[4,7,8] allowing the visualization of atypical melanocytes beyond clinically visible margins (Figure 1A). RCM is also indicated for defining LM margins given the horizontal spread of LM.[4] In addition, because RCM does not degrade specimens, further histopathologic examination is possible. Therefore, to help delineate LM margins, the authors suggest a new procedure that combines the "spaghetti" technique with in vivo RCM.

Materials and Methods

The Ethics Committee of the University Hospital of Saint Etienne (France) approved our study.

Patients

Patients were recruited from the Department of Dermatology and underwent surgery in the Department of Maxillofacial and Plastic Surgery, University Hospital of Saint Etienne.

The inclusion criterion was LM of the head histologically proven using biopsy. The exclusion criterion was inoperability. Thirty-three consecutive subjects were included from March 2011 to April 2013 (17 male, 16 female) with an average age of 74 (range 39 90).

Imaging Protocol

The surgical margins of the LM lesions were outlined using in vivo RCM (VivaScope 3000, CALIBER, MAVIG GmbH, München, Germany) in the Department of Dermatology on the same day of or the day before surgery. Examination using in vivo RCM was performed through the entire depth of the epidermis and papillary dermis every 4 μm. The area of a confocal microscopy field is 1,000 by 1,000 μm.

A diagnosis of positive margins with RCM was made according to at least one bright, large (>20 μm), round or dendritic cell in the epidermidis

(Figure 2). A diagnosis of negative margin was made in the absence of these atypical cells.

Marking began at the visual limits of LM, defined by the clinical examination and dermoscopy, and moved upward to obtain a first malignant cell free examination. The following investigations were performed circumferentially, moving closer by 5 mm to the visual limits if the analysis was negative and moving away by 5 mm if malignant cells were found. This spacing of 5 mm corresponds to the size of the tip of the VivaScope 3000 camera. When applied to the skin, this tip creates a temporary footprint that serves as a transitional benchmark for the next exploration, with the tip applied adjacent to the mark that the previous exploration left.

A mark was made on the analyzed area using a dermographic pen as a dot in the center of the skin footprint of the camera after quickly mopping up the interface oil used for the RCM examination. These dots were interconnected by a line, drawn using a dermographic pen and then stained with a solution of fuchsin ink (1.25 g fuchsin, 25 g silver nitrate, 375 mL 90° alcohol, supplemented with water to obtain 480 mL of solution) to avoid any possible deletion during preoperative disinfection of the skin. The outline of the lesion was marked (Figures 1 and 3A). Two operators, well trained in the use of RCM, were needed to perform the marking. Approximately 30 minutes was required to perform RCM-guided margin detection.

Surgical Excision

We proceeded under local anesthesia to the excision of the border of the lesion marked by RCM in accordance with the "spaghetti" technique

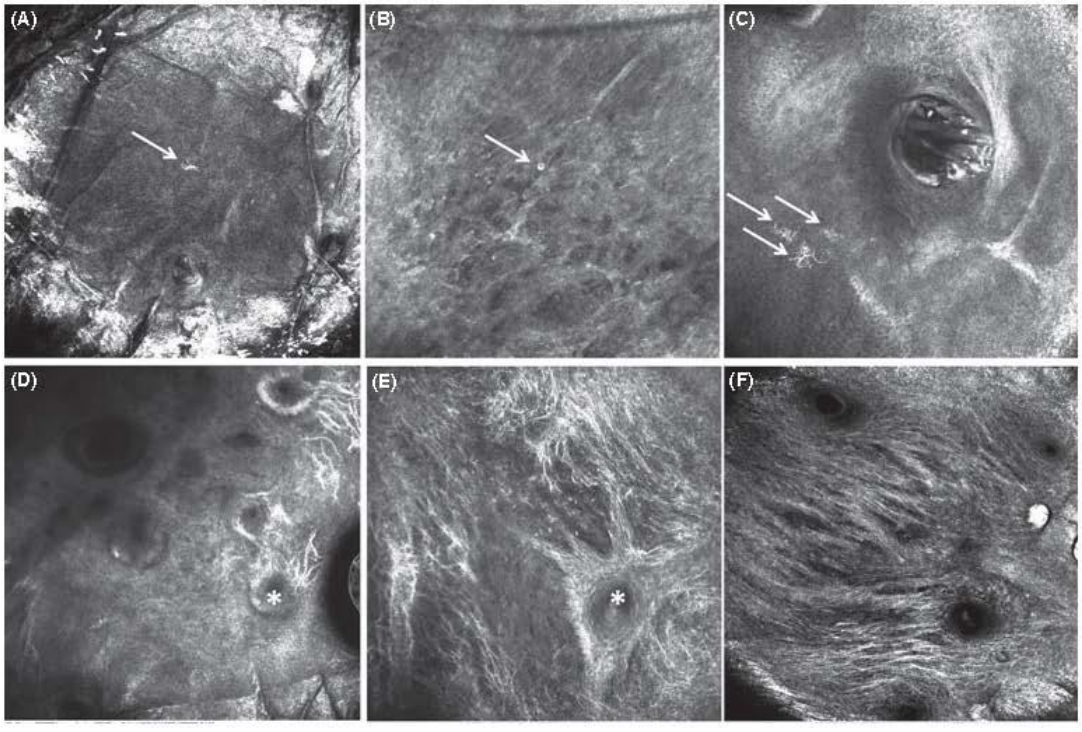

Figure 2. The reflectance confocal microscopy aspect of lentigo maligna can vary from the presence of one (A, B) or sparse (C) large, bright, dendritic (A, C) or round cells in the epidermidis to the presence of a large proliferation of these atypical cells (D, E, F), mainly around hair follicles (asterisk).

previously described[6] (Figures 3 and 4). We excised a 2-mm-wide strip of skin (the "spaghetti") around the lesion using a dedicated double-bladed knife (scalpel double 5, reference 304515, Dexter, Argenteuil, France), leaving the lesion in place. The excision margin of the "spaghetti" was immediately sutured. The "spaghetti" was then oriented and sent to the Department of Pathology for histologic examination. If the excision was not tumor-free, new "spaghetti" limited to the affected area was resected using the same technique. This procedure was repeated until we obtained tumor-free "spaghetti."

Complete excision of the lesion and reconstruction by skin graft or local flap were then performed together in a second surgical procedure. The pathologic examination of the lesion provided a definitive histologic diagnosis and was used to define the minimum clear margin. When final histology showed tumor invading the dermis, corresponding to lentigo malignant melanoma (LMM), an extra excision 1 cm from the initial margin of the lesion was performed.

Histological Examination

The "spaghetti" was divided into several samples after orientation points were inked. Each sample was placed separately in paraffin and examined in longitudinal sections stained with hemalum-eosin-safran and monoclonal anti-Melan-A, clone A103 (Dako, Glostrup, Denmark). The central tumor was examined after paraffin embedding, sectioning perpendicular to the long axis (vertical serial sections) every 3 mm, and staining with hemalum-eosin-safran and MelanA. The length of the first piece of "spaghetti," the percentage in length of invasion by the tumor, and the minimum margin observed after complete excision (minimum distance of the tumor from the outer margin outlined by the "spaghetti") of the lesion were measured.

Follow-up

Follow-up consisted of clinical and RCM examination after an average of 10 months (range 4 25 months) in 27 patients.

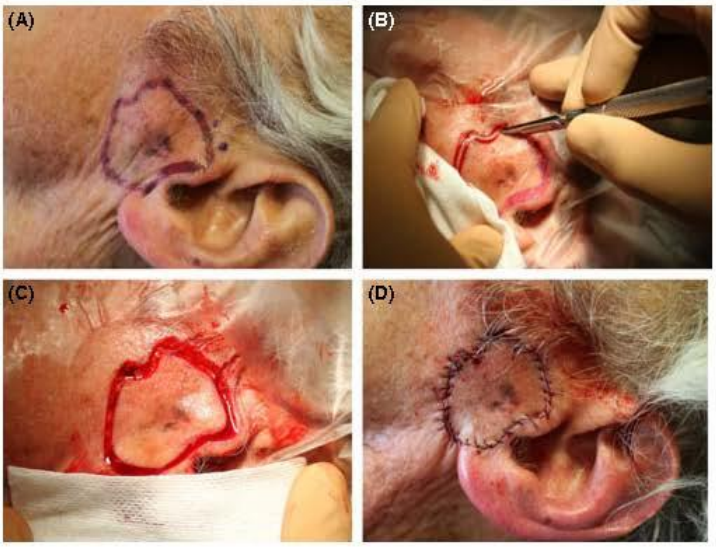

Figure 3. Photographic sequence of the procedure combining reflectance confocal microscopy (RCM) with the "spaghetti" technique. (A) Outlining surgical margins after in vivo RCM examination. (B) Excision of the piece of "spaghetti" using a dedicated double-bladed knife. (C) Appearance after resection of the "spaghetti." (D) Immediate suture of excised margins.

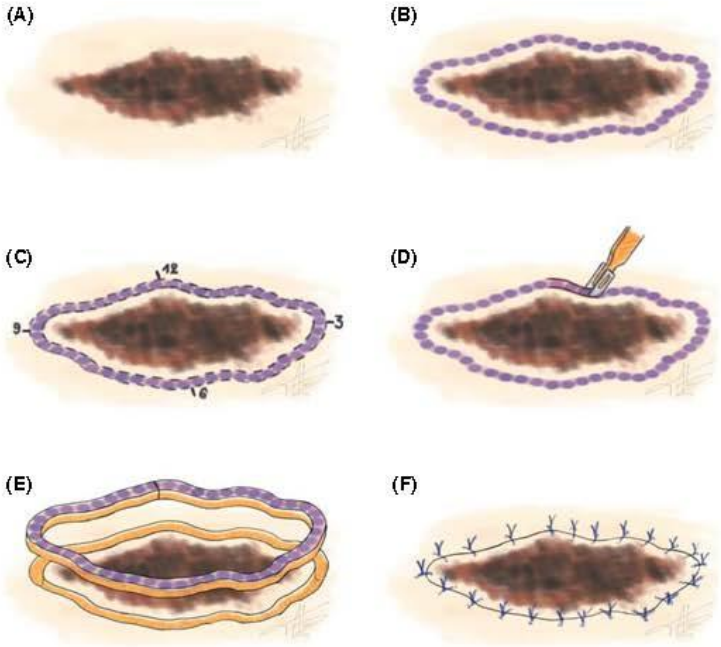

Figure 4. Modus operandi: diagram. (A) Initial lesion. (B) Outlining surgical margins after in vivo reflectance confocal microscopy examination. (C) Orientation of the piece of "spaghetti." (D) and (E) excision of the piece of "spaghetti" using a dedicated double-bladed knife. (F) Immediate suture of excised margins.

Statistical Analysis

Student's test was performed with R (R software version 2.12.2, cran.r-project.org).

Results

The results obtained are summarized in Table 1. Thirty-three cases were studied. Twelve cases were LM or LMM recurrences. In all cases, the margin outlined using RCM did not correspond to what the clinical and dermatoscopic examination suggested, and in all tumors, it was more than 5 mm beyond the clinically visible pigmentation at least at one point. The number of pieces of "spaghetti" per tumor ranged from one to three (average 1.2 ± 0.5 for all 33 tumors, 1.1 ± 0.3 for only the LM recurrences). Excision of the first piece of "spaghetti" in a tumor-free area was obtained in 28 of 33 patients. In the first 8 patients, the number of pieces of "spaghetti" per tumor was on average 1.5 ± 0.7, whereas for the following 25 patients, it was 1.08 ± 0.3 (significantly different, $p = 0.04$). The total length of the first piece of "spaghetti" was 3,158 mm; 683 mm for the first 10 patients and 2,475 mm for the following 23. The average minimum margin observed after complete excision (minimum distance of the tumor from the outer margin outlined by the piece of "spaghetti") was 2.7 mm (range 0 5 mm). Six of 33 tumors were LMM, with a Breslow index of <1 mm, and had an extra excision 1 cm from the initial margin of the lesion. Patients number 10, 31, and 33 refused any further surgical procedures after the first piece of "spaghetti," which was tumor free in all three cases. None of the 27 patients for whom follow-up data were available have shown any recurrence.

Discussion

LM has a high recurrence rate after excision[5,9] because of its characteristic subclinical extension. Based on consensus opinion, a 5-mm margin is

TABLE 1. Results

Patient	*Location*	*Melanoma Recurrence Before Our Technique,* n	*Pieces of Spaghetti,* n	*Length of First Piece of Spaghetti, mm*	*Length of Invaded Area(s) in the First Spaghetti, mm (% of Length)*	*Final Histologic Diagnosis*	*Minimum Lateral Margins on the Final Tumor Excision, mm*	*Follow-Up, Months*
1	Temple	2	1	65	–	LMM (Breslow 0.37 mm)	1.5	25
2	Cheek	1	2	111	1.2 and 3.4 (4.1)	LM	1	24
3	Upper eyelid	1	1	92	–	LM	2	22
4	Nose	–	3	37	0.9 (2.4)	LM	2	11
5	Nose	–	1	87	–	LMM (Breslow 0.6 mm)	3	16
6	Cheek	–	1	51	–	LM	3	10
7	Cheek	1	1	105	0.47 (0.5)	LMM (Breslow 0.25 mm)	6	18
8	Glabella	–	2	45	0.5 and 0.1 (1.3)	LM	0	NA
9	Lower eyelid	–	1	80	–	LM	1	12
10	Cheek	–	1	10	–	NA	NA	14
11	Cheek	–	1	189	–	LMM (Breslow 0.32 mm)	2	6
12	Nose	3	1	42	–	LM	0.3	5
13	Cheek	–	1	100	–	LM	5	13
14	Cheek	–	1	131	–	LM	3	9
15	Cheek	–	2	75	–	LM	5	8
16	Cheek	1	1	113	–	LMM (Breslow 0.52 mm)	4	10
17	Cheek	1	1	129	–	LM	0	NA
18	Temple	–	1	127	–	LM	0	10
19	Cheek	–	1	79	–	LM	0.5	7
20	Temple	–	1	74	–	LM	1	4
21	Cheek	1	1	207	–	LMM (Breslow 0.97 mm)	1	6
22	Cheek	–	1	68	–	LM	2	7
23	Cheek	1	1	135	–	LM	2	6
24	Cheek	–	1	51	–	LM	5	NA
25	Temple	–	2	201	0.1 (0.5)	LM	1	7
26	Nose	–	1	75	–	LM	3	10
27	Cheek	1	1	65		LM	3	NA
28	Nose	–	1	93	–	LM	4	9

TABLE 1. Continued

Patient	Location	Melanoma Recurrence Before Our Technique, n	Pieces of Spaghetti, n	Length of First Piece of Spaghetti, mm	Length of Invaded Area(s) in the First Spaghetti, mm (% of Length)	Final Histologic Diagnosis	Minimum Lateral Margins on the Final Tumor Excision, mm	Follow-Up, Months
29	Lower eyelid	–	1	96	–	LM	4	8
30	Temple	–	1	75	–	LM	5	NA
31	Cheek	–	1	145	–	LM	NA	8
32	Cheek	1	1	100	–	LM	4	8
33	Cheek	1	1	105	–	LM	NA	NA

LM, lentigo maligna; LMM, lentigo malignant melanoma; NA, not available.

recommended for melanoma in situ,[10] although numerous studies have demonstrated that a 5-mm margin is insufficient in LM in 45% to 60% of cases,[2,11–17] and Breuninger and colleagues[18] have shown the persistence of tumoral melanocytes in 54% of LM excised using 0.5-cm margins.

According to the guidelines of the American Academy of Dermatology,[19] alternative surgical approaches may be considered for LM; >0.5-cm margins may be necessary particularly for large lesions on the head and neck. The French Society of Dermatology recommends a margin of 1 cm for LM, and if this measure is not feasible for anatomic or functional reasons, a 0.5-cm margin is acceptable, with histologic control of the entire margin using MMS or a staged excision technique.[20]

MMS[5,21] is used in few centers because it requires significant logistics and trained operators. Moreover, it is based on frozen-section processing with frequent morphologic alterations of keratinocytes, such as the formation of halos, which makes them difficult to differentiate from melanocytes.[17]

The staged excision is easier to perform and, unlike MMS, has the great advantage of being based on paraffin-embedded specimens.[1,12–17,22,23] This technique is easy to perform and provides satisfactory histologic control of the margins, although it has the disadvantage of relying on visual analysis of the limits of the lesion to determine the first excision margin at the discretion of the operator. In addition, it entails a phase when the wound remains open, which patients and their families object to.

The "spaghetti" technique, inspired by the "perimeter" technique,[14] has been described more recently.[6] This technique can accurately outline the limits of LM and save skin tissue. It consists of the resection of a 2-mm skin strip (the "spaghetti") on the periphery of the lesion, with a margin of 3 to 5 mm beyond its visual limits while leaving the lesion in place. Histologic analysis of the "spaghetti" is performed, and the procedure is repeated until a tumor-free piece of "spaghetti" is obtained. The "spaghetti" wound is immediately sutured to reduce the risk of wound infection, to simplify local care, and to facilitate returning home between two stages. The "spaghetti" technique is inexpensive, easy to perform, and performed under local anesthesia, although it has the drawback of relying on visual analysis of the lesion limits to determine the margin of resection, as well as the staged excision.

To address the problem of the clinical definition of lesion extent, dermoscopy, Wood's light examina-

tion, and in vivo RCM[4,24] can be useful techniques. In vivo RCM is a noninvasive imaging technique, reported for the first time in dermatology in 1995,[25] which is now used for the diagnosis of pigmented skin lesions.[26–29] It allows in vivo exploration of the different layers of the epidermis up to the superficial dermis, with nearly histologic resolution. RCM has two great advantages over dermoscopy and Wood's light examination; it allows single tumoral melanocytic cells beyond the pigmented area to be identified, and it is suitable for amelanotic lesions.[30]

We therefore decided to optimize the "spaghetti" technique by combining it with RCM to define the surgical margins of LM precisely. RCM was found particularly useful in cases of severely sun-damaged skin with solar lentigo overlapping the melanoma area (Figure 1B) and in cases of subtle pigmentation, such as in LM recurrences (Figure 1C). The number of pieces of "spaghetti" per tumor ranged from one to three (average 1.2). Although most patients needed only one piece of "spaghetti," two pieces was necessary in four cases, and three were required in one case. Our results suggest better performance than with the "spaghetti" technique not coupled with in vivo RCM, in which the number of pieces of "spaghetti" ranged from one to four (average 1.5),[6] although even if our technique required fewer excisions than the RCM unassisted "spaghetti" technique, no conclusions can be drawn because of the lack of detailed data such as the number of pieces of "spaghetti" per case, the length of the piece of "spaghetti," and the relative length of invaded spaghetti in the previous study. Our results seem also to be superior to those obtained using the staged excision technique,[12–15] although these data cannot be compared in statistical analysis because of the small number of cases.

There was a learning curve in our study. Despite a high failure rate for the first 8 patients (average number of pieces of "spaghetti" 1.5), the remaining 25 patients mostly required only one piece (average 1.08). The significant higher failure rate at the beginning might have been due to the initial difficulty in identifying single atypical melanocytes under RCM.

A diagnosis of positive margins with RCM was made in the presence of at least one bright, large (>20 μm), round or dendritic cell in the epidermidis. The main criteria for the diagnosis of LM suggested by Guitera and colleagues, consisting of nonedged papillae and round large pagetoid cells,[27] were therefore not followed because we did not observe the architecture and cytology of the entire lesion but observed only the margins of LM, where only mild cytologic atypia may be present.

Guitera and colleagues considered only round pagetoid cells to diagnose LM, because large dendritic cells can represent melanocytic hyperplasia in actinic keratosis, solar lentigo, and inflammatory lesions, but in our experience, the presence of a single large dendritic cell should be considered part of the tumor when outlining LM margin. Characteristically, large bright dendritic cells were mostly found around follicle openings that should be carefully examined.

As Guitera and colleagues described, we could not differentiate LM from LMM because atypical nucleated cells within the papillae can be found in both conditions; this is probably because of the difficulty in determining the exact site of the cells (junctional or dermal) on RCM, especially because the dermoepidermal junction is less visible on the face and is partially distorted in many cases of LM. In addition, LM is often a subtle diagnosis on RCM, as with pathology slides. When more than one piece of "spaghetti" was required, only few atypical cells were present on histologic examination, and the additional pieces of "spaghetti" were limited to a restricted area (<5 mm, 0.5–4.1% of the total length of the first piece of "spaghetti") with a decrease in size with experience over time. Moreover, some of these cases were characterized by LM that extended far beyond the clinically visible area, making the examination even more challenging.

Final histologic examination allowed us to confirm the high accuracy of in vivo RCM. The average minimum clear margin (minimum distance of the tumor from the margin outlined by the piece of "spaghetti) found on the final excision of the tumor was 2.7 mm, suggesting the possibility of extremely precise excision of the lesion, close to its real limits.

The combination of the "spaghetti" technique and in vivo RCM is currently used in our department for all patients with facial LM and seems to give promising results. It allows us to limit the risk of excision in invaded areas, to spare tissue, and to perform a single surgical resection of the tumor with immediate reconstruction and absence of an open wound, which is a source of discomfort for patients. RCM has the advantage of being noninvasive but requires the in vivo RCM camera and close collaboration between dermatologists, surgeons, and pathologists for successful performance. The expected benefit is reduction or avoidance of further surgical treatments because of reduced recurrence. This benefit, largely suggested by this preliminary study, should nonetheless be confirmed in a larger number of cases with longer follow-up, especially to compare the incidence of recurrence with that of conventional techniques.

References

1. Agarwal-Antal N, Bowen GM, Gerwels JW. Histologic evaluation of lentigo maligna with permanent sections: implications regarding current guidelines. J Am Acad Dermatol 2002;47:743 8.
2. Osborne JE, Hutchinson PE. A follow-up study to investigate the efficacy of initial treatment of lentigo maligna with surgical excision. Br J Plast Surg 2002;55:611 5.
3. McKenna JK, Florell SR, Goldman GD, Bowen GM. Lentigo maligna/lentigo maligna melanoma: current state of diagnosis and treatment. Dermatol Surg 2006;32:493 504.
4. Chen C-SJ, Elias M, Busam K, Rajadhyaksha M, et al. Multimodal in vivo optical imaging, including confocal microscopy, facilitates presurgical margin mapping for clinically complex lentigo maligna melanoma. Br J Dermatol 2005;153:1031 6.
5. Barlow RJ, White CR, Swanson NA. Mohs' micrographic surgery using frozen sections alone may be unsuitable for detecting single atypical melanocytes at the margins of melanoma in situ. Br J Dermatol 2002;146:290 4.
6. Gaudy-Marqueste C, Perchenet A-S, Taséi A-M, Madjlessi N, et al. The "spaghetti technique": an alternative to Mohs surgery or staged surgery for problematic lentiginous melanoma (lentigo maligna and acral lentiginous melanoma). J Am Acad Dermatol 2011;64:113 8.
7. Busam KJ, Hester K, Charles C, Sachs DL, et al. Detection of clinically amelanotic malignant melanoma and assessment of its margins by in vivo confocal scanning laser microscopy. Arch Dermatol 2001;137:923 9.
8. Curiel-Lewandrowski C, Williams CM, Swindells KJ, Tahan SR, et al. Use of in vivo confocal microscopy in malignant melanoma: an aid in diagnosis and assessment of surgical and nonsurgical therapeutic approaches. Arch Dermatol 2004;140:1127 32.
9. Wildemore JK 4th, Schuchter L, Mick R, Synnestvedt M, et al. Locally recurrent malignant melanoma characteristics and outcomes: a single-institution study. Ann Plast Surg 2001;46:488 94.
10. Goldsmith LA, Askin FB, Chang AE, Cohen C, et al. Diagnosis and treatment of early melanoma. NIH Consensus Development Conference. Consens Statement 1992;10:1 25.
11. Pitman GH, Kopf AW, Bart RS, Casson PR. Treatment of lentigo maligna and lentigo maligna melanoma. J Dermatol Surg Oncol 1979;5:727 37.
12. Bub JL. Management of lentigo maligna and lentigo maligna melanoma with staged excision: a 5-year follow-up. Arch Dermatol 2004;140:552 8.
13. Hazan C, Dusza SW, Delgado R, Busam KJ, et al. Staged excision for lentigo maligna and lentigo maligna melanoma: a retrospective analysis of 117 cases. J Am Acad Dermatol 2008;58:142 8.
14. Mahoney M-H, Joseph M, Temple CLF. The perimeter technique for lentigo maligna: an alternative to Mohs micrographic surgery. J Surg Oncol 2005;91:120 5.
15. Bosbous MW, Dzwierzynski WW, Neuburg M. Staged excision of lentigo maligna and lentigo maligna melanoma: a 10-year experience. Plast Reconstr Surg 2009;124:1947 55.
16. Huilgol SC, Selva D, Chen C, Hill DC, et al. Surgical margins for lentigo maligna and lentigo maligna melanoma: the technique of mapped serial excision. Arch Dermatol 2004;140:1087 92.
17. Abdelmalek M, Loosemore MP, Hurt MA, Hruza G. Geometric staged excision for the treatment of lentigo maligna and lentigo maligna melanoma: a long-term experience with literature review. Arch Dermatol 2012;148:599 604.
18. Breuninger H, Schlagenhauff B, Stroebel W, Schaumburg-Lever G, et al. Patterns of local horizontal spread of melanomas: consequences for surgery and histopathologic investigation. Am J Surg Pathol 1999;23:1493 8.
19. Bichakjian CK, Halpern AC, Johnson TM, Foote Hood A, et al. Guidelines of care for the management of primary cutaneous melanoma. J Am Acad Dermatol 2011;65:1032 47.
20. Négrier S, Saiag P, Guillot B, Verola O, et al. Guidelines for clinical practice: standards, Options and Recommendations 2005 for the management of adult patients exhibiting an M0 cutaneous melanoma, full report. National Federation of Cancer Campaign

Centers. French Dermatology Society. Update of the 1995 Consensus Conference and the 1998 Standards, Options, and Recommendations. Ann Dermatol Venereol 2005;132:1053 85.

21. Temple CLF, Arlette JP. Mohs micrographic surgery in the treatment of lentigo maligna and melanoma. J Surg Oncol 2006;94:287 92.

22. Johnson TM, Headington JT, Baker SR, Lowe L. Usefulness of the staged excision for lentigo maligna and lentigo maligna melanoma: the "square" procedure. J Am Acad Dermatol 1997;37:758 64.

23. Moehrle M, Dietz K, Garbe C, Breuninger H. Conventional histology vs. three-dimensional histology in lentigo maligna melanoma. Br J Dermatol 2006;154:453 9.

24. Guitera P, Moloney FJ, Menzies SW, Stretch JR, et al. Improving management and patient care in lentigo maligna by mapping with in vivo confocal microscopy. JAMA Dermatol 2013;3:1 7.

25. Rajadhyaksha M, Grossman M, Esterowitz D, Webb RH, et al. In vivo confocal scanning laser microscopy of human skin: melanin provides strong contrast. J Invest Dermatol 1995;104:946 52.

26. Guitera P, Pellacani G, Longo C, Seidenari S, et al. In vivo reflectance confocal microscopy enhances secondary evaluation of melanocytic lesions. J Invest Dermatol 2009;129:131 8.

27. Pellacani G, Guitera P, Longo C, Avramidis M, et al. The impact of in vivo reflectance confocal microscopy for the diagnostic accuracy of melanoma and equivocal melanocytic lesions. J Invest Dermatol 2007;127:2759 65.

28. Gerger A, Hofmann-Wellenhof R, Samonigg H, Smolle J. In vivo confocal laser scanning microscopy in the diagnosis of melanocytic skin tumours. Br J Dermatol 2009;160:475 81.

29. Koller S, Wiltgen M, Ahlgrimm-Siess V, Weger W, et al. In vivo reflectance confocal microscopy: automated diagnostic image analysis of melanocytic skin tumours. J Eur Acad Dermatol Venereol 2011;25:554 8.

30. Guitera P, Pellacani G, Crotty KA, Scolyer RA, et al. The impact of in vivo reflectance confocal microscopy on the diagnostic accuracy of lentigo maligna and equivocal pigmented macules of the face. J Invest Dermatol 2010; 130(8):2080 91.

Address correspondence and reprint requests to: Thomas Alix, MD, Department of Maxillofacial and Plastic Surgery, University Hospital of Saint-Étienne, 42055 Saint-Étienne Cedex 2, France, or e-mail: alix.thomas.cmf@gmail.com

3- Imagerie non invasive in vivo et processus infectieux cutanéomuqueux et phanérien

Lorsque nous avons commencé à nous intéresser à l'apport de la MCIV pour la prise en charge des malades suspects d'infections parasitaires 5 articles seulement avaient été publiés concernant la gale et 8 autres à propos de différentes formes de teignes. Aussi l'épidémie de gale qui a sévi en France, concomitamment à l'acquisition des caméra de MCIV, nous a de fait amenée à travailler de fait sur ce sujet avec pas moins de 8 articles publiés.
Par ailleurs la gale nous a ouvert à la possibilité d'étudier tous les autres processus infectieux parasitaires, mais aussi de ce qui paraissait hors de portée de la microscopie confocale, les infections à virus et notamment les virus du groupe herpès et même les bactéries en l'occurrence le T pallidum. Avoir pu visualiser un vivo l'agent pathogène de la syphilis n'a pas été pour le dermatologue vénérologue que je suis, sans une certaine émotion.
De plus l'acquisition de caméra d'OCT nous a conduit à réaliser l'exploration de processus parasitaire avec ces nouveaux dispositifs. Cette expérience stéphanoise dans le domaine de la visualisation en MICV des processus infectieux cutanéo-muqueux nous a conduit à publier des articles de synthèses sur ce sujet et une discussion de collaboration avec un laboratoire pharmaceutique australien est en cours quant à la caractérisation de l'efficacité d'un nouvel antiparasitaire (discussion sous couvert du secret actuellement)

3.a Imagerie non invasive in vivo in vivo et processus infectieux cutanéomuqueux et phanérien des parasites

3.a 1 Reflectance confocal microscopy for quantification of Sarcoptes scabiei in Norwegian scabies

3.a 2 Rapid diagnosis of scabies by manual confocal reflectance microscopy

3.a 4 On the feasibility of confocal microscopy for the diagnosis of scabies

3.a 5 Diagnosis of scabies by high-magnification dermoscopy: the "delta-wing jet" appearance of Sarcoptes scabiei

3.a 6 Inefficacy of alcohol-based hand rub on mites in a patient with hyperkeratotic scabies

3.a 7 Tinea corporis diagnosed by reflectance confocal microscopy

3.a 8 Hair dermatophytosis diagnosed by reflectance confocal microscopy: six cases

3.a 9 Dermoscopy and confocal microscopy for in vivo detection and characterization of Dermanyssus gallinae mite.

3.a 10 Unusual reflectance confocal microscopy findings during the examination of a perianal nevus: pinworms.

3.a 11 Videodermoscopy compared to reflectance confocal microscopy for the diagnosis of scabies

3.a 12 Dermoscopy, confocal microscopy and optical coherence tomography for the diagnosis of bedbug infestation

3.a 1 Reflectance confocal microscopy for quantification of Sarcoptes scabiei in Norwegian scabies

Background and Objectives

In vivo reflectance-mode confocal microscopy (RCM) can be used for the diagnosis of scabies. This study quantifies S. scabiei and its eggs and droppings in a patient affected by Norwegian Scabies (NS), and describes their distribution within the epidermis and in different body areas.

Methods

Different skin sites were randomly chosen in four sections (head, upper limbs, trunk and inferior limbs) of the body surface area (BSA) to acquire a total of 60 RCM z-stacks. The number of mites and eggs, the presence of droppings, as well as the minimum epidermal depth at which mites, eggs and faeces were detectable, was established for each z-stack. The total number of mites and eggs on the entire BSA was calculated considering the weighted mean for the four sections of the B S A .

Results

A total of 15.8 millions of S. scabiei and 7.2 millions of eggs were calculated. Mites, eggs and faeces were homogeneously distributed all over the body surface. Droppings, easily recognized by the RCM, were present in more than an half of the analyzed cutaneous sites and were associated with the presence of parasites (chi-squared test, P = 0.002).

Conclusions

Our study illustrates the ability of RCM to identify, locate, and quantify the various forms of S. scabies in human skin. NS is an extremely contagious disease, considering that the number of mites can be around 15.8 millions. Moreover, all areas of the body are parasitized in NS, including the face.

DOI: 10.1111/j.1468-3083.2012.04555.x JEADV

ORIGINAL ARTICLE

Reflectance confocal microscopy for quantification of *Sarcoptes scabiei* in Norwegian scabies

E. Cinotti,[†,‡] J.L. Perrot,[†] B. Labeille,[†] P. Vercherin,[§] C. Chol,[†] E. Besson,[†] F. Cambazard[†,*]

[†]Service de Dermatologie Hôpital Nord, Cedex 2, Saint Etienne, France
[‡]San Martino Hospital, Di.S.Sal, Viale Benedetto XV, Genova, Italy
[§]Service de Santé Publique et de l'Information Médicale, Hôpital Nord, Cedex 2, Saint Etienne, France
*Correspondence: F. Cambazard. E-mail: frederic.cambazard@chu-st-etienne

Abstract

Background and Objectives *In vivo* reflectance-mode confocal microscopy (RCM) can be used for the diagnosis of scabies. This study quantifies *S. scabiei* and its eggs and droppings in a patient affected by Norwegian Scabies (NS), and describes their distribution within the epidermis and in different body areas.

Methods Different skin sites were randomly chosen in four sections (head, upper limbs, trunk and inferior limbs) of the body surface area (BSA) to acquire a total of 60 RCM z-stacks. The number of mites and eggs, the presence of droppings, as well as the minimum epidermal depth at which mites, eggs and faeces were detectable, was established for each z-stack. The total number of mites and eggs on the entire BSA was calculated considering the weighted mean for the four sections of the BSA.

Results A total of 15.8 millions of *S. scabiei* and 7.2 millions of eggs were calculated. Mites, eggs and faeces were homogeneously distributed all over the body surface. Droppings, easily recognized by the RCM, were present in more than an half of the analyzed cutaneous sites and were associated with the presence of parasites (chi-squared test, $P = 0.002$).

Conclusions Our study illustrates the ability of RCM to identify, locate, and quantify the various forms of *S. scabiei* in human skin. NS is an extremely contagious disease, considering that the number of mites can be around 15.8 millions. Moreover, all areas of the body are parasitized in NS, including the face.

Received: 25 November 2011; Accepted: 29 March 2012

Conflict of interests

None declared.

Funding sources

None declared.

Introduction

Norwegian scabies (NS) is a widespread cutaneous infestation of *Sarcoptes scabiei* that manifests with extensive erythema, hyperkeratosis and scaling of the skin, especially on hands and feet. The condition is most frequently seen in individuals with compromised immune systems as well as those with decreased sensory functions. Thousands to millions of mites[1] have often been reported to be in a person affected by NS but this number had never been proved.

In vivo reflectance-mode confocal microscopy (RCM) is an optical imaging technique that allows non-invasive, high-resolution cutaneous imaging. It permits to view horizontal images of the skin at a cellular level resolution from the surface to the papillary dermis.[2]

It has already been used to identify *S. scabiei* and its eggs and droppings in the skin,[3] but there are no reports on the use of this technique in NS.

The objective of this study was to quantify the presence of *S. scabiei* and of its eggs and droppings in a patient affected by an erythrodermic form of NS (Fig. 1), describing their distribution within the epidermis and in different body areas.

Materials and methods

Confocal imaging was performed with a near-infrared reflectance confocal laser scanning microscope (VivaScope 3000, Lucid Inc., Henrietta, NY, USA). Each given image corresponds to a horizontal skin section of 0.5 mm × 0.5 mm (0.25 mm^2) at a selected depth. Series of images (z-stacks), focused at regularly placed intervals of 4.56 μm through the depth of the epidermis (z axis), were acquired within the same section of the skin. Each z-stack consisted of 37 images from the epidermal surface to the upper dermis.

The body surface area (BSA) of the patient was divided into four sections: head, upper limbs, trunk and inferior limbs. In each

Figure 1 Clinical presentation of the patient affected by Norwegian scabies. (a) Extensive cutaneous hyperkeratosis and crusting of the abdomen (with a significant umbilical hernia) and (b) the right hand.

section, different skin sites were randomly chosen (10, 23, 10 and 17 sites in the head, upper limbs, trunk and inferior limbs respectively) to acquire a total of 60 z-stacks.

Under RCM adult *S. scabiei* is seen as a dishomogeneous refractive structure, with an ovoid body and short legs. Females are 400 × 300 μm in size, while males are just over half these sizes. Eggs are dishomogeneous refractive ovoid bodies of 200 × 100 μm in diameter and droppings appear as highly refractive roundish bodies of around 15 μm in diameter.

The number of *S. scabiei* and of its eggs, as well as the presence of its droppings and the minimum depth at which it was possible to observe these three findings were assessed by three dermatologists (Fig. 2).

To estimate the total number of mites and eggs present in all the body surface, we calculated the mean number (x) per z-stack in the head (x_h), upper limbs (x_u), trunk (x_t) and inferior limbs (x_i), assigning a weight to each of these values, according to the extension of the respective body areas (head, upper limbs, trunk and inferior limbs respectively represent 10%, 20%, 30%, 40% of the BSA). We also considered that each z-stack corresponds to an area of 0.25 mm^2 ($0.25*10^{-6}m^2$) of the BSA.

Therefore, the total number of mites and eggs was calculated using the following formula: [Total number = $(0.1* x_h + 0.2 *x_u + 0.3 *x_t + 0.4 x_i) * BSA /(0.25*10^{-6})$].

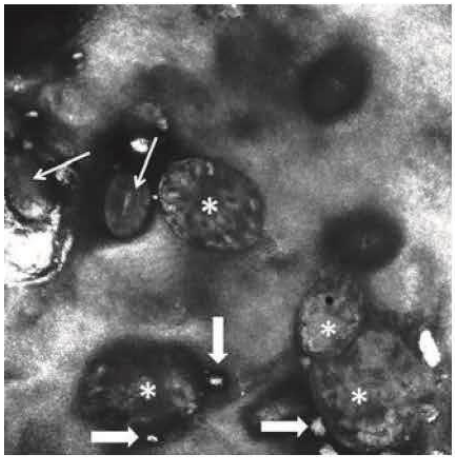

Figure 2 A Reflectance Confocal Microscopy image showing Sarcoptes scabiei mites (asterisks), with their eggs (thin arrows) and droppings (thick arrows).

Results

Mites, droppings and eggs were found in 66%, 58%, and 22%, of z-stacks respectively. The range and the mean of the number of mites and eggs per z-stack (corresponding to an area of 0.25 mm^2 of body surface), and of the minimum depth at which mites, eggs and droppings were detectable in the different body areas, are reported in Table 1.

The mean number of mites per z-stack in the head, upper limbs, trunk and inferior limbs was respectively 0.8, 2.1, 2.5 and 1.8. Therefore, considering a BSA equal to 2 m^2 for our patient

Table 1 Mean number and depth of mites, eggs and droppings in different body areas

	Head	Upper limbs	Trunk	Inferior limbs
Number of z-stacks	10	17	10	23
Mean (SD) number of mites	0.8 (0.9)	1.8 (1.7)	2.5 (2.8)	2.1 (2.0)
Mean (SD) number of eggs	0.5 (1.0)	1.1 (1.8)	0.9 (1.6)	0.9 (1.5)
Depth (SD) of mites (in μm)	61 (34)	61 (24)	52 (43)	70 (40)
Depth (SD) of eggs (in μm)	36 (19)	52 (23)	52 (43)	79 (23)
Depth (SD) of droppings (in μm)	75 (26)	37 (15)	30 (33)	43 (34)

Mean and standard deviation (SD) per z-stack (corresponding to the observation of an area of 0.25 mm^2 of body surface) of the number of mites and eggs, and of the minimum depth at which mites, eggs and droppings were detectable in the different body areas (head, upper limbs, trunk and inferior limbs).

(with a height of 170 cm and a weight of 100 kg), the total number of mites, calculated with the previously reported formula in the 'Materials and methods' section, was equal to 15.8 millions.

Using the same formula and a mean value of eggs per z-stack in the head, upper limbs, trunk and inferior limbs, respectively of 0.5, 1.1, 0.9 and 0.9, the total number of eggs was established to be 7.2 millions. Droppings were associated to the presence of parasites in 75% of the cases, and a statistically significant association was observed between the presence of mites and their droppings (chi-squared test, $P = 0.002$).

Concerning the minimum skin depth at which different findings were detectable, there was a significant difference in the skin depth of mites, droppings and eggs, being droppings the most superficial ($\bar{x}$ droppings depth = 41 μm; SD = 30), and mites the deepest ($\bar{x}$ mites depth = 61 μm; SD = 34) (Kruskal–Wallis test, $P < 0.002$).

Finally, no significant association between the number of mites and eggs and a specific body site was observed (Kruskal–Wallis test, $P > 0.05$).

Discussion

In this study we used RCM to evaluate the number and distribution of parasites and eggs in NS. We calculated the total number of mites being 15.8 millions and this high number should remind us how much NS is contagious. However, our count is an approximation of the real value because we evaluated a surface of 60×0.25 mm^2 (15 mm^2) of 2 m^2 of BSA.

We wanted to assess if it is more frequent to find a mite rather than an egg or an excrement when performing a skin examination, and we found that mites (66% of z-stacks) were more frequent than its faeces (58% of z-stacks) or eggs (22% of z-stacks).

We also evaluated the minimum depth at which mites, eggs and droppings were detectable, to suggest the clinician the minimum depth at which skin scraping should be performed. We observed that parasites ($\bar{x}$ mite depth = 61 μm; SD = 34), eggs ($\bar{x}$ egg depth = 52 μm; SD = 29) and droppings ($\bar{x}$ faeces depth = 41 μm; SD = 30) were superficial, and in some cases they were at the stratum corneum level. There was no relation between the minimum depth of mites and those of eggs or droppings (Pearson coefficient test, $P > 0.05$). In fact, droppings and eggs were more superficial than mites and we explained this aspect hypothesizing that, being the eggs and droppings an inert material, they might migrate to the surface following the differentiation of the keratinocytes.

Droppings were associated with the presence of parasites in 75% of cases and chi-squared test highlighted a relation between the presence of droppings and mites (chi-squared test, $P = 0.002$). This is particularly important because faecal pellets are easily detectable at RCM, as they appear as hyperefractive balls in the surface of the epidermis, and may indicate the presence of an underlying mite. At the contrary, the presence of eggs was not associated with that of mites (chi-squared test, $P > 0.05$). In addition we compared the ratio between the number of parasites and eggs, measured on skin scrapings trough optical microscopy, to that calculated by '*in vivo*' RCM, and found that there is a portion of eggs that are visible to optical microscopy but not to RCM.

The distribution of mites and eggs was homogeneous in the entire body surface. Therefore, we confirmed that in NS the entire body surface is affected, differently from classical forms of scabies, where face is spared.

In conclusion, our study illustrates the ability of RCM to identify, locate, and quantify the various forms of *S. scabiei* in human skin. Our study confirms that the number of mites in NS is enormous, emphasizing that this disease is highly contagious.

Acknowledgments

We thank Dr Pierre Flori (Parasitology Department of Hôpital Nord of Saint Etienne) for helping us in differentiating the parasites on skin scrapings.

References

1 Kolar KA, Rapini RP. Crusted (Norwegian) scabies. *Am Fam Physician* 1991; 44: 1317–1321.
2 Branzan AL, Landthaler M, Szeimies RM. *In vivo* confocal scanning laser microscopy in dermatology. *Lasers Med Sci* 2007; **22**: 73–82.
3 Longo C, Bassoli S, Monari P *et al.* Reflectance-mode confocal microscopy for the in vivo detection of *Sarcoptes scabiei*. *Arch Dermatol* 2005; 141: 1336.

3.a 2 Rapid diagnosis of scabies by manual confocal reflectance microscopy

Annales de dermatologie et de v n r ologie (2012) **139**, 502—505

Disponible en ligne sur SciVerse ScienceDirect www.sciencedirect.com

Elsevier Masson France EM|consulte www.em-consulte.com

Formation médicale continue

DOCUMENT ICONOGRAPHIQUE

Diagnostic rapide de la gale au moyen d'une cam ra manuelle de microscopie confocale par r flectance

Rapid diagnosis of scabies by manual confocal reflectance microscopy

J.-L. Perrot[a], E. Cinotti[a], B. Labeille[a,*], C. Trau[b], H. Rab rin[c], P. Flori[c], F. Cambazard[a]

[a] *Service de dermatologie, hopital Nord, CHU de Saint- tienne, 42055 Saint- tienne cedex 2, France*
[b] *Service de pharmacie, hopital Nord, CHU de Saint- tienne, 42055 Saint- tienne cedex 2, France*
[c] *Service de parasitologie, hopital Nord, CHU de Saint- tienne, 42055 Saint- tienne cedex 2, France*

Reçu le 13 mars 2012 ; accept le 29 mars 2012
Disponible sur Internet le 2 juin 2012

Nous avons observ cinq cas de gale au cours des trois premiers mois de l'ann e 2011, dans lesquels l'utilisation de la cam ra manuelle pour microscopie confocale in vivo a confirm le diagnostic.

Observations

Observation 1 : une femme de 90 ans vivant en r sidence pour personnes g es souffrait d'une maladie d'Alzheimer et d'une pemphigo de bulleuse diagnostiqu e en juillet 2010 sur les crit res cliniques histologiques et immunologiques. Le prurit et les bulles disparaissaient rapidement avec des applications quotidiennes de cr me de dipropionate de b tam thasone, mais en novembre 2010, un prurit r cidivait, principalement localis aux plis interdigitaux des mains et sur la poitrine. Pour confirmer la suspicion clinique de gale, l'examen en microscopie confocale par reflectance tait r alis au moyen de la cam ra manuelle (VivaScope 3000, Lucid). Les formes adultes de *Sarcoptes scabiei* (*S. scabiei*), ainsi que les œufs et d jections taient rapidement observ es dans les sillons (Fig. 1A) des plis interdigitaux. L'examen a pris moins de deux minutes. Les d jections de *S. scabiei* apparaissaient comme des amas tr s distincts de granules tr s r flectants mesurant entre 9 et 13 µm de diam tre (Fig. 2). Facilement reconnaissables, elles mettaient rapidement sur la piste du sarcopte adulte. Observation 2 : un homme de 87 ans se plaignait depuis six mois d'un prurit g n ralis , particuli rement intense au niveau de la poitrine et des plis interdigitaux. Pour confirmer la suspicion clinique de gale, taient faits d'une part, un examen en microscopie optique du produit de grattage interdigital de la main droite et, d'autre part, un examen en microscopie confocale sur les espaces interdigitaux de la main gauche en utilisant la cam ra manuelle. L'examen en microscope optique ne montrait pas de signes de gale, mais en microscopie confocale des formes adultes de *S. scabiei*, des œufs et des d jections taient trouv s. L'examen en microscopie confocale avait pris moins d'une minute. Observation 3 : une petite fille de trois ans souffrait d'un prurit (principalement localis aux plis interdigitaux des mains et sur la poitrine) depuis deux semaines. Un examen en microscopie

* Auteur correspondant.
Adresse e-mail : bruno.labeille@chu-st-etienne.fr (B. Labeille).

0151-9638/$ — see front matter
http://dx.doi.org/10.1016/j.annder.2012.03.021

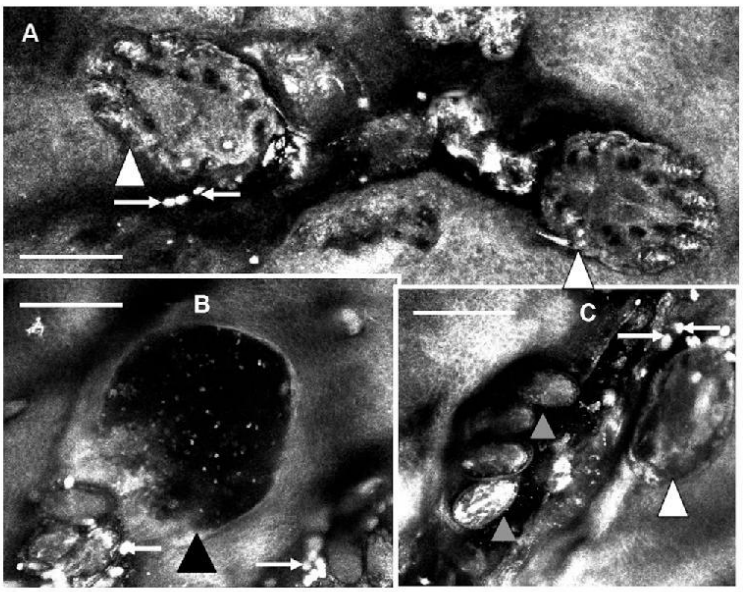

Figure 1. Examen en microscopie confocale in vivo au moyen de la cam ra manuelle (VivaScope 3000, Lucid) de plusieurs patients atteints de gale (trait blanc = 200 µm). A. Parasite adulte (triangle blanc) et d jections caract ristiques (fl che blanche). B. V sicule perl e (triangle noir) et d jections caract ristiques (fl che blanche). C. Parasite adulte (triangle blanc), œufs (triangle gris) et d jections caract ristiques (fl che blanche).

optique du mat riel de grattage interdigital d'une main permettait de d tecter des œufs et des d jections de *S. scabiei* apr s sept minutes d'examen. Au m me endroit, l'examen en microscopie confocale demandait moins d'une minute pour trouver *S. scabiei* dans une v sicule perl e (Fig. 1B). Observation 4 : un enfant de six ans pr sentait des pustules palmoplantaires et un prurit g n ralis depuis cinq mois. Un examen en microscopie optique de deux pr l vements par grattage de pustules plantaires de chaque pied ne permettait pas de confirmer la suspicion clinique de gale. Cependant, l'examen en microscopie confocale des plantes trouvait en moins d'une minute la pr sence de *S. scabiei*, de ses œufs et d jections (Fig. 1C). Observation 5 : une femme de 71 ans souffrait de prurit depuis trois mois avec une atteinte pr dominante de la poitrine. Seul un examen en microscopie confocale a t r alis qui mettait en vidence *S. scabiei*, ses œufs et d jections en moins d'une minute.

Commentaires

Un diagnostic de certitude de gale n'est pas seulement important pour les patients, mais aussi pour les mesures d'hygi ne et de pr vention vis- -vis de l'entourage, tout sp cialement dans les r sidences m dicalis es de personnes g es qui sont expos es une diffusion pid mique de la gale. Toutefois, il n'est pas toujours facile d'obtenir la preuve parasitologique du diagnostic [1]. La m thode diagnostique de r f rence habituelle est l'examen en microscopie optique d'un pr l vement obtenu par grattage cutan sur lequel on cherche identifier les formes adultes, les nymphes, les larves, les œufs et/ou les d jections de *S. scabiei*. Cette technique prend du temps. Sa sensibilit a t tablie 90 % [2], mais elle est probablement moindre dans la pratique courante. Actuellement, la m thode en microscopie optique est souvent remplac e par l'examen pimicroscopique qui montre le « signe du delta » qui repr - sente la portion c phalique du parasite [3]. Cependant, ce signe est parfois difficile d tecter, et les espaces interdigitaux qui sont l'une des zones les plus touch es par la gale sont impossibles explorer avec le dermoscope du fait de la largeur excessive de l'objectif.

L'examen en microscopie confocale par r flectance de *S. scabiei* a t rapport pour la premi re fois en 2005 [4]. Au d but, tait utilis e pour la microscopie confocale in vivo une cam ra qui n' tait pas tr s appropri e au diagnostic de gale du fait de sa grande taille, de sa faible mobilit , et de la n cessit de fixer l'objectif sur la peau par un adh sif. Actuellement, la mise disposition d'une cam ra manuelle pour la microscopie confocale par r flectance in vivo (VivaScope 3000) permet un diagnostic rapide et facile de la gale gr ce un appareil compact manipulable d'une seule main, muni d'une fibre optique flexible qui permet de l'orienter dans toutes les directions, et d'un objectif de petite taille utilisable dans les plis. Ce dispositif permet l'examen rapide de nombreuses zones augmentant ainsi la capacit de d tection du parasite.

Nous avons illustr les diff rentes formes parasitaires selon leur mode de d tection, par biopsie cutan e (Fig. 2A), par examen au microscope optique du produit de grattage

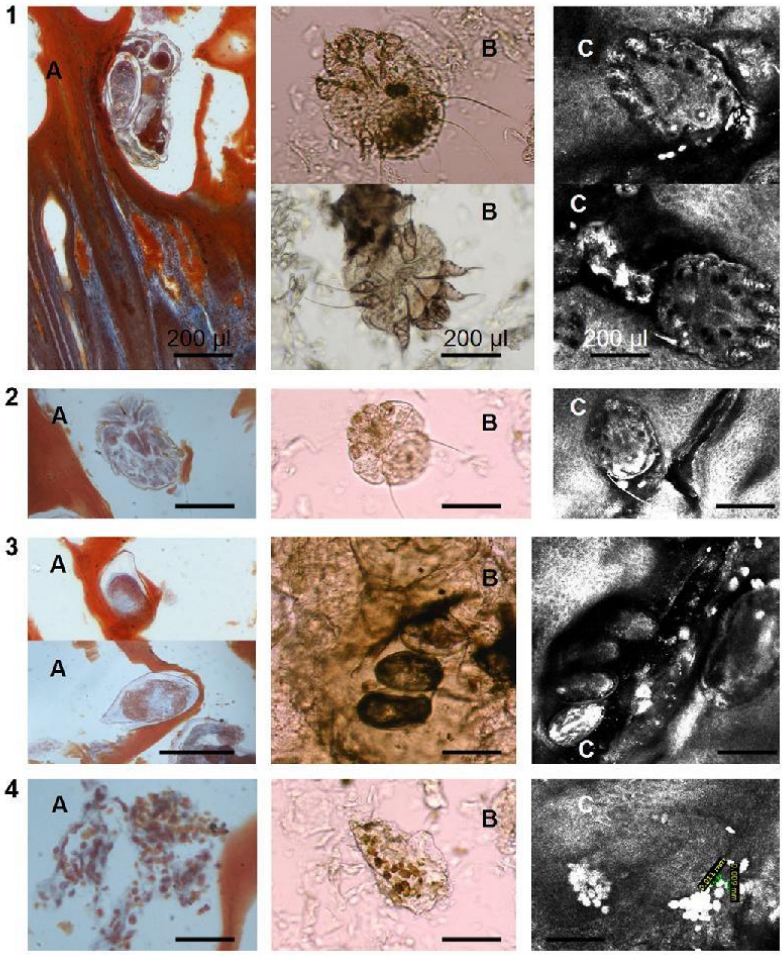

Figure 2. Morphologie comparative de parasite adulte (2,1), larve (2,2), œufs (2,3), et d jections caract ristiques (2,4) par (A) biopsie cutan e et examen histopathologique, (B) grattage cutan et examen en microscopie optique avec coloration au chlorazol noir, et (C) examen en microscopie confocale par r flectance (VivaScope 3000, Lucid) (trait noir = 200 µm), 2-1 : *Sarcoptes scabiei* adulte ; 2-2 : larves de *Sarcoptes scabiei* ; 2-3 : œufs de *Sarcoptes scabiei* ; 2-4 : d jections caract ristiques.

(Fig. 2B), et par microscopie confocale in vivo (Fig. 2C). La microscopie confocale a une haute r solution et elle peut identifier les diff rents segments du parasite tels que le rostre et les longs cils l'extr mit des pattes. De plus, bien que la morphologie des diff rents stades de d veloppement de *S. scabiei* soit semblable, l'examen en microscopie confocale permet de distinguer les formes adultes des formes larvaires d'apr s leur taille (les larves sont plus petites que les adultes) et d'apr s le nombre de paires de pattes (pour les adultes deux paires de pattes l'avant et deux paires de pattes l'arri re, pour les larves deux paires de pattes l'avant et une paire de pattes l'arri re). La morphologie des œufs est caract ristique. Celle des d jections aussi qui ont une forme de granules quadrangulaires et hyper-r flectants, qui peuvent tre un signal utile de la pr sence proximit du parasite adulte (Fig. 1, Fig. 2).

En conclusion, la microscopie confocale par r flectance in vivo est une m thode facile rapide et pr cise pour le diagnostic de la gale en permettant l'examen des diff rentes couches de l' piderme sur de multiples sites corporels. Comme la microscopie confocale par r flectance est faite par le dermatologue lui-m me, l'examen peut tre suivi imm diatement de la prescription du traitement dans le d roulement d'une consultation de routine.

D claration d'int r ts

Les auteurs d clarent ne pas avoir de conflit d'int r t en relation avec cet article.

R f rences

[1] Chosidow O. Scabies and pediculosis. Lancet 2000;355:819—26.
[2] Dupuy A, Dehen L, Bourrat E, Lacroix C, Benderdouche M, Dubertret L, et al. Accuracy of standard dermoscopy for diagnosing scabies. J Am Acad Dermatol 2007;56:53—62.
[3] Argenziano G, Fabbrocini G, Delfino M. Epiluminescence microscopy. A new approach to in vivo detection of *Sarcoptes scabiei*. Arch Dermatol 1997;133:751—3.
[4] Longo C, Bassoli S, Monari P, Seidenari S, Pellacani G. Reflectance-mode confocal microscopy for the in vivo detection of *Sarcoptes scabiei*. Arch Dermatol 2005;141:1336.

3.a 4 On the feasibility of confocal microscopy for the diagnosis of scabies

Annales de dermatologie et de v n r ologie (2013) 140, 215—219

ELSEVIER MASSON

Disponible en ligne sur SciVerse ScienceDirect www.sciencedirect.com

Elsevier Masson France EM|consulte www.em-consulte.com

LETTRES LA R DACTION

Microscopie confocale pour le diagnostic de la gale : questions sur la faisabilit

On the feasibility of confocal microscopy for the diagnosis of scabies

Nous avons appr ci l' ditorial de Chosidow et Sbidian [1] qui a permis de relancer le d bat sur la gale et qui nous donne l'opportunit de r pondre aux questions laiss es ouvertes par les auteurs sur le diagnostic par microscopie confocale par r flectance (MCR) in vivo.

Peut-on distinguer les sarcoptes morts des sarcoptes vivants ? Contrairement l'examen microscopique de squames recueillies par grattage au vaccinostyle qui peut provoquer une absence de mouvement du sarcopte par le traumatisme au cours de la proc dure, la MCR est une m thode non invasive qui permet d'observer les parasites dans toutes leurs fonctions vitales : mouvements, p ristaltisme de l'intestin [2] et d f cation.

De plus, les acariens se trouvent souvent avec leurs mati res f cales derri re eux, ce qui indique qu'ils ont r cemment d f qu et qu'ils sont vivants. Les acariens, les excr ments et les œufs se trouvant dans la partie la plus superficielle de la peau, les parasites morts disparaissent rapidement du fait du renouvellement de l' piderme [3]. Toutefois, nous avons pu observer que les parasites morts non seulement sont immobiles, mais qu'ils ont un aspect hyperrefl tant, avec des contours flous et une perte de visibilit des structures internes (Fig. 1).

Qu'en est-il de la d contamination entre chaque utilisation ? La d contamination concerne la fois la machine, les op rateurs et la salle o l'examen est effectu . Pour la machine, nous utilisons un film transparent jetable (Visulin®, Paul Hartmann AG, Allemagne) que nous appliquons sur l'embout de la cam ra dans tous les cas o le diagnostic de gale est fortement suspect , par exemple en pr sence des sillons caract ristiques. Dans les cas o le film transparent n'a pas t appliqu (utilisation courante de l'appareil pour exclure une gale en cas de prurit s v re chez des patients pr sentant des l sions de prurigo), la d contamination est faite a posteriori, si le diagnostic de gale est finalement retenu. On d sinfecte alors l'embout de la camera avec une double d tersion par lingette usage unique contenant du did cyldim thylammonium chloride (Sani-Cloth Active®, PDI, Royaume-Uni) et ensuite par lingette contenant de l'alcool isopropylique 70 % (Alkotip®, Servoprax, Allemagne). Les lingettes ont des propri t s virucides, fongicides, bact ricides, mais leur capacit antiparasitaire n'a pas t d montr e. En revanche, le geste de nettoyage m canique effectu plusieurs reprises avec deux types de lingettes diff rents sur la surface lisse de l'embout permet l' limination physique des parasites. La protection de l'op rateur est faite avec des gants et une blouse manches longues. Apr s l'examen, la salle doit galement tre nettoy e, en particulier dans le cas de gale hyperk ratosique avec un nombre lev (millions) de parasites [3].

L'utilisation est-elle ais e ? Le diagnostic de la gale en MCR est simple. La MCR permet une visualisation de composants cellulaires dans la peau une r solution comparable celle de l'histologie conventionnelle. La morphologie des parasites adultes, des œufs et des d jections sont caract ristiques [3,4]. De plus, la mise disposition d'une cam ra manuelle pour la MCR in vivo (VivaScope® 3000, LUCID, distribu en Europe par MAVIG) permet un diagnostic facile

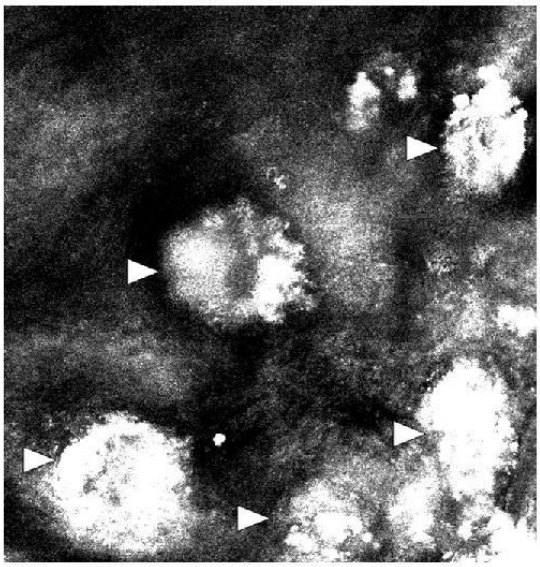

Figure 1. Microscopie confocale in vivo. L'examen en microscopie confocale in vivo au moyen de la cam ra manuelle (VivaScope 3000, Lucid) montre des parasites morts (triangle blanc) qui ont un aspect hyperrefl tant, avec des contours flous et une perte de visibilit des structures internes.

et rapide de la gale gr ce un appareil compact manipulable d'une seule main, muni d'une fibre optique flexible qui permet de l'orienter dans toutes les directions, et d'un objectif de petite taille utilisable dans les plis [4].

Cette nouvelle m thode est-elle reproductible chez un m me op rateur et entre plusieurs op rateurs? Dans une tude effectu e dans notre service, le nombre de parasites, d'œufs et d'excr ments a t valu par trois dermatologues chez un patient ayant une gale hyperk ratosique; les r sultats des trois comptages taient superposables. Il reste d montrer la m me reproductibilit dans les cas de gale petit nombre de sarcoptes.

Le co t est-il un facteur limitant? Le co t de la machine est un facteur limitatif. Mais dans les centres o existe d j une telle machine, le diagnostic de la gale peut tre une application de plus. En outre, dans un futur proche, le co t des machines est destin baisser avec leur diffusion, comme ce fut le cas pour les pimicroscopes. En Europe, 120 machines sont d j install es.

Enfin, en ce qui concerne la sensibilit de l'instrument pour le diagnostic de la gale, avec des images proches de l'histologie et l'utilisation d'une cam ra manuelle qui permet de se d placer rapidement sur la peau en explorant plusieurs sites de l sions en peu de temps, la technique de MCR offre une tr s bonne sensibilit pour la recherche du parasite in vivo. Cependant, l' tude de ses performances comparativement la recherche du parasite au microscope optique sur lame serait int ressante.

D claration d'int r ts

Les auteurs d clarent ne pas avoir de conflits d'int r ts en relation avec cet article.

R f rences

[1] Chosidow O, Sbidian E. La gale: une reconnaissance m rit e! Ann Dermatol Venereol 2012;139:425—7.
[2] Levi A, Mumcuoglu KY, Ingber A, Enk CD. Assessment of Sarcoptes scabiei viability in vivo by reflectance confocal microscopy. Lasers Med Sci 2011;26:291—2.
[3] Cinotti E, Perrot JL, Labeille B, Vercherin P, Chol C, Besson E, et al. Reflectance confocal microscopy for quantification of Sarcoptes scabiei in Norwegian scabies. J Eur Acad Dermatol Venereol 2012 May 23, http://dx.doi.org/10.1111/j.1468-3083.2012.04555.x. [Epub ahead of print].
[4] Perrot JL, Cinotti E, Labeille B, Trau C, Rab rin H, Flori P, et al. Diagnostic rapide de la gale au moyen d'une cam ra manuelle de microscopie confocale par r flectance. Ann Dermatol Venereol 2012;139:502—5.

E. Cinotti , J.-L. Perrot , B. Labeille*, F. Cambazard
Service de dermatologie, h pital Nord, CHU, 42055 Saint- tienne cedex 2, France

*Auteur correspondant.
Adresse e-mail : bruno.labeille@chu-st-etienne.fr (B. Labeille)

Reçu le 18 juillet 2012 ; accept le 13 novembre 2012
Disponible sur Internet le 11 janvier 2013
http://dx.doi.org/10.1016/j.annder.2012.11.007

La t l dermatologie dans la prise en charge des patients en milieu carc ral : exp rience d'un centre r gional

Teledermatology in the management of skin diseases in prison inmates: Experience in central France

La diminution du nombre de m decins imposera dans un futur proche l'utilisation de plus en plus fr quente des techniques de t l m decine pour r pondre la demande de prise en charge des patients loign s des structures de soin. La loi 94-43 du 18 janvier 1994 fait entrer les soins en prison dans la norme des soins dispens s la population g n rale. La prise en charge des patients dans le milieu p nitentiaire reste toutefois moins performante par rapport la population g n rale. En pratique, cette prise en charge mobilise souvent plusieurs agents de la force publique qui doivent accompagner le d tenu pour sa consultation [1]. cela s'ajoutent bien s r des d lais de consultations de plus en plus longs, li s l'appauvrissement actuel de la densit m dicale, qui rendent parfois impossible une prise en charge m dicale correcte.

Le but de notre tude tait d'estimer l'int r t de la t l - consultation en dermatologie dans la prise en charge des dermatoses pr sent es par des patients provenant du milieu carc ral.

Mat riel et m thodes

Nous avons eu recours au syst me de t l transmissions utilis dans le centre hospitalier du Mans pour les r unions de visioconf rence. Ce syst me relie notre tablissement d'autres centres hospitaliers et hospitalo-universitaires et, depuis 2010, la nouvelle prison de Coulaines situ e 10 km du centre hospitalier. Depuis sa mise en place, toutes les consultations dermatologiques ont t r alis es par t l dermatologie. Nous disposons d'un cran t l visuel Samsung HD 1900 × 1200 dans le service de dermatologie et dans une salle de consultation du centre p nitentiaire. l'aide d'un bo tier reli un c blage en fibre optique (r seau Internet s curis), chaque pi ce est dot e d'une cam ra de visioconf rence (Polycom™) permettant une visualisation en mode paysage (visualisation de la moiti de la salle).

Nos patients provenaient de la nouvelle prison de Coulaines, qui a une capacit d'accueil de 400 personnes. L'organisation carc rale comporte deux quartiers de maison d'arr t d'hommes majeurs de 150 et 181 places, cinq cellules pour personnes mobilit r duite, un quartier de semi-libert de 40 places (situ l'ext rieur du mur d'enceinte) et un quartier d'accueil de 30 places. Deux m decins g n ralistes (1,5 quivalent temps plein) sont charg es des patients de la prison dans le cadre d'une UCSA (Unit de consultation et soins ambulatoires). Une dizaine des 186 centres UCSA de France sont d j dot s d'un syst me de t l m decine.

En cas de difficult s diagnostiques ou th rapeutiques, une t l consultation tait assur e par un des praticiens du service de dermatologie du centre hospitalier du Mans. La consultation se d roulait dans le centre p nitentiaire, le d tenu accompagn d'un m decin g n raliste tant en

3.a 5 Diagnosis of scabies by high-magnification dermoscopy: the "delta-wing jet" appearance of Sarcoptes scabiei

Annales de dermatologie et de v n r ologie (2013) 140, 722–724

ELSEVIER MASSON

Disponible en ligne sur SciVerse ScienceDirect www.sciencedirect.com

Elsevier Masson France EM|consulte www.em-consulte.com

LETTRES LA R DACTION

Diagnostic de la gale par pimicroscopie fort grossissement : l'aspect « en deltaplane » de *Sarcoptes scabiei*

Diagnosis of scabies by high-magnification dermoscopy: The ''delta-wing jet'' appearance of *Sarcoptes scabiei*

Le signe du deltaplane est devenu un signe classique pour le diagnostic de la gale en pimicroscopie [1]. Ce signe est discret, et parfois difficile diff rencier des l sions de grattage. Comparativement la microscopie confocale, qui donne rapidement des images tr s d taill es de l'anatomie du parasite [2,3], l'examen pimicroscopique peut sembler frustrant. Cependant, on a observ que le plus fort grossissement du vid odermatoscope augmentait la sp cificit de l'examen, permettant d'avoir des images plus identifiables des parasites.

Observations

Nous avons pris l'habitude de comparer les images en pimicroscopie (FotoFinder Systems, Allemagne) et en microscopie confocale (VivaScope 1500 et 3000, Lucid Inc, Rochester, New York, distribu en Europe par MAVIG, Allemagne) et dans quelques cas de gale profuse, on a pu v rifier la bonne concordance de ce signe du deltaplane (Fig. 1) avec la visualisation du parasite au microscope confocal (Fig. 2). On s'est aussi aperçu qu'avec des prises de vue pimicroscopiques au plus fort grossissement (70 ×), on obtenait en r alit l'image du parasite entier, donc bien plus que les images de deltaplane obtenues au grossissement habituel (20 ×). De plus, l'examen fort grossissement permet l'identification des larves, des œufs et des d jections du parasite, surtout quand ils sont group s. L'identification du parasite ou des œufs au fort grossissement permet une certitude du diagnostic, similaire ce qu'on obtient par microscopie confocale (Fig. 2).

Nous avons ramen les images de microscopie confocale et de vid omicroscopie une chelle comparable pour mieux voir les correspondances et les diff rences (Fig. 2). Bien que la microscopie confocale permette de d tailler l'anatomie du parasite avec une r solution de quelques microns, l' pimicroscopie fort grossissement montre aussi le m me contour ovo de du sarcopte et de ses œufs, et la forme allong e du sillon avec de la k ratine l'int rieur.

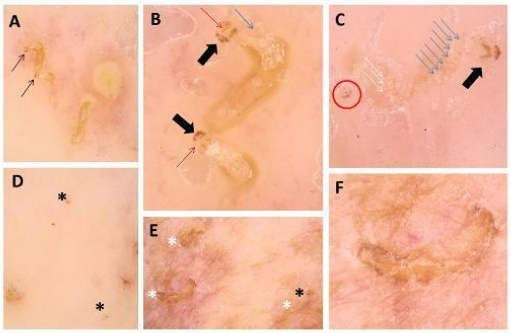

Figure 1. Examen en pimicroscopie par FotoFinder d'un patient atteint de gale faible (A, 20 ×) et fort (B et C, 70 ×) grossissement. A. Signe du deltaplane (fl che noire) ; B. Le triangle du deltaplane correspond l'extr mit c phalique du parasite (fl che noire) et est suivi par une partie ovo de (fl che rouge) correspondant au reste du corps du parasite, qui appara t blanch tre avec un contenu organique brun tre de chaque c t . Un œuf est visible (fl che bleue). C. Parasite adulte (fl che noire), larve (cercle rouge), œufs visibles dans le sillon comme des corps ovo des transparents la p riph rie brun tre (fl che bleue) et d jections visibles comme des petits corps ronds blanc opaque (fl che blanche). Images de l sions de grattage en pimicroscopie par FotoFinder faible (D, E; 20 ×) et fort (F; 70 ×) grossissement. D et E. L sions de grattage qui apparaissent comme des petites l sions brun tres (ast risque noir) qui peuvent simuler le triangle du deltaplane associ es une desquamation pouvant simuler un sillon (ast risque blanc). F. fort grossissement, on peut exclure que la l sion desquamative en figure E soit associ e un parasite.

De plus, la vid omicroscopie permet d'appr cier la t te comme partie anatomique bien d finie du parasite, tout comme la microscopie confocale. Pour ce qui concerne les organes l'int rieur du sarcopte, ils apparaissent en pimicroscopie comme deux bandes parall les brun fonc , alors qu'en microscopie confocale, on trouve bien une sym trie du corps du parasite mais sans une stricte concordance avec ces structures.

Commentaires

Le signe du deltaplane correspond la t te de *Sarcoptes scabiei*, visible en pimicroscopie sous la forme d'un triangle brun tre. Ce signe est discret, et parfois difficile diff rencier des l sions de grattage qui apparaissent comme des

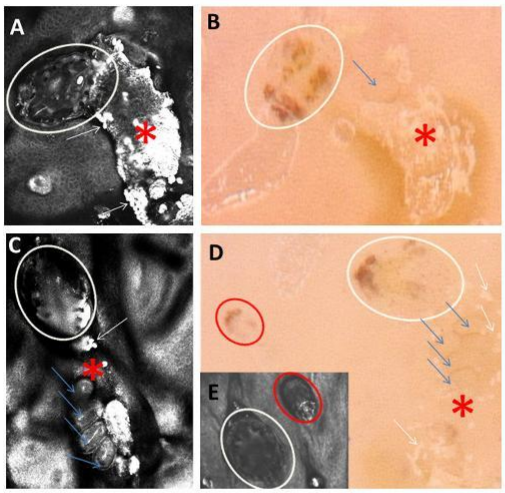

Figure 2. Examen en microscopie confocale in vivo au moyen de la cam ra manuelle (VivaScope 3000, Lucid Inc, distribu en Europe par MAVIG) (A, C, E) d'une gale compar avec l'examen en pimicroscopie par FotoFinder fort grossissement 70 × (B, D). Parasites adultes (cercle blanc), larves (cercle rouge), sillons (ast - risque rouge), œufs (fl che bleue) et d jections caract ristiques (fl che blanche).

petites taches rouge tres ou brun tres (Fig. 1). Une image lin aire blanch tre, correspondant au sillon du sarcopte, peut tre pr sente en association au triangle et peut aider le rep rer. Cependant, cette image n'est pas n cessaire pour tablir le signe du deltaplane car des parasites peuvent tre trouv s distance des sillons et elle n'est pas non plus sp cifique de gale, car les l sions de grattage peuvent se confondre avec un sillon d shabit (Fig. 1). On propose donc de se servir du fort grossissement du vid odermatoscope pour identifier le corps des parasites, ses œufs et ses d jections pour confirmer le diagnostic de gale.

En conclusion, si une exploration des zones suspectes en pimicroscopie trouve le signe du deltaplane, le fort grossissement du deltaplane permet d'achever le diagnostic parasitologique en l'absence de microscope confocal.

D claration d'int r ts

Les auteurs d clarent ne pas avoir de conflits d'int r ts en relation avec cet article.

R f rences

[1] Argenziano G, Fabbrocini G, Delfino M. Epiluminescence microscopy. A new approach to in vivo detection of *Sarcoptes scabiei*. Arch Dermatol 1997;133:751—3.

[2] Perrot JL, Cinotti E, Labeille B, Trau C, Rab rin H, Flori P, et al. Diagnostic rapide de la gale au moyen d'une cam ra manuelle de microscopie confocale par r flectance. Ann Dermatol Venereol 2012;139:502—5.

[3] Cinotti E, Perrot JL, Labeille B, Vercherin P, Chol C, Besson E, et al. Reflectance confocal microscopy for quantification of *Sarcoptes scabiei* in Norwegian scabies. J Eur Acad Dermatol Venereol 2013;27:e176—8.

E. Cinotti , J.-L. Perrot , B. Labeille*, F. Cambazard
Service de dermatologie, h pital Nord, CHU de Saint- tienne, 42055 Saint- tienne cedex 2, France

*Auteur correspondant.
Adresse e-mail : bruno.labeille@chu-st-etienne.fr (B. Labeille)

Reçu le 7 décembre 2012 ;
accept le 10 avril 2013
Disponible sur Internet le 3 juin 2013

http://dx.doi.org/10.1016/j.annder.2013.04.097

Carcinome basocellulaire apr s « r juv nation » par injection de plasma autologue riche en plaquettes

Basal cell carcinoma following platelet-rich plasma injection for skin rejuvenation

Une femme de 79 ans consultait pour une l sion du menton de d couverte r cente. Elle tait de phototype 3 et avait eu des expositions solaires importantes. Ses ant c dents m dicaux consistaient en une hypertension art rielle et un cancer du sein, et son traitement comportait du valsartan. Elle n'avait pas connaissance de cas de m lanome ou de carcinome cutan dans sa famille. L'examen de l'ensemble du t gument montrait deux k ratoses actiniques du nez et de la joue droite, trait es par cryoth rapie l'azote liquide, ainsi que deux l sions infiltr es en regard du pli mentonnier et sur la paupi re sup rieure droite. L'examen histologique des biopsies cutan es puis des pi ces d'ex r se concluait deux carcinomes basocellulaires, dans une forme micronodulaire infiltrante pour la l sion du menton, et dans une forme nodulaire pour la l sion de la paupi re.

Notre attention tait attir e par la r alisation par un m decin esth tique, huit mois avant la survenue de la l sion du menton, d'une injection intradermique mentonni re de plasma autologue riche en plaquettes (PRP). L'interrogatoire de la patiente r v lait l'absence de toute l sion cutan e du menton pr existant l'injection. Aussi ce cas soul ve-t-il la question d'une possible association entre cette injection et la survenue ult rieure du carcinome basocellulaire (CBC) du menton. Ce cas a t d clar au r seau de vigilance en dermatologie esth tique et correctrice (Vigi-DEC).

Discussion

Le PRP s'obtient par centrifugation du sang total issu d'une ponction veineuse, permettant une s paration et une concentration des plaquettes. L'enrichissement en plaquettes est de l'ordre de 300 700 %, aboutissant une concentration d'environ un million de plaquettes par microlitre. Avant r injection, le PRP est activ par adjonction de thrombine recombinante ou de calcium, afin d'obtenir la d granulation des plaquettes [1,2]. L'utilisation du PRP en th rapeutique repose sur la pr sence de nombreux

3.a 6 Inefficacy of alcohol-based hand rub on mites in a patient with hyperkeratotic scabies.

Background.
The World Health Organization is strongly promoting alcohol-based hand rubs to interrupt transmission of pathogens within the healthcare environment, and in some hospitals they are being recommended in cases of scabies. How- ever, there are no studies that demonstrate the efficacy of such hand rubs against scabies.
Aim.
To evaluate the viability of *Sarcoptes scabiei* after the application of various topical antiseptics used for hand hygiene, and the effect of hand washing on the number of parasites present on the skin surface of a patient with scabies.
Methods.
We applied three different topical antiseptics (two alcohol-based and one povidone–iodine-based) to the skin of one hand that was affected by scabies, and took a skin scraping of each area to evaluate the viability of the mites over time. A skin scraping of a control area without antiseptic application was also taken. We also tested the antiseptics directly on the mites. Statistical comparison between the percentages of vital mites in the different samples was assessed using the $X^{(2)}$ test. We also captured a dermoscopic image of the other hand before and after hand washing to count the number of parasites on the skin surface.
Results. Topical antiseptics did not reduce the number of living mites compared with control skin, and hand washing did not reduce the number of parasites on the skin surface.
Conclusions.
Application of topical antiseptics does not reduce the viability of *S. scabiei*, and is therefore unable to prevent the transmission of scabies. The useful- ness of hand washing in preventing transmission of scabies to new subjects remains to be investigated.

Experimental dermatology • **Original article**

CED
Clinical and Experimental Dermatology

Inefficacy of alcohol-based hand rub on mites in a patient with hyperkeratotic scabies

E. Cinotti,[1] J. L. Perrot,[1] B. Labeille,[1] H. Maguet,[2] C. Couzan,[1] P. Flori[2] and F. Cambazard[1]

Departments of [1]Dermatology and [2]Parasitology, University Hospital of Saint-Etienne, Saint-Etienne, France

doi:10.1111/ced.12467

Summary

Background. The Wold Health Organization is strongly promoting alcohol-based hand rubs to interrupt transmission of pathogens within the healthcare environment, and in some hospitals they are being recommended in cases of scabies. However, there are no studies that demonstrate the efficacy of such hand rubs against scabies.

Aim. To evaluate the viability of *Sarcoptes scabiei* after the application of various topical antiseptics used for hand hygiene, and the effect of hand washing on the number of parasites present on the skin surface of a patient with scabies.

Methods. We applied three different topical antiseptics (two alcohol-based and one povidone–iodine-based) to the skin of one hand that was affected by scabies, and took a skin scraping of each area to evaluate the viability of the mites over time. A skin scraping of a control area without antiseptic application was also taken. We also tested the antiseptics directly on the mites. Statistical comparison between the percentages of vital mites in the different samples was assessed using the χ^2 test. We also captured a dermoscopic image of the other hand before and after hand washing to count the number of parasites on the skin surface.

Results. Topical antiseptics did not reduce the number of living mites compared with control skin, and hand washing did not reduce the number of parasites on the skin surface.

Conclusions. Application of topical antiseptics does not reduce the viability of *S. scabiei*, and is therefore unable to prevent the transmission of scabies. The usefulness of hand washing in preventing transmission of scabies to new subjects remains to be investigated.

Introduction

The World Health Organization is strongly promoting alcohol-based hand rubs to interrupt transmission of infectious diseases between patients and within the healthcare environment.[1] In some hospitals, application of an alcohol-based hand rub before and after entering the room of a patient affected by scabies is recommended.[2] However, there are no studies demonstrating the efficacy of alcohol-based hand rubs for scabies, and some authors claim that these products can even increase scabies transmission by inducing a false sense of security in healthcare workers.[3] To our knowledge, the efficacy of compounds based on topical alcohol, chlorexidine digluconate or povidone–iodine against *Sarcoptes scabiei* has not yet been closely studied.

The aim of this study was to evaluate the viability of *S. scabiei* after the application of alcohol-based, chlorexidine digluconate-based, and povidone–iodine-based topical antiseptics usually used for hand hygiene. Moreover, we evaluated if hand washing was able to reduce the number of parasites on the skin surface by mechanical disturbance.

Correspondence: Dr Elisa Cinotti, Department of Dermatology, Hôpital Nord Saint-Etienne, 42055 Saint Etienne Cedex 2, France
E-mail: elisacinotti@gmail.com

Conflict of interest: the authors declare that they have no conflicts of interest.

Accepted for publication 26 April 2014

Materials and methods

Patient

We evaluated a 91-year-old patient with hyperkeratotic scabies, which had been diagnosed by clinical examination and reflectance confocal microscopy.[4]

Evaluation of the efficacy of hand washing and topical antiseptics against *Sarcoptes scabiei*

We evaluated the survival of *S. scabiei* after use of hand washing, after the application of three different antiseptics to the patient's skin, and after immersion of the mites in the three antiseptics in *ex vivo* conditions.

We took dermoscopic images of a skin area on the patient's right hand before and after hand washing with water and a soap (Phagoderm®; Phagogène, Nantes, France) composed of water, potassium cocoate, glycerine and coconut oil.

We applied the three antiseptics to an area of 1 cm^2 on the patient's left hand (Fig. 1). Three antiseptics are usually used in our department for hand hygiene: an alcohol gel (Aniosgel 85 NPC®; Anios, Lille-Hellemmes, France) containing 755 mL/L ethanol; a chlorexidine scrub (Gilbert scrub®; Gilbert, Hérouville Saint-Clair, France) containing 5% ethanol and 4% chlorexidine digluconate, and an iodine scrub (Betadine®; Meda, Paris, France) containing 4% povidone–iodine. The first antiseptic is a 'leave-on' product while the two other antiseptics need to be rinsed off after an appropriate length of time. Simulating the habitual conditions for use of such products in clinical practice, we rinsed off the two latter products, and left the alcohol gel to dry.

Figure 1 Areas of application of the three topical antiseptics to the left hand of a patient affected by hyperkeratotic scabies.

Subsequently, we took a skin scraping from each of the three tested areas and from a control area of the same hand that did not have antiseptic application. We then evaluated the four samples under optical microscopy to count the total number of *S. scabiei* and the number of mites showing leg movements (considered living mites) per sample at time 0 (before application) and after 3, 17, and 44 h.

We also took four additional skin scrapings of the other (right) hand to collect parasites: three of the samples were immersed in one of the three different antiseptic solutions (Aniosgel 85 NPC®, Gilbert® scrub and Betadine® scrub), and one served as control. We subsequently evaluated the four samples under optical microscopy to count the total number of *S. scabiei* and the number of mites showing leg movements per sample at time 0 and after 24 h.

All samples were stored in sterile Petri dishes in a room with controlled temperature (22°C). Counting was performed by three of the investigators (EC, JLP and HM) working as a team.

Statistical analysis

Statistical comparison between the percentage of vital mites in the eight samples with and without the antiseptic application at the different times was assessed using the χ^2 test in Excel (Microsoft Corp., Redmond, WA, USA). $P < 0.05$ was considered statistically significant.

Results

Evaluation of the efficacy of hand washing against *Sarcoptes scabiei*

Dermoscopic images of the patient's right hand were taken (Fig. 2) before and after hand washing, and we counted the number of parasites visible in the two images (Fig. 3).

Evaluation of the efficacy of topical antiseptics against *Sarcoptes scabiei*

The total number of mites and the number of the moving mites visible under optical microscopy in each of the eight skin-scraping samples were counted. Table 1 indicates the survival rate of mites after application of the three different antiseptics on the skin,

Figure 2 Dermoscopic examination of the right hand of a patient affected by hyperkeratotic scabies.

and Table 2 indicates the survival rate of mites directly immersed in the same three antiseptic solutions under *ex vivo* conditions.

Application of any of the topical antiseptic solutions to the skin did not affect the viability of the mites. No statistically significant difference was observed for the percentage of vital mites in the four specimens taken from the treated and untreated skin (χ^2 values of 2.14, 1.46, 0.51, 4.41 at time 0, 3, 17 and 44 h, respectively, with a χ^2 tabulated value of 7.82 for $P = 0.05$ in a χ^2 table with three degrees of freedom). The mobility concerned both nymphs and adult mites. The rate of moving mites in the samples treated with topical antiseptics showed a trend similar to the control sample over time. Mite mobility decreased from time 0 to 17 h,

Table 1 Survival of *Sarcoptes scabiei* after topical application of three different antiseptics on the skin compared with the control sample.

		Vital mites	
	Total mites, *n*	*n*	%
0 h (baseline)			
Control	41	29	70
Alcohol	47	46	98
Chlorhexidine	46	43	93
Povidone iodine	45	38	84
3 h		0	
Control	45	32	71
Alcohol	48	42	88
Chlorhexidine	46	43	93
Povidone iodine	47	39	83
17 h		0	
Control	38	18	47
Alcohol	51	27	53
Chlorhexidine	46	27	59
Povidone iodine	44	23	52
44 h			
Control	17	7	41
Alcohol	54	40	74
Chlorhexidine	55	39	71
Povidone iodine	56	28	50

All mites were counted under optical microscopy at time 0 (baseline) and 3, 17 and 44 h in skin scrapings taken from the skin of a patient with scabies treated with different antiseptics. The control area was not treated.

and then slightly increased at 44 h, probably due to the hatching of eggs and the consequent appearance of new mites.

Immersion of mites in any of the antiseptic solutions also did not affect mite viability. No statistically significant difference was observed for the percentage of vital

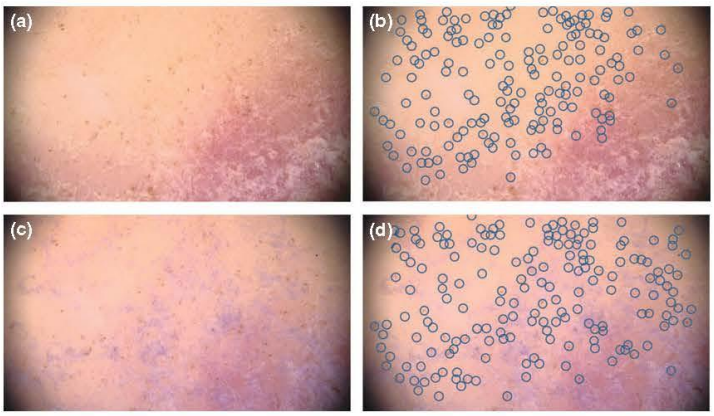

Figure 3 Dermoscopic images of an area on the right hand of a patient affected by hyperkeratotic scabies (a) before and (c) after hand washing with topical antiseptics. (b, d) *Sarcoptes scabiei* mite (blue circle).

Table 2 Survival of *Sarcoptes scabiei* after incubation in one of three different antiseptics in *ex vivo* conditions compared with the control sample.

		Vital mites	
	Total mites, *n*	*n*	%
T0			
Control	17	11	65
Alcohol	15	11	73
Chlorhexidine	12	10	83
Povidone iodine	21	16	76
T24			
Control	17	6	35
Alcohol	15	3	20
Chlorhexidine	13	3	23
Povidone iodine	21	4	19

All mites were counted under optical microscopy at time 0 (baseline) and 24 h in skin scrapings taken from the skin and immersed in different antiseptics. The control area was not treated.

mites in the three specimens incubated with the antiseptics compared with the control value (χ^2 values of 0.35 and 1.21 at time 0 and 24 h, respectively, with a χ^2 tabulated value of 7.82 for $P = 0.05$ in a χ^2 table with three degrees of freedom).

Evaluation of the efficacy of hand washing against *Sarcoptes scabiei*

Dermoscopy showed 167 mites before hand washing and 177 mites after hand washing.

Discussion

Application of topical antiseptics, specifically, hand rubs containing alcohol, chlorexidine digluconate or povidone–iodine, which are usually used by healthcare workers to prevent transmission of pathogens within the healthcare environment, are not able to reduce the viability of *S. scabiei*. In our study, the viability of *S. scabiei* was measured as the ratio of moving parasites to the total number of parasites present on skin scrapings from a patient with hyperkeratotic scabies. None of the samples taken from the skin treated with three different antiseptic solutions or the samples directly immersed in the three antiseptic solutions in *ex vivo* conditions showed any statistically significant difference in the ratio of moving to immobile parasites compared with the control samples that were not treated with any antiseptic solution.

Topical antiseptics have virucidal, fungicidal and bactericidal properties, but their antiparasitic activity has not been demonstrated, and consequently topical antiseptics should not be recommended to prevent scabies transmission. Moreover, the antiparasitic action is even more questionable for topical antiseptics that need to be rinsed off, because even topical acaricides that are known to be highly effective against scabies (e.g. benzyl benzoate and permethrin) require prolonged application (at least 8 h or overnight) in order to kill the mites.

Antiseptic wipes might be sufficient to clean instruments used for the diagnosis of scabies such as dermoscopes or confocal microscopes because of the mechanical disturbance caused by rubbing against a smooth surface,[5] whereas the skin surface is uneven. Nevertheless, it is better to use a disposable transparent film applied to the tip of a camera[5] or similar instrument, or to sterilize the tip if possible whenever the diagnosis of scabies is suspected.

Bellissimo-Rodrigues *et al.*[3] hypothesized that the replacement of hand washing with alcohol-based hand rubs could facilitate scabies dissemination, and suggested the use of traditional hand hygiene techniques instead, in order to prevent transmission of scabies between either staff or patients. Our study showed that hand washing is not able to reduce the number of mites present on the skin surface as measured by dermoscopy before and after hand washing. Moreover, hand washing resulted in greater superficial exposure of the parasites because it eliminated superficial scales, which might possibly increase the transmission of the mites. In addition, our group observed in a previous work[6] that *S. scabiei* can be found at different depths in the skin, and elimination of the more superficial parasites may not be sufficient to prevent the transmission of scabies. The mechanical gesture of hand washing required for the two rinse-off antiseptics that were used in our study also did not reduce either the number or the viability of mites. Therefore, our study showed that hand washing is not sufficient to reduce the number or viability of parasites present on the skin surface of a patient affected by scabies. However, from our study we cannot conclude that hand washing by a person who comes into contact with a patient with scabies is ineffective in reducing the transmission of the disease. It is possible that the mechanical cleansing provided by hand washing with soap can wash away the few parasites that have just come into contact with the new subject and are located more superficially compared with those in an overt case of infection.

Our study has some limitations. First, we measured the viability of mites based on their motility, and therefore we could have missed some living mites that were not moving. However, relying solely on the mobility of the parasites, we found that neither the antiseptic solutions nor the mechanical cleansing by hand washing significantly reduced the number of mobile parasites compared with the control sample. A second limitation of the study is that we evaluated a case of hyperkeratotic scabies so that we could collect a large number of mites, but it could be that our results would not be applicable in cases of less profuse scabies. In fact, it is conceivable that the hyperkeratosis associated with more severe scabies may constitute a barrier to the penetration of antiseptics into the skin. However, hyperkeratosis is often discontinuous even in severe scabies, as showed by the dermoscopical results of our patient (Fig. 2). Furthermore, the fact that the parasites could even survive immersion in the pure antiseptic solutions in *ex vivo* conditions provides support that topical application of an antiseptic is not effective for any form of scabies.

To confirm our results, *in vivo* experiments should be carried out, but these are difficult to achieve. For example, studies that might provide interesting results include infecting volunteers with parasites treated with different antiseptic solutions in order to evaluate the infective capacity of the mites, or evaluating the transmission of scabies from a patient washed with soap and water to a person coming into skin contact with the patient.

Conclusion

Topical antiseptic hand rubs are not able to prevent scabies transmission. Hand washing does not seem to reduce the number of parasites on the skin surface of a patient affected by scabies, but additional studies should be performed to evaluate if hand washing can decrease scabies transmission.

What's already known about this topic?

- No studies have evaluated the efficacy of alcohol-based hand rubs for scabies.

What does this study add?

- Application of topical antiseptics (alcohol, chlorexidine and povidone–iodine), usually used by healthcare workers to prevent transmission of pathogens within the healthcare environment, are not able to reduce the viability of *S. scabiei*.

References

1 Marcel J-P, Alfa M, Baquero F *et al.* Healthcare-associated infections: think globally, act locally. *Clin Microbiol Infect* 2008; **14**: 895–907.
2 Gale, Précautions spécifiques, Plate-forme régionale d'Hygiène Hospitalière des provinces Namur-Luxembourg, 2006. Available at: http://www.health.belgium.be (accessed 7 November 2013).
3 Bellissimo-Rodrigues F, Silva MFI, de Souza RP, de Oliveira e Castro P de T. Alcohol-based hand rub and nosocomial scabies. *Infect Control Hosp Epidemiol* 2008; **29**: 782–83.
4 Perrot JL, Cinotti E, Labeille B *et al.* Rapid diagnosis of scabies by manual confocal reflectance microscopy. *Ann Dermatol Venereol* 2012; **139**: 502–5.
5 Cinotti E, Perrot JL, Labeille B, Cambazard F. On the feasibility of confocal microscopy for the diagnosis of scabies. *Ann Dermatol Venereol* 2013; **140**: 215–16.
6 Cinotti E, Perrot JL, Labeille B *et al.* Reflectance confocal microscopy for quantification of Sarcoptes scabiei in Norwegian scabies. *J Eur Acad Dermatol Venereol* 2013; **27**: e176–8.

3.a 7 Tinea corporis diagnosed by reflectance confocal microscopy

Annales de dermatologie et de v n r ologie (2014) 141, 150—152

Disponible en ligne sur ScienceDirect www.sciencedirect.com

Elsevier Masson France EM|consulte www.em-consulte.com

Formation médicale continue

FICHE TH MATIQUE / MICROSCOPIE CONFOCALE PAR R FLECTANCE

Dermatophytose de la peau glabre diagnostiqu e par microscopie confocale

Tinea corporis diagnosed by reflectance confocal microscopy

E. Cinotti[a], J.L. Perrot[a], B. Labeille[a,*], A. Moragues[a], H. Raberin[b], P. Flori[b], F. Cambazard[a,c], au nom du groupe imagerie cutan e non invasive de la Soci t française de dermatologie

[a] *Service de dermatologie, h pital Nord, CHU de Saint- tienne, 42055 Saint- tienne cedex 2, France*
[b] *Service de parasitologie, h pital Nord, CHU de Saint- tienne, 42055 Saint- tienne cedex 2, France*
[c] *Facult de m decine Jacques-Lisfranc, universit de Saint- tienne, 15, rue Ambroise-Par , 42023 Saint- tienne, France*

Reçu le 15 octobre 2013 ; accept le 29 novembre 2013
Disponible sur Internet le 13 janvier 2014

Observation

Un patient de 32 ans nous a t adress pour une dermatose tr s prurigineuse, voluant depuis environ un an. Le patient avait t trait sans b n fice par acitr tine pour une ventuelle maladie de Darier suspect e en raison de l sions k ratosiques sur le visage et le d collet .

l'examen clinique, des macules ryth matosquameuses aux bords bien limit s, tendues taient pr sentes sur le d collet (Fig. 1), le cou, le visage, la zone pubienne, les fesses et la face ant rieure des cuisses (Fig. 2). Ces aspects taient vocateurs d'une dermatophytose de la peau glabre.

Microscopie confocale par r flectance

Un examen en microscopie confocale (MC) (Vivascope 3000®; Caliber, tats-Unis, New York, distribu en France par Mavig, Munich) tait r alis pour confirmer le diagnostic de dermatophytose de la peau glabre. En quelques minutes, il mettait en vidence dans la couche corn e et granuleuse des structures fines (d'environ 10 µm de diam tre), allong es, hyper-refl tantes et en serpentin (Fig. 3 et 4). Ces aspects taient vocateurs de filaments myc liens. Nous avons ensuite proc d au d collement la curette de quelques squames de la l sion du d collet pour une analyse ex vivo conventionnelle. L'examen microscopique direct par pr paration d'hydroxyde de potassium (KOH) et de noir chlorazole (Fig. 5) a confirm le diagnostic de dermatophytose, et une culture fongique a permis d'identifier *Trichophyton rubrum*.

* Auteur correspondant.
Adresse e-mail : bruno.labeille@chu-st-etienne.fr (B. Labeille).

0151-9638/$ — see front matter
http://dx.doi.org/10.1016/j.annder.2013.11.007

Figure 1. Aspect clinique des l sions du d collet .

Figure 2. Aspect clinique des l sions des cuisses.

Commentaires

La tinea corporis repr sente une infection de la peau glabre par des dermatophytes. Elle se manifeste par des l sions ryth mato-squameuses, annulaires volution centrifuge tr s prurigineuses. L'aspect clinique est souvent voca-teur, mais des examens compl mentaires sont n cessaires pour affirmer le diagnostic. Les techniques conventionnelles pour identifier les dermatophytes sont l'examen direct au microscope optique et la culture fongique. L'examen micro-scopique direct est relativement long et peut donner des r sultats faussement n gatifs en cas de pauci-parasitisme ou erreur d' chantillonnage. La culture fongique n cessite plusieurs semaines et son diagnostic est tardif. R cemment, la MC in vivo a t propos e pour le diagnostic des der-matophytoses, avec l'avantage de ne pas n cessiter de pr l vement des squames pour une analyse ex vivo. De plus, elle est rapide et permet d' valuer toute la surface d'une l sion cutan e et pas seulement les squames pr lev es pour l'analyse ex vivo conventionnelle.

La MC in vivo a t utilis e pour la premi re fois pour l'identification de champignons en 1994 par Pi rard et al. [1] dans un cas d'onychomycose. En 2000, Hong-charu et al. [2] ont montr que la MC in vivo et ex vivo pouvait tre plus rapide que l'examen microscopique

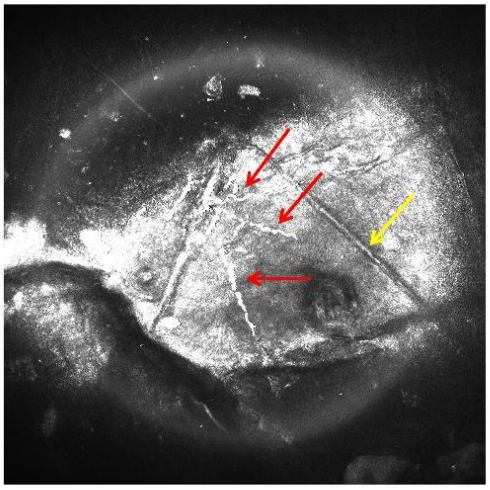

Figure 3. Examen en microscopie confocale de la couche corn e de l' piderme : filaments myc liens avec un aspect en structures fines (diam tre d'environ 10 µm), allong es, hyper-refl tantes et en serpentin (fl che rouge). Un sillon cutan (fl che jaune) est aussi pr sent dans l'image et peut tre diff renci des filaments fon-giques par sa r flectance inhomog ne (hyper-refl tant au milieu et hypo-refl tant sur les c t s) ainsi que par sa lin arit .

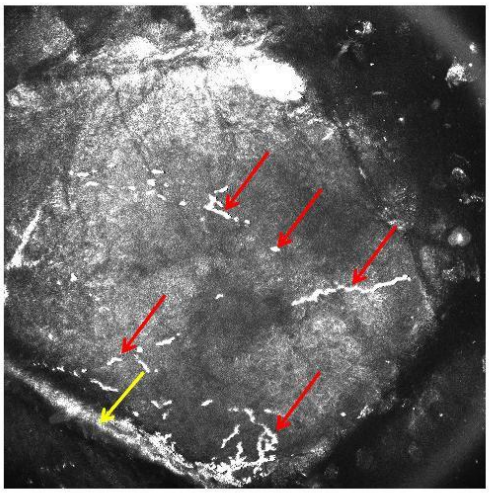

Figure 4. Examen en microscopie confocale de la partie superfi-cielle de la couche granuleuse de l' piderme : filaments myc liens hyper-refl tants de longueurs diff rentes (fl che rouge). Un sillon cutan (fl che jaune) est aussi pr sent dans l'image.

direct classique avec pr paration KOH pour le diagnostic d'onychomycose. En 2001, Markus et al. [3] ont signal le premier cas de diagnostic de tinea corporis par MC in vivo. La sup riorit de la MC in vivo sur l'examen microscopique direct classique avec pr paration KOH pour le diagnostic

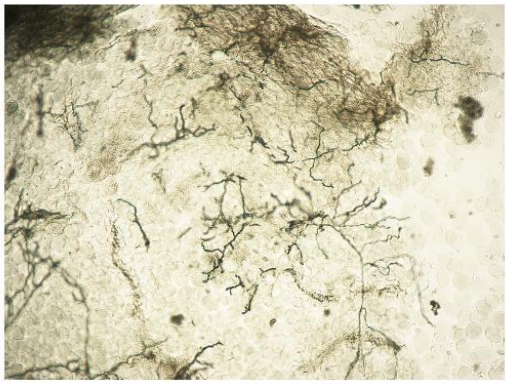

Figure 5. L'examen au microscope optique montre des filaments fongiques.

de dermatophytose a r cemment t rapport e par Rothmund et al. [4] dans une tude prospective sur 50 patients avec suspicion d'onychomycoses des orteils, (sensibilit 79 % contre 74 %, et sp cificit de 81 % contre 76 %) et par Liansheng et al. [5] dans un essai sur 55 patients atteints de tinea corporis (sensibilit 89,1 % vs 80,0 %). Hui et al. [6] ont trouv une sensibilit plus faible de la MC pour les dermatophytoses cutan es dans une tude prospective sur 45 cas qui comparait la MC aux cas positifs en examen microscopique direct classique avec pr paration KOH (64 % de sensibilit chez 22 patients avec tinea manus et pedis ; 83 % de sensibilit dans 23 cas de tinea cruris). La MC a t aussi utilis e pour confirmer le diagnostic clinique de tinea incognita par Turan et al. [7] qui ont montr sa sup riorit en termes de sensibilit par rapport la culture. En particulier, les auteurs ont utilis la MC in vivo trois longueurs d'onde diff rentes (785, 658, 445 nm) et les meilleures images des filaments fongiques ont t obtenues 445 nm.

Les filaments myc liens sont facilement identifiables en MC par leur aspect en structures fines, allong es et hyper-refl tantes. Dans notre cas ils avaient une forme en serpentin. Ils peuvent aussi tre plus lin aires [3,6,7] et arboriformes [6,7]. Les dermatophytes doivent tre recherch s dans la couche corn e et dans la partie superficielle de la couche granuleuse. Les sillons cutan s sont visibles dans ces couches cutan es en MC et doivent tre diff renci s des filaments fongiques. En effet ils pr sentent une r flectance inhomog ne (hyper-refl tant au milieu et hypo-refl tant sur les c t s), ils sont strictement lin aires, et ils forment des structures rhombo des par leur enchev trement.

Markus et al. [3] ont identifi les filaments fongiques par MC apr s application d'une goutte de KOH sur la peau l sionnelle. Cependant, dans notre exp rience et dans celle de Turan et al. [7] cette proc dure n'est pas n cessaire. Les tudes de la litt rature [5—7] ont utilis la camera fixe (VivaScope 1500®), mais dans notre exp rience, la camera manuelle permet aussi d'obtenir de belles images et a l'avantage de permettre une acquisition plus rapide.

En conclusion, la MC est une nouvelle technique non invasive et rapide qui peut confirmer le diagnostic de dermatophytose. De plus, cette technique pourrait s'av rer utile pour une valuation non invasive des r ponses th rapeutiques. Toutefois, des tudes suppl mentaires doivent tre r alis es pour la comparer aux techniques conventionnelles et pour valuer si, sur la base des images de MC, il est possible d'orienter le diagnostic vers tel ou tel type de dermatophytes.

D claration d'int r ts

Les auteurs d clarent ne pas avoir de conflits d'int r ts en relation avec cet article.

R f rences

[1] Pi rard GE, Arrese JE, Pierre S, Bertrand C, Corcuff P, L v que JL, et al. Diagnostic microscopique des onychomycoses. Ann Dermatol Venereol 1994;121:25—9.
[2] Hongcharu W, Dwyer P, Gonzalez S, Anderson RR. Confirmation of onychomycosis by in vivo confocal microscopy. J Am Acad Dermatol 2000;42:214—6.
[3] Markus R, Huzaira M, Anderson RR, Gonz lez S. A better potassium hydroxide preparation? In vivo diagnosis of tinea with confocal microscopy. Arch Dermatol 2001;137:1076—8.
[4] Rothmund G, Sattler EC, Kaestle R, Fischer C, Haas CJ, Starz H, et al. Confocal laser scanning microscopy as a new valuable tool in the diagnosis of onychomycosis — comparison of six diagnostic methods. Mycoses 2013;56:47—55.
[5] Liansheng Z, Xin J, Cheng Q, Zhiping W, Yanqun L. Diagnostic applicability of confocal laser scanning microscopy in tinea corporis. Int J Dermatol 2013;52:1281—2.
[6] Hui D, Xue-cheng S, Ai-e X. Evaluation of reflectance confocal microscopy in dermatophytosis. Mycoses 2013;56:130—3.
[7] Turan E, Erdemir AT, Gurel MS, Yurt N. A new diagnostic technique for tinea incognito: in vivo reflectance confocal microscopy. Report of five cases. Skin Res Technol 2013;19:e103—7.

acceptable adverse effect profile and can induce sustained remission.

G.-Y. Chu,[1] S. C.-S. Hu,[1] C.-C. E. Lan[1,2,*]
[1]Department of Dermatology, Kaohsiung Medical University Hospital, College of Medicine , [2]Department of Dermatology, Kaohsiung Municipal Ta-Tung Hospital, Kaohsiung Medical University, Kaohsiung, Taiwan
*Correspondence: Dr. C.-C. E. Lan. E-mail: laneric@cc.kmu.edu.tw

References

1 Khachemoune A, Janjua SA, Guldbakke KK. Inflammatory linear verrucous epidermal nevus: a case report and short review of the literature. *Cutis* 2006; **78**: 261 267.
2 Vissers WH, Muys L, Erp PE *et al.* Immunohistochemical differentiation between inflammatory linear verrucous epidermal nevus (ILVEN) and psoriasis. *Eur J Dermatol* 2004; 14: 216 220.
3 Jesionek-Kupnicka D, Chomiczewska-Skóra D, Rotsztejn H. Influence of phototherapy in psoriasis on Ki-67 antigen expression: a preliminary study. *Pol J Pathol* 2013; 64: 96 103.

DOI: 10.1111/jdv.12554

Hair dermatophytosis diagnosed by reflectance confocal microscopy: six cases

Editor

Reflectance confocal microscopy (RCM) is an emerging imaging technique that has been used to diagnose skin[1 3] and nail[4] dermatophytosis. Moreover, it has been recently applied to the study of hair[5,6] but not of hair dermatophytosis. We report four cases of tinea capitis and two of tinea barbae diagnosed by *in vivo* or *ex vivo* RCM and the first conidia imaged by RCM.

Major clinical, RCM, optical microscopy and cultural features are reported in Table 1. RCM examination was performed during the dermatological consultation without the use of any particular staining. *In vivo* RCM examination (VivaScope3000®, CALIBER, distributed in Europe by MAVIG GmbH) was performed in case of superficial non-suppurated lesions (Fig. 1), whereas *ex vivo* examination (VivaScope 2500®) was performed when there were suppuration and crusts (Fig. 2). *Ex vivo* RCM was performed immediately after the hair collection: loose hairs that could be painlessly removed were selected and, whenever not available, hairs were collected by gently plucking the hair root with sterile forceps. *In vivo* or *ex vivo* RCM examination took approximately 5 min per patient. RCM examination showed the presence of roundish homogeneous (5 10 μm in size) hyper-reflective structures corresponding to conidia around the proximal part of the hair shaft in all cases (Figs 1, 2). In *in vivo* conditions conidia had a compact organization, whereas in *ex vivo* conditions they were more disperse. In two cases sparse elongated hyper-reflective structures outside the hair shafts, corresponding to hyphae, could also be identified. Dermatophytes inside the medulla of the hair shaft could not be identified.

Conventional optical microscopic examination with blue lactophenol solution confirmed the presence of conidia outside the hair shaft in all cases, but could find hyphae in only one case. The culture, performed on Sabouraud's dextrose agar containing chloramphenicol (0.05%) and cycloheximide (0.5%), showed the presence of *Microsporum canis* or *Trichophyton mentagrophytes*.

In our case series, we could confirm in few minutes the diagnosis of hair dermatophytosis by using RCM during the

Table 1 Clinical features of the six hair dermatophytosis with their respective findings of reflectance confocal microscopy, optical microscopy and cultural examination.

Case number	Age/ sex	Site of the lesions	Evolution	Clinical presentation	Wood's light examination	*In vivo* RCM	*Ex vivo* RCM	Optical microscopy examination	Cultural examination
1	5/F	Scalp	2 months	Two scaly patches of alopecia	Green	Ectothrix conidia	NA	Ectothrix conidia	*Microsporum canis*
2	7/M	Scalp	1 month	One scaly patch of alopecia	Green	Ectothrix conidia	NA	Ectothrix conidia	*Microsporum canis*
3	6/F	Scalp	15 days	Abscess	Negative	NA	Ectothrix conidia	Ectothrix conidia	*Trichophyton Mentagrophytes*
4	54/M	Beard	15 days	Abscess	Negative	NA	Ectothrix conidia and hyphae	Ectothrix conidia	*Trichophyton Mentagrophytes*
5	28/M	Beard	1 month	Abscesses	Green	NA	Ectothrix conidia	Ectothrix conidia	*Microsporum canis*
6	4/M	Scalp	1 month	One patch of alopecia with pustules	Green	Ectothrix conidia and hyphae	NA	Ectothrix conidia and hyphae	*Microsporum canis*

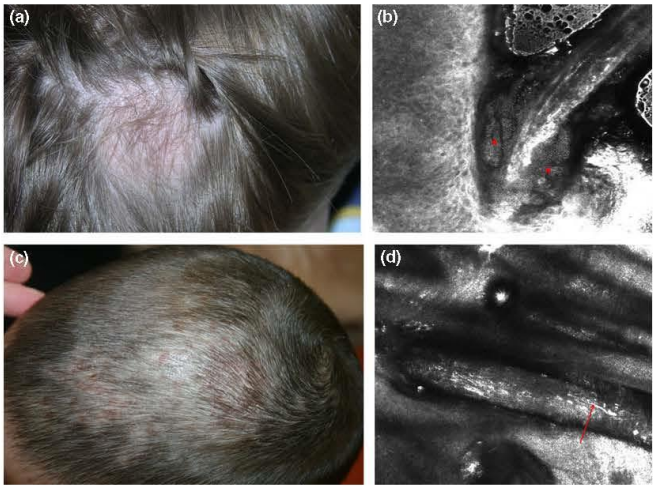

Figure 1 Two cases of tinea capitis due to *Microsporum canis*. (a, c) Clinical aspect with patchy alopecia. (b, c) *In vivo* reflectance confocal microscopy aspect with conidia (red asterisk) and hyphae (red arrow).

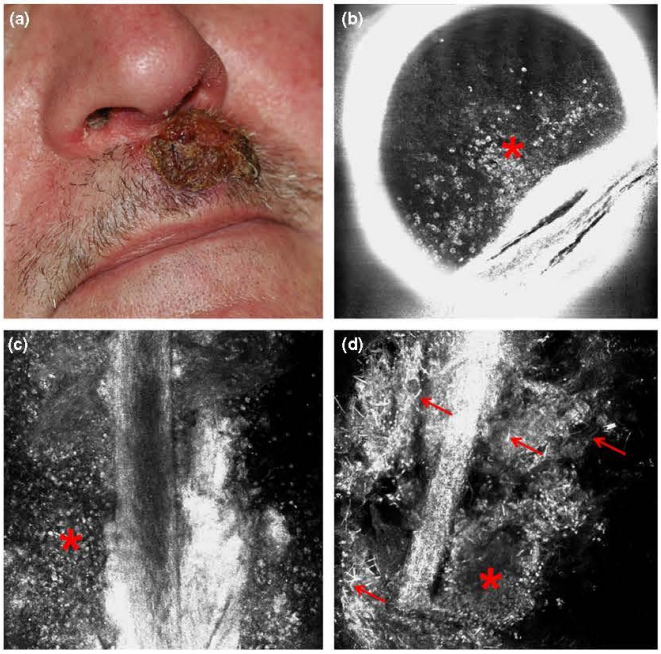

Figure 2 Tinea barbae due to *Trichophyton Mentagrophytes*. (a) Clinical aspect with an inflammatory crusted patch. (b) *Ex vivo* reflectance confocal microscopy aspect with conidia (red asterisk) and hyphae (red arrow).

dermatological consultation, and could quickly initiate an appropriate treatment without waiting for the conventional mycological examination. In contrast, conventional fungal cultures require long incubation periods of 1 5 weeks[7] and optical microscopy is usually performed with a particular staining such as KOH or blue lactophenol with an incubation of around 10 30 min[8,9] to increase its sensitivity.

In vivo RCM has the additional advantage, compared to conventional optical microscopy and cultures, of being non-invasive and not limited to the analysis of the extracted hair, being able to explore the entire lesion, thus reducing false negative cases. However, *in vivo* examination cannot be performed in case of suppuration or crusting that give artefacts. *Ex vivo* RCM examination avoids the problem of movements in children and is not very invasive because the collection of the hair, in case of hair dermatophytosis due to the parasitic involvement, is usually not painful.

In conclusion, this study shows that RCM can identify hair dermatophytes and that conidia are 'visible' under RCM due to their high reflectance. Further studies are needed to define the RCM features of different types of dermatophytes and to compare RCM performances with the conventional techniques. Although at present RCM cannot replace the current diagnostic standards for hair dermatophytosis, it may be successfully used as an additional tool to facilitate the diagnosis and indicate the need for further investigation of the patient.

E. Cinotti,[1,*] J.L. Perrot,[1] B. Labeille,[1] H. Raberin,[2] P. Flori,[2] F. Cambazard[1]

[1]Department of Dermatology, University Hospital of Saint-Etienne, Saint Etienne, France, [2]Department of Parasitology, University Hospital of Saint-Etienne, Saint Etienne, France

*Correspondence: E. Cinotti. E-mail: elisacinotti@gmail.com

References

1 Slutsky JB, Rabinovitz H, Grichnik JM, Marghoob AA. Reflectance confocal microscopic features of dermatophytes, scabies, and demodex. *Arch Dermatol* 2011; **147**: 1008.
2 Hui D, Xue-cheng S, Ai-e Xu. Evaluation of reflectance confocal microscopy in dermatophytosis. *Mycoses* 2013; **56**: 130 133.
3 Liansheng Z, Xin J, Cheng Q *et al.* Diagnostic applicability of confocal laser scanning microscopy in tinea corporis. *Int J Dermatol* 2013; **52**: 1281 1282.
4 Cinotti E, Fouilloux B, Perrot JL, Labeille B, Douchet C, Cambazard F. Confocal microscopy for healthy and pathological nail. *J Eur Acad Dermatol Venereol* 2013; doi: 10.1111/jdv.12330. [Epub ahead of print].
5 Rudnicka L, Olszewska M, Rakowska A. In vivo reflectance confocal microscopy: usefulness for diagnosing hair diseases. *J Dermatol Case Reports* 2008; **2**: 55 59.
6 Scope A, Benvenuto-Andrade C, Agero A-LC *et al.* In vivo reflectance confocal microscopy imaging of melanocytic skin lesions: consensus terminology glossary and illustrative images. *J Am Acad Dermatol* 2007; **57**: 644 658.
7 Tampieri MP. Update on the diagnosis of dermatomycosis. *Parassitologia* 2004; **46**: 183 186.
8 Rothmund G, Sattler EC, Kaestle R *et al.* Confocal laser scanning microscopy as a new valuable tool in the diagnosis of onychomycosis - comparison of six diagnostic methods. *Mycoses* 2013; **56**: 47 55.
9 Grillot R. Techniques de diagnostic biologique des mycoses. In Les mycoses humaines: Démarche diagnostique (Grillot R, ed). Elsevier, Paris: Collection Option Bio, 1996;3: 221.

DOI: 10.1111/jdv.12557

Widespread erythema ab igne caused by hot bathing

Editor

Erythema ab igne (EAI) is caused by frequent exposure to heat, usually infrared radiation.[1] Although it may be seen anywhere on the body, most cases are localized. It typically affects the thighs and lower legs of individuals who sit in front of heaters or fires. Recently, laptop computer-induced EAI has been frequently reported.[2] The cultures of bathing are unique in each culture throughout the world. In Japan, bathtub is more popular than shower. Furthermore, the temperature of bath water in Japan is usually hotter than that in Europe. Nevertheless, there are no English literatures with EAI caused by bathing, from Japan. Lin *et al.* reported a case due to frequent hot bathing, who was affected in the lower extremities.[3] We present here a widespread EAI on the body caused by hot bathing.

A 50-year-old man was referred to our hospital with net-like pigmented skin eruptions on his trunk and legs that had been present for a year. There were no subjective symptoms. He had not been receiving topical ointments or other medications. Physical examination revealed reticulated pigmented eruptions on both the lower extremities, the buttocks and the trunk, with a clear border on the chest (Fig. 1). No skin ulcerations, papules, or indurations were detected. He showed no peripheral circulatory disturbance in the palpable dorsalis pedis artery pulse. The complete blood count, serum chemistry profile, liver function test, complement and urinalysis were normal. Anti-nuclear antibody was positive, with a titer of 1 : 40. Anti-double-stranded DNA antibody and cryoglobulin were negative. A skin biopsy was taken from a pigmented lesion on the left leg. The microscopic findings showed mild superficial perivascular lymphocytic infiltration, dermal pigmentation and a dyskeratotic cells in the epidermis, but not vasculitis (Fig. 2). In the dermis, inner lumen of eccrine duct was obstructed or slender (Fig. 2). On further questioning, he reported taking a very hot bath (approximately 45°C for 30 min) every day for the previous 2 years. The distribution of the pigmented lesions corresponded to the areas that were

3.a 9 Dermoscopy and confocal microscopy for in vivo detection and characterization of Dermanyssus gallinae mite.

Dermoscopy and confocal microscopy for in vivo detection and characterization of *Dermanyssus gallinae* mite

Elisa Cinotti, MD,[a] Bruno Labeille, MD,[a] Charlotte Bernigaud, MD,[b] Fang Fang, DVM,[c] Christelle Chol, MD,[a] René Chermette, DVM,[c] Jacques Guillot, DVM, PhD,[c] Frédéric Cambazard, PhD,[a] and Jean-Luc Perrot, MD[a]
Saint-Etienne, Créteil, and Maisons-Alfort, France

Key words: dermatonyssus; dermoscopy; entodermoscopy; imaging; in vivo reflectance confocal microscopy; parasite.

CLINICAL PRESENTATION

A 92-year-old woman was evaluated for the possibility of scabies. She presented small itchy purpuric macules and papules on the trunk and limbs (Fig 1). A careful examination found small red parasites moving on the skin.

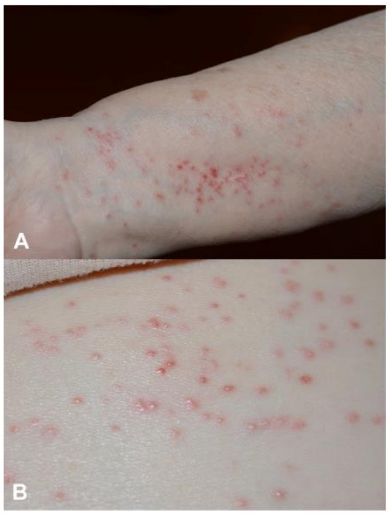

Fig 1. Clinical appearance: purpuric papules with a vesicular center on the forearm (**A**) and the thigh (**B**).

DERMOSCOPIC AND REFLECTANCE CONFOCAL MICROSCOPY APPEARANCE

Dermoscopy showed dilated vessels on an erythematous background in correspondence of the macules and papules (Fig 2, *A*). Reflectance confocal microscopy demonstrated the presence of intraepidermal vesicles (Fig 2, *C*). Both techniques allowed us to better characterize the parasites as 650- × 1000-μm ovoid bodies with 8 legs (Fig 2, *B* and *D*).

From the Department of Dermatology, University Hospital of Saint-Etienne[a]; Department of Dermatology, University Hospital of Créteil[b]; and Department of Parasitology, Veterinary College of Alfort.[c]
Funding sources: None.
Conflicts of interest: None declared.

Reprint requests: Elisa Cinotti, MD, Department of Dermatology, University Hospital of Saint-Etienne, 42055 Saint Etienne Cedex 2, France. E-mail: elisacinotti@gmail.com.
J Am Acad Dermatol 2015;73:e15-6.
0190-9622/$36.00

http://dx.doi.org/10.1016/j.jaad.2015.03.022

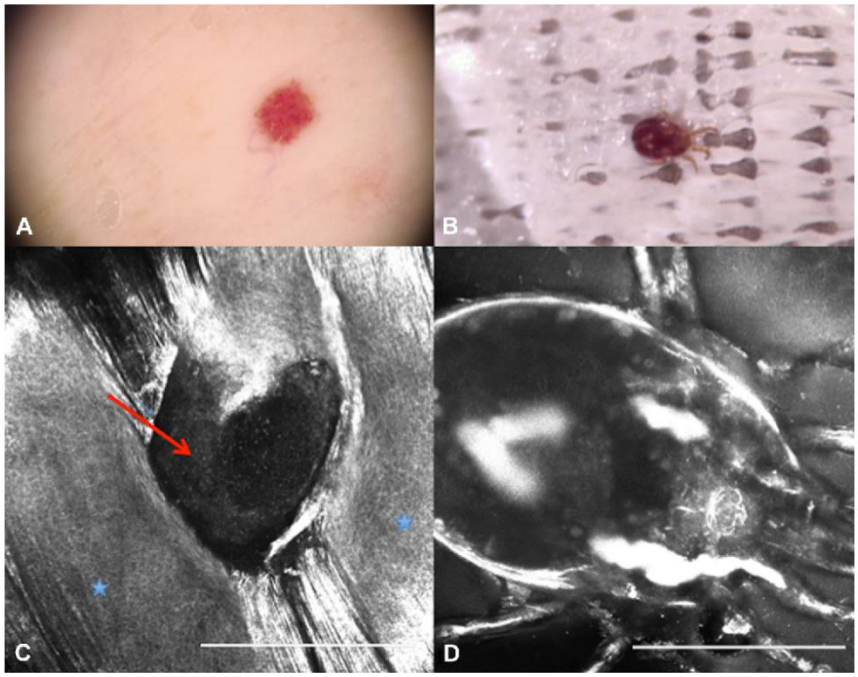

Fig 2. Dermocopic (**A** and **B**) and reflectance confocal microscopy (RCM) (**C** and **D**) images of the skin lesions (**A** and **C**) and of *Dermanyssus gallinae* (**B** and **D**). **A**, Erythematous background with dilated vessels. **C**, Intraepidermal vesicle (*red arrow*). *Dermanyssus gallinae* appears as a bright red (**B**) mite with an ovoid body (**B** and **D**). The parasite was identified by dermoscopy and RCM on the skin of the patient and was then placed in a container to capture these images. Scale bar = 500 μm.

DIAGNOSIS

Skin lesions corresponded to bites from *Dermanyssus gallinae* that were identified directly on the skin of the patient thanks to dermoscopy and reflectance confocal microscopy. This hematophagous ectoparasite affects birds and occasionally human beings in direct contact with birds. Moreover, mites have been reported to enter buildings from pigeon nests via windows or air-conditioning systems, such in our case where the patient had no direct contact with any animals.[1] Unfed adult mites measure approximately 400 × 700 μm and are grayish white but increase to greater than 1 mm and become bright red and brown[1] when engorged as in our case.

KEY MESSAGE

Parasites from *Dermanyssus* genus can cause a pruritic dermatitis that can be misdiagnosed as scabies and unnecessarily treated with ectoparasiticides.[1] These mites are temporary visitors to human skin and the identification and removal of their source is necessary to cure the patients. Dermoscopy and reflectance confocal microscopy can help their identification. In our patient, parasites were easily removed from the skin by showering and washing clothes.

REFERENCE

1. Gavrilović P, Kecman V, Jovanović M. Diagnosis of skin lesions caused by *Dermanyssus gallinae* in five patients. *Int J Dermatol.* 2015;54:207-210.

3.a 10 Unusual reflectance confocal microscopy findings during the examination of a perianal nevus: pinworms.

K. Imafuku,[1,*] K. Yoshino,[1] K. Ishiwata,[1] S. Otobe,[1] S. Tsuboi,[1] K. Ohara,[1] H. Hata[2]
[1]Tokyo Metropolitan Cancer and Infectious Diseases Center, Komagome Hospital, Tokyo, Japan, [2]Department of Dermatology, Hokkaido University Graduate School of Medicine, Sapporo, Japan
*Correspondence: K. Imafuku. E-mail: imafukukeisuke@gmail.com

References

1 Hodi FS, O'Day SJ, McDermott DF *et al.* Improved survival with ipilimumab in patients with metastatic melanoma. *N Engl J Med* 2010; **363**: 711 723.
2 Robert C, Long GV, Brady B *et al.* Nivolumab in previously untreated melanoma without BRAF mutation. *N Engl J Med* 2015; **372**: 320 330.
3 Chapman PB, Hauschild A, Robert C *et al.* Improved survival with vemurafenib in melanoma with BRAF V600E mutation. *N Engl J Med* 2011; **364**: 2507 2516.
4 Harding JJ, Pulitzer M, Chapman PB. Vemurafenib sensitivity skin reaction after ipilimumab. *N Engl J Med* 2012; **366**: 866 868.
5 Johnson DB, Wallender EK, Cohen DN *et al.* Severe cutaneous and neurologic toxicity in melanoma patients during vemurafenib administration following anti-PD-1 therapy. *Cancer Immunol Res* 2013; **1**: 373 377.

DOI: 10.1111/jdv.13331

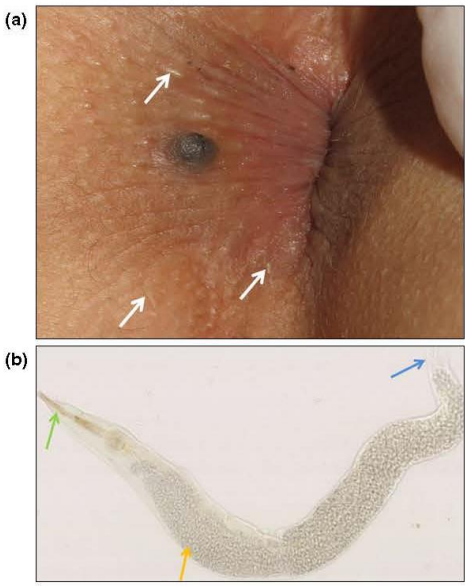

Figure 2 Clinical aspect (a) of the perianal nevus and pinworms (white arrow) and optical microscopy examination (b) of a pinworm. The pharynx (green arrow), the eggs (yellow arrow) and the anus (blue arrow) are visible.

Unusual reflectance confocal microscopy findings during the examination of a perianal nevus: pinworms

Editor

During the reflectance confocal microscopy (RCM) examination of a perianal nevus of a child with the hand-held camera Vivascope 3000® (Caliber, New York, USA, distributed in Europe by MAVIG GmbH, München, Germany) we observed fusiform structures, about 300 μm in diameter, plenty of tightly packed, hyper-reflective ovoid bodies of around 50 μm per 20 μm in size (Fig. 1), which were too ovoid to be melanocytes. Moreover, the fusiform structure that contained these bodies was unusual in the skin.

A clinical examination of the naevus and the peripheral healthy skin allowed the identification of elongated white structures moving on the skin surface (Fig. 2a) suggestive of pinworms which are one of the most common intestinal parasitosis.[1] A conventional microscopic examination could confirm the presence of pinworms (Fig. 2b).

The RCM aspect of pinworms had never been reported. RCM can confirm the presence of the parasite and its eggs, visible as ovoid hyper-reflective bodies. RCM features of pinworms should be known when examining the perianal region to recognize these possible incidental findings.

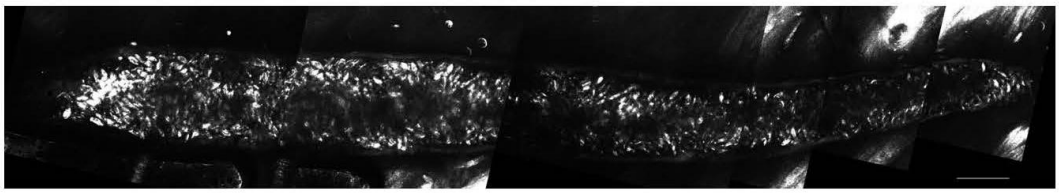

Figure 1 Reflectance confocal microscopy examination of a pinworm. Scale bar=200 μm. RCM images are stitched together to reconstruct the entire parasite. Eggs are visible inside the parasite body.

E. Cinotti,[1,*] B. Labeille,[1] F. Cambazard,[1] P. Flori,[2] H. Raberin,[2] J. L. Perrot[1]
[1]Department of Dermatology, University Hospital of Saint-Etienne 42055, Saint Etienne, France, [2]Department of Parasitology, University Hospital of Saint-Etienne 42055, Saint Etienne, France
*Correspondence: E. Cinotti. E-mail: elisacinotti@gmail.com

Reference

1 Guidetti C, Ricci L, Vecchia L. Prevalence of intestinal parasitosis in Reggio Emilia (Italy) during 2009. *Infez Med* 2010; **18**: 154–161.

DOI: 10.1111/jdv.13333

Penile ulceration: a rare manifestation of cutaneous crohn's successfully treated with subcutaneous methotrexate

Editor

A 41-year-old man was referred to the joint dermatology/genitourinary clinic with a 2-month history of penile ulcers. He had a complicated history of perianal and colorectal Crohn's disease. This was previously treated by the gastroenterologist with Infliximab but was ineffective, Azathioprine of which he was intolerant and 6-mercaptopurine. Initially, the latter was partially effective then less so requiring a subtotal colectomy with end ileostomy.

The ulcers started 4 months after being on Adalimumab, started for Crohn's related spondylarthropathy. Examination revealed numerous painful ulcers on the ventral and dorsal glans penis (Fig. 1). There were no oral lesions. Histology from one of the penile ulcers revealed dense granulomatous inflammation with prominent epithelioid granulomas, multinucleate giant cells and a mixed inflammatory infiltrate. Direct immunofluorescence was negative. Apart from one positive, repeated swabs for herpes simplex virus (HSV) were negative. Sexually transmitted infection screen for syphilis, gonorrhoea, chlamydia and HIV were negative. His chest X-ray was unremarkable.

He underwent panproctocolectomy for ongoing active Crohn's of the rectal stump but unfortunately developed wound dehiscence. An extensive perineal ulcer with indurated erythematous edges gradually extended to the subscrotal area. Oral methotrexate, prescribed by his rheumatologist at a dose of 15 mg a week orally for 2 months, was ineffective. This was followed by Etanercept 25 mg subcutaneously twice a week, which improved his ulcers but worsened his arthritis and was stopped after 6 weeks. Adalimumab was restarted but his arthritis worsened and was stopped.

Figure 1 Showing numerous painful ulcers on glans penis and inner foreskin.

Given the ongoing penile ulceration and extending perineal wound, subcutaneous methotrexate was prescribed gradually building to a maintenance dose of 25 mg once a week. There has been resolution of the penile ulcers (Fig. 2) with sustained remission over 2 years and slower near complete healing of the perineal wound. His gastrointestinal Crohn's has remained inactive since his panproctocolectomy and his spondylarthropathy has been partially controlled on subcutaneous methotrexate.

Given the histology and ongoing ulceration despite HSV prophylaxis with valciclovir, the penile ulcers and perineal wound dehiscence was in keeping with cutaneous Crohn's. Metastatic cutaneous Crohn's lesions are found in areas anatomically distant from the gastrointestinal tract, separated by normal skin. It can affect any area of the skin and the penile involvement in cutaneous Crohn's is rare.[1] Clinical features affecting penile skin include ulceration either on the glans (corona or subcoronal area), dorsal or lateral penis[2,3] and also penile oedema. Cutaneous Crohn's is more frequently observed in patients with colon or colorectal involvement than in those with involvement of the small intestine alone. Clinical course is usually independent from the intestinal disease.[2] Treatment of bowel disease is not always followed by improvement of the cutaneous lesions.

This man's penile ulcers have been resistant to treatment complicated by worsening of arthritic symptoms with anti-TNF therapy. Treatment of ulcerative penile crohn's remains controversial. Topical[3] or oral corticosteroids[1,2] (CS), topical tacrolimus,[4] oral thalidomide,[3] methotrexate,[1] and a combination of oral CS, metronidazole and aminosalicylates[2,5] have been suggested in case reports only.

Patients with Crohn's disease have reduced the bioavailability with oral methotrexate compared with subcutaneous administration.[6] This case highlights the rare manifestations of cutaneous Crohn's and the use of methotrexate particularly by

3.a 11 Videodermoscopy compared to reflectance confocal microscopy for the diagnosis of scabies.

Introduction

Reflectance confocal microscopy (RCM) and dermoscopy have recently been suggested for non-invasive diagnosis of scabies. However, there are large studies on diagnostic accuracy for scabies only with dermoscopy at low (10x) and high (100–1000 x) magnification.

Objective

Our study evaluated the diagnostic accuracy, for the diagnosis of scabies, of RCM and videodermoscopy at intermediate (209 and 709) magnification, which is usually found in commercially available videodermoscopes.

Methods

Patients with a presumptive diagnosis of scabies were prospectively enrolled during 20 months and examined by RCM and videodermoscopy at intermediate magnification. The specificity of RCM was considered 100% because RCM can identify the anatomical details of the parasites.

Results A total of 148 patients were enrolled. Videodermoscopy showed a higher sensitivity for scabies than RCM (95% vs. 92%) and a specificity of 97%.

Conclusions

Videodermoscopy at intermediate magnification, and RCM are both highly accurate for the diagnosis of scabies. If the two devices are available, it would be better to perform videodermoscopy first, that is more sensitive, and then RCM to confirm the diagnosis.

DOI: 10.1111/jdv.13676 JEADV

SHORT REPORT

Videodermoscopy compared to reflectance confocal microscopy for the diagnosis of scabies

E. Cinotti,* B. Labeille, F. Cambazard, A.C. Biron, C. Chol, A. Leclerq, C. Jaffelin, J.L. Perrot

Dermatology Department, University Hospital of Saint-Etienne, Saint-Etienne, France
*Correspondence: E. Cinotti. E-mail: elisacinotti@gmail.com

Abstract

Introduction Reflectance confocal microscopy (RCM) and dermoscopy have recently been suggested for non-invasive diagnosis of scabies. However, there are large studies on diagnostic accuracy for scabies only with dermoscopy at low (10×) and high (100–1000×) magnification.

Objective Our study evaluated the diagnostic accuracy, for the diagnosis of scabies, of RCM and videodermoscopy at intermediate (20× and 70×) magnification, which is usually found in commercially available videodermoscopes.

Methods Patients with a presumptive diagnosis of scabies were prospectively enrolled during 20 months and examined by RCM and videodermoscopy at intermediate magnification. The specificity of RCM was considered 100% because RCM can identify the anatomical details of the parasites.

Results A total of 148 patients were enrolled. Videodermoscopy showed a higher sensitivity for scabies than RCM (95% vs. 92%) and a specificity of 97%.

Conclusions Videodermoscopy at intermediate magnification, and RCM are both highly accurate for the diagnosis of scabies. If the two devices are available, it would be better to perform videodermoscopy first, that is more sensitive, and then RCM to confirm the diagnosis.

Received: 30 October 2015; Accepted: 2 March 2016

Conflict of Interest

None declared.

Funding sources

None

Introduction

Scabies can mimic a variety of skin diseases and the diagnosis based only on clinical criteria is prone to error.[1] *Ex vivo* optical microscope examination of scales obtained by skin scraping was so far the standard procedure for the diagnosis of scabies.[2] However, this technique can give false negative results when only few parasites are present.[3] Recently, dermoscopy[1,4–9] and reflectance confocal microscopy (RCM)[10–12] have been suggested for the diagnosis of this infestation. Different from optical microscopy, these techniques are non-invasive and are performed *in vivo*, with the consequent advantage of being faster and suitable for an extensive examination of the body surface.

Two studies[1,6] demonstrated that the sensitivity of hand-held dermoscopy at low (10×) magnification for the diagnosis of scabies is non-inferior[6] and even higher[1] than that of optical microscopy. Dermoscopy specificity was much lower than the 100% of optical microscopy, but two other studies[13,14] suggested that higher magnification (up to 1000×) could improve dermoscopy specificity.

Our study compared the diagnostic accuracy of RCM and dermoscopy performed at intermediate (20× and 70×) magnification, which is usually found in commercially available videodermoscopes, as well as the time required for the diagnosis.

Material and methods

Patients

All patients referred to the Dermatology Department of the University Hospital of Saint-Etienne (France) for a clinical suspicion of scabies and all patients with a clinical diagnosis of scabies established by a dermatologist in our department were prospectively enrolled from the 10 October 2013 to the 10 June 2015.

Study design

Sex and age, presence of highly pigmented skin, signs and symptoms (severe itch, absence of skin lesions, papules, vesicles, pustules, burrows, plaques and nodules) and positive history of atopic dermatitis in the last year were recorded.

The diagnosis of scabies was performed at clinical examination, at first without imaging devices and then with dermoscopy and RCM. Patients were examined separately by three dermatologists. The first one only performed the clinical examination and gave the clinical diagnosis. The others, experts in dermoscopy and RCM, gave the imaging diagnosis: one used videodermoscopy first and then RCM; the other performed a RCM examination followed by videodermoscopy. The selection of the body sites to be examined was left to the discretion of the investigator.

The time necessary for the dermoscopic and the RCM diagnosis of scabies was recorded starting from the moment when the investigator placed the probe on the skin, after performing a clinical examination of the patient to identify the possible lesions to be examined. A duration of 10 min per patient was necessary to affirm the absence of scabies.

Dermoscopy

Dermoscopy was performed with a videodermoscope (FotoFinder Systems GmbH, Bad Birnbach, Germany) at ×20 magnification as initial screening and at ×70 to confirm the presence of the mite[5] (Fig. 1a c). A positive dermoscopy diagnosis of scabies was established whenever a mite was visible. The presence of eggs and droppings at ×70 magnification were additional elements to confirm the diagnosis of scabies but were not used (if alone) as a positive criterion.

Reflectance confocal microscopy

RCM examination was carried out with the hand-held VivaScope 3000® camera (Caliber, New York, NY, USA, distributed in Europe by MAVIG GmbH, Munich, Germany). A positive RCM diagnosis of scabies was established whenever mites and/or eggs were visible[11,12] (Fig. 1d f). Droppings were used as a signal of a nearby presence of a parasite. However, they were not used for the diagnosis of scabies in order to avoid the risk of having false positive results induced by the presence of artefacts.

Final diagnosis of scabies

The final diagnosis of scabies was established by comparing the results of the four examinations performed by the two investigators and basing on the clinical evolution after 3 weeks. RCM was considered 100% specific. A patient was considered to be affected by scabies if RCM was positive or if he responded to the anti-parasitic treatment. A patient was not considered affected by scabies if he responded to a treatment different from the anti-parasitic one (for example in case of eczema, prurigo and dyshidrosis, a steroid cream was prescribed).

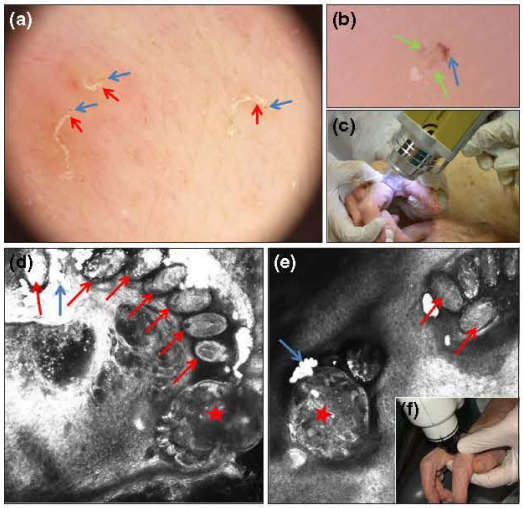

Figure 1 Videodermoscopy (a–c) at ×20 and ×70 magnification and reflectance confocal microscopy (RCM) (d–f) examination of scabies. The 'delta wing sign', a triangular brown structure corresponding to the fore portion of the *Sarcoptes scabiei* (blue arrow) usually found at the end of a burrow (red arrow), is visible at ×20 magnification (a). At ×70 magnification (b) it is possible to better identify the brown cephalic portion of the parasite (blue arrow) followed by its ovoid body with two brownish parallel bands (green arrow). 70× magnification is particularly useful when the burrow behind the parasite is absent and a parasite might be misinterpreted as a crust. The videodermoscope used for the examination is showed (c). RCM (d and e) shows adult females of *Sarcoptes scabies* (red asterisk) present with a not homogeneously refractive ovoid body, droppings (blue arrow) and eggs (red arrow). The hand-held reflectance confocal microscope used for the examination is showed (f).

Data analysis

The *t*-test and the chi-square test (corrected for continuity when necessary) were used to compare the demographic and clinical features of the patients with and without scabies.

The sensitivity, specificity, positive and negative predictive values and 95% confidence intervals of videodermoscopy and RCM were established by comparing the results of these two techniques to the final diagnosis of scabies performed following the criteria detailed in the previous paragraph. Results of dermoscopy and RCM performed with the different orders, considering the two investigators altogether, were compared among them using the chi-square test and Mc Nemar's test. These results were also compared to the final diagnosis of scabies using the chi-square test. In order to compare the diagnostic skills of the two investigators, results of dermoscopy and RCM performed with the different orders by each investigator were compared by the chi-square test. A *P*-value less than 0.05 was considered statistically significant.

Results

Clinical features

Clinical data are reported in Table 1.

Hundred and forty-eight consecutive patients were enrolled. Thirty-two patients had ≤12 years and 9 ≤ 1 year. Hundred and forty patients were sent for a suspicion of scabies; five out of these were already treated for scabies. Eight patients were sent with other diagnoses (five eczema, one pruritus associated with pregnancy, one psoriasis, one hand-foot and mouth disease) but had clinical lesions evocative of scabies.

In total, 52% of the patients had scabies. Demographic data of patients with and without scabies were not statistically different.

The presence of vesicles ($P = 0.0058$) was associated with scabies, whereas the presence of plaques ($P = 0.0025$) was more commonly found in patients not affected by scabies. Burrows were present in most patients with scabies (73%). Eight patients had a personal history of atopic dermatitis in the last year, but this aspect could not allow to differentiate patients with eczema from those with scabies. Only three patients were phototype VI.

Diagnostic accuracy of dermoscopy and RCM

The diagnostic properties of the two devices are shown in Table 2. The first investigator performed dermoscopy first, and then RCM in 73 cases and inversely in 75 cases; the second investigator performed the opposite sequence. The mean time to diagnose positive cases by dermoscopy or RCM with the different orders was less than 1 min for both devices. Both techniques showed an excellent accuracy. A statistically significant difference among the results of videodermoscopy and RCM performed in the two different orders was not found. However, dermoscopy performed before RCM showed the best sensitivity (95%). Moreover, when we compared the results of each test with the final diagnosis of scabies, dermoscopy performed as the first examination had the lowest chi-square value (chi-square value 0.054, $P = 0.8161$), indicating a lower difference with the final diagnosis of scabies. No inter-investigator difference was found.

Table 1 Clinical features of the examined patients

	No scabies* ($n = 71$)	Scabies ($n = 77$)	Total ($n = 148$)
Demographic data			
Men (%)	20 (28)	28 (36)	48 (32)
Women (%)	51 (72)	49 (64)	100 (68)
Mean age (range)	47 year (3 months to 96 year)	33 year (1 months to 96 years)	40 year (1 months to 96 years)
Median age	29 year	23 year	47 year
Symptoms and signs			
Severe itch	71 (100)	77 (100)	148 (100)
Absence of skin lesions (%)	12 (17)	7 (9)	19 (13)
Burrows (%)	1 (1)	56 (73)	57 (39)
Papules (%)	20 (28)	31 (40)	51 (34)
Vesicles (%)	10 (14)	27 (35)	37 (25)
Pustules (%)	3 (4)	2 (3)	5 (3)
Plaques (%)	8 (11)	0	8 (5)
Nodules (%)	0	3 (4)	3 (2)
Severe excoriations (%)	29 (41)	8 (10)	37 (25)
Phototype IV (%)	0	3 (4)	3 (2)
Atopic dermatitis in the last year (%)	5 (7)	3 (4)	8 (5)
Diagnosis performed by non-dermatologists			
Possible scabies (%)	68 (96)	67 (87)	135 (91)
Resistance to anti-scabies treatment (%)	2 (3)	3 (4)	5 (3)
No scabies (%)	1	7 (9)	8 (5)
Clinical diagnosis performed in our department			0
Scabies (%)	7 (10)	51 (66)	58 (39)
Possible scabies (%)	25 (35)	20 (35)	45 (30)
Low chance for scabies (%)	8 (11)	4 (11)	12 (8)
No scabies (%)	31 (44)	2 (44)	33 (22)

*Patients not affected by scabies had: eczema (atopic dermatitis and irritant contact dermatitis; 39 cases, including 4 cases with irritant contact dermatitis induced by anti-scabies treatment), folliculitis (3 cases), prurigo (12 cases, including 3 cases induced by insect bites), pruritus *sine materia* (14 cases), urticaria (1 case), viral exanthema (1 case) and dyshidrosis (1 case).

Table 2 Comparison of dermoscopy and reflectance confocal microscopy accuracy for the diagnosis of scabies

	DS before RCM	DS after RCM	RCM before DS	RCM after DS
Diagnostic properties: value (95% confident interval)*				
Sensitivity	95 (87–98)	91 (82–96)	92 (84–96)	93 (86–97)
Specificity	97 (90–99)	100 (95–100)	100†	100†
Positive predictive value	97 (90–100)	100 (94–100)	100†	100†
Negative predictive value	95 (86–98)	91 (82–96)	92 (83–97)	93 (85–98)
Duration of the procedure in patients with scabies: mean (standard deviation) score in seconds	45 (95)	41 (66)	60 (100)	57 (65)

*Results obtained considering all together the data of the two investigators.
†RCM 100% specificity was defined by the authors beforehand because mites and/or eggs are well defined under RCM and could not be misunderstood with other cutaneous structures.
DS, dermoscopy; RCM, reflectance confocal microscopy.

Dermoscopy had a specificity of 97% and 100%, respectively, when used before or after RCM. In fact, the previous use of RCM confirmed the presence of the parasites.

Discussion

This study showed an excellent diagnostic accuracy for scabies of intermediate magnification videodermoscopy and RCM, better than what reported for dermoscopy at ×10 magnifications.[1,6]

Videodermoscopy was found to be slightly more sensitive than RCM. However, RCM also allowed to diagnose scabies in two negative cases at dermoscopy, identifying some parasites that were deeper in the epidermis.

Since mites and/or eggs are well defined under RCM and could not be misunderstood with other cutaneous structures, RCM was considered 100% specific. Videodermoscopy performed before RCM gave false positive results in only two cases: one with an excoriated lesion that resembled a mite and another corresponding to a patient already treated for scabies (Fig. 2a). These two cases pointed out that, although much more specific than low magnification dermoscopy, 70× magnification videodermoscopy cannot always give a diagnosis of certainty.

Post-therapeutic studies using high-magnification dermoscopy have suggested that dying mites can be seen as an amorphous material[7,15] that could be indicative of mite decomposition. However, in our study we could find this aspect also in viable mites (Fig. 2b).

RCM has the advantage over dermoscopy of being able to clearly differentiate living from dead parasites in case of post-treatment follow-up. In fact, RCM can show the parasite's movements in addition to the anatomical differences induced by the treatment.[10] Interestingly, it has been reported that videodermoscopy at 500 1000× magnifications can also identify the movements of the mite in the skin[14] but not the peristaltic movements.

Notably, both hand-held RCM and videodermoscopy are not time consuming. The main limitation of these techniques is the price. However, our study shows that dermatology departments already equipped with these devices can benefit from their use in suspected scabies.

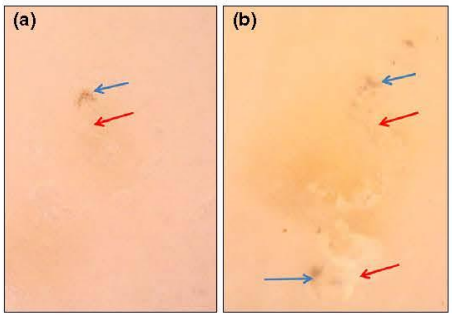

Figure 2 Equivocal images of *Sarcoptes scabies* under videodermoscopy at ×70 magnifications presenting as amorphous material. The fore portion of the mite (blue arrow) and the burrow behind (red arrow) are visible. The first case (a) corresponds to a false positive case in a patient already treated for scabies (dead mite) and the second case (b) corresponds to an affected patient before treatment (viable mites). In both cases with dead (a) or viable (b) mites, the mite contours are blurred.

Our study suggests that if both videodermoscopy and RCM devices are available, it is better to start with videodermoscopy that allows the exploration of a bigger area (area of observation with a diameter of 15 mm instead of 0.9 mm) and then perform RCM on the suspected areas in order to confirm the presence of the parasites and possibly establish their viability after treatment.

References

1 Walter B, Heukelbach J, Fengler G *et al.* Comparison of dermoscopy, skin scraping, and the adhesive tape test for the diagnosis of scabies in a resource-poor setting. *Arch Dermatol* 2011; 147: 468 473.
2 Wendel K, Rompalo A. Scabies and pediculosis pubis: an update of treatment regimens and general review. *Clin Infect Dis* 2002; 35: S146 S151.

3 Leung V, Miller M. Detection of scabies: a systematic review of diagnostic methods. *Can J Infect Dis Med Microbiol* 2011; **22**: 143 146.
4 Argenziano G, Fabbrocini G, Delfino M. Epiluminescence microscopy. A new approach to in vivo detection of Sarcoptes scabiei. *Arch Dermatol* 1997; **133**: 751 753.
5 Cinotti E, Perrot J-L, Labeille B *et al.* Diagnosis of scabies by high-magnification dermoscopy: the "delta-wing jet" appearance of Sarcoptes scabiei. *Ann Dermatol Vénéréol* 2013; **140**: 722 723.
6 Dupuy A, Dehen L, Bourrat E *et al.* Accuracy of standard dermoscopy for diagnosing scabies. *J Am Acad Dermatol* 2007; **56**: 53 62.
7 Micali G, Lacarrubba F, Tedeschi A. Videodermatoscopy enhances the ability to monitor efficacy of scabies treatment and allows optimal timing of drug application. *J Eur Acad Dermatol Venereol* 2004; **18**: 153 154.
8 Brunetti B, Vitiello A, Delfino S, Sammarco E. Findings in vivo of Sarcoptes scabiei with incident light microscopy. *Eur J Dermatol* 1998; **8**: 266 267.
9 Bauer J, Blum A, Sönnichsen K, Metzler G, Rassner G, Garbe C. Nodular scabies detected by computed dermatoscopy. *Dermatology* 2001; **203**: 190 191.
10 Cinotti E, Perrot J-L, Labeille B, Cambazard F. On the feasibility of confocal microscopy for the diagnosis of scabies. *Ann Dermatol Vénéréol* 2013; **140**: 215 216.
11 Cinotti E, Perrot JL, Labeille B *et al.* Reflectance confocal microscopy for quantification of Sarcoptes scabiei in Norwegian scabies. *J Eur Acad Dermatol Venereol* 2013; **27**: e176 e178.
12 Perrot J-L, Cinotti E, Labeille B *et al.* Rapid diagnosis of scabies by manual confocal reflectance microscopy. *Ann Dermatol Vénéréol* 2012; **139**: 502 505.
13 Lacarrubba F, Musumeci ML, Caltabiano R, Impallomeni R, West DP, Micali G. High-magnification videodermatoscopy: a new noninvasive diagnostic tool for scabies in children. *Pediatr Dermatol* 2001; **18**: 439 441.
14 Micali G, Lacarrubba F, Lo Guzzo G. Scraping versus videodermatoscopy for the diagnosis of scabies: a comparative study. *Acta Derm Venereol* 1999; **79**: 396.
15 Haas N, Sterry W. The use of ELM to monitor the success of antiscabietic treatment. Epiluminescence light microscopy. *Arch Dermatol* 2001; **137**: 1656 1657.

3.a 12 Dermoscopy, confocal microscopy and optical coherence tomography for the diagnosis of bedbug infestation

LETTER TO THE EDITOR

Dermoscopy, confocal microscopy and optical coherence tomography for the diagnosis of bedbug infestation

Editor

A 33-year-old woman suffering from rosacea presented with outbreaks of itchy plaques on her face and limbs that curiously improved when she was far from home during summer holidays (Fig. 1). Dermoscopy (FotoFinder Systems GmbH, Bad Birnbach, Germany) showed petechiae (Fig. 2a) and reflectance confocal microscopy (RCM; Vivascope 3000®, Caliber, New York, USA, distributed in Europe by MAVIG GmbH, München, Germany) showed intraepidermal vesicles (Fig. 2b) suggesting parasite bites. RCM found *Demodex folliculorum* (Fig. 2c) that could have been responsible for rosacea. However, a careful examination with dermoscopy identified a brown oval-shaped

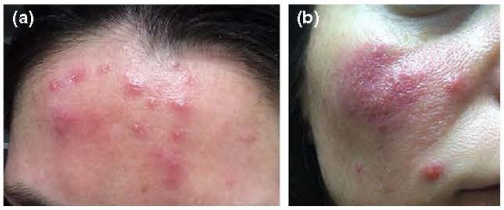

Figure 1 Bedbug infestation. Clinical appearance: papules and pustules confluent in violaceous oedematous plaques on the face.

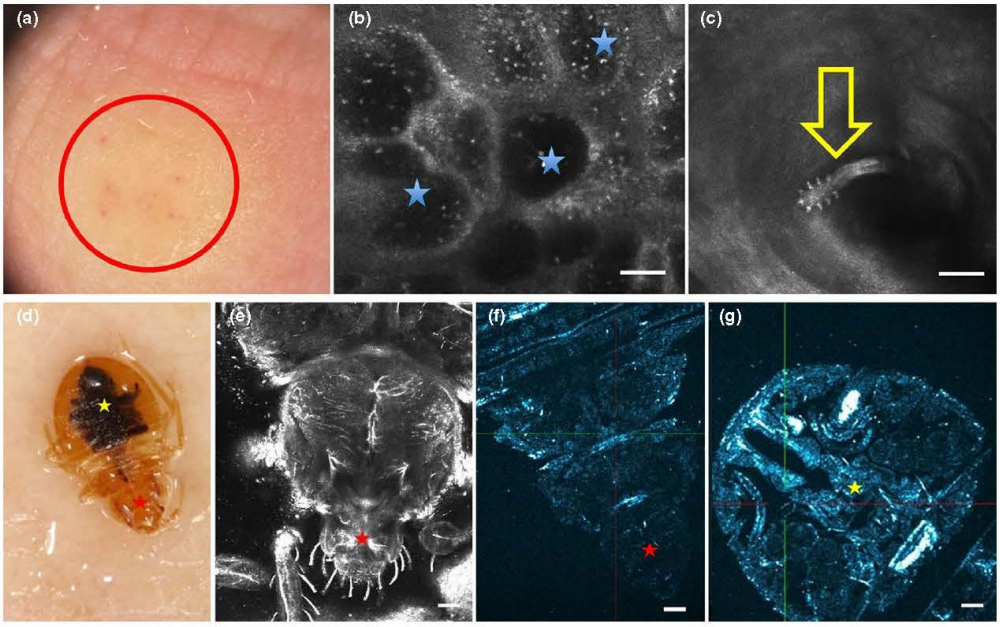

Figure 2 Bedbug infestation. Dermoscopy (a, d), reflectance confocal microscopy (RCM) (b, c, e) and high-definition optical coherence tomography (HD-OCT) (f, g) examination. Dermoscopy showed petechiae (A, red circle). RCM demonstrated the presence of intraepidermal vesicles (B, blue star) and a *Demodex folliculorum* (c) coming out from a facial hair follicle (yellow arrow) probably due to the severe skin inflammation caused by bedbugs. A third-stage nymph of *Cimex lectularius* was identified by dermoscopy (d), RCM (e) and HD-OCT (f, g). RCM and HD-OCT allowed to identify the details of its forepart (red star) and abdomen (yellow star). Scale bar = 100 μm.

wingless insect on the skin (Fig. 2d) and RCM and high-definition optical coherence tomography (HD-OCT; Skintell®; Agfa Gevaert, Antverpen, Belgium) allowed to better characterize the parasite (Fig. 2e g) as a nymph of *Cimex lectularius*.

Parasite bite reactions are often non-specific and new non-invasive imaging devices can help in the diagnosis by showing blood extravasation and microscopic signs of inflammation.[1 3] Moreover, they help the exact identification of the hematophagus parasite[1 3] as in our case where a bedbug infestation was diagnosed. Dermoscopy can be used as an initial screening in order to detect the parasites and RCM and HD-OCT can be used to highlight their anatomical features.

Bedbugs are visible on the body of the host when feeding.[4] Face and limbs are the most affected since hosts are typically bitten at night on exposed skin.[4] Disinfestation of the house and topical treatment such as corticosteroids are necessary to cure the patients. Interestingly, RCM also showed *Demodex folliculorum*, possibly responsible for the previous long standing rosacea, with a different RCM aspect from usual (Fig. 2c). Under RCM, *Demodex folliculorum* were visible in all their length as under the *ex vivo* optical microscope because they were not inside facial hair follicles but were coming out from them probably due to the severe skin inflammation.

E. Cinotti,[1,*] M. Espinasse,[2] B. Labeille,[1] F. Cambazard,[1] J.L. Perrot[1]

[1]Department of Dermatology, University Hospital of St-Etienne, Saint-Etienne, France, [2]Department of Ophthalmology, University Hospital of St-Etienne, Saint-Etienne, France

*Correspondence: E. Cinotti. E-mail: elisacinotti@gmail.com

References

1 Cinotti E, Labeille B, Cambazard F, Perrot JL. Reflectance confocal microscopy in infectious diseases. *G Ital Dermatol Venereol* 2015; **150**: 575 583.
2 Cinotti E, Perrot JL, Labeille B, Cambazard F. Reflectance confocal microscopy for cutaneous infections and infestations. *J Eur Acad Dermatol Venereol* 2016; **30**: 754 763.
3 Cinotti E, Labeille B, Bernigaud C *et al.* Dermoscopy and confocal microscopy for in vivo detection and characterization of Dermanyssus gallinae mite. *J Am Acad Dermatol* 2015; **73**: e15 e16.
4 Fallen RS, Gooderham M. Bedbugs: an update on recognition and management. *Skin Therapy Lett* 2011; **16**: 5 7.

DOI: 10.1111/jdv.13956

3.b Imagerie non invasive in vivo in vivo et processus infectieux cutanéo-muqueux et phanérien des virus

3.b 1 First identification of the herpes simplex virus by skin-dedicated ex vivo fluorescence confocal microscopy during herpetic skin infections.

Background.
Skin-dedicated *ex vivo* fluorescence confocal microscopy (FCM) has so far been used to identify cutaneous tumours on freshly excised samples using acridine orange as fluorochrome.
Aim.
To use FCM for a new indication, namely, the identification of the herpes simplex virus (HSV) in skin lesions, using fluorescent antibodies.
Methods. Six roof samples from skin vesicles suspicious for HSV lesions were incubated with anti-HSV-1 and anti-HSV-2 antibodies coupled with fluorescein isothiocanate, and examined under skin-dedicated *ex vivo* FCM. The positive controls were swabs taken from the floor of each vesicle and observed under conventional direct fluorescence assay (DFA) and by viral cultures. Roof samples from three bullae of bullous pemphigoid were the negative controls.
Results.
Using *ex vivo* FCM, the samples from the lesions clinically suspicious for HSV infection were seen to be fluorescent after incubation with anti-HSV-1, and were negative after incubation with anti-HSV-2 antibodies. Conventional DFA with a n optical microscope and cultures confirmed the presence of HSV-1 i n f e c t i o n .
Conclusions.
By using fluorescent antibodies to identify precise structures, *ex vivo* FCM can be used for indications other than tumour identification. More specifically, it can be an additional diagnostic tool for HSV infection.

3.b 1 First identification of the herpes simplex virus by skin-dedicated ex vivo fluorescence confocal microscopy during herpetic skin infections.

Experimental dermatology • **Original article**

CED
Clinical and Experimental Dermatology

First identification of the herpes simplex virus by skin-dedicated *ex vivo* fluorescence confocal microscopy during herpetic skin infections

E. Cinotti,[1] J. L. Perrot,[1] B. Labeille,[1] N. Campolmi,[2,3] G. Thuret,[2,3,4] N. Naigeon,[3] T. Bourlet,[5] S. Pillet[5] and F. Cambazard[1]

Departments of [1]Dermatology, [2]Ophthalmology and [5]Virology, University Hospital of Saint-Etienne, Saint-Etienne, France; [3]Department of Biology, Engineering and Imaging of Corneal Graft Laboratory, Jean Monnet University, Saint-Etienne, France; and [4]French University Institute, Boulevard Saint-Michel, Paris, France

doi:10.1111/ced.12546

Summary

Background. Skin-dedicated *ex vivo* fluorescence confocal microscopy (FCM) has so far been used to identify cutaneous tumours on freshly excised samples using acridine orange as fluorochrome.

Aim. To use FCM for a new indication, namely, the identification of the herpes simplex virus (HSV) in skin lesions, using fluorescent antibodies.

Methods. Six roof samples from skin vesicles suspicious for HSV lesions were incubated with anti-HSV-1 and anti-HSV-2 antibodies coupled with fluorescein isothiocyanate, and examined under skin-dedicated *ex vivo* FCM. The positive controls were swabs taken from the floor of each vesicle and observed under conventional direct fluorescence assay (DFA) and by viral cultures. Roof samples from three bullae of bullous pemphigoid were the negative controls.

Results. Using *ex vivo* FCM, the samples from the lesions clinically suspicious for HSV infection were seen to be fluorescent after incubation with anti-HSV-1, and were negative after incubation with anti-HSV-2 antibodies. Conventional DFA with an optical microscope and cultures confirmed the presence of HSV-1 infection.

Conclusions. By using fluorescent antibodies to identify precise structures, *ex vivo* FCM can be used for indications other than tumour identification. More specifically, it can be an additional diagnostic tool for HSV infection.

A skin-dedicated *ex vivo* fluorescence confocal microscope (FCM) has recently been developed, which carries the advantage over other microscopes of being able to analyse freshly excised samples without any further cutting. Until now, it has been used directly on fresh tissue for the identification of skin tumour margins, as an attractive alternative to frozen histopathology during Mohs micrographic surgery.[1,2] Several fluorescent agents have been tested, including acridine orange, fluorescein, patent blue, methylene blue, Nile blue and toluidine blue, but only acridine orange is used in practice, as it provides strong contrast for cells by staining nuclear DNA.[1,2]

We report on the use of this microscope for a new indication, i.e. the identification of the herpes simplex virus (HSV) in skin lesions, and on the use of fluorescent antibodies for this procedure.

Methods

We first examined the ability of the technique to identify HSV-2 by using anti HSV-2 fluorescent monoclonal antibodies (D^3DFA HSV Identification and Typing Kit; Diagnostic Hybrids, Athens, OH, USA) with a skin-dedicated *ex vivo* FCM (VivaScope 2500®

Correspondence: Dr Elisa Cinotti, Hôpital Nord Saint-Etienne, 42055 Saint Etienne Cedex 2, France
E-mail: elisacinotti@gmail.com

Conflict of interest: the authors declare that they have no conflicts of interest.

Accepted for publication 30 June 2014

CALIBER, distributed in Europe by Mavig GmbH, Munich, Germany) on five experimentally infected corneas taken from cadavers (data not shown) which, unlike skin, are homogeneously transparent and are not prone to any associated inflammatory reaction because the infection is induced under *ex vivo* conditions.

We then collected roof samples from six vesicles clinically suggestive of HSV-induced lesions from three different patients (two samples per patient): (i) a 30 year-old woman with recurrent labial HSV (Fig. 1a), (ii) a 66 year-old woman receiving vemurafenib for a metastatic melanoma with suspected Kaposi–Juliusberg eruption (Fig. 1b) and (iii) a 18-year-old man with recurrent HSV infection of the ear (Fig. 1c) and concurrent erythema multiforme major (Fig. 1d). The control skin samples were roof samples from bullous pemphigoid bullae from two patients. Specimens were obtained within 3 days from the first appearance of cutaneous lesions, and the vesicles/bullae were deroofed with a sterile scalpel.

The samples were incubated for 20 min with monoclonal anti-HSV-1 and anti-HSV-2 antibodies (one sample per patient was tested with anti-HSV-1 and one with the anti-HSV-2 antibody) coupled to fluorescein isothiocyanate (D^3DFA HSV Identification and Typing Kit; Diagnostic Hybrids), and then rinsed with phosphate buffered saline (pH 7.0–7.6). This procedure was performed in a dark room to avoid loss of fluorescence. Samples were examined under skin-dedicated *ex vivo* FCM (VivaScope 2500®) using the fluorescence mode (wavelength of incident light at 488 nm and filter blocking wavelengths below 500 nm).

We also took swabs from the floor of each vesicle and from control lesions for HSV-1 and HSV-2 detection by conventional direct fluorescence assay (DFA) under an optical microscope and by viral culture. Histological examination was also performed for the second and third patients.

Results

The samples from the lesions that were clinically suspicious for HSV infection were fluorescent after incubation with anti-HSV-1 antibodies both under *ex vivo* FCM (Fig. 2) and conventional DFA with an optical microscope, but were nonfluorescent after incubation with anti-HSV-2 antibodies. Viral cultures confirmed HSV-1 infection. The control samples were nonfluorescent under *ex vivo* FCM after incubation with anti-HSV-1 and anti-HSV-2 antibodies, and their viral cultures and conventional DFA were also negative for HSV infection. Histological examination of the second and third patients found the characteristic appearance of herpetic infection.

Discussion

HSV eruptions are most often clinically typical and do not require any complementary investigation. Few

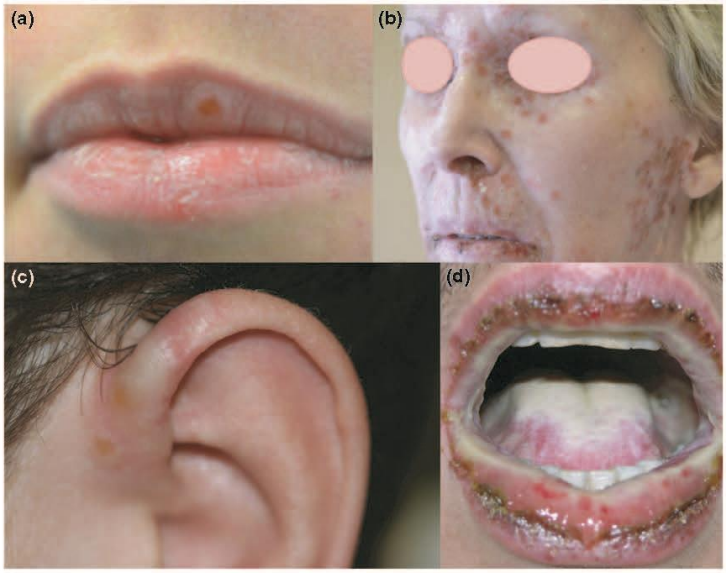

Figure 1 (a) Recurrent vesicles of the lip in patient 1, (b) diffuse excoriated vesicles in patient 2, who was receiving vemurafenib for metastatic melanoma and (c) recurrent vesicles of the ear in patient 3, who also had (d) concurrent erythema multiforme major.

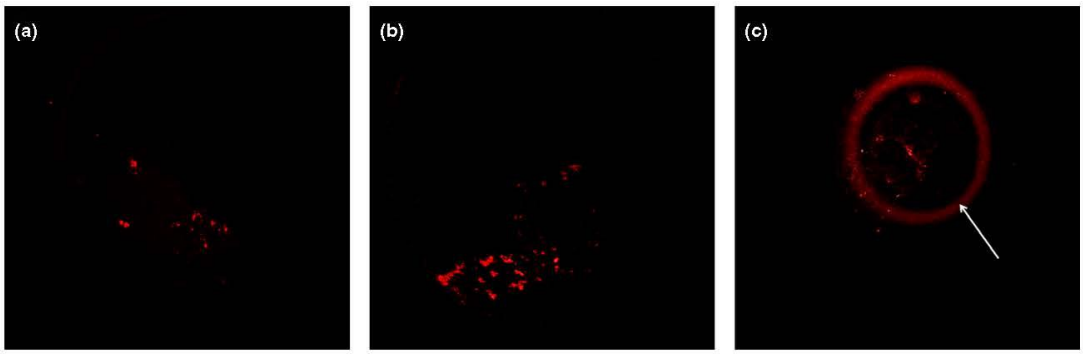

Figure 2 *Ex vivo* fluorescence confocal microscope (FCM) examination of the roof of three herpetic vesicles taken from the patient [(a) patient 1, (b) patient 2 and (c) patient 3] shown in Fig. 1 revealed bright (false red colour has been applied to a greyscale image) structures corresponding to epidermal cells infected by herpes simplex virus-1. The staining was performed with fluorescein isothiocyanate-labelled anti-HSV-1 antibodies and the tissue examined under FCM. The white arrow (c) indicates a ring, which was an artefact induced by image acquisition in a superficial layer. An FCM image corresponds to an area of 750 × 750 μm.

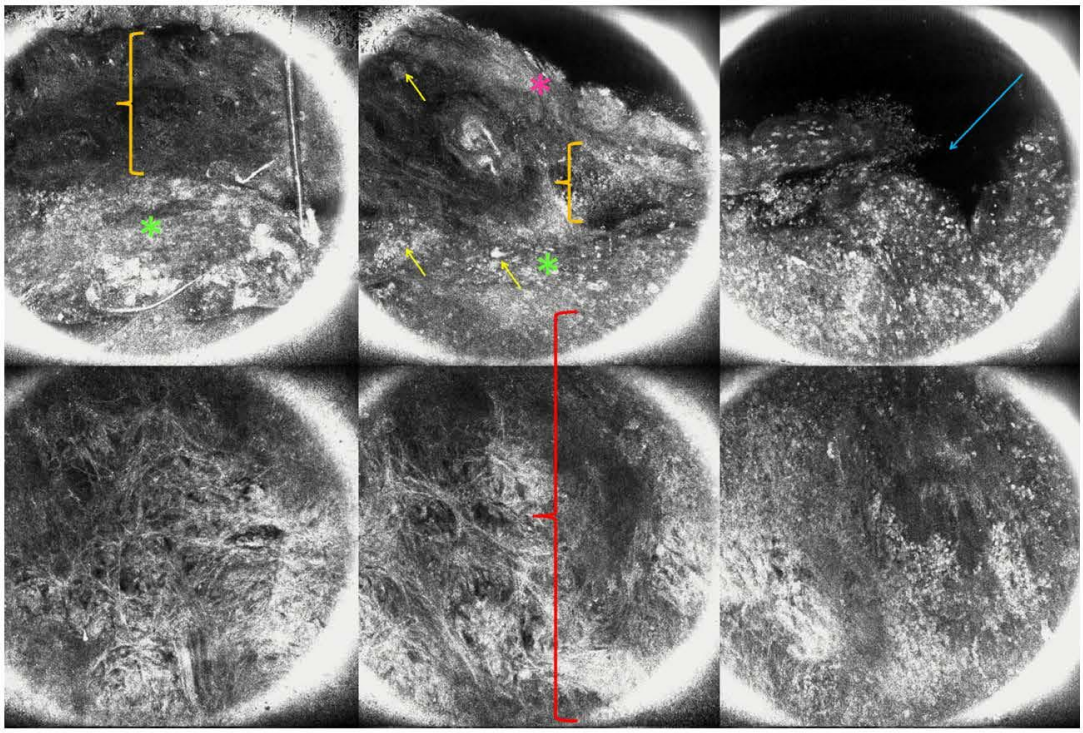

Figure 3 *Ex vivo* reflectance confocal microscope examination of a skin biopsy from a vesicle showed an intraepidermal cavity (orange curly bracket), large acantholytic keratinocytes (yellow arrow) and erosion (blue arrow), all signs of herpes simplex virus-1 infection (mosaic reconstruction). The roof (pink asterisk) and the floor (green asterisk) of the intraepidermal vesicle are visible in the image, as well as the superficial dermis (red curly bracket). A fluorescence confocal microscopy image corresponds to an area of 750 × 750 μm.

cases are atypical, and these occur mostly when there is a pre-existing skin disease or if the patient is immunocompromised. In some cases, a precise diagnosis is crucial for proper patient management, as it was in two of our patients. Patient 2 presented with diffuse vesicles on photoexposed areas, which were suggestive of HSV infection but could also be the result of direct adverse effects of vemurafenib. Patient 3 presented with vesicles on one ear, as well as febrile mucous membrane erosions and severe conjunctivitis prior to amoxicillin treatment, and it was difficult to assess whether the erythema multiforme major was triggered by HSV recurrence or the antibiotic treatment, or both. In such cases, the diagnosis requires investigations such as Tzanck cytodiagnosis, DFA, viral cultures, PCR or a histological examination to confirm the herpetic infection.

Debarbieux *et al.*[3] used *in vivo* reflectance confocal microscopy (RCM) to identify the herpes virus in two patients: a 25-year-old woman with Kaposi–Juliusberg eruption and a 71-year-old woman with herpes zoster infection. In both cases, examination of the pustules revealed intraepidermal cavities with acantholytic cells admixed with large cells with several darker roundish areas inside, consistent with HSV-infected plurinucleated keratinocytes. There was a high concordance with the histopathology and cytology findings. *In vivo* RCM is noninvasive and quick, while *ex vivo* FCM is minimally invasive and time-consuming because collection of the roof of the vesicles is sufficient to identify the virus; the whole procedure took about 30 min (20 min for incubation), and was performed during the patient's examination. *Ex vivo* FCM can typify HSV, and no expertise is needed to interpret the findings, as the test is positive if fluorescence is produced, and negative if there are black images without fluorescence. Conversely, *in vivo* RCM images need to be interpreted by dermatologists trained in pathology to identify the correct differential diagnosis (e.g. Darier disease).[3] As *ex vivo* FCM is also coupled with a reflectance microscope, cytological signs of HSV infection can be found in reflectance mode. Lastly, *ex vivo* FCM can also detect HSV in necrotic and/or inflamed tissue, which would normally hinder the detection of the cytopathic signs of HSV under RCM. In the current study, we were able to identify the cytological signs of HSV infection under *ex vivo* RCM in the skin biopsies that were later examined histopathologically (Fig. 3), but these signs were less evident on the roofs of the vesicles, consisting mainly of amorphous necrotic material and acantholytic cells (Fig. 4).

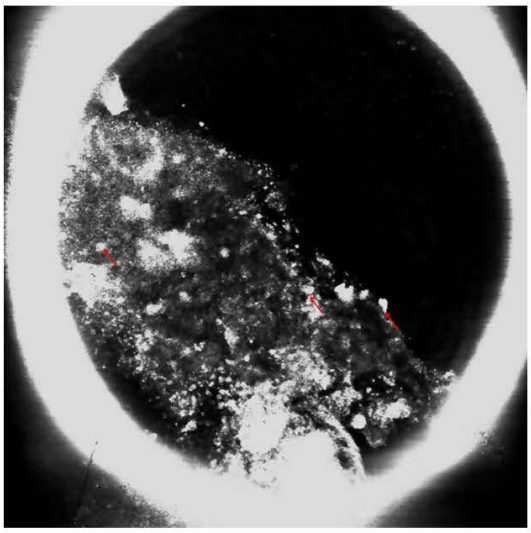

Figure 4 *Ex vivo* reflectance confocal microscope examination of a roof of a herpes simplex virus-induced vesicle showed acantholytic keratinocytes (red arrow). A fluorescence confocal microscopy image corresponds to an area of 750 × 750 μm.

To our knowledge, this is the first time that skin-dedicated *ex vivo* FCM has been used for a virological application. Identification of HSV is usually performed with alternative procedures (Tzanck cytodiagnosis, DFA, cultures or PCR),[4,5] which are not inferior to *ex vivo* FCM. The cost of FCM is the main drawback of this method, and for the moment, the diagnosis of HSV infection by FCM is only feasible in dermatology departments that are already equipped with a FCM for the study of skin tumours. However, this technique seems a very good solution for these departments, and a diagnosis can be reached in 30 min.

Our application opens new perspectives for the use of skin-dedicated *ex vivo* FCM. In the future, we could use different fluorescent antibodies to identify different anatomical structures, as used for immunohistochemistry. *Ex vivo* FCM devices could also be used for diagnosis of autoimmune bullous diseases because, compared with conventional direct immunofluorescence under an optical microscope, this technique can use data from both fluorescence and reflectance images, and study an entire biopsy specimen without cutting. Although skin-dedicated *ex vivo* FCM is only at its inception, with < 10 machines having been sold worldwide, the possibility of using fluorescent antibodies may increase its application. There are commercially available fluorescent monoclonal antibody staining kits for the detection of various viruses (such

as cytomegalovirus and varicella zoster) and for different skin structures with a short incubation time of approximately 15–30 min.

Conclusion

This is the first report of use of skin-dedicated *ex vivo* FCM to identify virus infections, and shows that this device can be used for indications other than tumour identification.

What's already known about this topic?

- Skin-dedicated *ex vivo* FCM has so far been used only for the identification of cutaneous tumours, using acridine orange as fluorochrome.

What does this study add?

- This is the first time that fluorescent antibodies have been used with skin-dedicated *ex vivo* FCM.
- This is the first study to have identified HSV using this microscope.

References

1 Bennàssar A, Vilata A, Puig S *et al.* Ex vivo fluorescence confocal microscopy for fast evaluation of tumour margins during Mohs surgery. *Br J Dermatol* 2014; **170**: 360–5.
2 Gareau DS, Jeon H, Nehal KS *et al.* Rapid screening of cancer margins in tissue with multimodal confocal microscopy. *J Surg Res* 2012; **178**: 533–8.
3 Debarbieux S, Depaepe L, Poulalhon N *et al.* Reflectance confocal microscopy characteristics of eight cases of pustular eruptions and histopathological correlations. *Skin Res Technol* 2013; **19**: e444–52.
4 Cohen PR. Tests for detecting herpes simplex virus and varicella-zoster virus infections. *Dermatol Clin* 1994; **12**: 51–68.
5 Singh A, Preiksaitis J, Ferenczy A, Romanowski B. The laboratory diagnosis of herpes simplex virus infections. *Can J Infect Dis Med Microbiol* 2005; **16**: 92–8.

3.b 2 Role of in vivo and ex vivo confocal microscopy and of optical coherence tomography as a ids in the diagnosis of molluscum contagiosum

Annales de dermatologie et de v n r ologie (2016) 143, 564—566

Disponible en ligne sur ScienceDirect www.sciencedirect.com

Elsevier Masson France EM|consulte www.em-consulte.com

Formation médicale continue

FICHE TH MATIQUE / MICROSCOPIE CONFOCALE PAR R FLECTANCE

Apport de la microscopie confocale in et ex vivo et de la tomographie en coh rence optique dans le diagnostic du molluscum contagiosum

Role of in vivo and ex vivo confocal microscopy and of optical coherence tomography as aids in the diagnosis of molluscum contagiosum

E. Cinotti[a,*], B. Labeille[a], C. Douchet[b], M. Chovet[a], C. Habougit[b], F. Cambazard[a], J.-L. Perrot[a], Groupe imagerie cutan e non invasive de la Soci t fran aise de dermatologie

[a] *Service de dermatologie, h pital universitaire de Saint- tienne, 42055 Saint- tienne cedex 2, France*
[b] *Laboratoire d'anatomopathologie, h pital universitaire de Saint- tienne, 42055 Saint- tienne cedex 2, France*

Reçu le 23 décembre 2015 ; accept le 5 février 2016
Disponible sur Internet le 20 mai 2016

Observation

Une enfant de 11 ans tait adress e par son m decin g n raliste pour l' valuation d'une tumeur du cuir chevelu acquise depuis 3 mois. L'anamn se ne trouvait pas d'ant c dent remarquable.

Nous constations une tumeur unique et blanch tre de 11 mm de diam tre localis e en r gion occipitale basse (Fig. 1a).

L'examen en dermatoscopie retrouvait des gros globules blanch tres au sein d'une structure homog ne ros e avec quelques fines t langiectasies et une micro-ulc ration excentr e (Fig. 1b).

Microscopie confocale par r flectance

Un examen en microscopie confocale (MC) par r flectance (Vivascope 3000® ; Caliber Inc., New York, tats-Unis, distribu en France par Mavig, Munich) tait r alis pour orienter le diagnostic de façon non invasive chez cette enfant. Il mettait en vidence une micro-ulc ration (Fig. 2a) et des grosses cellules arrondies peu refl tantes d'aspect de grains de grenade (Fig. 2b) regroup es en lobules au sein de l' piderme.

* Auteur correspondant.
Adresse e-mail : elisacinotti@gmail.com (E. Cinotti).

http://dx.doi.org/10.1016/j.annder.2016.02.030

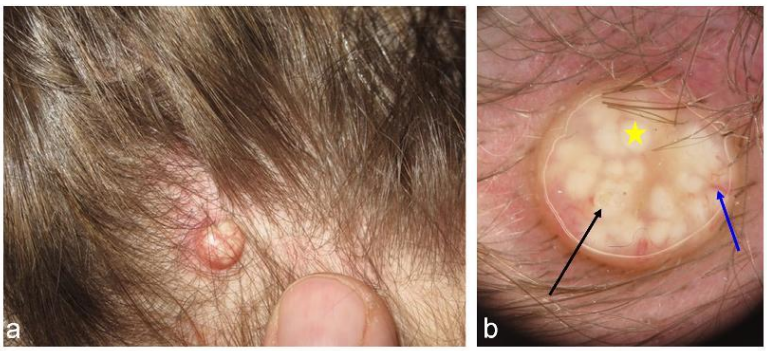

Figure 1. Aspect clinique (a) : tumeur blanch tre avec t langiectasies en surface. Aspect dermoscopique (b) : gros globules blanch tres (toile) au sein d'une structure homog ne ros e avec quelques fines t langiectasies (fl che bleue) et une micro-ulc ration excentr e (fl che noire).

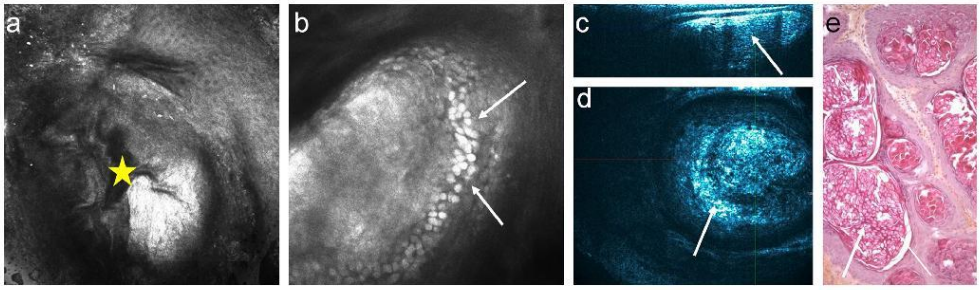

Figure 2. Aspect en microscopie confocale in vivo (a et b), aspect en tomographie de coh rence optique haute d finition (OCT HD) en coupe sagittale (c) et en coupe transversale (d) et examen histologique comparatif (h matoxyline- osine, 10 ×) (e). La microscopie confocale in vivo trouve un crat re superficiel (toile jaune) (a) et des grosses cellules rondes irr guli res hyper-refl tantes (b) (fl ches blanches) sous-jacent un pith lium normal (b). L'examen en OCT HD retrouve sur la coupe sagittale du mat riel hyper-refl tant (fl che blanche) sous-jacent un pith lium normal (c) et sur la coupe transversale (d) un nodule bien limit constitu de grosses cellules rondes hyper-refl tantes (fl che blanche). L'examen histologique (e) montre des k ratinocytes de grande taille ronds regroup s en amas (fl che blanche).

Tomographie par coh rence optique

Ensuite, un examen par tomographie de coh rence optique haute d finition (OCT HD) (Skintell® ; Agfa Gevaert, Antverpen, Belgique) mettait en vidence des grandes cellules rondes hyper-refl tantes (Fig. 2d), regroup es en amas ronds appendus l' piderme (Fig. 2c, d).

Microscopie confocale ex vivo

Une biopsie tait r alis e. Un examen en MC ex vivo tait alors effectu vis e iconographique, pr alablement l'examen histologique. Cet examen tait r alis en r flectance 830 nm puis en fluorescence 488 nm apr s application d'acridine orange 2 %. Il montrait des cellules arrondies de grande taille spontan ment refl tantes (Fig. 3a) mais aussi fluorescentes 488 nm (Fig. 3b), qui s'ouvraient dans un crat re dilat rempli de mat riel k ratosique confirmant le diagnostic de molluscum contagiosum. L'examen histologique d finitif en h matoxyline- osine validait ce diagnostic (Fig. 2e et 3c).

Commentaires

Le molluscum contagiosum est fr quent chez l'enfant. Toutefois, notre observation est inhabituelle car il s'agissait d'une l sion unique de grande taille de localisation particuli re (cuir chevelu). La dermoscopie ne montrait pas la classique architecture ombiliqu e dans la partie centrale, mais des gros globules blanch tres qui peuvent tre observ s dans le formes g antes [1]. Le molluscum contagiosum se caract rise l'examen histologique par des k ratinocytes de grande taille, arrondis, cons quence de l'action cytopathog ne du pox virus. Ces cellules sous l'action de l'acantholyse progressive induite par le virus forment une exulc ration avec un crat re central prenant un aspect en grenade. La MC et l'OCT HD in vivo nous ont permis de mettre en vidence un aspect caract ristique de

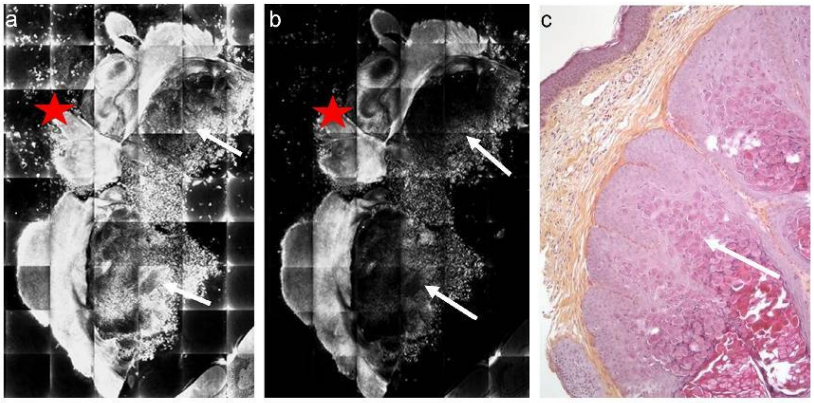

Figure 3. Aspect en microscopie confocale ex vivo par r flectance (a) et par fluorescence 488 nm avec application d'acridine orange 2% (b) et examen histologique correspondant (h matoxyline- osine 4×) (c). L'examen en microscopie confocale ex vivo montre des k ratinocytes de grande taille regroup s en amas (fl ches blanches) refl tant spontan ment en mode r flectance et fluorescent 488 nm formant une exulc ration avec un crat re (toile rouge). L'examen histologique montre un pith lium acanthosique avec des k ratinocytes de grande taille caract ris s par des inclusions osinophiliques intracytoplasmiques et acantholyse progressive (fl che blanche).

molluscum contagiosum similaire l'examen anatomopathologique.

Nous n'avons pas trouv dans la litt rature de description de molluscum contagiosum en MC ex vivo ni en OCT HD, et peu de descriptions en microscopie confocale in vivo [2—4]. Il s'agit pourtant d'un diagnostic particuli rement ais tant en MC qu'en OCT HD ce qui en fait une l sion de diagnostic simple pour les « confocalistes » d butants. Il nous ne semble pas qu'une des m thodes in vivo utilis es (MC ou OCT HD) soit sup rieure l'autre pour affirmer ce diagnostic m me si aucune tude n'a t conduite ce sujet dans la litt rature.

D claration de liens d'int r ts

Les auteurs d clarent ne pas avoir de liens d'int r ts.

R f rences

[1] Mun JH, Ko HC, Kim BS, Kim MB. Dermoscopy of giant molluscum contagiosum. J Am Acad Dermatol 2013;69:e287—8.
[2] Scope A, Benvenuto-Andrade C, Gill M, Ardigo M, Gonzalez S, Marghoob AA. Reflectance confocal microscopy of molluscum contagiosum. Arch Dermatol 2008;144:134.
[3] Cinotti E, Perrot JL, Labeille B, Cambazard F. Reflectance confocal microscopy for cutaneous infections and infestations. J Eur Acad Dermatol Venereol 2016;30:754—63.
[4] Cinotti E, Labeille B, Cambazard F, Perrot JL. Reflectance confocal microscopy in infectious diseases. G Ital Dermatol Venereol 2015;150:575—83.

3.c Imagerie non invasive in vivo in vivo et processus infectieux cutanéo-muqueux et phanérien des bactéries

The role of reflectance confocal microscopy in the diagnosis of secondary syphilis of the vulva and anus: A first case report

Annales de dermatologie et de v n r ologie (2016) 143, 687—690

Disponible en ligne sur ScienceDirect www.sciencedirect.com

Elsevier Masson France EM|consulte www.em-consulte.com

CAS CLINIQUE

Apport de la microscopie confocale par r flectance dans le diagnostic de syphilides ano-vulvaires, premier cas relat

The role of reflectance confocal microscopy in the diagnosis of secondary syphilis of the vulva and anus: A first case report

A. Leclercq[a], E. Cinotti[a,*], B. Labeille[a], B. Cribier[b], A.C. Biron[a], C. Vermersch[c], J. Montlouis[c], F. Cambazard[a], J.L. Perrot[a], groupe imagerie cutan e non invasive de la Soci t fran aise de dermatologie

[a] *Service de dermatologie, h pital universitaire de Saint-Etienne, 42055 Saint-Etienne cedex 2, France*
[b] *Service de dermatologie et laboratoire de dermatopathologie, h pitaux universitaires de Strasbourg, 67091 Strasbourg cedex, France*
[c] *Service de gyn cologie, h pital universitaire de Saint-Etienne, 42055 Saint-Etienne cedex 2, France*

Reçu le 27 juin 2016 ; accept le 12 juillet 2016
Disponible sur Internet le 25 août 2016

MOTS CL S
Microscopie confocale par r flectance ;
In vivo ;
Imagerie non invasive ;
Syphilis ;
Treponema pallidum

R sum

Observation. — Nous rapportons le cas d'une patiente de 18 ans, enceinte, qui pr sentait des syphilides ano-g nitales et plantaire, une pharyngite, un intertrigo ryth mateux finement squameux naso-g nien et une perl che.

Microscopie confocale par r flectance. — Un examen en microscopie confocale in vivo (Vivascope 3000® ; Caliber Inc, Rochester, NY, tats-Unis, distribu en France par Mavig, Munich) des papules g nitales montrait des b tonnets allong s hyper-refl tants au sein du derme papillaire voquant des spiroch tes. La s rologie sanguine TPHA-VDRL et l'examen immunohistologique permettaient de confirmer le diagnostic.

* Auteur correspondant.
Adresse e-mail : elisacinotti@gmail.com (E. Cinotti).

http://dx.doi.org/10.1016/j.annder.2016.07.010

Commentaire. — Nous avons pu identifier pour la premi re fois au sein des syphilides des structures en b tonnets alternants r guli rement des zones hyper-refl tantes et non refl tantes, correspondant aux spires des tr pon mes visualis es en microscopie fond noir et qui ne peuvent pas tre confondues avec une autre structure cellulaire.

KEYWORDS
Reflectance confocal microscopy;
In vivo;
Non-invasive imaging;
Syphilis;
Treponema pallidum

Summary
Patients and methods. — Herein we report the case of an 18-year-old pregnant patient presenting with plantar and ano-genital lesions of syphilis, pharyngitis, erythematosus and scalynasolabial intertrigo and angular cheilitis.
Reflectance confocal microscopy. — In vivo reflectance confocal microscopy examination (Vivascope 3000®; Caliber Inc, Rochester, NY, USA, distributed in France by Mavig, Munich) of ano-genital lesions enabled us to identify hyper-reflective elongated rods in the papillary dermis suggesting spirochetes. The diagnosis was confirmed by TPHA and VDRL as well as immunohistological examination.
Comments. — We identified for the first time rod shaped structures in ano-genital lesions of secondary syphilis, regularly alternating hyper-reflective and non-reflective areas corresponding to helix-shaped treponemes visualized by darkfield microscopy, which may not be confused with other cell structures.

Observation

Une jeune femme roumaine de 18 ans nous tait adress e pour une suspicion de syphilis g nitale. Elle tait enceinte (20 semaines d'am norrh e) et n'avait pas d'ant c dent m dical notable. Nous constations la pr sence de papules ryth mateuses ano-g nitales (Fig. 1a). Le reste de l'examen permettait de constater une pharyngite (Fig. 1b), des maculo-papules plantaires ryth mateuses discr tement cuivr es cercl es par une bordure finement squameuse (Fig. 1c), un intertrigo ryth mateux finement squameux naso-g nien (Fig. 1d) et une perl che (Fig. 1d). L'interrogatoire ne rapportait pas de chancre syphilitique pr alable. Nous voquions donc une syphilis secondaire.

Microscopie confocale par r flectance

Un examen en microscopie confocale (MC) in vivo (Vivascope 3000® ; Caliber Inc, Rochester, NY, tats-Unis, distribu en France par Mavig, Munich) tait r alis pour confirmer le diagnostic lors de la consultation. L'examen des papules g nitales en MC in vivo montrait des b tonnets allong s hyper-refl tants au sein du derme papillaire voquant des spiroch tes (Fig. 2a). Ces b tonnets taient caract ris s par l'alternance r guli re d'hyper- et d'hypo-r flectance, en moyenne 10 alternances (Fig. 2b). Leur taille tait mesur e entre 8 et 15 microm tres. Un traitement par p nicilline retard tait alors d but sans tarder.

Les s rologies demand es lors de la consultation confirmaient le diagnostic : TPHA positif 40 960, et VDRL positif et quantifi 64 U.

L'examen immunohistologique de la biopsie d'une syphilide vulvaire avec marquage sp cifique des tr pon mes (anticorps *polyclonal biocare*) permettait d'identifier des nombreux spiroch tes dans l' piderme profond et le derme (Fig. 2c).

La recherche des autres infections sexuellement transmissibles tait n gative.

Commentaires

Un examen en MC in vivo a t r alis afin d'obtenir une confirmation du diagnostic en temps r el, lors de la consultation. Ceci l'instar de l'examen en microscopie fond noir du chancre syphilitique qui permet de caract riser le tr pon me sous la forme d'une bact rie mobile tr s fine (10 μm de long sur 0,2 μm de large), h lico dale, aux spires tr s serr es et r guli rement espac es au nombre de 6 12.

Or si de nombreux articles ont permis d'identifier des parasites en MC [1—13], ou l'aspect en MC des cons quences cytopathog nes d'une atteinte virale [14—16], les bact ries ont une taille qui chappe pour la majorit d'entre elles la discrimination de la MC in vivo. Ainsi ce jour un seul article a relat l'identification en MC in vivo de *Treponema pallidum* [17] au sein d'un chancre syphilitique primaire. Mais cet article est critiquable car ce qui est montr comme *T. pallidum* pourrait correspondre des parois cellulaires des k ratinocytes [12]. En revanche, dans notre observation sont identifi es des structures en b tonnets alternants r guli rement des zones hyper-refl tantes et non refl tantes, correspondant aux spires visualis es en microscopie fond noir et qui ne peuvent pas tre confondues avec une paroi

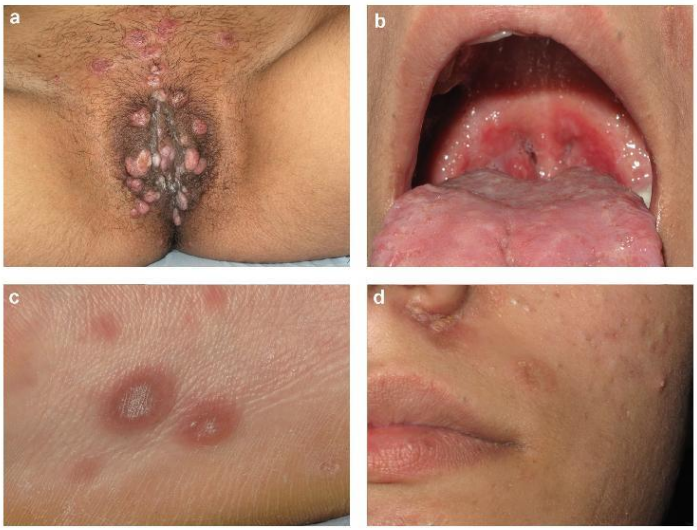

Figure 1. Aspect clinique. Papules ryth mateuses g nitales (a) ; pharyngite (b) ; maculo-papules plantaires ryth mateuses discr tement cuivr es cercl es par une bordure finement squameuse (c) ; intertrigo ryth mateux finement squameux naso-g nien, perl che et l sions acn iformes du menton (d).

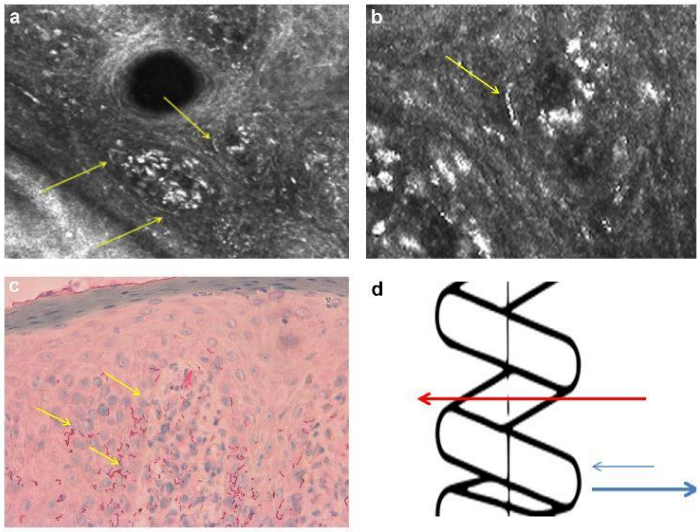

Figure 2. Aspect en microscopie confocale (MC) par r flectance in vivo (a) avec agrandissement en zoom num rique (b), aspect histologique (c), anticorps anti-*Treponema pallidum* et sch ma explicatif de l'alternance r flectance non-r flectance (d). La MC par r flectance in vivo (a et b) et l'examen immunohistochimique avec des anticorps anti-tr pon me (c) montrent des b tonnets (fl ches jaunes). Les b tonnets sont refl tants en MC in vivo (a), avec une alternance r guli re d'hyper- et hypo-r flectance (c). Le sch ma (d) montre la diff - rence de r flectance selon la quantit de spire travers e ; la fl che rouge correspond un signal hypo-refl tant alors que les fl ches bleues correspondent un signal hyper-refl tant.

des k ratinocytes. La partie hyper-refl tante correspond la partie la plus dense en mati re bact rienne (Fig. 2d).

Seule la mobilit mise en vidence en microscopie fond noire n'a pu tre constat e sur des p riodes d'examen de stricte immobilit de la cam ra de 30 secondes. Cependant, la MC a l'avantage sur le fond noir de pouvoir identifier les bact ries qui sont dans la partie basale de l' piderme et dans le derme et non seulement celles qui sont en surface. Il y a enfin une concordance anatomique quant la localisation des *T. pallidum* dans le derme comme le confirme la confrontation anatomo-confocale.

En conclusion, m me s'il s'agit du premier cas rapport d'identification de *T. pallidum* au sein d'une syphilide, cette observation montre qu'il s'agit d'un diagnostic simple et rapide r aliser en MC in vivo, une sorte de microscopie fond noir applicable m me certaines l sions secondaires.

D claration de liens d'int r ts

Les auteurs d clarent ne pas avoir de liens d'int r ts.

R f rences

[1] Leclercq A, Cinotti E, Labeille B, Perrot JL, Cambazard F. Ex vivo confocal microscopy: a new diagnostic technique for mucormycosis. Skin Res Technol 2016;22:203—7.

[2] Cinotti E, Fouilloux B, Perrot JL, Labeille B, Douchet C, Cambazard F. Confocal microscopy for healthy and pathological nail. J Eur Acad Dermatol Venereol 2014;28:853—8.

[3] Cinotti E, Perrot JL, Labeille B, Raberin H, Flori P, Cambazard F. Hair dermatophytosis diagnosed by reflectance confocal microscopy: six cases. J Eur Acad Dermatol Venereol 2015;29:2257—9.

[4] Cinotti E, Perrot J-L, Labeille B, Cambazard F. Diagnostic de la gale par pimicroscopie fort grossissement : l'aspect « en deltaplane » de Sarcoptes scabiei. Ann Dermatol Venereol 2013;140:722—3.

[5] Cinotti E, Perrot J-L, Labeille B, Cambazard F. Microscopie confocale pour le diagnostic de la gale : questions sur la faisabilit . Ann Dermatol Venereol 2013;140:215—6.

[6] Cinotti E, Perrot JL, Labeille B, Vercherin P, Chol C, Besson E, et al. Reflectance confocal microscopy for quantification of Sarcoptes scabiei in Norwegian scabies. J Eur Acad Dermatol Venereol 2013;27:e176—8.

[7] Perrot J-L, Cinotti E, Labeille B, Trau C, Rab rin H, Flori P, et al. Diagnostic rapide de la gale au moyen d'une cam ra manuelle de microscopie confocale par r flectance. Ann Dermatol Venereol 2012;139:502—5.

[8] Forest F, Cinotti E, Habougit C, Gingu n C, Perrot J-L, Labeille B, et al. Rapid characterization of human brain aspergillosis by confocal microscopy on a thick squash preparation. Cytopathology 2016;27:221—2.

[9] Forest F, Cinotti E, Yvorel V, Habougit C, Vassal F, Nuti C, et al. Ex vivo confocal microscopy imaging to identify tumor tissue on freshly removed brain sample. J Neurooncol 2015;124:157—64.

[10] Pharaon M, Gari-Toussaint M, Khemis A, Zorzi K, Petit L, Martel P, et al. Diagnosis and treatment monitoring of toenail onychomycosis by reflectance confocal microscopy: prospective cohort study in 58 patients. J Am Acad Dermatol 2014;71:56—61.

[11] Cinotti E, Labeille B, Bernigaud C, Fang F, Chol C, Chermette R, et al. Dermoscopy and confocal microscopy for in vivo detection and characterization of Dermanyssus gallinae mite. J Am Acad Dermatol 2015;73:e15—6.

[12] Cinotti E, Perrot JL, Labeille B, Cambazard F. Reflectance confocal microscopy for cutaneous infections and infestations. J Eur Acad Dermatol Venereol 2016;30:754—63.

[13] Cinotti E, Labeille B, Cambazard F, Perrot JL. Reflectance confocal microscopy in infectious diseases. G Ital Dermatol E Venereol 2015;150:575—83.

[14] Cinotti E, Perrot JL, Labeille B, Campolmi N, Thuret G, Naigeon N, et al. First identification of the herpes simplex virus by skin-dedicated ex vivo fluorescence confocal microscopy during herpetic skin infections. Clin Exp Dermatol 2015;40:421—5.

[15] Debarbieux S, Moulin C, Thomas L, Groupe imagerie cutan e non invasive de la Soci t française de dermatologie. Infection virus zona varicelle. Ann Dermatol Venereol 2014;141:476—7.

[16] Debarbieux S, Depaepe L, Poulalhon N, Dalle S, Balme B, Thomas L. Reflectance confocal microscopy characteristics of eight cases of pustular eruptions and histopathological correlations. Skin Res Technol 2013;19:e444—52.

[17] Venturini M, Sala R, Semenza D, Santoro A, Facchetti F, Calzavara-Pinton P. Reflectance confocal microscopy for the in vivo detection of Treponema pallidum in skin lesions of secondary syphilis. J Am Acad Dermatol 2009;60:639—42.

3.d articles de synthèse

3.d.1 Reflectance confocal microscopy in infectious diseases.

In vivo reflectance confocal microscope (RCM) is a high- resolution non-invasive imaging technique that was initially focused on the diagnosis of skin cancers. A rising number of other indications have been later described for the diagnosis and management of inflammatory and infectious dermato- logical disorders. RCM can identify cutaneous parasites that are not visible to naked eye such as *Sarcoptes scabiei* and *Demodex folliculorum* and it allows to better identify the dif- ferent body parts of bigger parasites such as ticks. Fungal filaments can also be identified as elongated bright structures in the cutaneous upper layers. RCM cannot observe virus directly. However, the cytopathic effect associated with some virus can be recognized. In addition of being helpful for the diagnosis and follow-up after treatment, thanks to its non- invasiveness, RCM allows pathophysiological studies.

5127-MD

???

G ITAL DERMATOL VENEREOL 2015;150:1-2

Reflectance confocal microscopy in infectious diseases

E. CINOTTI, B. LABEILLE, F. CAMBAZARD, J. L. PERROT

Dermatology Department, University Hospital of Saint-Etienne, Cedex 2, Saint Etienne, France

***In vivo* reflectance confocal microscope (RCM) is a high-resolution non-invasive imaging technique that was initially focused on the diagnosis of skin cancers. A rising number of other indications have been later described for the diagnosis and management of inflammatory and infectious dermatological disorders. RCM can identify cutaneous parasites that are not visible to naked eye such as *Sarcoptes scabiei* and *Demodex folliculorum* and it allows to better identify the different body parts of bigger parasites such as ticks. Fungal filaments can also be identified as elongated bright structures in the cutaneous upper layers. RCM cannot observe virus directly. However, the cytopathic effect associated with some virus can be recognized. In addition of being helpful for the diagnosis and follow-up after treatment, thanks to its non-invasiveness, RCM allows pathophysiological studies.**

KEY WORDS: Microscopy, confocal - Infection - Prasitic diseases - Mycoses - Scabies - Virus.

In vivo reflectance confocal microscope (RCM) is a high-resolution non-invasive imaging technique that was initially focused on the diagnosis of skin neoplasms.[1, 2] A rising number of other indications have been later described for the diagnosis and management of inflammatory and infectious dermatological disorders. Here, we report the possible indication of RCM for cutaneous infections and infestations. RCM has a lateral resolution of 1.25µm and an axial resolution of 5 µm. This means that structures with bigger size than 1.25µm could theoretically be identified. Most skin parasites are well visible under RCM because they are large and sometimes also visible to naked eye. Virus could not be identified because they are too small. However, viral cytopathic effects can be observed on keratinocytes. Theoretically, bacteria could also be identified but a clear demonstration of a bacteria under RCM has not yet been provided. Recently, the handheld compact camera (VivaScope3000®, CALIBER, New York, NY, USA, distributed in Europe by the company MAVIG GmbH, Munich, Germany) has been introduced on the market, permitting flexible movements in all directions and allowing a fast and easy diagnosis of skin and appendages infections and infestations in clinical routine.[3-6]

In order to prevent any contagion risk during the RCM examination, a disposable sterile transparent film (for example Visulin, Paul Hartmann AG, Germany) should be applied to the tip of the handheld camera. If the traditional wide probe (VivaScope1500®) is used there is no need to use a sterile film because the examination is made with a disposable plastic interface.

Confocal microscopy and viral infections

RCM has been used to identify the cytopathic effects of *herpes simplex and varicella-zoster herpes virus* [7, 8] and *molluscipoxvirus* [9] in the skin. In case

Corresponding author: J. L. Perrot, University Hospital of Saint-Etienne, Cedex 2, 42055 Saint Etienne, France.
E-mail: j.luc.perrot@gmail.com

of *herpes virus* infection, RCM shows the presence of pleomorphic large keratinocytes and multinucleated giant cells corresponding to *herpes virus*-infected keratinocytes and intra-epidermal vesicles with acantholytic keratinocytes (Figure 1). In case of *molluscipoxvirus* infection, RCM shows a round, well-circumscribed lesion with central round cystic areas separated by fine septa and filled with hyperrefractive roundish bodies corresponding to the characteristic eosinophilic inclusion bodies (molluscum bodies) at the histopathological examination (Figure 2).[9] The cutaneous lesions induced by these viruses are most often clinically evident and do not require any complementary investigation. Atypical cases mostly occur in association with other skin diseases such as Darier's disease and atopic dermatitis, or in the case of immunocompromised patients. In such cases, further investigations such as Tzanck cytodiagnosis, direct fluorescence assay, viral cultures, PCR or histopathological examination could be useful. RCM could be an alternative new technique that could help the clinicians in the diagnosis. It has the advantages of being able to image the entire affected cutaneous surface and of

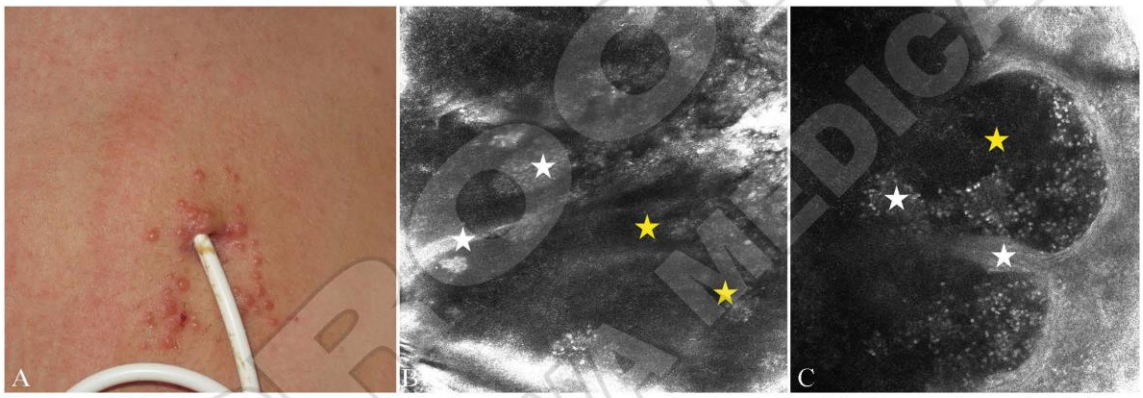

Figure 1.—Clinical (A) and reflectance confocal microscopy (B, C) aspect of an *herpes virus* infection around a surgical drainage. Confocal microscopy shows intra-epidermal vesicles with acantholytic keratinocytes (yellow stars). Remnants of the normal epidermis that is going to flake are visible (white stars).

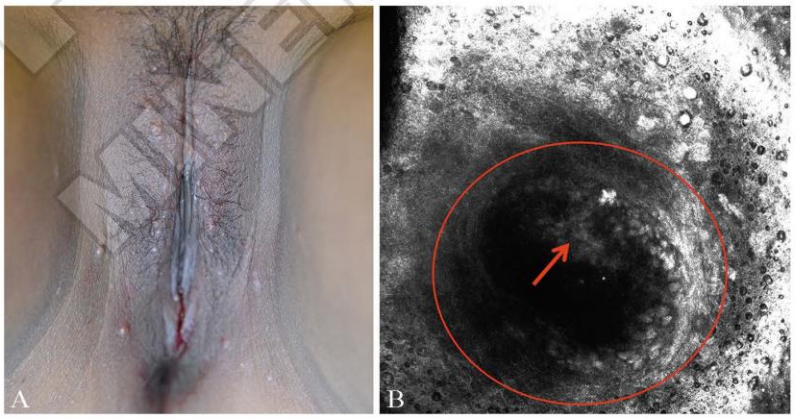

Figure 2.—Clinical (A) and reflectance confocal microscopy (B) aspect of a *molluscipoxvirus* infection. Confocal microscopy shows the presence of an intra-epidermal cavity (red circle) plenty of large roundish bodies (red arrow).

being non-invasive and quick. Interestingly, RCM can also identify subtle epidermal changes in an early pre-vesicular stage allowing an early treatment (Figure 3). Physiological studies can also be performed, for example to investigate the viral effects on a same location over time. RCM dedicated to the genital mucosa has also been used for an early diagnosis of vaginal intraepithelial neoplasia[10] and in our experience we could identify with the hand-held device dedicated to the skin the cytopathic effect induced by *human papillomavirus* in the other part of the vagina of few patients. In our experience it was not possible to identify the cytopathic effect of *human papillomavirus in common warts* with the characteristics large vacuolated cells. We suppose that this apsct could be related to the marked hyperkeratosis and acanthosis that reduces the resolution of RCM images in the underlying epidermal layers. However, papillomatosis of the filiform variants can be observed (Figure 4).

In our experience it could also be used to identify intraepidermal vesicles and few ballooned cells in case of atypical cases of hand, foot and mouth disease caused by *coxsackievirus* infection (Figure 5).

Confocal microscopy and cutaneous bacterial infections

Treponema pallidum has been described by RCM in cutaneous lesions of secondary syphilis [11] as bright particles intermingled with keratinocytes. However, it is difficult to differentiate these particles from the hyper-reflective cell membranes of keratinocytes.

Figure 3.—Clinical (A) and reflectance confocal microscopy (B) aspect of a *varicella-zoster herpes virus* infection in a clinically pre-vesicular stage. Confocal microscopy shows small intra-epidermal vesicles (yellow arrows and yellow star).

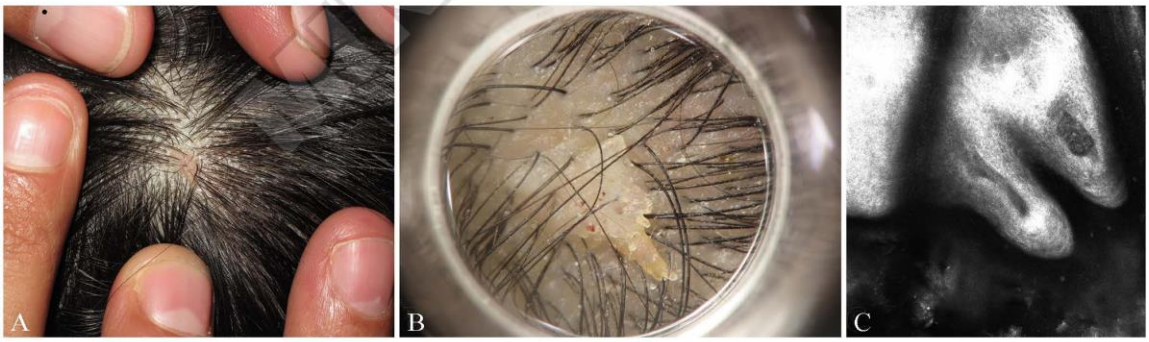

Figure 4.—Clinical (A), dermoscopical (B) and reflectance confocal microscopy (C) aspect of filiform wart of the scalp.

Figure 5.—Clinical (A, B) and reflectance confocal microscopy (C) aspect of a coxsackievirus infection in an adult. Reflectance confocal microscopy shows intraepidermal vesicles (C, red circle) and few ballooned cells.

Confocal microscopy and superficial mycosis

RCM can also be used to identify filaments, pseudofilaments and conidia on skin, and mucosa, and in skin appendages (Figures 6, 7). Filaments and pseudofilaments appear as thin, hyper-reflective, longitudinal structures with a serpentine shape (Figure 6),[5, 6, 12] whereas Conidia are hyper-reflective small roundish bodies.[12] Septa can also be identified.[13]

Fungi should be searched in the upper part of the epidermis, and are more easily visible at the skin surface where there is the bright ring artifact given by the tip of the confocal placed on the skin. Their identification is easier in nails because the nail plate is mainly a homogeneous hyporeflective medium (Figure 7).[6] In the hairs they could be identified but they should be differentiated from the normal structure of the hair shaft that gives longitudinal bright reflections.[12] Comparing to established diagnostic techniques (light microscopic examination with potassium hydroxide preparation and fungal culture), in vivo RMC has the advantages of 1) being non-invasive; 2) not requiring a skin sample for ex vivo analysis; 3) being performed immediately without any preparation; 4) evaluating the entire surface of a lesion and not just the scales removed for a conventional ex vivo analysis. Therefore, RCM can give a real time diagnosis during the dermatological consultation and to initiate an appropriate treatment without waiting for the conventional mycological examination.[5, 14]

The identification of fungi requires experience because fungi can be mistaken for cell membranes of keratinocytes and inversely. However, a better diag-

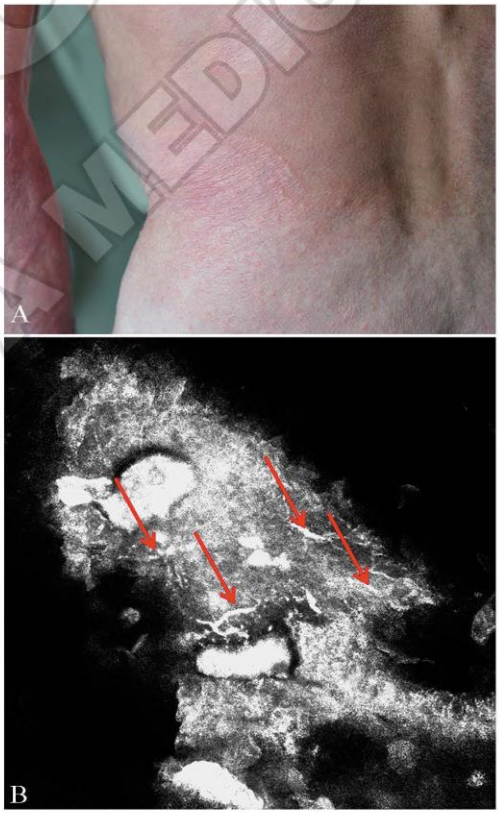

Figure 6.—Clinical (A) and reflectance confocal microscopy (B) aspect of a dermatophytosis. Dermatophytes are easily identified under reflectance confocal microscopy as thin, high-reflective, longitudinal structures with a linear shape (red arrows).

Figure 7.—Clinical (A) and reflectance confocal microscopy aspect of an onychomycosis (B).

nostic accuracy of *in vivo* RCM than conventional microscopic examination has been found in a prospective trial on 50 toes suspicious of onychomycosis, (sensitivity 79% *versus* 74% and specificity 81% *versus* 76%)[15] and in a trial on 55 patients affected by tinea corporis (sensitivity 89.1% *versus* 80.0%)[13]. Recent studies confirmed the high specificity of RCM[14,16] but found a lower sensitivity for both onychomycosis (52.9% of sensitivity in a series of 58 patients)[14] and skin dermatophytosis (64% of sensitivity in 22 patients with *tinea manus* and *pedis*; 83% of sensitivity in 23 cases of *tinea cruris*).[16] Turan *et al.*[17] demonstrated the utility of RCM in 5 cases of *tinea incognito*, for which RCM was found to be more sensitive than cultural examination.

Confocal microscopy and parasitosis

Sarcoptes scabiei (Figure 8),[3, 4, 17-19, 19-21] *Demodex folliculorum* (Figure 9),[20, 22-26] *Pyemotes ventricosus*[27] *and Ixodes* (Figure 10)[28] have been identified by RCM. The identification of *S. scabiei* by RCM was first reported in 2005.[18] *S. scabiei* is characterized by an inhomogeneously refractive ovoid body and short legs (Figure 8).[4, 21] Adult females are 400x300 µm in size, while males are just over half this size.[4, 21] Eggs are hypo-refractive, 200x100 µm, ovoid structures with a hyper-refractive thin wall.[4, 21] Droppings are a useful sign for a nearby presence of a parasite:[21] in fact they are easy to be identified since they are numerous, superficial and hyper-reflective roundish bodies of around 15 µm in diameter.

RCM can confirm the diagnosis of scabies in cases that are doubtful at dermoscopy and it can be used for the follow-up after treatment. In fact, it allows to distinguish living mites from dead ones, that do not move and lose their vital functions (intestinal peristalsis, defecation),[3, 19, 29] and because they have a hyper-reflecting appearance, with homogenization of internal structures.[3]

RCM is also suitable for pathophysiological studies, being able to show the exact localization of parasites, their eggs and droppings in the epidermis, and their activity over time.[21]

Demodex folliculorum is easy to be recognized by RCM, being located upside down within the follicular infundibulum and appearing as a small (5 µm in diameter) round body with a hyper-reflective contour, corresponding to the horizontal section of the parasite, or as a lengthy cone-shaped structure when it is met a little sideways (Figure 9).[20, 22, 23] Multiple parasites are usually grouped within the same hair follicle. *Demodex brevis* has not been so far identified by RCM, probably because it is located at the lower portion of the hair follicle close to sebaceous ducts, an area that cannot be investigated by this technique due to the penetration depth limited to about 200-300 µm.[30]

The *Demodex folliculorum* count using RCM has been demonstrated to be higher in patients affected by rosacea than in healthy controls.[23, 25]

RCM gives higher numbers of parasites if com-

Figure 8.—Clinical (A,B), dermoscopical (B, 20x; C, 70x) and reflectance confocal microscopy (RCM) (D,E) aspect of a case of scabies of a newborn. RCM shows a pearly vesicle at the end of a burrow (D, white circle) and a *Sarcoptes scabies* mite (E, red circle) in the acral skin characterized by the presence of acrosyringia (E, yellow arrow).

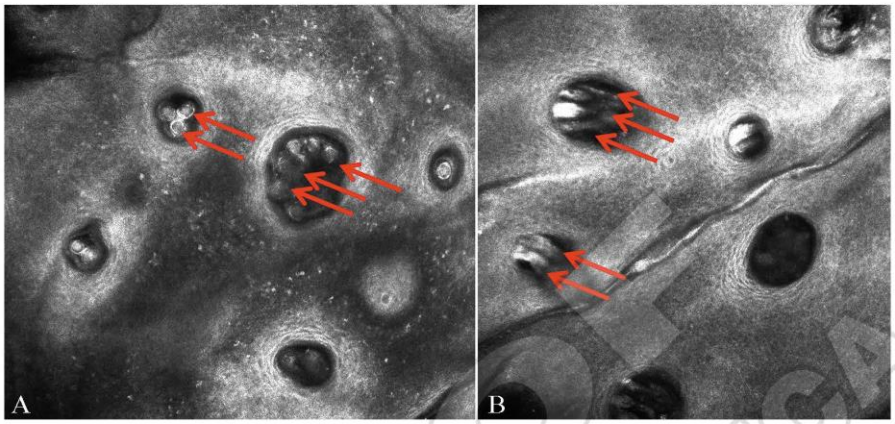

Figure 9.—Under reflectance confocal microscopy, *Demodex folliculorum* (A,B; red arrow) appears as a small round body with a hyper-reflective contour, corresponding to the horizontal section of the parasite (A), or as a lengthy cone-shaped structure when it is met a little sideways (B). Multiple parasites are grouped within the same hair follicle.

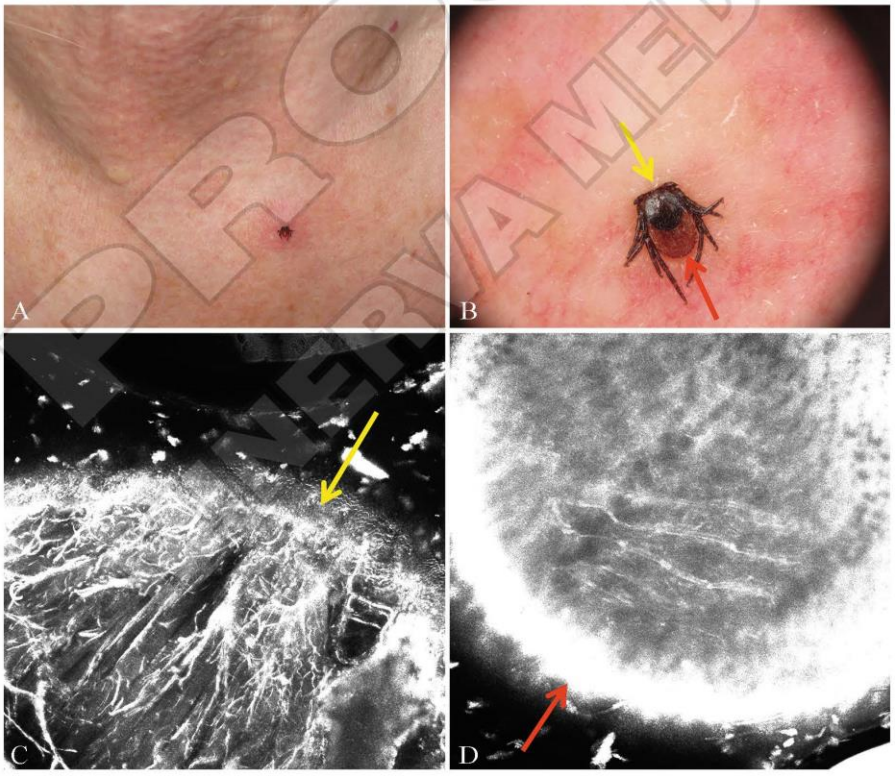

Figure 10.—Clinical (A), dermoscopical (B) and reflectance confocal microscopy (C,D) aspect of a *Ixodes* infestation. Reflectance confocal microscopy can identify different segments of the parasite such as rostrum (C, yellow arrow) and the gut (D, red arrow).

pared to standardized superficial skin biopsy (SSSB) that has been so far the gold standard diagnostic test to detect Demodex mites. In fact, in SSSB only superficial layers of skin are scraped off and examined, whereas RCM can identify all the mites directly on the skin, inside the follicle, reaching mites that are hidden inside elongated and hyperkeratotic follicles and that would not be counted on SSSB.[24, 30]

RCM has also been used to identify *Pyemotes ventricusus*, an ectoparasite of arthropod larvae invading furniture [27] and responsible for a pruritic cutaneous rash. However, the quality of the published image does not allow to confirm that the RCM image corresponds to this parasite.

Leishmania is too small to be identified by RCM. However, it is possible to observe a dermal inflammatory infiltrate with multinucleated cells in case of cutaneous Leishmaniasis[31]. RCM could be also useful to study the anatomical details of some parasites visible to the naked eye, such as ticks and lice (Figure 10). In our experience RCM is also helpful to identified *Dermanyssus gallinae* (data under publication). Moreover, RCM can be used to differentiate either the hypostome [28] or other tick body parts left in the skin from a simple hemorrhagic crust or a traumatized hyperpigmented skin lesion.

Conclusions

In conclusion, in vivo RCM can be used to diagnose in real-time, without causing discomfort to the patient and without requiring any further equipment or laboratory devices several cutaneous infestations and infections. In particular RCM can identify cutaneous parasites that are not visible to naked eye such as *Sarcoptes scabiei* and *Demodex folliculorum* and it allows to better identify the different body parts of bigger parasites such as ticks. Fungi can also be identified but their recognition is more difficult. RCM cannot direct observes virus. However, cytopathic effect associated with some virus such as *herpes virus* is easy to be recognized. As RCM examination is quick and performed by the dermatologist himself, it may be immediately followed by the prescription of treatment in the course of a routine consultation. Being non-invasive, RCM is also suitable for follow-up after therapy and for studies of physiology and pathogenesis with repeated examinations over time.

References

1. Guitera P, Menzies SW, Longo C, Cesinaro AM, Scolyer RA, Pellacani G. In vivo confocal microscopy for diagnosis of melanoma and basal cell carcinoma using a two-step method: analysis of 710 consecutive clinically equivocal cases. J Invest Dermatol 2012;132:2386-94.
2. Pellacani G, Pepe P, Casari A, Longo C. Reflectance confocal microscopy as a second-level examination in skin oncology improves diagnostic accuracy and saves unnecessary excisions: a longitudinal prospective study. Br J Dermatol 2014;171:1044-51.
3. Cinotti E, Perrot J-L, Labeille B, Cambazard F. On the feasibility of confocal microscopy for the diagnosis of scabies. Ann Dermatol Vénéréologie 2013;140:215-6.
4. Perrot J-L, Cinotti E, Labeille B, Trau C, Rabérin H, Flori P *et al.* Rapid diagnosis of scabies by manual confocal reflectance microscopy. Ann Dermatol Vénéréologie 2012;139:502-5.
5. Cinotti E, Perrot JL, Labeille B, Moragues A, Raberin H, Flori P *et al.* Tinea corporis diagnosed by reflectance confocal microscopy. Ann Dermatol Vénéréologie 2014;141:150-2.
6. Cinotti E, Fouilloux B, Perrot JL, Labeille B, Douchet C, Cambazard F. Confocal microscopy for healthy and pathological nail. J Eur Acad Dermatol Venereol 2014; 28:853-8
7. Goldgeier M, Alessi C, Muhlbauer JE. Immediate noninvasive diagnosis of herpesvirus by confocal scanning laser microscopy. J Am Acad Dermatol 2002;46:783-5.
8. Abraham LS, Costa MC, Agozzino M, Amorosi B, Cota C, Ardigo M. In vivo reflectance confocal microscopy for varicella prompt diagnosis and treatment in a severely immunosuppressed patient. Skin Res Technol 2012;18:386-8.
9. Scope A, Benvenuto-Andrade C, Gill M, Ardigo M, Gonzalez S, Marghoob AA. Reflectance confocal microscopy of molluscum contagiosum. Arch Dermatol 2008;144:134.
10. Tan J, Quinn MA, Pyman JM, Delaney PM, McLaren WJ. Detection of cervical intraepithelial neoplasia in vivo using confocal endomicroscopy. Int J Obstet Gynaecol 2009;116:1663-70.
11. Venturini M, Sala R, Semenza D, Santoro A, Facchetti F, Calzavara-Pinton P. Reflectance confocal microscopy for the in vivo detection of Treponema pallidum in skin lesions of secondary syphilis. J Am Acad Dermatol 2009;60:639-42.
12. Cinotti E, Perrot JL, Labeille B, Raberin H, Flori P, Cambazard F. Hair dermatophytosis diagnosed by reflectance confocal microscopy: six cases. J Eur Acad Dermatol Venereol JEADV 2014 May 22.
13. Liansheng Z, Xin J, Cheng Q, Zhiping W, Yanqun L. Diagnostic applicability of confocal laser scanning microscopy in tinea corporis. Int J Dermatol 2013;52:1281-2.
14. Pharaon M, Gari-Toussaint M, Khemis A, Zorzi K, Petit L, Martel P *et al.* Diagnosis and treatment monitoring of toenail onychomycosis by reflectance confocal microscopy: prospective cohort study in 58 patients. J Am Acad Dermatol 2014;71:56-61.
15. Rothmund G, Sattler EC, Kaestle R, Fischer C, Haas CJ, Starz H *et al.* Confocal laser scanning microscopy as a new valuable tool in the diagnosis of onychomycosis - comparison of six diagnostic methods. Mycoses 2013;56:47-55.
16. Hui D, Xue-cheng S, Ai-e Xu. Evaluation of reflectance confocal microscopy in dermatophytosis. Mycoses 2013;56:130-3.
17. Turan E, Erdemir AT, Gurel MS, Yurt N. A new diagnostic technique for tinea incognito: in vivo reflectance confocal microscopy. Report of five cases. Skin Res Technol 2013;19:e103-107.
18. Longo C, Bassoli S, Monari P, Seidenari S, Pellacani G. Reflectance-mode confocal microscopy for the in vivo detection of Sarcoptes scabiei. Arch Dermatol 2005;141:1336.
19. Levi A, Mumcuoglu KY, Ingber A, Enk CD. Assessment of Sarcoptes scabiei viability in vivo by reflectance confocal microscopy. Lasers Med Sci 2011;26:291-2.
20. Slutsky JB, Rabinovitz H, Grichnik JM, Marghoob AA. Reflectance confocal microscopic features of dermatophytes, scabies, and demodex. Arch Dermatol 2011;147:1008.

21. Cinotti E, Perrot JL, Labeille B, Vercherin P, Chol C, Besson E *et al.* Reflectance confocal microscopy for quantification of Sarcoptes scabiei in Norwegian scabies. J Eur Acad Dermatol Venereol 2013;27:e176-178.
22. Longo C, Pellacani G, Ricci C, De Pace B, Argenziano G, Zalaudek I. In vivo detection of Demodex folliculorum by means of confocal microscopy. Br J Dermatol 2012;166:690-2.
23. Sattler EC, Maier T, Hoffmann VS, Hegyi J, Ruzicka T, Berking C. Noninvasive in vivo detection and quantification of Demodex mites by confocal laser scanning microscopy. Br J Dermatol 2012;167:1042-7.
24. Veasey J, Framil V, Ribeiro A, Lellis R. Reflectance confocal microscopy use in one case of Pityriasis follicularum: a Demodex folliculorum analysis and comparison to other diagnostic methods. Int J Dermatol 2014;53:e254-257.
25. Turgut Erdemir A, Gurel MS, Koku Aksu AE, Bilgin Karahalli F, Incel P, Kutlu Haytoğlu NS *et al.* Reflectance confocal microscopy vs. standardized skin surface biopsy for measuring the density of Demodex mites. Skin Res Technol 2014;20:435-9.
26. Yuan C, Wang X-M, Guichard A, Lihoreau T, Sophie M-M, Lamia K *et al.* Comparison of Reflectance Confocal Microscopy and Standardized skin surface biopsy for three different lesions in a pityriasis folliculorum patient. Br J Dermatol 2014;172:1440-2.
27. Del Giudice P, Blanc-Amrane V, Bahadoran P, Caumes E, Marty P, Lazar M *et al.* Pyemotes ventricosus dermatitis, southeastern France. Emerg Infect Dis 2008;14:1759-61.
28. Erdoğan S, Dorittke P, Kardorff B. Identification of a foreign body--tick (Ixodes)--with confocal laser scan microscopy (CLSM) in comparison to histology in a mouse model. J Dtsch Dermatol Ges 2012;10:277-8.
29. Levi A, Mumcuoglu KY, Ingber A, Enk CD. Detection of living Sarcoptes scabiei larvae by reflectance mode confocal microscopy in the skin of a patient with crusted scabies. J Biomed Opt 2012;17:060503.
30. Sattler EC, Maier T, Hoffmann VS, Ruzicka T, Berking C. Noninvasive in vivo detection and quantification of Demodex mites by confocal laser scanning microscopy: reply from the authors. Br J Dermatol 2013;169:213-5.
31. Alarcon I, Carrera C, Puig S, Malvehy J. In vivo Confocal Microscopy Features of Cutaneous Leishmaniasis. Dermatol 2014;228:121-4.

Conflicts of interest.—The authors certify that there is no conflict of interest with any financial organization regarding the material discussed in the manuscript.

3.d 2 Reflectance confocal microscopy for cutaneous infections and infestations

Reflectance confocal microscopy (RCM) is a high-resolution emerging imaging technique that allows non-invasive diagnosis of several cutaneous disorders. A systematic review of the literature on the use of RCM for the study of infections and infestations has been performed to evaluate the current use of this technique and its possible future applications in this field. RCM is particularly suitable for the identification of *Sarcoptes scabies*, *Demodex folliculorum*, *Ixodes*, *Dermatophytes* and *Candida species* in the clinical practice and for the follow-up after treatment. The cytopathic effect of *herpes simplex virus*, *varicella zoster virus* and *molluscipoxviru*s is also detectable by this imaging technique even in a pre-vesicular stage. In addition, thanks to its non-invasiveness, RCM allows pathophysiological studies.

DOI: 10.1111/jdv.13254 JEADV

REVIEW ARTICLE

Reflectance confocal microscopy for cutaneous infections and infestations

E. Cinotti,* J.L. Perrot, B. Labeille, F. Cambazard

Dermatology Department, University Hospital of Saint-Etienne, Saint Etienne, France
*Correspondence: E. Cinotti. E-mail: elisacinotti@gmail.com

Abstract

Reflectance confocal microscopy (RCM) is a high-resolution emerging imaging technique that allows non-invasive diagnosis of several cutaneous disorders. A systematic review of the literature on the use of RCM for the study of infections and infestations has been performed to evaluate the current use of this technique and its possible future applications in this field. RCM is particularly suitable for the identification of *Sarcoptes scabies*, *Demodex folliculorum*, *Ixodes*, *Dermatophytes* and *Candida species* in the clinical practice and for the follow-up after treatment. The cytopathic effect of *herpes simplex virus*, *varicella zoster virus* and *molluscipoxvirus* is also detectable by this imaging technique even in a pre-vesicular stage. In addition, thanks to its non-invasiveness, RCM allows pathophysiological studies.

Received: 9 January 2015; Accepted: 6 March 2015

Conflicts of Interest

None declared.

Introduction

Reflectance confocal microscopy (RCM) is an emerging technique, which optically sections the living tissue at various depths, to image horizontal layers of the skin and appendages with resolution at a cellular level and without alteration of the tissue surface. The use of RCM in dermatology was first reported roughly 20 years ago[1,2] and was initially focused on the diagnosis of skin cancer. A rising number of other indications have been later described for the diagnosis and management of dermatological disorders.

Here, we summarize the literature on the RCM use for cutaneous infections and infestations. Search terms employed were 'reflectance confocal microscopy', 'confocal microscopy', 'laser-scanning confocal microscopy', 'skin', 'nail', 'hair', 'infection', 'parasitosis', 'mycosis', 'dermatophytosis', 'virus', 'bacteria', 'parasite', 'scabies ', '*Sarcoptes scabiei*', '*Demodex folliculorum*', 'rosacea', '*Pyemotes ventricosus*', 'tick', '*herpes virus*' and 'molluscum contagiosum'.

In vivo reflectance confocal microscopy devices

Two *in vivo* devices dedicated to the skin are available: VivaScope® 1500 and 3000 (CALIBER, New York, USA, distributed in Europe by the company MAVIG GmbH, Munich, Germany). They both allow a real-time and non-invasive examination. Initially, the diagnosis of skin parasitosis[3 6] and infections[7] was made by the fixed camera VivaScope® 1500, the first to be produced, but not very suitable for this purpose due to its large size, low mobility and the need to fix the lens to the skin by means of an adhesive ring. Recently, the provision of a hand held compact camera (VivaScope® 3000) permitting flexible movements in all directions has allowed a fast and easy diagnosis. Moreover, it enables the examination of all body areas due to its smaller tip, thus increasing the detection capability of infectious agents.[8 11]

Confocal microscopy and parasitosis

Sarcoptes scabiei,[4,6,8,11,12,12 14] *Demodex folliculorum*,[3 5,15 17] *Pyemotes ventricosus*[18] *and Ixodes*[19] have been identified using RCM (Fig. 1 and 2). The optical microscopic examination of a specimen obtained from skin scraping is the reference technique to identify parasites, eggs and/or droppings in case of scabies. However, this technique is time consuming and can give false-negative results.[20] Currently, this method is often replaced by dermoscopy, which shows the 'delta-wing jet' sign that corresponds to the cephalic portion of *S. scabiei* and its furrow.[3] Nevertheless, this sign is sometimes difficult to detect, and some locations such as inter-digital spaces, one of the most affected sites, are impossible to be explored by the dermoscope due to the excessive tip size.[8]

The identification of *S. scabiei* by RCM was first reported in 2005[6] and the introduction of the handheld camera allowed the use of this technique for the diagnosis of scabies in clinical routine.[8,11] Under RCM, *S. scabiei* presents with an inhomogeneously refractive ovoid body and short legs[11,14] (Fig. 1b,c). Adult females are 400 × 300 μm in size, while males are just

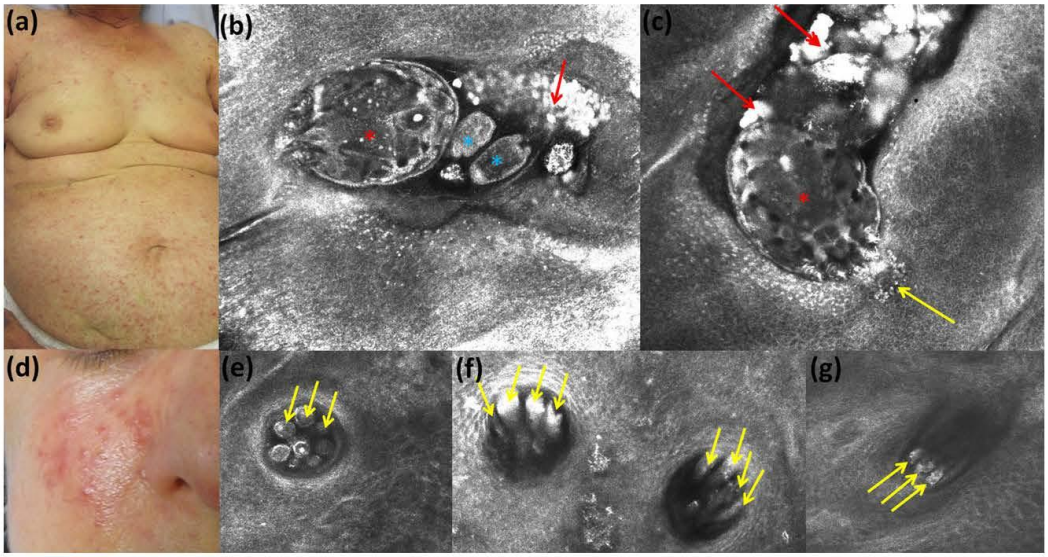

Figure 1 Clinical and reflectance confocal microscopy aspect of a case of scabies (a–c) and rosacea (d–g). Under confocal microscopy adult females of *Sarcoptes scabies* (red asterisk) present with an inhomogeneously refractive ovoid body (b,c), with a furrow behind them full of eggs (b, blue asterisk) and droppings (b,c; red arrow).In particular, it is possible to observe *Sarcoptes scabies* digging its furrow using its rostrum and saliva (c, yellow arrow).Under confocal microscopy, *Demodex folliculorum* (e.g. yellow arrow) appears as a small round body with a hyper-reflective contour, corresponding to the horizontal section of the parasite (e), or as a lengthy cone-shaped structure when it is met a little sideways (f,g). Multiple parasites are grouped within the same hair follicle.

over half this size.[11,14] Eggs are hypo-refractive, 200 × 100 μm, and have ovoid structures with a hyper-refractive thin wall[11,14] (Fig. 1b).In addition, although, the morphology of different developmental stages of *S. scabiei* is similar, examination by RCM allows to distinguish adults from larvae according to their size (larvae are smaller than adults) and number of pairs of legs (four pairs of legs for adults and three pairs of legs for larvae).[11] Droppings are easily identified as they are superficial hyper-reflective roundish bodies of around 15 μm in diameter that can be a useful signal of a nearby presence of an adult parasite[14] (Fig. 1b,c).

Unlike dermoscopy, RCM can be used for the follow-up after treatment, being a non-invasive real-time examination that allows to distinguish living mites from the dead ones as all the vital functions of the parasites are visible, from intestinal peristalsis to defecation.[8,12,21] Moreover, dead parasites can be recognized not only because they don't move but also because they have a hyper-reflecting appearance, with blurred edges and homogenization of internal structures.[8]

The parasitological confirmation of scabies is vital for patients, environmental hygiene and prevention measures.RCM is also suitable for pathophysiological studies, being able to show the exact localization of parasites, their eggs and droppings in the epidermis, and their activity over time (Fig. 1c).It even allows to count them.[14]

Demodex mites are thought to play a pathogenic role when they are present in excessive number and are implicated in several skin conditions such as rosacea, demodecidosis and pityriasis folliculorum.[3,15] So far the gold-standard diagnostic test to detect Demodex mites and confirm the diagnosis of related dermatitis is the standardized superficial skin biopsy (SSSB) technique, which utilizes cyanoacrylate glue on a glass slide to extract the content of facial hair follicles. However, this technique may cause discomfort to the patient.

Demodex folliculorum is easy to be recognized by RCM, being located upside down within the follicular infundibulum and appearing as a small (5 μm in diameter) round body with a hyper-reflective contour, corresponding to the horizontal section of the parasite, or as a lengthy cone-shaped structure when it is met a little sideways[3 5] (Fig. 1 e g).Multiple parasites are usually grouped within the same hair follicle. *Demodex brevis* has not been identified by RCM so far, probably because it is located at the lower portion of the hair follicle, close to sebaceous ducts, an area that cannot be investigated by this technique as the penetration depth is limited to about 200 300 μm.[22]

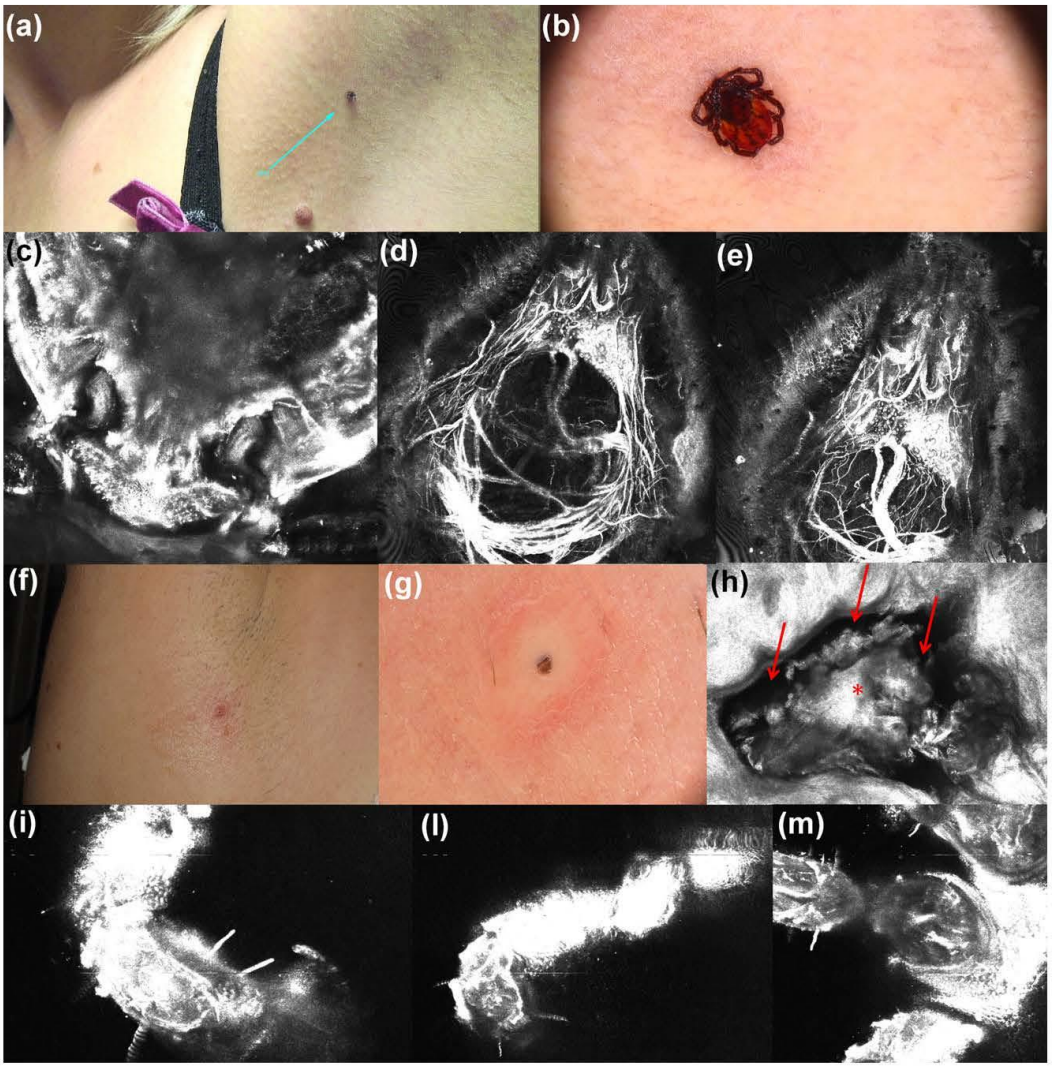

Figure 2 Clinical, dermoscopical and the reflectance confocal microscopy aspect of a *Ixodes* infestation (a–h) and reflectance confocal microscopy of a *Pediculus humanus* (i–m). A tick that is clinically (a) and dermoscopically (b) evident is observed under confocal microscopy (c–e) that can identify different segments of the parasite such as rostrum (c) and gut (d,e). The presence of a possible remnant of a tick identified by clinical (f) and dermoscopical (g) examination is confirmed by confocal microscopy (h) showing a leg of the tick (red asterisk) inside a skin hole (red arrow). The distal (i, l) and proximal (m) part of the legs of a louse are identified under confocal microscopy.

Sattler *et al.*[5] examined 25 patients with facial rosacea and 25 healthy controls by RCM and found a significant difference ($p < 0.0001$) in the mean number of mites (94.2 and 22.4 per 5 mm^2 area and 0.7 0.8 and 0.1 0.2 per follicle in the patients and controls respectively). Lacey *et al.*[23] criticized this study assuming on a false-positive identification of Demodex mites by

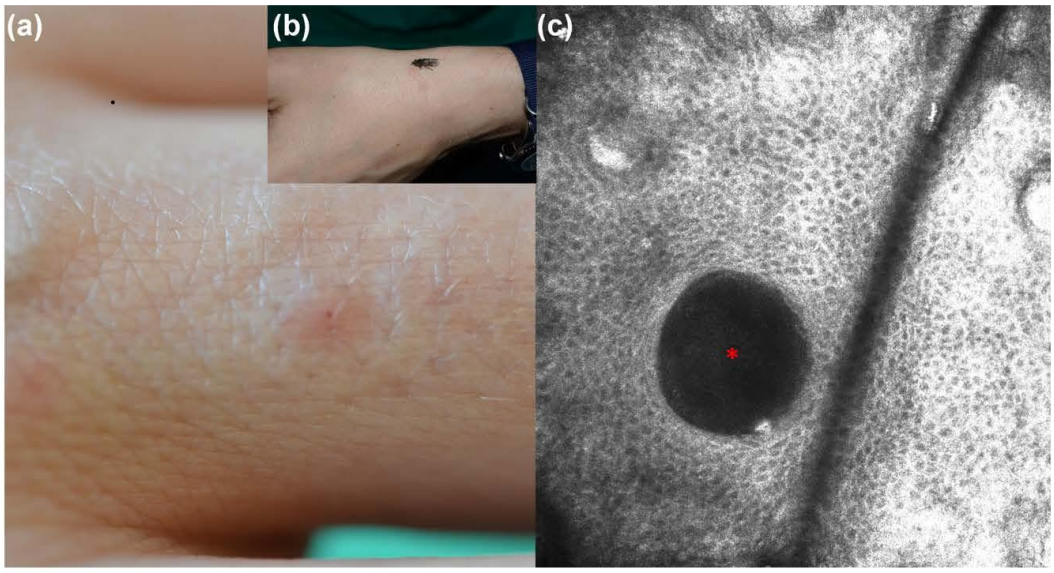

Figure 3 Clinical and reflectance confocal microscopy aspect of an horsefly bite. The clinical image (a) shows a non-specific inflammatory reaction on a finger, possibly corresponding to a horsefly (b) bite; hypothesis confirmed by confocal microscopy showing a well-defined round hole in the epidermis (c, red asterisk).

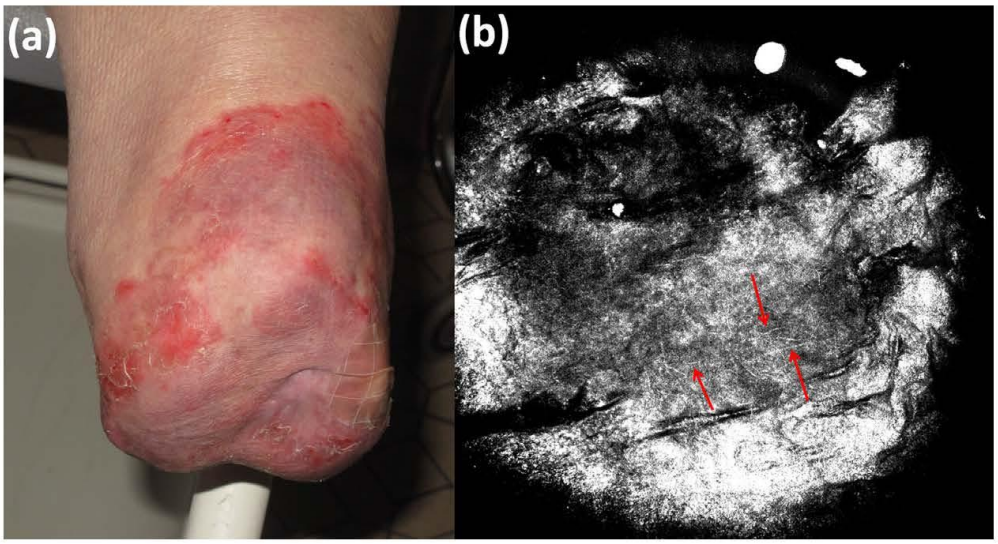

Figure 4 Clinical (a) and reflectance confocal microscopy (b) aspect of a dermatophytosis on a stump. Dermatophytes are easily identified under reflectance confocal microscopy as thin, high-reflective and longitudinal structures with a linear shape (red arrow).

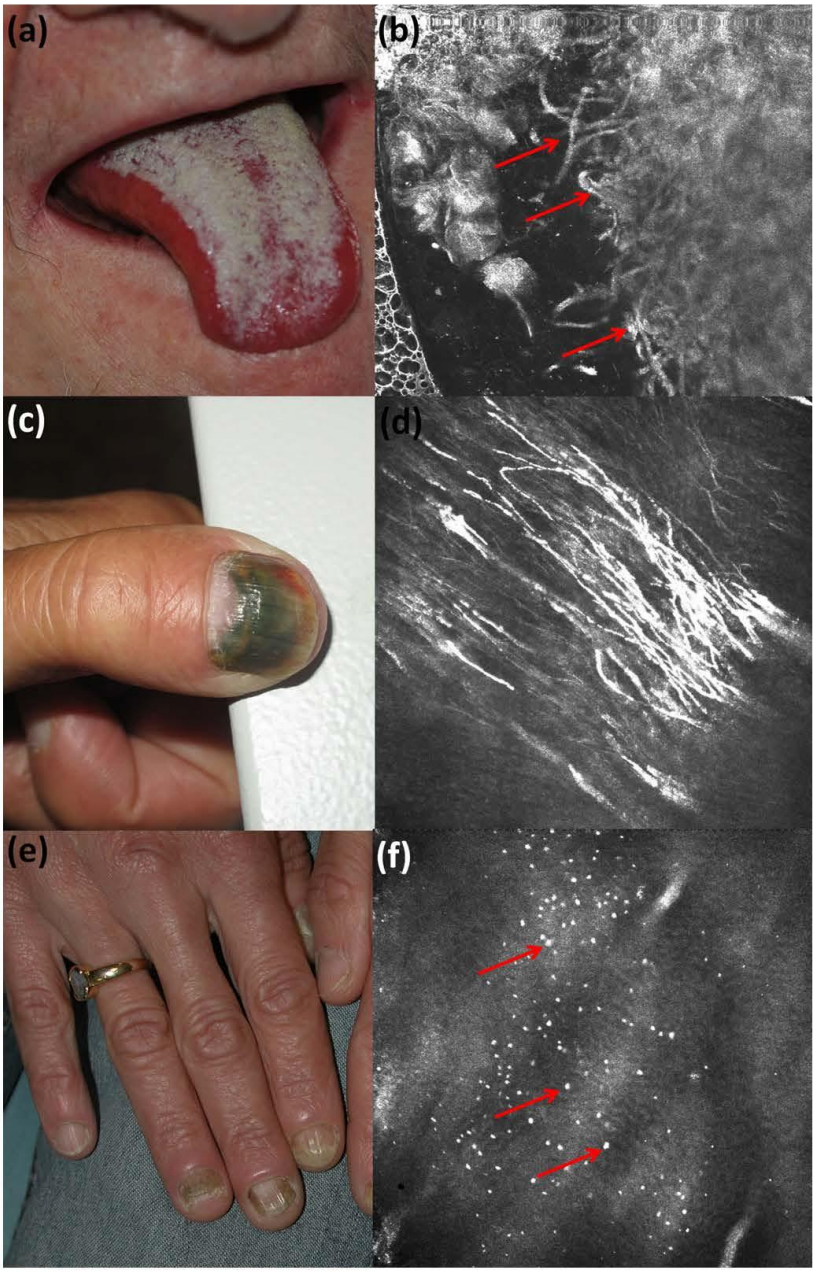

Figure 5 Clinical and reflectance confocal microscopy aspect of an oral mucosa (a–b) and nail (c–f) Candida infection. Confocal microscopy shows pseudofilaments (b, d); indicated by red arrows in figure b and conidia (f), red arrow.

RCM due to the large number of mites identified by RCM, compared to standard observations by SSSB. However, the number of mites cannot be compared with these two different diagnostic methods as in SSSB only superficial layers of skin are scraped off and examined, whereas RCM can identify all the mites directly on the skin, inside the follicle, reaching mites that are hidden inside the elongated and hyper-keratotic follicles and these would not be counted on SSSB.[15,22]

Turgut Erdemir *et al.*[16] performed another study on 48 affected patients (40 by pityriasis folliculorum and eight by rosacea) and on 47 healthy controls and confirmed the capacity of RCM to discriminate between affected and healthy control patients by finding a higher mean number of mites in the patients (2.63 ± 0.77 and 0.77 ± 0.98 mites per follicle in patients and controls respectively, $p < 0.001$). In addition, the authors performed SSSB on the same subjects and obtained a number of mites lower than that found using RCM (15.33 ± 18.1 and 409.8 ± 209.2 mites per 10 mm^2 with SSSB and RCM respectively, $p < 0.001$). Moreover, they showed a better precision of RCM (100%) compared with SSSB (85.7%) for the detection of increased Demodex in affected subjects.

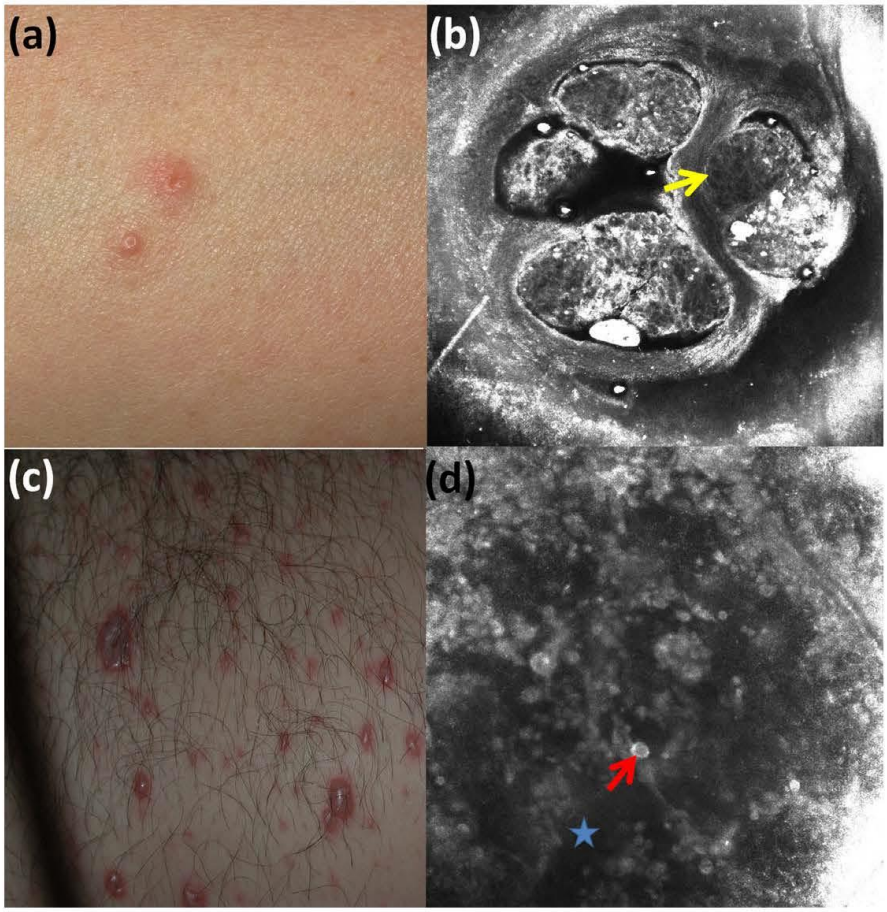

Figure 6 Clinical and reflectance confocal microscopy aspect of a *molluscipoxvirus*(a, b) and *varicella-zoster herpes virus*(c, d) infection in two adult patients. Confocal microscopy shows the presence of intra-epidermal cavities (blue star) with large acantholytic cells (yellow and red arrow) .

RCM has also been used to identify *Pyemotes ventricosus*, an ectoparasite of arthropod larvae invading furniture.[18] This parasite is responsible for a pruritic erythematous rash with maculopapules with a central microvesicle sometimes associated with lymphangitis. Del Giudice *et al.*[18] showed by RCM an ovoid body of intermediate reflectance with morphological features suggestive of *P. ventricosus* inside a cutaneous microvesicle of an infested patient. However, the quality of the published image does not allow confirming that the RCM image corresponds to this parasite. Moreover, the RCM identification of this parasite was not reproduced on other lesions from the same patients or from other patients and the parasite was not identified by using other techniques.

One case of cutaneous Leishmaniasis was also observed under RCM[24]: a dermal inflammatory infiltrate with multinucleated cells was visible.RCM could be also useful to study the anatomical details of some parasites that are visible to the naked eye, such as ticks and lice (Fig. 2). Moreover, RCM can be used to differentiate either the hypostome[19] or other tick body parts on the skin from a simple haemorrhagic crust or a traumatized hyper-pigmented skin lesion (Fig. 2). Using RCM, we can also identify the skin hole caused by the sting of an insect by allowing to rapidly differentiate insect bites from other inflammatory dermatoses (Fig. 3).

Confocal microscopy and superficial mycosis

Conventional techniques to confirm the clinical diagnosis of superficial mycosis are direct light microscopic examination and fungal culture. Direct microscopic examination can give false-negative results in case of low fungal load or sampling error, whereas the fungal culture is time consuming. *In vivo* RMC has been recently used for the diagnosis of dermatophytosis with the advantage of (i) being non-invasive, (ii) requiring no skin sample for *ex vivo* analysis, (iii) being performed on the spot without any previous preparation, (iv) evaluating the entire lesion surface and not just the scales removed for a conventional *ex vivo* analysis.

Therefore, RCM can allow to confirm the diagnosis of dermatophytosis during the dermatological consultation and to initiate an appropriate treatment without waiting for the conventional mycological examination.[25,26] Dermatophytes are easily identified under RCM in the skin, the nail plate and hairs due to their particular appearance as thin, high-reflective and longitudinal structures with a serpentine shape[9,10,25] (Fig. 4).

In vivo RCM was first used for the identification of fungi in 1994 by Piérard *et al.*[27] in a case of onychomycosis. In 2000 Hongcharu *et al.*[28] showed that using *in vivo* and *ex vivo* RCM could be faster than the conventional potassium hydroxide preparation for the diagnosis of onychomycosis, and in 2001 Markus *et al.*[29] reported the first case of *in vivo* RCM diagnosis of tinea corporis. The superiority of *in vivo* RCM to potassium hydroxide preparation for the diagnosis of dermatophytosis has been later reported by Rothmund *et al.*[30] in a prospective trial on 50 toes suspicious of onychomycosis, (sensitivity 79% versus 74% and specificity 81% versus 76%) and by Liansheng *et al.*[31] in a trial on 55 patients affected by tinea corporis (sensitivity 89.1% vs 80.0%). Recent studies confirmed the high specificity of RCM[26,32] but found a lower sensitivity for both onychomycosis (52.9% of sensitivity in a series of 58 patients)[26] and skin dermatophytosis (64% of sensitivity in 22 patients with tinea manus and pedis; 83% of sensitivity in 23 cases of tinea cruris).[32] Turan *et al.*[13] demonstrated the utility of RCM in five cases of *tinea incognito*, for which RCM was found to be more sensitive than cultural examination.

Our group recently demonstrated the possibility of RCM use not only to identify filaments but also conidia, which

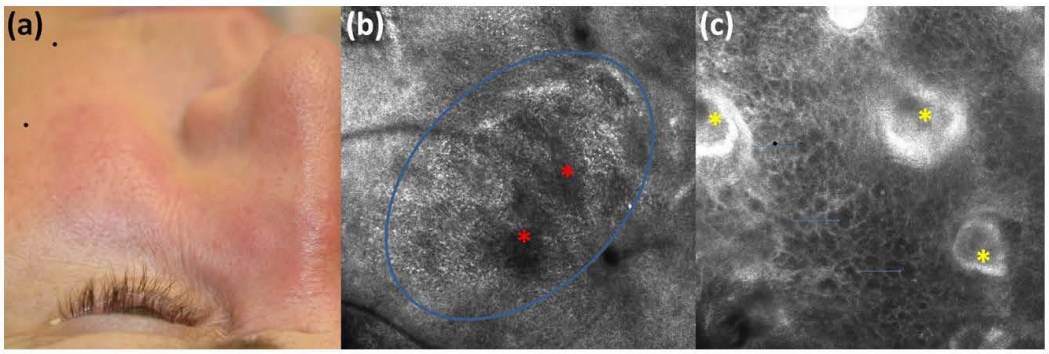

Figure 7 Clinical (a) and reflectance confocal microscopy (b, c) aspect of a *varicella-zoster herpes virus* infection in a pre-vesicular stage. Confocal microscopy shows a subtle acatholysis in the epidermis (red asterisk and blue circle) and large keratinocytes (blue arrow). Hair follicles are marked by yellow asterisks.

corresponds to roundish hyper-reflective bright structures.[10] The RCM aspect of yeasts in onychomycosis has been reported only by Arrese *et al.*,[33] while few cases of nail infestation by moulds have been included in the series of Pharaon *et al.*,[26] but no specific features are described. In our experience it is possible to identify Candida's pseudofilaments and/or conidia on oral mucosa and nails (Fig. 5).

Confocal microscopy and cutaneous bacterial infections

Venturini *et al.*[7] identified *Treponema pallidum* by RCM in cutaneous lesions, clinically suggestive of secondary syphilis, of three patients, disclosing bright particles intermingled with keratinocytes. However, the published images are of poor resolution: these particles did not have a spiral shape

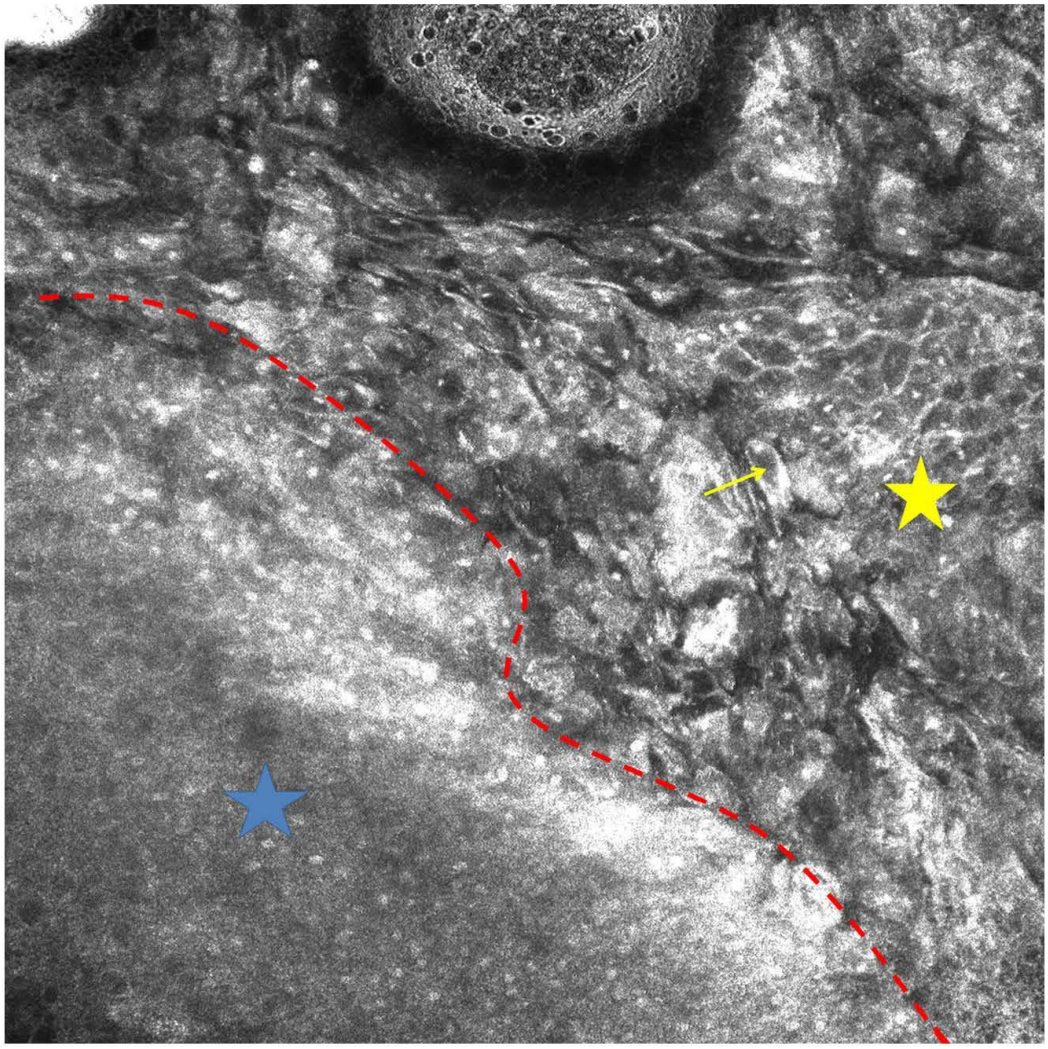

Figure 8 Reflectance confocal microscopy aspect of a vaginal intra-epithelial neoplasia with large keratinocytes (yellow arrow). The red dotted line separates the normal mucosa (blue star) from the pathological mucosa (yellow star).

and are difficult to differentiate from the normal keratinocytes.

Confocal microscopy and viral infections

RCM has also been used to identify the cytopatic effects of *herpes simplex and varicella-zoster herpes virus*[34,35] and *molluscipoxvirus*[36] in the skin (Fig. 6). In first two infections, RCM shows the presence of intra-epidermal cavities with acantholytic cells admixed with pleomorphic large keratinocytes and multinucleated giant cells corresponding to *herpes virus*-infected keratinocytes. In case of *molluscipoxvirus* infection, RCM shows a round, well-circumscribed lesion with central round cystic areas filled with brightly refractive material corresponding to the characteristic eosinophilic inclusion bodies (molluscum bodies) of the histopathological examination.[36] The cutaneous lesions induced by these viruses are most often clinically typical and do not require any complementary investigation. Few cases are atypical, mostly in the case of a pre-existing skin disease or in immuno-compromised patients, where the diagnosis requires investigations such as Tzanck cytodiagnosis, direct fluorescence assay, viral cultures, PCR or histopathological examination. Compared with standard techniques, RCM has the advantages of being non-invasive and quick, and able to image the entire affected cutaneous surface. Moreover, it can be useful for a non-invasive diagnosis in an early pre-vesicular stage (Fig. 7). Physiological studies can also be performed, for example, to investigate the viral effects on a same location over time. However, up to date, RCM has only been employed in few cases of herpetic infection and in one case of molluscum contagiosum, and its sensitivity and specificity in atypical cases remain to be evaluated.

Confocal microscopy for the diagnosis of virus-induced neoplasia and neuropathy

RCM could be also be used for an early diagnosis of vaginal intra-epithelial neoplasia with cytopathic effect induced by *human papillomavirus* (Fig. 8). RCM has also been used for quantitative assessment of distal sensory polyneuropathy associated with human immunodeficiency virus by measuring the density per mm^2 of the Meissner Corpuscles at the volar side of the hand and foot.[37]

Contagion risk associated with the confocal microscopy examination

In case of a suspected infection or infestation, a disposable transparent film (for example Visulin ®, Paul Hartmann AG, Germany) should be applied on the tip of the RCM camera. If this film is not used, a decontamination of the tip of the camera should be performed with a disposable virucidal, fungicidal and bactericidal cleansing wipe(for example Sani-Cloth Active®, PDI, UK, or Alkotip®, Servoprax, Germany). This wipe has no proved activity against parasites, but the mechanical cleaning action, repeatedly performed on the smooth surface of the tip, allows their elimination.

Conclusions

In conclusion, *in vivo* RCM can be used to detect the cutaneous parasites (mainly *Sarcoptes scabiei*, *Demodex folliculorum* and *Ixodes)* and fungi (mainly dermatophytes) and to identify the cytopathic effects associated with virus in real-time, within a few minutes, without causing discomfort to the patient and without requiring any further equipment or laboratory devices. As RCM examination is quick and performed by the dermatologist himself, it can be immediately followed by the prescription of the treatment in the course of a routine consultation. The cost of the machine is a limiting factor. However, for the dermatological centers where there is already such a machine for the detection of skin tumours, infestations and infections are additional possible diagnostic applications. Being non-invasive, RCM is also suitable for follow-up after therapy and for study of physiology and pathogenesis with repeated examinations over time. Further studies are needed to compare the RCM performances with that of the conventional diagnostic techniques.

References

1 Piérard GE. *In vivo* confocal microscopy: a new paradigm in dermatology. *Dermatology* 1993; **186**: 4 5.
2 Corcuff P, Bertrand C, Leveque JL. Morphometry of human epidermis *in vivo* by real-time confocal microscopy. *Arch Dermatol Res* 1993; **285**: 475 481.
3 Longo C, Pellacani G, Ricci C, De Pace B, Argenziano G, Zalaudek I. *In vivo* detection of Demodex folliculorum by means of confocal microscopy. *Br J Dermatol* 2012; **166**: 690 692.
4 Slutsky JB, Rabinovitz H, Grichnik JM, Marghoob AA. Reflectance confocal microscopic features of dermatophytes, scabies, and demodex. *Arch Dermatol* 2011; **147**: 1008.
5 Sattler EC, Maier T, Hoffmann VS, Hegyi J, Ruzicka T, Berking C. Noninvasive *in vivo* detection and quantification of Demodex mites by confocal laser scanning microscopy. *Br J Dermatol* 2012; **167**: 1042 1047.
6 Longo C, Bassoli S, Monari P, Seidenari S, Pellacani G. Reflectance-mode confocal microscopy for the *in vivo* detection of Sarcoptes scabiei. *Arch Dermatol* 2005; **141**: 1336.
7 Venturini M, Sala R, Semenza D, Santoro A, Facchetti F, Calzavara-Pinton P. Reflectance confocal microscopy for the *in vivo* detection of Treponema pallidum in skin lesions of secondary syphilis. *J Am Acad Dermatol* 2009; **60**: 639 642.
8 Cinotti E, Perrot J-L, Labeille B, Cambazard F. On the feasibility of confocal microscopy for the diagnosis of scabies. *Ann Dermatol Venereol* 2013; **140**: 215 216.
9 Cinotti E, Fouilloux B, Perrot JL, Labeille B, Douchet C, Cambazard F. Confocal microscopy for healthy and pathological nail. *J Eur Acad Dermatol Venereol* 2014; **28**: 853 858.
10 Cinotti E, Perrot JL, Labeille B, Raberin H, Flori P, Cambazard F. Hair dermatophytosis diagnosed by reflectance confocal microscopy: six cases. *J Eur Acad Dermatol Venereol* 2014; doi: 10.1111/jdv.12557. [e-pub ahead of print].
11 Perrot J-L, Cinotti E, Labeille B *et al.* Rapid diagnosis of scabies by manual confocal reflectance microscopy. *Ann Dermatol Venereol* 2012; **139**: 502 505.

12 Levi A, Mumcuoglu KY, Ingber A, Enk CD. Assessment of Sarcoptes scabiei viability *in vivo* by reflectance confocal microscopy. *Lasers Med Sci* 2011; **26**: 291 292.
13 Turan E, Erdemir AT, Gurel MS, Yurt N. A new diagnostic technique for tinea incognito: *in vivo* reflectance confocal microscopy. Report of five cases. *Skin Res Technol* 2013; **19**: e103 e107.
14 Cinotti E, Perrot JL, Labeille B *et al.* Reflectance confocal microscopy for quantification of Sarcoptes scabiei in Norwegian scabies. *J Eur Acad Dermatol Venereol* 2013; **27**: e176 e178.
15 Veasey J, Framil V, Ribeiro A, Lellis R. Reflectance confocal microscopy use in one case of Pityriasis folliculorum: a Demodex folliculorum analysis and comparison to other diagnostic methods. *Int J Dermatol* 2014; **53**: e254 e257.
16 Turgut Erdemir A, Gurel MS, Koku Aksu AE *et al.* Reflectance confocal microscopy vs. standardized skin surface biopsy for measuring the density of Demodex mites. *Skin Res Technol* 2014; **20**: 435 439.
17 Yuan C, Wang X-M, Guichard A *et al.* Comparison of reflectance confocal microscopy and standardized skin surface biopsy for three different lesions in a pityriasis folliculorum patient. *Br J Dermatol* 2015; **172**: 1440 1442.
18 Del Giudice P, Blanc-Amrane V, Bahadoran P *et al.* Pyemotes ventricosus dermatitis, southeastern France. *Emerg Infect Dis* 2008; **14**: 1759 1761.
19 Erdoğan S, Dorittke P, Kardorff B. Identification of a foreign body tick (Ixodes) with confocal laser scan microscopy (CLSM) in comparison to histology in a mouse model. *J Dtsch Dermatol Ges* 2012; **10**: 277 278.
20 Dupuy A, Dehen L, Bourrat E *et al.* Accuracy of standard dermoscopy for diagnosing scabies. *J Am Acad Dermatol* 2007; **56**: 53 62.
21 Levi A, Mumcuoglu KY, Ingber A, Enk CD. Detection of living Sarcoptes scabiei larvae by reflectance mode confocal microscopy in the skin of a patient with crusted scabies. *J Biomed Opt* 2012; **17**: 060503.
22 Sattler EC, Maier T, Hoffmann VS, Ruzicka T, Berking C. Noninvasive *in vivo* detection and quantification of Demodex mites by confocal laser scanning microscopy: reply from the authors. *Br J Dermatol* 2013; **169**: 213 215.
23 Lacey N, Forton FMN, Powell FC. Demodex quantification methods: limitations of confocal laser scanning microscopy. *Br J Dermatol* 2013; **169**: 212 213.
24 Alarcon I, Carrera C, Puig S, Malvehy J. *In vivo* confocal microscopy features of cutaneous leishmaniasis. *Dermatol Basel Switz.* 2014; **228**: 121 124.
25 Cinotti E, Perrot JL, Labeille B *et al.* Tinea corporis diagnosed by reflectance confocal microscopy. *Ann Dermatol Venereol* 2014; **141**: 150 152.
26 Pharaon M, Gari-Toussaint M, Khemis A *et al.* Diagnosis and treatment monitoring of toenail onychomycosis by reflectance confocal microscopy: prospective cohort study in 58 patients. *J Am Acad Dermatol* 2014; **71**: 56 61.
27 Piérard GE, Arrese JE, Pierre S *et al.* Microscopic diagnosis of onychomycoses. *Ann Dermatol Venereol* 1994; **121**: 25 29.
28 Hongcharu W, Dwyer P, Gonzalez S, Anderson RR. Confirmation of onychomycosis by *in vivo* confocal microscopy. *J Am Acad Dermatol* 2000; **42**: 214 216.
29 Markus R, Huzaira M, Anderson RR, González S. A better potassium hydroxide preparation? *In vivo* diagnosis of tinea with confocal microscopy. *Arch Dermatol* 2001; **137**: 1076 1078.
30 Rothmund G, Sattler EC, Kaestle R *et al.* Confocal laser scanning microscopy as a new valuable tool in the diagnosis of onychomycosis - comparison of six diagnostic methods. *Mycoses* 2013; **56**: 47 55.
31 Liansheng Z, Xin J, Cheng Q, Zhiping W, Yanqun L. Diagnostic applicability of confocal laser scanning microscopy in tinea corporis. *Int J Dermatol* 2013; **52**: 1281 1282.
32 Hui D, Xue-cheng S, Ai-e X. Evaluation of reflectance confocal microscopy in dermatophytosis. *Mycoses* 2013; **56**: 130 133.
33 Arrese J-E, Quatresooz P, Piérard-Franchimont C, Piérard G-E. Nail histomycology. Protean aspects of a human fungal bed. *Ann Dermatol Venereol* 2003; **130**: 1254 1259.
34 Goldgeier M, Alessi C, Muhlbauer JE. Immediate noninvasive diagnosis of herpesvirus by confocal scanning laser microscopy. *J Am Acad Dermatol* 2002; **46**: 783 785.
35 Abraham LS, Costa MC, Agozzino M, Amorosi B, Cota C, Ardigo M. *In vivo* reflectance confocal microscopy for varicella prompt diagnosis and treatment in a severely immunosuppressed patient. *Skin Res Technol* 2012; **18**: 386 388.
36 Scope A, Benvenuto-Andrade C, Gill M, Ardigo M, Gonzalez S, Marghoob AA. Reflectance confocal microscopy of molluscum contagiosum. *Arch Dermatol* 2008; **144**: 34.
37 Almodovar JL, Schifitto G, McDermott MP, Ferguson M, Herrmann DN. HIV neuropathy: an *in vivo* confocal microscopic study. *J Neurovirol.* 2012; **18**: 503 510.

4- Imagerie non invasive des phanères

Il s'agit d'un sous chapitre beaucoup plus court que les autres avec seulement 1 article de synthèse**.** Toutefois les phanères ont été sources de travaux rapportés dans le sous chapitre précédent consacré aux infection cutanéomuqueuses avec la description de la teigne de la barbe et des cheveux ainsi que de différents type d'infections fungique de l'appareil unguéal. Par ailleurs nos travaux préliminaires non encore publiés sur l'étude de l'appareil unguéal en échographie ultra haute définition nous laissent espérer un champ d'investigation très large pour un avenir proche

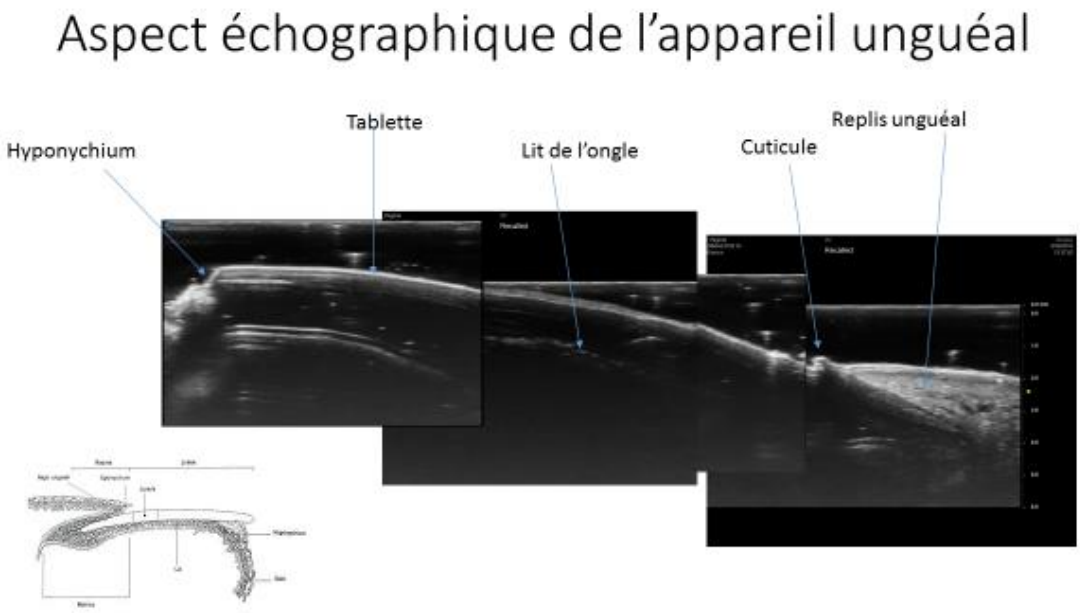

Confocal microscopy for healthy and pathological nail.

Nail diseases are often annoying for the patient and diagnostically challenging for dermatologists. New imaging techniques are of high interest in the diagnosis of nail disorders to reduce the number of nail biopsies. Confocal microscopy is a high-resolution emerging imaging technique that can be used to explore the entire body surface, includ- ing skin, mucosa, hair and nails. A systematic review of the literature concerning the use of confocal microscopy for the study of either healthy or pathological nail has been performed to evaluate the current use of this technique and possible future applications. Confocal microscopy is particularly suitable for nails because it allows a non-invasive *in vivo* exami- nation of this sensitive body area, and nail plate transparency permits to image up to the nail bed with an easy identifica- tion of corneocytes. Confocal microscopy can play a role in the diagnosis of onychomycosis and melanonichia, and in the study of drug penetration through the nail plate. It could be used in the future as a non-invasive procedure for the investigation of different nail diseases, such as psoriasis and lichen planus. Further application could be the intra-opera- tive *ex vivo* examination of nail specimens to outline tumour margins to assist surgery.

DOI: 10.1111/jdv.12330 JEADV

REVIEW ARTICLE

Confocal microscopy for healthy and pathological nail

E. Cinotti,[1,*] B. Fouilloux,[1] J. L. Perrot,[1] B. Labeille,[1] C. Douchet,[2] F. Cambazard[1]

[1]Dermatology Department and [2]Pathology Department, University Hospital of Saint-Etienne, Saint-Etienne, France
*Correspondence: E. Cinotti. E-mail: elisacinotti@gmail.com

Abstract Nail diseases are often annoying for the patient and diagnostically challenging for dermatologists. New imaging techniques are of high interest in the diagnosis of nail disorders to reduce the number of nail biopsies. Confocal microscopy is a high-resolution emerging imaging technique that can be used to explore the entire body surface, including skin, mucosa, hair and nails. A systematic review of the literature concerning the use of confocal microscopy for the study of either healthy or pathological nail has been performed to evaluate the current use of this technique and possible future applications. Confocal microscopy is particularly suitable for nails because it allows a non-invasive *in vivo* examination of this sensitive body area, and nail plate transparency permits to image up to the nail bed with an easy identification of corneocytes. Confocal microscopy can play a role in the diagnosis of onychomycosis and melanonichia, and in the study of drug penetration through the nail plate. It could be used in the future as a non-invasive procedure for the investigation of different nail diseases, such as psoriasis and lichen planus. Further application could be the intra-operative *ex vivo* examination of nail specimens to outline tumour margins to assist surgery.
Received: 22 August 2013; Accepted: 6 November 2013

Conflicts of interest
None declared.

Funding sources
None declared.

Introduction
Confocal laser-scanning microscopy (CLSM) is an emerging technique which optically sections living tissue at various depths, to image horizontal layers of the skin[1] with resolution at a cellular level and without alteration of the tissue surface. Four devices dedicated to the skin are available, two work *in vivo* (VivaScope® 1500 and 3000, CALIBER, New York, USA, distributed in Europe by the company MAVIG GmbH, Munich, Germany) and two *ex vivo* (VivaScope® 2000 and 2500, CALIBER, distributed in Europe by the company MAVIG GmbH). The use of CLSM in the field of dermatology, was first reported 20 years ago.[2,3] Recently, it has also been applied to the examination of skin appendages, like hairs[4] and nails.[5]

Confocal laser-scanning microscopy is particularly interesting for the diagnosis of nail disorders because the *in vivo* examination could allow to reduce the number of biopsies in this sensitive body site and the *ex vivo* device could assist surgery intra-operatively. Moreover, nail plate transparency allows deep penetration of CLSM that can image up to the nail bed.

Here, we summarize the literature on the use of confocal microscopy for the study of healthy and pathological nail.[5–14] The review was performed utilizing PubMed database. Search terms employed were 'nail', 'reflectance confocal microscopy', 'confocal microscopy' and 'onychomycosis'.

Confocal microscopy and normal nails
Kaufman *et al.*[5] were the first ones to use confocal microscope to study the ultrastructure of the nail and showed that the unique properties of confocal microscope make possible to explore the capillary nailfold and the nails up to the deeper layers of the nail plate. Sattler *et al.*[11] have recently investigated healthy nail plates with CLSM, obtaining resolution images better than those taken by Kaufman *et al.* using the mercury lamp confocal microscope. The depth to which the CLSM can penetrate optically corresponds to 200 300 μm for skin tissue, but is 400 500 μm[11] for the nails that are more transparent, probably due to fewer cell organelles absorbing the light and the lower refractive index of the nail unit.[11] CLSM is able to display single corneocytes and the integrity of their borders.

The nail plate can be scanned from the surface to the lower part adjacent to the underlying nail bed. Three different layers can be differentiated by CLSM according to the intensity of the reflection (Fig. 1). The superficial layer shows a brighter reflection, followed by a zone with slightly poorer signal, followed again by a brighter zone in the deepest part. The transition to

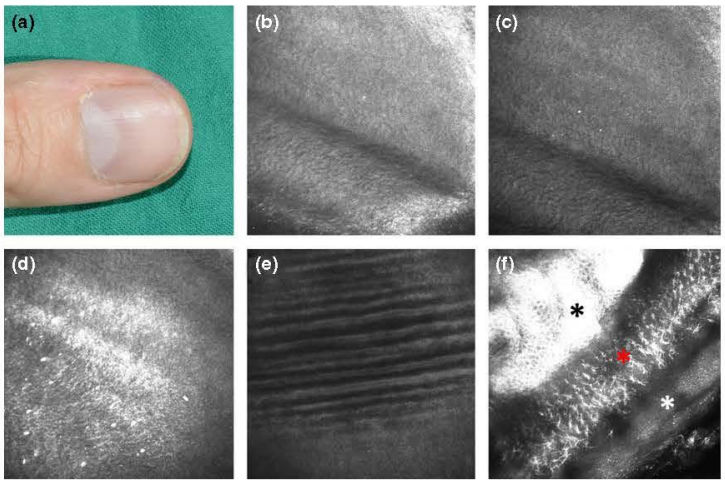

Figure 1 Clinical (a) and *in vivo* confocal laser-scanning microscopy (CLSM) aspect of a thumbnail plate (b, c, d, e, f). Three zones of different brightness can be differentiated going deeper into the nail plate: a bright surface (b), a dark central part (c) and a bright deepest part (d). The transition to the underlying nail bed is visible as wave-like structures, which are directed towards the fingertip. The transition between the proximal part of the nail plate and the skin (f) is characterized by stellate figures corresponding to epidermal keratinocytes sectioned obliquely (red asterisk) that continue into the normal honeycomb pattern of the epidermis (black asterisk) and by a grey stripe corresponding to the cuticle (white asterisk).

the underlying nail bed is visible only in thin nails (<500 μm) and displayed in wave-like structures, which are directed towards the fingertip (Fig. 1). The transition between the skin and the proximal part of the nail plate is characterized by a stripe corresponding to the cuticle, and by stellate figures corresponding to the membranes of keratinocytes sectioned obliquely on the skin side (Fig. 1).

Confocal microscopy and onychomycosis

In suspicion of an onycomycosis, before starting a therapy, the identification of the fungi from the affected nails is necessary because the treatment usually lasts several months, requiring systemic antifungal agents that may cause serious adverse effects. The methods currently used to confirm the clinical diagnoses of onychomycosis are direct microscopic examination and culture of nail clippings. These procedures are invasive, and often either yield negative results (e.g. microscopic examination) or are slow in giving a result (e.g. dermatophyte cultures). Moreover, accurate diagnosis depends on the expertise of laboratory staff and on the quality of the nail sample.[10]

Already in 1994, Piérard *et al.*[6] used *in vivo* confocal microscopy for onychomycosis. In 2000, Hongcharu *et al.*[8] first showed that *in vivo* CLSM could be faster than the conventional routine *ex vivo* potassium hydroxide (KOH) preparations in the diagnosis of onychomycosis and reported the *in vivo* CLSM diagnosis of toenail onychomycosis in a young man. The performance of this technique has been recently evaluated by Rothmund *et al.*[12] in a prospective trial on 50 patients, where CLSM was compared to the gold standard techniques (culture, Periodic acid-Schiff staining and Polymerase Chain Reaction) as tool in toe onychomycosis and showed a better sensitivity (79% vs. 74%) and specificity (81% vs. 76%) than KOH preparation. This study included different types of onychomycosis: distolateral subungual onychomycosis, total dystrophic onychomycosis, white onychomycosis and proximal sub-ungual onychomycosis.[12]

Dermatophytes can be easily observed in nail plate as network of lengthy structures with high reflection and the typical shape of hyphae (Fig. 2). CLSM aspect of yeasts has been reported only by Arrese *et al.*,[7] while moulds have not been described yet in nails, but are well characterized in other tissues under CLSM.[15]

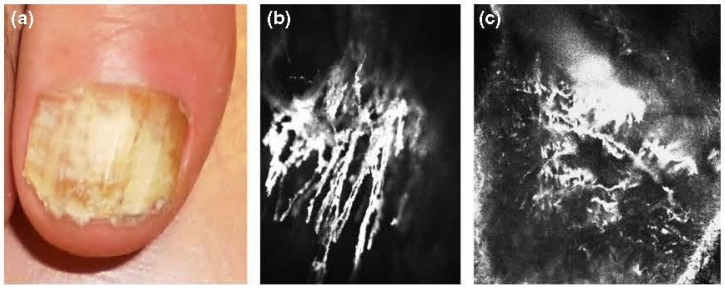

Figure 2 Clinical (a), *in vivo* (b) and *ex vivo* (c) CLSM aspect of an onychomycosis. CLSM shows characteristic highly reflective thick linear structures corresponding to hyphae.

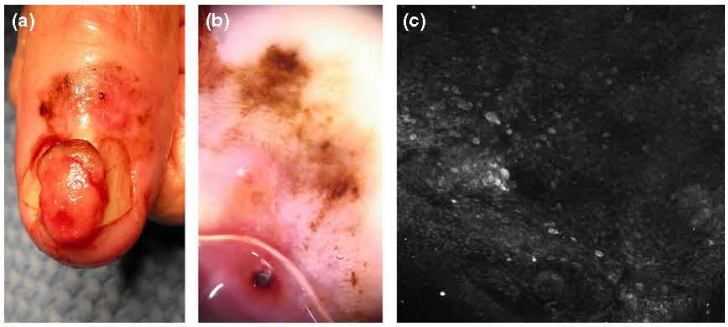

Figure 3 Clinical (a), dermoscopical (b) and *in vivo* CLSM (c) aspect of Hutchinson's sign in a sub-ungueal melanoma. *In vivo* CLSM shows hyperreflective roundish big cells corresponding to tumoral melanocytes.

For tinea corporis, the potassium hydroxide application is suggested before the CLSM[16] examination, but in onychomycosis hyphae can be observed directly without preparation. In addition, *in vivo* CLSM is not limited to the area of the nail clippings, but can explore the entire nail surface, being also able to demonstrate the location and density of the fungi.

Feuilhade de Chauvin *et al.*[10] stated that CLSM is powerful and rapid for the diagnosis of onychomycosis but it is complicated to use, making it unsuitable for routine use. However, we think that apart from the cost, this technique is simpler than routine procedure because it can be performed *in vivo* without taking a nail clipping. Moreover, the acquisition of images is fast, it takes just few minutes, especially if the handheld camera (VivaScope® 3000) is used, applied to the surface of the nail without being fixed to the tissue. Thus, the identification of hyphae is easy due to their particular shape and high reflectance.

In conclusion, *in vivo* CLSM is a new tool for the diagnosis of onychomycosis, non-invasive, fast and easy to perform, that allows to identify the fungi without any sampling or peculiar preparation of the nails.

Confocal microscopy and melanonychia

Although dermoscopy adds some elements[17] to help the distinction between benign and malignant causes of nail pigmentation, the clinical diagnosis of sub-ungueal melanoma is often clinically challenging. CLSM has been shown to be useful in discriminating benign vs. malignant melanocytic lesions of the skin, and can image melanocytes of the Hutchinson's sign (Fig. 3), but cannot penetrate in the nail matrix *in vivo*, to allow a diagnosis of sub-ungueal melanoma in case of melanonychia.

Management of melanonychia recommends a nail matrix biopsy in suspicious cases and, in case of histological confirmation of melanoma, a surgical treatment should be subsequently performed. A technique to confirm a diagnosis of sub-ungual melanoma intra-operatively could therefore be helpful to avoid this two steps procedure.

At the moment, there is no accurate way to confirm a diagnosis of sub-ungueal melanoma intra-operatively. Histopathological examination of the nail matrix is not possible extemporaneously because the size of the specimen is quite small and the diagnosis usually requires immunostaining. However, recent studies showed that the eponychium could be reclined during the nail biopsy procedure to better visualize the nail matrix pigmentation and to perform intra-operative dermoscopy[18] and CLSM.[19]

Hirata *et al.*[18] described four intra-operative dermoscopic patterns of the nail matrix pigmentation which had better

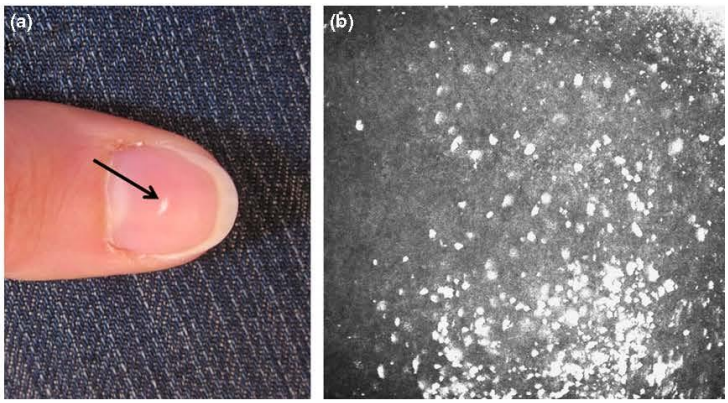

Figure 4 Clinical (a) and *in vivo* CLSM (b) aspect of leukonychia. *In vivo* CLSM shows detachment of single hyperreflective corneocytes.

sensitivities and specificities for the aetiological diagnosis of longitudinal melanonychias than patterns observed by nail plate dermoscopy. However, some difficulties persist. For example, the so-called 'regular brown lines pattern', which was usually associated with a naevus, was also observed in two cases of early melanoma, illustrating the diagnostic difficulties between benign melanocytic hyperplasia and early melanoma.

Debarbieux *et al.*[19] evaluated the feasibility of intra-operative imaging of the nail matrix by both *in vivo* and *ex vivo* CLSM. In nine patients presented with clinical and dermoscopical suspicion of sub-ungueal melanoma, CLSM was performed *in vivo* on the pigmented area of the matrix, after it had been exposed by reclination of the nail plate, and/or *ex vivo* on the fresh tissue biopsy. CLSM revealed sufficiently atypical cytological and architectural features to accurately suggest the correct final diagnosis of melanoma in seven cases. A good correlation between intra-operatively CLSM and histopathology was found: melanoma was diagnosed in seven of eight cases proven to be melanomas by histological examination and lentigo was diagnosed in one case confirmed by histological examination. The authors suggest that CLSM is a promising tool for the intra-operative diagnosis of melanonychia because it combines the advantages of dermoscopy (non-invasive examination of the whole pathological area without alteration of the tissue surface) and histopathology (resolution at a cellular level). *Ex vivo* examination can be used either alone or as a complementary technique if the data provided by *in vivo* intra-operative examination are not diagnostic. Moreover, the same group[20] also demonstrated that perioperative CSLM can differentiate pigmented squamous cell carcinoma presenting as melanonychia striata from melanoma.

A great advantage of CSLM, compared to dermoscopy for the diagnosis of skin melanoma, is that CSLM also recognizes amelanotic melanocytes, but this aspect has not been studied yet for sub-ungueal melanoma. In addition, although *in vivo* CLSM is not able to image melanocytes of the nail bed, in the future it might be a useful tool to exclude the diagnosis of melanonychia not caused by a melanocytic proliferation but due to an alteration of the nail plate, e.g.related to onychomycosis or iterative friction.

Confocal microscopy and leukonychia

Sattler *et al.*[11] showed the CLSM aspect of leukonychia, where in contrast to the regularity of a normal nail, a detachment of single hyperreflective corneocytes could be seen (Fig. 4). Further study should be performed to investigate CLSM features of leukonychia in different conditions, such as trauma, lichen planus, onychomycosis and drug intake, to evaluate if there are differences either in the aspect or amount or depth of diskeratotic corneocytes to better understand the pathophysiologic mechanisms that cause nail white discoloration.

Confocal microscopy and inflammatory disorders of the nail

There are no studies about the CLSM diagnosis of the inflammatory disorders of the nail. In our experience on few cases of nail psoriasis, we could observe a delamination of the nail plate, better visible on the lateral margins and large hyperreflective irregular areas on the surface and inside the nail plate, likely corresponding to areas of keratin densification (Fig. 5). However, in case of nail psoriasis and lichen planus, we can expect to find the same nail plate changes that have already been described under the histological examination such as neutrophilic infiltration, serum crusts and parakeratosis for psoriasis and orthokeratosis with focal parakeratosis and serum crusts for lichen

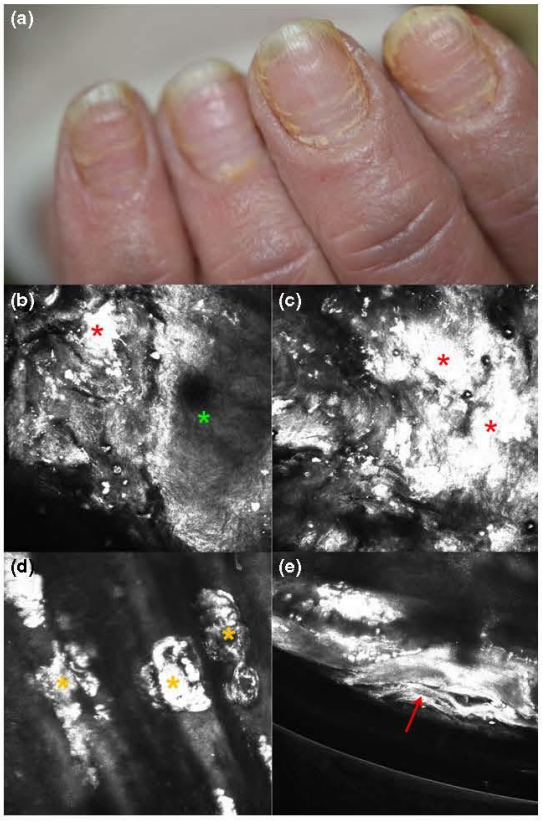

Figure 5 Clinical (a) and *in vivo* CLSM (b–e) aspect of nail psoriasis. *In vivo* CLSM shows large hyperreflective irregular areas on the surface of the nail plate (red asterisk) (b, c) and inside the nail plate (yellow asterisk) (d), likely corresponding to areas of keratin densification. Normal nail plate is also visible (green asterisk). Delamination of the nail plate can be seen on the lateral margins of the nail plate (red arrow) (e).

planus.[21,22] In the skin, leucocytes are well visible under CLSM as hyperreflective homogeneous roundish cells and parakeratosis can also be identified by CLSM,[23] and we can speculate that these aspects could also be recognizable in the nail. In addition, in the presence of a thin nail plate with an underlying nail bed visible at CLSM, we could expect to see an inflammatory infiltration at the dermal epidermal junction in case of lichen planus of the nail, similarly of what can be found in the skin.[24]

Confocal microscopy and nail research applications

Confocal laser-scanning microscopy has also been applied in the research. Dutet *et al.*[13] studied ungual penetration of sodium fluorescein and nile blue chloride by *ex vivo* fluorescence CLSM and found that fluorescent markers penetrated 7 12% of the nail thickness and iontophoresis (the application of low-intensity electrical currents) increased penetration of both markers compared to passive diffusion. Therefore, CLSM can be used to evaluate drug delivery of topical nail therapies, e.g. for onychomycosis and nail psoriasis, where nail penetration is the major limitation.

Confocal laser-scanning microscopy has also been used to measure nail plate thickness before a manicure gel application and after its removal to prove that the removal of the gel induced a nail thinning.[7] However, we think that CLSM is not a suitable technique for measuring the nail thickness because in thick nails the transition between the nail plate and bed is blurred, and it is not possible to clearly determine its exact depth.

Ex vivo confocal microscopy and nails

There are no reports about the use of *ex vivo* confocal devices dedicated to the skin to study the nails. Debarbieux *et al.*[19] used the *in vivo* device for the *ex vivo* examination of the nail biopsies of sub-ungueal melanoma. However, this procedure has the limitation that the specimen is not fixed, tends to move, and is difficult to be oriented, differently from the *ex vivo* device.

In our experience, images of healthy nail obtained with the *ex vivo* CLSM device are similar to *in vivo* CLSM, with the advantage of gathering more information at greater depth as specimens can be observed also from the lower side. Dermatophytes are also visible and show similar characteristics of *in vivo* CLSM (Fig. 2). Tumoral cell proliferations, like glomic tumour and squamous cell carcinoma[20] can be recognized (Fig. 6) and in the feature *ex vivo* CLSM could be a promising technique to help control tumours margins intra-operatively.

Limitations of confocal microscopy for nail imaging

The cost of CLSM is a limit for a wide use of this technology. Then, there is the limited penetration depth of about 400 500 μm,[11] that although better than in the skin does not allow to clearly image *in vivo* the nail bed and reach the nail matrix.

The convex surface of the nail and the concavity of the transition between the nail plate and the surrounding skin make difficult to place and hold the device during *in vivo* imaging. To overcome this technical problem, the handheld CLSM device (VivaScope® 3000) with ultrasound gel used as interface, is more suitable because no extra window is needed and the ultrasound gel allows adapting the tip of the device to the irregular surface to be observed.

Conclusions

In conclusion, due to its natural transparency, nail plate is particularly suitable for the CLSM examination. Nails can be imaged at a cellular level resolution without fixing or staining, *in vivo* or *ex vivo*.

Confocal laser-scanning microscopy is a promising technique for the diagnosis onychomycosis, being faster and more accurate than the conventional microscope used in KOH preparations. At the moment mainly dermathophytes have been observed in nails under CLSM; in the future it should be evaluated if dermathophytes can be distinguished from yeasts and moulds. CSLM can

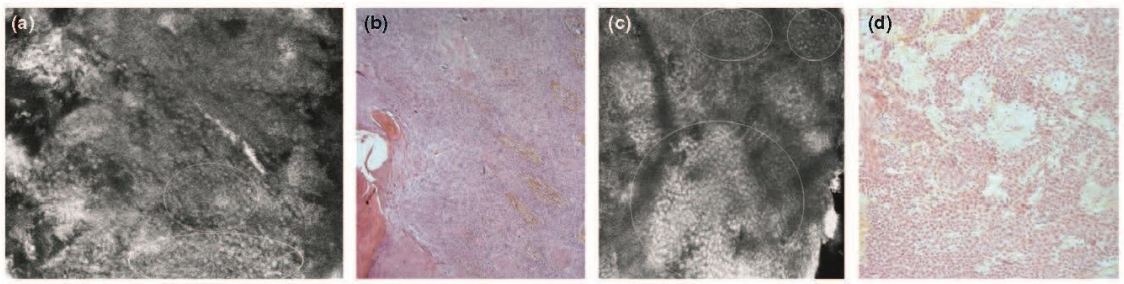

Figure 6 *Ex vivo* CLSM (a) and histological (b) aspect of a nail bed squamous cell carcinoma and *ex vivo* CLSM (c) and histological (d) aspect of a nail bed glomic tumour. Tumoral cells are visible as a homogeneous compact proliferation of refractive medium size roundish cells (white circles).

also play a role in the intra-operative diagnosis of sub-ungueal melanoma, and in the research field fluorescence CLSM can study the drug penetration through the nail plate.

In the future, *in vivo* CLSM could be used as a non-invasive procedure for the study of different nail diseases, such as psoriasis and lichen planus to better understand the anatomical alteration and their pathogenesis. Further application of CLSM could be the *ex vivo* evaluation of non-pigmented nail lesions to distinguish inflammatory diseases from tumours and identify tumour surgical margins.

References

1 Nwaneshiudu A, Kuschal C, Sakamoto FH *et al.* Introduction to confocal microscopy. *J Invest Dermatol* 2012; **132**: e3.

2 Piérard GE. In vivo confocal microscopy: a new paradigm in dermatology. *Dermatology* 1993; **186**: 4 5.

3 Corcuff P, Bertrand C, Leveque JL. Morphometry of human epidermis in vivo by real-time confocal microscopy. *Arch Dermatol Res* 1993; **285**: 475 481.

4 Rudnicka L, Olszewska M, Rakowska A. In vivo reflectance confocal microscopy: usefulness for diagnosing hair diseases. *J Dermatol Case Rep* 2008; **2**: 55 59.

5 Kaufman SC, Beuerman RW, Greer DL. Confocal microscopy: a new tool for the study of the nail unit. *J Am Acad Dermatol* 1995; **32**: 668 670.

6 Piérard GE, Arrese JE, Pierre S *et al.* Microscopic diagnosis of onychomycoses. *Ann Dermatol Venereol* 1994; **121**: 25 29.

7 Chen AF, Chimento SM, Hu S, *et al.* Nail damage from gel polish manicure. *J Cosmet Dermatol* 2012; 11: 27 29.

8 Hongcharu W, Dwyer P, Gonzalez S, Anderson RR. Confirmation of onychomycosis by in vivo confocal microscopy. *J Am Acad Dermatol* 2000; **42**: 214 216.

9 Arrese J-E, Quatresooz P, Piérard-Franchimont C, Piérard GE. Nail histomycology. Protean aspects of a human fungal bed. *Ann Dermatol Venereol* 2003; **130**: 1254 1259.

10 Feuilhade de Chauvin. M. New diagnostic techniques. *J Eur Acad Dermatol Venereol* 2005; **19**: 20 24.

11 Sattler E, Kaestle R, Rothmund G, Welzel J. Confocal laser scanning microscopy, optical coherence tomography and transonychial water loss for in vivo investigation of nails. *Br J Dermatol* 2012; **166**: 740 746.

12 Rothmund G, Sattler EC, Kaestle R *et al.* Confocal laser scanning microscopy as a new valuable tool in the diagnosis of onychomycosis - comparison of six diagnostic methods. *Mycoses* 2013; **56**: 47 55.

13 Dutet J, Delgado-Charro MB. Assessment of iontophoretic and passive ungual penetration by laser scanning confocal microscopy. *Pharm Res* 2012; **29**: 3464 3474.

14 Gupta AK, Ryder JE, Summerbell RC. Onychomycosis: classification and diagnosis. *J Drugs Dermatol* 2004; **3**: 51 56.

15 Brasnu E, Bourcier T, Dupas B *et al.* In vivo confocal microscopy in fungal keratitis. *Br J Ophthalmol* 2007; **91**: 588 591.

16 Markus R, Huzaira M, Anderson RR, González S. A better potassium hydroxide preparation? In vivo diagnosis of tinea with confocal microscopy. *Arch Dermatol* 2001; **137**: 1076 1078.

17 Blum A, Simionescu O, Argenziano G *et al.* Dermoscopy of pigmented lesions of the mucosa and the mucocutaneous junction: results of a multicenter study by the International Dermoscopy Society (IDS). *Arch Dermatol* 2011; **147**: 1181 1187.

18 Hirata SH, Yamada S, Enokihara MY *et al.* Patterns of nail matrix and bed of longitudinal melanonychia by intraoperative dermatoscopy. *J Am Acad Dermatol* 2011; **65**: 297 303.

19 Debarbieux S, Hospod V, Depaepe L *et al.* Perioperative confocal microscopy of the nail matrix in the management of in situ or minimally invasive subungual melanomas. *Br J Dermatol* 2012; **167**: 828 836.

20 Fernandes Massa A, Debarbieux S, Depaepe L *et al.* Pigmented squamous cell carcinoma of the nail bed presenting as a melanonychia striata: diagnosis by perioperative reflectance confocal microscopy. *Br J Dermatol.* 2013; **169**: 198 199.

21 Grover C, Reddy BSN, Uma Chaturvedi K. Diagnosis of nail psoriasis: importance of biopsy and histopathology. *Br J Dermatol* 2005; **153**: 1153 1158.

22 Grover C, Chaturvedi UK, Reddy BSN. Role of nail biopsy as a diagnostic tool. *Indian J Dermatol Venereol Leprol* 2012; **78**: 290 298.

23 Moscarella E, Longo C, Zalaudek I, Argenziano G, Piana S, Lallas A. Dermoscopy and confocal microscopy clues in the diagnosis of psoriasis and porokeratosis. *J Am Acad Dermatol* 2013; **69**: e231 e233.

24 Moscarella E, González S, Agozzino M, Sánchez-Mateos JLS, Panetta C, Contaldo M *et al.* Pilot study on reflectance confocal microscopy imaging of lichen planus: a real-time, non-invasive aid for clinical diagnosis. *J Eur Acad Dermatol Venereol* 2012; **26**: 1258 1265.

5- imagerie non invasive cutanéomuqueuse et de l'appareil oculaire
5.a imagerie non invasive de l'appareil oculaire

Il s'agit de la partie la plus originale de notre activité d'imagerie non invasive. Nous avons, en effet, d'une part utilisé une caméra de MCIV dans un usage qui n'avait pas été celui évoqué initialement par ses concepteurs, et d'autre part, nous avons établi une étroite collaboration entre deux disciplines sans liens particuliers jusque-là, et de plus, mis en place ce que l'on peut considérer, comme une intime collaboration entre ces 2 équipes avec partage de matériel et de compétences humaines dans un but de recherche et de pratique clinique. En effet, nous avons utilisé la caméra Vivascope 3000 pour réaliser l'exploration de l'appareil oculaire antérieur. Cette caméra (dotée d'un laser de classe 1 dans le proche infra-rouge) nous permet de réaliser une exploration qu'aucun autre dispositif de MICV dédié à l'ophtalmologie ne peut faire. Il faut signaler que les 2 systèmes de MICV dédiés à l'imagerie microscopique non invasive ophtalmologique sont conçus pour l'examen de la cornée. Ainsi seule une petite partie de l'appareil oculaire peut être étudié. Or nous avons pu explorer la cornée, la conjonctive bulbaire et toute la paupière : son versant cutané, muqueux et son bord libre.Or Jamais une caméra de MICV dédiée à l'ophtalmologie n'avait pu réaliser tous ces examens. Les communications et les publications ont été nombreuses. Un protocole CCPPRB « InnovEYE » à l'instigation du Pr G Thuret, 4 thèses de médecine et un Master 2 ont par ailleurs été consécutifs de ces travaux.

De ce travail de recherche a découlé :
- la mise en place d'une consultation multidisciplinaire de microscopie confocale dermato-ophtalmologique unique en son genre, ayant donné lieu à plus de 600 examens avec des patients adressés de bien au-delà de la région Rhône-Alpes.
- la mise en place d'une consultation multidisciplinaire de microscopie confocale Allergo-dermato-ophtalmologique elle aussi unique en son genre.
- 1 interne d'ophtalmologie par semestre effectue (depuis mai 2016) 3 demi-journée de travail en dermatologie dans le cadre de l'activité de la microscopie confocale, sous ma responsabilité. Des articles sous forme de fiches iconographiques pour les annales de dermatologie vénéréologie sont publiés lors de chacun des semestres en plus de travaux plus ambitieux.
- 1 autre interne d'ophtalmologie par semestre effectue (depuis novembre 2017) 2 demi-journée de travail en dermatologie dans le cadre de l'activité de la microscopie confocale-allergologique toujours sous ma responsabilité

Les projets en cours de réalisation restent multiples :
- Une étude sur l'utilité de la dermatoscopie de contact pour l'exploration des tumeurs conjonctivales et du bord libre des paupières
- Une étude sur la faisabilité de l'exploration en fluorescence au moyen de la caméra Vivascope 1500 des structures oculaires après injection IV de fluorescéine
- Un travail avec le Dr Ch. Schwab ophtalmologiste de l'Université de Graz,qui est venu se former durant 1 semaine dans le service à la MICV de l'appareil oculaire antérieur.

- De multiples projets sont en gestation concernant l'exploration échographique en ultra haute définition de l'appareil oculaire antérieur, qui pourront être initiés lors de l'acquisition de l'échographe en cours d'achat., ainsi une étude sur l'exploration de la paupière et des tumeurs associées

Ci-dessous une de nos premières images de paupière en échographie HD issue du cours d'initiation que je vais réaliser pour les futurs internes en poste dans le module échographie de l'appareil oculaire antérieur

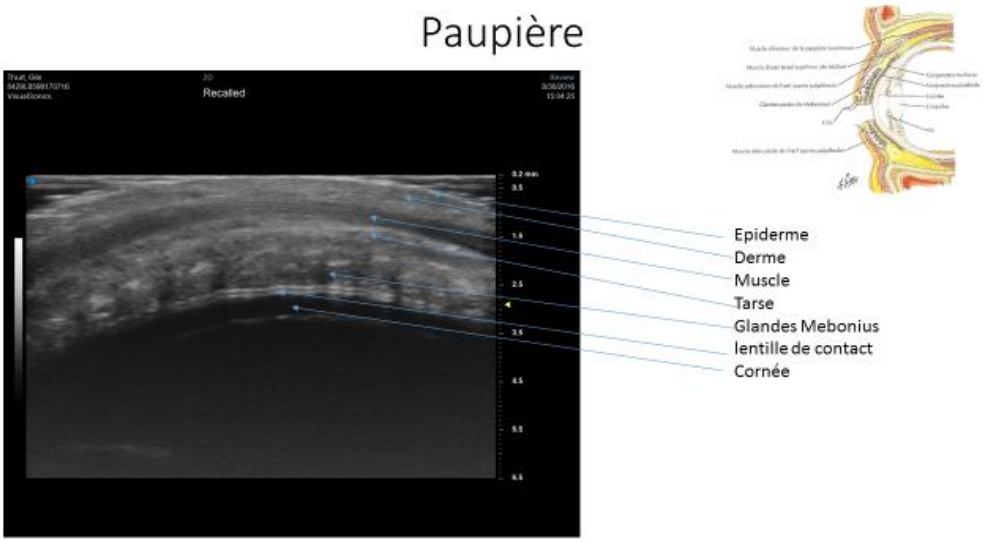

Mais aussi sur l'exploration des tumeurs de la sclère et plus particulièrement les nævus, mélanomes et carcinomes épidermoïdes ainsi que les mélanomes de la choroïde.

Ci-dessous une de nos premières images de l'angle irido-cornéen en échographie HD issue du cours d'initiation que je vais réaliser pour les futurs internes en poste dans le module échographie de l'appareil oculaire antérieur

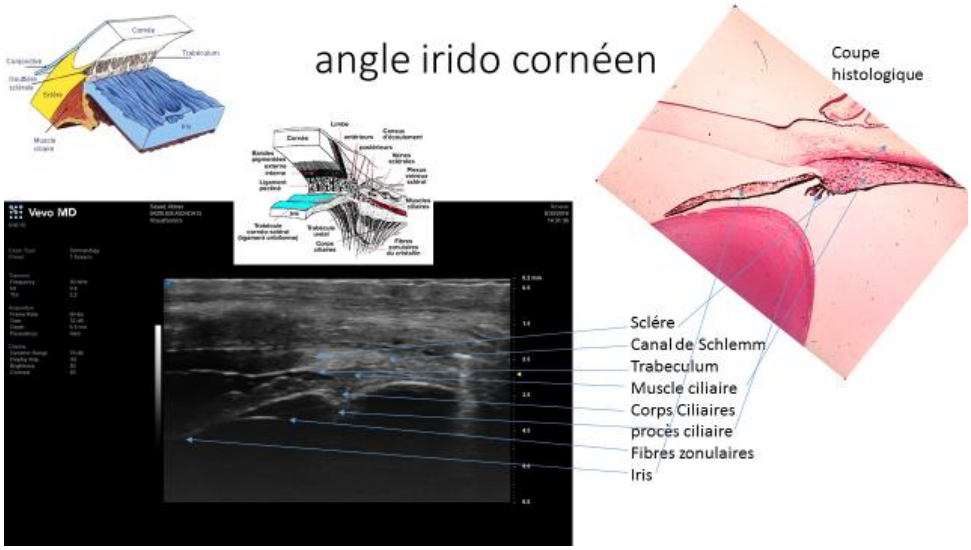

5.a 1 The role of in vivo confocal microscopy in the diagnosis of eyelid margin tumors: 47 cases

Background :
Handheld in vivo reflectance confocal microscopy (IVCM) is a new imaging method that allows noninvasive diagnosis of cutaneous tumors but to date it has not been used in the study of eyelid tumors.

Objective:
We sought to evaluate the suitability of IVCM for eyelid margin tumors.

Methods:
We prospectively evaluated the IVCM features of 47 eyelid margin lesions, clinically suspicious of malignancy; 35 of these were excised whereas the other 12, with no IVCM malignant features, were followed up for at least 1 year. Clinical, IVCM, and histologic diagnoses were compared.

Results:
IVCM showed sensitivity and specificity of 100% and 69.2%, respectively, for malignancy (basal cell carcinoma, squamous cell carcinoma, and melanoma). The follow-up of the 12 nonexcised lesions did not show any clinical p r o g r e s s i o n .

Limitations:
The lesions showing neither clinical nor IVCM features for malignancies were not biopsied in view of the potential functional and aesthetic consequences of eyelid margin surgery.

Conclusion:
Used with a handheld dermatology-specific microscope, IVCM can play a role in the noninvasive diagnosis of eyelid margin lesions. Further studies are needed to better define diagnostic criteria of eyelid tumors and improve the specificity of this technique.

ORIGINAL ARTICLE

The role of in vivo confocal microscopy in the diagnosis of eyelid margin tumors: 47 cases

Elisa Cinotti, MD,[a] Jean Luc Perrot, MD,[a] Nelly Campolmi, MD,[b,d] Bruno Labeille, MD,[a] Marine Espinasse, MD,[b,d] Damien Grivet, MD,[b,d] Gilles Thuret, PhD,[b,d,e] Philippe Gain, MD, PhD,[b,d] Catherine Douchet, MD,[c] Fabien Forest, MD,[c] Maher Haouas, MD,[b] and Frédéric Cambazard, PhD[a]
Saint-Etienne and Paris, France

Background: Handheld in vivo reflectance confocal microscopy (IVCM) is a new imaging method that allows noninvasive diagnosis of cutaneous tumors but to date it has not been used in the study of eyelid tumors.

Objective: We sought to evaluate the suitability of IVCM for eyelid margin tumors.

Methods: We prospectively evaluated the IVCM features of 47 eyelid margin lesions, clinically suspicious of malignancy; 35 of these were excised whereas the other 12, with no IVCM malignant features, were followed up for at least 1 year. Clinical, IVCM, and histologic diagnoses were compared.

Results: IVCM showed sensitivity and specificity of 100% and 69.2%, respectively, for malignancy (basal cell carcinoma, squamous cell carcinoma, and melanoma). The follow-up of the 12 nonexcised lesions did not show any clinical progression.

Limitations: The lesions showing neither clinical nor IVCM features for malignancies were not biopsied in view of the potential functional and aesthetic consequences of eyelid margin surgery.

Conclusion: Used with a handheld dermatology-specific microscope, IVCM can play a role in the noninvasive diagnosis of eyelid margin lesions. Further studies are needed to better define diagnostic criteria of eyelid tumors and improve the specificity of this technique. (J Am Acad Dermatol http://dx.doi.org/10.1016/j.jaad.2014.05.060.)

Key words: basal cell carcinoma; eyelid; eyelid margin; in vivo; melanoma; mucosa; reflectance confocal microscopy; tumor.

The clinical diagnosis of eyelid margin tumors is often challenging and surgical excision in this area may have both functional and aesthetic consequences, along with being technically complex for surgeons. New imaging techniques are of high interest in the diagnosis of eyelid margin tumors to minimize the number of unnecessary surgical excisions. We investigated whether in vivo reflectance confocal microscopy (IVCM), an emerging, noninvasive, and high-resolution imaging technique, used for cutaneous and conjunctival cancers, may help physicians detect eyelid margin tumors. To our knowledge, we present the largest series of eyelid margin tumors described from a clinical standpoint

Abbreviations used:

BCC: basal cell carcinoma
IVCM: in vivo reflectance confocal microscopy
SCC: squamous cell carcinoma

From the Departments of Dermatology,[a] Ophthalmology,[b] and Pathology,[c] University Hospital of St-Etienne; Laboratory Biology, Engineering and Imaging of Corneal Graft, Jean Monnet University, Saint-Etienne[d]; and French University Institute, Paris.[e]

Funding sources: None.
Conflicts of interest: None declared.
Accepted for publication May 27, 2014.

Reprints not available from the authors.
Correspondence to: Elisa Cinotti, MD, Department of Dermatology, University Hospital of St-Etienne, 42055 Saint Etienne Cedex 2, France. E-mail: elisacinotti@gmail.com.

Published online July 3, 2014.
0190-9622/$36.00

http://dx.doi.org/10.1016/j.jaad.2014.05.060

and the first investigated by IVCM with a histopathologic correlation.

METHODS

A total of 45 consecutive patients (19 female, 36 male; average age 64 years, range 13-94 years) presenting with a total of 47 eyelid margin tumor lesions were recruited at the Department of Dermatology, University Hospital of Saint-Étienne, France, between January 2011 and June 2013. Clinical and IVCM diagnoses were established by a team of 3 dermatologists (E. C., J. L. P., B. L.) and 2 ophthalmologists (D. G., M. E.).

IVCM examination was carried out with a handheld microscope for skin imaging (VivaScope 3000, Caliber ID, Rochester, NY, distributed in Europe by MAVIG GmbH, Munich, Germany) equipped with an 830-nm diode laser and high optical resolution (horizontal and vertical axis: 1.25 μm and 5 μm, respectively). Each image corresponds to a horizontal 1- × 1-mm section.

Before the examination, topical anesthesia was administered using oxybuprocaine hydrochloride (1.6 mg/0.4 mL) and tetracaine hydrochloride 1% applied in the lower conjunctival sac of the eye and a transparent ophthalmic gel of carbomer 974P (Gel larme Théa, Théa, Clermont-Ferrand, France) was applied to the ocular region to be examined. A disposable sterile transparent film (Visulin, Paul Hartmann AG, Heidenheim, Germany) was applied to the tip of the IVCM. The total duration of IVCM examination was approximately 5 to 10 minutes per lesion.

Before imaging the tumors, IVCM was also used to observe and assess the normal eyelid margin of the other eye.

Basal cell carcinoma (BCC) was diagnosed when at least 2 of the following criteria were present: dark silhouette, lobular nests or trabecular structures of tightly packed cells, peripheral palisading of elongated cells, peritumoral clefts, convoluted and dilated blood vessels, and polarized elongated keratinocytes (streaming) of the overlying skin.[1,2] Squamous cell carcinoma (SCC) was diagnosed when there was evidence of an atypical honeycomb and/or a disarranged pattern of the spinous-granular layer of the epidermis.[3] This diagnosis was further confirmed by the presence of horizontal and dilated blood vessels. Melanoma was diagnosed when at least 1 bright, large (>20 μm) and roundish pagetoid cell or widespread infiltration of large (>20 μm) dendritic pagetoid cells was evident, whereas solar lentigo was diagnosed when IVCM detected an increased density of dermal papillae surrounded by a bright monomorphic layer of cells (cordlike rete ridges).[4] The presence of junctional and/or dermal nests of homogeneous cells, with absence of: (1) pagetoid cells, (2) atypical cells at the dermoepidermal junction, (3) disarrangement of the epidermal layer, and (4) cerebriform nests led to the diagnosis of nevus.[2]

A surgical excision and a histologic examination were performed in 35 cases that were clinically and/or IVCM suspicious for malignancies. The correlation between the 2 methods (IVCM and histology) was assessed to calculate the sensitivity and specificity of IVCM for the diagnosis of malignant eyelid margin tumors, and in particular of BCC, SCC, and melanoma. We also calculated Cohen kappa and weighted kappa correlation coefficients for both diagnoses ($k < 0$ no agreement, 0-0.20 slight, 0.21-0.40 fair, 0.41-0.60 moderate, 0.61-0.80 substantial, and 0.81-1 almost perfect agreement). Nonbiopsied lesions were then monitored for at least 12 months.

CAPSULE SUMMARY

- We evaluated the suitability of in vivo confocal microscopy for the diagnosis of eyelid margin tumors.
- We found a high sensitivity and specificity of in vivo confocal microscopy for eyelid margin tumors in a series of 47 cases.
- The use of in vivo confocal microscopy for the diagnosis of eyelid lesions can avoid unnecessary surgical excisions.

RESULTS

IVCM features of the tumor-free mucosa varied according to the area of the eyelid margin. Three main different areas were identified: the cutaneous outer part, the mucous intermediate part, and the inner tarsal conjunctiva. Although the first resembled normal-appearing skin, the mucous intermediate part was characterized by: (1) the absence of stratum corneum and stratum granulosum, (2) the absence of papillae, and (3) prominent chorion capillaries. The same features were evident in the tarsal conjunctiva with the exception of: (1) a thinner epithelium (3-4 cell layers) made of cuboidal medium reflective cells, and (2) a prominent inflammatory infiltrate of bright cells.

The clinical features and the IVCM and histologic diagnoses of the lesions are reported in Table I (available at http://www.jaad.org). Sixteen lesions proved clinically challenging for both dermatologists and ophthalmologists whereas 3 further malignancies (1 BCC and 2 melanomas) were clinically diagnosed as benign lesions.

Table II. Correlation among clinical, in vivo reflectance confocal microscopy, and histologic features

Clinical diagnosis	Histopathological diagnosis	IVCM concordant with histopathological diagnosis	IVCM discordant with histopathological diagnosis	Sensitivity and specificity of IVCM
Melanoma, nevus, or lentigo	Melanoma	5	0	Sensitivity of IVCM for melanoma: 100% (5/5)
Melanoma, nevus, or lentigo	Not melanoma	7	2	Specificity of IVCM for melanoma: 77.7% (7/9)
BCC	BCC	14	0	Sensitivity of IVCM for BCC: 100% (14/14)
BCC	Not BCC	3	2	Specificity of IVCM for BCC: 60% (3/5)
SCC	SCC	3	0	Sensitivity of IVCM for SCC: 100% (3/3)
SCC	Not SCC	0	0	Specificity of IVCM for SCC: NA
All diagnosis	Malignant tumor	22	0	Sensitivity of IVCM for malignant tumor: 100% (22/22)
All diagnosis	Not malignant tumor	9	4	Specificity of IVCM for malignant tumor: 69.2% (9/13)

BCC, Basal cell carcinoma; *IVCM*, in vivo reflectance confocal microscopy; *NA*, not available; *SCC*, squamous cell carcinoma.

Considering all 35 excised lesions, IVCM showed a sensitivity of 100% and a specificity of 69.2% for malignant tumors (Table II). Cohen kappa and weighted kappa coefficients for the IVCM and histopathological diagnoses of all malignancies were 0.74 and 0.81, respectively. Of the 21 lesions with a clinical diagnosis of likely BCC, 19 were excised and their histologic examination showed 14 BCCs (Fig 1), 1 solar lentigo, 1 SCC, 2 dermal nevi, and 1 nodular hidradenoma. IVCM matched all 14 histologic diagnoses of BCC, showing a sensitivity of 100% for BCC, but it overdiagnosed BCC in 1 case of dermal nevus and in the case of nodular hidradenoma (Fig 2), showing a specificity of 60% for BCC. Cohen kappa and weighted kappa coefficients for IVCM and histopathological diagnoses of BCC were 0.69 and 0.77, respectively. Of the 24 cases with a clinical diagnosis of melanoma (9), nevi (11), and lentigo (4), 14 were excised and histologic examination showed 5 melanomas (Fig 3), 6 nevi, 1 lentigo, 1 melanoacanthoma, and 1 folliculitis. IVCM diagnosis was in agreement with the histologic examination in all 5 cases of melanoma, showing a sensitivity of 100% for melanoma, but it overdiagnosed melanoma in 1 case of lentigo and in 1 case of melanoacanthoma, showing a specificity of 77.7% for melanoma. Cohen kappa and weighted kappa coefficients between IVCM diagnosis and histopathological diagnosis of melanoma were 0.77 and 0.79, respectively. IVCM and histologic examination confirmed the diagnosis in all 3 cases of suspected SCC on clinical examination (one of these was also counted as suspected BCC because the clinical diagnosis was BCC vs SCC); IVCM showed therefore a sensitivity of 100% for SCC.

Nonbiopsied lesions were diagnosed by IVCM as 8 nevi, 2 lentigines (Fig 4), and 2 scars at the site of excision of the BCC and showed no changes after consecutive clinical and IVCM monitoring for at least 12 months.

DISCUSSION

Our study showed that skin-specific handheld IVCM can be a new tool for the noninvasive diagnosis of eyelid margin tumors. Two IVCMs are currently available to explore the eye surface: a 4-slit scanning confocal microscope (Confoscan, Nidek, Gamagori, Japan) and a laser-scanning confocal microscope (Heidelberg Retina Tomograph,[5,6] Heidelberg Engineering GmbH, Heidelberg, Germany). Because of their limited ease of handling, both these microscopes are mostly used to view the cornea and more rarely the conjunctiva. We used the skin-specific handheld VivaScope 3000 imager (Caliber ID) for the first time, to our knowledge, to explore the eyelid margin. This handy device, equipped with a smaller tip and suitable for the whole ocular area, has been recently applied to the imaging of the mucosa.[7,8] It is fitted with a class-1B diode laser, which is not harmful to the eye, with an 830-nm wavelength, which does not induce ocular glare. Examination is best performed on a compliant patient who should not move his/her eyes excessively, with ongoing adjustment of the position of the camera by the operator.

Before starting our study we explored the normal eyelid margin. Some of the IVCM features of the

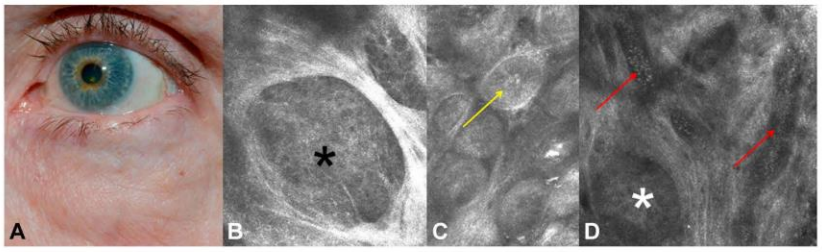

Fig 1. Clinical (**A**) and in vivo reflectance confocal microscopy (IVCM) (**B** to **D**) aspects of a basal cell carcinoma of the eyelid margin. IVCM shows dark silhouettes (*asterisks*), lobular nests of tightly packed cells (*yellow arrow*), and dilated vessels (*red arrows*).

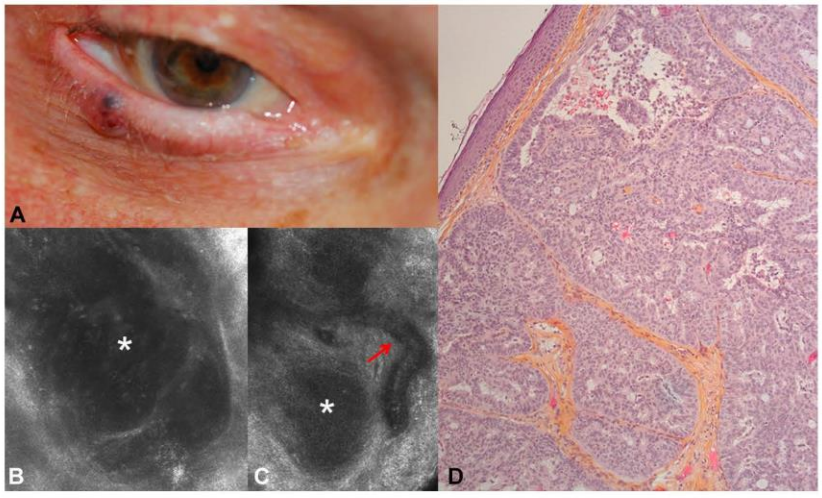

Fig 2. Clinical (**A**), in vivo reflectance confocal microscopy (IVCM) (**B** and **C**), and histopathological (**D**) aspects of the nodular hidrocystoma of the inferior eyelid margin that was misdiagnosed as basal cell carcinoma by IVCM. IVCM shows dark silhouettes containing scattered different refractive cells (*asterisks*) and dilated vessels (*red arrow*). (**D**, Hematoxylin-eosin stain; original magnification: ×4.)

normal eyelid margin had already been described by Knop et al[9] who used the Heidelberg Engineering GmbH device to examine 4 patients. We were able to identify 3 distinct anatomic areas under IVCM and obtained high resolution images, comparable with those achievable in the skin.

Given the lack of IVCM-validated criteria to diagnose tumoral lesions with the handheld VivaScope 3000 microscope (Caliber ID) in the eyelid margin area, we defined new criteria based on those used for tumoral skin lesions with the VivaScope 1500 device (Caliber ID), and on our personal experience. We were unable to use the usual architectural criteria for the IVCM diagnosis of melanoma because: (1) unlike the VivaScope 1500 (Caliber ID), the handheld VivaScope 3000 camera (Caliber ID) does not enable the "mosaic" reconstruction of images in the x-y directions, and (2) unlike the skin, the epithelium-dermal junction of the mucosal part of the eyelid-margin is flat, without papillae.

Using our diagnostic criteria, IVCM showed an excellent sensitivity (100%) for BCC, SCC, and melanoma. In most malignant tumors it confirmed the clinical diagnosis, whereas in 5 cases of BCC the clinical diagnosis was uncertain; 1 case of BCC and 2 cases of melanoma were clinically diagnosed as benign lesions. IVCM is extremely useful to confirm the clinical diagnosis of eyelid margin tumors and in clinically challenging cases. IVCM is equally useful during the follow-up after surgery of tumors from the eyelid margin, an area where surgical margins are often small for anatomic reasons. In our series IVCM confirmed the diagnosis of recurrent BCC in

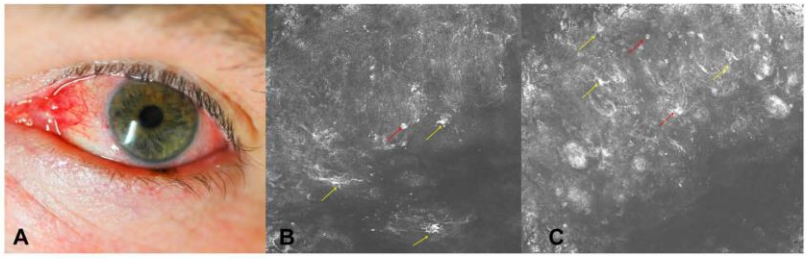

Fig 3. Clinical (**A**) and in vivo reflectance confocal microscopy (IVCM) (**B** and **C**) aspects of a melanoma of the inferior eyelid margin. IVCM shows pagetoid roundish cells (*red arrows*) and dendritic cells (*yellow arrows*) in the epithelium.

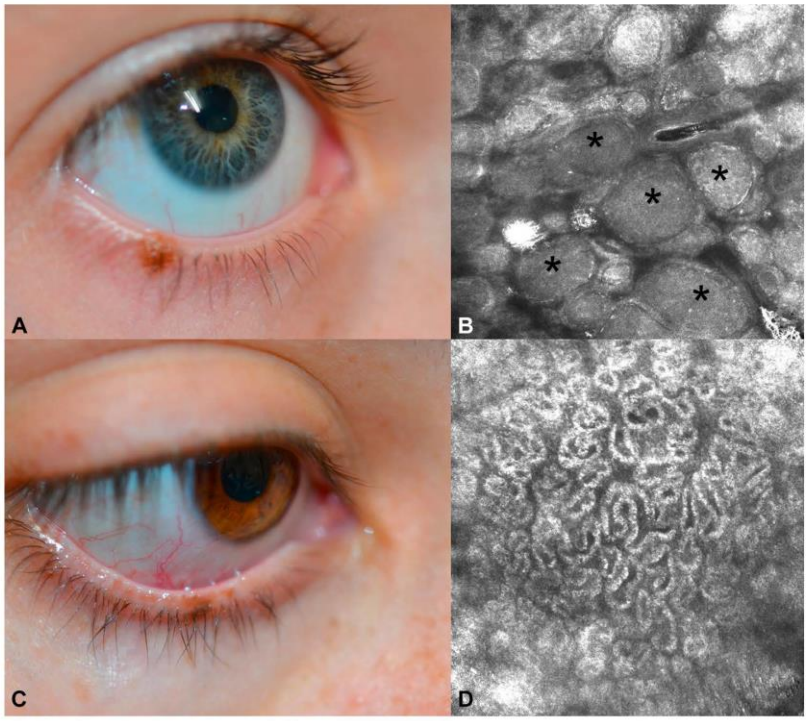

Fig 4. Clinical (**A**) and in vivo reflectance confocal microscopy (IVCM) (**B**) aspects of a nevus and clinical (**C**) and IVCM (**D**) aspects of a lentigo of the eyelid margin. IVCM of the dermal nevus (**B**) shows dermal nests of melanocytes (*asterisks*) and IVCM of the lentigo shows increased density of dermal papillae surrounded by a bright monomorphic layer of cells (cordlike rete ridges) typical of a lentigo (**D**).

2 patients but excluded it in 2 other patients who did not show any clinical progression at 12 months' follow-up.

The specificity of IVCM for malignant skin cancer of the eyelid ranged from 60% for BCC to 77.7% for melanoma and could not be assessed for SCC. IVCM correctly diagnosed as benign 5 lesions suspicious for melanoma, but it overdiagnosed BCC in a dermal nevus and in a nodular hidradenoma (Fig 2) and it overdiagnosed melanoma in a lentigo and a melanoacanthoma.

The case of a dermal nevus misdiagnosed as BCC by IVCM clinically presented as a pink papule with large telangiectases suggestive of BCC. IVCM showed dark silhouettes and horizontal dilated blood vessels, but the lesion lacked other

characteristic features of BCC. Retrospectively we found that the dark silhouettes evidenced by IVCM were small and not typical of BCC, which was in line with the small nests of melanocytes in the papillary dermis shown by the histologic examination. The case of nodular hidradenoma, diagnosed as BCC by IVCM (Fig 2), presented with a translucent skin-colored papule and focal pigmentation, clinically suggestive of pigmented BCC. There are no reports of the IVCM aspect of nodular hidradenoma, a rare benign tumor of sweat gland derivation.[10] Histologically it can mimic BCC because it is multilobular; is composed of closely arranged cells; and although centered in the dermis, can have epidermal connections. The differential diagnosis with BCC can be assessed by the presence of cystic areas and ductlike structures, but the retrospective analysis of our IVCM images did not allow us to clearly identify these structures. IVCM showed dark silhouettes and linear dilated blood vessels, but all the other criteria of BCC were absent. Unlike BCC stroma, stroma among lobules was delicate and not very reflective.

To improve the specificity of the diagnosis of BCC, we should better characterize the shape and size of the dark silhouettes of BCC, to differentiate them from those likely to be found in cases of benign adnexal tumors. We should also determine whether dilated blood vessels, very suspicious for BCC in the skin, should remain a diagnostic criterion for eyelid margin BCC.

The 2 cases that were misdiagnosed as melanoma by IVCM showed focal large pagetoid roundish bright cells (lentigo) or an intraepithelial widespread infiltrate of large dendritic cells (melanoacanthoma). In addition, small dendritic cells were observed in the lentigo. We speculated that pagetoid cells were actually at the basal epithelial layer, but we pinpointed their exact location incorrectly because of continuous eye movements and the curved eyelid margin surface. The histologic examination showed large activated melanocytes in the basal epithelial layer corresponding to the lentigo and focal atrophy of the epithelium, resulting in a more superficial position of the basal melanocytes. To our knowledge, melanoacanthoma has never been described under IVCM and it involves a benign proliferation of slightly pigmented keratinocytes and melanocytes that rarely affect the eyelid.[11] These melanocytes are typically large and highly dendritic, not confined to the basal layer and found throughout the tumor lobules.[12] In our case there was a marked proliferation of melanocytes that rendered the differential diagnosis challenging with melanoma in situ, by both IVCM and histologic examination. IVCM images were highly concordant with the histologic sections, which showed a widespread proliferation of dendritic melanocytes in an acanthotic epithelium. Melanocytes were homogeneously distributed within the lesion and this aspect can provide a clue for the diagnosis of melanoacanthoma.

Of the 5 cases of melanoma, large pagetoid cells were present in two, large dendritic cells in one, and both were present in the other two. Four of the 5 patients with eyelid margin melanoma had a history of ocular melanoma, which shows how useful IVCM is as an imaging technique to monitor these patients.

Considering the excellent sensitivity of IVCM for eyelid margin tumors and the fact that eyelid margin surgery is troublesome for patients, we decided not to excise 12 lesions considered benign clinically and by IVCM (2 scars of excised BCC, 8 nevi, and 2 lentigines). No clinical progression in all these lesions was shown by the follow-up to at least 12 months.

In conclusion, our preliminary study strongly suggests that handheld IVCM can be efficiently used for a noninvasive investigation of the eyelid margin. IVCM has shown excellent sensitivity and good specificity for eyelid margin BCC, SCC, and melanoma. In addition, we have shown that with skin-specific handheld IVCM it is possible to examine both the skin and the conjunctiva, with the added benefit of dermatologists and ophthalmologists sharing the same device in a medical facility.[13] Larger studies are needed to validate our data and to better define the diagnostic ability of this imaging technique.

Innov-EYE Project, Interregional Rhône-Alpes Auvergne Clinical Research Group funded a project on an atlas on eyelid tumors explored by IVCM that helped us to carry out this study.

REFERENCES

1. Nori S, Rius-Díaz F, Cuevas J, Goldgeier M, Jaen P, Torres A, et al. Sensitivity and specificity of reflectance-mode confocal microscopy for in vivo diagnosis of basal cell carcinoma: a multicenter study. J Am Acad Dermatol 2004;51:923-30.
2. Guitera P, Menzies SW, Longo C, Cesinaro AM, Scolyer RA, Pellacani G. In vivo confocal microscopy for diagnosis of melanoma and basal cell carcinoma using a two-step method: analysis of 710 consecutive clinically equivocal cases. J Invest Dermatol 2012;132:2386-94.
3. Rishpon A, Kim N, Scope A, Porges L, Oliviero MC, Braun RP, et al. Reflectance confocal microscopy criteria for squamous cell carcinomas and actinic keratoses. Arch Dermatol 2009;145:766-72.
4. Langley RGB, Burton E, Walsh N, Propperova I, Murray SJ. In vivo confocal scanning laser microscopy of benign lentigines: comparison to conventional histology and in vivo characteristics of lentigo maligna. J Am Acad Dermatol 2006;55:88-97.
5. Niederer RL, McGhee CNJ. Clinical in vivo confocal microscopy of the human cornea in health and disease. Prog Retin Eye Res 2010;29:30-58.

6. Wang Y, Le Q, Zhao F, Hong J, Xu J, Zheng T, et al. Application of in vivo laser scanning confocal microscopy for evaluation of ocular surface diseases: lessons learned from pterygium, meibomian gland disease, and chemical burns. Cornea 2011; 30(Suppl):S25-8.
7. Cinotti E, Perrot JL, Labeille B, Adegbidi H, Cambazard F. Reflectance confocal microscopy for the diagnosis of vulvar melanoma and melanosis: preliminary results. Dermatol Surg 2012;38:1962-7.
8. Cinotti E, Perrot JL, Labeille B, Douchet C, Mottet N, Cambazard F. Laser photodynamic treatment for in situ squamous cell carcinoma of the glans monitored by reflectance confocal microscopy. Australas J Dermatol 2014; 55:72-4.
9. Knop E, Knop N, Zhivov A, Kraak R, Korb DR, Blackie C, et al. The lid wiper and muco-cutaneous junction anatomy of the human eyelid margins: an in vivo confocal and histological study. J Anat 2011;218:449-61.
10. Soua Y, Mohamed M, Belhajali H, Njim L, Youssef M, Zakhama A, et al. Nodular hidradenoma. Ann Dermatol Venereol 2013; 140:152-3.
11. Spott DA, Heaton CL, Wood MG. Melanoacanthoma of the eyelid. Arch Dermatol 1972;105:898-9.
12. Shankar V, Nandi J, Ghosh K, Ghosh S. Giant melanoacanthoma mimicking malignant melanoma. Indian J Dermatol 2011;56:79-81.
13. Cinotti E, Perrot JL, Labeille B, Espinasse M, Ouerdane Y, Boukenter A, et al. Optical diagnosis of a metabolic disease: cystinosis. J Biomed Opt 2013;18:046013.

Table 1. Patient demographics and clinical, in vivo confocal microscopy, and histologic diagnosis of the eyelid margin tumors

Patient no.	Sex	Age, y	Eyelid margin	Size, mm	Clinical features	Evolution, y	Clinical diagnosis	IVCM diagnosis	Histologic diagnosis	Correlation IVCM/ histology
1	M	73	Inferior	5	Nodule, skin colored and focally pigmented	1	BCC	BCC	BCC	Yes
2	F	67	Inferior	2	Macule, skin colored, itchy	1	BCC?	BCC	BCC	Yes
3	F	79	Inferior	3	Erosion on the scar of a previous excised BCC	1	Recurrent BCC?	BCC	BCC	Yes
4	M	69	Inferior	2	Papule, erythematous	0.5	BCC? Dermal nevus?	BCC	BCC	Yes
5	F	71	Inferior	4	Papule, erythematous	2	BCC	BCC	BCC	Yes
6	F	13	Inferior	3	Papule, erythematous	1	BCC	BCC	BCC	Yes
7	M	78	Inferior	3	Papule, skin colored and focally pigmented	1	BCC	BCC	BCC	Yes
8	F	86	Inferior	8	Nodule, skin colored	2	BCC	BCC	BCC	Yes
9	M	81	Inferior	3	Erosion	1	BCC?	BCC	BCC	Yes
10	M	84	Inferior	2	Macule, erythematous	0.5	BCC	BCC	BCC	Yes
11	F	64	Inferior	3	Macule, erythematous	1	Recurrent BCC?	BCC	BCC	Yes
12	M	54	Inferior	4	Macule, translucent	1	BCC	BCC	BCC	Yes
13	M	83	Superior	3	Nodule, yellowish	0.5	Epidermal cyst	BCC	BCC	Yes
14	F	78	Inferior	3	Nodule, yellowish	1	BCC	BCC	BCC	Yes
15	M	73	Inferior	2	Papule, gray	3	BCC?	Solar lentigo	Solar lentigo	Yes
16	M	79	Inferior	6	Nodule, erythematous	2	BCC? SCC?	SCC	SCC	Yes
17	M	65	Inferior	3	Papule, skin colored	0.5	BCC?	BCC or annexal tumor	Dermal nevus	No
18	F	66	Superior	4	Papule, skin colored	20, Recently enlarged	BCC? Dermal nevus?	Dermal nevus	Dermal nevus	Yes
19	M	80	Inferior	3	Nodule, skin colored and focally pigmented	1	BCC	BCC	Nodular hydradenoma	No
20	F	79	Inferior	2	Eroded papule	<0.5	Recurrent BCC?	Scar	NA	NA
21	M	87	Inferior	4	Scar	0.5	Recurrent BCC?	Scar	NA	NA
22	F	47	Inferior	4	Flat papule, dark brown	3, Recently enlarged	Melanoma	Nevus	Dermal nevus	Yes
23	M	50	Inferior	4	Flat papule, light brown	1	Melanoma?	Folliculitis	Folliculitis	Yes
24	M	27	Inferior	4	Papule, dark brown	2	Melanoma?	Compound nevus	Compound nevus	Yes
25	F	62	Inferior	4	Papule, light brown, recently itchy	10	Melanoma?	Dermal nevus	Dermal nevus	Yes
26	F	42	Superior	4	Macule, light brown	2	Melanoma	Melanoma	Melanoma	Yes
27	F	73	Inferior	5	Macule, light brown	10	Melanoma	Melanoma	Melanoma	Yes
28	M	64	Inferior	3	Macule, light brown	9 mo	Nevus	Melanoma	Melanoma	Yes
29	M	46	Inferior	3	Macule, light brown	?	Lentigo	Melanoma	Melanoma	Yes
30	F	94	Inferior	4	Macule, light brown	10	Melanoma	Melanoma	Melanoma	Yes
31	M	60	Inferior	2	Macule, light brown	10	Lentigo	Melanoma	Lentigo	No
31	M	60	Inferior	2	Macule, erythematous	10	Nevus	Compound nevus	Compound nevus	Yes
32	M	71	Inferior (lateral lesion)	3	Papule, 3 mm, skin colored	Since childhood	Congenital nevus	Compound nevus	Compound nevus	Yes
33	F	67	Inferior (lateral lesion)	2	Nodule, erythematous	3	Nevus	Melanoma	Melanoacanthoma	No
34	F	62	Inferior	4	Papule, light brown, recently itchy	10	Melanoma?	Dermal nevus	Dermal nevus	Yes
35	F	88	Superior	10	Nodule, yellowish, keratotic	0.5	SCC	SCC	SCC	Yes
36	M	69	Inferior	4	Atrophic scar, erythematous	0.6	Recurrent SCC	Recurrent SCC	SCC	Yes
37	F	41	Inferior	3	Macule, light brown	9	Nevus	Dermal nevus	NA	NA
38	F	20	Inferior	3	Macule, light brown	3	Nevus	Dermal nevus	NA	NA
38	F	20	Inferior	5	Macule, light brown	3	Lentigo	Lentigo	NA	NA
39	M	13	Inferior	3	Papule, light brown	Since childhood	Congenital nevus	Congenital nevus	NA	NA
40	F	66	Superior	5	Nodule, skin colored	20, Recently enlarging	Dermal nevus	Compound nevus	NA	NA
41	F	21	Inferior	3	Nodule, dark brown	Since childhood, recently enlarging	Melanoma vs nevus?	Dermal nevus	NA	NA
42	M	77	Superior	5	Papule, erythematous	?	Nevus	Dermal nevus	NA	NA
43	M	65	Inferior	2	Papule, erythematous, focally pigmented	5	Nevus?	Dermal nevus	NA	NA
44	M	62	Inferior	3	Macule, light brown	1	Lentigo	Lentigo	NA	NA
45	M	73	Inferior	2	Macule, light brown	2	Nevus	Compound nevus	NA	NA

BCC, Basal cell carcinoma; *F*, female; *IVCM*, in vivo reflectance confocal microscopy; *M*, male; *NA*, not available; *SCC*, squamous cell carcinoma.

5.a 1bis The role of in vivo confocal microscopy in the diagnosis of eyelid margin tumors: 47 cases : reply from the author

The role of in vivo confocal microscopy in the diagnosis of eyelid margin tumors: Reply from the authors

To the Editor: We recently reported a new noninvasive imaging method called "in vivo reflectance confocal microscopy (IVCM)" for the diagnosis of eyelid margin tumors.[1] Lee et al[2] stated that sensitivity and specificity were enough to demonstrate the diagnostic accuracy for IVCM in our study and that Cohen kappa and weighted kappa should not be used.

The aim of our study was to compare IVCM to histologic examination for the diagnosis of eyelid tumors. Sensitivity and specificity analysis were carried out to compare IVCM to the histologic examination, used as gold standard. The results obtained showed a good IVCM diagnostic accuracy.

In addition we used Cohen kappa and weighted kappa coefficients that did not represent independent statistical findings, but they strengthened the hypothesis that both IVCM and the histologic examination lead to similar results. We assumed that IVCM and histologic examination were 2 unrelated diagnostic methods of similar weight and found a good interdevice agreement.

Elisa Cinotti, MD,[a] Jean-Luc Perrot, MD,[a] Nelly Campolmi, MD,[b,c] Bruno Labeille, MD,[a] Marine Espinasse, MD,[b,c] Damien Grivet, MD,[b,c] Gilles Thuret, PhD,[b,c,d] Philippe Gain, MD, PhD,[b,c] Catherine Douchet, MD,[e] Fabien Forest, MD,[e] Maher Haouas, MD,[b] and Frédéric Cambazard, PhD[a]

Departments of Dermatology,[a] Ophthalmology,[b] and Pathology,[e] University Hospital of Saint-Etienne; Laboratory Biology, Engineering, and Imaging of Corneal Graft, EA2512, Jean Monnet University, Saint-Etienne[c]; and French University Institute, Boulevard Saint-Michel, Paris,[d] France

Funding sources: None.

Conflicts of interest: None declared.

Correspondence to: Elisa Cinotti, MD, Dermatology Department, University Hospital of Saint-Etienne, 42055 Saint Etienne Cedex 2, France

E-mail: elisacinotti@gmail.com

REFERENCES

1. Cinotti E, Perrot JL, Campolmi N, et al. The role of in vivo confocal microscopy in the diagnosis of eyelid margin tumors: 47 cases. *J Am Acad Dermatol.* 2014;71:912-918.
2. Lee JH, Park Y-G. Re: The role of in vivo confocal microscopy in the diagnosis of eyelid margin tumors: 47 cases. *J Am Acad Dermatol.* 2015;72:e121.

http://dx.doi.org/10.1016/j.jaad.2015.01.013

5.a 2 Handheld reflectance confocal microscopy for the diagnosis of conjunctival tumors

Purpose:
To evaluate whether the handheld in vivo reflectance confocal microscopy that has been r e c e n t l y developed for the study of skin tumors is suitable for the diagnosis of conjunctival tumors.

Design:
Prospective study, observational case series.

Method: We prospectively evaluated the reflectance confocal microscopy features of 53 conjunctival lesions clinically suspicious for tumors of 46 patients referred to the University Hospital of Saint-Etienne (France) by using the handheld device. Twenty-three lesions were excised (3 nevi, 10 melanomas, 5 squamous cell carcinoma, 2 lymphomas, and 3 pinguecula/pterygium) while the other 30, presenting no reflectance confocal microscopy malignant features, were under follow-up for at least 1 year. Clinical reflectance confocal microscopy and histologic diagnosis were compared.

Results:
In vivo reflectance confocal microscopy diagnosis was in agreement with the histologic diagnosis in all cases and none of the lesions that were not excised show any clinical progression under follow-up.

Conclusion:
In vivo reflectance confocal microscopy with a handheld dermatology-dedicated microscope can play a role in the noninvasive diagnosis of conjunctival lesions. Further studies should be performed to better define the diagnostic ability of this technique.

Handheld Reflectance Confocal Microscopy for the Diagnosis of Conjunctival Tumors

ELISA CINOTTI, JEAN-LUC PERROT, BRUNO LABEILLE, NELLY CAMPOLMI, MARINE ESPINASSE, DAMIEN GRIVET, GILLES THURET, PHILIPPE GAIN, CATHERINE DOUCHET, CAROLINE ANDREA, MAHER HAOUAS, AND FRÉDÉRIC CAMBAZARD

• PURPOSE: To evaluate whether the handheld in vivo reflectance confocal microscopy that has been recently developed for the study of skin tumors is suitable for the diagnosis of conjunctival tumors.
• DESIGN: Prospective study, observational case series.
• METHODS: We prospectively evaluated the reflectance confocal microscopy features of 53 conjunctival lesions clinically suspicious for tumors of 46 patients referred to the University Hospital of Saint-Etienne (France) by using the handheld device. Twenty-three lesions were excised (3 nevi, 10 melanomas, 5 squamous cell carcinoma, 2 lymphomas, and 3 pinguecula/pterygium) while the other 30, presenting no reflectance confocal microscopy malignant features, were under follow-up for at least 1 year. Clinical reflectance confocal microscopy and histologic diagnosis were compared.
• RESULTS: In vivo reflectance confocal microscopy diagnosis was in agreement with the histologic diagnosis in all cases and none of the lesions that were not excised show any clinical progression under follow-up.
• CONCLUSION: In vivo reflectance confocal microscopy with a handheld dermatology-dedicated microscope can play a role in the noninvasive diagnosis of conjunctival lesions. Further studies should be performed to better define the diagnostic ability of this technique. (Am J Ophthalmol 2015;159:324–333. © 2015 by Elsevier Inc. All rights reserved.)

THE CLINICAL DIAGNOSIS OF CONJUNCTIVAL TUMORS is often challenging,[1 4] and in case of clinical doubt of malignant tumor excision is mandatory. However, a surgical excision in this area may have functional or aesthetic consequences for the patient and may be technically complex for the surgeon. New imaging techniques are of high interest in the diagnosis of conjunctival tumors to reduce the number of unnecessary surgical excisions. In vivo reflectance confocal microscopy is a noninvasive, high-resolution imaging technique that has been demonstrated to be useful for the diagnosis of conjunctival tumors.[2,5 9] However, this technique is not extensively used, mainly owing to the difficulty of acquiring the images, especially because reflectance confocal microscopes dedicated to ophthalmology have limited numbers of degrees of freedom and limited possibilities of mechanical displacement. We investigated whether the handheld reflectance confocal microscope that has been developed for the cutaneous tumors, and which has been demonstrated to be applicable to the study of the genital[10 13] and the oral[13,14] mucosa with easy and quick examinations, could play a role in the diagnosis of conjunctival tumors. We present a series of conjunctival tumors described from a clinical standpoint and the first that has been investigated by the handheld in vivo reflectance confocal microscope.

Accepted for publication Oct 29, 2014.
From the Departments of Dermatology (E.C., J.-L.P., B.L., C.A., F.C.), Ophthalmology (N.C., M.E., D.G., G.T., P.G., M.H.), and Pathology (C.D.), University Hospital of Saint-Etienne, Saint-Etienne, France; Biology, Engineering and Imaging of Corneal Graft Laboratory, EA2521, Jean Monnet University (N.C., M.E., D.G., G.T., P.G.), Saint-Etienne, France; and Institut Universitaire de France (G.T.), Paris, France.
Inquiries to Elisa Cinotti, Dermatology Department, University Hospital of Saint-Etienne, 42055 Saint-Etienne Cedex 2, France; e-mail: elisacinotti@gmail.com

METHODS

FORTY-SIX PATIENTS (24 FEMALE, 22 MALE, AVERAGE AGE 53 years, range 13-94 years) presenting with a total of 53 conjunctival lesions suggestive of tumors were recruited at the Dermatology Department of the University Hospital of Saint-Etienne, France, between January 1, 2011 and June 30, 2013. Clinical and in vivo reflectance confocal microscopy diagnosis were prospectively established together by 2 ophthalmologists (D.G., E.M.) and 3 dermatologists (E.C., J.-L.P., B.L.). Tumors confined to the eyelid margin were excluded owing to the particular features of this area of transition between the tarsal conjunctiva and the skin.

A slit-lamp examination was performed to establish the clinical diagnosis. In vivo reflectance confocal microscopy examination was carried out with the handheld microscope dedicated to skin (VivaScope 3000; Caliber, Rochester, New York, USA, distributed in Europe by MAVIG GmbH, München, Germany) (Figure 1), which uses an 830-nm class 1B (classification CDRH—Center for Devices and Radiological Health) diode laser not harmful to eyes, with a wavelength that does not induce ocular glare. This system has a high optical resolution (horizontal and vertical axis: 1.25 μm and 5 μm, respectively) and allows

0002-9394/$36.00
http://dx.doi.org/10.1016/j.ajo.2014.10.031

visualization of tumors up to 250 μm in depth from the epithelial surface of the conjunctiva. Each image corresponds to a horizontal section of 1 mm × 1 mm. Before the ocular examination, topical anesthesia was performed with oxybuprocaine hydrochloride 1.6 mg/0.4 mL and tetracaine hydrochloride 1% applied into the lower conjunctival sac of the eye and a transparent ophthalmic gel of Carbomer 974P (Gel larme; Théa, Clermont-Ferrand, France) was placed on the ocular region to be examined. A disposable sterile transparent film (Visulin; Paul Hartmann AG, Heidenheim, Germany) was applied on the reflectance confocal microscope tip. In some cases an eyelid retractor was used to prevent blinking. Examinations were performed on patients in supine position. Reflectance confocal microscopy examination time per lesion was around 5-10 minutes.

An institutional review board approval was obtained (institutional review board at the University Hospital of Saint-Etienne, France, number IORG0007394; study filed under reference number IRBN332014/CHUSTE). A patient informed consent was always obtained orally during the first consultation and before this examination.

Before imaging the tumors, the normal conjunctiva of the contralateral eye was also observed under in vivo reflectance confocal microscopy and features of normal conjunctiva were assessed. We examined both benign and malignant conjunctival tumors, including nevi, primary acquired melanosis (PAM), melanomas, extrascleral growth of uveal melanomas, squamous cell carcinomas (SCC), and lymphomas. Moreover, some cases of pinguecula and pterygium were also observed when in doubt of SCC. Two cases of nevus of Ota were also examined to exclude the presence of areas of malignant transformation.

The in vivo reflectance confocal microscopy diagnosis of nevus was determined in the presence of junctional and/or stromal hyperreflective homogeneous medium-sized (10-20 μm), roundish cells organized in nests, with the absence of (1) pagetoid cells, (2) atypical cells at the epithelium-stromal junction, and (3) disarrangement of the epithelial layers.[15] The presence of stromal pseudocyst-like structures partly filled with monomorphous material allowed diagnosis of the epithelial-cystic nevus. Lesions with hyperreflective cells confined to the basal layer of the epithelium[16] and/or small (<20 μm) pagetoid dendritic cells at in vivo reflectance confocal microscopy were diagnosed as PAM without atypia, whereas lesions with hyperreflective cells throughout the epithelium and large pagetoid dendritic cells (>20 μm) were diagnosed as PAM with atypia.[5] The in vivo reflectance confocal microscopy diagnosis of conjunctival melanoma and extrascleral growths of uveal melanomas were established in the presence of large (>20 μm) dendritic or roundish hyperreflective cells at the epithelial-stromal junction and/or in the stroma associated with the possible presence of large pagetoid cells.

The in vivo reflectance confocal microscopy diagnosis of SCC was made in the presence of large (>20 μm) epithelial cells[17] and/or a disarranged pattern of the epithelium.

FIGURE 1. In vivo reflectance confocal microscopy examination of the conjunctiva using the handheld microscope dedicated to the skin.

The presence of horizontal and dilated blood vessels and the presence of abundant dendritic cells was an additional criterion that confirmed the SCC diagnosis. Pinguecula and pterygium were diagnosed in the absence of epithelial atypia and the subepitehlial presence of degenerated stromal collagen that presented with a coiled shape and a fibrovascular proliferation, respectively. Increased leukocytes (small hyperrefractive roundish homogeneous cells) in the stroma were an additional finding.

Mucosa-associated lymphoid tissue (MALT) lymphoma was diagnosed in the presence of a normal epithelium and abundant small hyperrefractive roundish cells corresponding to lymphocytes in the stroma.

A surgical excision and a histopathologic examination were performed in 20 cases clinically and/or in vivo reflectance confocal microscopy suspicious for malignant tumors (melanoma, SCC, MALT lymphoma). In addition, the first 3 cases of nevi were excised to perform a histopathologic examination considering that the in vivo reflectance confocal microscopy aspect of the conjunctival nevi had never been described using the handheld camera.

The correlation between in vivo reflectance confocal microscopy and the histopathologic examination was evaluated. Lesions that were not biopsied because considered benign at in vivo reflectance confocal microscopy examination were then monitored for at least 12 months.

RESULTS

IN VIVO REFLECTANCE CONFOCAL MICROSCOPY FEATURES of the normal conjunctiva were the presence of (1) 3-6

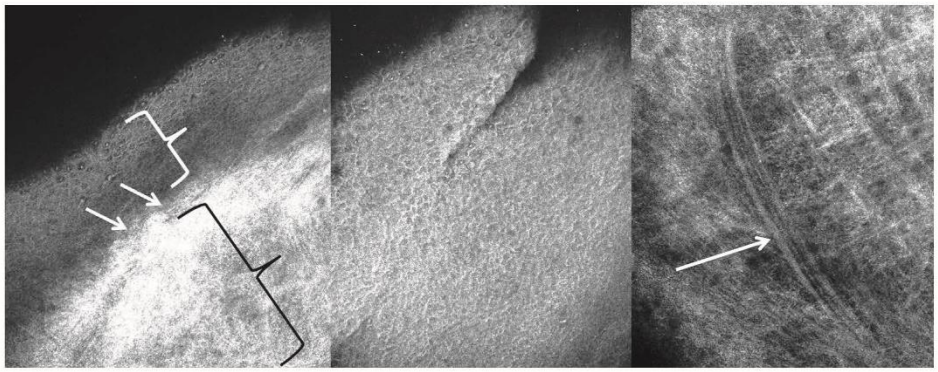

FIGURE 2. In vivo reflectance confocal microscopy features of the normal conjunctiva. Thanks to the convexity of the ocular surface it is possible to obtain a vertical section of the conjunctiva (Left), which show the epithelium (white bracket), the stroma (black bracket), and a flat epithelial-stromal junction (arrow). The epithelium (Center) is composed by polygonal medium size cells with hyperreflective membranes, hyporeflective cytoplasm, and medium reflective round nuclei. In the stroma (Right) elongated hyperreflective structures are organized in a dense meshwork (corresponding to collagen fibers) and prominent capillaries (arrow) are visible.

layers of polygonal medium-size (10 μm) cells with hyperreflective membranes, hyporeflective cytoplasm, and medium reflective round nuclei in the epithelium, (2) a flat epithelial-stromal junction and (3) elongated hyperreflective structures organized in a dense meshwork (corresponding to collagen fibers) and prominent capillaries in the stroma (Figure 2). The movement of blood cell flow could be observed in real time inside blood capillaries.

The clinical features, the in vivo reflectance confocal microscopy, and the histopathologic diagnosis of the lesions are reported in the Table. Considering all the 23 excised lesions (Figures 3 and 4), 12 lesions were clinically challenging, and 3 cases of melanomas were clinically diagnosed as benign lesions, whereas in vivo reflectance confocal microscopy diagnosis was in agreement with the histologic diagnosis in all cases, including 10 melanomas, 5 SCC, and 2 MALT lymphomas.

The 30 lesions that were not biopsied were diagnosed by in vivo reflectance confocal microscopy as 20 nevi (including 7 nevi with epithelial-cystic inclusions), 2 nevus of Ota (Figure 5), 2 pterygium, and 6 PAM without atypia (Figure 6), and showed no changes following consecutive clinical and in vivo reflectance confocal microscopy monitoring for at least 12 months. No complications such as ocular inflammation and/or infections and/or mechanical trauma were found using this imaging technique.

DISCUSSION

OUR STUDY SHOWED THAT HANDHELD IN VIVO REFLECTance confocal microscope dedicated to skin can be a new tool for a noninvasive diagnosis of conjunctival tumors. Two in vivo reflectance confocal microscopes are currently available to explore the ocular surface: the Confoscan 4 slit-scanning confocal microscope (Nidek, Gamagori, Japan) and the in vivo reflectance confocal microscope Heidelberg Retina Tomograph (HRT),[18,19] in association with the Rostock Cornea Module (Heidelberg Engineering GmbH, Heidelberg, Germany). Differently from the in vivo reflectance confocal microscope dedicated to skin, these devices do not have a handheld probe but present a hinged support for the camera that renders more difficult the precise alignment with the region of interest. Because of this limitation in the handiness, they are mainly used to visualize cornea and, more rarely, the conjunctiva near the axis.[20] There are only few studies[2,5–9] about their use for conjunctival tumors. One study[5] evaluated 28 melanocytic tumors, 1 article described a case of lymphoma,[9] and all the other publications are about squamous neoplasia.[2,6–8,21]

For the first time we used the handheld in vivo reflectance confocal microscope dedicated to skin (VivaScope 3000) to explore the conjunctiva. This device, thanks to its ease of handling (handheld probe of small size, light weight, equipped with manual control buttons to move in the vertical axis of the tissue) and its small tip, has been recently applied to the imaging of the mucosa[10,12,13] and was suitable for the examination of the whole ocular area. VivaScope 3000 is expensive, but the same device can be shared between dermatologists and ophthalmologists, as we demonstrated that it can be used for both skin and eye. Most of the largest dermatologic centers already have this device.

Examination is best performed on a cooperative patient who should not excessively move his eyes, while the operator continuously adapts the position of the camera. During our study we also explored the normal conjunctiva that presented with similar features to those described for the Heidelberg device.[22–24]

TABLE. Clinical Features and Handheld Reflectance Confocal Microscopy and Histologic Diagnosis of the Conjunctival Lesions

Patient Number	Sex	Age	Location	Size (mm)	Clinical Feature	Evolution (Years)	Clinical Diagnosis	Confocal Microscopy Diagnosis	Histologic Diagnosis	Confocal Microscopy/Histology Correlation
1	M	78	Bulbar	2 × 2	Dark brown flat papule	0.5	Melanoma?	Melanoma	Melanoma	Yes
2	F	73	Bulbar/tarsal	5 × 3	Multiple macules, light brown	10	Melanoma	Melanoma	Melanoma	Yes
3	F	94	Bulbar	4 × 3	Multiple macules, dark brown	10	Melanoma	Melanoma	Melanoma	Yes
4	F	42	Bulbar	3 × 2	Light brown macule	2	Melanoma	Melanoma	Melanoma	Yes
4	F	42	Tarsal	4 × 2	Light brown macule	2	Melanoma	Melanoma	Melanoma	Yes
5	M	64	Bulbar	3 × 3	Red macule	9 months	Pinguecula?	Melanoma	Melanoma	Yes
5	M	64	Tarsal	3 × 4	Brown macule	9 months	Nevus?	Melanoma	Melanoma	Yes
5	M	64	Bulbar	2	Brown macule	3 months	Melanoma?	Melanoma	Melanoma	Yes
5	M	64	Tarsal	3 × 6	Brown macule	10 months	Melanoma	Melanoma	Melanoma	Yes
6	F	66	Limbal	6 × 8	Black flat papule	7	Nevus?	Melanoma	Melanoma	Yes
7	M	60	Caruncle	4 × 3	Pink papule	NA	Nevus	Compound nevus	Compound nevus	Yes
8	F	19	Limbal	1 × 1	Brown macule	1	Nevus	Subepithelial nevus	Subepithelial nevus	Yes
9	M	59	Bulbar	10 × 6	Brown macule	10	Nevus	Epithelial-cystic nevus	Epithelial-cystic nevus	Yes
10	M	81	Limbal	3 × 2	Flat rose papule	0.5	SCC?	SCC	SCC in situ	Yes
11	F	55	Limbal/bulbar	9 × 10	Red macule	1	SCC	SCC	SCC in situ	Yes
12	F	47	Limbal	5 × 5	Pink macule	NA	SCC	SCC	SCC	Yes
13	M	73	Limbal	5 × 5	Reddish papule	1 month	SCC	SCC	SCC	Yes
14	M	77	Limbal	5 × 5	Pink nodule	0.5	SCC?	SCC	SCC	Yes
15	F	59	Limbal	3 × 3	Whitish nodule	10	SCC?	Pinguecula	Pinguecula	Yes
16	F	69	Limbal	4 × 3	Whitish nodule	2	SCC?	Pterygium	Pinguecula	Yes
17	M	71	Limbal	3 × 4	Pink papule	1	SCC?	Pinguecula	Pinguecula	Yes
18	M	73	Tarsal	8 × 5	Pink patch	1 month	MALT lymphoma?	MALT lymphoma	MALT lymphoma	Yes
19	F	64	Tarsal	4 × 3	Pink papules	0.5	MALT lymphoma?	MALT lymphoma	MALT lymphoma	Yes
20	M	51	Bulbar	3 × 2	Brown macule	3 months	Melanoma?	Junctional nevus	NA	NA
21	M	56	Limbal	1 × 1	Light brown macule	Congenital	Nevus	Dermal nevus	NA	NA
22	F	71	Caruncle	2 × 2	Light brown papule	5	Nevus	Subepithelial nevus	NA	NA
23	M	17	Limbal/bulbar	8 × 5	Brown-yellow patch	Congenital	Nevus	Compound nevus	NA	NA
24	F	23	Caruncle	3 × 1	Brown macule	NA	Nevus	Junctional nevus	NA	NA
25	M	58	Bulbar	7 × 6	Flat brown papule	48	Nevus	Epithelial-cystic nevus	NA	NA
26	F	33	Bulbar	4 × 4	Macule with a light and dark brown pigmentation	Congenital	Nevus	Junctional nevus	NA	NA
27	F	28	Bulbar	5 × 5	Brown patch	10	Epithelial-cystic nevus	Epithelial-cystic nevus	NA	NA
28	F	32	Bulbar	1.5	Brown papule	2	Nevus	Epithelial-cystic nevus	NA	NA
29	F	84	Bulbar	2 × 4	Light brown macule	1	Nevus	Epithelial-cystic nevus	NA	NA
30	M	61	Caruncle	15 × 7	Brown macule	45	Nevus	Epithelial-cystic nevus	NA	NA
31	M	31	Limbal		Brown macule	5	Nevus	Epithelial-cystic nevus	NA	NA

Continued on next page

TABLE. Clinical Features and Handheld Reflectance Confocal Microscopy and Histologic Diagnosis of the Conjunctival Lesions (*Continued*)

Patient Number	Sex	Age	Location	Size (mm)	Clinical Feature	Evolution (Years)	Clinical Diagnosis	Confocal Microscopy Diagnosis	Histologic Diagnosis	Confocal Microscopy/Histology Correlation
32	M	17	Limbal	7 × 5	Erythematous macule	10	Nevus	Subepithelial nevus	NA	NA
33	M	68	Bulbar	5 × 3	Flat light brown papule	10	Epithelial-cystic nevus	Epithelial-cystic nevus	NA	NA
34	M	51	Bulbar	3 × 2	Brown papule	10	Epithelial-cystic nevus	Epithelial-cystic nevus	NA	NA
35	M	41	Bulbar	3	Light brown macule	10	Racial melanosis	Compound nevus	NA	NA
35	M	41	Bulbar	2	Light brown macule	10	Racial melanosis	Compound nevus	NA	NA
35	M	41	Bulbar	2	Light brown macule	10	Racial melanosis	Compound nevus	NA	NA
36	F	13	Bulbar	6 × 4	Erythematous macule	Congenital, but recently enlarged	Nevus	Subepithelial nevus	NA	NA
37	M	27	Caruncule, conjunctive	1	Brown macule	3	Nevus	Subepithelial nevus	NA	NA
15	F	59	Bulbar		Brown and gray macules	NA	Nevus of Ota	Nevus of Ota	NA	NA
38	M	48	Bulbar	1 × 1	Brown and gray macules	Congenital	Nevus of Ota	Nevus of Ota	NA	NA
39	F	48	Bulbar	3 × 4	Multifocal light brown macule	10	PAM	PAM	NA	No
40	F	62	Limbal	2 × 1	Light brown macule	10	PAM	PAM	NA	NA
41	F	66	Tarsal	5	Light brown macule	0.5	PAM	PAM	NA	NA
42	F	33	Limbal	4	Light brown macule	10	PAM	PAM	NA	NA
43	F	40	Bulbar	10	Brown macule	6	Racial melanosis	PAM	NA	NA
44	F	29	Bulbar	3 × 4	Light brown macule	4	Racial melanosis	PAM	NA	NA
45	M	72	Limbal	5 × 2	Grayish nodule	NA	Pterygium vs SCC?	Pterygium	NA	NA
46	F	68	Limbal	2 × 2	Red nodule	10	Pterygium vs SCC?	Pterygium	NA	NA

MALT = mucosa-associated lymphoid tissue; NA = not available; PAM = primary acquired melanosis; SCC = squamous cell carcinoma.

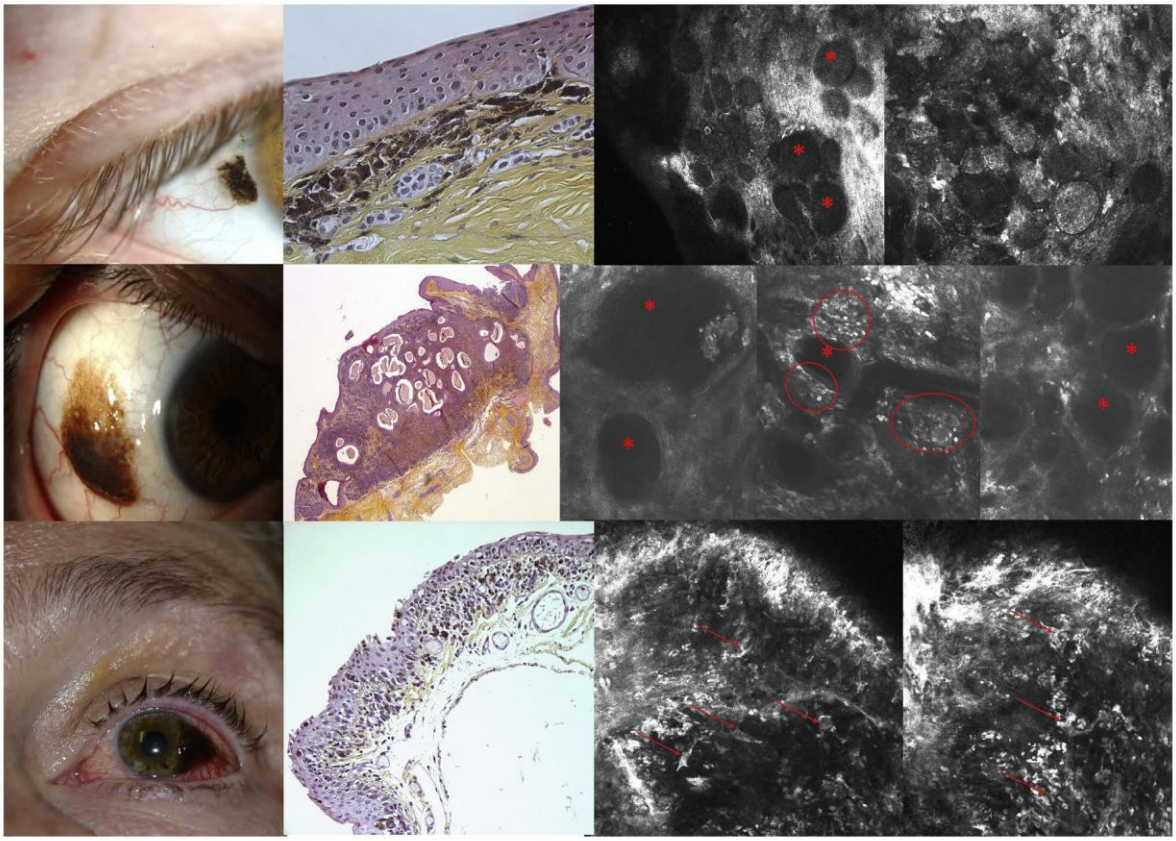

FIGURE 3. Clinical (Left), histologic (Center) and handheld reflectance confocal microscopy (Right) aspect of a subepithelial nevus (First line), an epithelial-cystic nevus (Second line), and a melanoma (Third line). Handheld reflectance confocal microscopy shows in the subepithelial nevus homogeneous nests of cells (red asterisk) in the stroma; in the epithelial-cystic nevus stromal pseudocyst-like structures (red asterisk) partly filled with monomorphous material surrounded by hyperreflective homogeneous cells (red circles); in the melanoma uneven large cells (red arrow) of different shape (roundish, dendritic and polygonal cells) in the epithelium. (Histologic stains: hematoxylin-eosin, first and third lines 20×, second line 4×.)

Given the lack of in vivo reflectance confocal microscopy validated criteria to diagnose tumors with the handheld VivaScope 3000 camera, in particular in the conjunctival area, we defined new criteria based on those used in the 2 studies of conjunctival tumors explored by the Heildelberg in vivo reflectance confocal microscope,[9,22] on in vivo reflectance confocal microscopy diagnostic criteria used for skin tumors[15,17] and for genital and oral mucosal[10,13] tumors, on histology of conjunctival tumors,[4,25] and on our personal experience.

Using our diagnostic criteria, in vivo reflectance confocal microscopy diagnosis was in agreement with histology in all cases, and in particular for SCC, melanoma, and MALT lymphoma. In vivo reflectance confocal microscopy was mostly used to confirm the clinical diagnosis of malignant tumors, but in 5 cases of SCC, 4 cases of melanoma, and 2 cases of lymphoma the clinical diagnosis was completely uncertain. Interestingly, it also found melanomas in 3 lesions that were not clinically suspicious for malignant tumors.

In all SCC we found large epithelial cells (Figure 4) and an abundant infiltrate of dendritic cells. Enlarged epithelial cells corresponding to neoplastic epitheliocytes could also be found by Falke and associates[2] in their in vivo reflectance confocal microscopy observation on a case of in situ SCC. Nguena and associates[21] recently reported a series of 26 SCC observed by in vivo reflectance confocal microscopy in a black population and could not find a statistically significant difference for the parameters that have been so far identified as characteristic of SCC (presence of irregular cell size, hyperreflectivity, prominent bright nucleoli, and mitotic figures) compared to 18 benign conjunctival lesions. Based on our experience we agree that hyperreflectivity, prominent bright nucleoli, and mitotic figures are not in vivo reflectance confocal microscopy valid criteria for SCC. Irregular cell size is a difficult criterion to be evaluated

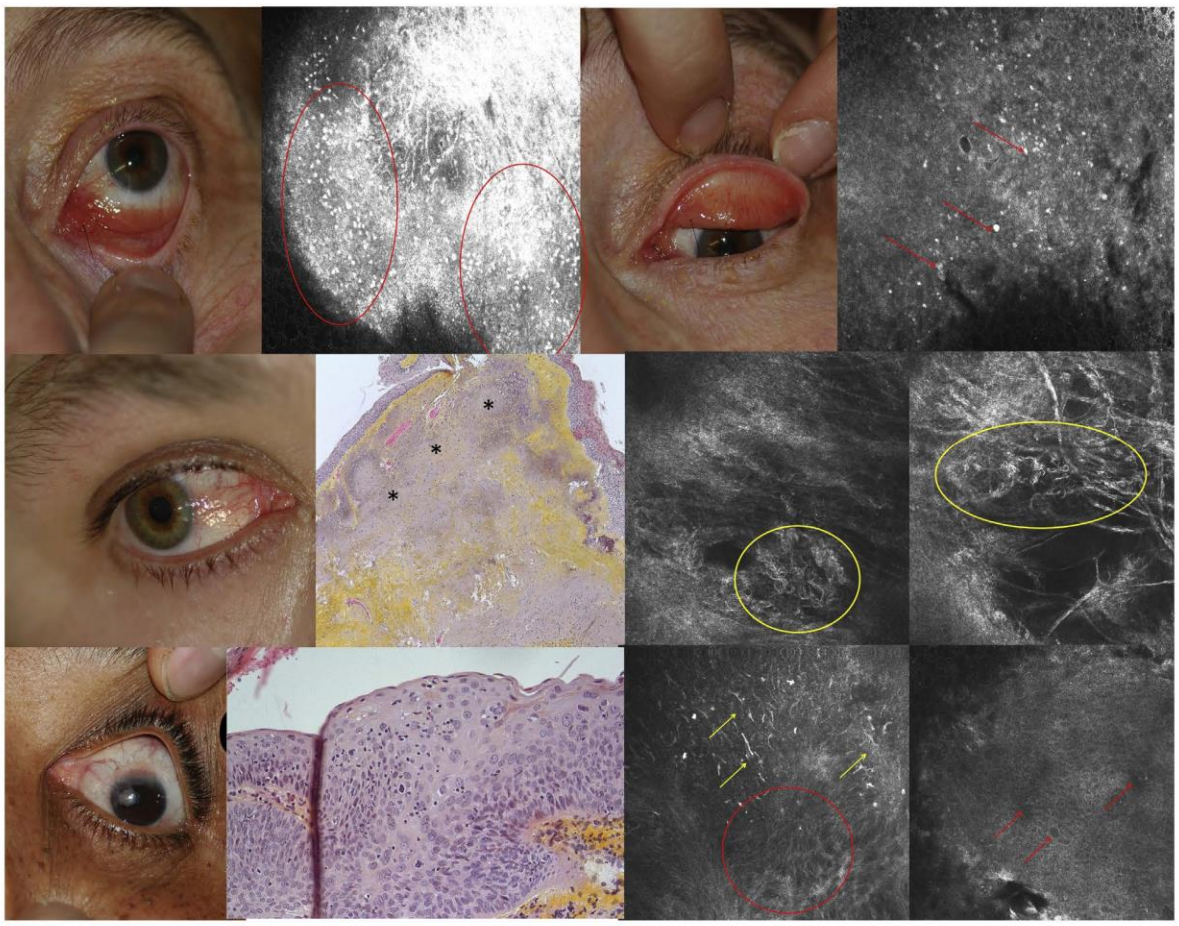

FIGURE 4. Clinical and handheld reflectance confocal microscopy appearance of a mucosa-associated lymphoid tissue lymphoma (First line) of the superior (Left) and inferior (Right) tarsal conjunctiva; clinical (Left), histologic (Center), and reflectance confocal microscopy (Right) appearance of a pinguecula (Second line); and a squamous cell carcinoma (Third line). Reflectance confocal microscopy shows in the lymphoma (First line) widespread small hyperrefractive roundish cells corresponding to tumoral lymphocytes in the stroma (red arrow and circle); in the pinguecula (Second line) degenerated stromal collagen with a coiled shape (yellow circle) that corresponds to homogenized areas of collagen in the histologic examination (black asterisk); in the squamous cell carcinoma (Third line) a disarranged pattern of the epithelium (red circle) with some large epithelial cells (red arrow) and abundant dendritic cells (yellow arrow). (Histologic stains: hematoxylin-eosin, second line 10×, third line 40×.)

because epitheliocytes are not completely regular in form and size in physiologic conditions; moreover, the extent of irregularity that is considered pathologic should be defined. For these reasons in our series we only look for the presence of large epithelial cells (>20 μm). In case of advanced SCC, the irregularity of the cells is more evident and a completely disarranged pattern can be observed, corresponding to epitheliocytes that are completely distorted in their shape and organization. However, we should notice that pterygium can sometimes present dysplastic and pleomorphic cells at histology.[26,27] Therefore, although in our small series epithelial cells of pterygium were not large in size and pleomorphic, and pterygium could be differentiated from SCC, large cells could be eventually found in these lesions, and this aspect could point out lesions with epithelial atypia that could be associated with ocular surface squamous neoplasia[27] and need surgical excision. We should also notice that in our study in vivo reflectance confocal microscopy images were interpreted in real time during the examination, whereas in the study of Nguena and associates[21] in vivo reflectance confocal microscopy images were read retrospectively masked to the clinical appearance.

In all cases of melanoma we found enlarged hyperreflective cells, roundish or dendritic, in the epithelium and/or the stroma, corresponding to malignant melanocytes (Figure 3). These cells were uneven in size and sometimes enlarged nuclei were visible as central hyporeflective areas.

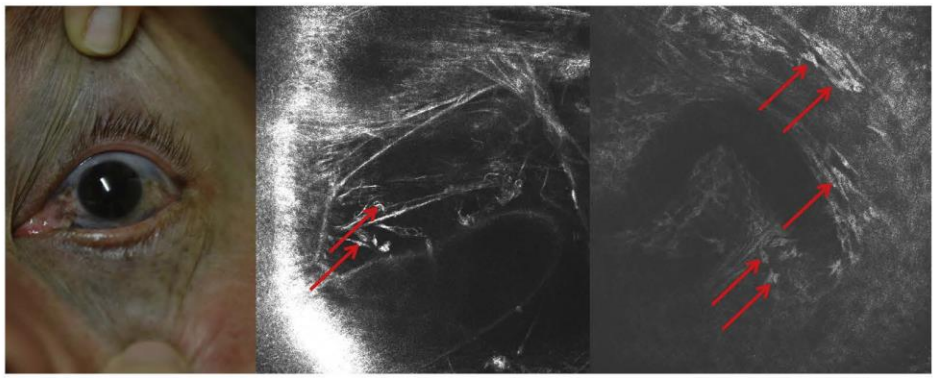

FIGURE 5. Clinical (Left) and handheld reflectance confocal microscopy (Center and Right) appearance of a nevus of Ota. Handheld reflectance confocal microscopy of the conjunctival part of the nevus showed large homogeneous dendritic bright cells (red arrow) between the collagen fibers.

FIGURE 6. Clinical (Left) and handheld reflectance confocal microscopy (Right) aspect of primary acquired melanosis without atypia. Handheld reflectance confocal microscopy shows homogeneous hyperreflective cells confined to the basal layer of the epithelium.

Messmer and associates[5] have already demonstrated in a study on 28 lesions that in vivo reflectance confocal microscopy had a high sensitivity and specificity for the melanocytic lesions of the conjunctiva, finding a sensitivity of 89% and a specificity of 100% for melanoma. They misdiagnosed only 1 lesion over 28, diagnosing PAM with atypia in a challenging lesion that histology classified as melanoma/PAM with atypia. With our study we confirmed the diagnostic ability of in vivo reflectance confocal microscopy for melanocytic lesions and we confirmed that in vivo reflectance confocal microscopy can also identify melanocytes as hyperreflective cells in amelanotic melanocytic lesions (3 in our series, 1 melanoma and 2 nevi). Concerning the 6 patients with conjunctival melanomas, 3 had a previous history of ocular melanoma (2 uveal, 1 of the eyelid), and 4 had a multifocal conjunctival involvement, indicating that in vivo reflectance confocal microscopy can be a useful imaging technique to monitor patients with a history of melanoma and multifocal lesions.

The in vivo reflectance confocal microscopy aspect of MALT lymphoma has already been reported by Pichierri and associates,[9] consisting of highly reflective small-size roundish cells arranged diffusely or in nests at epithelial and subepithelial conjunctival levels. In our 2 cases we found the same kind of cells in the stroma (Figure 4), but in vivo reflectance confocal microscopy could not identify cytologic atypia in order to distinguish tumoral from inflammatory cells. Therefore, in vivo reflectance confocal microscopy could point out the necessity of a histologic examination in case of an evocative aspect of lymphoma, but the final diagnosis should be left to histology.

Considering the excellent diagnostic ability with the use of in vivo reflectance confocal microscopy for conjunctival malignant tumors and the fact that conjunctival surgery could be disturbing for the patient, we decided not to excise 30 lesions that were considered benign by in vivo reflectance confocal microscopy. These lesions were diagnosed as nevus in 20 cases, a nevus of Ota in 2 cases, pterygium

in 2 cases, and PAM without atypia in 6 cases. The follow-up during at least 12 months of all these lesions did not show any clinical progression. In the 2 cases of nevus of Ota the exploration of the entire nevus was possible, differently from what is done performing focal biopsies of clinically suspicious areas. The aspect of nevus of Ota (Figure 5) has never been described using in vivo reflectance confocal microscopy, and we found large homogeneous dendritic bright cells between the collagen fibers that could be either isolated or grouped in clusters and could also be found in apparently uninvolved conjunctiva. The absence of malignant transformation was assessed by the absence of polymorphic hyperreflective cells, uneven in size and shape, suggestive of malignant melanocytes.

In conclusion, our pilot study strongly suggests that handheld in vivo reflectance confocal microscopy can be efficiently employed for a noninvasive and rapid investigation of the conjunctiva, including melanoma, SCC, and MALT lymphoma. To date, the diagnosis of conjunctival lesions has been based on the slit-lamp appearance and surgery was performed in all suspicious cases. In our series most lesions could be accurately diagnosed clinically by their slit-lamp appearance, but some were either under- or over-diagnosed. Handheld in vivo reflectance confocal microscopy is an additional tool that can add information to the clinical examination in order to proceed with more evidence to the surgical excision. Although in vivo reflectance confocal microscopy does not replace histologic examination for definitive diagnosis, it can avoid unnecessary surgery in patients who cannot undergo surgery, such as elderly or debilitated patients. Moreover, in cases of large or multifocal lesions it allows exploration of an entire lesion differently from a biopsy.

Larger multicenter studies should now be performed to validate our data and better define the diagnostic capability of handheld in vivo reflectance confocal microscopy. In particular, diagnosis performances should be compared with ophthalmologic in vivo reflectance confocal microscopy, and management using this advanced handheld in vivo reflectance confocal microscopy should be compared to the conventional management using slit-lamp examination and biopsies.

ALL AUTHORS HAVE COMPLETED AND SUBMITTED THE ICMJE FORM FOR DISCLOSURE OF POTENTIAL CONFLICTS OF INTEREST and the following were reported. G.T. and P.G. are consultants for Théa Laboratories and Quantel Medical. J.-L.P., B.L., and F.C. are consultants for Leo Pharma, Pierre Fabre, LVMH, MSD, Amgen, Pfizer, and Roche Laboratories. Funding was provided through the Groupement Interregional pour la recherche Clinique Rhône-Alpes Auvergne (GIRCI RAA) (Lyon, France) 2012 Young Investigator award. Contributions of authors: design and conduct of the study (E.C., J.-L.P., B.L., N.C., M.E., D.G., G.T., P.G., C.D., C.A., F.C.); collection of data, management (E.C., J.-L.P., B.L., N.C., M.E., D.G., G.T., P.G., C.D., C.A., M.H.); analysis and interpretation of the data (E.C., J.-L.P., B.L.); preparation of the manuscript (E.C.); review and approval of the manuscript (E.C., J.-L.P., B.L., N.C., M.E., D.G., G.T., P.G., C.D., C.A., M.H., F.C.).

REFERENCES

1. Maschi C, Caujolle J-P, Liolios I, Costet C. Benign conjunctival tumors. *J Fr Ophtalmol* 2013;36(9):796–802.
2. Falke K, Zhivov A, Zimpfer A, Stachs O, Guthoff RF. Diagnosis of conjunctival neoplastic lesions by confocal in-vivo microscopy. *Klin Monatsblätter* Für Augenheilkd 2012; 229(7):724–727.
3. Folberg R, Jakobiec FA, Bernardino VB, Iwamoto T. Benign conjunctival melanocytic lesions. Clinicopathologic features. *Ophthalmology* 1989;96(4):436–461.
4. Ranty M-L, Quintyn J-C, Uro-Coste E, Delisle M-B. Ocular conjunctival pathology. A ten-year retrospective study in Toulouse-Rangueil University Hospital and literature review. *Ann Pathol* 2012;32(3):170–176.
5. Messmer EM, Mackert MJ, Zapp DM, Kampik A. In vivo confocal microscopy of pigmented conjunctival tumors. *Graefes Arch Clin Exp Ophthalmol* 2006;244(11):1437–1445.
6. Duchateau N, Hugol D, D'Hermies F, et al. Contribution of in vivo confocal microscopy to limbal tumor evaluation. *J Fr Ophtalmol* 2005;28(8):810–816.
7. Xu Y, Zhou Z, Xu Y, et al. The clinical value of in vivo confocal microscopy for diagnosis of ocular surface squamous neoplasia. *Eye (Lond)* 2012;26(6):781–787.
8. Parrozzani R, Lazzarini D, Dario A, Midena E. In vivo confocal microscopy of ocular surface squamous neoplasia. *Eye (Lond)* 2011;25(4):455–460.
9. Pichierri P, Martone G, Loffredo A, Traversi C, Polito E. In vivo confocal microscopy in a patient with conjunctival lymphoma. *Clin Experiment Ophthalmol* 2008;36(1):67–69.
10. Cinotti E, Perrot JL, Labeille B, Adegbidi H, Cambazard F. Reflectance confocal microscopy for the diagnosis of vulvar melanoma and melanosis: preliminary results. *Dermatol Surg* 2012;38(12):1962–1967.
11. Cinotti E, Chol C, Perrot JL, Labeille B, Forest F, Cambazard F. Anal melanosis diagnosed by reflectance confocal microscopy. *Australas J Dermatol* 2013; http://dx.doi.org/10.1111/ajd.12096.
12. Cinotti E, Perrot JL, Labeille B, Douchet C, Mottet N, Cambazard F. Laser photodynamic treatment for in situ squamous cell carcinoma of the glans monitored by reflectance confocal microscopy. *Australas J Dermatol* 2014; 55(1):72–74.
13. Debarbieux S, Perrot JL, Erfan N, et al. Reflectance confocal microscopy of mucosal pigmented macules: a review of 56 cases including 10 macular melanoma. *Br J Dermatol* 2014; 170(6):1276–1284.
14. Erfan N, Hofman V, Desruelles F, et al. Labial melanotic macule: a potential pitfall on reflectance confocal microscopy. *Dermatol Basel Switz* 2012;224(3):209–211.
15. Guitera P, Menzies SW, Longo C, Cesinaro AM, Scolyer RA, Pellacani G. In vivo confocal microscopy for diagnosis of melanoma and basal cell carcinoma using a two-step method: analysis of 710 consecutive

clinically equivocal cases. *J Invest Dermatol* 2012;132(10): 2386–2394.
16. Langley RGB, Burton E, Walsh N, Propperova I, Murray SJ. In vivo confocal scanning laser microscopy of benign lentigines: comparison to conventional histology and in vivo characteristics of lentigo maligna. *J Am Acad Dermatol* 2006;55(1):88–97.
17. Rishpon A, Kim N, Scope A, et al. Reflectance confocal microscopy criteria for squamous cell carcinomas and actinic keratoses. *Arch Dermatol* 2009;145(7):766–772.
18. Niederer RL, McGhee CNJ. Clinical in vivo confocal microscopy of the human cornea in health and disease. *Prog Retin Eye Res* 2010;29(1):30–58.
19. Wang Y, Le Q, Zhao F, Hong J, et al. Application of in vivo laser scanning confocal microscopy for evaluation of ocular surface diseases: lessons learned from pterygium, meibomian gland disease, and chemical burns. *Cornea* 2011;30(Suppl 1):S25–S28.
20. Zhivov A, Stachs O, Kraak R, Stave J, Guthoff RF. In vivo confocal microscopy of the ocular surface. *Ocul Surf* 2006; 4(2):81–93.
21. Nguena MB, van den Tweel JG, Makupa W, et al. Diagnosing ocular surface squamous neoplasia in East Africa: case-control study of clinical and in vivo confocal microscopy assessment. *Ophthalmology* 2014;121(2):484–491.
22. Messmer EM, Mackert MJ, Zapp DM, Kampik A. In vivo confocal microscopy of normal conjunctiva and conjunctivitis. *Cornea* 2006;25(7):781–788.
23. Efron N, Al-Dossari M, Pritchard N. In vivo confocal microscopy of the palpebral conjunctiva and tarsal plate. *Optom Vis Sci* 2009;86(11):E1303–E1308.
24. Efron N, Al-Dossari M, Pritchard N. In vivo confocal microscopy of the bulbar conjunctiva. *Clin Experiment Ophthalmol* 2009;37(4):335–344.
25. Shields CL, Shields JA. Tumors of the conjunctiva and cornea. *Surv Ophthalmol* 2004;49(1):3–24.
26. Golu T, Mogoantă L, Streba CT, et al. Pterygium: histological and immunohistochemical aspects. *Romanian J Morphol Embryol Rev* 2011;52(1):153–158.
27. Chui J, Coroneo MT, Tat LT, Crouch R, Wakefield D, Di Girolamo N. Ophthalmic pterygium. *Am J Pathol* 2011; 178(2):817–827.

5.a 3 In vivo confocal microscopy of pine processionary caterpillar hair-induced keratitis.

MS NO: CORNEA-D-14-00691

CASE REPORT

In Vivo Confocal Microscopy of Pine Processionary Caterpillar Hair–Induced Keratitis

Rémy Jullienne, MD, Zhiguo He, PhD,† Pierre Manoli, MD,* Damien Grivet, MD,* Elisa Cinotti, MD,‡ Jean Luc Perrot, MD,‡ Bruno Labeille, MD,‡ Frédéric Cambazard, MD,‡ Philippe Gain, MD, PhD,*† and Gilles Thuret, MD, PhD*†§*

Purpose: Multimodal imaging of processionary caterpillar hair induced keratitis with anterior segment optical coherence tomography and in vivo confocal microscopy.

Methods: Case report.

Results: A 25-year-old woman presented with acute keratitis induced by multiple tiny processionary caterpillar hairs. She initially experienced severe pain and moderate vision loss, which gradually improved within a few weeks. Diagnosis was confirmed by in vivo confocal microscopy showing a pathognomonic image strictly comparable with ex vivo microscopy photography.

Conclusions: To the best of our knowledge, this is the first case of corneal in vivo confocal imaging of a caterpillar hair with confirmation by ex vivo microscopy.

Key Words: cornea, human, in vivo confocal microscopy, keratitis, caterpillar hair

(*Cornea* 2014;00:1 3)

The pine processionary caterpillar, *Thaumetopoea pityocampa*, is a forest pest and human health hazard affecting the eyes, skin, and respiratory tract. Global warming has caused its range to extend northward,[1] and further human populations are now exposed to it in late winter and early spring. Pathogenesis is attributed to the thousands of microscopic hairs covering the caterpillar's body, which are truly airborne weapons. The adverse reaction is linked to the mechanical effect of the harpoon-shaped hairs, to direct toxicity of thaumetopoein toxin present inside the setae, and to an allergic immunoglobulin E-mediated reaction to various caterpillar proteins.[2] Ocular exposure gives variable manifestations referred to as *ophthalmia nodosa*: unspecific conjunctivitis, keratitis, uveitis, vitritis, retinochoroiditis, or endophthalmitis.[3] Diagnosis is based on direct visualization of the hairs, clinical history, and environmental conditions. We evaluate multimodal anterior segment imaging of processionary caterpillar hair–induced keratitis in a young adult and describe the pathognomonic aspect in in vivo confocal microscopy (IVCM).

CASE REPORT

We report the case of a 25-year-old woman who presented at our clinic in February 2014 with severe acute pain, photophobia, and loss of vision in her left eye since that morning. She had no past medical or ocular history and worked in a horse-riding school. She had been cleaning the stable 1 hour before the foreign body sensation started, and the pain gradually increased over the next few hours. On admission, her best-corrected visual acuity was 20/50 in her left eye and 20/20 in her right eye. Slit-lamp examination of her left eye was remarkable for a cluster of approximately 50 tiny linear foreign bodies embedded in the epithelium and stroma (Fig. 1), associated with corneal edema, conjunctival chemosis, and eyelid edema. The foreign bodies were located at varying stromal depth, but none was observed inside the anterior chamber by gonioscopy. Intraocular pressure and fundus examination were normal. The right eye was normal.

We initially performed multimodal anterior segment imaging comprising anterior segment optical coherence tomography (AS-OCT) using the Spectralis Anterior Segment Module (Heidelberg Engineering GmbH, Heidelberg, Germany), specular microscopy (SP3000; Topcon, Tokyo, Japan), and IVCM using 2 devices: (1) the Heidelberg Retina Tomograph III Rostock Cornea Module (Heidelberg), an ophthalmic IVCM, and (2) the VivaScope 3000 (Caliber, New York, distributed in Europe by MAVIG GmbH, Munich, Germany), a handheld dermatological IVCM, working with a 830-nm diode laser, which we pioneered for use in ophthalmological examination. Corneal contact IVCM examinations were performed under topical anesthesia. All these tests were repeated during the follow-up. The patient was immediately administered topical dexamethasone, tobramycin, and lubricant eye drops every hour, cycloplegia with atropine 3 times daily, and pain medications. Daily subconjunctival injection of dexamethasone was also given during the first 3 days. On examination, prominent corneal nerves were visible around the caterpillar hairs. Gentle epithelial debridement under general anesthesia was scheduled the next day; the patient refused local anesthesia. During surgery, only 20% of the hairs could be removed and a few intact specimens were sent to our laboratory

Received for publication October 1, 2014; revision received November 9, 2014; accepted November 23, 2014. Published online ahead of print XX XX, XXXX.

From the *Department of Ophthalmology, University Hospital, Saint-Etienne, France; †Corneal Graft Biology, Engineering and Imaging Laboratory, EA2521, Federative Institute of Research in Sciences and Health Engineering, Faculty of Medicine, Jean Monnet University, Saint-Etienne, France; ‡Department of Dermatology, University Hospital, Saint-Etienne, France; and §Institut Universitaire de France, Paris, France.

The authors have no funding or conflicts of interest to disclose.

Reprints: Gilles Thuret, MD, PhD, Corneal Graft Biology, Engineering and Imaging Laboratory, EA 2521, SFR143, Faculty of Medicine, Jean Monnet University, 15, Rue Ambroise Paré, F 42023 Saint-Etienne Cedex 2, France (e-mail: gilles.thuret@univ-st-etienne.fr).

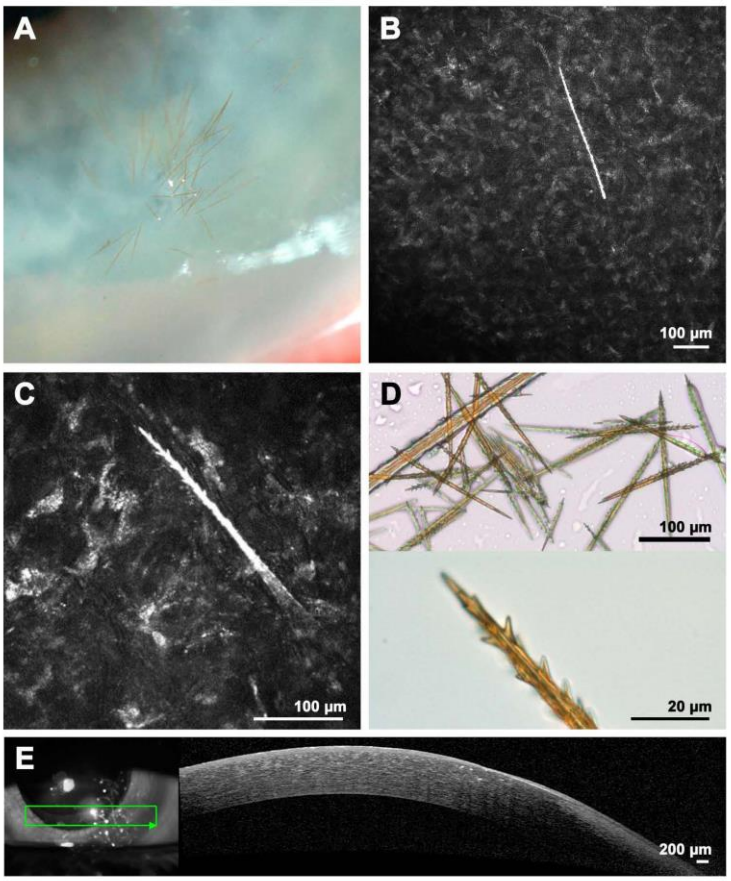

FIGURE 1. Multimodal imaging of the caterpillar hairs. A, Slit-lamp examination of the inferior part of the cornea (magnification, ×30). At admission, a cluster of tiny brown spindle-shaped foreign bodies was clearly visible. B, IVCM performed with the handheld dermatological Vivascope 3000 showed a linear highly hyperreflective foreign body with serrated edges within the stroma, measuring 430 μm long, at a depth of 150 μm, corresponding to a caterpillar hair. C, Heidelberg HRTIII-RCM IVCM showing another caterpillar hair with small spikes clearly visible at the edges and oriented toward the tip. D, For comparison, bright field microscopy of caterpillar hairs removed from a caterpillar, showing hairs of different sizes (top) and zoom on the end of 1 hair removed from the cornea revealing identical spikes protruding from the stalk (bottom). E, Anterior segment OCT Heidelberg showing several hyperreflective points with posterior shadows lying within the anterior stroma.

for microscopic photography (IX81; Olympus, Tokyo, Japan). The remaining hairs were too deep within the stroma and were thus closely observed.

IVCM revealed the very particular aspect of the caterpillar hairs, which was strictly identical to the specimens sent for microscopic photography (Fig. 1). AS-OCT showed hyperreflective spots corresponding to foreign bodies at various depths inside the stroma. Specular microscopy on both eyes was unremarkable. After 4 days, corneal edema had resolved and a minor foreign body sensation persisted. Visual acuity had improved to 20/25. The topical dexamethasone and tobramycin dosage was gradually reduced over time. At 4 months follow-up, no intracamerular or vitreous migration was observed. Some hairs had spontaneously extruded, whereas others formed epithelial and stromal scars.

DISCUSSION

IVCM is extremely useful for exploring anterior segment diseases. In our case, the IVCM images obtained were pathognomonic for processionary caterpillar hairs. This diagnosis was highly suspected after slit-lamp examination, and then confirmed by IVCM. In situations such as edematous cornea or inflammatory conjunctival granuloma, foreign bodies may not be easily visible on slit lamp, therefore IVCM could be useful for initial workup and be repeated during follow-up. Our patient was tested with 2 IVCMs: a standard ophthalmic IVCM and a handheld dermatology Vivascope 3000 (larger examination field), initially designed for dermatologists but which we pioneered for use in routine ophthalmological examination as its handling allows easy exploration of the whole ophthalmological sphere (eyeball surface and adnexa). We are presently investigating a range of anterior segment diseases in daily practice by combining the advantages of each machine. IVCM is not readily available in all eye centers; however, specific training and practice in image acquisition and analysis are needed.[8] Furthermore, both IVCMs that we use require corneal contact, which causes

AU1

great discomfort in patients with pain, photophobia, and eyelid edema.

The pathognomonic microscopic aspect of the hair, consisting of a series of spike-like structures fixed to the central stalk and oriented toward the tip, was clearly visualized by IVCM and by laboratory microscopy. This image was similar in all aspects to the structure of *Thaumetopoea pityocampa* hairs described previously.[5] This specific harpoon shape partly explains its pathogenesis, facilitating stromal penetration though barely accessible for surgical removal. Indeed, when the hairs were pulled out with forceps, most broke into smaller fragments inside the stroma, which may accentuate the inflammatory reaction by releasing additional toxins.

Caterpillar hair–induced keratitis is associated with massive inflammatory response that needs high doses of topical corticosteroids.[6] In such conditions, as with infectious or inflammatory keratitis, corneal nerve enlargement is frequently observed. These nerves are clearly visible by IVCM, and their characteristics have previously been described in different conditions.[7] These caterpillar hairs should not be mistaken for enlarged corneal nerves by IVCM. The sole description of the IVCM aspect of a caterpillar hair in the literature[8] may be misleading, because it is more suggestive of a prominent corneal nerve. The IVCM characteristics of corneal nerves and of caterpillar hair should be distinguished according to size, reflectivity, presence of branching, tip shape, and presence of spikes on the central stalk. The hairs are usually 100 to 500 μm long with very high reflectivity, no branching, a triangular tip, and pathognomonic spikes.

We also performed AS-OCT to assess the depth of the hairs inside the cornea, which was described as the main risk factor for intraocular penetration in a series of 544 cases of caterpillar hair–induced ophthalmitis.[9] AS-OCT was initially useful to locate the most superficial hairs potentially accessible to surgical removal, and was repeated during follow-up to monitor posterior progression of the hairs. Specular microscopy was performed to observe any corneal endothelial damage, as previously reported,[10] but endothelial cell density did not significantly decrease in our patient.

To the best of our knowledge, this is the first description of pathognomonic IVCM images of pine processionary caterpillar hairs. Ophthalmologists should be aware of this ocular hazard, which due to climate change is increasingly common in western and northern Europe.

REFERENCES

1. Battisti A, Stastny M, Netherer S, et al. Expansion of geographic range in the pine processionary moth caused by increased winter temperatures. *Ecol Appl.* 2005;15:2084–2096.
2. Vega J, Vega JM, Moneo I. Skin reactions on exposure to the pine processionary caterpillar (Thaumetopoea pityocampa) [in Spanish]. *Actas Dermosifiliogr.* 2011;102:658–667.
3. Cadera W, Pachtman MA, Fountain JA, et al. Ocular lesions caused by caterpillar hairs (ophthalmia nodosa). *Can J Ophthalmol.* 1984;19:40–44.
4. Patel DV, McGhee CN. Quantitative analysis of in vivo confocal microscopy images: a review. *Surv Ophthalmol.* 2013;58:466–475.
5. Petrucco Toffolo E, Zovi D, Perin C, et al. Size and dispersion of urticating setae in three species of processionary moths. *Integr Zool.* 2014;9:320–327.
6. Portero A, Carreño E, Galarreta D, et al. Corneal inflammation from pine processionary caterpillar hairs. *Cornea.* 2013;32:161–164.
7. Cruzat A, Pavan-Langston D, Hamrah P. In vivo confocal microscopy of corneal nerves: analysis and clinical correlation. *Semin Ophthalmol.* 2010;25:171–177.
8. Fournier I, Saleh M, Beynat J, et al. Cornea imagery and keratitis caused by processionary caterpillar hairs. *J Fr Ophtalmol.* 2011;34:164–167.
9. Sengupta S, Reddy PR, Gyatsho J, et al. Risk factors for intraocular penetration of caterpillar hair in ophthalmia nodosa: a retrospective analysis. *Indian J Ophthalmol.* 2010;58:540–543.
10. Campolmi N, Gauthier AS, Cinotti E, et al. Specular microscopic analysis of endothelial wound healing after trauma from pine processionary caterpillar hairs: Pediatric case report. *J Fr Ophtalmol.* 2014;37:e83–e85.

5.a 4 Contribution of reflectance confocal microscopy in the diagnosis of eyelid dermal nevus

Annales de dermatologie et de vénéréologie (2015) 142, 226—228

ELSEVIER MASSON

Disponible en ligne sur ScienceDirect www.sciencedirect.com

Elsevier Masson France EM|consulte www.em-consulte.com

Formation médicale continue

DOCUMENT ICONOGRAPHIQUE

Apport de la microscopie confocale par réflectance dans le diagnostic de nævus dermique palpébral

Contribution of reflectance confocal microscopy in the diagnosis of eyelid dermal nevus

E. Cinotti[a,*], J.-L. Perrot[a], B. Labeille[a], D. Grivet[c], C. Habougit[b], C. Douchet[b], F. Cambazard[a], Groupe imagerie cutanée non invasive/ICNI de la SFD

[a] *Service de dermatologie, hôpital universitaire de Saint-Étienne, 42055 Saint-Étienne cedex 2, France*
[b] *Service d'anatomopathologie, hôpital universitaire de Saint-Étienne, 42055 Saint-Étienne cedex 2, France*
[c] *Service d'ophtalmologie, hôpital universitaire de Saint-Étienne, 42055 Saint-Étienne cedex 2, France*

Reçu le 1er octobre 2014 ; accepté le 9 janvier 2015
Disponible sur Internet le 23 février 2015

Observation

Un homme de 76 ans était adressé par son ophtalmologue pour une tumeur ancienne du bord libre de la paupière inférieure droite ayant augmenté de taille récemment et occasionnant une gêne mécanique. Il s'agissait d'une tumeur rosée de 5 mm de diamètre et il n'y avait pas de madarose en regard (Fig. 1). Le patient avait pour principal antécédent un mélanome dorsal de type SSM mesurant 0,37 mm d'épaisseur opéré il y 8 ans.

* Auteur correspondant.
Adresse e-mail : elisacinotti@gmail.com (E. Cinotti).

http://dx.doi.org/10.1016/j.annder.2015.01.003

Un examen en dermatoscopie montrait des télangiectasies fines en périphérie de la tumeur sur un fond homogène blanchâtre avec présence de structures à type de granulations et de globules bruns irréguliers répartis de manière asymétrique.

Microscopie confocale par réflectance

Un examen en microscopie confocale (MC) in vivo (Vivascope 3000®; Caliber Inc., Rochester, NY, États-Unis, distribué en France par Mavig, Munich) était réalisé pour orienter le diagnostic. On constatait la présence d'un épiderme d'aspect en nid d'abeille régulier sans présence de cel-

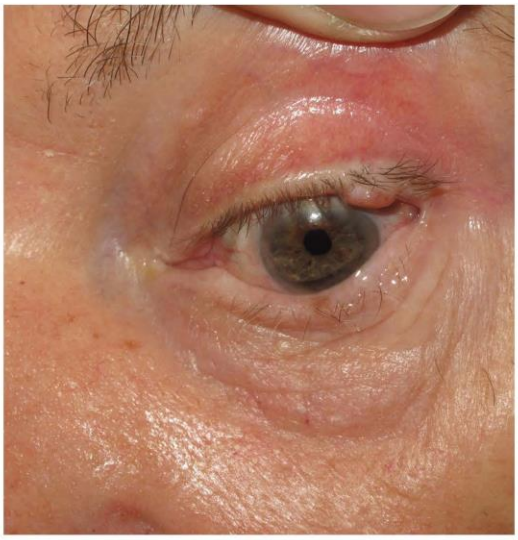

Figure 1. Examen clinique de la tumeur rosée du bord libre de la paupière supérieure gauche.

lule pagétoïde. Dans le derme superficiel on mettait en évidence la présence d'amas de grosses cellules rondes, hyper-reflétantes, monomorphes et cohésives dans des papilles dermiques élargies. On ne retrouvait pas de cellule atypique (de forme et taille irrégulières) à la jonction dermo-épidermique (JDE) et dans le derme superficiel (Fig. 2A), aspect qui a été confirmé par l'examen histologique (Fig. 2B).

Une exérèse par résection pentagonale transfixiante de la paupière supérieure gauche était réalisée sous anesthésie locale du fait de la gêne mécanique engendrée par l'augmentation de taille de la tumeur.

Nous avons procédé à un examen en MC ex vivo peropératoire d'une tranche de section sagittale de la tumeur. Nous constations la présence d'amas de cellules hyper-reflétantes régulières dans le derme superficiel sans présence de cellule pagétoïde ni de prolifération mélanocytaire atypique à la JDE et dans le derme (Fig. 3A).

Un examen histologique était ensuite réalisé sur la pièce d'exérèse qui montrait (Fig. 2B et 3B) la présence d'amas mélanocytaires réguliers dans le derme superficiel.

Commentaires

Un examen en MC in vivo a été réalisé compte tenu de l'augmentation de taille récente de la lésion et de l'aspect dermatoscopique chez un patient ayant comme principal antécédent l'exérèse d'un mélanome. En particulier, nous avons utilisé le MC à type de camera portable qui grâce à son petit embout permet l'examen des zones d'accès difficile comme les muqueuses. La MC a permis de visualiser des amas intradermiques de cellules denses (« clods ») [1] sans prolifération cellulaire atypique au sein de l'épiderme, de la JDE et du derme [2]. Les cellules nævi ques se présentaient comme des cellules hyper-reflétantes rondes, homogènes en taille et forme, cohésives, différentes des cellules de mélanome qui ont une forme et une taille irrégulières. Le diagnostic de mélanome a pu être éliminé devant l'absence de cellules atypiques (irrégulières en taille et forme, de taille encore plus importante) dans l'épiderme, à la JDE ou dans le derme. D'autre part, le diagnostic de carcinome basocellulaire a pu être éliminé devant l'absence d'amas cellulaires à bord palissadique, peu reflétants, appendus à l'épiderme et volontiers entourés par des arcs périphériques optiquement vides [3,4].

Pour l'examen des muqueuses, il est nécessaire d'appliquer sur l'embout de la camera un film de protection transparent stérile et du gel larme [3] qui a des propriétés optiques différentes de l'huile utilisée sur la peau mais celle-ci occasionnerait des sensations de brûlures oculaires. L'utilisation de ces dispositifs donne des images de 'résolution un peu moindre par rapport à celles

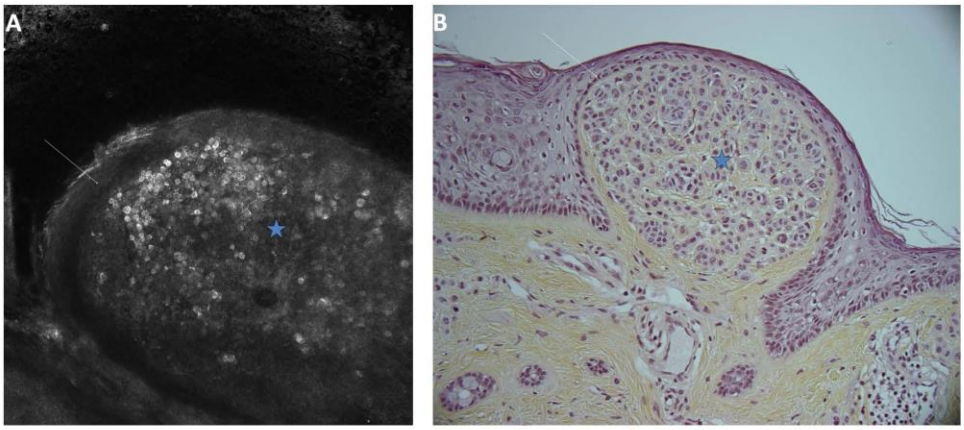

Figure 2. Aspect en microscopie confocale par réflectance in vivo (A) et en histologie (B) du nævus dermique. La microscopie confocale par réflectance in vivo (A) et l'examen histologique (B) avec coloration hématoxyline éosine (grossissement × 20) montrent un épiderme normal (flèche blanche) sans cellule atypique et des amas intradermiques de cellules nævi ques rondes régulières (étoiles).

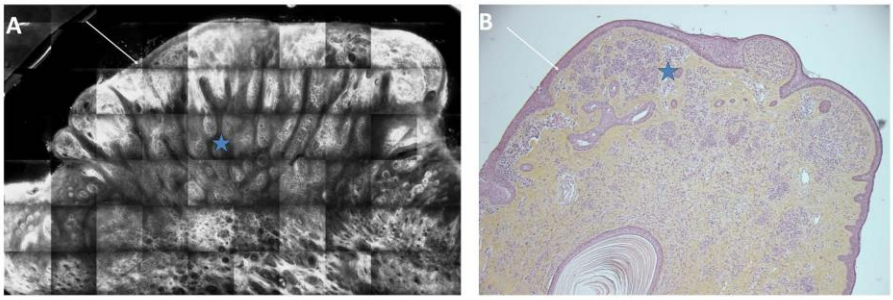

Figure 3. Aspect en microscopie confocale par réflectance ex vivo (A) et en histologie (B) du nævus dermique. La microscopie confocale par réflectance ex vivo d'une section sagittale (A) et l'examen histologique avec coloration hématoxyline éosine (grossissement × 10) montrent un épiderme normal sans cellule atypique (flèche blanche) et des amas intradermiques de cellules nævuques rondes régulières (étoiles).

habituellement obtenues pour la peau, mais suffisante pour reconnaître les différents types de cellules.

La MC ex vivo peropératoire nous a permis de trouver un aspect superposable à la MC in vivo. De plus, elle nous a permis d'observer la partie profonde de la tumeur, confirmant l'absence de prolifération tumorale atypique dans le derme profond, ce qui n'est pas possible en MC in vivo où l'observation arrive à 250 μm.

Notre groupe a récemment mis en valeur l'utilité de la MC in vivo pour les tumeurs du bord libre de la paupière où le diagnostic clinique et dermatoscopique est souvent difficile [3]. La paupière peut être le site de différentes tumeurs malignes d'origine épithéliale, mésenchymateuse, lymphoprolifératives, et endocrine [5] qui nécessitent souvent une biopsie ou une exérèse pour un diagnostic de certitude. En particulier en cas de nodule rosé ferme, le diagnostic différentiel entre nævus dermique, carcinome basocellulaire et tumeur annexielle peut être difficile comme dans notre cas [6]. L'exérèse des lésions de la paupière est complexe car elle doit préserver la fonction dynamique et de protection du globe oculaire, elle doit garantir le maintien d'un film lacrymal et d'un drainage lacrymal suffisant et doit tenir compte de l'aspect esthétique [5]. La MC in vivo peut permettre de limiter les biopsies et les exérèses diagnostiques avec un examen non invasif. D'autre part, la MC ex vivo peut permettre de confirmer le diagnostic et de contrôler les marges d'exérèse en phase peropératoire, avant la fermeture chirurgicale, en limitant les ré-interventions.

Déclaration d'intérêts

Les auteurs déclarent ne pas avoir de conflits d'intérêts en relation avec cet article.

Références

[1] Pellacani G, Scope A, Farnetani F, Casaretta G, Zalaudek I, Moscarella E, et al. Towards an in vivo morphologic classification of melanocytic nevi. J Eur Acad Dermatol Venereol 2014;28:864—72.
[2] Kanitakis J, Bahadoran P, Braun R, Debarbieux S, Labeille B, Perrot JL, et al. La microscopie confocale par réflectance in vivo en dermatologie : proposition de terminologie en langue française. Ann Dermatol Venereol 2013;140:678—86.
[3] Cinotti E, Perrot JL, Campolmi N, Labeille B, Espinasse M, Grivet D, et al. The role of in vivo confocal microscopy in the diagnosis of eyelid margin tumors: 47 cases. J Am Acad Dermatol 2014;71:912—8.
[4] Debarbieux S, Harou O, Thomas L, Au nom du groupe imagerie cutanée non invasive de la Société française de dermatologie. Carcinome baso cellulaire. Ann Dermatol Venereol 2013;140:725—7.
[5] Dekmezian MS, Cohen PR, Sami M, Tschen JA. Malignancies of the eyelid: a review of primary and metastatic cancers. Int J Dermatol 2013;52:903—26.
[6] Morel X, Meyer A, Le Rouic JF, Tahn Trong T, Behar-Cohen F, Halhal M, et al. Nevus mimicking a basal cell carcinoma of the eyelid. J Fr Ophtalmol 2002;25:657—60.

5.a 5 In vivo confocal microscopy for eyelids and ocular surface: a new horizon for dermatologists.

In vivo confocal microscopy for eyelids and ocular surface: a new horizon for dermatologists

TO THE EDITOR: In vivo confocal microscopy (IVCM) is an emerging non-invasive diagnostic technique that offers the evaluation of external body tissues at real time, with cellular resolution, and is increasingly used in dermatology for the examination of the skin.[1, 2] Until now dermatologists did not use IVCM to investigate the eye, although the eyelid, the ciliary margin and the conjunctiva also belong to the dermatologic field. Two IVCM are currently available in ophthalmology: the Confoscan 4 slit scanning confocal microscope (Nidek, Gamagori, Japan) and the laser scanning confocal microscope Heidelberg Retina Tomograph [3, 4] equipped with the Rostock Cornea Module (Heidelberg engineering GmbH, Heidelberg, Germany). These devices are mainly used to visualise cornea and more rarely the conjunctiva located near the sclerocorneal limbus. Because of limitations in the handiness of both microscopes, the rest of the conjunctiva, the ciliary margin and the entire eyelid have never been extensively studied.

We used for the first time the two IVCM dedicated to skin (VivaScope 1500 and 3000, Lucid Inc, Rochester, New York, distributed in Europe by MAVIG Gmb11, München, Germany) to explore eyelid and conjunctiva.

The handled camera (HC) VivaScope 3000, thanks to its good handiness, enables an easy exploration of the whole ocular area, in particular the palpebral conjunctiva (Figure 1), the ciliary margin, the lacrimal punctum, the internal and external canthi, and both surfaces of the eyelids comprising the Meibomian glands. All these regions have almost never been explored by IVCM before because of the limited mobility of devices available at present for ophthalmology. Of course, like both ophthalmology IVCM, the HC also enables examining cornea and bulbar conjunctiva. The IVCM aspect of the conjunctiva is analogue to the skin (Fig. 1) due to the similar anatomy of these tissues. The conjunctiva is formed by a stratified squamous epithelium with polygonal cells with hyper-reflective membranes that are analogue to skin keratinocytes, and by a stroma (lamina propria) with collagen fibers and vessels that is similar to the skin dermis. The main differences are that the epithelium is non-keratinized and therefore no stratum granulosum and corneum are present, that there are no hair follicles, and that the conjunctival stroma is less reflective than dermis under IVCM.

The multilaser camera (MLC) VivaScope 1500 permits examination in both reflectance and fluorescence with three different wavelength (488, 658 and 785 nm), thus fundamentally differing from the previous devices that have only one light source and do not allow fluorescence acquisition.

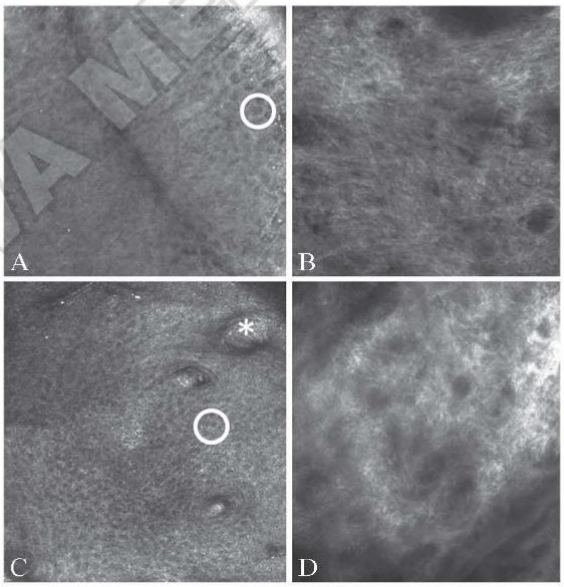

Figure 1.—*In vivo* confocal microscopy (IVCM) (VivaScope 3000) aspect of normal conjunctiva (A, B) compared with normal skin (~~B, C~~). The conjunctiva is composed by a stratified squamous epithelium (A) with polygonal cells with hyper-reflective membranes (~~white~~ circle) that are analogue to skin keratinocytes (~~red~~ circle) (C), and by an underlying stroma (B) that is similar to the skin dermis (D). Unlike the conjunctiva, in the skin hair follicles are present (C) (asterisk), and the dermal collagen (D) is more thick and more reflective ~~(B)~~.

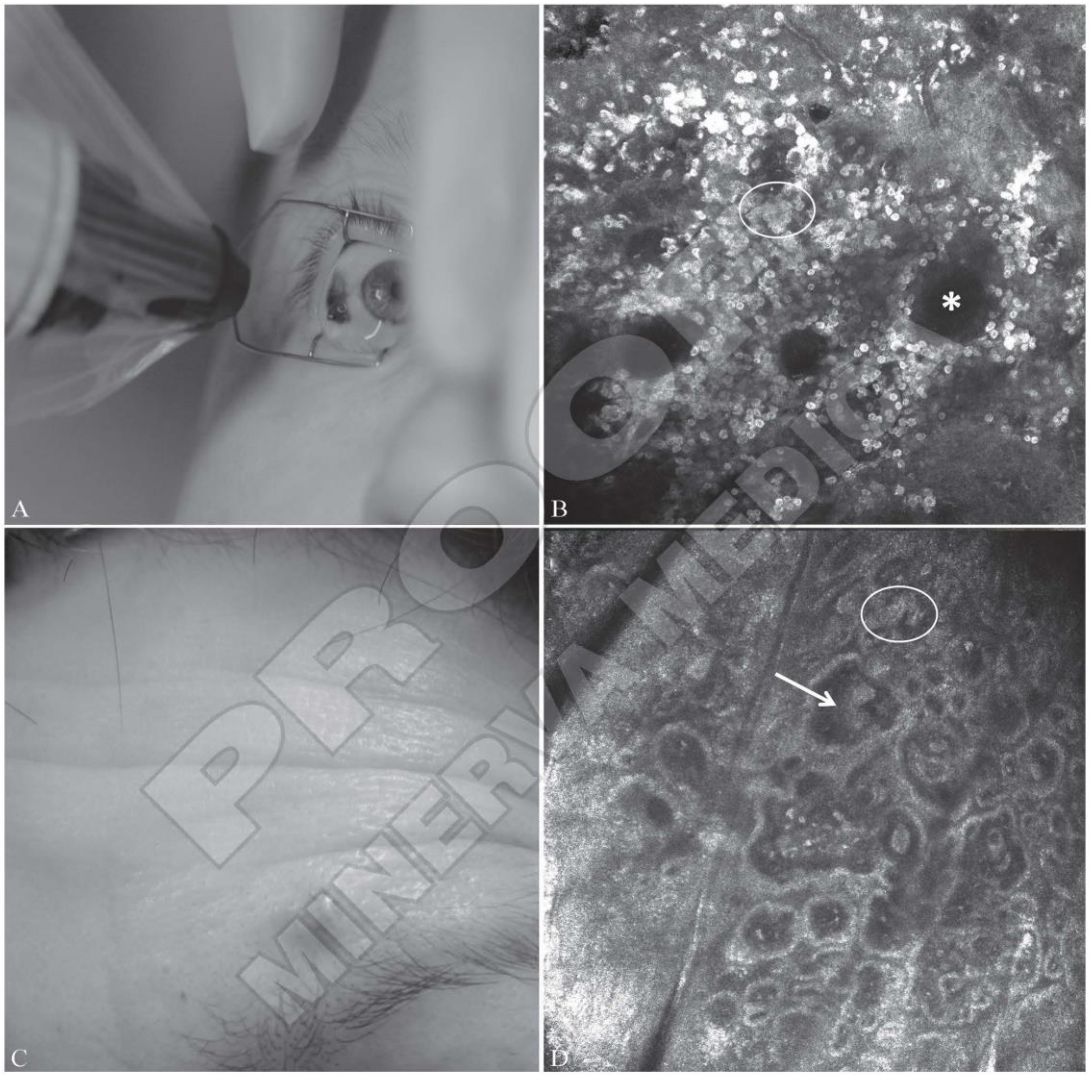

Figure 2.—Clinical and IVCM aspect of a conjunctival compound nevus (A, B) compared with a skin (C, D) compound nevus. Under IVCM, conjunctival nevus (B) shows sheets and small nests (~~red~~ circle) of hyper-reflective nevocytes in the epithelium and lamina propria, and dark cysts (asterisks) characteristic of benign conjuctival nevi. Under IVCM, skin nevus (~~B~~) shows nests of hyper-reflective melanocytes at the dermoepidermal junction (~~white~~ circle) and in the dermal papillae (arrow).

In order to use the MLC, we created an adapter between its tip and the ocular surface to reduce the diameter of the current tip made for the skin, while preserving its optic qualities. In addition, to avoid abrupt or involuntary movements of the patient, the investigator and the head of the camera, which could be dangerous for the ocular surface, we use a

chin support for the patient and created a hinged support for the MLC that allows 5 degrees of liberty and therefore a precise alignment in front of the region of interest.

We explored normal eyelid, conjunctiva and cornea, and neoplastic (squamous cell carcinomas, basal cell carcinomas, lentigos, nevi and melanomas), inflammatory, infectious and storage disease with ocular involvement. All the suspected malignant lesions have been excised and the histological examination confirmed the IVCM diagnosis in all cases.

We obtain high resolution images, comparable to those achievable with the skin (Figures 1, 2), but contrary to what happens in the skin, the lack of the stratum corneum on the mucosal surface enables to preserve the same optical resolution on the deeper layers.

The ~~MC~~ allows to explore the fluorescence characteristics of the ocular apparatus either spontaneously or after topical instillation or intravenous injection of fluorochromes already used in routine by ophthalmologists. Fluorochromes specifically stain cellular or tissular components that are unlikely to be discriminate only by reflectance confocal images.

In addition, there is a medico-economic interest of the ophthalmology applications of the IVCM devices initially dedicated to the skin: the same machine can be shared by dermatologists and ophthalmologists with a better cost benefit ratio for medical centers.

In conclusion, our preliminary experience suggests that IVCM used until now to examine the skin can be employed for the ocular surface and ocular adnexa analysis, establishing a connection between dermatology and ophthalmology in this field. Larger studies are now needed to evaluate these applications.

E. CINOTTI
Department of Dermatology,
University Hospital of Saint Etienne,
Saint Etienne, France
elisacinotti@gmail.com

J.-L. PERROT
Department of Dermatology,
University Hospital of Saint Etienne,
Saint Etienne, France

B. LABEILLE
Department of Dermatology,
University Hospital of Saint Etienne,
Saint Etienne, France

G. THURET
Department of Ophthalmology,
University Hospital of Saint Etienne,
Saint Etienne, France

M. ESPINASSE
Department of Ophthalmology,
University Hospital of Saint Etienne,
Saint Etienne, France

D. GRIVET
Department of Ophthalmology,
University Hospital of Saint Etienne,
Saint Etienne, France

P. GAIN
Department of Ophthalmology,
University Hospital of Saint Etienne,
Saint Etienne, France

C. DOUCHET
Department of Pathology,
University Hospital of Saint Etienne,
Saint Etienne, France

N. CAMPOLMI
Department of Ophthalmology,
University Hospital of Saint Etienne,
Saint Etienne, France

F. CAMBAZARD
Department of Dermatology,
University Hospital of Saint Etienne,
Saint Etienne, France

G ITAL DERMATOL VENEREOL 2014;149:1-2

References

1. Longo C, Zalaudek I, Argenziano G, Pellacani G. New directions in dermatopathology: in vivo confocal microscopy in clinical practice. Dermatol Clin 2012;30:799-814.
2. Ulrich M, Lange-Asschenfeldt S, Gonzalez S. Clinical applicability of in vivo reflectance confocal microscopy in dermatology. G Ital Dermatol Venereol 2012;147:171-8.
3. Wang Y, Le Q, Zhao F, Hong J, Xu J, Zheng T et al. Application of in vivo laser scanning confocal microscopy for evaluation of ocular surface diseases: lessons learned from pterygium, meibomian gland disease, and chemical burns. Cornea 2011;30:S25-8.
4. Niederer RL, McGhee CN. Clinical in vivo confocal microscopy of the human cornea in health and disease. Prog Retin Eye Res 2010;29:30-58.

5.a 6 In Vivo and Ex Vivo Confocal Microscopy for the Management of a Melanoma of the Eyelid Margin.

References

1. Yamamoto K. Treatment of thin linear scars on the scalp. Dermatol Surg 2015;41:1433–5.
2. Yamamoto K. Double trichophytic closure with wavy two-layered closure for optimal hair transplantation scar. Dermatol Surg 2012;38:664–9.
3. Rassman WR, Pak JP, Kim J, Estrin NF. Scalp micropigmentation: a concealer for hair and scalp deformities. J Clin Aesthet Dermatol 2014; 8:35–42.

NICOLE E. ROGERS, MD
Department of Dermatology
Tulane University School of Medicine
New Orleans, Louisiana

The author has indicated no significant interest with commercial supporters.

In Vivo and Ex Vivo Confocal Microscopy for the Management of a Melanoma of the Eyelid Margin

The clinical diagnosis of melanocytic tumors and in particular of malignant melanoma (MM) is hampered by diagnostic problems resulting in unnecessary surgical excision or, worse, in missed diagnosis of MM. In vivo reflectance confocal microscopy (RCM) has shown to be a useful tool for the diagnosis of eyelid margin tumors and in particular of melanocytic tumors, due to the high reflectance of melanin.[1] Ex vivo RCM has been recently used to evaluate the margins of cutaneous tumors directly in freshly excised tissue.[2,3] Therefore, this technique could be of great interest in eyelid surgery to control surgical margins. The authors report a case of an eyelid margin MM diagnosed by in vivo RCM and whose surgical margins were evaluated by ex vivo RCM in a perioperative setting.

A 65-year-old man was referred to the Ophthalmology Department of the University Hospital of Saint-Étienne for a pigmented tumor on the upper left eyelid margin rapidly growing for 6 months. Suspecting a malignancy, the patient was examined by a multidisciplinary team of ophthalmologists and dermatologists. The clinical examination revealed a 10 × 5mm dark brown tumor on the upper eyelid margin of the left eye (Figure 1A). Dermoscopy (FotoFinder Systems GmbH; Bad Birnbach, Germany) and RCM were performed applying a disposable transparent film (Visulin; Paul Hartmann AG, Germany) on the tip of both devices. Dermoscopy showed a structureless brown-gray pigmentation with some darker blotches, especially around the eyelash follicles (Figure 1B). In vivo RCM examination of the tumor was performed using the hand-held VivaScope 3000 confocal microscope (Caliber, New York, NY, distributed in Europe by MAVIG GmbH; Munich, Germany) after topical anesthesia with one drop of oxybuprocaine hydrochloride 1.6 mg/0.4 mL. Reflectance confocal microscopy

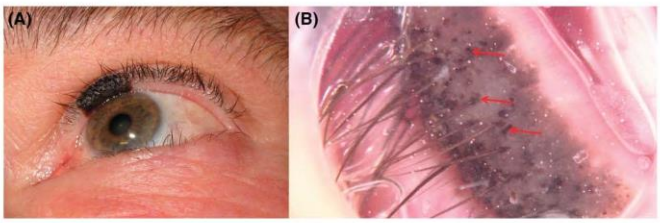

Figure 1. (A) Clinical examination revealed a 10 × 5mm dark brown tumor on the upper eyelid margin of the left eye. (B) Dermoscopy showed a structureless brown-gray pigmentation with some darker blotches (red arrows).

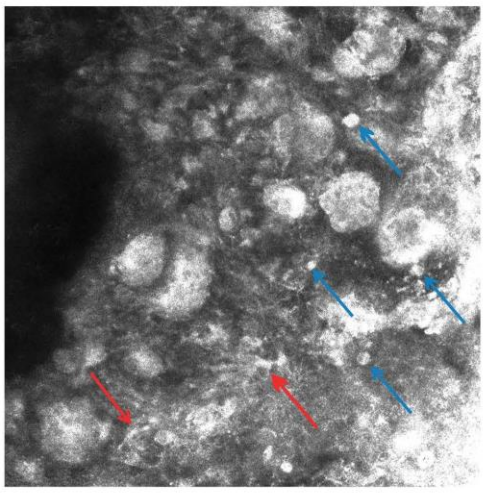

Figure 2. In vivo RCM examination showed a disarranged epithelium with large hyperreflective roundish (blue arrows) and denditric (red arrows) pagetoid cells.

examination showed a disarranged epithelium with large hyperreflective dendritric and roundish pagetoid cells and large hyperreflective polymorphic cells in the superficial chorion (Figure 2). In particular, these atypical cells also invaded the eyelash follicles. These features were indicative of a diagnosis of MM and supported the indication for surgical excision. A full-thickness pentagonal resection with a 2-mm lateral margin was performed under local anesthesia. The excised tissue was examined by ex vivo RCM using the VivaScope 2500 confocal microscope (Caliber, distributed in Europe by MAVIG GmbH). Ex vivo RCM showed the same atypical hyperreflective cells observed by in vivo RCM, thus confirming the diagnosis of MM (Figure 3), and the architecture of the entire tumor and found tumor-free margins allowing a direct surgical closure. A subsequent histopathological examination (Figure 4) showed a proliferation of large melanocytes with nuclear atypia and large nucleoli in the epithelium and the superficial chorion, with consumption of the epidermis, in both the cutaneous and conjunctival sides. A massive invasion of eyelash follicles was also visible. Histopathological examination confirmed the diagnosis of MM with a Breslow index of 0.47 mm and tumor-free surgical margins.

Discussion

Malignant melanoma is an aggressive tumor whose diagnosis can be challenging, especially in the eyelid

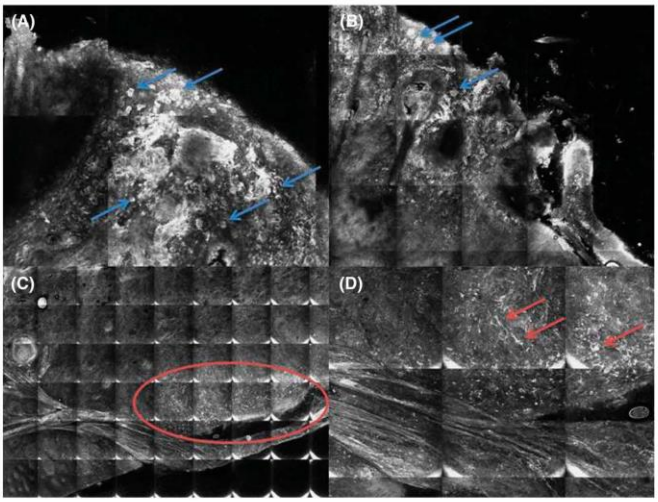

Figure 3. Ex vivo RCM examination of the conjunctival side showing large hyperreflective roundish (blue arrows) (A and B) and dendritic cells (red arrows and circle) (C and D).

References

1. Cinotti E, Perrot JL, Campolmi N, Labeille B, et al. The role of in vivo confocal microscopy in the diagnosis of eyelid margin tumors: 47 cases. J Am Acad Dermatol 2014;71:912–8.
2. Bennàssar A, Carrera C, Puig S, Vilalta A, et al. Fast evaluation of 69 basal cell carcinomas with ex vivo fluorescence confocal microscopy: criteria description, histopathological correlation, and interobserver agreement. JAMA Dermatol 2013; 149:839–47.
3. Longo C, Rajadhyaksha M, Ragazzi M, Nehal K, et al. Evaluating ex vivo fluorescence confocal microscopy images of basal cell carcinomas in Mohs excised tissue. Br J Dermatol 2014;171: 561–70.
4. Cinotti E, Perrot J-L, Labeille B, Campolmi N, et al. Handheld reflectance confocal microscopy for the diagnosis of conjunctival tumors. Am J Ophthalmol 2015;159:324–33.

ELISA CINOTTI, MD
Departments of Dermatology
University Hospital of Saint-Étienne
Saint-Étienne, France

MAHER HAOUAS, MD
Departments of Ophtalmology
University Hospital of Saint-Étienne
Saint-Étienne, France

DAMIEN GRIVET, MD
Departments of Ophtalmology
University Hospital of Saint-Étienne
Saint-Étienne, France

JEAN LUC PERROT, MD
Departments of Dermatology
University Hospital of Saint-Étienne
Saint-Étienne, France

The authors have indicated no significant interest with commercial supporters.

Use of Bone Anchor Systems for the Reconstruction of Medial Canthal Tendon

The bony insertion of the medial canthal tendon (MCT) may be disrupted after trauma or as a result of ablative surgery. An inadequate reattachment may result in medial canthal dystopia. To avoid this deformity, it is important to accurately identify the anatomic insertion point of the MCT and to achieve a secure fixation of the tendon at the medial orbital wall.[1,2]

Various techniques have been described for medial canthopexy, being the transnasal suture the most frequently used. Some surgeons have proposed the use of ipsilateral techniques, as the stainless steel screw or titanium miniplates. However, these methods of fixation either require extensive dissection of the nasal bones, are technically difficult, or prone to infections.[1,3]

In the 1980s, intraosseous fixation devices with an incorporated suture were developed. Currently, there are several designs of these anchoring systems, being the Mitek Anchor Systems (MAS)[4] the most commonly used by dermatology surgeons.

The MAS (Mitek Surgical Products, Inc., Westwood, MA) was developed for ligamentous or tendinous reconstruction in orthopedic surgery.[1–5] Subsequently, this system has been used in facial reconstructive surgery as an alternative method for fixation of soft tissues to the facial skeleton, such as the cervicofacial rotation-advancement flaps, in the reconstruction of the nasolabial fold, or mainly in the medial and lateral canthopexy.[3–5]

Materials and Methods

The MAS include different types of anchors. The authors have used 3 of them, all include the device and the drill bit, so that no additional material is needed:

(1) Mini QUICKANCHOR Plus (DePuy Mitek, Inc, Raynham, MA), features a titanium alloy anchor with a hole for suture placement and 2 opposing arcs on each side of the anchor made of nickel–titanium, which confers elasticity and shape memory, a braided absorbable suture 2/0 (Orthocord), a drill bit (2.4 mm), and an inserter. The suture is introduced into the hole using the accessory inserter.
(2) LUPINE Loop Plus and MINILOK QUICKANCHOR Plus (DePuy Mitek, Inc) (Figure 1). These 2

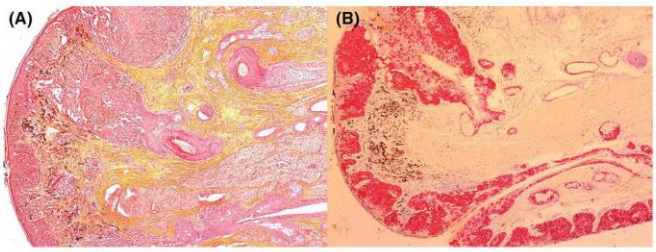

Figure 4. (A) Histopathological examination showing atypical melanocytic nests in the epithelium and superficial chorion (Hematoxylin-eosin stain, ×4). (B) Immunohistocytochemical analysis reveals that chorium and eyelash follicles are invaded by melanocytes (Melan-A staining ×4).

margin where the conjunctival side can be clinically difficult to explore.

In this case, the clinical aspect caused the authors' concern because of the rapid growth and hyperpigmentation of the lesion. Dermoscopy showed a structureless dark pigmentation with a perifollicular intensification that was difficult to interpret since no study describes the dermoscopic features of eyelid margin lesions. The authors' suspicion of MM was confirmed by in vivo RCM and they were able to proceed to the surgical excision of the tumor without previous biopsy.

Two recent studies have assessed the diagnostic accuracy of in vivo RCM for melanocytic lesions of the eyelid margin[1] and the conjunctiva[4] and have come to the conclusion that the use of this novel technique provides a significant improvement in MM detection. In a series of 47 eyelid margin tumors including 5 MMs, 100% sensitivity and 77.7% specificity for MM have been found.[1] In particular, RCM allowed the diagnosis of MM in 2 lesions of this series that were not clinically evocative of malignancy. As signs of malignancy were able to be identified (large pagetoid cells and polymorphic melanocytes), RCM may be instrumental in confirming the clinical diagnosis of MM and avoiding the excision of benign melanocytic lesions in the absence of these signs.

Ex vivo RCM is a new diagnostic imaging procedure that enables rapid diagnosis of cutaneous lesions with cellular resolution and may represent an attractive alternative to the extemporaneous histopathological examination of freshly excised tissue.[2,3] In this case, the authors found a high correlation between in vivo RCM, ex vivo RCM, and histopathological examination; all three showed the presence of large pagetoid melanocytes and their extension along the epithelium of eyelash follicles and the chorion. The authors also found a good correlation with dermoscopy. The structureless pigmentation corresponded to the extensive melanocytic proliferation and the darker blotches corresponded to superficial nests of melanocytes, especially around eyelash follicles.

Although the diagnostic ability of in vivo RCM is well known for cutaneous MM, ex vivo RCM has not been used so far for the diagnosis of MM. Previous studies have found an excellent correlation between ex vivo RCM and histopathology for basal cell carcinoma.[2,3] The authors' case report suggests that this correlation could be also valid for melanocytic tumors. Ex vivo RCM produces high magnification images of an area of 2 cm in diameter, larger than a conventional optical microscopy examination. This feature is particularly valuable to assess the overall architecture of the lesion and verify whether surgical margins are tumor-free. Micrographic eyelid surgery using the ex vivo RCM examination of fresh excised tissue is highly desirable in eyelid skin surgery, where excessive surgical excision can be irksome for patients and technically challenging for surgeons. In conclusion, both in vivo and ex vivo RCM show promise for the diagnosis and the surgical management of MM of the eyelid margin and further studies are needed to confirm the usefulness of RCM in this specific body site.

5.a 7 The role of reflectance confocal microscopy and optical coherence tomography in the diagnosis of epithelial-cystic conjunctival nevus

Annales de dermatologie et de vénéréologie (2016) 143, 653—656

Disponible en ligne sur ScienceDirect www.sciencedirect.com

Elsevier Masson France EM|consulte www.em-consulte.com

FICHE THÉMATIQUE / MICROSCOPIE CONFOCALE PAR RÉFLECTANCE

Apport de la microscopie confocale par réflectance et de l'imagerie en cohérence optique dans le diagnostic de nævus conjonctival de Parinaud

The role of reflectance confocal microscopy and optical coherence tomography in the diagnosis of epithelial-cystic conjunctival nevus

M. Kaspi[a], C. Habougit[b], D. Grivet[a], J.M. Dumollard[b], C. Douchet[b], A. Singer[a], G. Thuret[a], P. Gain[a], B. Labeille[c], E. Cinotti[c,*], J.L. Perrot[c]

[a] *Service d'ophtalmologie, hôpital universitaire de Saint-Etienne, 42055 Saint-Etienne cedex 2, France*
[b] *Service d'anatomopathologie, hôpital universitaire de Saint-Etienne, 42055 Saint-Etienne cedex 2, France*
[c] *Service de dermatologie, hôpital universitaire de Saint-Etienne, 42055 Saint-Etienne cedex 2, France*

Reçu le 24 mars 2016 ; accepté le 3 mai 2016
Disponible sur Internet le 28 juin 2016

Formation médicale continue

Observation

Un homme de 53 ans était adressé en consultation multidisciplinaire de dermato-ophtalmologie pour une lésion conjonctivale pigmentée de l'œil droit, ayant présenté une modification de taille et de pigmentation en quelques mois. Cette lésion était stable depuis plus de 20 ans. Le principal antécédent du patient était un mycosis fongoïde diagnostiqué 5 ans auparavant et traité par bexatorene.

Macroscopiquement, on constatait une lésion unique de la conjonctive bulbaire de l'œil droit mesurant 7 mm par 3 mm, bien limitée, de couleur marron foncé (Fig. 1). L'examen ophtalmologique à la lampe à fente, révélait la présence de structures arrondies translucides évocatrices de microkystes (Fig. 1). L'examen en dermoscopie trouvait la présence de globules bruns foncés confluant dans une pigmentation homogène (Fig. 1).

Tomographie par cohérence optique

L'examen en tomographie par cohérence optique (OCT) de non-haute définition (Vivosight®, Michelson Diagnostics Ltd,

* Auteur correspondant.
Adresse e-mail : elisacinotti@gmail.com (E. Cinotti).

http://dx.doi.org/10.1016/j.annder.2016.05.001

Figure 1. Aspect clinique (a), à la lampe à fente (b) et dermoscopique (c). Des microkystes sont visibles (flèche bleue) (b). La dermoscopie (c) trouve des globules bruns confluents dans un patron homogène.

Maidstone, comté de Kent, Grande Bretagne) montrait une tumeur conjonctivale tissulaire contenant des structures non reflétantes correspondant à des microkystes au sein desquels étaient visibles des corps arrondis reflétants (Fig. 2).

Microscopie confocale par réflectance

L'examen en microscopie confocale (MC) par réflectance in vivo (Vivascope 3000® ; Caliber Inc, Rochester, NY, États-Unis, distribué en France par Mavig, Munich) montrait des amas de cellules rondes hyper-reflétantes homogènes associés à des espaces microkystiques contenant eux-mêmes des petites cellules hyper-reflétantes (Fig. 3). L'aspect évoquait un nævus conjonctival dit de Parinaud.

Malgré le caractère rassurant de l'examen en MC, une exérèse était pratiquée à la demande du patient, pour raison esthétique et pour s'affranchir d'une surveillance ultérieure. L'examen histopathologique confirmait le diagnostic de nævus conjonctival de Parinaud (Fig. 2) : nous constations des thèques jonctionnelles régulières constituées de mélanocytes non atypiques, sans migration pagétoïde, avec de nombreux récessus pseudo-kystiques (Fig. 4). Le tissu conjonctif sous-jacent renfermait de vastes nappes de mélanocytes avec un gradient de maturation conservé, sans activité mitotique notable (Fig. 4). Lors de l'étude immunohistochimique, les cellules tumorales exprimaient de manière diffuse et intense le MelanA (Dako, A103) au niveau jonctionnel et dans le chorion (Fig. 4) confirmant le caractère composé de ce nævus.

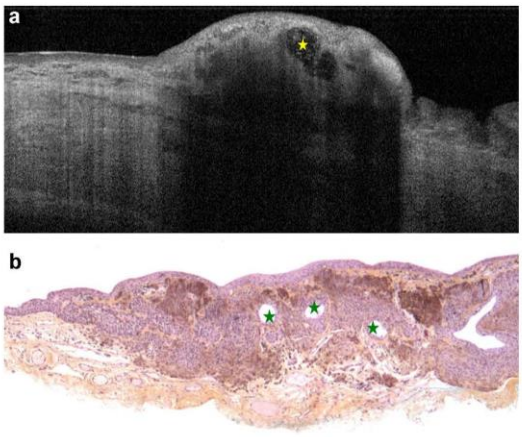

Figure 2. Examen en tomographie par cohérence optique (OCT) (a) comparé à l'examen histologique (b). L'OCT montre une lésion tissulaire avec des microkystes contenant des corps arrondis reflétants (étoile jaune). L'examen histopathologique (coloration hématoxiline-éosine ; × 50) montre un nævus composé conjonctival avec récessus pseudo-kystiques (étoiles vertes) (b).

Commentaires

Les tumeurs pigmentées de la conjonctive sont identifiables lors d'un examen clinique minutieux ; celles-ci représenteraient entre 23 % [1] et 50 % [2,3] de toutes les lésions conjonctivales. Le nævus conjonctival est la plus fréquente des tumeurs conjonctivales pigmentées [4,5], représentant 50 % [2,3] à 63 % [5] de celles-ci. Il est typiquement localisé sur la conjonctive bulbaire (entre 65,9 % et 81 %) [1–3,6]. Il est unique et bien limité [7], avec une taille médiane de 3 à 5 mm [6]. Cette tumeur pigmentée apparaît dans l'enfance ou l'adolescence [2,4,5,8] et est relativement stable dans le temps. Cependant, une modification de pigmentation ou de taille s'observe dans environ 10 % des cas [4–6,8] ; ce qui a été le cas chez notre patient. La pigmentation est variable ; 16 à 30 % des nævus sont achromiques [5,6,8,9]. Les nævus conjonctivaux sont discrètement en relief car ils contiennent dans 50 à 65 % des cas des microkystes, visibles en lampe à fente [4–6,8]. Le taux de transformation d'un nævus conjonctival en mélanome est inférieur à 1 % [4]. Le diagnostic clinique de nævus conjonctival n'est pas évident. Celui-ci est correctement posé moins d'une fois sur deux [9], ce qui souligne l'utilité des examens paracliniques tels que l'OCT et le MC.

En OCT, le nævus conjonctival a habituellement un profil légèrement en relief, n'infiltre pas la sclère, et contient des pseudo-kystes hypo-reflétants [4,5,10]. À notre connaissance, nous rapportons la première utilisation de l'OCT (Vivosight®), habituellement à usage dermatologique, pour l'exploration d'un nævus conjonctival.

En MC, des cellules hyper-reflétantes homogènes de taille moyenne sont organisées en amas au niveau de la membrane basale et du stroma (Fig. 3). Des pseudo-kystes hypo-reflétants contenant des petites cellules homogènes peuvent être présents au sein du nævus. Pour poser le diagnostic de nævus il est aussi nécessaire de ne pas observer

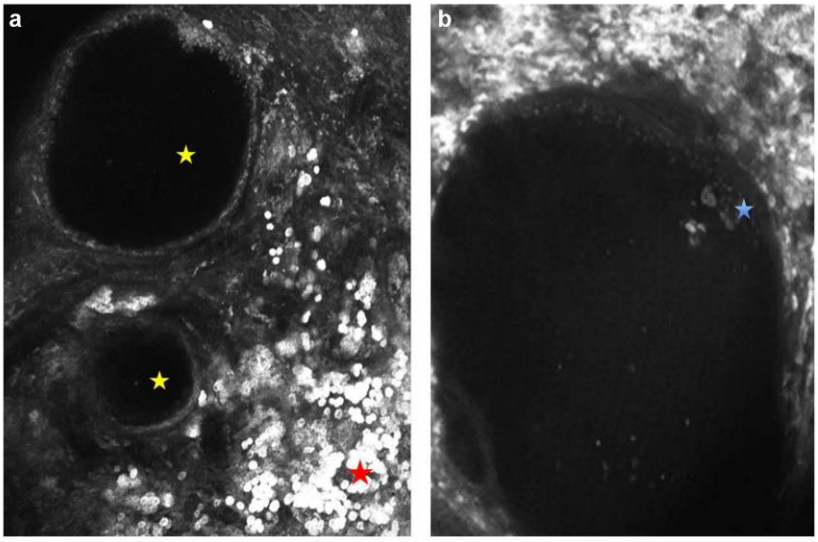

Figure 3. Aspect en microscopie confocale (MC) par réflectance in vivo : amas de cellules rondes hyper-reflétantes (étoile rouge) (a) et microkystes (étoiles jaunes) (a). En grossissant l'image en MC (b) des corps hyper-reflétants sont visibles à l'intérieur des cavités (étoile bleue).

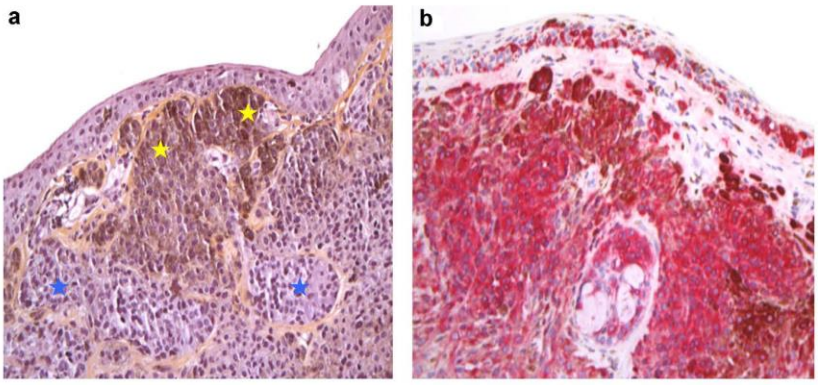

Figure 4. Aspect histopathologique (coloration hématoxiline-éosine ; × 100) (a) de nævus composé conjonctival avec thèques jonctionnelles (étoiles jaunes) et thèques du chorion (étoiles bleues). L'immunohistochimie (anticorps anti-MelanA ; × 100) conforte le caractère composé et mélanocytaire de la lésion (b).

de mélanocyte atypique, de cellule pagétoïde et de désorganisation épithéliale [9,11].

L'histologie corrobore les signes observés en OCT et MC :

- la présence de thèques de mélanocytes non atypiques à la jonction épithélium-chorion et dans le chorion permet la classification en nævus « composé » ;
- les inclusions kystiques sont formées par l'invagination de l'épithélium conjonctival ; dont la lumière est remplie par le mucus sécrété.

Le volume des kystes peut varier, ce qui peut occasionner une modification de taille de la lésion, présente chez notre patient.

Ainsi, en complément d'un examen clinique rigoureux (complété par un suivi photographique), l'OCT et la MC sont des outils de choix pour le diagnostic et le suivi des nævus conjonctivaux. Il existe des appareils d'OCT et de MC adaptés à l'ophtalmologie mais en pratique, d'utilisation peu aisée, voire impossible pour les lésions éloignées de la cornée et du limbe. Ainsi, nous avons été les premiers à utiliser le MC et l'OCT dédiés à la peau pour un usage ophtalmologique [11—13] permettant d'analyser la totalité de la surface conjonctivale bulbaire et tarsale.

Ces nouveaux appareils d'imagerie sont particulièrement utiles car ils permettent de confirmer le critère de bénignité, et d'éviter ainsi une exérèse chirurgicale inutile en cas de modification non maligne d'un nævus conjonctival.

Déclaration de liens d'intérêts

Les auteurs déclarent ne pas avoir de liens d'intérêts.

Références

[1] Elshazly LH. A clinopathologic study of excised conjunctival lesions. Middle East Afr J Ophtalmol 2011;18:48—54.

[2] Novais GA, Fernandes BF, Belfort RN, Castiglione E, Cheema DP, Burnier MN. Incidence of melanocytic lesions of the conjunctiva in a rewiew of 10675 ophtalmic specimens. Int J Surg Pathol 2010;18:60—3.

[3] Shields CL, Demirci H, Karatza E, Shields JA. Clinical survey of 1643 melanocytic and nonmelanocytic conjunctival tumors. Ophtalmology 2004;111:1747—54.

[4] Shields CL, Shields JA. Tumors of the conjunctiva and cornea. Surv Ophtalmol 2004;49:3—24.

[5] Maschi C, Caujolle JP, Liolios I, Costet C. Tumeurs conjonctivales bénignes. J Fr Ophtalmol 2013;36:796—802.

[6] Shields CL, Fasiuddin AF, Mashayekhi A, Shields JA. Conjunctival nevi: clinical features and natural course in 410 consecutive patients. Arch Ophtalmol 2004;122:167—75.

[7] Farber M, Schutzer P, Mihm MC. Pigmented lesions of the conjunctiva. J Am Acad Dermatol 1998;38:971—8.

[8] Levy Gabriel C. Taches suspectes de la conjonctive. J Fr Ophtalm 2010;33:125—30.

[9] Messmer EM, Mackert MJ, Zapp DM, Kampik A. In vivo confocal microscopy of pigmented conjunctival tumors. Graefes Arch Clin Exp Ophtalmol 2006;244:1437—45.

[10] Buchwald HJ, Müller A, Kampmeier J, Lang GK. Optische Kohärenztomographie versus Ultraschallbiomikroskopie bei Bindehaut- und Lidtumoren. Klin Monbl Augenheilkd 2003;220:822—9.

[11] Cinotti E, Perrot JL, Labeille B, Campolmi N, Espinasse M, Grivet D, et al. Handheld reflectance confocal microscopy for the diagnosis of conjunctival tumors. Am J Ophtalmol 2015;159:324—33.

[12] Cinotti E, Perrot JL, Campolmi N, Labeille B, Espinasse M, Grivet D, et al. The role of in vivo confocal microscopy in the diagnosis of eyelid margin tumors: 47 cases. J Am Acad Dermatol 2014;71:912—8.

[13] Cinotti E, Perrot JL, Labeille B, Thuret G, Espinasse M, Grivet D, et al. In vivo confocal microscopy for eyelids and ocular surface: a new horizon for dermatologistes. G Ital Dermatol E Venereol 2015;150:127—9.

5.a 8 The role of reflectance confocal microscopy in the diagnosis of ocular-cutaneous erucism or dermatitis and keratitis induced by pine processionary caterpillar hairs

Annales de dermatologie et de vénéréologie (2016) 143, 860—862

Disponible en ligne sur ScienceDirect www.sciencedirect.com

Elsevier Masson France EM|consulte www.em-consulte.com

Formation médicale continue

FICHE THÉMATIQUE / MICROSCOPIE CONFOCALE PAR RÉFLECTANCE

Apport de la microscopie confocale par réflectance dans le diagnostic d'érucisme oculocutané ou réaction aux poils de chenilles processionnaires

The role of reflectance confocal microscopy in the diagnosis of ocular-cutaneous erucism or dermatitis and keratitis induced by pine processionary caterpillar hairs

J.-L. Perrot[a], R. Julienne[b], M. Kaspi[b], B. Labeille[a], D. Grivet[b], A. Vercherin[c], F. Cambazard[a], E. Cinotti[a,*], au nom du groupe imagerie cutanée non invasive de la Société française de dermatologie

[a] *Service de dermatologie, hôpital universitaire de Saint-Étienne, 42055 Saint-Étienne cedex 2, France*
[b] *Service d'ophtalmologie, hôpital universitaire de Saint-Étienne, 42055 Saint-Étienne cedex 2, France*
[c] *Service d'anatomopathologie, institut de pathologie du Forez, 11, rue de la République, 42001 Saint-Étienne, France*

Reçu le 18 avril 2016 ; accepté le 26 juillet 2016
Disponible sur Internet le 19 septembre 2016

Observation

Un homme âgé de 64 ans, sans antécédent particulier, était adressé à notre consultation pour une dermatose très prurigineuse évoluant depuis 5 jours. L'interrogatoire trouvait, d'une part, une marche en forêt par beau temps, inhabituellement chaud pour la saison, en février 2016 dans les Monts du Forez quelques heures avant le début des symptômes, et d'autre part, la participation à des travaux de maçonnerie durant les 8 jours précédents.

Nous constatons à l'entrée dans le service 6 jours après le début des symptômes des micropapules érythémateuses confluentes dans des placards fixes et quelques pustules sur les membres (Fig. 1a) et le décolleté. Les lésions n'avaient pas de topographie compatible avec une photodermatose même si elles prédominaient sur les zones découvertes. L'examen en dermatoscopie des papules trouvait une structure homogène rosée bien limitée non spécifique (Fig. 1b). Le patient se plaignait également d'une sensation de prurit mono-oculaire sans signe clinique évident (Fig. 1c). Devant

* Auteur correspondant.
Adresse e-mail : elisacinotti@gmail.com (E. Cinotti).

http://dx.doi.org/10.1016/j.annder.2016.07.013

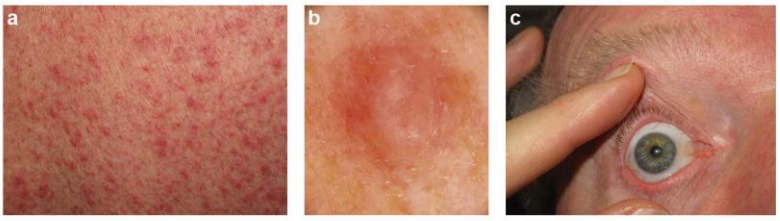

Figure 1. Aspect clinique cutané (a) et oculaire (c) et aspect dermoscopique d'une papule cutanée (b).

l'intensité des symptômes, une biopsie cutanée pour examen histologique avait été réalisée par un dermatologue en ambulatoire et elle mettait en évidence une dermo-épidermite à éosinophiles avec folliculite.

Microscopie confocale par réflectance in vivo

L'examen en microscopie confocale par réflectance in vivo (MCIV) (Vivascope 3000® ; Caliber Inc, Rochester, NY, États-Unis, distribué en France par Mavig, Munich) d'une papulopustule trouvait un épiderme à type de nid d'abeille régulier sans cellule anormale et une folliculite (Fig. 2a). L'aspect en MCIV était similaire à celui de la biopsie cutanée précédemment réalisée (Fig. 2b, c). L'examen en MCIV de la cornée après anesthésie locale avec du chlorhydrate d'oxybutaïne (laboratoire Théa, Clermont-Ferrand, France) montrait la présence de quelques structures réflétantes linéaires de grande taille à type de harpon ainsi qu'une réflectance anormalement marquée des kératocytes (Fig. 3). Nous pouvions donc poser le diagnostic d'atteinte oculocutanée par contact avec des poils de chenilles processionnaires du pin. Une corticothérapie locale oculaire et cutanée a permis de soulager en quelques jours le malade.

Commentaires

L'aspect clinique et le contexte épidémiologique étaient compatibles avec une réaction aux poils de chenille processionnaire du pin, nommée érucisme (du latin eruca : chenille) ou lépidoptérisme (qui a trait à la famille des papillons), par contact avec des poils urticants de chenilles. Cependant, une dermite allergique de contact au ciment était un autre diagnostic possible. Nous avons confirmé le diagnostic par l'examen en MCIV de la cornée du malade qui a permis de visualiser de manière formelle des poils de chenille processionnaire du pin d'hiver (*Thaumetopoea pityocampa*). En effet, le milieu transparent de la cornée permet d'identifier les poils urticants qui sont spontanément reflétants en MCIV malgré leur petite taille. Inversement, ces poils ne peuvent pas être vus à l'examen histologique d'une biopsie cutanée, faute de révélation optique par un marqueur spécifique.

Les poils urticants se distinguent aisément des nerfs cornéens, seule structure linéaire présente naturellement dans la cornée, par leur structure barbelée. Les nerfs sont beaucoup plus longs (plusieurs centaines de microns) et présentent souvent des embranchements caractéristiques (Fig. 3a). Au sein des structures barbelées des poils de *T. pityocampa* sont contenues les substances qui occasionnent les manifestations cliniques, dont la

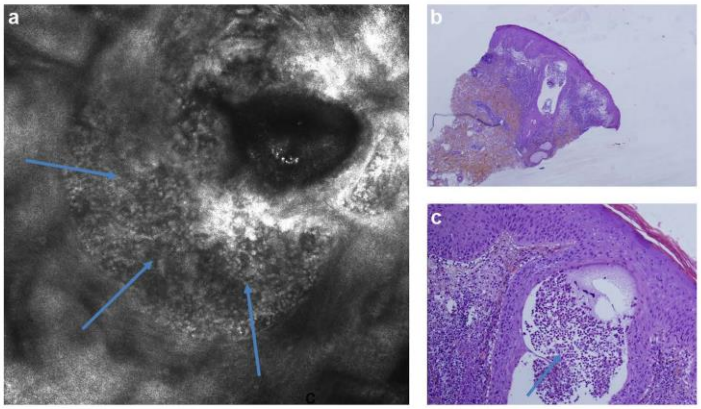

Figure 2. Examen en microscopie confocale in vivo (MCIV) (a) et examen histologique d'une papulopustule (hématoxyline-éosine, b × 2 et c × 10). La MCIV et l'examen histologique montrent une folliculite (flèches bleues) sans mise en évidence de poils urticants.

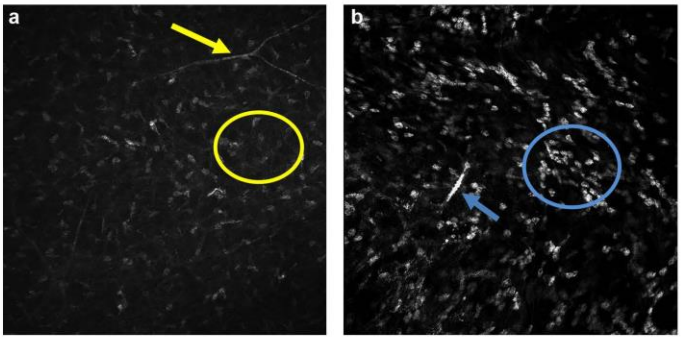

Figure 3. Examen en microscopie confocale in vivo (MCIV) de la cornée saine (a) et pathologique (b). La MCIV montre un poil urticant sous forme de harpon (b : flèche bleue) bien différent d'un axone, fin, beaucoup plus long, embranché et moins reflétant (a : flèche jaune). La réflectance des kératocytes du stroma cornéen est plus intense (b : cercle bleu) dans la cornée atteinte par rapport à la cornée saine controlatérale (a : cercle jaune).

thaumétopéine, substance histaminolibératrice, et des protéases [1].

Il s'agit à notre connaissance de la deuxième identification en MCIV des poils urticants de *T. pityocampa* dans la cornée [2]. Toutefois, compte tenu de la vaste dissémination de *T. pityocampa* en France et d'un nombre de colonies en constante augmentation, probablement du fait du réchauffement climatique [3], cette dermato-zoonose est appelée à se multiplier. De plus, les citadins ne font pas forcement attention à la présence de cocons des colonies de *T. pityocampa* dans les branches de pin au-dessus d'eux lors des balades de fin d'hiver et de printemps.

Une approche mixte dermato-ophtalmologique est nécessaire pour aborder ce type de pathologie, d'autant que la MCIV par caméra manuelle Vivascope 3000® utilisée en dermatologie est particulièrement adaptée à l'examen en MCIV de l'appareil oculaire antérieur [4,5].

Déclaration de liens d'intérêts

Les auteurs déclarent ne pas avoir de liens d'intérêts.

Références

[1] Bonamonte D, Foti C, Vestita M, Angelini G. Skin reactions to pine processionary caterpillar *Thaumetopoea pityocampa* Schiff. Sci World J 2013;27:867431.
[2] Jullienne R, He Z, Manoli P, Grivet D, Cinotti E, Perrot JL, et al. In vivo confocal microscopy of pine processionary caterpillar hair-induced keratitis. Cornea 2015;34:350—2.
[3] Robinet C, Laparie M, Rousselet J. Looking beyond the large-scale effects of global change: local phenologies can result in critical heterogeneity in the pine processionary moth. Front Physiol 2015;6:334.
[4] Cinotti E, Perrot JL, Campolmi N, Labeille B, Espinasse M, Grivet D, et al. The role of in vivo confocal microscopy in the diagnosis of eyelid margin tumors: 47 cases. J Am Acad Dermatol 2014;71:912—8.
[5] Cinotti E, Perrot JL, Labeille B, Campolmi N, Espinasse M, Grivet D, et al. Handheld reflectance confocal microscopy for the diagnosis of conjunctival tumors. Am J Ophthalmol 2015;159:324—33.

5.b Imagerie des muqueuses

Il s'agit du premier travail innovant publié par notre équipe. En effet les muqueuses n'avaient jamais été explorées en MCIV auparavant. Ce travail a donné lieu à une première communication à Lisbonne lors de la réunion de l'International Confocal World Group en 2011.

En effet seules les tumeurs pigmentées cutanées avaient fait l'objet d'étude en MCIV, parce qu'elles étaient plus fréquentes et parce que leur examen en MICV était très complexe. Ceci d'une part pour des raisons techniques liées à l'anatomie de la vulve et d'autre part à la nécessité d'avoir une caméra adaptée. Mais aussi comme nous allions le publier par la suite parce que l'interprétation des images obtenue est complexe, différente en partie de celles de la peau.

Cette activité de recherche a abouti à la création d'une consultation mixte multidisciplinaire de microscopie confocale dermato-gynécologique portant essentiellement sur la prise en charge de tumeurs pigmentés génitales mais aussi dans une moindre mesure de la plaque aréolo-mamelonaire dont l'aspect en MICV est là aussi différent de celui de la peau.

5.b 1 Reflectance confocal microscopy for the diagnosis of vulvar melanoma and melanosis: preliminary results

Background:
In the early stages, vulvar melanoma can mimic vulvar melanosis and therefore the diagnosis is often late and carries a poor prognosis. In vivo reflectance-mode confocal microscopy (RCM) is an emerging technique that allows noninvasive high-resolution imaging of the skin and mucosa, but it has not been employed in the study of genital pigmentation.

Objective
To analyze the characteristics of vulvar melanosis and vulvar melanoma using RCM to define the confocal aspects that allow a correct differential diagnosis.

Method and materials

Features of eight melanoses and two melanomas of the vulva were analyzed using RCM. RCM diagnosis was then compared with clinical and histologic diagnosis.

Results
Two major characteristics are associated with vulvar melanosis: papillae rimmed by bright monomorphous cells and possible presence of a few dendritic bright cells in the basal layer of the epithelium. Two major features of vulvar melanoma have been identified: atypical cells in the epithelium and loss of normal architecture of chorion papillae.

Conclusions
Reflectance Confocal Microscopy can play a role in noninvasive differentiation between vulvar melanoma and vulvar melanosis, but further broader studies are needed to validate our observations.

Reflectance Confocal Microscopy for the Diagnosis of Vulvar Melanoma and Melanosis: Preliminary Results

Elisa Cinotti, MD,*† Jean Luc Perrot, MD,* Bruno Labeille, MD,* Huges Adegbidi, MD,* and Frédéric Cambazard, PhD*

BACKGROUND In the early stages, vulvar melanoma can mimic vulvar melanosis and therefore the diagnosis is often late and carries a poor prognosis. In vivo reflectance-mode confocal microscopy (RCM) is an emerging technique that allows noninvasive high-resolution imaging of the skin and mucosa, but it has not been employed in the study of genital pigmentation.

OBJECTIVE To analyze the characteristics of vulvar melanosis and vulvar melanoma using RCM to define the confocal aspects that allow a correct differential diagnosis.

METHODS AND MATERIALS Features of eight melanoses and two melanomas of the vulva were analyzed using RCM. RCM diagnosis was then compared with clinical and histologic diagnosis.

RESULTS Two major characteristics are associated with vulvar melanosis: papillae rimmed by bright monomorphous cells and possible presence of a few dendritic bright cells in the basal layer of the epithelium. Two major features of vulvar melanoma have been identified: atypical cells in the epithelium and loss of normal architecture of chorion papillae.

CONCLUSIONS Reflectance Confocal Microscopy can play a role in noninvasive differentiation between vulvar melanoma and vulvar melanosis, but further broader studies are needed to validate our observations.

The authors have indicated no significant interest with commercial supporters.

The clinical differential diagnosis between melanosis and melanoma of the vulva is challenging. Melanosis is a benign pigmented lesion of the mucosa characterized by hyperpigmented basal keratinocytes. Despite its benign behavior, on clinical grounds it may show overlapping features with malignant melanoma, particularly when occurring on genitalia, possibly being characterized by asymmetry, variegated pigmentation from light to dark brown, irregular borders, multifocality, and large size.[1]

Vulvar melanoma is rare but is the second most common cause of vulvar malignancy (10% of all malignant vulvar tumors).[2] In the early stages, it can present as a brown macule simulating melanosis. Therefore, in most cases, it is diagnosed at an advanced stage, being a polypoid, ulcerated, bleeding tumor with thick dermal invasion and poor prognosis. Moreover, melanoma can be amelanotic and thus less visible and often misdiagnosed. Dermoscopy adds some criteria for a correct diagnosis, but because it is insufficient in many cases, biopsy and histopathologic examination are necessary.[3] In particular, dermoscopic features of vulvar melanomas have been reported in only 17 cases, so the number of evaluated melanomas is too small to establish the utility of dermoscopy in the diagnosis of vulvar melanoma.[4]

*Department of Dermatology, Hôpital Nord, Saint Etienne, France; †Dermatology Department, University Hospital of Genoa, Genoa, Italy

ISSN: 1076-0512 • Dermatol Surg 2012;38:1962–1967 • DOI: 10.1111/dsu.12009

In vivo reflectance-mode confocal microscopy (RCM) is an emerging technique that allows for noninvasive high-resolution imaging of the skin and the mucosa, with good sensitivity (97%) and specificity (83%) for the diagnosis of skin melanoma,[5,6] but, as far as we know, it has never been employed to study genital pigmentation.

We present a small series of patients, describe the RCM features of melanosis and melanoma of the vulva, and identify the RCM characteristics that allowed us to establish the differential diagnosis between these two entities.

Materials and Methods

We evaluated 10 pigmented genital lesions from nine women recruited at the Dermatology Department of Hôpital Nord (Saint Etienne, France) between May 2011 and October 2011. Clinical, RCM, and histopathologic features were examined.

Lack of elevation, bilateralism, and the presence of homogeneous brown pigmentation were considered clinical aspects suggestive of melanosis, whereas a single, large, raised, ulcerated lesion with irregular blue-black pigmentation and jagged edges was suggestive of melanoma.

Confocal imaging was performed using a reflectance confocal microscope (VivaScope 3,000, Lucid Inc., Henrietta, NY), which uses an 830-nm diode laser and has high optical resolution (horizontal axis, 1.25 μm; vertical axis, 5 μm). Each image corresponds to a 0.5- by 0.5-mm horizontal section (0.25 mm^2). Series of images (*z*-stacks) focused at regularly 4.56-μm placed intervals through the depth of the epithelium (*z* axis) were also acquired within the same section of mucosa.

Because no studies had analyzed the vulva using RCM before, we first assessed the RCM features of clinically noninvolved vulvas in the same group of patients.

Given the lack of specific criteria to diagnose pigmented lesions in this site, our first RCM diagnosis was based on the criteria used for pigmented skin lesions and on personal experience. After performing the RCM examination, biopsies were taken from all of the vulvar lesions to compare our RCM diagnosis with the histopathologic diagnosis, and then RCM images were reassessed to establish the confocal characteristics of melanosis and melanoma in our case series.

The RCM images were described using the terms previously summarized in a consensus terminology glossary.[7]

Results

Our observation included eight vulvar melanoses and two vulvar melanomas in nine women. One vulvar melanoma also showed urethral invasion. In all cases, the RCM diagnosis corresponded to the histopathologic one.

Before starting RCM analysis of the pigmented lesions, we observed non-clinically involved vulvar mucosa in the same group of patients to establish their characteristics. Confocal microscopy features of the non-clinically involved mucosa (Figure 1) were honeycomb pattern of the epithelium, wide interpapillary spaces at the epithelial–chorion junction (papillae grouped in small clusters separated by wide interpapillary hyporefractive areas because of the presence of large rete ridges), edged papillae with a roundish (ringed pattern) or elongated shape (which we named "draped pattern" because it was reminiscent of a draped fabric) rimmed by monomorphous bright cells, and the possible presence of dendritic bright cells around the chorion papillae (not more than 1 or 2 cells per RCM image).

Clinical characteristics of the eight melanoses are reported in Table 1. The mean age of the patients was 56 (range 26–89). Lesions were multifocal in all cases except one, and the great majority were located on the labia minora. Clinical diagnosis was

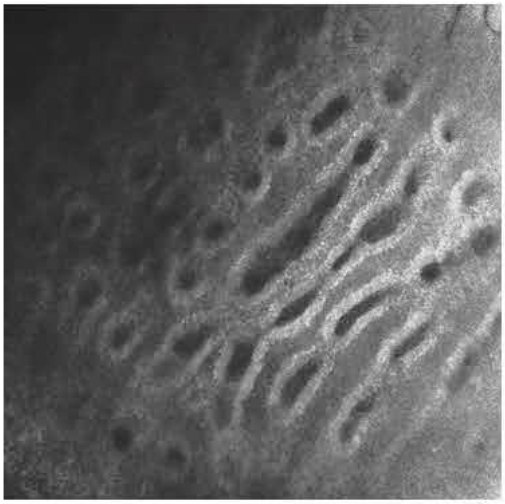

Figure 1. Reflectance-mode confocal microscopy image of clinically noninvolved mucosa.

not evident in three cases (cases 1, 3, and 4), in which one lesion was located on the surgical scar of a previous melanoma excision (case 1), and two lesions had extensive dark brown pigmentation with irregular borders (cases 3 and 4).

All eight cases of melanosis had the same RCM characteristics observed in non-clinically involved vulval mucosa, but the cells around the edged papillae were more refractive (Figure 2). Moreover, dendritic cells around the papillae were present in only one case, and in this case, they were more numerous than in non-clinically involved vulval mucosa. Edged papillae with a ringed pattern were found in half of the patients, and the "draped pattern" was found in the other half. No atypical bright cells were detected in the suprabasal layer of the epithelium. In the case of multifocal lesions, we observed all of the different parts of the lesions and found that the RCM appearance could be reproduced.

The two melanomas were multifocal and were observed in two patients (aged 41 and 74). The clinical characteristics of the different parts of these tumors are shown in Table 2. The first vulvar melanoma comprised an invasive and an in situ near part, and the other comprised an in situ vulvar lesion and an invasive urethral tumor and was a recurrence of a previous in situ vulvar melanoma diagnosed 4 years earlier. The clinical diagnosis was evident only in the invasive part of the first melanoma (Figure 3A). The urethral part of the second melanoma was amelanotic.

Reflectance Confocal Microscopy of the invasive part of the first melanoma showed a disarranged pattern (disarray of the normal architecture of the epithelium with unevenly distributed bright granular particles and cells) in the suprabasal layers of the epithelium (Figure 3B); roundish and, more rarely, spindle bright atypical cells in the epithelium; and roundish nucleated cells distributed in sheet-like structures (Figure 3C) at the epithelium chorion junction consistent with atypical melanocytic proliferation in single units destroying the normal

TABLE 1. Clinical Characteristics of Eight Cases of Melanosis

Patient	*Age*	*Site*	*Bilateral*	*Multifocal*	*Color*	*Diameter > 6 mm†*	*Raised*
1*	74	Labium majus	No	No	Light brown	No	No
2	33	Labia minora	Yes	Yes	Dark brown	Yes	No
3	45	Labia minora	Yes	Yes	Light and dark brown	No	No
4	26	Labia minora	Yes	Yes	Light and dark brown	Yes	No
5	51	Perineum	No	Yes	Light brown	No	No
6	53	Labia minora	Yes	Yes	Light brown	Yes	No
7	89	Labia minora	Yes	Yes	Light brown	Yes	No
8	80	Labia minora	Yes	Yes	Dark brown	Yes	No

*Patient 1 also developed a melanoma.
†In case of multifocal lesions, we considered the size of the largest one.

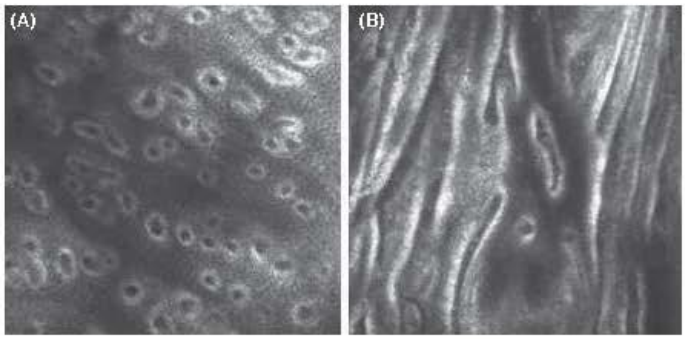

Figure 2. Reflectance mode confocal microscopy images of vulvar melanosis taken at the epithelium chorion junction show edged papillae rimmed by small and monomorphous bright cells with a roundish shape (ringed pattern) (A) or an elongated shape (draped pattern) (B).

TABLE 2. Clinical and Histologic Characteristics of the Different Parts of the Two Multifocal Melanomas

Patient	*Age*	*Site*	*Color*	*Diameter > 6 mm*	*Raised*	*Histologic Features*
1*	41	Left labium majus and minor	Black, grey, red	Yes	Yes (focal)	Invasive
		Left labium minor	Grey	No	No	In situ
2	74	Left labium minor	Light brown	No	No	In situ
		Urethral orifice	Normal mucosa color	Yes	Yes	Invasive

*Patient 1 also developed a melanosis.

architecture of the chorion papillae (totally disarranged papillae).

On RCM, the in situ part of the previous melanoma (Figure 3A) showed a disarranged pattern of the suprabasal layers of the epithelium with large dendritic cells (Figure 3D) and nonedged papillae at the chorion–epithelial junction with few atypical bright cells (Figure 3E).

On RCM (Figure 3F), the second vulvar melanoma (Figure 3G) showed a disarranged epithelium with large hyperreflective dendritic cells consistent with atypical melanocytes.

The urethral part had a large number of bright cells in the epithelium, most small and suggestive of inflammatory cells and some large, consistent with melanocytes. In this case, clinical diagnosis (because the lesion was amelanotic) and histopathologic diagnosis were challenging, and only the use of melanocytic markers, suggested by the RCM examination, allowed the histopathologic diagnosis of invasive melanoma.

Discussion

The clinical differential diagnosis of vulvar lesions is not always easy, and in two-thirds of our patients, we were unable to establish a correct clinical diagnosis. Unlike clinical diagnosis, RCM diagnosis correlated well with histopathologic findings in all 10 cases.

The RCM pattern of normal skin and pigmented cutaneous lesions cannot be applied to the vulva. Therefore, we first had to establish the confocal microscopy features of the non-clinically involved vulvar mucosa (Table 3). Papillae are rimmed by monomorphous bright cells, a pattern that in the

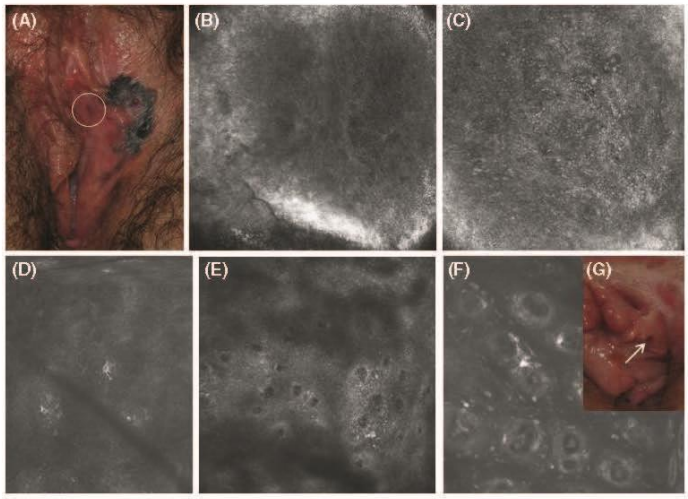

Figure 3. Reflectance-mode confocal microscopy (RCM) images of vulvar melanomas. Clinical image of the first vulvar melanoma, comprising an invasive and an in situ adjacent part (circled) (A). RCM images of the invasive part of the melanoma show a disarranged pattern in the suprabasal layers of the epithelium (B) and areas of atypical roundish cells distributed in sheet-like structures, corresponding to a melanocytic proliferation in single units at the epithelium–chorion junction (C). RCM images of the in situ part of the melanoma (the circled tumor in figure A) show large, hyperreflective dendritic cells in the epithelium (D) and nonedged papillae, with some atypical brighter cells at the epithelium–chorion junction (E). RCM (F) and clinical (inset) (G) views of the in situ recurrence of melanoma of the other patient. RCM (F) shows atypical spindle and dendritic cells around the papillae.

TABLE 3. Reflectance Confocal Microscopic Features of Clinically Noninvolved Mucosa, Melanosis, and Melanoma of the Vulva

	Clinically Noninvolved Mucosa	*Melanosis*	*Melanoma*
Epithelium	Honeycomb pattern	Honeycomb pattern	Disarranged pattern. Roundish, spindle, or dendritic pagetoid cells
Epithelium chorion junction	1. Papillae: • In clusters, separated by wide interpapillary spaces • Rimmed by bright cells • With a roundish (ringed) or elongated (draped) form. 2. Rare dendritic cells around the papillae	Same characteristics of normal mucosa but brighter cells around the papillae and occasionally more dendritic cells around the papillae	Disarranged papillae. Atypical cells in sheet-like structures.

skin is typical of lentigo and indicates greater pigmentation of basal keratinocytes of the mucosa. Characteristically, it is possible to find rare dendritic bright cells around the papillae, possibly indicating a slight increase in melanocytes or Langerhans cells in the basal layer of the epidermis. These cells can be differentiated from atypical cells found in melanoma because, in melanoma, they are present in larger numbers; they are larger in size, with shorter and thicker dendrites; and they are located around nonedged, irregular papillae.

All eight cases of melanosis showed the RCM characteristics observed in clinically uninvolved mucosa, but the cells around the edged papillae were more refractive (Table 3). Melanosis is characterized

by higher melanin content of basal keratinocytes, corresponding to a greater brightness of these cells.

In vulvar melanoma, we always found two of the RCM characteristics of skin melanoma: atypical cells and loss of the normal chorion papillae architecture. These two aspects were always associated and were never found in melanosis (Table 3).

Atypical cells are large cells with a bright cytoplasm and an often evident hyporefractive nucleus corresponding to neoplastic melanocytes. They can have a dendritic or a spindle or roundish shape and are often pleomorphic and scattered in the epithelium. Atypical cell infiltration destroys papillae architecture at the epithelium–chorion junction, leading first to the formation of nonedged papillae (papillae without precise boundaries) and then to totally disarranged papillae with sheet-like structures of atypical cells (sheets of isolated cells).

Reflectance Confocal Microscopy is particularly useful for the diagnosis of vulvar lesions because it is noninvasive, and if larger studies confirm its accuracy in the diagnosis of pigmented lesions of the vulva, it will obviate the need for biopsies in this sensitive part of the body. This technique also enables earlier diagnosis of melanoma because it allows early noninvasive examination of vulvar lesions, without waiting for clinical changes necessary to warrant a biopsy at a stage when lesions may already be advanced. Vulvar melanosis and melanoma are often multifocal, and RCM allows analysis of all of the different parts of the lesions, identifying the most significant areas to be biopsied and reducing the number of biopsies.

In our case of urethral melanoma, the clinical diagnosis was not clear, because the color of the lesion was the same as normal mucosa, but RCM allowed us to detect some atypical large bright cells, indicating a possible melanocytic tumor. This indicates that RCM is also an excellent method for the diagnosis of achromic melanoma.

Reflectance Confocal Microscopy is also important in the follow-up of vulvar melanoma, in which it can help decide whether to perform a biopsy of a new pigmented lesion. For example, in one of our cases, RCM allowed us to easily diagnose a melanosis that had developed on the surgical scar of a previous melanoma excision and to exclude melanoma recurrence.

In conclusion, our preliminary data show that RCM seems promising for differentiating vulvar melanoma from vulvar melanosis, even in clinically controversial lesions. This needs to be followed up by prospective studies including early melanomas to establish the diagnostic performance of RCM in pigmented lesions of the genitalia.

References

1. Mannone F, De Giorgi V, Cattaneo A, Massi D, et al. Dermoscopic features of mucosal melanosis. Dermatol Surg 2004;30:1118 23.
2. Moxley KM, Fader AN, Rose PG, Case AS, et al. Malignant melanoma of the vulva: an extension of cutaneous melanoma? Gynecol Oncol 2011;122:612 7.
3. Ronger-Savle S, Julien V, Duru G, Raudrant D, et al. Features of pigmented vulval lesions on dermoscopy. Br J Dermatol 2011;164:54 61.
4. Ferrari A, Zalaudek I, Argenziano GP, Buccini P, et al. Dermoscopy of pigmented lesions of the vulva: a retrospective morphological study. Dermatology 2011;222:157 66.
5. Pellacani G, Cesinaro AM, Seidenari S. Reflectance-mode confocal microscopy of pigmented skin lesions improvement in melanoma diagnostic specificity. J Am Acad Dermatol 2005;53:979 85.
6. Gerger A, Hofmann-Wellenhof R, Samonigg H, Smolle J. In vivo confocal laser scanning microscopy in the diagnosis of melanocytic skin tumours. Br J Dermatol 2009;160:475 81.
7. Scope A, Benvenuto-Andrade C, Agero AL, Malvehy J, et al. In vivo reflectance confocal microscopy imaging of melanocytic skin lesions: consensus terminology glossary and illustrative images. J Am Acad Dermatol 2007;57:644 58.

Address correspondence and reprint requests to:
Frédéric Cambazard, PhD, Hôpital Nord Saint-Etienne, 42055 Saint Etienne, Cedex 2, France, or
e-mail: frederic.cambazard@chu-st-etienne.fr

5.b 2 Anal melanosis diagnosed by reflectance confocal microscopy

Abstract

Until now, *in vivo* reflectance-mode confocal micros- copy (IVCM) has been applied only to pigmented lesions of the vulvar and oral mucosa, but not to anal mucosa lesions. We present the first case in which IVCM has been used to diagnose anal melanosis. Clinical and dermoscopic features were of concern while IVCM found the draped pattern already described for genital melanosis. IVCM adds information to the clinical and dermatoscopic examination and allows skin biopsies to be avoided. Further studies are needed to define the IVCM features of anal melanosis and to compare the performance of IVCM with the findings of histological examinations.

Australasian Journal of Dermatology

Australasian Journal of Dermatology (2013) ••, ••–••

doi: 10.1111/ajd.12096

BRIEF REPORT

Anal melanosis diagnosed by reflectance confocal microscopy

Elisa Cinotti,[1] Christelle Chol,[1] Jean Luc Perrot,[1] Bruno Labeille,[1] Fabien Forest[2] and Frédéric Cambazard[1]

[1]*Dermatology and* [2]*Pathology Department, University Hôpital of Saint Etienne, Saint Etienne, France*

ABSTRACT

Until now, *in vivo* reflectance-mode confocal microscopy (IVCM) has been applied only to pigmented lesions of the vulvar and oral mucosa, but not to anal mucosa lesions. We present the first case in which IVCM has been used to diagnose anal melanosis. Clinical and dermoscopic features were of concern while IVCM found the draped pattern already described for genital melanosis. IVCM adds information to the clinical and dermatoscopic examination and allows skin biopsies to be avoided. Further studies are needed to define the IVCM features of anal melanosis and to compare the performance of IVCM with the findings of histological examinations.

Key words: anus, confocal microscopy, dermatoscopy, melanosis, mucosa.

INTRODUCTION

In vivo reflectance-mode confocal microscopy (IVCM) is an emerging technique that provides non-invasive high-resolution imaging of the skin, thus allowing the diagnosis of pigmented lesions with a specificity of 97.6% for melanoma.[1] It has recently been applied to pigmented lesions of the vulvar[2] and oral[3] mucosa, specifically to differentiate between melanosis and melanoma. We present the first case in which IVCM was used to diagnose a pigmented anal lesion.

Correspondence: Dr Elisa Cinotti. University Hospital of Saint Etienne, 42055 Saint Etienne Cedex 2, France. Email: elisacinotti@gmail.com

Elisa Cinotti, MD. Christelle Chol, MD. Jean Luc Perrot, MD. Bruno Labeille, MD. Fabien Forest, MD. Frédéric Cambazard, PhD.

All authors contributed in drafting the manuscript.

Conflict of interest: none

Submitted 25 February 2013; accepted 4 July 2013.

CASE REPORT

A 48-year-old HIV-positive patient presented with an acquired pigmentation of the anal mucosa. The patient had been monitored once a year by anoscopy since the discovery, in 2000, of anal condylomas without evidence of pigmented lesions. A clinical examination showed the presence of a brown to black, asymmetric, 3 × 8 mm in diameter macule on the anal verge with an adjacent whitish area on one side (Fig. 1). Careful examination of the oral and genital mucous membranes and nails did not reveal any other pigmentation.

When examined dermoscopically using ultrasound gel, the lesion appeared asymmetric. One half was pigmented and the other was non-pigmented. The pigmented part presented with structureless brown and grey areas and a subtle brown network at the periphery, whereas the non-pigmented part was characterised by a homogeneous white background with several linear vessels (Fig. 2). An IVCM examination was carried out with a handheld VivaScope 3000 camera (Caliber, New York, USA) and a disposable sterile transparent film (Visulin, Paul Hartmann AG, Germany) applied to the tip of the IVCM. The IVCM showed a honeycomb pattern of the epidermis, with hyper-refractive elongated dermal papillary rings, composed of homogeneous round cells and no atypical cells (Fig. 3) suggestive of melanosis. Given the rapid evolution of the lesion, its asymmetry, its dermoscopic features, the immunosuppressive state of the patient and the fact that the IVCM aspect of anal melanosis had never been described before, surgical excision and a histological examination followed and confirmed the diagnosis reached with IVCM (Fig. 4).

DISCUSSION

Melanosis is the most common pigmented lesion of the mucosa and its correct diagnosis is necessary as it can be clinically indistinguishable from a superficial melanoma.[4]

Abbreviation:

IVCM	*in vivo* reflectance-mode confocal microscopy

Figure 1 Clinical aspect of the pigmented macule on the anal verge.

Figure 2 Dermoscopic examination of the anal verge lesion shows structureless brown, grey and white areas, a subtle brown network and linear vessels.

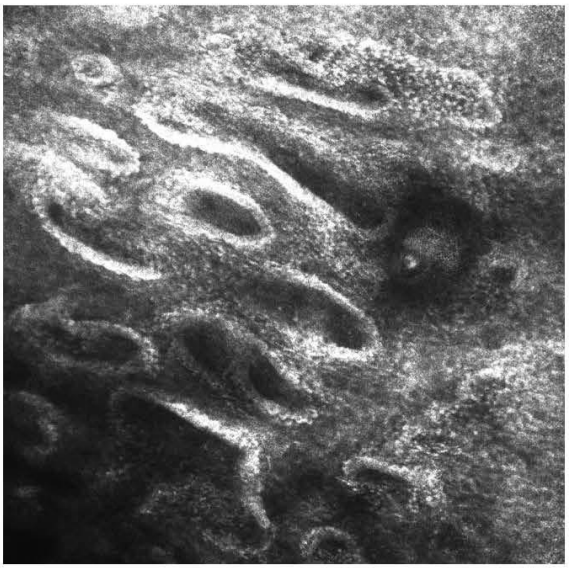

Figure 3 *In vivo* reflectance-mode confocal microscopy examination of the anal verge lesion shows a honeycomb pattern of the epidermis, with hyper-refractive elongated dermal papillary rings, composed of homogeneous round cells and no atypical cells.

Melanoma of the mucosa is rare but prognosis is poor as it develops in sites rich in blood and lymphatic vessels.[4] Furthermore, diagnosis of mucosal melanoma is often delayed because histological examinations in this delicate area are avoided until the appearance of clinical changes that warrant a biopsy, by which time lesions already may be advanced.

Dermoscopy adds information to the clinical examination[4,5] but the particular localisation of mucosal lesions, especially in the anal area, may prevent the use of a large tip and may require the use of ultrasound gel that may alter the identification of the pigment network.[6] Two diagnostic models have been identified by the International Dermoscopy Society for genital lesions: the presence of structureless zones inside the lesions that are blue, grey or white in colour (the first model) and the presence of a blue, grey, or white colour (the second model), with a sensitivity of 100% and a specificity of 82.2% and 64.3% for melanoma, respectively.[5] Using both models our lesion would have been diagnosed as melanoma.

IVCM provides additional information that facilitates the correct diagnosis[7] as it is particularly appropriate for the mucosa, thanks to the handheld device with a small 5 mm^2 tip. Our case of anal melanosis had a typical draped pattern appearance, already described by our team[2] in the vulvar mucosa and characterised by elongated papillae with homogeneous hyper-reflective basal cells. The IVCM had not allowed us to differentiate exactly between the pigmented and non-pigmented parts. In fact, in order to observe the entire architecture of the lesion and to make a direct comparison with the dermatoscopic aspect we should have used the VivaScope 1500 device, but its larger tip does not allow the exploration of the perianal region. Equipped with a smaller tip, the handheld VivaScope 3000 camera is handy and allows the exploration of the whole perianal region. It does not however enable a mosaic reconstruction of the images in the x-y direction to provide an overview of the entire lesion. The histological examination showed parakeratosis and scant pigmentation of basal keratinocytes in the whitish area of the lesion (Fig. 4), which may be explained by mechanical trauma in this particular body site.

In conclusion, IVCM could allow skin biopsies to be avoided and could lead to the detection of early melanomas in the anal region. Further studies are needed to define the IVCM features of melanosis and early melanoma of the anal

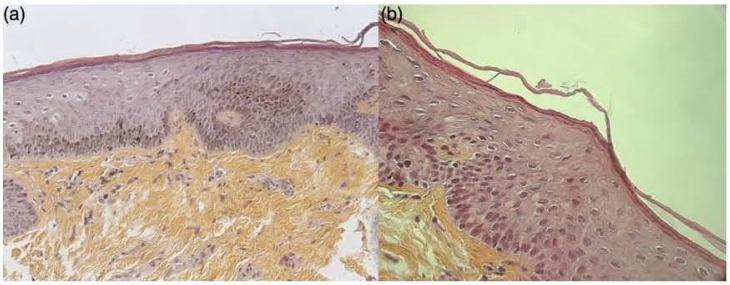

Figure 4 Histological examination shows (a) hyperpigmented keratinocytes in the basal layer of the epithelium (haematoxylin–eosin stain ×20) in the pigmented part of the anal verge lesion and (b) parakeratosis and reduced pigmentation of basal keratinocytes (haematoxylin–eosin stain ×40) in the non-pigmented part of the lesion.

mucosa to compare the performance of IVCM with the findings of histological examinations.

REFERENCES

1. Gerger A, Koller S, Kern T *et al.* Diagnostic applicability of *in vivo* confocal laser scanning microscopy in melanocytic skin tumors. *J. Invest. Dermatol.* 2005; **124**: 493–8.
2. Cinotti E, Perrot JL, Labeille B *et al.* Reflectance confocal microscopy for the diagnosis of vulvar melanoma and melanosis: preliminary results. *Dermatol. Surg.* 2012; **38**: 1962–7.
3. Erfan N, Hofman V, Desruelles F *et al.* Labial melanotic macule: a potential pitfall on reflectance confocal microscopy. *Dermatology* 2012; **224**: 209–11.
4. Lin J, Koga H, Takata M *et al.* Dermoscopy of pigmented lesions on mucocutaneous junction and mucous membrane. *Br. J. Dermatol.* 2009; **161**: 1255–61.
5. Blum A, Simionescu O, Argenziano G *et al.* Dermoscopy of pigmented lesions of the mucosa and the mucocutaneous junction: results of a multicenter study by the International Dermoscopy Society (IDS). *Arch. Dermatol.* 2011; **147**: 1181–7.
6. Tasli L, Oguz O. The role of various immersion liquids at digital dermoscopy in structural analysis. *Indian J. Dermatol. Venereol. Leprol.* 2011; **77**: 110.
7. Carrera C, Puig S, Malvehy J. In vivo confocal reflectance microscopy in melanoma. *Dermatol. Ther.* 2012; **25**: 410–22.

5.b 3 The contribution of reflectance confocal microscopy in the diagnosis of Paget's disease of the breast

Annales de dermatologie et de v n r ologie (2013) 140, 829—832

ELSEVIER MASSON

Disponible en ligne sur ScienceDirect www.sciencedirect.com

Elsevier Masson France EM|consulte www.em-consulte.com

FICHE TH MATIQUE / MICROSCOPIE CONFOCALE PAR R FLECTANCE

Apport de la microscopie confocale par r flectance dans le diagnostic de la maladie de Paget mammaire

The contribution of reflectance confocal microscopy in the diagnosis of Paget's disease of the breast

E. Cinotti, J.L. Perrot, B. Labeille*, F. Cambazard, au nom du groupe imagerie cutan e non invasive de la Soci t fran aise de dermatologie

Service de dermatologie, h pital Nord, CHU, 42055 Saint- tienne cedex 2, France

Reçu le 15 juillet 2013 ; accept le 4 octobre 2013
Disponible sur Internet le 20 novembre 2013

Observation

Une patiente de 61 ans tait adress e pour un examen annuel de ses nævus. Pendant l'examen, nous avons observ une papule k ratosique de 2 mm de diam tre sur le mamelon droit, r cidivante depuis 8 mois. La mammographie, l' chographie mammaire et l'examen gyn cologique pratiqu s trois mois auparavant taient consid r s comme normaux. L'examen clinique et dermoscopique (Fig. 1) tait non sp cifique.

Microscopie confocale par r flectance

Un examen en microscopie confocale (Vivascope 3000®; Lucid Inc, Rochester, NY, tats-Unis, distribu en France par Mavig, Munich) tait r alis pour orienter le diagnostic de façon non invasive compte tenu de la topographie. Il mettait en vidence la disparition de la structure habituelle du mamelon, savoir un patron en nid d'abeille r gulier dans l' piderme et des anneaux de cellules hyper-refl tantes r guli rement r parties la jonction dermo- pidermique (Fig. 2), et il montrait des zones optiquement vides correspondant des grandes cellules rondes peu refl tantes et des cellules hyper-refl tantes avec halo sombre p riph rique (Fig. 3). Dans la couche basale de l' piderme, ces zones hypo-refl tantes taient larges (Fig. 4) en raison de la confluence de cellules de Paget qui pr dominent dans les couches profondes de l' piderme. Des cellules inflammatoires hyper-refl tantes et des cellules dendritiques taient aussi pr sentes (Fig. 5). Ces aspects taient typiquement vocateurs d'une maladie de Paget du mamelon, confirm e histologiquement dans un second temps (Fig. 6).

Commentaires

La maladie de Paget correspond un ad nocarcinome intra- pidermique [1] impliquant le mamelon et la peau anog nitale (maladie de Paget extra-mammaire). Elle est souvent difficile diagnostiquer cliniquement car elle peut simuler une dermatite de contact ou une infection. En r gle

* Auteur correspondant.
Adresse e-mail : bruno.labeille@chu-st-etienne.fr (B. Labeille).

0151-9638/$ — see front matter
http://dx.doi.org/10.1016/j.annder.2013.10.029

Figure 1. L'examen clinique (gauche) et dermoscopique (droite).

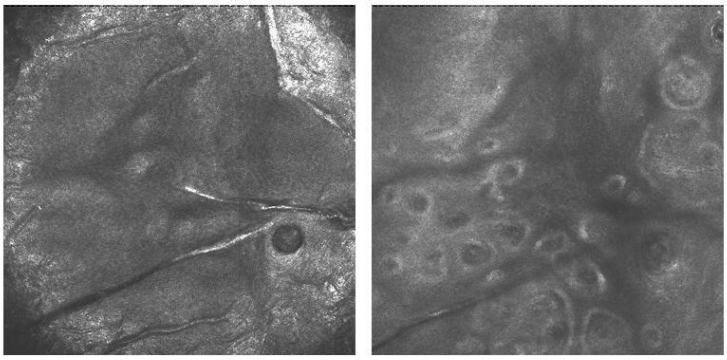

Figure 2. Aspect en microscopie confocale par r flectance d'un mamelon normal : patron en nid d'abeille r gulier dans l' piderme (gauche) et anneaux de cellules hyper-refl tantes la jonction dermo- pidermique (droite).

g n rale, on observe une plaque prurigineuse ryth mateuse et squameuse ou cro teuse. Un mauvais diagnostic peut entra ner un retard dans le traitement appropri et un pronostic d favorable.

Dans notre cas, l'aspect clinique tait peu vocateur et le diagnostic a t sugg r par l'examen en microscopie confocale (MC).

La maladie de Paget est caract ris e en MC comme en histologie par la pr sence de cellules de Paget : grosses cellules, arrondies, g n ralement 1,5 2 fois plus grandes que les k ratinocytes voisins, dans l' piderme. En MC les cellules de Paget se pr sentent soit comme des zones arrondies et sombres intra- pidermiques (il s'agit alors de cellules peu refl tantes [2]) (Fig. 3 et 4), soit comme une structure

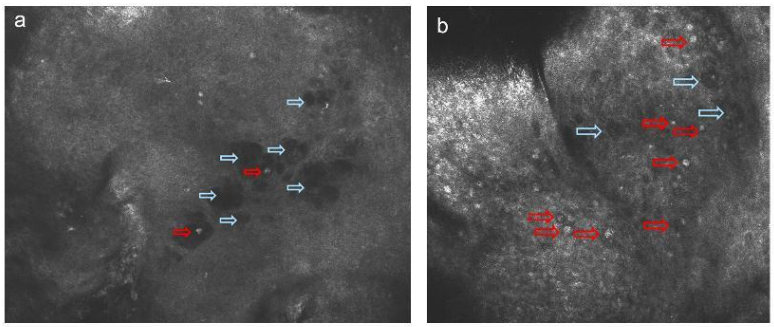

Figure 3. L'examen en microscopie confocale par r flectance montre des structures sombres et arrondies (fl che bleue) et des structures « en cible » avec une zone centrale ronde hyper-refl tante entour e par un grand halo sombre (fl che rouge) dans l' piderme, correspondant toutes les deux des cellules de Paget.

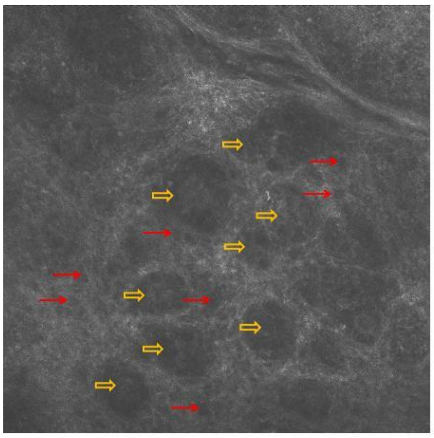

Figure 4. Les cellules de Paget peuvent tre isol es (fl che rouge) ou appara tre sous forme de gros amas de cellules (fl che jaune).

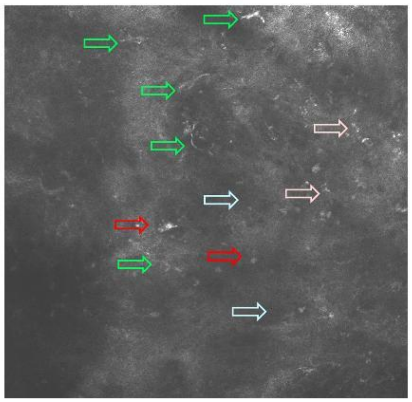

Figure 5. Des particules r fl chissantes, correspondant un infiltrat inflammatoire (fl che rose), et des cellules dendritiques (fl che verte) sont m lang es aux cellules de Paget (cavit s sombres — fl che bleue — et structures « en cible » — fl che rouge).

« en cible » avec une zone centrale ronde hyper-refl tante entour e par un halo sombre [2]. Le double aspect des cellules de Paget en MC, sombre et « en cible », est connu dans la litt rature [2,3], mais la corr lation avec l'examen histopathologique, o les cellules de Paget ont des caract ristiques tinctoriales plut t homog nes, n'est pas claire. Des hypoth ses existent concernant l'aspect « en cible » : le halo sombre pourrait correspondre aux fentes qu'on trouve l'examen histologique parmi les cellules de Paget, possiblement de nature mucineuse [2], ou au cytoplasme des cellules autour d'un gros noyau refl tant [3]. En cas de maladie de Paget pigment e, les cellules de Paget sont hyper-refl tantes [4].

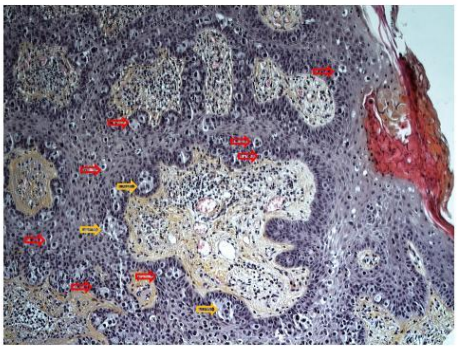

Figure 6. L'examen histologique montre de multiples cellules de grande taille en migration pag to de (fl che rouge). Ces cellules sont dot es d'un cytoplasme p le abondant et d'un noyau tr s volumineux anisocaryotique. Dans certains territoires, elles se rassemblent en petits amas (fl che jaune).

Les cellules de Paget peuvent tre trouv es dans toutes les couches de l' piderme, mais en g n ral, elles pr dominent dans les couches profondes de l' piderme, basale et suprabasale. [2]. Les cellules peuvent tre isol es ou appara tre sous forme d'amas de cellules plus ou moins grands (Fig. 5). Parfois les nids sont nombreux et remplacent presque compl tement l'architecture normale de l' piderme ; cet aspect est le plus souvent trouv dans les cas de maladie de Paget associ s un ad nocarcinome invasif sous-jacent [2]. Aux cellules de Paget peuvent s'associer des particules refl tantes, correspondant un infiltrat inflammatoire, des cellules dendritiques hyper-refl tantes, correspondant des cellules dendritiques r actionnelles ou des m lanocytes normaux [2,4] (Fig. 6).

M me si une biopsie est un acte peu traumatique, imposer ce geste sur le mamelon, notre patiente, avec comme seul argument une papule k ratosique, de 2 mm^2, r cidivante, alors qu'un bilan gyn cologique r cent tait normal, n cessitait des arguments suppl mentaires que la MC a pu nous offrir.

L'identification de cellules atypiques, pag to des, nous donne des l ments en faveur d'un cancer cutan et nous permet d' liminer une dermite de contact [5]. En effet, dans la dermite de contact, l' piderme pr sente un patron en nid d'abeille r gulier, parsem des multiples structures arrondies nettement d limit es, sombres, contenant des particules hyper-refl tantes qui correspondent aux micro-v sicules contenant des k ratinocytes n crotiques. De plus, le caract re non invasif de cet examen est particuli rement int ressant dans le marquage pr op ratoire des marges de ce type de l sions [3]. En revanche, l'examen en MC ne permet pas toujours d' liminer un diagnostic de m lanome, o on trouve souvent des cellules pag to des arrondies de grande taille et de r flectivit variable comme dans la maladie de Paget [4,6].

En conclusion, la MC est une technique non invasive qui peut apporter une aide diagnostique pr cieuse dans les formes d butantes de la maladie de Paget qui se localisent

dans des zones sensibles telles que les seins et la r gion anog nitale.

D claration d'int r ts

Les auteurs d clarent ne pas avoir de conflits d'int r ts en relation avec cet article.

R f rences

[1] Dalberg K, Hellborg H, W rnberg F. Paget's disease of the nipple in a population based cohort. Breast Cancer Res Treat 2008;111:313—9.

[2] Guitera P, Scolyer RA, Gill M, Akita H, Arima M, Yokoyama Y, et al. Reflectance confocal microscopy for diagnosis of mammary and extramammary Paget's disease. J Eur Acad Dermatol Venereol 2013;27:e24—9.

[3] Pan Z-Y, Liang J, Zhang Q-A, Lin J-R, Zheng Z-Z. In vivo reflectance confocal microscopy of extramammary Paget disease: diagnostic evaluation and surgical management. J Am Acad Dermatol 2012;66:e47—53.

[4] Longo C, Fantini F, Cesinaro AM, Bassoli S, Seidenari S, Pellacani G. Pigmented mammary Paget disease: dermoscopic, in vivo reflectance-mode confocal microscopic, and immunohistochemical study of a case. Arch Dermatol 2007;143:752—4.

[5] Richtig E, Ahlgrimm-Siess V, Arzberger E, Hofmann-Wellenhof R. Non-invasive differentiation between mamillary eczema and Paget disease by in vivo reflectance confocal microscopy on the basis of two case reports. Br J Dermatol 2011;165:440—1.

[6] Scope A, Benvenuto-Andrade C, Agero A-LC, Malvehy J, Puig S, Rajadhyaksha M, et al. In vivo reflectance confocal microscopy imaging of melanocytic skin lesions: consensus terminology glossary and illustrative images. J Am Acad Dermatol 2007;57:644—58.

5.b 4 Reflectance confocal microscopy of mucosal pigmented macules: a review of 56 cases including 10 macular melanomas.

Background

Although most mucosal pigmented macules are benign; it can be clinically challenging to rule out an early melanoma. Reflectance confocal microscopy (RCM) is a noninvasive imaging technique useful in discriminating between benign and malignant skin lesions.

Objectives

To describe the confocal aspects of benign and malignant mucosal pigmented macules with histopathological correlations.

Methods We retrospectively reviewed the confocal images of 56 labial or genital pigmented macules including 10 macular melanomas. According to the retrospective nature of the study, we evaluated the recorded images chosen by the physicians that performed the RCM examination for each case.

Results

In benign macules, the most frequently observed pattern was a ringed pattern characterized by round or polycyclic papillae, with a hyper-reflective basal layer; another pattern was characterized by sparse bright dendritic cells in the basal layer, the basal epithelial cells being otherwise less reflective. Roundish cells, a high density of dendritic cells with atypias and intraepithelial bright cells were clues to the presence of malignancy.

Conclusions

Reflectance confocal microscopy seems to be a valuable tool to noninvasively differentiate benign from malignant mucosal pigmented macules and target biopsies in cases of equivocal features.

BJD
British Journal of Dermatology

Reflectance confocal microscopy of mucosal pigmented macules: a review of 56 cases including 10 macular melanomas

S. Debarbieux,[1] J.L. Perrot,[2] N. Erfan,[3] S. Ronger-Savlé,[4] B. Labeille,[2] E. Cinotti,[2] L. Depaepe,[5] N. Cardot-Leccia,[6] J.P. Lacour,[3] L. Thomas,[1] P. Bahadoran[3,7,8] and for the Groupe d'Imagerie Cutanée Non Invasive de la Société Française de Dermatologie

[1]Departments of Dermatology [4]Gynaecology and [5]Dermatopathology, Centre Hospitalier Lyon Sud, Pierre Bénite, France
[2]Department of Dermatology, Hôpital Nord, Saint Etienne, France
[3]Department of Dermatology, Hôpital Archet 2, Nice, France
[6]Department of Pathology, Hopital Pasteur, Nice, France
[7]Centre de Recherche Clinique, CRC, Nice, France
[8]INSERM U 1065, Equipe 1, Nice, France

Correspondence
Sebastien Debarbieux.
E-mail: sebastien.debarbieux@chu-lyon.fr

Accepted for publication
16 December 2013

Funding sources
This work is supported in part by grants from Lyon 1 University (to L.T.), the Hospices Civils de Lyon (to L.T.) and the ligue contre le cancer du Rhone (to L.T.).

Conflicts of interest
None declared.

DOI 10.1111/bjd.12803

Summary

Background Although most mucosal pigmented macules are benign, it can be clinically challenging to rule out an early melanoma. Reflectance confocal microscopy (RCM) is a noninvasive imaging technique useful in discriminating between benign and malignant skin lesions.

Objectives To describe the confocal aspects of benign and malignant mucosal pigmented macules with histopathological correlations.

Methods We retrospectively reviewed the confocal images of 56 labial or genital pigmented macules including 10 macular melanomas. According to the retrospective nature of the study, we evaluated the recorded images chosen by the physicians that performed the RCM examination for each case.

Results In benign macules, the most frequently observed pattern was a ringed pattern characterized by round or polycyclic papillae, with a hyper-reflective basal layer; another pattern was characterized by sparse bright dendritic cells in the basal layer, the basal epithelial cells being otherwise less reflective. Roundish cells, a high density of dendritic cells with atypias and intraepithelial bright cells were clues to the presence of malignancy.

Conclusions Reflectance confocal microscopy seems to be a valuable tool to noninvasively differentiate benign from malignant mucosal pigmented macules and target biopsies in cases of equivocal features.

What's already known about this topic?

- Reflectance confocal microscopy (RCM) features of skin pigmented lesions are well documented but it is not known whether they can be extrapolated to mucosal pigmented lesions.

What does this study add?

- We describe the RCM patterns observed in benign and malignant pigmented macules.
- Knowledge of these patterns can avoid unnecessary biopsies and help to target biopsies appropriately.

Mucosal pigmentation is a common cause of referral to dermatologists. It can affect the vulva, the glans penis or the buccal mucosa, especially the lip. Benign melanotic macules are the most frequent cause of mucosal pigmentation. In most cases, their small size, homogeneous pigmentation and lack of extension are suggestive of benignity. However, due to an atypical clinical presentation, such as irregularity, nonhomogeneous pigmentation, large size or recent onset or enlargement, some cases are clinically challenging. Although dermoscopy can be helpful,[1 4] a biopsy is usually required in such cases to rule out an early melanoma. Indeed vulvar melanomas account for approximately 10% of vulvar malignancies.[5] Melanomas of the lip or of the oral cavity and melanomas of the glans penis presenting as flat pigmented macules, though less frequent, have also been reported.[2,3,6 9] Such lesions can initially present as brown macules simulating a benign pigmentation which can lead to a misdiagnosis or a late diagnosis.[2,3,6]

Reflectance confocal microscopy (RCM) is a noninvasive technique of skin imaging, which provides high-resolution images of the upper 250 μm of the skin, and is useful in discriminating between benign and malignant skin lesions.[10 12]

To our knowledge, the confocal presentation of mucosal pigmented macules has been reported in only two preliminary studies; according to these studies, it seems that some of these lesions harbour specific features that are not observed in the skin.[13,14]

The purpose of our study was to describe comprehensively the RCM features of benign mucosal melanotic macules and of macular mucosal melanomas.

Patients and methods

The confocal images of 54 consecutive patients with a mucosal macular pigmentation were retrospectively evaluated. Fourteen patients (12 with melanotic macules and two with melanomas) who have previously been reported[13,14] were included, as additional confocal features were analysed in the present study. The pigmentation affected the oral mucosa (lip or gingiva) or the genital area (vulva or glans penis). This study has not been registered in a public trial registry because it does not 'prospectively assigns human subjects to intervention or comparison groups to evaluate the cause and effect relationship between a medical intervention and a health outcome'. As data were collected retrospectively and patients' management was not modified, according to the French law (n°2004-806, 9th August 2004), this study did not need to be approved by a research ethics committee. After giving their informed consent, each patient underwent a confocal imaging examination (VivaScope® 3000, Lucid Inc., Henrietta, NY, U.S.A.) which provided 0·5 × 0·5 mm or 1 × 1 mm horizontal sections of the thickness of the epithelium from its surface to the upper chorion. For that purpose, the optical window of the device was covered with a translucent dressing (Tegaderm®; 3M, Cergy-Pontoise, France). Histopathological study was performed for 31 lesions, including 21 benign macules and 10 melanomas. Lesions that were not biopsied showed no suspicious features clinically or under dermoscopy and no changes following consecutive digital monitoring for at least 12 months. In addition, for eight pathology-benign lesions where dendritic cells were identified by RCM, immunostaining with MelanA (Biotech®; Kosice, Slovakia) and CD1a (DakoCytomation®, Carpinteria, U.S.A.) was performed and the number of stained cells per mm length of epithelium was counted. Immunostaining with MelanA and CD1a were also performed on normal lips from two patients undergoing lip resection for nonmelanoma skin cancer to serve as the control.

Results

Pigmentation affected the lower lip in 21 cases, the upper lip in two cases, both upper and lower lip in one case, the vulva in 20 cases, the glans penis in 10 cases and the gingiva in two cases. Altogether, there were 46 cases of benign melanotic macules and 10 cases of *in situ* or minimally invasive lentiginous malignant melanoma (Table 1). In benign macules, confocal microscopy showed polycyclic or ringed papillae or the previously described 'draped pattern'[14] in 38 cases (83%) (Figs 1, 2). Bright dendritic cells around papillae, intercalated between epithelial basal cells which were often weakly reflective, were observed in 26 cases (56%) (Fig. 3).

Table 1 Anatomic sites and diagnosis of 56 pigmented mucosal lesions

	Melanotic macule	Melanoma	Total
Lips	22	2[a]	24 (43%)
Vulva	12	8	20 (36%)
Glans penis	10	0	10 (18%)
Gingiva	2	0	2 (3%)
Total	46 (82%)	10 (18%)	56 (100%)

[a]Both on the upper lip.

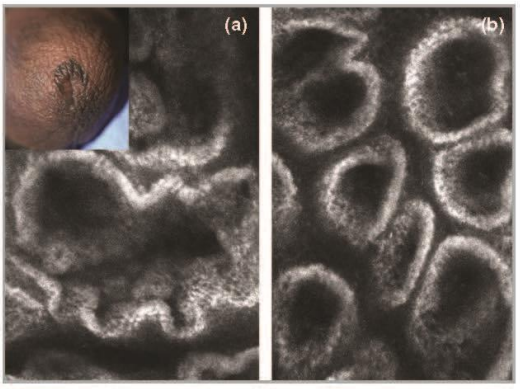

Fig 1. Melanotic macule of the glans penis: reflectance confocal microscopy images of polycyclic (a) or round (b) papillae rimmed by a layer of highly reflective epithelial cells.

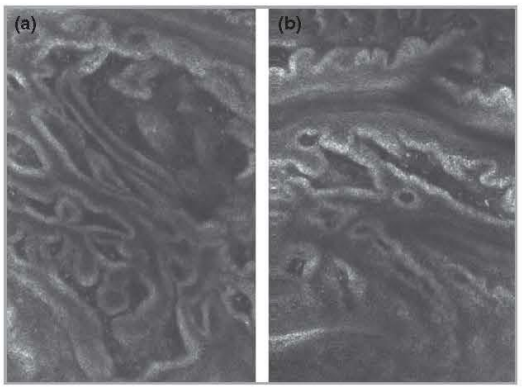

Fig 2. Melanotic macule of the vulva: reflectance confocal microscopy images of draped pattern characterized by elongated papillae rimmed by a layer of reflective epithelial cells.

The two features coexisted in 20 cases (43%). Dendritic cells mainly had a stellate, triangular or fusiform shape (Fig. 4), a roundish shape being observed exceptionally. Dendritic cells were most frequently observed in the lip (19 cases, 86% of the melanotic macules of the lip), occasionally in the vulva (five cases, 42% of the melanotic macules of the vulva) and rarely in the glans (one case, 10% of the melanotic macules of the glans), while the frequency could not be assessed on gingiva (one of two melanotic macules). For this feature, the difference between the lip and other mucosal locations was statistically significant ($P < 0{\cdot}001$, chi-squared test; SPSS, SPSS Inc., Chicago, IL, U.S.A.). In most cases, the density of dendritic cells was low: the maximum number of dendritic cells per papilla was ≤ two in 11 cases, ≤ four in 20 cases, with four in six cases, nearly exclusively on the lip (one case on the vulva). Sparse intraepithelial dendritic cells were observed exceptionally, exclusively on the lip. No roundish bright cells were observed in the epithelium. Finally, plump bright cells corresponding to melanophages were observed within the papillae in 16 cases (35%). Regarding the eight cases of melanotic macules with dendritic cells under RCM for which immunostaining with CD1a and Melan-A was performed, there was no correlation between the density of dendritic cells observed by RCM and the density of either Langerhans cells or melanocytes on the biopsied area. We performed the same CD1a and Melan-A immunostaining on two samples of normal lip. The density of melanocytes was slightly higher in labial melanotic macules than in control biopsies, although not the density of Langerhans cells.

Ten cases were macular melanomas (two on the upper lip, eight on the vulva); in most malignant cases, the confocal appearance was strikingly different from melanotic macules (Tables 2 and 3); cytologically, roundish cells and fusiform cells were predominant; roundish cells were seen in all cases, even if they were not always the predominant type; fusiform cells sometimes showed a plump appearance (Figs 5, 6). Basal dendritic cells were focally numerous, leading to a 'pearl-necklace' appearance when the cells were rather roundish (Figs 5, 6) or a continuous proliferation of atypical enlarged bright cells (Fig. 7). Intraepithelial bright cells were observed in all cases; they were also focally numerous (Figs 5, 6), although they were sparse in two cases. They were mostly fusiform or roundish. In three cases, sheets of atypical fusiform and/or roundish cells were observed (Fig. 6). Nests of melanocytes were observed in three cases (Fig. 8), and sheets of atypical cells were observed in the chorion in one case. In one case, the features described above were irregularly distributed over the pigmented macule, some areas exhibiting features consistent with a benign lentigo (polycyclic papillae,

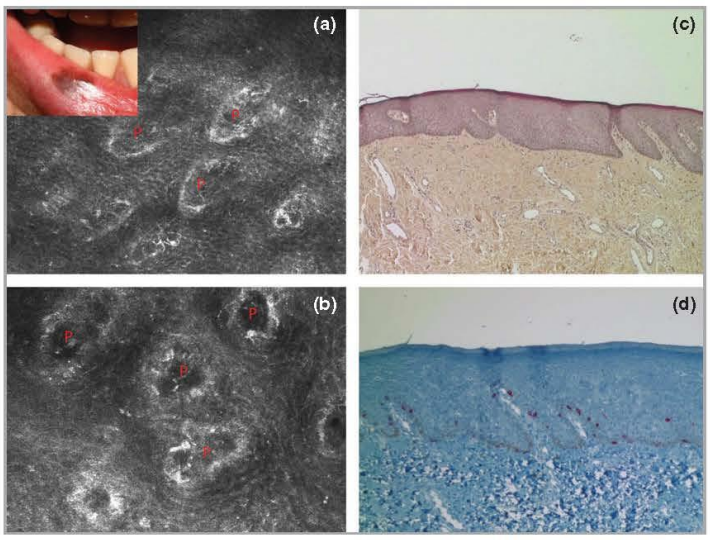

Fig 3. Melanotic macule of the lower lip. (a, b) Reflectance confocal microscopy appearance characterized by the absence of a hyper-reflective basal layer and the presence of two or three bright dendritic cells per papilla in the basal layer (P, papilla). (c) Histopathology (haematoxylin and eosin staining, ×4) shows acanthosis and no melanocytic hyperplasia in the basal layer. (d) MelanA staining (×10) shows absence of melanocytic hyperplasia in the basal layer.

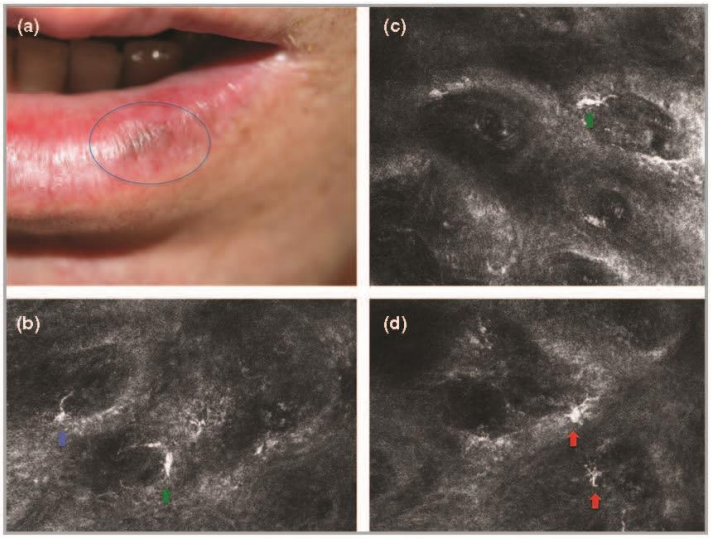

Fig 4. Different types of dendritic basal cells in a melanotic macule of the lower lip. (a) Clinical appearance (pigmentation in the blue circle). (b, c, d) Reflectance confocal microscopy images showing occasional dendritic cells in the basal layer of the epithelium: fusiform (green arrow), stellate (red arrow) or triangular (blue arrow).

Table 2 Frequency of confocal patterns associated with benign and malignant mucosal lesions

	Basal layer patterns			Intraepithelial patterns	
	Polycyclic or ringed papillae or draped pattern	Basal dendritic cells	Basal nests	Intraepithelial dendritic cells	Sheets of atypical cells
Melanotic macules	+++	+ (sparse, ≤4 per papilla, mainly stellate or triangular, occasionally fusiform)	−	+/− (stellate or triangular, occasionally fusiform)	−
Melanoma	+	+++ (numerous,mainly roundish and fusiform)	+	++ (mainly roundish and fusiform)	+

+++, Very frequent; ++, frequent; +, occasional; +/−, rare; −, never.

Table 3 Reflectance confocal microscopy features of the melanoma cases

	Location	Basal dendritic cells	Nests	Intraepithelial dendritic cells	Sheets of atypical cells	Other features
Case1	Vulva	+++ (fusiform and roundish)	−	+++ (fusiform and roundish)	+	
Case 2	Vulva	+++ (fusiform and occasionally roundish)	+	++ (fusiform and roundish)	+	
Case 3	Vulva	++ to +++ (fusiform and occasionally roundish)	+	±, to ++ (fusiform, stellate and occasionnally roundish)	−	Heterogeneously distributed features
Case 4	Vulva	+++ (roundish and fusiform)	−	+++ (roundish and fusiform)	−	Pearl-necklace appearance around papillae
Case 5	Vulva	++ to +++ (roundish)	+	++ to +++ (roundish)	+	
Case 6	Vulva	+++ (roundish and fusiform)	−	+++ (roundish)	−	
Case 7	Cervix and vagina	+++ (roundish and fusiform)	−	++ (roundish and fusiform)	+	
Case 8	Vulva	+, focally +++ Stellate and triangular, rarely roundish	−	−	−	Foci of irregular bright thickening of the basal layer
Case 9	Upper lip	++ (roundish)	+	± to ++ (roundish)	−	Pearl-necklace appearance around papillae
Case 10	Upper lip	+++ (fusiform and occasionally roundish)	−	++ (fusiform)	−	

+++, Numerous; ++, moderate; +, occasional; ±, rare; −, absent.

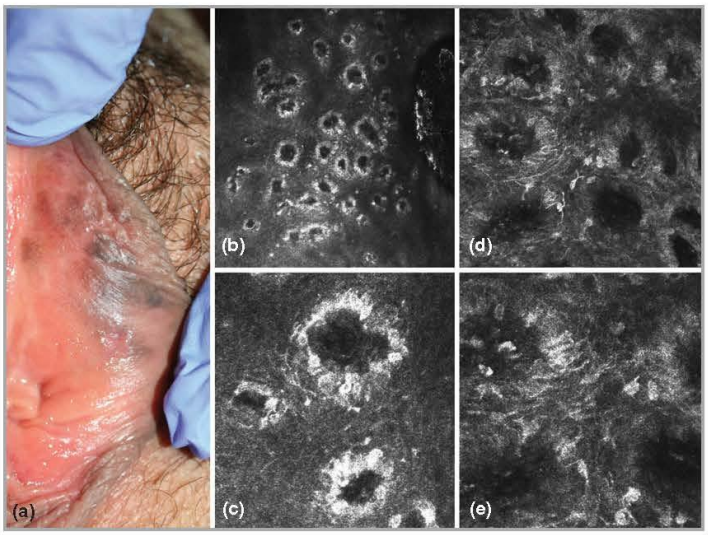

Fig 5. (a) Large heterogeneous vulvar pigmentation corresponding to an *in situ* melanoma. (b, c) Numerous roundish bright cells around the papillae showing a pearl-necklace appearance under reflectance confocal microscopy (RCM). (d, e) Numerous intra-epithelial bright cells with fusiform or roundish shape under RCM. (b, d, low magnification; c, e, high magnification).

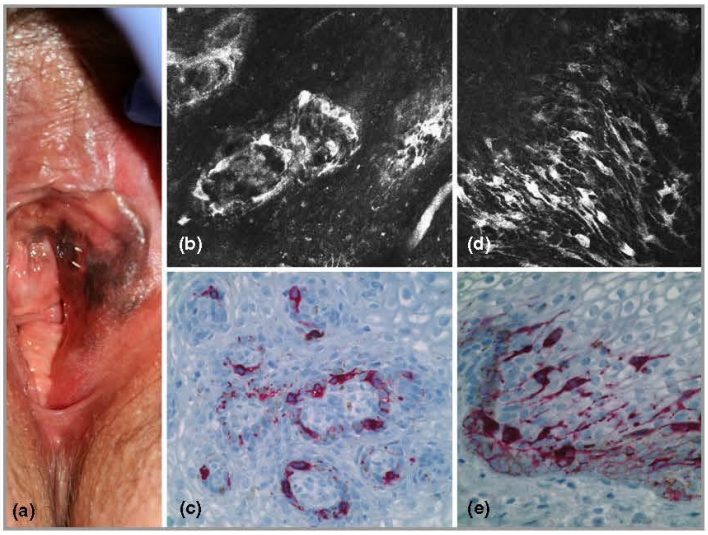

Fig 6. (a) Large heterogeneous vulvar pigmentation corresponding to a minimally invasive melanoma (0·27 mm). (b) Large atypical (mainly roundish) bright cells around the papillae under reflectance confocal microscopy (RCM). (c) MelanA staining (×10) shows the corresponding pathological appearance: melanocytic hyperplasia is mainly localized in the basal layer of the epithelium. (d) Sheets of atypical fusiform bright cells within the epithelium shown by RCM; (e) MelanA staining (×20) shows the corresponding pathological appearance.

rare basal dendritic cells) whereas atypical roundish bright cells (occasionally intraepithelial) were observed in other areas (Fig. 9). Interestingly enough, in two cases, the pathological features of a punch biopsy performed before RCM included atypias but did not wholly suggest a melanoma, whereas RCM strongly indicated malignancy, which was subsequently confirmed pathologically. Finally, one case was particularly challenging (Fig. 10), because RCM was inconclusive initially. Excision was performed and the lesion was diagnosed pathologically as a mainly *in situ* melanoma with focally isolated melanoma cells in the papillae. RCM images were then re-examined and we could identify foci with occasional roundish cells in the basal layer, foci of irregular bright thickening of the basal layer, corresponding to aggregated bright cells larger than epithelial cells, and occasional bright roundish nucleated cells in some papillae, not typical of melanophages and rather suggestive of melanoma cells.

Discussion

Labial or genital pigmented macules are commonly observed in daily practice. Although most mucosal pigmented macules are benign, rare cases correspond to early lentiginous mucosal melanomas. RCM is a painless, noninvasive imaging technique, and mucous membranes are easily accessible to confocal examination thanks to a handheld device.[13 15] RCM

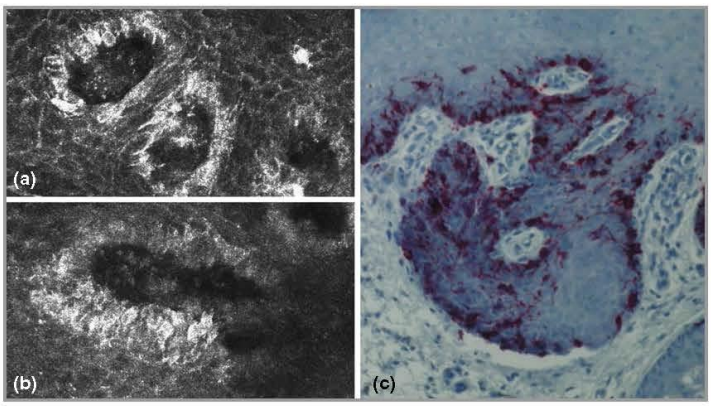

Fig 7. *In situ* melanoma. (a, b) Continuous proliferation of atypical enlarged bright roundish, fusiform and triangular/stellate cells in the basal layer under reflectance confocal microscopy. (c) MelanA staining (×10) shows the corresponding pathological appearance.

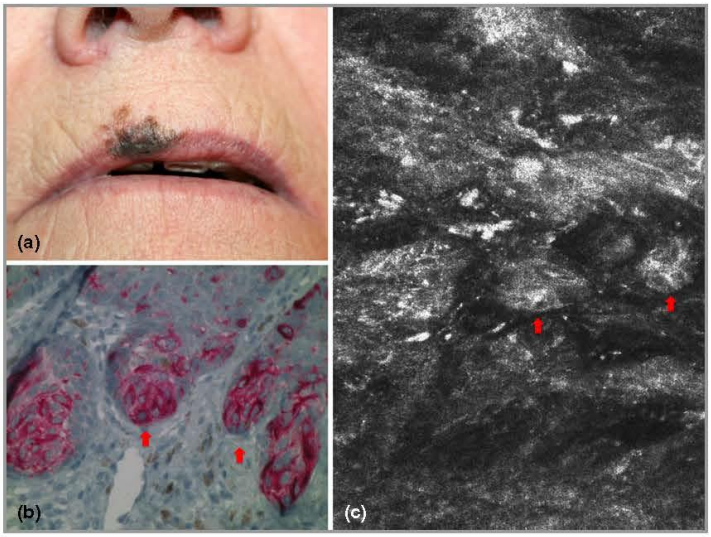

Fig 8. (a) Heterogenous upper lip pigmentation corresponding to a minimally invasive melanoma (0·35 mm). (b) MelanA staining (×20) shows nests of melanocytes within the epithelial digitations (red arrows). (c) The corresponding reflectance confocal microscopy image with nests of aggregated large nucleated bright cells (red arrows).

criteria for benign and malignant melanocytic lesions have been extensively described for the skin,[10 12] but it has never been stated whether these criteria could be extended to mucosae. To date, there are only scant reports about RCM features of mucosal pigmented lesions. Erfan *et al.*[13] reported the RCM features of four labial melanotic macules and highlighted the presence of sometimes numerous dendritic bright cells at the dermoepithelial junction, a feature which is commonly observed in lentiginous melanomas developed on chronically sun-exposed skin, especially on the face.[10] However, histopathology did not reveal any suspicious melanocytic hyperplasia and was in favour of a benign lentigo in each case. Cinotti *et al.*[14] reported their experience on 10 pigmented lesions of the vulva, eight of which were benign melanotic macules. They concluded that benign macules are characterized by either a ringed (roundish shape of the papillae) or a draped (elongated shape of the papillae) pattern, the papillae being rimmed by highly reflective monomorphous epithelial cells. However, they noticed dendritic cells around the papillae in one case.

Here we present RCM features of benign and malignant pigmented mucosal macules. The main limitation of our study is its retrospective nature. RCM is indeed a dynamic procedure and the recorded images are chosen by the physician who performs the examination, which could induce a bias. Also, lesions with otherwise benign clinical and dermoscopic[2,3] criteria were not always biopsied, therefore, we ensured that these lesions were stable both by history and follow-up. However, we confirmed on a large series of cases that a ringed or a draped pattern with polycyclic papillae is the most often observed feature in benign mucosal pigmentation, which is in agreement with the RCM pattern (polycyclic-edged papillae) classically observed in skin lentigines.[16] However, the presence of dendritic cells in the basal layer of the epithelium is not such a rare event, especially on the lip where it was observed in 86% of the cases of our series; it is less frequent on the

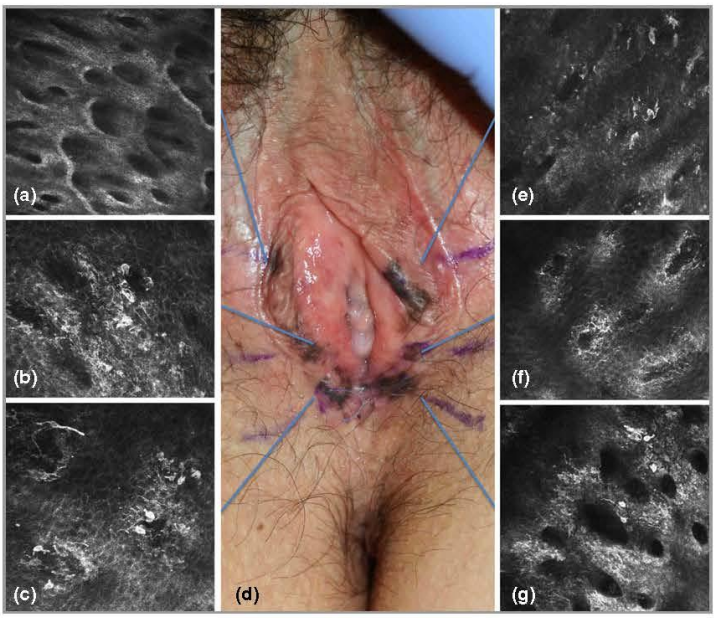

Fig 9. (d) Large heterogenous pigmentation corresponding to an *in situ* melanoma. (a, b, c, e, f, g) Reflectance confocal microscopy images of different areas highlighting the heterogeneity of the different features described. (a) Polycyclic-edged papillae rimmed by bright epithelial basal cells; such an appearance is suggestive of a lentigo. (f) Quite numerous bright dendritic cells in the basal layer of the papillae; the density of these cells is rather unusual for a lentigo, but such an appearance is not typically suggestive of a melanoma. (b, c, e, g) Variable density of basal and intraepithelial roundish and fusiform bright cells, suggestive of a melanoma.

vulva and rarely observed on the glans penis. In most cases, the density of such cells is low. Importantly, in our experience there were no atypical roundish cells, and bright dendritic cells were observed exceptionally in the suprabasal layers of the epithelium; however, considering this was a retrospective study, we cannot rule out the possibility that these cells were truly close to the top of papillae that were not visible on single images. This pattern, characterized by the presence of sparse dendritic cells in the basal layer, with up to four (occasionally more) dendritic cells per papilla, and the possible absence of hyper-reflective epithelial basal cells, must be known in order to avoid overdiagnosis of melanoma.

On chronically sun-exposed skin, the presence of pagetoid roundish atypical cells is much more predictive of a lentigo maligna than the presence of pagetoid dendritic cells;[12] bright dendritic cells under RCM can indeed correspond to either melanocytes or Langerhans cells, whereas roundish atypical bright cells always correspond to atypical melanocytes.[17] Our observations did not allow us to determine the nature of the dendritic cells observed in our cases of labial macules and genital pigmented macules, and why these dendritic cells were predominantly observed on the lips. To clarify the identity of these dendritic cells, we performed an immunohistochemical study on melanotic macules, but it did not show any striking correlation between the density of either Langerhans cells or melanocytes and the presence of dendritic cells under RCM. A comparison with normal lip samples suggested that dendritic cells might correspond to melanocytes but the low number of control biopsies and the lack of RCM examination in these samples does not allow a definitive conclusion and a more comprehensive study comparing RCM and immunohistochemistry on pigmented and unpigmented mucosae is needed.

Moreover, histologically, the melanocyte count is usually normal in labial melanotic macules,[18 20] although a higher number of melanocytes than usual has rarely been reported in cases of macular pigmentation of Laugier and Hunziker.[20] However, it is possible that the melanin load in melanocytes could be more important in mucosal melanotic macules than in normally pigmented mucosa,[9,18,19] and could increase the contrast under RCM between basal epithelial cells and melanocytes, thereby highlighting their dendricity. Of note, in the benign cases of our series, basal dendritic cells observed under RCM were stellate, triangular or fusiform shaped cells with no atypia, which is consistent with this hypothesis.

On the other hand, in the melanoma group, the presence of cytological (roundish shape, plump appearance of fusiform cells) and architectural atypias (high density of dendritic cells in the basal layer, pagetoid cells, sheet-like proliferation of cells, pearl-necklace appearance around papillae, presence of melanocyte nests) are correlated to the previously reported histopathological characteristics[9] of early mucosal melanoma and to the pathological data observed in our patients (Figs 5 10). On the whole, the presence of roundish bright cells, a high density of atypical dendritic cells and the presence of intraepithelial bright cells were particularly relevant features in our experience. It is noteworthy, however, that in the so-called lentiginous pattern[9] of *in situ* mucosal melanomas, the cytological atypias can be subtle and most architectural criteria can be missing under RCM, giving more importance to the density of dendritic and/or atypical cells in the basal layer.

In conclusion, this study shows that melanotic macules and early mucosal melanomas have mostly distinct RCM features. The presence of dendritic cells in both situations may be confusing and requires a comprehensive analysis of

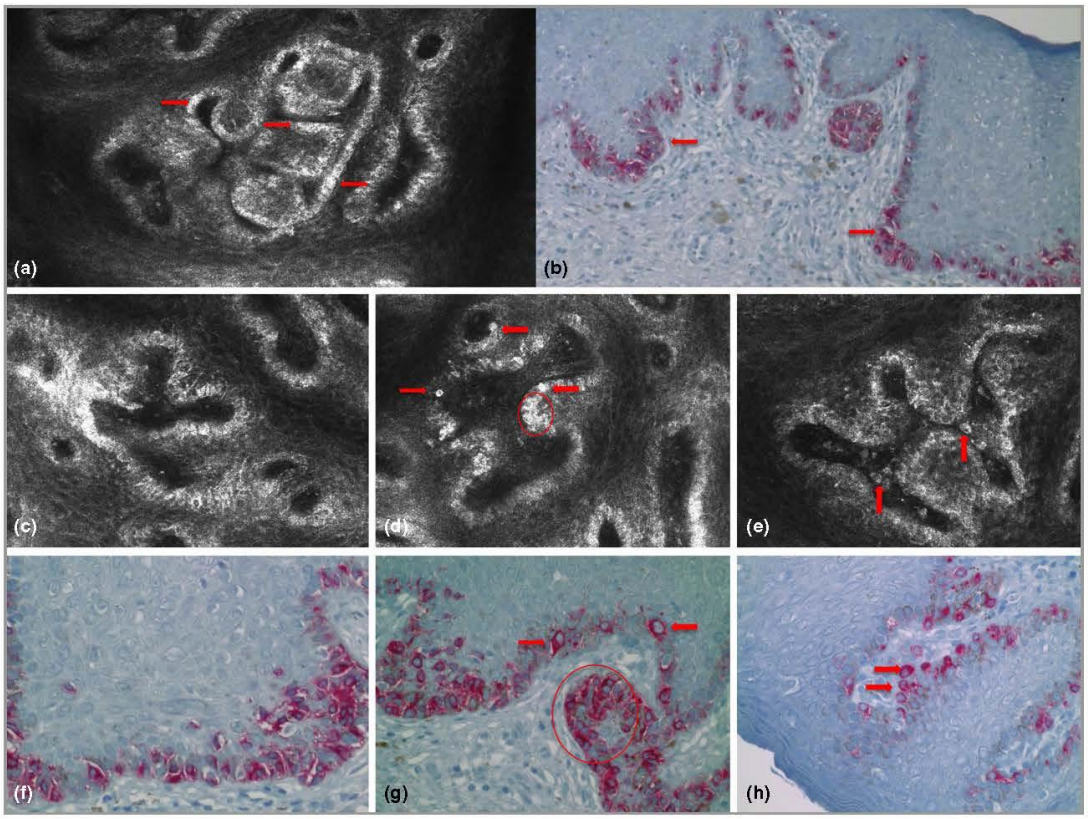

Fig 10. A case of lentiginous mucosal melanoma. (a) At first glance, the polycyclic papillae and the brightness of the basal layer could be suggestive of a melanotic macule; however, note the irregularity of the brightness with foci of thickening (arrows) and presence of dendrites shown by reflectance confocal microscopy (RCM). (b) MelanA staining (×20) shows the corresponding pathological appearance with a dense nearly continuous lentiginous proliferation of melanocytes in the basal layer; they are quite small, which explains how they can be missed under RCM because of the brightness of adjacent basal epithelial cells. However, they are aggregated in some places (red arrows), which explains the irregularity of the brightness and foci of thickening under RCM. (c) Note the density of the bright dendritic cells in the basal layer under RCM. (f) MelanA staining (×40) shows corresponding pathological appearance. (d) Occasional roundish cells are identified (red arrows), as well as foci of aggregation of bright cells in the epithelial digitations (red circle) under RCM. (g) MelanA staining (×40) shows corresponding pathological appearance: occasional larger melanoma cells are present (red arrows), corresponding to roundish bright cells under RCM. Aggregation of melanocytes at the tip of epithelial digitations (red circle). (e) Occasional roundish nucleated cells in the papillae (red arrows), not typically suggestive of melanophages under RCM. (h) MelanA staining (×40) shows corresponding pathological appearance of melanoma cells (red arrows).

their shape, density and localization. These results suggest that RCM could be a useful tool to discriminate between melanotic macules and mucosal melanomas or to target biopsies in case of suspicious lesions. Nevertheless, there may remain difficult cases because of unusually numerous basal dendritic cells by RCM, with neither atypia nor other features suggestive of melanoma on RCM and pathological examination. It is worth prospectively following such cases clinically and with RCM in order to determine their long-term outcome.

Acknowledgments

The authors are indebted to Kevin Zorzi, BSc, for his help in the statistical analysis of data.

References

1 Mannone F, De Giorgi V, Cattaneo A *et al.* Dermoscopic features of mucosal melanosis. *Dermatol Surg* 2004; **30**:1118–23.
2 Lin J, Koga H, Takata M, Saida T. Dermoscopy of pigmented lesions on mucocutaneous junction and mucous membrane. *Br J Dermatol* 2009; **161**:1255–61.
3 Blum A, Simionescu O, Argenziano G *et al.* Dermoscopy of pigmented lesions of the mucosa and the mucocutaneous junction: results of a multicenter study by the International Dermoscopy Society (IDS). *Arch Dermatol* 2011; **147**:1181–7.
4 Ronger-Savle S, Julien V, Duru G *et al.* Features of pigmented vulval lesions on dermoscopy. *Br J Dermatol* 2011; **164**:54–61.
5 Moxley KM, Fader AN, Rose PG *et al.* Malignant melanoma of the vulva: an extension of cutaneous melanoma? *Gynecol Oncol* 2011; **122**:612–17.

6 Eisen D, Voorhees JJ. Oral melanoma and other pigmented lesions of the oral cavity. J Am Acad Dermatol 1991; **24**:527–37.
7 Betti R, Menni S, Crosti C. Melanoma of the glans penis. Eur J Dermatol 2005; **15**:113–15.
8 Hankins CL, Kotwal S, Majumder S et al. Multifocal melanoma of the glans penis. Plast Reconstr Surg 2006; **118**:33e–8e.
9 Saida T, Kawachi S, Takata M et al. Histopathological characteristics of malignant melanoma affecting mucous membrane: a unifying concept of histogenesis. Pathology 2004; **36**:404–13.
10 Pellacani G, Guitera P, Longo C et al. The impact of in vivo reflectance confocal microscopy for the diagnostic accuracy of melanoma and equivocal melanocytic lesions. J Invest Dermatol 2007; **127**:2759–65.
11 Pellacani G, Farnetani F, Gonzalez S et al. In vivo confocal microscopy for detection and grading of dysplastic nevi: a pilot study. J Am Acad Dermatol 2012; **66**:e109–21.
12 Guitera P, Pellacani G, Crotty KA et al. The impact of in vivo reflectance confocal microscopy on the diagnostic accuracy of lentigo maligna and equivocal pigmented and nonpigmented macules of the face. J Invest Dermatol 2010; **130**:2080–91.
13 Erfan N, Hofman V, Desruelles F et al. Labial melanotic macule: a potential pitfall on reflectance confocal microscopy. Dermatology 2012; **224**:209–11.
14 Cinotti E, Perrot JL, Labeille B et al. Reflectance confocal microscopy for the diagnosis of vulvar melanoma and melanosis: Preliminary results. Dermatol Surg 2012; **38**:1962–7.
15 Alessi SS, Nico MM, Fernandes JD, Lourenço SV. Reflectance confocal microscopy as a new tool in the in vivo evaluation of desquamative gingivitis: patterns in mucous membrane pemphigoid, pemphigus vulgaris and oral lichen planus. Br J Dermatol 2013; **168**:257–64.
16 Langley RG, Burton E, Walsh N et al. In vivo confocal scanning laser microscopy of benign lentigines: comparison to conventional histology and in vivo characteristics of lentigo maligna. J Am Acad Dermatol 2006; **55**:88–97.
17 Hashemi P, Pulitzer MP, Scope A et al. Langerhans cells and melanocytes share similar morphologic features under in vivo reflectance confocal microscopy: a challenge for melanoma diagnosis. J Am Acad Dermatol 2012; **66**:452–62.
18 Ho KK, Dervan P, O'Loughlin S, Powell FC. Labial melanotic macule: a clinical, histopathologic, and ultrastructural study. J Am Acad Dermatol 1993; **28**:33–9.
19 Gupta G, Williams RE, Mackie RM. The labial melanotic macule: a review of 79 cases. Br J Dermatol 1997; **136**:772–5.
20 Moore RT, Chae KA, Rhodes AR. Laugier and Hunziker pigmentation: a lentiginous proliferation of melanocytes. J Am Acad Dermatol 2004; **5** (Suppl):S70–4.

5.b 5 Reflectance confocal microscopy for the diagnosis of vulvar naevi: six cases

Background and objectives

The differential diagnosis between vulvar naevi and melanoma is challenging. *In vivo* reflectance-mode confocal microscopy (RCM) is an emerging technique that allows non-invasive high-resolution imag- ing of the skin and mucosa. It has recently been used for the study of vulvar melanosis and melanoma, but it has not been so far employed for the diagnosis of genital naevi. The objective of this study is to evaluate RCM features of vulvar naevi and to compare them with dermoscopical and histopathological aspects.

Methods

Clinical, dermoscopical, *in vivo* RCM and histological features of six vulvar naevi were evaluated.

Results The clinical and/or dermoscopical aspects were suspicious in all six cases. RCM showed a blue naevus, an atypical genital naevus, a junctional naevus and three compound naevi that were later confirmed by histological examination. In one compound naevus, RCM showed focal cytological atypia and architectural irregularity without clear fea- tures of malignancy, confirmed by histological examination.

Conclusions Reflectance-mode confocal microscopy can play a role in non-invasive diagnosis of vulvar naevi, but further broader studies are required to validate our observations.

SHORT REPORT

Reflectance confocal microscopy for the diagnosis of vulvar naevi: six cases

E. Cinotti,[1,*,†] C. Couzan,[1] J.L. Perrot,[1,†] B. Labeille,[1,†] P. Bahadoran,[2,3,4,†] S. Puig,[5] M. Wantz,[6,†] A. Vicente-Villa,[7] C. Habougit,[8] C. Butori,[9] F. Cambazard[1,†]

[1]Dermatology Department, University Hospital of Saint-Etienne, Saint-Etienne Cedex 2, France
[2]Dermatology Department, Hôpital Archet 2, Nice, France
[3]Centre de Recherche Clinique, CRC Nice, France
[4]INSERM U 1065, Equipe 1, Nice, France
[5]Dermatology Department, University Hospital of Barcelona, Barcelona, Spain
[6]Dermatology Department, Hôpital Saint Vincent de Paul, GHICL, Lille, France
[7]Dermatology Department, Hospital Sant Joan de Deu, Barcelona, Spain
[8]Pathology Department, University Hospital of Saint-Etienne, Saint-Etienne, France
[9]Pathology Department, Hôpital Archet 2, Nice, France
*Correspondence: E. Cinotti. E-mail: elisacinotti@gmail.com

Abstract

Background and objectives The differential diagnosis between vulvar naevi and melanoma is challenging. *In vivo* reflectance-mode confocal microscopy (RCM) is an emerging technique that allows non-invasive high-resolution imaging of the skin and mucosa. It has recently been used for the study of vulvar melanosis and melanoma, but it has not been so far employed for the diagnosis of genital naevi. The objective of this study is to evaluate RCM features of vulvar naevi and to compare them with dermoscopical and histopathological aspects.

Methods Clinical, dermoscopical, *in vivo* RCM and histological features of six vulvar naevi were evaluated.

Results The clinical and/or dermoscopical aspects were suspicious in all six cases. RCM showed a blue naevus, an atypical genital naevus, a junctional naevus and three compound naevi that were later confirmed by histological examination. In one compound naevus, RCM showed focal cytological atypia and architectural irregularity without clear features of malignancy, confirmed by histological examination.

Conclusions Reflectance-mode confocal microscopy can play a role in non-invasive diagnosis of vulvar naevi, but further broader studies are required to validate our observations.

Received: 1 April 2014; Accepted: 18 November 2014

Conflicts of interest

None declared.

Funding sources

None declared.

Introduction

Clinical differential diagnosis between vulvar naevi and melanoma is challenging. Dermoscopy adds some elements[1–4] for a correct diagnosis, but has limitations. *In vivo* reflectance-mode confocal microscopy (RCM) is an emerging technique that allows for non-invasive high-resolution imaging of the skin[5] and mucosa.[6–9] The contrast in RCM images relies on the differences in the refractivity of the tissue. In particular, melanin and melanosomes have a high refractive index and appear bright in RCM, being easy to identify. This is why RCM is particularly suitable for melanocytic lesions. We present the first six cases of vulvar naevi observed by RCM.

Materials and methods

Vulvar lesions of six different patients were evaluated by clinical, dermoscopical and *in vivo* RCM examination after being either incidentally discovered during self-examination (case 2, 3 and 6), or annual gynaecological check-up (case 1), or noticed by parents in case of children (case 4 and 5). No other pigmented lesions were present on oral mucous membranes and nails. One patient presented with multiple genital pigmented lesions.

†Groupe Imagerie Cutanée Non Invasive, Société Française de Dermatologie.

High-definition (HD) dermoscopy was performed with the HD dermoscope Canon PowerShot® G10 camera (FotoFinder Systems GmbH, Bad Birnbach, Germany) and Dermlite Foto (3GEN, San Juan Capistrano, CA, USA) combined with a Canon camera (Canon Powershot®; Canon, New York, NY, USA).

In vivo RCM examination was carried out with the handheld VivaScope 3000® camera (Caliber, New York, NY, USA, distributed in Europe by MAVIG GmbH, Munich, Germany) which uses a laser with a wavelength of 830 nm that causes no damage to tissue but limits the imaging depth to 200 300 μm. Each given image corresponds to a horizontal 1 mm × 1 mm section of the mucosa at a selected depth.

The tip of both the dermoscope and the *in vivo* reflectance-mode confocal microscope were covered by a disposable sterile transparent film (Visulin®; Paul Hartmann AG, Heidenheim, Germany) to prevent possible transmission of infections. Ultrasound gel was used as immersion liquid for both dermoscopy and *in vivo* RCM.

The RCM diagnosis was made independently by three investigators for the first three cases and by one investigator for the other three.

Results

Major clinical features are reported in Table 1. In all cases RCM diagnosed benign naevus. A 100% concordance was found for the three cases evaluated by different investigators.

All lesions were excised due to the suspicious clinical and/or dermoscopical features (Fig. 1) and the histopathological examination confirmed the RCM diagnosis.

Reflectance confocal microscopy features compared to histological findings

Case 1 *In vivo* RCM examination showed hyper-reflective cells with a plump cellular body and long dendrites intermingled with hyper-reflective and elongated collagen fibres in the superficial chorion suggestive of blue naevus (Fig. 2a).

The histological examination showed the same proliferation of dendritic cells in the superficial chorion (Fig. 2b), thus confirming the diagnosis of blue naevus.

Case 2 *In vivo* RCM examination showed large junctional nests of large roundish hyper-reflective melanocytes that were characteristically dyshesive (Fig. 2c). Histology found the same type of nests (Fig. 2d) and showed that these melanocytes were hyperpigmented and had prominent nucleoli. Both RCM and histology also showed a lichenoid infiltrate at the junction. The lesion was diagnosed by both RCM and histopathology as atypical genital naevus.

Case 3 and 4 *In vivo* RCM (Fig. 3a,c) and histopathological (Fig. 3b,d) examinations found regular melanocytic nests at the junction and in the chorion. In particular, under RCM junctional nests were well visible in both cases, whereas chorion nests were well visible in case 4, as roundish homogeneous aggregates of hyper-reflective cells, and less evident in case 3 where melanocytes were less reflective (Fig. 3a).

Case 5 *In vivo* RCM showed high-density and confluent junctional and chorion nests of melanocytes of different size and refractivity (Fig. 3e). A proliferation of focal roundish and dendritic large hyper-reflective cells corresponding to atypical melanocytes were also present in the basal layer of the epidermis. Histopathological examination showed a compound naevus with cytological and architectural atypia associated with lichen sclerosus (Fig. 3f).

Case 6 *In vivo* RCM showed edged papillae lined by hyper-reflective cells for all vulvar macules, except for one that presented with lentiginous junctional proliferation of melanocytes and junctional nests of bright cells (Fig. 3g). Histopathological

Table 1 Clinical features of the four cases with dermoscopical, reflectance confocal microscopy and histological diagnosis

Patient number	Age/ Sex	Location	Clinical aspect	Dermoscopical diagnosis	RCM diagnosis	Histological diagnosis
1	70 yr/F	Left labia majora	Dark brown macule, 6 × 6 mm	Blue naevus or melanoma	Blue naevus	Blue naevus
2	30 yr/F	Left labia majora	Bluish macule, 8 × 4 mm	Blue naevus or melanoma	Genital atypical naevus	Genital atypical naevus
3	13 yr/F	Left labia majora	Asymmetrical brown macule, 8 × 8 mm	Melanoma	Compound naevus	Compound naevus
4	13 mo	Left labia majora	Dark brown macule, 10 × 10 mm	Melanoma	Compound naevus	Compound naevus
5	10 yr/F	Right labia majora	Asymmetrical brown macule, 8 × 8 mm	Melanoma	Compound naevus	Compound naevus
6	72/F	Left labia minor	Brown macule, 4 × 4 mm	Melanosis	Junctional naevus	Junctional naevus

yr, years; mo, months.

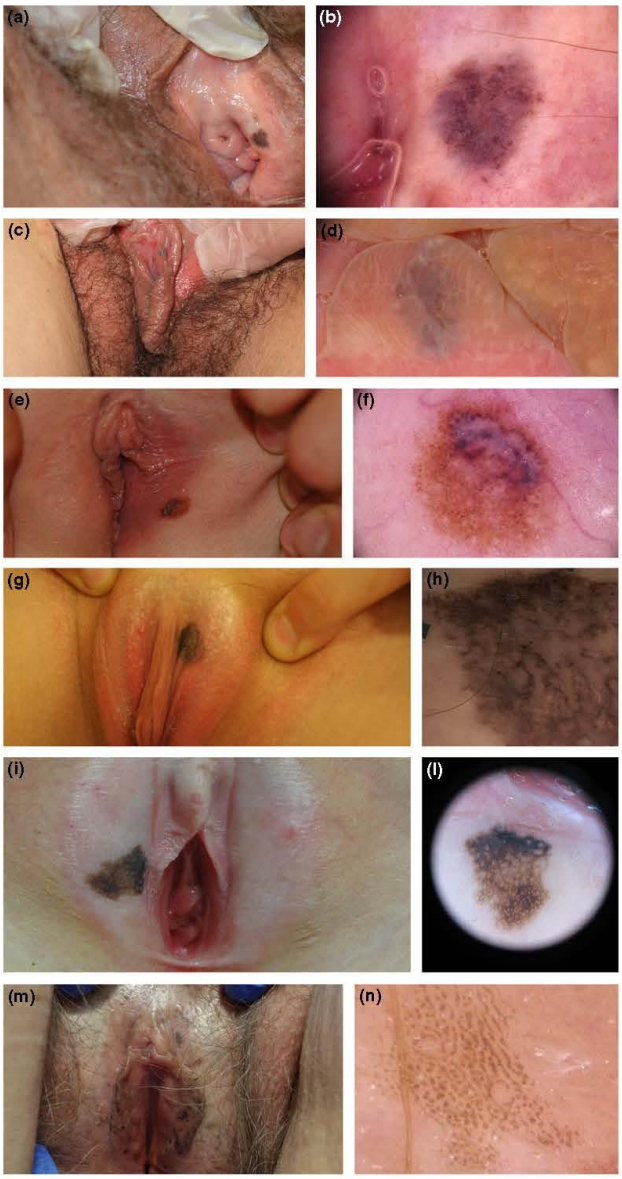

Figure 1 Clinical (a,c,e,g,i,m) and dermoscopical (b,d,f,h,l,n) aspects of the six naevi. HD dermoscopy showed in case 1 (b) brown globules and streaks with a remnant of broken pigment network, irregularly distributed on a grey background where grey dots were hardly to be seen; in case 2 bluish areas separated by white structures (d); in case 3 (f) an asymmetrical lesion with regular brown globules on the cutaneous side and a peripheral whitish area with bluish dots and globules on the mucosal side, and a central reticular depigmentation; in case 4 (h) brown polygonal structures, brown and grey globules and homogeneous areas; in case 5 (l) a brown and reticular cutaneous side and a bluish and homogeneous mucosal side with irregularly distributed brown and grey dots; and in case 6 (n) a polycircular pattern.

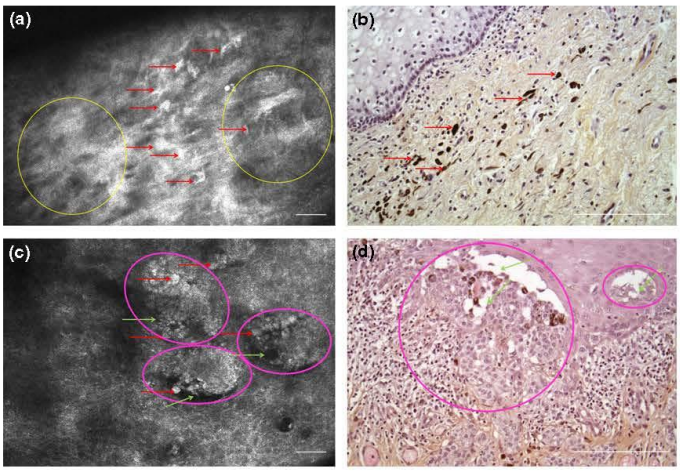

Figure 2 *In vivo* reflectance confocal microscopy (RCM) and histopathological aspects of the naevi 1 and 2. *In vivo* RCM shows in case 1 (a, image of the superficial chorion) a proliferation of hyper-reflective cells (red arrows) with a plump cellular body and long dendrites in the chorion (yellow circles indicate collagen fibres in the chorion); in case 2 (c, image of the epithelial-chorion junction) large dyshesive (hypo-reflective clefts among cells are indicated by green arrows) junctional nests (pink circles) of large roundish hyper-reflective melanocytes (red arrows). Histopathological examination with haematoxylin and eosin stain (20×) shows in case 1 (b) a proliferation of fusiform dendritic cells in the superficial chorion (red arrows), irregularly distributed parallel to the epithelium and in case 2 (d) confluent, crowded and dyshesive (clefts among cells are indicated by green arrows) nests (pink circles) of hyper-pigmented and fusiform melanocytes at the epithelium-chorion junction and in the chorion. Scale bar: 100 μm.

examination confirmed the diagnosis of junctional naevus (Fig. 3h).

Discussion

Vulvar naevi are rare[10] and the literature about their clinical and dermoscopical features is very poor.[1 4,10] In all of our cases the clinical aspect was suspicious and in the first five patients dermoscopy showed worrying features.

All the cases suspicious at dermoscopy showed polychromia and a polymorphous pattern that are more likely associated with melanoma.[1,2] Four cases presented melanoma-specific criteria (case 1: irregular globules; case 2: blue-white veil; case 3: reticular depigmentation, regression structures consisting of irregular dots and globules and grey dots; and case 5: regression structures consisting of irregular dots and grey dots). Basing on the algorithm of Ronger-Savle *et al.*[2] our five lesions suspicious at dermoscopy should be removed. Using the models identified by the International Dermoscopy Society for genital lesions,[4] three of our lesions (n. 2, 3 and 5 for model I and n. 1, 2, 3 for model II) would be diagnosed as melanoma.

Reflectance-mode confocal microscopy provides additional information to the clinical and dermoscopical examination facilitating the correct diagnosis of melanocytic lesions and is particularly appropriate for the mucosa, thanks to the handheld device.[7] We recently identified four major RCM features of vulvar melanoma:[6,7] a high density of basal hyper-reflective dendritic cells, numerous pagetoid bright large cells in the epithelium (mainly roundish or fusiform), loss of normal architecture of chorion papillae and sheets of atypical cells in the chorion. In our series of vulvar naevi we did not find any of these features in five of six cases. In one case (case 5) we found the focal presence of atypical cells at the basal layer of the epithelium and the loss of normal architecture of chorion papillae, but these microscopical aspects, not typical of a naevus, were also found at histopathological examination.

In our case 1, RCM showed regular dendritic cells between collagen bundles in the chorion, characteristic of blue naevus.[11] At a first observation this lesion could have been misdiagnosed as melanoma due to the presence of large hyper-reflective cells, irregularly distributed in the chorion, but careful examination showed that these cells were homogeneous and all presented a lanceolate body, characteristic for blue naevi.

In our case 2 RCM and histology showed homogeneous large junctional nests, curiously dyshesive, characteristic for atypical genital naevus. Atypical genital naevus represents 3 20% of the vulvar naevi,[1,12] has a benign behaviour,[13,14] and may raise concern for a diagnosis of melanoma because of its peculiar histopathological aspect with large discohesive junctional nests,

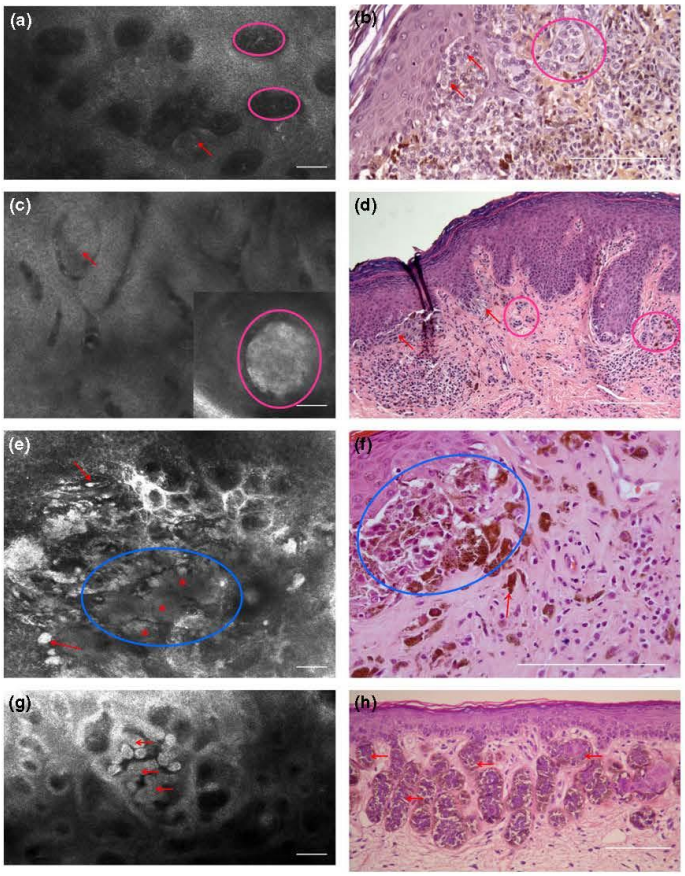

Figure 3 *In vivo* reflectance confocal microscopy (RCM) and histopathological aspects of the naevi 3, 4, 5 and 6. *In vivo* RCM images of the epithelium-chorion junction shows in case 3 and 4 (a, c) junctional (red arrows) and chorion (pink circles) nests of melanocytes; in case 5 (e) atypical cells at the epithelium-chorion junction (red arrows) and homogeneous dense and confluent nests of melanocytes (blue circle; red asterisks indicate single nests); in case 6 (g) junctional (red arrow) nests of melanocytes. Histopathological examination with haematoxylin and eosin stain shows in case 3 (b) and 4 (d) junctional (red arrows) and chorion nests (pink circles; b 20× and d 10×); in case 5 (f) a compound naevus with large confluent nests (blue circle) and large hyper-pigmented melanocytes (red arrow; 20×); and in case 6 (h) small junctional nests (red arrows; 10×). Scale bar: 100 μm.

lentiginous growth, possible mild cytological atypia and pagetoid spread.[12,15] Moreover, an inflammatory infiltrate is often present as in our case.[15] Recognition of this unusual entity and its RCM and histological features is important to avoid over-diagnosis of melanoma. However, the histological differential diagnosis with melanoma is not always easy and we suggest a surgical excision in case of a similar aspect under RCM until large series are described.

In our case 3, RCM aspect was completely reassuring in contrast to the worrying clinical and dermoscopical appearance, probably induced by the special location at the junction between the mucosa and skin.

Our cases 4 and 5, characterized by a similar clinical suspicious aspect, concerned children. RCM is particularly interesting in children, being a non-invasive procedure, and in both cases allowed to exclude melanoma. In case 5, the contemporary presence of cytological and architectural atypia (irregular and confluent nests with non-homogeneous cellularity) at RCM examination was suggestive of histological dysplasia, but the lack of pagetoid cells and the focality of the atypia allowed to exclude

a melanoma, as for atypical naevi of the skin.[16] The architectural and cytological atypia in case 5 could also be explained by the co-existence of lichen sclerosus.

Case 6 highlights one of the main advantages of RCM: the handheld camera is handy and enables the exploration of the whole vulvar region being also suitable for multifocal lesions and allowing to spare multiple biopsies.

In conclusion, RCM could help in the differential diagnosis of pigmented lesions of female genitalia and avoid genital biopsies. In all our six cases the clinical and/or dermoscopical aspects were suspicious, whereas RCM was in favour of naevus. Main limitations of the technique in addition to the availability of the machine and its cost are 1) the loss of image resolution going in depth, that could render more difficult the diagnosis of deep melanoytic proliferations like in blue naevi where the distinction of melanocytes and collagen fibres, both elongated and hyper-reflective can be difficult to an untrained eye, 2) the difficulty to identify melanocytes in the chorion when they are poorly reflecting as in our case 3, and 3) the inability to identify nuclear and nucleolar atypia. Further studies are required to define the RCM features of vulvar naevi and to compare them with skin naevi and vulvar melanoma.

Acknowledgement

None.

References

1 Ferrari A, Zalaudek I, Argenziano G *et al.* Dermoscopy of pigmented lesions of the vulva: A retrospective morphological study. *Dermatology* 2011; **222**: 157 166.
2 Ronger-Savle S, Julien V, Duru G, Raudrant D, Dalle S, Thomas L. Features of pigmented vulval lesions on dermoscopy. *Br J Dermatol* 2011; **164**: 54 61.
3 Virgili A, Zampino MR, Marzola A, Corazza M. Vulvar melanocytic nevi: a dermoscopic investigation. *Dermatology* 2010; **221**: 55 62.
4 Blum A, Simionescu O, Argenziano G *et al.* Dermoscopy of pigmented lesions of the mucosa and the mucocutaneous junction: results of a multicenter study by the International Dermoscopy Society (IDS). *Arch Dermatol* 2011; **147**: 1181 1187.
5 Longo C, Zalaudek I, Argenziano G, Pellacani G. New directions in dermatopathology: in vivo confocal microscopy in clinical practice. *Dermatol Clin* 2012; **30**: 799 814, viii.
6 Debarbieux S, Perrot JL, Erfan N *et al.* Reflectance confocal microscopy of mucosal pigmented macules: a review of 56 cases including 10 macular melanoma. *Br J Dermatol* 2014; **170**: 1276 1284.
7 Cinotti E, Perrot JL, Labeille B, Adegbidi H, Cambazard F. Reflectance confocal microscopy for the diagnosis of vulvar melanoma and melanosis: preliminary results. *Dermatol Surg* 2012; **38**: 1962 1967.
8 Cinotti E, Perrot JL, Labeille B, Douchet C, Mottet N, Cambazard F. Laser photodynamic treatment for in situ squamous cell carcinoma of the glans monitored by reflectance confocal microscopy. *Australas J Dermatol* 2014; **55**: 72 74.
9 Cinotti E, Chol C, Perrot JL, Labeille B, Forest F, Cambazard F. Anal melanosis diagnosed by reflectance confocal microscopy. *Australas J Dermatol* 2014; **55**: 286 288.
10 Rock B, Hood AF, Rock JA. Prospective study of vulvar nevi. *J Am Acad Dermatol* 1990; **22**: 104 106.
11 Puig S, Di Giacomo TB, Serra D *et al.* Reflectance confocal microscopy of blue nevus. *Eur J Dermatol* 2012; **22**: 552 553.
12 Brenn T. Atypical genital nevus. *Arch Pathol Lab Med* 2011; **135**: 317 320.
13 Clark WH Jr, Hood AF, Tucker MA, Jampel RM. Atypical melanocytic nevi of the genital type with a discussion of reciprocal parenchymal-stromal interactions in the biology of neoplasia. *Hum Pathol* 1998; **29**: S1 S24.
14 Gleason BC, Hirsch MS, Nucci MR *et al.* Atypical genital nevi. A clinicopathologic analysis of 56 cases. *Am J Surg Pathol* 2008; **32**: 51 57.
15 Ribé A. Melanocytic lesions of the genital area with attention given to atypical genital nevi. *J Cutan Pathol* 2008; **35**: S24 S27.
16 Pellacani G, Farnetani F, Gonzalez S *et al.* In vivo confocal microscopy for detection and grading of dysplastic nevi: a pilot study. *J Am Acad Dermatol* 2012; **66**: e109 e121.

5 c Articles de synthèse
5.c1 Reflectance confocal microscopy for mucosal diseases

G ITAL DERMATOL VENEREOL 2015;150:585-93

Reflectance confocal microscopy for mucosal diseases

E. CINOTTI [1], B. LABEILLE [1], F. CAMBAZARD [1], G. THURET [2], P. GAIN [2], J. L. PERROT [1]

[1]Dermatology Department
University Hospital of Saint-Etienne
Saint Etienne, France
[2]Opthalmology Department
University Hospital of Saint-Etienne
Saint Etienne, France

Non-invasive, real-time microscopic imaging using *in vivo* reflectance confocal microscopy (RCM) has been demonstrated to be a useful tool for the evaluation of skin diseases and in particular for skin neoplasms. Recently, the RCM devices dedicated to the skin have also been applied to perform "virtual biopsies" of the oral, genital and ocular mucosa. In fact, mucosa is a sensitive area where non invasive imaging techniques are of high interest in order to spare biopsies and excisions. Mucosa is particularly suitable for RCM because of its thin or absent cornified layer and its thin epithelium that allows a deeper penetration of the laser with the consequent possibility of exploring deeper tissue levels. Besides, being useful for the diagnosis, RCM may be helpful to identify the area to be biopsied in case of large or multifocal lesions and may be regarded as a complementary technique for non invasive assessment of treatment efficacy.

The RCM features of healthy mucosa are described and a revision of the literature of the mucosal diseases that can be diagnosed by RCM has been performed.

KEY WORDS: Confocal microscopy - Mucous membrane - Mouth mucosa - Vulva - Eye.

Non-invasive, real-time microscopic imaging using *in vivo* reflectance confocal microscopy (RCM) has been demonstrated to be a useful tool for the evaluation of skin diseases and in particular for skin neoplasms.[1-3] Recently, the RCM devices dedicated to the skin have been also applied to perform "virtual biopsies" of the mucosa. In fact, mucosa is a sensitive area where non invasive imaging techniques are of high interest in order to spare biopsies and excisions. The diagnosis of mucosal cancer and inflammatory diseases is often challenging, requiring surgical biopsies to study the sampled tissue histologically. Mucosal biopsies can be painful and associated with bleeding and functional problems such as difficulties in eating and speaking in the oral site, difficulties in urinating and defecating in the genital area and difficulties in seeing in the ocular area. Furthermore, although the wounds of the mucosa heal rapidly, consequent scars are often associated with a feeling of discomfort in the vulvar area.

Mucosa is particularly suitable for RCM because of its thin or absent cornified layer and its thin epithelium that allows a deeper penetration of the laser with the consequent possibility of exploring deeper tissue levels. Moreover, the absence of the stratum corneum determines a higher resolution in the upper layers than in the skin, having a better-detailed visualization of the cellular morphology.

Reflectance confocal microscopy devices for the examination of the mucosa

Recently, the two devices dedicated to the skin VivaScope 3000® and 1500® (Caliber, New York, USA, distributed in Europe by Mavig, Munich, Ger-

Corresponding author: E. Cinotti, University Hospital of Saint-Etienne, Cedex 2, 42055 Saint Etienne, France.
E-mail: elisacinotti@gmail.com.

many) have been applied to the study of the mucosa. The examination of the mucosa is better performed with the handheld (HH) VivaScope 3000® than with the traditional wide probe (TWP) VivaScope 1500®. HH-RCM has 3 main advantages compared to the TWP-RCM: 1) it is handy to use an optical fiber wiring the optical source to the detector; 2) it is directly applied to the lesion to be examined and it does not need the fixation on the mucosa through a metal ring; and 3) it has a smaller tip (5 mm in diameter the first version of the HH device, 1.5 cm the second version of the HH device and 2 cm the TWP) (Figure 1), enabling to access to body sites with curved surfaces inaccessible to the TWP. In addition, image acquisition is faster (1-3 minutes per skin lesion *versus* 10-20 minutes).

The resolution of the TWP-RCM and HH-RCM is the same (1.25 µm in the horizontal axis and 5 µm in the vertical one). HH-RCM provides images of 1x1 mm, whereas TWP-RCM gives individual images of 500x500 µm and mosaics of merged individual images up to 8x8 mm. Therefore, the main disadvantage of HH-RCM is that users must be able to identify their current position in the lesion and mentally reconstruct the architecture of it in real time, because there is no possibility to acquire mosaics images. It should be noticed that the TWP device permits examination in both reflectance and fluorescence mode with three different wavelengths (488, 658 and 785 nm) that can be useful for the ocular examination, thus differing from the HH device that has only one light source of 830 nm and does not allow fluorescence acquisition. In order to use the TWP for the ocular mucosa, an adapter should be placed between the tip and the ocular surface.[4, 5]

If the HH device is used, a disposable sterile transparent film (for example Visulin, Paul Hartmann AG, Heidenheim, Germany) should be applied to the tip of the RCM. As for TWP-RCM there is no need to use a sterile film, because the examination is made with a disposable plastic interface that is fixed to the metallic ring applied on the mucosa.

In addition to VivaScope 3000® and 1500®, there are several RCM devices dedicated to the oral [6-8] or genital mucosa [9] that have been developed during the last 20 years. Some of them allow an endoscopical examination because they are small and can be introduced in the oral cavity or the vagina. Two RCM devices dedicated to the ocular surface exist too: the Confoscan 4 slit scanning confocal microscope (Nidek, Gamagori, Japan) and the laser scanning confocal microscope Heidelberg Retina Tomograph equipped with the Rostock Cornea Module (Heidelberg engineering GmbH, Heidelberg, Germany).[10] However, all these devices dedicated to the mucosa have specific indications and are rarely used by dermatologists because they are less suitable for the study of the skin.

Figure 1.—Comparison of the two reflectance confocal microscopes dedicated to the skin: the traditional wide probe VivaScope 1500® (left) and the handheld probe VivaScope 3000® (right).

Healthy oral and genital mucosa

Several studies have been conducted on the RCM aspect of healthy oral mucosa, evaluating all its parts: lips, cheek, gingivae and tongue.[7, 8, 11-13] Few studies evaluated the normal genital mucosa under RCM.[9, 14-16]

The images offered by RCM correlate with histologic findings, with the difference that RCM provides horizontal sections and histology provides vertical sections of the tissue. Moreover, in the superficial layers of the epithelium, RCM imaging provides greater cellular detail than histology.[8, 11]

The normal mucosa is similar to the skin with an epithelium corresponding to the epidermis and a *lamina propria* corresponding to the dermis. The epithelium has the same honeycomb pattern of the epidermis, characterized by polygonal cells with a hyperreflective outer part (mainly corresponding to the cellular membrane) and a hypo-reflective inner part

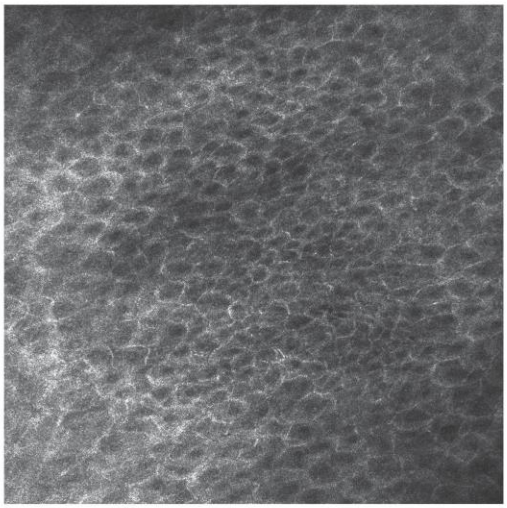

Figure 2.—Reflectance confocal microscopy aspect of the normal mucosal epithelium (image from the glans, handheld confocal microscope VivaScope 3000®).

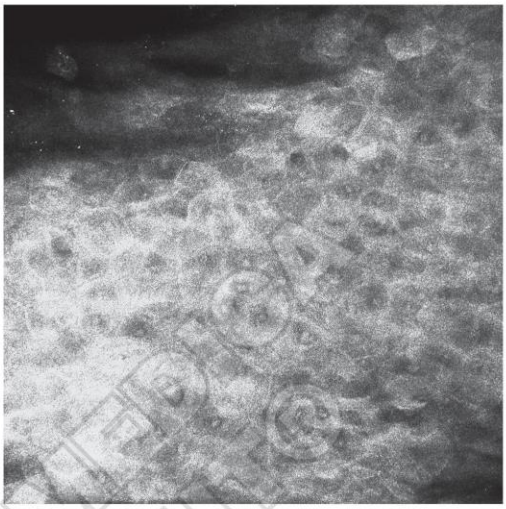

Figure 3.—Reflectance confocal microscopy aspect of the superficial layer of the mucosal epithelium with visible bright nuclei inside the cells (image from the glans, handheld confocal microscope VivaScope 3000®).

(mainly corresponding to the cytoplasm) (Figure 2). Differently from the skin, nuclei are easily visible in many areas of the upper layers. They appeared as bright large round structures in the center of the cells (Figure 3). Moreover, cell membranes are more demarcated and visible than in the skin. The stratum corneum is thin (in the areas of transition between the skin and the mucosa) or absent and numerous flaking cells are visible at the surface (Figure 3).

The *lamina propria* consists of bright collagen fibers arranged in bundles. Papillae are less evident than in the skin due to the often flattened epithelium. When papillae are visible, they are surrounded by bright roundish cells corresponding to the basal keratinocytes that could be slightly more pigmented (and therefore more bright) than the suprabasal cells (Figure 4). Vessels are better seen than in the skin due to the deeper penetration of the laser in the mucosa: they could be horizontal or vertical (Figure 5). When papillae are present, capillaries are vertical and their horizontal sections can be appreciated inside the papillae. Small bright cells corresponding to erythrocytes moving inside blood vessels can be easily distinguished.

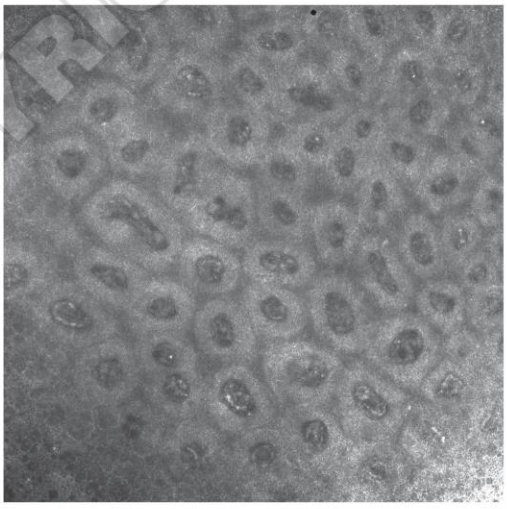

Figure 4.—Reflectance confocal microscopy aspect of the normal papillae of the glans mucosa (handheld confocal microscope VivaScope 3000®).

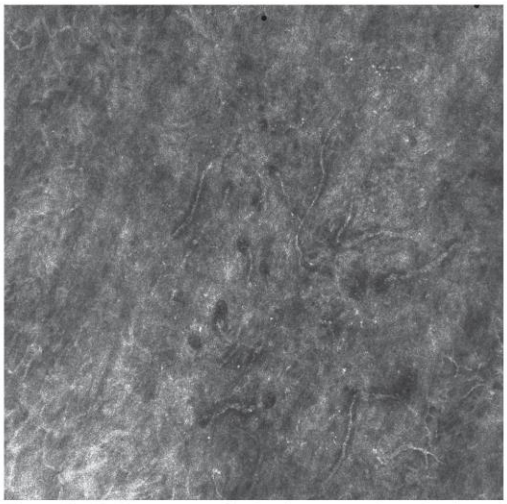

Figure 5.—Reflectance confocal microscopy shows horizontal vessels in the stroma of the glans mucosa (handheld confocal microscope VivaScope 3000®).

Healthy ocular mucosa

The conjunctival mucosa is similar to the oral and genital one under RCM. It has a multilayer non-keratinized stratified epithelium characterized by an honeycomb pattern and a stroma with hyper-reflective collagen fibers.[5] Notably, the HH camera dedicated to the skin, thanks to its good handiness, enables an easy exploration of the whole ocular surface, in particular the ciliary margin, the lacrimal punctum (Figure 6A-C), the internal and external canthi, and both surfaces of the eyelids comprising the Meibomian glands (Figure 7A, B). All these regions have hardly never been explored by RCM before, because of the limited mobility of devices available at present for ophthalmology. Of course, as both ophthalmology RCM devices, the HH camera also enables examining cornea and bulbar conjunctiva.

The cornea is compose by different layers: the epithelium, the Bowman's membrane, the stroma, the Descemet's membrane and the endothelium that can be easily recognized under RCM (Figure 8A-E). Interestingly, nerves are visible in the stroma (Figure 8A-E). Notably, differently from the skin, where the maximum penetration is at around 250 μm, images of the cornea can be taken up to a depth of 1000 μm (the technical limit of the RCM dedicated to the skin) because this tissue is transparent and allows a deeper penetration of the laser.

Pathological genital and oral mucosa

Several studies evaluated the *in vivo* RCM features of epithelial malignancies of the vulvar mucosa,[9, 17-19] and only few studies evaluated these neoplasms in the oral [6, 20] and male genital mucosa.[15, 16] Cervical intraepithelial neoplasia (CIN) is characterized under RCM by an increase in nuclear density and nuclear size, and by cellular atypia.[9] In a study of 15 patients the sensitivity for detection of CIN

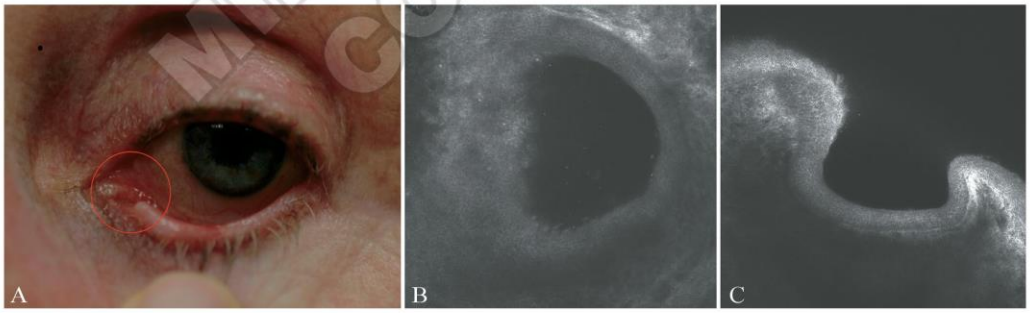

Figure 6.—Clinical presentation and reflectance confocal microscopy aspect of the lacrimal punctum obtained with the handheld confocal microscope VivaScope 3000®; A) aspect (red circle); B) transversal view; and C) sagittal view.

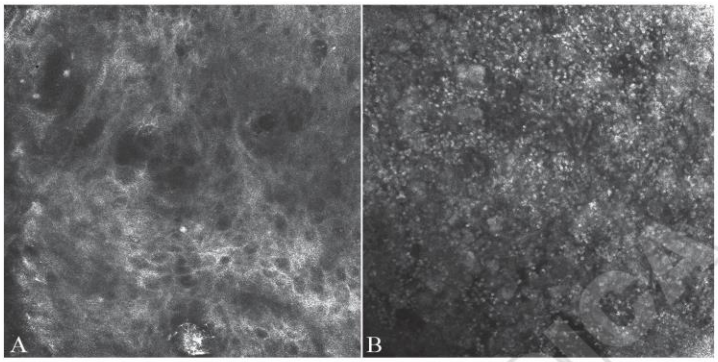

Figure 9.—Reflectance confocal microscopy features of *in situ* SCC and zoon plasma cell balanitis of the glans with the hand-held confocal microscope VivaScope 3000®. A) *In situ* SCC is characterized by an atypical honeycomb pattern with a disarranged epithelium; B) zoom plasma cell balanitis is characterized by small bright cells in the lower part of the epithelium and stroma.

tiate melanoma from the more frequent melanosis.[14, 23] This device is particularly useful to detect early melanoma that can clinically mimic melanosis presenting as a small size, homogenous pigmented macule.

Melanoses are characterized by the presence of chorion papillae rimmed by bright monomorphous cells corresponding to hyper-pigmented basal keratinocytes. Papillae can be ringed (roundish shaped) or draped (elongated shaped) or polycyclic (formed by more semicircles) (Figure 10 A, D).[14, 23, 24] Mucosal melanoma is characterized by four major features: high density of basal hyper-reflective dendritic cells, presence of pagetoid bright large cells in the epithelium (mainly roundish or fusiform with plump body), loss of normal architecture of chorion papillae, and sheet-like proliferation of atypical cells in the chorion.[14, 23]

The differential diagnosis of melanosis and melanoma could be sometimes difficult due to the possible presence of dendritic bright cells in the basal layer of the epithelium of melanoses, indicating a slight increase in melanocytes or Langerhans cells. However, some details can help the differentiation of these cells from atypical melanocytes found in melanoma, because in melanoma they are present in larger numbers; they are larger in size, with shorter and thicker dendrites; and they are located around nonedged, irregular papillae. Moreover, dendritic cells in melanoses mainly have a stellate, triangular or fusiform shape and are exceptionally roundish.[23] Dendritic cells are mainly found in the oral mucosa, as showed by a study of the French group of non invasive imaging (Groupe Imagerie Cutanée Non Invasive), that found dendritic cells in 86% of the cases from the lip.[23]

Mucosal nevi have been evaluated only in the vulvar area,[25] and they have the same features than skin nevi, except for atypical genital nevi. Atypical genital nevus is characterized by large junctional nests of large roundish hyperreflective melanocytes that are characteristically dyshesive.[25]

RCM is also important in the follow-up of vulvar melanoma, in which it can help to decide whether to perform a biopsy of a new pigmented lesion. RCM allows to easily diagnose a melanosis that develops on the surgical scar of a previous melanoma excision and to identify or exclude melanoma recurrences.[14]

As for the breast,[26] genital Paget disease is one more good indication for RCM that shows hyporeflective large cells inside the epithelium corresponding to Paget cells. In particular RCM can be used to for the diagnosis, definition of surgical margins and follow-up after treatment of this neoplasia.

RCM has also been used for the diagnosis of inflammatory oral mucosal disorders.[27, 28] Alessi *et al.*[28] demonstrated that RCM can distinguish mucous membrane pemphigoid, pemphigus vulgaris and lichen planus in case of desquamative gingivitis in a series of 25 patients and he found a good RCM-histopathological correlation. Intraepidermal and subepidermal clefts are visible in case of autoimmune

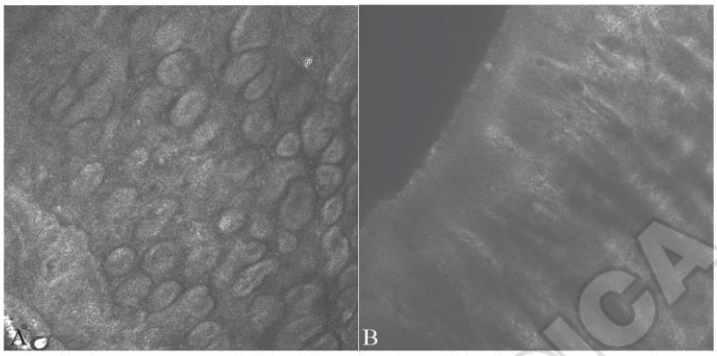

Figure 7.—Reflectance confocal microscopy aspect of the Meibomian glans with the handheld confocal microscope VivaScope 3000®; A) transversal view; and B) sagittal view.

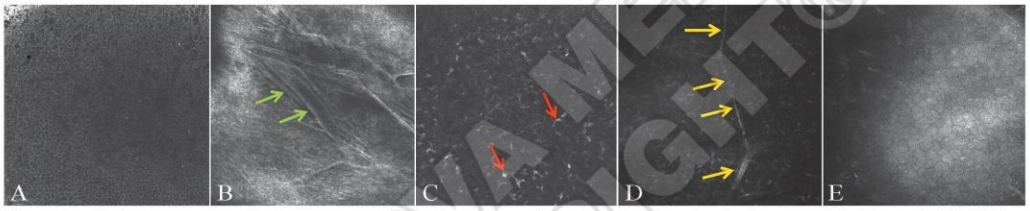

Figure 8.—Reflectance confocal microscopy aspect of the cornea with the handheld confocal microscope VivaScope 3000®. Different layers are visible: the epithelium. 8.—A) the Bowman's membrane; B) with its collagen fibers (green arrows); C) the stroma with sparsely distributed keratocytes (red arrows); D) nerves (yellow arrows); and E) the endothelium, a monolayer of cuboidal cells.

was 97% and the specificity for predicting the grade of abnormality was 80% for normal-CIN1 and 93% for CIN2-CIN3.[9]

Concerning the oral epithelial cancers, Anuthama *et al.*[13] demonstrated by *ex vivo* RCM extensive variations in cell size, nuclear size and nuclear morphology in oral SCC. Maitland *et al.*[6] evaluated 8 squamous cell carcinomas (SCC) by *in vivo* RCM and showed disorganized and irregular structures. However, specific features of SCC could not be defined in this study. Agozzino *et al.*[20] pointed out the usefulness of RCM to select the site of biopsy in case of suspected oral SCC and described the presence of targetoid-like structures located at different epithelial layers as an additional sign of mucosal SCC.

Arzberger *et al.*[16] evaluated 15 cases of erythematous lesions of the male genital mucosa in order to define RCM features that can differentiate *in situ* SCC from Zoon plasma cell balanitis, a benign idiopathic inflammatory disease of the glans and prepuce (Figure 9A, B). They examined 6 cases of *in situ* SCC and 9 cases of Zoon plasma cell balanitis. The most relevant RCM criteria for SCC were atypical honeycomb pattern, disarranged epidermal pattern (Figure 9A, B) and round nucleated cells. Zoon plasma cell balanitis showed a nucleated honeycomb pattern, small bright cells in the upper dermis (Figure 9A, B) and vermicular vessels. RCM has also been used by our group to monitor laser photodynamic treatment [15] for *in situ* SCC of the glans over time in a total non-invasive modality.

One case of verruciform xanthoma of the glans has also been described under RCM, showing large hyperreflecting cells in the dermal papillae corresponding to histiocytic foam cells at histology.[21]

RCM is a promising tool for the differential diagnosis of pigmented lesions in the genital and oral mucosa,[14, 22-24] and in particular to differen-

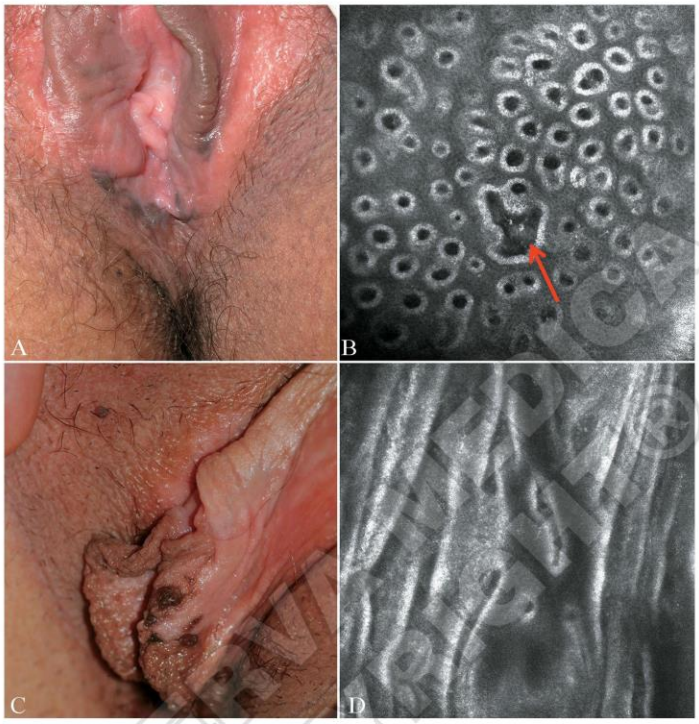

Figure 10.—Clinical and reflectance confocal microscopy (RCM) aspect of vulvar melanoses with the hand held confocal microscope VivaScope 3000®. A, C) clinical aspect; B, D) under RCM, melanoses are characterized by the chorion papillae rimmed by bright monomorphous cells corresponding to hyper-pigmented basal keratinocytes. Papillae can be ringed (roundish shape), or draped (elongated shape), or polycyclic (formed by more semicircles; red arrow).

bullous diseases, whereas lichen planus is characterized by a dense inflammatory infiltrate in the superficial dermis obscuring the epithelial-chorion junction.

Inflammatory cells are well visible under RCM as small bright roundish bodies. Lymphocytes can be distinguished from granulocytes and macrophages from their size. However, it is not possible to differentiate different types of granulocytes (neutrophils, basophils and eosinophils) in the inflammatory infiltrate.

RCM has been used to image ectopic sebaceous glands (Fordyce granules) of the lip in patients with the Muir-Torre Syndrome (MTS),[29] and it has been suggested that their identification may constitute an additional parameter for the diagnosis of MTS. Ectopic sebaceous glands appear under RCM with multiple round or oval hyper-refractive cells organized in lobules.

Pathological ocular mucosa

Numerous studies performed with the RCM dedicated to ophthalmology describe the features of ocular mucosa diseases.[30, 31] Our group described the features of lentigo, primary acquired melanosis, nevi, basal cell carcinoma, SCC, melanoma and lymphoma of eyelid margin and conjunctiva under RCM dedicated to the skin.[4, 5, 10, 32] These lesions are simi-

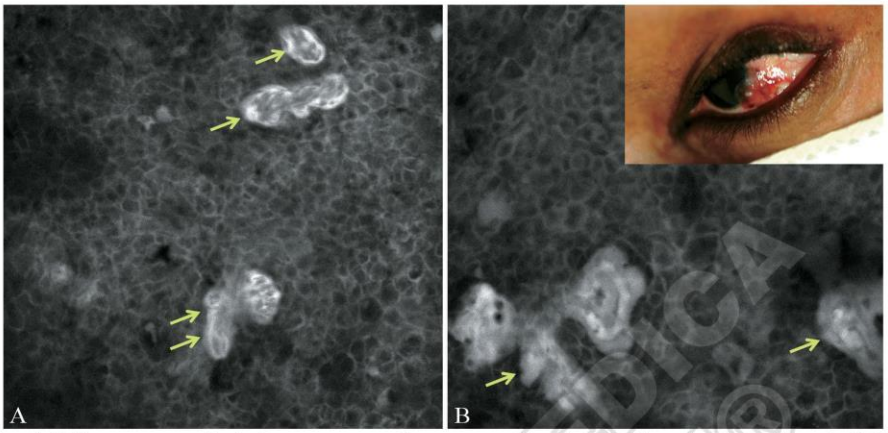

Figure 11.—A, B) Fluorescence confocal microscopy aspect of a squamous cell carcinoma of the conjunctiva performed with VivaScope 1500® (488 nm) showed a longer persistence of the fluorescence in the squamous cell carcinoma islands (green arrows) compared to the surrounding healthy tissue in case of intravenous fluorescein injection.

lar to the cutaneous counterparts. However, it should be noticed that compared to the skin: 1) dilated vessels are common in normal conjunctiva and are less specific for malignancy; 2) inflammatory cells are common in the stroma of the normal conjunctiva; 3) dendritic cells can be found in the normal epithelium of the conjunctiva, especially in case of primary acquired melanosis; 4) nevi of the conjunctiva often have a cystic aspect; and 5) melanoma of the conjunctiva are invasive, whereas *in situ* melanoma are named primary acquired melanosis with atypia in ophthalmology. RCM can also be used to diagnose ocular infections from *Acanthamoeba* and filamentous fungi,[33] and to diagnose storage disease with ocular involvement, such as cystinosis.[4] RCM can also confirm the diagnosis of irritant contact dermatitis to pine processionary caterpillar hair, because processionary caterpillar hairs can be identified in the cornea.[34] In the skin it was not possible to identify these hairs because the skin is more inhomogeneous and less transparent than the cornea.

Interestingly, TWP-RCM dedicated to the skin permits to explore the fluorescence characteristics of the ocular apparatus either spontaneously or after topical instillation or intravenous injection of fluorochromes already used in routine by ophthalmologists. Fluorochromes specifically stain cellular or tissular components that are unlikely to be discriminate only by reflectance confocal images. Notably, we observed that intravenous injected fluoresecin stay longer in the tumoral tissue than in the normal mucosa (Figure 11 A-C).

Conclusions

RCM provides additional information to the clinical and dermoscopical examination facilitating the correct diagnosis of mucosal tumoral and inflammatory diseases. RCM allows sparing biopsies and excisions in this sensitive area and could lead to the detection of early tumors. Moreover, RCM may be useful to identify the area to be biopsied in case of large or multifocal lesions and may be regarded as a complementary technique for non invasive assessment of treatment efficacy.

References

1. Guitera P, Menzies SW, Longo C, Cesinaro AM, Scolyer RA, Pellacani G. In vivo confocal microscopy for diagnosis of melanoma and basal cell carcinoma using a two-step method: analysis of 710 consecutive clinically equivocal cases. J Invest Dermatol 2012;132:2386-94.

2. Alarcon I, Carrera C, Palou J, Alos L, Malvehy J, Puig S. Impact of in vivo reflectance confocal microscopy on the number needed to treat melanoma in doubtful lesions. Br J Dermatol 2014;170:802-8.
3. Pellacani G, Pepe P, Casari A, Longo C. Reflectance confocal microscopy as a second-level examination in skin oncology improves diagnostic accuracy and saves unnecessary excisions: a longitudinal prospective study. Br J Dermatol 2014;171:1044-51.
4. Cinotti E, Perrot JL, Labeille B, Espinasse M, Ouerdane Y, Boukenter A *et al*. Optical diagnosis of a metabolic disease: cystinosis. J Biomed Opt 2013;18:046013.
5. Cinotti E, Perrot JL, Labeille B, Thuret G, Espinasse M, Grivet D *et al*. In vivo confocal microscopy for eyelids and ocular surface: a new horizon for dermatologists. G Ital Dermatol Venereol 2015;150:127-9.
6. Maitland KC, Gillenwater AM, Williams MD, El-Naggar AK, Descour MR, Richards-Kortum RR. In vivo imaging of oral neoplasia using a miniaturized fiber optic confocal reflectance microscope. Oral Oncol 2008;44:1059-66.
7. Jabbour JM, Bentley JL, Malik BH, Nemechek J, Warda J, Cuenca R *et al*. Reflectance confocal endomicroscope with optical axial scanning for in vivo imaging of the oral mucosa. Biomed Opt Express 20141;5:3781-91.
8. White WM, Rajadhyaksha M, González S, Fabian RL, Anderson RR. Noninvasive imaging of human oral mucosa in vivo by confocal reflectance microscopy. The Laryngoscope 1999;109:1709-17.
9. Tan J, Quinn MA, Pyman JM, Delaney PM, McLaren WJ. Detection of cervical intraepithelial neoplasia in vivo using confocal endomicroscopy. BJOG Int J Obstet Gynaecol 2009;116:1663-70.
10. Cinotti E, Perrot J-L, Labeille B, Campolmi N, Espinasse M, Grivet D *et al*. Handheld reflectance confocal microscopy for the diagnosis of conjunctival tumors. Am J Ophthalmol 2015;159:324-33.e1.
11. García-Hernández A, Roldán-Marín R, Iglesias-Garcia P, Malvehy J. In Vivo noninvasive imaging of healthy lower lip mucosa: a correlation study between high-definition optical coherence tomography, reflectance confocal microscopy, and histology. Dermatol Res Pract 2013;2013:205256.
12. Contaldo M, Agozzino M, Moscarella E, Esposito S, Serpico R, Ardigò M. In vivo characterization of healthy oral mucosa by reflectance confocal microscopy: a translational research for optical biopsy. Ultrastruct Pathol 2013;37:151-8.
13. Anuthama K, Sherlin HJ, Anuja N, Ramani P, Premkumar P, Chandrasekar T. Characterization of different tissue changes in normal, betel chewers, potentially malignant lesions, conditions and oral squamous cell carcinoma using reflectance confocal microscopy: correlation with routine histopathology. Oral Oncol 2010;46:232-48.
14. Cinotti E, Perrot JL, Labeille B, Adegbidi H, Cambazard F. Reflectance confocal microscopy for the diagnosis of vulvar melanoma and melanosis: preliminary results. Dermatol Surg Off Publ Am Soc Dermatol Surg Al 2012;38:1962-7.
15. Cinotti E, Perrot JL, Labeille B, Douchet C, Mottet N, Cambazard F. Laser photodynamic treatment for in situ squamous cell carcinoma of the glans monitored by reflectance confocal microscopy. Australas J Dermatol 2014;55:72-4.
16. Arzberger E, Komericki P, Ahlgrimm-Siess V, Massone C, Chubisov D, Hofmann-Wellenhof R. Differentiation between balanitis and carcinoma in situ using reflectance confocal microscopy. JAMA Dermatol 2013;149:440-5.
17. Carlson K, Pavlova I, Collier T, Descour M, Follen M, Richards-Kortum R. Confocal microscopy: imaging cervical precancerous lesions. Gynecol Oncol 2005;99:S84-88.
18. Schomacker KT, Meese TM, Jiang C, Abele CC, Dickson K, Sum ST *et al*. Novel optical detection system for in vivo identification and localization of cervical intraepithelial neoplasia. J Biomed Opt 2006;11:34009.
19. Tan J, Delaney P, McLaren WJ. Confocal endomicroscopy: a novel imaging technique for in vivo histology of cervical intraepithelial neoplasia. Expert Rev Med Devices 2007;4:863-71.
20. Agozzino M, Bhasne P, Franceschini C, Vincenza G, Catricalà C, Ardigò M. Noninvasive, in vivo assessment of oral squamous cell carcinoma. Br J Dermatol 2014;170:754-6.
21. Arzberger E, Oliveira A, Hofmann-Wellenhof R, Zalaudek I, Cerroni L, Komericki P. Dermoscopy and reflectance confocal microscopy in verruciform xanthoma of the glans penis. J Am Acad Dermatol 2015;72:e147-9.
22. Erfan N, Hofman V, Desruelles F, Passeron T, Ortonne JP, Lacour JP *et al*. Labial melanotic macule: a potential pitfall on reflectance confocal microscopy. Dermatol Basel Switz 2012;224:209-11.
23. Debarbieux S, Perrot JL, Erfan N, Ronger-Savlé S, Labeille B, Cinotti E *et al*. Reflectance confocal microscopy of mucosal pigmented macules: a review of 56 cases including 10 macular melanoma. Br J Dermatol 2014;170:1276-84.
24. Cinotti E, Chol C, Perrot JL, Labeille B, Forest F, Cambazard F. Anal melanosis diagnosed by reflectance confocal microscopy. Australas J Dermatol 2014;55:286-8.
25. Cinotti E, Couzan C, Perrot JL, Labeille B, Bahadoran P, Puig S *et al*. Reflectance confocal microscopy for the diagnosis of vulvar naevi: six cases. J Eur Acad Dermatol Venereol JEADV 2014 [Epub ahead of print].
26. Cinotti E, Perrot JL, Labeille B, Cambazard F, Groupe imagerie cutanée non invasive de la Société française de dermatologie. [The contribution of reflectance confocal microscopy in the diagnosis of Paget's disease of the breast]. Ann Dermatol Vénéréologie 2013;140:829-32 [Article in French].
27. Ardigo M, Donadio C, Franceschini C, Catricalà C, Agozzino M. Interest of reflectance confocal microscopy for inflammatory oral mucosal diseases. J Eur Acad Dermatol Venereol JEADV 2014 J [Epub ahead of print].
28. Alessi SS, Nico MMS, Fernandes JD, Lourenço SV. Reflectance confocal microscopy as a new tool in the in vivo evaluation of desquamative gingivitis: patterns in mucous membrane pemphigoid, pemphigus vulgaris and oral lichen planus. Br J Dermatol 2013;168:257-64.
29. Ponti G, Meschieri A, Pollio A, Ruini C, Manfredini M, Longo C *et al*. Fordyce granules and hyperplastic mucosal sebaceous glands as distinctive stigmata in Muir-Torre syndrome patients: characterization with reflectance confocal microscopy. J Oral Pathol Med 2014 [Epub ahead of print].
30. Messmer EM, Mackert MJ, Zapp DM, Kampik A. In vivo confocal microscopy of normal conjunctiva and conjunctivitis. Cornea 2006;25:781-8.
31. Messmer EM, Mackert MJ, Zapp DM, Kampik A. In vivo confocal microscopy of pigmented conjunctival tumors. Graefes Arch Clin Exp Ophthalmol Albrecht Von Graefes Arch Für Klin Exp Ophthalmol 2006;244:1437-45.
32. Cinotti E, Perrot JL, Campolmi N, Labeille B, Espinasse M, Grivet D *et al*. The role of in vivo confocal microscopy in the diagnosis of eyelid margin tumors: 47 cases. J Am Acad Dermatol 2014;71:912-8.
33. Labbé A, Khammari C, Dupas B, Gabison E, Brasnu E, Labetoulle M *et al*. Contribution of in vivo confocal microscopy to the diagnosis and management of infectious keratitis. Ocul Surf 2009;7:41-52.
34. Jullienne R, He Z, Manoli P, Grivet D, Cinotti E, Perrot JL *et al*. In vivo confocal microscopy of pine processionary caterpillar hair-induced keratitis. Cornea 2015;34:350-2.

Conflicts of interest.—The authors certify that there is no conflict of interest with any financial organization regarding the material discussed in the manuscript.

Epub ahead of print on June 23, 2015.

Confocal Microscopy for Special Sites and Special Uses

Elisa Cinotti, MD, PhD*, Bruno Labeille, MD,
Frédéric Cambazard, PhD, Jean-Luc Perrot, MD

KEYWORDS

• Reflectance confocal microscopy • Special sites • Mucosa • Nail • Tumor • Infection • Parasites • Microcirculation

KEY POINTS

- The in vivo hand-held reflectance confocal microscopy camera allows one to explore skin appendages and oral, genital, and ocular mucosa.
- In vivo and ex vivo confocal microscopy is not only valuable to identify skin cancers but also for the diagnosis of skin infections and inflammatory diseases.
- In vivo reflectance confocal microscopy can be used to guide presurgical mapping of skin tumors.
- Confocal microscopy can provide videos that are particularly useful to study the cutaneous microcirculation.

Video content accompanies this article at http://www.derm.theclinics.com.

INTRODUCTION

In vivo reflectance confocal microscopy (RCM) was initially developed in dermatology for the evaluation of skin neoplasms. Recently, a hand-held (HH) camera (VivaScope 3000, Caliber, Rochester, NY; distributed in Europe by Mavig GmbH, Munich, Germany) has been developed expanding the applications of RCM. HH-RCM has three main advantages compared with the traditional wide probe (TWP) VivaScope 1500: (1) it is handy because it uses an optical fiber wiring the optical source to the detector, (2) it does not need fixation on the skin through a metal ring, and (3) it has a smaller tip (5 mm in diameter in the first version of the HH device, 1.5 cm in the second version of the HH device, and 2 cm in the TWP), enabling access to body sites with curved surfaces inaccessible to the TWP.[1]

All these advantages have enabled the use of RCM for the study of the whole body skin, of the mucosa, and of the skin appendages. The HH-RCM has increased the use of RCM in clinical practice because of faster image acquisition (1–3 minutes per lesion vs 10–20 minutes).[1] Moreover, it has allowed the use of RCM for a rapid diagnosis of cutaneous inflammatory and infectious diseases and of epithelial cancers that do not require the architectural information provided by the mosaic image reconstruction of the TWP.[2,3]

HH-RCM can be compared with modern dermoscopy, which started with the evaluation of tumors and now has been demonstrated to be a useful noninvasive diagnostic tool for a wide range of skin diseases.

A new field of confocal microscopy has also been opened by the development of an ex vivo device dedicated to the skin (VivaScope 2500,

Funding Sources: None.
Conflict of Interest: None.
Dermatology Department, University Hospital of Saint-Etienne, Cedex 2, Saint-Etienne, 42055, France
* Corresponding author.
E-mail address: elisacinotti@gmail.com

Dermatol Clin 34 (2016) 477–485
http://dx.doi.org/10.1016/j.det.2016.05.010

Caliber; distributed in Europe by Mavig GmbH). This new device has been conceived for the evaluation of cutaneous tumor margins in real-time, directly on freshly excised tissue in a perioperative setting. However, further applications are possible, such as the diagnosis of infectious diseases.

SPECIAL SITES

Mucosa, nails, and hairs can be examined by RCM. All these body sites are sensitive areas where noninvasive imaging techniques are of high interest to spare biopsies and excisions. RCM has a limit in the laser penetration depth and for this reason acral skin has not been initially investigated. However, in our experience RCM could also be useful in this area.

Genital and Oral Mucosa

Mucosa is particularly suitable for RCM because of its thin or absent cornified layer, which allows a deeper penetration of the laser and a resolution in the upper layers higher than in the skin. Thus, RCM permits a better-detailed visualization of the cellular morphology.[1]

RCM is a promising tool for the differential diagnosis of pigmented lesions in the genital and oral mucosa[4–6] and in particular to differentiate early melanoma from the more frequent melanosis.[4,5] Melanoses correspond to the benign hyperpigmentation of basal keratinocytes and are characterized under RCM by the presence of chorion papillae rimmed by hyperreflective monomorphous cells corresponding to hyperpigmented basal keratinocytes[4–6] (**Fig. 1**). Mucosal melanoma is characterized by four major features: (1) high density of basal hyperreflective dendritic cells, (2) presence of pagetoid bright large cells in the epithelium (mainly roundish or fusiform with plump body), (3) loss of normal architecture of chorion papillae, and (4) sheet-like proliferation of atypical cells in the chorion.[4,5]

RCM is also helpful for the differential diagnosis between in situ squamous cell carcinoma (SCC) and Zoon plasma cell balanitis, a benign idiopathic inflammatory disease.[7] RCM criteria for mucosal SCC are similar to those used in the skin: atypical honeycomb pattern and disarranged epidermal pattern. Moreover RCM can be used to monitor laser photodynamic treatment of in situ SCC of the glans over time in a total noninvasive modality.[8]

Ocular Mucosa

Our group first applied the RCM devices dedicated to dermatology to the study of the ocular mucosa.[9] HH-RCM can explore the whole cornea and conjunctiva surface, including the ciliary margin, the lacrimal punctum, the internal and external canthi, and both surfaces of the eyelids comprising the meibomian glands.[1] These regions have not previously been explored by RCM, because of the limited mobility of devices available for ophthalmology (Confoscan 4 slit-scanning confocal microscope, Nidek, Gamagori, Japan; and Heidelberg Retina Tomograph in association

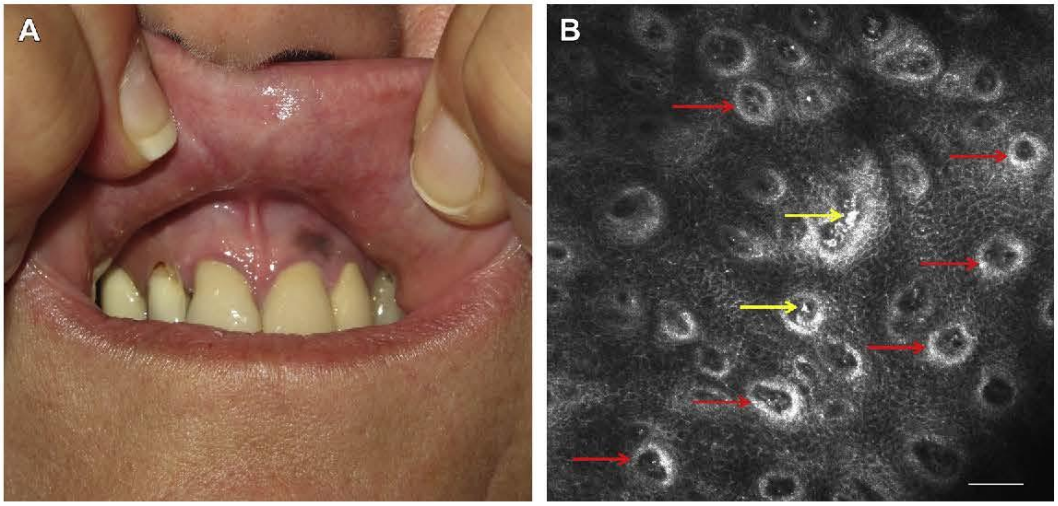

Fig. 1. Clinical (*A*) and in vivo RCM (*B*) aspect of a gingival melanosis. RCM shows roundish chorion papillae rimmed by hyperreflective cells (*B, red arrows*) at the epithelium-chorion junction. Some melanophages are visible inside the papillae (*B, yellow arrows*). Scale bar: 100 μm.

with the Rostock Cornea Module, Heidelberg Engineering GmbH, Heidelberg, Germany). RCM dedicated to the skin can diagnose lentigo (**Fig. 2**), primary acquired melanosis, nevi, basal cell carcinoma (BCC), SCC, melanoma, and lymphoma of eyelid margin and conjunctiva[9–12] with criteria similar to the cutaneous counterparts. However, compared with the skin (1) dilated vessels are common in normal conjunctiva and are less specific for malignancy; (2) inflammatory cells are common in the stroma of the normal conjunctiva; (3) dendritic cells can be found in the normal epithelium of the conjunctiva, especially in case of primary acquired melanosis; (4) nevi of the conjunctiva often have a cystic aspect; and (5) melanoma of the conjunctiva are invasive, whereas in situ melanoma are named primary acquired melanosis with atypia in ophthalmology.[1] RCM can also be used to diagnose ocular infections[1] and storage diseases with ocular involvement, such as cystinosis[12] and Fabry disease.[13] RCM can show the signs of postradiation blepharitis (**Fig. 3**) and can indicate foreign body material, such as pine processionary caterpillar hair in the cornea[14] and suture thread remaining in the eyelid after surgery and causing inflammation (**Fig. 4**).

Nail

The nail plate transparency allows a deep penetration of RCM that can image up to the nail bed in case of thin nails (<500 μm).[15] RCM can diagnose onychomycosis and could be used in the future as a noninvasive procedure for the investigation of different inflammatory nail diseases, such as psoriasis and lichen planus.[15] It is unable to directly explore the nail matrix located deep under the eponychium. However, it also helps in case of melanonichia to distinguish subungueal melanoma from lentigo and nevi because the matrix can be observed by reclining the eponychium.[15] In our experience RCM is also useful to confirm the diagnosis of periungueal and subungueal pyogenic granuloma, by showing a lobulated proliferation of capillary-sized vessels with possible secondary ulceration, hemorrhage, and inflammatory infiltrate (**Fig. 5**).

Palms and Soles

Under RCM normal acral skin has a specific aspect: epidermal ridges appear as broad parallel bands with a regular honeycomb pattern, and furrows as parallel dark areas disrupting the honeycomb pattern (**Fig. 6**).[16] The openings of sweat ducts appear as hyperreflective circles plugged in lines inside the honeycomb pattern (see **Fig. 6**). When the image plan is not exactly parallel to the skin surface, the longitudinal section of acrosyringia can be seen as hyperreflective elongated coiled structures.

Although the presence of a thick corneum layer makes more difficult the examination of this region, RCM can help to diagnose acral lentiginous melanoma by showing inhomogeneous pagetoid cells with a particular tropism for acrosyringia.[16] However, acral lentiginous melanoma diagnosis cannot be excluded in the absence of RCM signs because early acral lentiginous melanoma can present only subtle atypia, such as slight proliferation of atypical melanocytes at the dermal-epidermal junction that may not be identified under RCM.[16] The superficial part of the stratum corneum can also be scraped off with a scalpel to have a deeper RCM examination in this special area.

SPECIAL USES

Infections and Infestations

RCM has a lateral resolution of up to 1.25 μm. This means that structures larger than 1.25 μm could

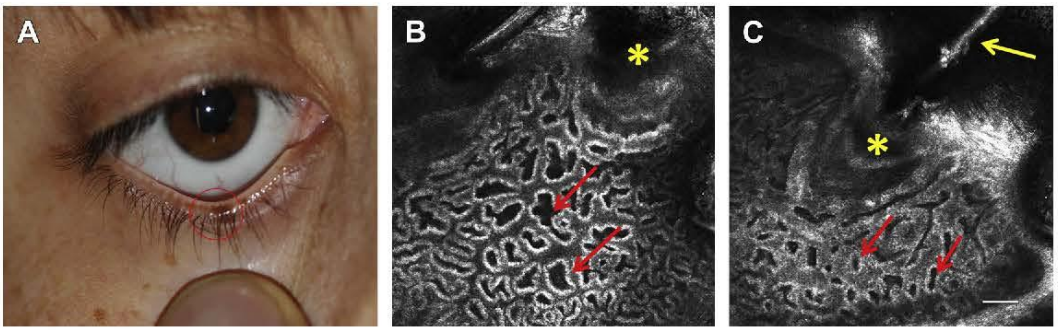

Fig. 2. Clinical (*A, red circle*) and in vivo RCM (*B, C*) aspect of an eyelid margin lentigo. RCM shows polycyclic and elongated dermal papillae rimmed by hyperreflective cells (*B, C, red arrows*) at the epidermal-dermal junction. An orifice of an eyelash (*B, C, yellow asterisk*) and the eyelash shaft (*C, yellow arrow*) are visible. Scale bar: 100 μm.

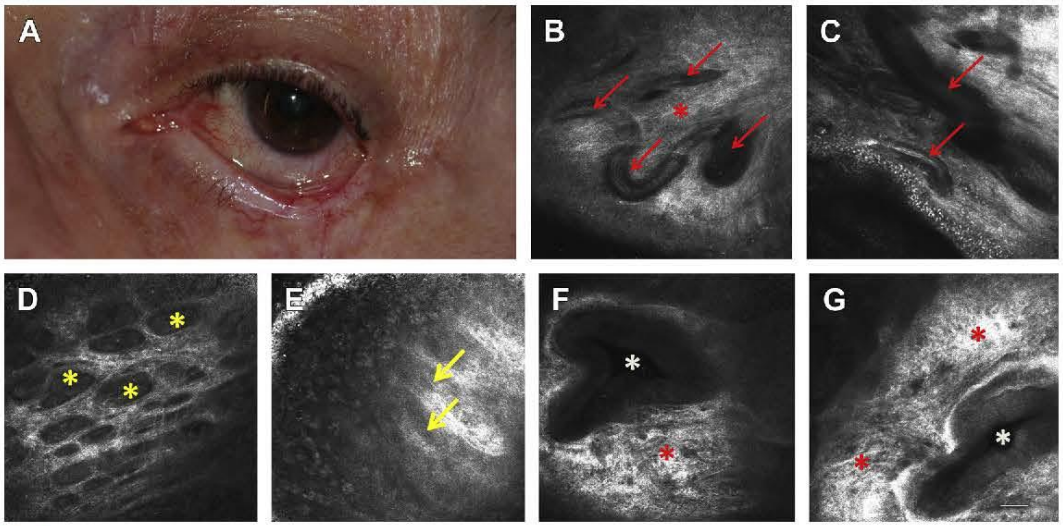

Fig. 3. Clinical (*A*) and in vivo RCM (*B–G*) aspect of postradiation blepharitis. RCM shows teleangectatic vessels (*B, C, red arrows*), fibrosis (*B, F, G, red asterisks*), alteration of meibomian glands in a transversal (*D*) and sagittal (*E*) view (*D, yellow asterisks; E, yellow arrows*), and distortion of the lacrimal punctum (*F, G, white asterisk*). Scale bar: 100 μm.

theoretically be identified. Parasites, such as *Sarcoptes scabiei* (**Fig. 7**), *Demodex folliculorum*, *Pyemotes ventricosus*, *Ixodes*, *Dermanyssus gallinae*, *Pediculus humanus*, pinworms, and *Pulex irritans* (**Fig. 8**), have been observed under RCM.[2,17–19] Some parasites are already visible to the naked eye but RCM can identify their different body parts helping the precise identification of the species (see **Fig. 8**). RCM can also quantify parasites, define their exact localization, and assess their viability after treatment.[20,21]

Some bacteria could also be theoretically identified, whereas virus cannot be observed because they are too small. However, viral cytopathic effects on keratinocytes can be observed in case of molluscipoxvirus, coxsackievirus, human papillomavirus, and herpes simplex and varicella-zoster herpes virus infection.[17]

RCM can also be used to identify filaments, pseudofilaments, and conidia on skin, and mucosa, and in skin appendages in case of mycosis. Filaments and pseudofilaments appear as thin,

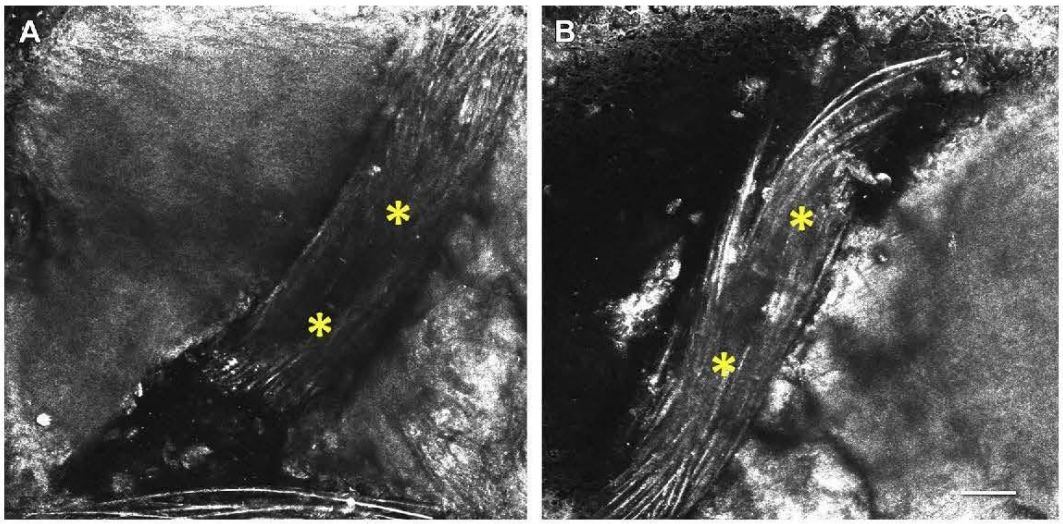

Fig. 4. In vivo RCM (*A, B*) aspect of a suture thread (*yellow asterisks*) that causes persistent blepharitis after eyelid surgery. Scale bar: 100 μm.

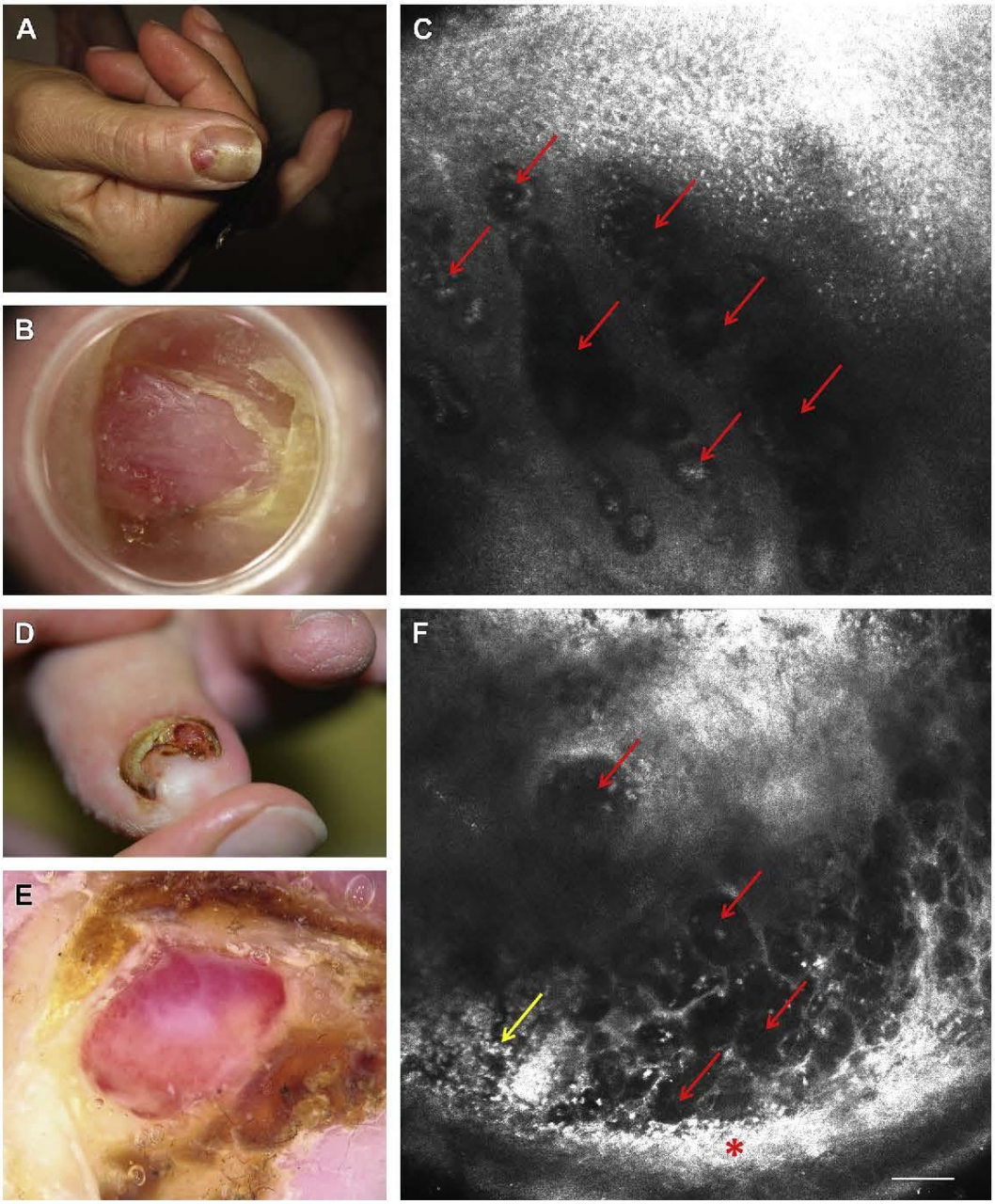

Fig. 5. Clinical (*A, D*), dermoscopical (*B, E*), and RCM (*C, F*) aspect of two cases of ungueal pyogenic granuloma. RCM shows a lobulated proliferation of capillary-sized vessels (*red arrows*), an inflammatory infiltrate (*yellow arrow*), and a well-defined hyperreflective collarette around the lesion (*red asterisk*). Scale bar: 100 μm.

hyperreflective, longitudinal structures with a serpentine shape,[15,22,23] whereas conidia are hyperreflective small roundish bodies.[23] RCM can confirm the diagnosis of mycosis during the clinical examination of patients avoiding them to wait for the microscopic and cultural examinations (**Fig. 9**).

Tumor Mapping

RCM can help surgery by indicating cutaneous tumor margins, especially in case of large BCC, lentigo maligna, and Paget disease. Our group developed a technique combining the staged excision of the "spaghetti type" and RCM[24,25] to

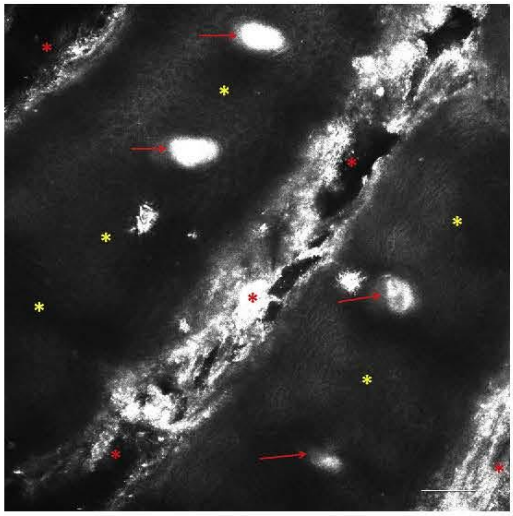

Fig. 6. In vivo RCM aspect of the normal epidermis from the acral skin. Ridges appear as broad parallel bands with a regular honeycomb pattern (*yellow asterisks*) and furrows as parallel hyperreflective (in the superficial portion filled of keratin) and hyporeflective (in the deeper portion) areas disrupting the honeycomb pattern (*red asterisks*). Acrosyringia appear as hyperreflective circles plugged in lines in the center of the ridges (*red arrows*). Scale bar: 100 μm.

Fig. 8. In vivo RCM shows different body parts of a human flea (*Pulux irritans*) (mosaic image reconstruction acquired with VivaScope 1500; *yellow arrow* cephalic portion and *red arrows* legs). Scale bar: 100 μm.

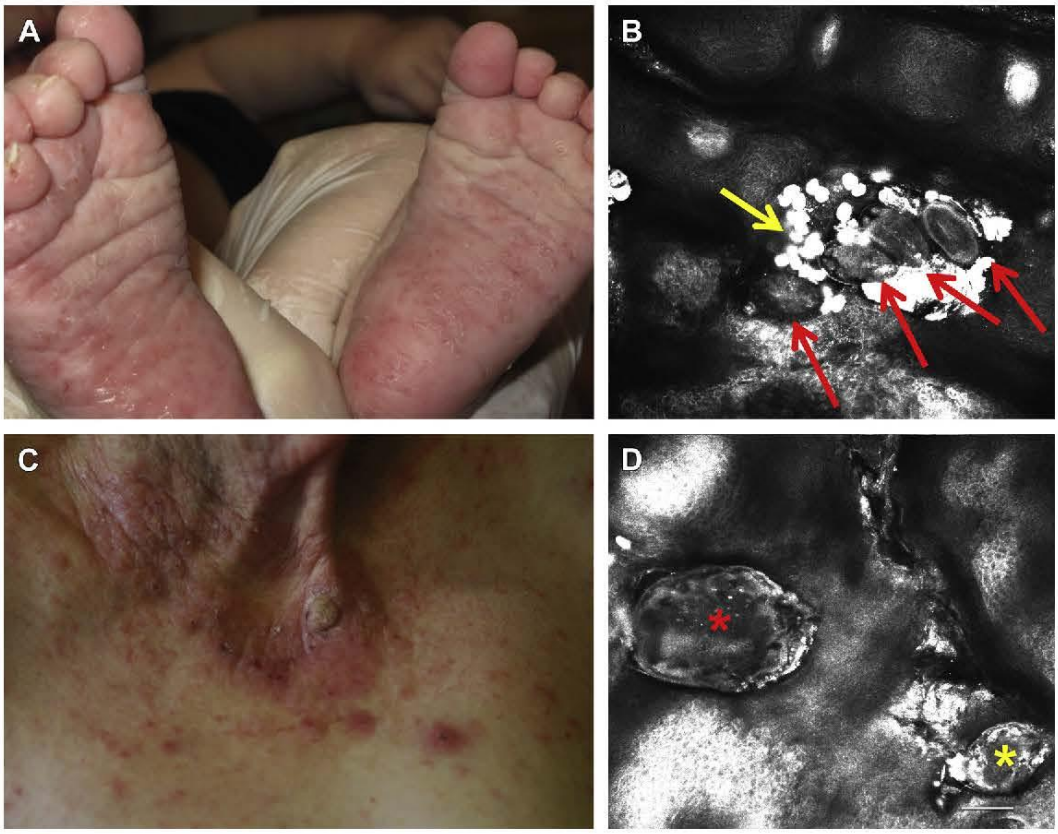

Fig. 7. Clinical (*A, C*) and in vivo RCM (*B, D*) aspect of two cases of scabies. RCM shows eggs (*B, red arrows*) and droppings (*B, yellow arrow*) and *Sarcoptes scabies* mites (*D, red asterisk* adult female and *yellow asterisk* larva). Scale bar: 100 μm.

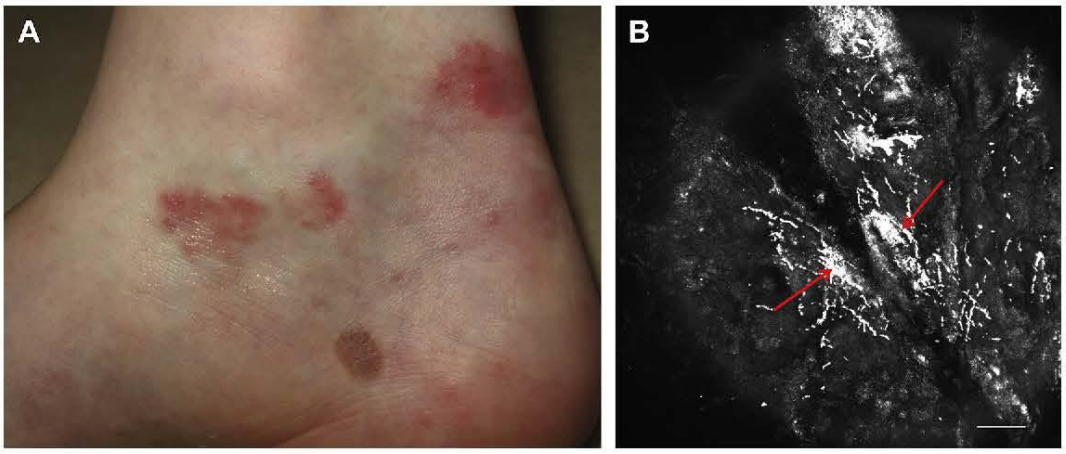

Fig. 9. Clinical (*A*) and in vivo RCM (*B*) aspect of a dermatophytosis. Dermatophytes are easily identified under RCM as thin, high-reflective, longitudinal structures with a linear shape (*red arrows*). Scale bar: 100 μm.

improve the definition of tumor margins. Subsequently, other groups invented new procedures, such as the combination of dermoscopy and RCM with a presurgical cut performed along the dermoscopical tumor margins before RCM examination.[26]

Understanding Clinical, Dermoscopic, and Histologic Features

Histology is the gold standard for examination of the architecture and cell components of the skin. However, histologic examination implies an invasive biopsy, requires a fixation that can alter the specimen, and is not always performed on the whole lesion. RCM has the advantage of being performed in vivo with possible direct correlation with the clinical and dermoscopic aspect. This is why RCM is of great interest in understanding the cellular substrate that is responsible for particular clinical and/dermoscopic features. For example, thanks to RCM, we could demonstrate that the gray color observed in mucosal melanoses is linked to the presence of melanophages.[27] Moreover, RCM showed that the clefts around the tumor islands of BCC are not artifacts induced by the tissue retraction following the fixation of the skin specimen but are present in vivo and correspond to mucin accumulation.[28] RCM could also add information to the histologic examination. For example, we observed that cells of Langerhans cell histiocytosis and epidermal Langerhans cells, which are considered different cell populations but are not possible to distinguish under histology, have different aspects under RCM.[29]

Videos

RCM produces real-time images that can be recorded as video with nine images per second. This modality is useful with HH-RCM to record the displacements of the operator, who "navigates" inside the skin. This is particularly interesting in case of large lesions and when the lesion architecture is important for the diagnosis.

Videos can also be useful to record in real-time blood cells circulating inside the lumina of dermal capillaries.[30] Blood cells appear as bright roundish spots inside roundish hyporeflective dermal capillaries. The capillaries appear in pairs, with the arterial and venous capillaries one next to the other. Our group quantified the capillary blood flow based on RCM videos in different vascular lesions.[31,32] Because microcirculation is a key element of tumor growth, quantification of blood flow could be helpful for the diagnosis of malignant tumors.

In case of parasitosis, videos also allow one to reconstruct the architecture of large parasites and to assess their viability through the identification of their movements, including intestinal peristalsis (Video 1) and defecation.

Ex Vivo Confocal Microscopy

Ex vivo confocal microscopy has been conceived for a fast alternative to frozen histopathology during Mohs micrographic surgery of cutaneous epithelial tumors. However, it is also useful for the diagnosis of melanocytic tumors and for tissues other than skin.[33,34] Moreover, it can be applied to the diagnosis of skin infections, such as herpes simplex[35] and mucormycosis.[36]

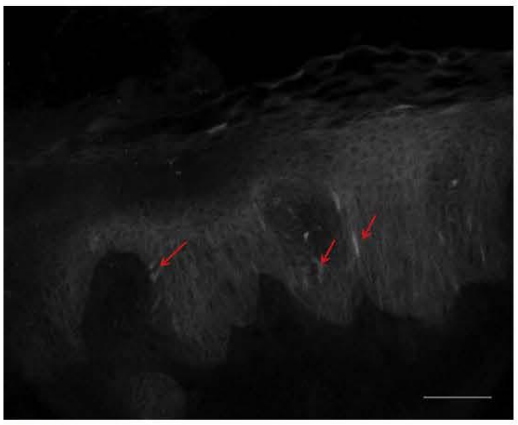

Fig. 10. Ex vivo fluorescence confocal microscopy of normal skin performed with a fluorescent antibody that target melanocytes allows to identify basal melanocytes (*red arrows*) that are usually not visible under reflectance confocal microscopy in nonpathologic conditions. Scale bar: 100 μm.

Because ex vivo confocal microscopy works with fluorescence and not only reflectance, in the future different fluorescent antibodies could be used to identify different cells and anatomic structures (**Fig. 10**), as used for immunohistochemistry in conventional histopathology.

SUPPLEMENTARY DATA

Supplementary data related to this article can be found at http://dx.doi.org/10.1016/j.det.2016.05.010.

REFERENCES

1. Cinotti E, Labeille B, Cambazard F, et al. Reflectance confocal microscopy for mucosal diseases. G Ital Dermatol Venereol 2015;150:585–93.
2. Cinotti E, Perrot JL, Labeille B, et al. Reflectance confocal microscopy for cutaneous infections and infestations. J Eur Acad Dermatol Venereol 2016;30:754–63.
3. Cinotti E, Jaffelin C, Charriere V, et al. Sensitivity of handheld reflectance confocal microscopy for the diagnosis of basal cell carcinoma: a series of 344 histologically proven lesions. J Am Acad Dermatol 2015;73:319–20.
4. Debarbieux S, Perrot JL, Erfan N, et al. Reflectance confocal microscopy of mucosal pigmented macules: a review of 56 cases including 10 macular melanoma. Br J Dermatol 2014;170:1276–84.
5. Cinotti E, Perrot JL, Labeille B, et al. Reflectance confocal microscopy for the diagnosis of vulvar melanoma and melanosis: preliminary results. Dermatol Surg 2012;38:1962–7.
6. Cinotti E, Chol C, Perrot JL, et al. Anal melanosis diagnosed by reflectance confocal microscopy. Australas J Dermatol 2014;55:286–8.
7. Arzberger E, Komericki P, Ahlgrimm-Siess V, et al. Differentiation between balanitis and carcinoma in situ using reflectance confocal microscopy. JAMA Dermatol 2013;149:440–5.
8. Cinotti E, Perrot JL, Labeille B, et al. Laser photodynamic treatment for in situ squamous cell carcinoma of the glans monitored by reflectance confocal microscopy. Australas J Dermatol 2014;55:72–4.
9. Cinotti E, Perrot JL, Labeille B, et al. In vivo confocal microscopy for eyelids and ocular surface: a new horizon for dermatologists. G Ital Dermatol Venereol 2015;150:127–9.
10. Cinotti E, Perrot JL, Campolmi N, et al. The role of in vivo confocal microscopy in the diagnosis of eyelid margin tumors: 47 cases. J Am Acad Dermatol 2014;71:912–8.e2.
11. Cinotti E, Perrot J-L, Labeille B, et al. Handheld reflectance confocal microscopy for the diagnosis of conjunctival tumors. Am J Ophthalmol 2015;159:324–33.e1.
12. Cinotti E, Perrot JL, Labeille B, et al. Optical diagnosis of a metabolic disease: cystinosis. J Biomed Opt 2013;18:046013.
13. Perrot J-L, Cinotti E, Labeille B, et al. In vivo confocal microscopy for the diagnosis of lysosomal storage diseases. Ann Dermatol Venereol 2014;141:784–5.
14. Jullienne R, He Z, Manoli P, et al. In vivo confocal microscopy of pine processionary caterpillar hair-induced keratitis. Cornea 2015;34:350–2.
15. Cinotti E, Fouilloux B, Perrot JL, et al. Confocal microscopy for healthy and pathological nail. J Eur Acad Dermatol Venereol 2014;28:853–8.
16. Cinotti E, Debarbieux S, Perrot JL, et al. Reflectance confocal microscopy features of acral lentiginous melanoma: a comparative study with acral nevi. J Eur Acad Dermatol Venereol 2016;30:1125–8.
17. Cinotti E, Labeille B, Cambazard F, et al. Reflectance confocal microscopy in infectious diseases. G Ital Dermatol Venereol 2015;150:575–83.
18. Cinotti E, Labeille B, Cambazard F, et al. Unusual reflectance confocal microscopy findings during the examination of a perianal nevus: pinworms. J Eur Acad Dermatol Venereol 2015. http://dx.doi.org/10.1111/jdv.13333.
19. Cinotti E, Labeille B, Bernigaud C, et al. Dermoscopy and confocal microscopy for in vivo detection and characterization of *Dermanyssus gallinae* mite. J Am Acad Dermatol 2015;73:e15–6.
20. Cinotti E, Perrot JL, Labeille B, et al. Reflectance confocal microscopy for quantification of *Sarcoptes scabiei* in Norwegian scabies. J Eur Acad Dermatol Venereol 2013;27:e176–8.

21. Cinotti E, Perrot J-L, Labeille B, et al. On the feasibility of confocal microscopy for the diagnosis of scabies. Ann Dermatol Venereol 2013;140:215–6.
22. Cinotti E, Perrot JL, Labeille B, et al. Tinea corporis diagnosed by reflectance confocal microscopy. Ann Dermatol Venereol 2014;141:150–2.
23. Cinotti E, Perrot JL, Labeille B, et al. Hair dermatophytosis diagnosed by reflectance confocal microscopy: six cases. J Eur Acad Dermatol Venereol 2015;29:2257–9.
24. Champin J, Perrot JL, Cinotti E, et al. In vivo reflectance confocal microscopy to optimize the spaghetti technique for defining surgical margins of lentigo maligna. Dermatol Surg 2014;40:247–56.
25. Terrier J-E, Tiffet O, Raynaud N, et al. In vivo reflectance confocal microscopy combined with the 'spaghetti' technique: a new procedure for defining surgical margins of genital Paget disease. Dermatol Surg 2015;41:862–4.
26. Venturini M, Gualdi G, Zanca A, et al. A new approach for pre-surgical margin assessment of basal cell carcinoma by reflectance confocal microscopy. Br J Dermatol 2016;174:380–5.
27. Cinotti E, Couzan C, Perrot JL, et al. In vivo confocal microscopic substrate of grey colour in melanosis. J Eur Acad Dermatol Venereol 2015;29:2458–62.
28. Ulrich M, Roewert-Huber J, González S, et al. Peritumoral clefting in basal cell carcinoma: correlation of in vivo reflectance confocal microscopy and routine histology. J Cutan Pathol 2011;38:190–5.
29. Cinotti E, Labeille B, Perrot JL, et al. Cells of Langerhans cell histiocytosis and epidermal Langerhans cells differ under reflectance confocal microscopy: first observation. Skin Res Technol 2014;20:385–7.
30. Cinotti E, Gergelé L, Perrot JL, et al. Quantification of capillary blood cell flow using reflectance confocal microscopy. Skin Res Technol 2014;20:373–8.
31. Perrot JL, Cinotti E, Labeille B, et al. Microscopie confocale et lésions vasculaires et analyse dynamique du débit vasculaire: un nouveau champ d'investigation de la microscopie confocale. Ann Dermatol Venereol 2014;141:S327–8.
32. Cinotti E, Perrot JL, Labeille B, et al. Reflectance confocal microscopy for the vascular flow analysis: a new field of exploration. Dermatol Pract Concept 2015;5:230.
33. Cinotti E, Haouas M, Grivet D, et al. In vivo and ex vivo confocal microscopy for the management of a melanoma of the eyelid margin. Dermatol Surg 2015;41:1437–40.
34. Forest F, Cinotti E, Yvorel V, et al. Ex vivo confocal microscopy imaging to identify tumor tissue on freshly removed brain sample. J Neurooncol 2015;124:157–64.
35. Cinotti E, Perrot JL, Labeille B, et al. First identification of the herpes simplex virus by skin-dedicated ex vivo fluorescence confocal microscopy during herpetic skin infections. Clin Exp Dermatol 2015;40:421–5.
36. Leclercq A, Cinotti E, Labeille B, et al. Ex vivo confocal microscopy: a new diagnostic technique for mucormycosis. Skin Res Technol 2016;22:203–7.

6- imagerie non invasive des maladies bulleuses

Peu de travaux ont porté sur sujet. J'ai participé à une étude comparant OCT non HD et MCIV pour la caractérisation des bulles lors de pemphigus et pemphigoïde, travail en finalisation avant publication en collaboration avec l'équipe italienne de Modena. Par ailleurs 2 fiches iconographiques à visée didactique ont été publiées dans les annales de dermatologie sur ce sujet sous mon contrôle par 1 interne du service.

Nous avons pu montrer l'intérêt de l'OCT notamment pour cibler le site des biopsies et le caractère multi-cloisonné de la bulle de la pemphigoïde.

6.1 The role of reflectance confocal microscopy and of optical coherence tomography in the diagnosis of pemphigus

Annales de dermatologie et de vénéréologie (2016) 143, 70—72

ELSEVIER MASSON

Disponible en ligne sur ScienceDirect www.sciencedirect.com

Elsevier Masson France EM|consulte www.em-consulte.com

Formation médicale continue

FICHE THÉMATIQUE / MICROSCOPIE CONFOCALE PAR RÉFLECTANCE

Apport de la microscopie confocale par réflectance et de la tomographie par cohérence optique dans le diagnostic de pemphigus

The role of reflectance confocal microscopy and of optical coherence tomography in the diagnosis of pemphigus

C. Couzan[a], J.L. Perrot[a], C. Habougit[b], B. Labeille[a], C. Douchet[b], F. Cambazard[a], E. Cinotti[a,*], Groupe d'imagerie cutanée non invasive de la Société française de dermatologie

[a] *Service de dermatologie, hôpital universitaire de Saint-Etienne, 42055 Saint-Etienne cedex 2, France*
[b] *Service d'anatomopathologie, hôpital universitaire de Saint-Etienne, 42055 Saint-Etienne cedex 2, France*

Reçu le 31 août 2015 ; accepté le 30 octobre 2015
Disponible sur Internet le 18 décembre 2015

Observation

Un homme âgé de 66 ans était adressé pour une dermatose extensive évoluant depuis 6 mois, au décours de la radiothérapie d'un adénocarcinome prostatique, et suspecte de psoriasis. Un impétigo, puis une gale avaient été évoqués préalablement. Leurs traitements s'étaient avérés inefficaces. Nous constations des lésions érythémato-squameuses thoraciques (Fig. 1a) d'extension lentement centrifuge, avec une atteinte plus récente des épaules, du cuir chevelu et du front. Il n'y avait pas d'atteinte des muqueuses. Le patient ne signalait pas de brûlure oculaire ou buccale. Il n'y avait pas de prise récente de nouveau médicament. L'examen en dermoscopie montrait des lésions croûteuses sur un fond érythémateux avec un patron vasculaire punctiforme (Fig. 1b).

Tomographie par cohérence optique et microscopie confocale par réflectance

La tomographie par cohérence optique (OCT) de non haute définition (HD) (Vivosight®, Michelson Diagnostics Ltd, Maidstone, comté de Kent, Grande-Bretagne) trouvait un clivage intra-épidermique (Fig. 2a). La microscopie confocale (MC) par réflectance in vivo (Vivascope 3000® ;

* Auteur correspondant.
Adresse e-mail : elisacinotti@gmail.com (E. Cinotti).

http://dx.doi.org/10.1016/j.annder.2015.10.591

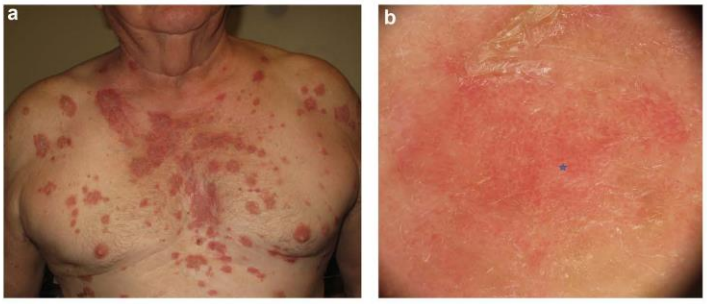

Figure 1. Examen clinique (a) et en dermoscopie (b). La dermoscopie (b) montre un patron vasculaire à type de points (étoile bleue).

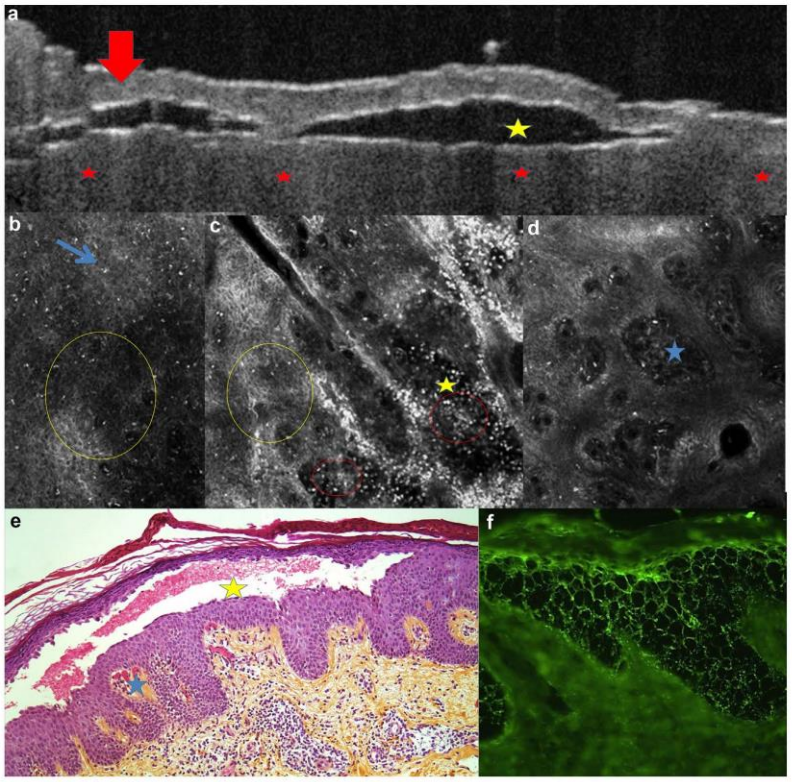

Figure 2. Examen en tomographie par cohérence optique (OCT) (a), en microscopie confocale (MC) par réflectance (b,c,d), histopathologique (e) et en immunofluorescence directe (IFD) (f). L'OCT (a) montre une bulle intra-épidermique (étoile jaune). Le toit de la bulle correspondant à la couche cornée et granuleuse de l'épiderme (flèche rouge) et les crêtes épidermiques (étoiles rouges) sont bien visibles. La MC (b,c,d) montre un épiderme en nid d'abeille irrégulier (cercles jaunes) des cellules inflammatoires intra-épidermiques (cellules de petite taille et hyper-reflétantes, flèche bleue), des kératinocytes détachés (cercle rouge), des clivages intra-épidermiques (étoile jaune) et des vaisseaux dilatés dans le derme (étoile bleue). L'examen histologique (e) montre un clivage intra-épidermique (étoile jaune) et des vaisseaux dilatés dans le derme (étoile bleue). L'examen en IFD (f) montre une fluorescence en maille intra-épidermique (anticorps anti-IgG).

Caliber Inc, Rochester, New York, États-Unis, distribué en France par Mavig, Munich, Allemagne) montrait un épiderme à type de nid d'abeille irrégulier, des cellules inflammatoires dans l'épiderme (petites cellules hyper-reflétantes) (Fig. 2b), des zones de clivage intra-épidermique et des cellules rondes acantholytiques (Fig. 2c). Nous observions la présence de vaisseaux dilatés au sommet des papilles dermiques (Fig. 2d). Un pemphigus était évoqué.

À l'issue de ces examens non invasifs une biopsie cutanée était réalisée sur une lésion de la partie latérale du tronc, dirigée par les constatations de la MC et de l'OCT. Elle montrait un décollement bulleux superficiel du corps muqueux de Malpighi (Fig. 2e). L'épiderme était acanthosique, psoriasiforme et le siège d'une acantholyse superficielle avec formation de bulles intra-épidermiques. La couche cornée était épaisse et focalement parakératosique avec des hématies. Nous ne notions pas d'effets cytopathogènes de type herpès-virus visibles. L'immunofluorescence cutanée directe réalisée sur peau péri-lésionnelle visualisait des dépôts intercellulaires en résille sur toute la hauteur de l'épiderme avec les anticorps anti-IgG et anti-C3 (Fig. 2f). L'examen en immunofluorescence directe permettait d'identifier la présence d'anticorps anti-desmogléine1 à un taux supérieur à 197 UA/mL. L'aspect histopathologique et en immunofluorescence était celui d'un pemphigus superficiel.

Commentaires

L'OCT [1] non HD permet une visualisation tridimensionnelle des deux premiers millimètres de l'épiderme. Il est particulièrement aisé et rapide de déterminer au moyen de l'OCT la présence et la topographie du décollement : intra-épidermique, ou dermo-épidermique [2], lors de l'examen clinique du malade. Il est ainsi possible d'examiner rapidement une grande surface cutanée pour identifier la zone la plus significative pour un examen additionnel en MC. L'OCT non HD n'a pas une capacité de discrimination cellulaire, à la différence de la MC qui permet d'identifier les cellules acantholytiques et les cellules inflammatoires dans l'épiderme en cas de pemphigus. L'aspect en MC du pemphigus a été peu rapporté. Nous avons trouvé 3 articles [3—5] qui décrivent les éléments séméiologiques suivants : perte du patron épidermique à type de nid d'abeille avec exocytose de cellules inflammatoires dans l'épiderme, décollement bulleux dans l'épiderme sous la forme d'un espace de clivage fin et sombre avec présence de cellules rondes détachées (cellules acantholytiques) et existence de vaisseaux dilatés au sommet des papilles dermiques.

Dans notre observation nous avons mis en évidence les 3 éléments séméiologiques du pemphigus en MC ce qui, compte tenu de l'aspect clinique et d'un clivage intra-épidermique en OCT, a permis d'évoquer avec une quasi-certitude lors de la consultation le diagnostic de pemphigus et de déterminer le meilleur site de la biopsie pour l'examen histologique. La MC peut apporter une aide diagnostique au cours d'autres dermatoses acantholytiques. Par exemple la MC peut montrer un clivage intra-épidermique dans la couche granuleuse ou épineuse avec présence de cellules acantholytiques à type de mur de brique ébranlé au cours de la maladie de Hailey-Hailey [6].

Si le diagnostic de certitude du pemphigus reste biologique et anatomopathologique, les méthodes modernes d'imageries MC et OCT permettent d'orienter rapidement le diagnostic clinique, de limiter les examens complémentaires et de choisir le site le plus approprié pour la biopsie cutanée.

Déclaration de liens d'intérêts

Les auteurs déclarent ne pas avoir de liens d'intérêts.

Références

[1] Marneffe A, Suppa M, Miyamoto M, Del Marmol V, Boone M. La tomographie par cohérence optique à haute définition : présentation de la technique et applications en dermatologie. Ann Dermatol Venereol 2015;142:452—5.
[2] Mogensen M, Morsy HA, Nurnberg BM, Jemec GB. Optical coherence tomography imaging of bullous diseases. J Eur Acad Dermatol Venereol 2008;22:1458—64.
[3] Kurzeja M, Rakowska A, Rudnicka L, Olszewska M. Criteria for diagnosing pemphigus vulgaris and pemphigus foliaceus by reflectance confocal microscopy. Skin Res Technol 2012;18:339—46.
[4] Alessi SS, Nico MM, Fernandes JD, Lourenço SV. Reflectance confocal microscopy as a new tool in the in vivo evaluation of desquamative gingivitis: patterns in mucous membrane pemphigoid, pemphigus vulgaris and oral lichen planus. Br J Dermatol 2013;168:257—64.
[5] Angelova-Fischer I, Pfeuti T, Zillikens D, Rose C. In vivo confocal laser scanning microscopy for non-invasive diagnosis of pemphigus foliaceus. Skin Res Technol 2009;15:40—4.
[6] Kurzeja M, Czuwara J, Rakowska A, Sicińska J, Maj M, Nasierowska-Guttmejer A, et al. Reflectance confocal microscopy as a non-invasive diagnostic tool for Hailey-Hailey disease. Skin Res Technol 2014;20:503—9.

6.2 Role of reflectance confocal microscopy and optical coherence tomography as aids in the diagnosis of pemphigoid gestationis

Annales de dermatologie et de vénéréologie (2016) 143, 483—485

Disponible en ligne sur ScienceDirect www.sciencedirect.com

Elsevier Masson France EM|consulte www.em-consulte.com

Formation médicale continue

FICHE THÉMATIQUE / MICROSCOPIE CONFOCALE PAR RÉFLECTANCE

Apport de la microscopie confocale par réflectance et de la tomographie en cohérence optique dans le diagnostic de pemphigoïde gestationis

Role of reflectance confocal microscopy and optical coherence tomography as aids in the diagnosis of pemphigoid gestationis

C. Couzan[a], E. Cinotti[a,*], B. Labeille[a], C. Habougit[b], C. Douchet[b], F. Cambazard[a], J.-L. Perrot[a], groupe imagerie cutanée non invasive de la Société française de dermatologie

[a] *Service de dermatologie, hôpital universitaire de Saint-Etienne, 42055 Saint-Étienne cedex 2, France*
[b] *Service d'anatomopathologie, hôpital universitaire de Saint-Etienne, 42055 Saint-Étienne cedex 2, France*

Reçu le 24 décembre 2015 ; accepté le 5 février 2016
Disponible sur Internet le 24 mai 2016

Observation

Une femme enceinte âgée de 22 ans, à 32 semaines d'aménorrhée, nous était adressée pour une dermatose prurigineuse évoluant depuis 2 mois. Les lésions étaient initialement localisées à l'ombilic. La surinfection d'un *piercing* ombilical, puis une toxidermie à la cloxacilline administrée pour traiter la surinfection du *piercing* et enfin une gale avaient été évoquées successivement par les médecins qui suivaient la patiente.

Nous constations à l'entrée dans le service des lésions érythémateuses, œdémateuses, pseudo-urticariennes sur la face antérieure de l'abdomen, les faces internes des 2 bras et sur les 2 cuisses (Fig. 1a). Le prurit était sévère. Il n'y avait pas d'atteinte des muqueuses ni de notion de souffrance obstétricale et de grossesse pathologique.

L'examen en dermoscopie montrait un patron érythémateux homogène sans vésicule (Fig. 1b).

Tomographie par cohérence optique

Un examen par tomographie de cohérence optique haute définition (OCT HD) (Skintell®; Agfa Gevaert, Antverpen Belgique) mettait en évidence un décollement

* Auteur correspondant.
Adresse e-mail : elisacinotti@gmail.com (E. Cinotti).

http://dx.doi.org/10.1016/j.annder.2016.02.029

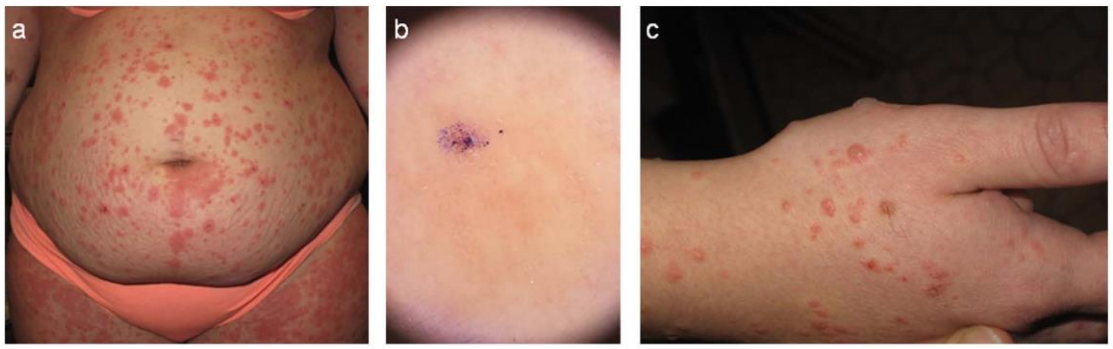

Figure 1. Examen clinique (a) et dermoscopique (b) initial et aspect clinique lors de l'éruption bulleuse (c). Le point violet sur l'image dermatoscopique (b) correspond à la zone de clivage cutané infraclinique.

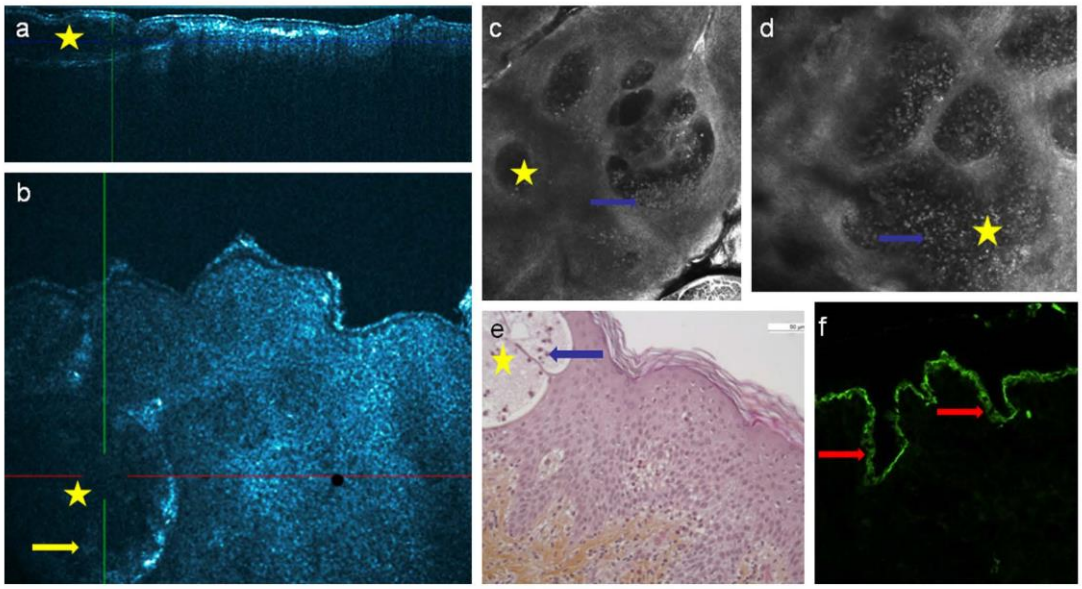

Figure 2. Tomographie de cohérence optique haute définition (OCT HD) en coupe sagittale (a) et en coupe transversale (b), microscopie confocale in vivo (c et d), examen histologique (e) et examen en immunofluorescence directe (IFD) (f). L'examen en OCT HD (a et b) montre une bulle sous-épidermique (étoile jaune) et des structures hyper-reflétantes à l'intérieur compatibles avec des cellules (flèche jaune). L'examen en microscopie confocale par réflectance au niveau de la couche épineuse (c) et au niveau de la jonction dermo-épidermique (d) montre des cavités hyporeflétantes sous-épidermiques (étoile jaune) parsemées de polynucléaires éosinophiles (flèche bleue). L'examen histopathologique (hématoxyline-éosine, 20 ×) (e) montre une bulle sous-épidermique (étoile jaune) avec un infiltrat éosinophilique (flèche bleue). L'examen en IFD (f) objective des dépôts linéaires d'anticorps anti-C3 (flèche rouge).

sous-épidermique (Fig. 2a, b) avec formation d'une cavité sombre contenant des structures hyper-reflétantes compatibles avec des cellules.

Microscopie confocale par réflectance

Un examen en microscopie confocale (MC) par réflectance in vivo (Vivascope 3000® ; Caliber Inc, Rochester, NY, États-Unis, distribué en France par Mavig, Munich) était ensuite réalisé sur une zone de décollement infraclinique. Cet examen montrait un clivage sous-épidermique avec des cavités hyporeflétantes remplies de petites cellules hyper-reflétantes et rondes (Fig. 2c, d). Une pemphigoïde gestationis était évoquée. Une biopsie cutanée était alors effectuée sur une lésion de la face interne de l'avant-bras en regard d'une zone de décollement sous-épidermique infraclinique (Fig. 1b, point violet).

L'examen histopathologique trouvait un décollement bulleux sous-épidermique avec un infiltrat éosinophilique et quelques kératinocytes nécrotiques (Fig. 2e). L'immunofluorescence cutanée directe montrait des dépôts linéaires de C3 (Fig. 2f), ce qui permettait de porter un diagnostic de pemphigoïde gestationis, confirmé

7- Elaboration d'outils pour améliorer au quotidien les instruments d'imagerie cutanéomuqueux

La pratique intensive de la microscopie confocale in et ex vivo nous a conduit à réfléchir à des améliorations techniques dans le but d'améliorer nos performances.

Ainsi a été créé un dispositif permettant d'étaler la totalité d'une pièce tissulaire prise entre 2 lames pour un examen en microscopie confocale ex vivo et éviter que des zones du prélèvement non en contact avec la lame ne puissent être analysée. Ce système simple a été nommé applaneur en français et tissue press en anglais.

Le deuxième dispositif que nous avons mis au point là encore en collaboration avec l'équipe du BiiGC et un embout stérilisable adaptée à la caméra Vivascope 3000.Là encore il s'agit d'un dispositif créé pour la première fois à St Etienne et qui répondait à toutes les questions soulevées quant à la prise en charge des mesures d'hygiènes pour l'exploration en MICV des muqueuses et des tumeurs ulcérées et micro-ulcérées

Le 3éme dispositif toujours d'invention stéphanoise est un embout stérilisable adapté à la caméra Vivascope 300 permettant d'optimiser le repérage des berges chirurgicales d'une tumeur en MICV. Il s'agit d'un embout dans le même matériaux que l'embout stérilisable décrit précédemment mais dont le rebord distal en périphérie de la lentille est très discrètement en relief pour créer une légère dépression cutanée après application ce qui nous indique parfaitement la circonférence de la zone explorer. Non seulement le marquage est plus précis mais un seul opérateur est nécessaire en lieu et place de 2 auparavant.Travaux en cours de publication

Enfin nous avons établi le cahier des charges d'un logiciel dont nous sommes propriétaire permettant de compter sur une vidéo où en direct lors du film en MICV du flux capillaire cutanéomuqueux le nombre de corpuscule (hématies isolées ou en amas) qui circulent en leur sein.
Une thèse de médecine en a été réalisé utilisant ce logiciel et qui a été présenté au 11th IEEE International Symposium on Medical Measurements and Applications, MeMeA 2016; University of Sannio Benevento en Italie en mai 2016.Ce logiciel a été prêté à l'université de Manchester pour des travaux sur la microcirculation de la peau des brûlés

7.1 Practical interest of in vivo reflectance confocal microscopy quantification of cutaneous vascular flow during iloprost treatment

Jaffélin C, Cinotti E., Perrot J.-L., Labeille B, Cambazard F, Tognetti L., Rubegni P., Pittet J.-C. Practical interest of in vivo reflectance confocal microscopy quantification of cutaneous vascular flow during iloprost treatment (Conference Paper). 11th IEEE International Symposium on Medical Measurements and Applications, MeMeA 2016; University of SannioBenevento; Italy; 15 May 2016 through 18 May 2016. 4 August 2016,
Article number 7533790.

Abstract:
Introduction: iloprost is a recommended treatment for several vascular diseases such as severe Raynaud's syndrome and digital ulcers in Systemic Sclerosis (SS). In vivo reflectance confocal microscopy (RCM) is a non-invasive imaging tool that can evaluate cutaneous microcirculation. The goal of this study was to observe, in real time, the effect of iloprost on cutaneous microcirculation by using RCM. Material and method: Five patients with microvascular diseases that needed iloprost were included. Administration speed started at 0.5 ng/kg/min until the maximum tolerated dosage. Recordings of capillary flow were done using RCM before treatment and at each change in the drug dosage. Results: The blood flow of the five patients demonstrated a significant increase from the dosage of 0.5 ng/kg/min. This significant variation did not exist at higher dosage. Discussion: This study suggests a precocious effect of iloprost in increasing the cutaneous vascular flow; this effect was not enhanced at higher drug dosage. Monitoring cutaneous capillary flow by in vivo RCM could then be of interest in optimizing iloprost dosage. This procedure will likely reduce the side effects of iloprost that are dose-dependent

7.2 The 'tissue press': a new device to flatten fresh tissue during ex vivo confocal microscopy examination.

Skin Research and Technology 2016; 0: 1–4
Printed in Singapore · All rights reserved
doi: 10.1111/srt.12293

Published by John Wiley & Sons Ltd
Skin Research and Technology

Letter to the Editor

The 'tissue press': a new device to flatten fresh tissue during *ex vivo* confocal microscopy examination

E. Cinotti[1], D. Grivet[2,3], B. Labeille[1], M. Solazzi[4], A. Bernard[3], F. Forest[5], M. Espinasse[2,3], F. Cambazard[1], G. Thuret[2,3,6], P. Gain[2,3] and J. L. Perrot[1]

[1]*Department of Dermatology, University Hospital of St-Etienne, Saint Etienne Cedex 2, France,* [2]*Department of Ophthalmology, University Hospital of St-Etienne, Saint Etienne Cedex 2, France,* [3]*Biology, Engineering and Imaging of Corneal Graft Laboratory, Institute of Research in Sciences and Health Engineering, EA2512, Jean Monnet University, Saint-Etienne, France,* [4]*PERCRO Laboratory, Scuola Superiore Sant'Anna, Pisa, Italy,* [5]*Department of Pathology, University Hospital of St-Etienne, Saint Etienne Cedex 2, France and* [6]*Institut Universitaire de France, Paris, France*

SKIN -dedicated *ex vivo* confocal microscopy (EVCM) VivaScope 2500® (Caliber, NY, USA, distributed in Europe by MAVIG GmbH, Munich, Germany) is a new device that allows evaluating in real-time cutaneous tumor margins, directly on freshly excised unfixed tissue in a perioperative setting (1–4).

One of the main limitations of this technique is the risk of false-negative results induced by an incorrect imaging of the whole sample due to the inability to properly flatten the fresh tissue. The outer faces of the specimen are the most informative areas for EVCM because: (i) the fluorescent dyes used to selectively stain cell organelles and to enhance contrast in tumors are more concentrated at the periphery because they do not penetrate in depth into fresh tissue; (ii) the resolution of the EVCM images is higher at the periphery because the signal is less attenuated; (iii) for cutaneous

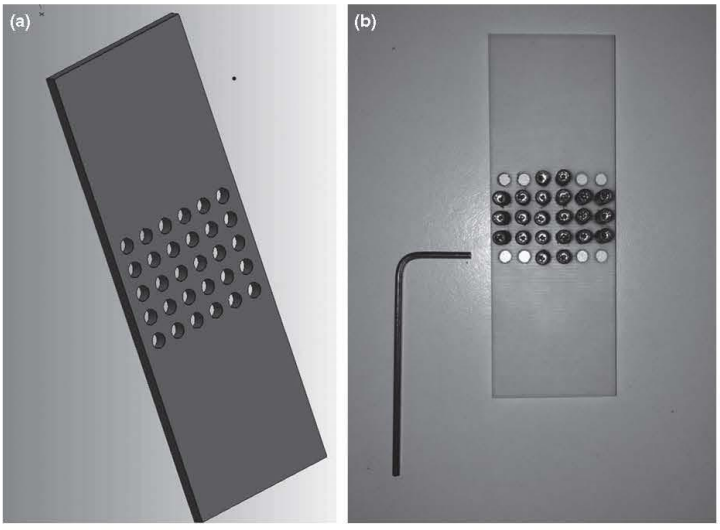

Fig. 1. The 'tissue press'. Lateral (a, drawing) and frontal (b) view of the device.

specimens, one outer side is the epidermis that must be carefully examined in case of superficial tumor (for instance, superficial basal cell carcinoma) and the opposite side is the lower part of the skin that can be infiltrated by other cancer types like sclerodermiform basal cell carcinoma. The standard procedure recommends flattening the tissue between two thick microscopy glass slides attached together by a small amount of silicon glue or modeling clay. The tissue mounted between the glass slides is placed on the EVCM that acquires z-stacks in the first 200 µm of the specimen. With this simple mount, a uniform pressure is evenly applied to the whole tissue that is, by nature, heterogeneous. The specimens are indeed entire surgical pieces or part of them, cut manually with a surgical blade. They are composed of tissue with different mechanical properties; their thickness and their surface are most often irregular. These irregularities prevent from a uniform stretch of the sample between the two glass slides and are

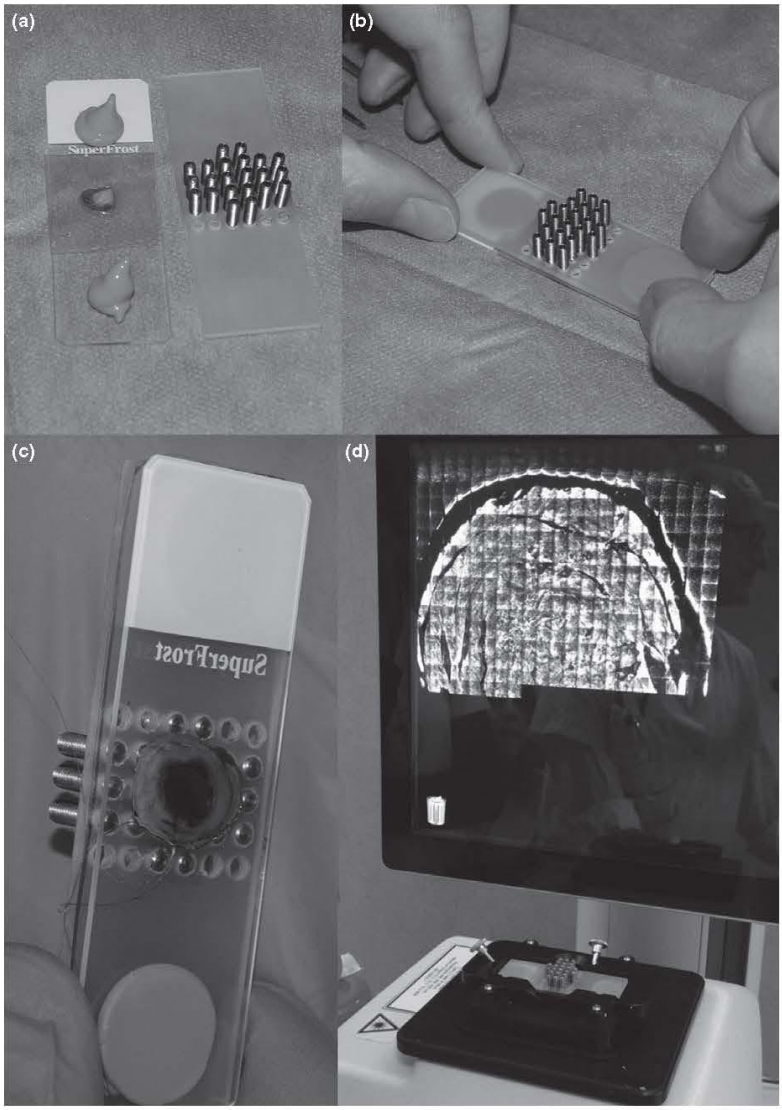

Fig. 2. Mounting procedure of the sample with the 'tissue press'. The tissue is placed on one conventional glass slide (a) and is covered by the plastic slide with the grub screws (b). The two slides are attached together by a silicon adhesive in their lateral part as it is done by the conventional procedure (b and c). The lower glass slide is placed in contact with the ex vivo confocal microscope stage (d).

responsible for artifacts during image acquisition: some parts are not in contact with the glass slide, others form folds and air bubble can be trapped between the glass slide and the tissue.

To facilitate the contact of the entire surface of the specimen with the glass slide facing the microscope objective, aqueous gel or silicone can be applied on the upper side of the tissue inducing the lower part to be adherent to the lower glass slide. However, these tips did not always enable us to obtain a homogeneous flattening of the tissue.

To solve this problem, we designed a specific device to flatten the tissue: the 'tissue press' (Fig. 1). We manufactured by rapid prototyping a plastic slide of the same size as the glass slide usually used to flatten the sample. This plastic slide has in its central part 30 tapped holes distributed on a 20 × 20 mm area, which corresponds to the maximum area that can be imaged by EVCM. In each hole, it is possible to place a flat point, hexagonal socket grub screw whose vertical position can be precisely adjusted with an Allen key. Each hole has a diameter of 2.5 mm to have a tradeoff between a good spatial resolution and a reasonable number of elements to be adjusted. The tissue to be examined is placed on one conventional glass slide and it is covered by a thin plastic sheet (a piece of a clear plastic folder for papers can be used) and by the plastic slide with the grub screws (Fig. 2). The grub screws exert their pressure on the plastic sheet and this pressure is then transmitted to the underlying tissue. The lower glass slide is placed in contact with the EVCM objective as usual. Since the EVCM

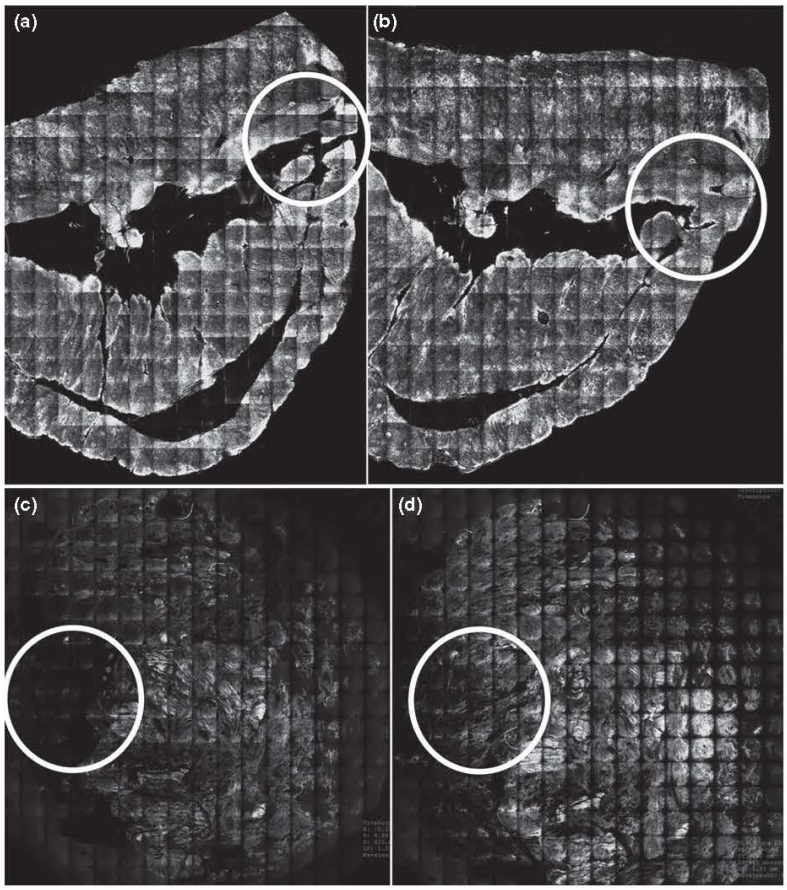

Fig. 3. Ex vivo confocal mosaic image before and after adjusting the grub screws of the 'tissue press'. The images before the adjustment of the grub screws (a and c) show some dark areas that disappeared after increasing the pressure on the corresponding area (circle) of the sample (b and d) by tightening the screws in the correspondent part of the specimen (a and b images of a lentigo maligna, reflectance mode, wavelength of the laser: 830 nm; b and c images of the bottom of a surgical excision of a basal cell carcinoma, fluorescence mode, wavelength of the laser: 488 nm).

analysis of tissue uses a laser beam coming from below the specimen, the slide of plastic with the grub screws does not alter the acquisition of the images because it is placed on the upper part of the tissue.

By gently adjusting the position of individual grub screws, the tissue can be flattened before and/or during the EVCM examination (Fig. 3). The adjustment can be performed keeping the sample mounted on the EVCM device and the effect of the adjustment can be observed in real-time through the EVCM images. Moreover, when mounting the tissue a drop of aqueous gel (Carbomer gel®, Gel Larmes Thea laboratories, Clermont-Ferrand, France) can be added between the inferior glass slide and the bottom of the tissue to facilitate their contact.

We tested our device on ten skin specimens and it allowed obtaining more complete mosaic images of the tissue after some local adjustments of the screws directly controlled by the image quality obtained in real-time. Our pathologist verified that this procedure did not damage the tissue for further histopathological examination.

In conclusion, our new device improves the quality of fresh tissue images obtained with the EVCM by locally correcting tissue distension.

Conflicts of interest

The authors declare not to have any conflicts of interest.

References

1. Chung VQ, Dwyer PJ, Nehal KS et al. Use of ex vivo confocal scanning laser microscopy during Mohs surgery for nonmelanoma skin cancers. Dermatol Surg 2004; 30: 1470 1478.
2. Bennàssar A, Vilata A, Puig S, Malvehy J. Ex vivo fluorescence confocal microscopy for fast evaluation of tumour margins during Mohs surgery. Br J Dermatol 2014; 170: 360 365.
3. Forest F, Cinotti E, Yvorel V et al. Ex vivo confocal microscopy imaging to identify tumor tissue on freshly removed brain sample. J Neurooncol 2015; 124: 157 164.
4. Cinotti E, Haouas M, Grivet D, Perrot JL. In vivo and ex vivo confocal microscopy for the management of a melanoma of the eyelid margin. Dermatol Surg 2015; 41: 1437 1440.

Address:
E. Cinotti
Hôpital Nord Saint-Etienne
42055 Saint Etienne Cedex 2
France
Tel: +33 (0)4.77.82.84.21
Fax: +33 (0)4.77.82.84.01
e-mail: elisacinotti@gmail.com

8- Spectrométrie Raman et microscopie confocale ex vivo

Ce chapitre semble à première vue, hors du champ de cette thèse dont l'objet principal est l'exploration optique in vivo du tégument cutanéomuqueux et de l'appareil oculaire antérieur. Toutefois il faut considérer qu'il s'agit de travaux préparatoires à l'exploration in vivo que l'on compte développer dans le service. Ainsi une demande pour une bourse dans le cadre d'un projet ANR (Chapitre E.1.) a été déposée en octobre 2016 pour réaliser l'intégration d'un spectromètre Raman dans un microscope confocal ou un OCT. D'autre part l'intégration d'un spectromètre Raman dans un appareil d'OCT ou de microscopie confocale a été validée comme étant un des axes prioritaires de développement hospitalo-universitaire du CHU de St Etienne.
De plus la microscopie confocale ex vivo est le prolongement de la microscopie confocale in vivo. En effet ces méthodes de microscopie confocale peuvent être intriquées dans le cadre de notre pratique clinique et ou notre activité de recherche concernant la chirurgie des tumeurs palpébrales et du lentigo malin notamment. Ainsi 2 articles ont été récemment soumis à des revues et sont en cours de relecture qui portent sur ses sujets.
Enfin l'examen en microscopie confocal ex vivo peut être considérer comme un travail préparatoire à de futures explorations in vivo ; notamment en ce qui concerne nos travaux sur le cerveau.
D'autre part la découverte et la mise en application de la spectrométrie Raman à la dermatologie a marqué une véritable transition dans notre façon d'aborder l'imagerie dermatologique. En effet cela nous a fait entrer de plein pied dans le monde l'optique et de la physique dure et surtout ceci nous a conduit à aborder l'imagerie dermatologique d'une matière totalement étrangère à la culture classique dermatologique, pour laquelle l'image se réduisait à la résultante de l'analyse optique du couple œil cerveau. Ainsi l'image « dermatologique » peut ne se présenter que sous la forme de d'une courbe traduisant l'effet Raman des différents constituants chimiques la composant. A la frustration du dermatologue liée à la perte des repères visuels classiques a répondu l'identification optique des constituants chimiques de la structure analysée.
Les possibilités offertes à la dermatologie entre autres sont gigantesques sous réserve de l'intrication d'un dispositif permettant le repérage microscopique non invasif in vivo de la cible.

Nos premiers travaux ont porté sur l'identification de corps étrangers dont du charbon ce qui pour une équipe stéphanoise était la moindre des choses. Cela nous a par ailleurs permis de réaliser la caractérisation purement optique d'une maladie métabolique mais aussi de démontrer la transformation d'un médicament : l'Ascabiol, lors de son contact avec certain type de récipients utilisés pour son application sur le corps humain, ce qui a occasionné une déclaration en pharmacovigilance et a modifié le RCP et la composition du produit ce qui a permis une amélioration globale de la santé des malades ayant à être traité par Ascabiol pour une gale.

8.1- Spectrométrie Raman

8.1.1 Optical diagnosis of a metabolic disease: cystinosis

Nephropathic cystinosis (NC) is a rare autosomal recessive storage disease characterized by the lysosomal accumulation of cystine crystals throughout the body, particularly in blood cells, the cornea, skin, kidneys, the central nervous system, and the muscles. The skin and the cornea are the most accessible sites to explore, and *in vivo* reflectance confocal microscopy (IVCM) helps identify crystals in both but does not provide any information to help define their composition. Raman spectroscopy (RS) allows cystine to be easily recognized thanks to its characteristic signature with a band at 499 cm^{-1}. Two dermatology confocal microscopes were used to visualize crystals in both the skin and the ocular surface of a cystinosis patient, and an *ex vivo* Raman examination of a skin
biopsy and of the cornea was performed and removed during a corneal graft to confirm the cystine composition of the crystals. Recently, RS has been performed *in vivo* and coupled with IVCM. In the future, it is suggested that crystals in NC and other deposits in storage diseases could be identified with this noninvasive *in vivo* technique that combines IVCM to recognize the deposits and RS to confirm their chemical nature

Journal of Biomedical Optics 18(4), 046013 (April 2013)

Optical diagnosis of a metabolic disease: cystinosis

Elisa Cinotti,[a] Jean Luc Perrot,[a] Bruno Labeille,[a] Marine Espinasse,[b,c] Youcef Ouerdane,[d] Aziz Boukenter,[d] Gilles Thuret,[b,c] Philippe Gain,[b,c] Nelly Campolmi,[b,c] Catherine Douchet,[e] and Frédéric Cambazard[a]
[a]University Hospital of St-Etienne, Department of Dermatology, 42055 Saint Etienne Cedex 2, France
[b]University Hospital of St-Etienne, Department of Ophthalmology, 42055 Saint Etienne Cedex 2, France
[c]Corneal Graft Biology, Engineering and Imaging Laboratory, EA2521, Federative Institute of Research in Sciences and Health Engineering, France
[d]Université Jean Monnet, Laboratoire Hubert Curien, CNRS UMR-5516, 42000 Saint Etienne, France
[e]University Hospital of St-Etienne, Department of Pathology, 42055 Saint Etienne Cedex 2, France

Abstract. Nephropathic cystinosis (NC) is a rare autosomal recessive storage disease characterized by the lysosomal accumulation of cystine crystals throughout the body, particularly in blood cells, the cornea, skin, kidneys, the central nervous system, and the muscles. The skin and the cornea are the most accessible sites to explore, and *in vivo* reflectance confocal microscopy (IVCM) helps identify crystals in both but does not provide any information to help define their composition. Raman spectroscopy (RS) allows cystine to be easily recognized thanks to its characteristic signature with a band at 499 cm^{-1}. Two dermatology confocal microscopes were used to visualize crystals in both the skin and the ocular surface of a cystinosis patient, and an *ex vivo* Raman examination of a skin biopsy and of the cornea was performed and removed during a corneal graft to confirm the cystine composition of the crystals. Recently, RS has been performed *in vivo* and coupled with IVCM. In the future, it is suggested that crystals in NC and other deposits in storage diseases could be identified with this noninvasive *in vivo* technique that combines IVCM to recognize the deposits and RS to confirm their chemical nature. [DOI: 10.1117/1.JBO.18.4.046013]

Keywords: confocal microscopy; nephropathic cystinosis; Raman; spectroscopy; skin; cornea; dermis; crystals; optic.

Paper 12808R received Dec. 19, 2012; revised manuscript received Feb. 26, 2013; accepted for publication Mar. 19, 2013; published online Apr. 22, 2013.

1 Introduction

Nephropathic cystinosis (NC) is a rare autosomal recessive storage disease characterized by lysosomal accumulation of cystine crystals throughout the body, particularly in blood cells, the cornea, skin, kidneys, the central nervous system and muscles.[1] Diagnosis and follow-up of NC are based on the demonstration and quantification of cystine crystal deposition. The concentration of cystine is normally assessed in blood cells, which is the gold standard for diagnosis.[1] However, the presence of crystals has also been investigated in the cornea,[2] the skin,[3] and in other tissues such as kidney[1] and intestinal mucosa.[4]

Thanks to *in vivo* reflectance confocal microscopy (IVCM), the cornea and skin crystals have recently become of greater interest because of the possibility of noninvasive identification and quantification in two easily accessible locations.[2,3] While IVCM provides high definition images of the crystals, but its optical principle does not help characterize their chemical composition and therefore cannot provide diagnostic certainty, with Raman spectroscopy (RS) coupled with a microscope, the chemical signature of particles can be determined in a biological sample.[5]

We combined IVCM and *ex vivo* RS for the examination of skin and cornea samples from a patient with NC to confirm the cystine composition of crystals. We present both optical devices and discuss their potential value in the diagnosis and follow-up of metabolic disorders.

Address all correspondence to: Elisa Cinotti, Hôpital Nord Saint-Etienne, 42055 Saint Etienne Cedex 2, France. Tel: +33 (0)4.77.82.84.21; Fax: +33 (0) 4.77.82.84.01; E-mail: elisacinotti@gmail.com

2 Materials and Methods

We examined a 36-year-old female patient with NC with mostly renal and corneal involvement and without clinically evident dermatological lesions except for skin xerosis. Forearm and eyelid skin, corneas (Fig. 1) and bulbar conjunctiva were analyzed by IVCM using a multilaser (488, 658, and 785 nm) Vivascope 1500 and a handheld monolaser Vivascope 3000 (Lucid Inc., New York, MAVIG GmbH, Munich, Germany). For the multilaser IVCM, we used an adapter between the tip and the ocular surface to reduce the diameter of the current tip made for the skin, while preserving its optic qualities (Fig. 2).

Ex vivo confocal RS (LabRAM ARAMIS, Horiba Jobin-Yvon, France) was later performed on two 5 mm punch biopsies taken from the forearm and on a corneal button retrieved during a penetrating keratoplasty. Both were immediately frozen in liquid nitrogen. The cornea was analyzed without further processing, while the skin biopsies were cut into 20 μm thick horizontal slices to make the crystals easier to identify in this uneven and nontransparent tissue. Randomly selected refringent crystals present in these tissues were scanned with RS (HeNe laser with a 150 μm pinhole) and identified by the optical microscope coupled to the RS. The control tissue consisted of randomly selected sites of crystal-free corneal stroma and skin dermis of the same patient.

3 Results

Multilaser and monolaser IVCM showed hyper-reflective bodies in the dermal layer of forearm and eyelid skin, in corneal stroma, and in bulbar conjunctiva (Fig. 3). Skin and conjunctiva particles

0091-3286/2013/$25.00

Fig. 1 Clinical aspect of the cornea. Cystine crystals accumulated in the cornea.

Fig. 2 Vivascope adaptor for the ocular surface. Adapted tip (arrow) for the ophthalmic application of Vivascope 1500.

were round or oval in shape and approximately 10 μm in diameter, while corneal particles were spindle-shaped, approximately 50 μm long and 10 μm thick. All wavelengths provided similar images. Crystals were slightly autofluorescent in the cornea at 785 nm.

Raman spectra from the corneal stroma and the skin dermis overlapped in different sites showing a spectrum of collagen.[6] Raman spectra obtained targeting refringent crystals (Fig. 4) found the optical profile of cystine[6] with vibrational fingerprints at wave numbers of 499, 542, 675, 785, 870, 960, 1340, 1383, and 1410 cm^{-1} (Fig. 5). The Raman spectrum of cystine was not modified by rotating the tissue samples or examining the samples after leaving them in the open air without fixative for 6 h. The Raman shift pic at 499 cm^{-1} was very high and was easily identified in the spectrum of the crystals, but was never found in the crystal-free corneal stroma and skin dermis of the same patient.

4 Discussion

We considered NC as a prototype storage disease characterized by the accumulation of materials with a perfectly well defined chemical composition in easily accessible tissues. Thanks to the IVCM and RS combination, we were able to exploit IVCM to characterize the deposits morphologically and RS to identify them chemically.

IVCM, an emerging technique that allows *in vivo* noninvasive high-resolution histomorphological analysis of skin, mucosa and ocular surface, has shown its usefulness in clinical practice and research,[7 11] and has recently been used to identify the presence of crystals in the cornea and skin of NC patients.[2,3,12] However, the identification of crystals in the cornea may not be sufficient for a diagnosis, since crystals within the cornea can also be identified by IVCM in other conditions, such as tyrosinemia, Schnyder dystrophy, Bietti crystalline dystrophy, multiple myelomas, and infectious crystalline keratopathy.[13 16] In the skin, IVCM identification of crystals appears to be more specific for NC,[3] but as yet it is not possible to state that such crystals are found only in NC, because no IVCM studies have been conducted in other storage diseases in the skin. The identification of crystals in both skin and eye samples suggest a systemic disease with material deposition in different tissues and could provide additional evidence for a diagnosis of NC.

The use of IVCM has also been suggested to quantify crystal deposition in order to monitor disease progression.[3] Also of note is that until now, IVCM of the skin and ocular surface had been performed with IVCM devices specifically designed for the use in dermatology and ophthalmology, respectively, whereas we used, for the first time, a skin-specific IVCM to examine both localizations concurrently. The Vivascope 3000 is a handheld laser scanning confocal microscope equipped with a class I 830 nm laser that can easily be used to acquire image stacks of the ocular surface. Thanks to our specific adaptation of an ophthalmology stand, the multilaser Vivascope 1500 can now also be used to examine the ocular surface using class I 658 and 785 nm lasers. All wavelengths provided similar images, but curiously, crystals were slightly autofluorescent in the cornea at 785 nm.

IVCM provides valuable morphological data, but, and this is its greatest limitation, it does not identify the chemical nature of the crystals. Conversely, RS is an optical technique that measures the vibrational motions of molecules to provide specific information on the molecular composition of a sample.[17] There are several potential applications of RS in different biomedical disciplines, such as studies on DNA, proteins, and cancer, as well as in dermatology[18] and ophthalmology.[17] This technique has also been recently used to analyze the correlation between chemical information and histological structures.[19]

RS lends itself particularly well to the study of cystine because this sulphur-containing amino acid presents a characteristic vibrational frequency of the S–S bond at 499 cm^{-1} that makes it easy to recognize.[6] Additional signals of cystine Raman spectrum are intense bands at wave numbers of 542, 613, 678, 785, 873, 967, 1341, 1385, and 1410 cm^{-1}.[6]

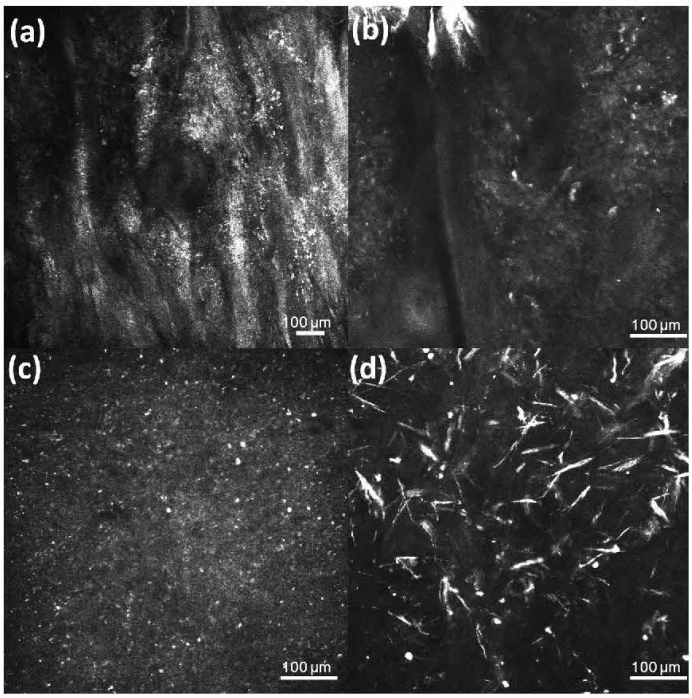

Fig. 3 *In vivo* confocal microscopy aspect of cystine crystals. Cystine crystals appear as roundish hyper-reflective bodies in the (a) eyelid, (b) forearm skin and (c) conjunctiva, but as spindle-shaped hyper-reflective bodies in the (d) cornea.

In our examinations, the amplitude of Raman shift peak at 499 cm^{-1} was very high and was easily identified in the spectrum, allowing a rapid identification of cystine. All other cystine characteristic bands have also been recognized in the spectra from the crystals of the cornea and of the skin, but due to their lower intensities, they were visible only with careful reading of the spectra. Characteristically, the same cystine signature was found in different crystals of both the skin and the cornea, demonstrating that exactly the same material is deposited in both tissues. The crystal-free corneal stroma and skin dermis of the same patient were used as control tissue and never presented the Raman shift peak at 499 cm^{-1}.

After rotating the tissue samples and therefore changing the inclination of the faces of the crystals within, the Raman spectrum did not change, demonstrating that the spectrum of cystine was not influenced by the orientation of the crystals. We also showed that the Raman examination was a reproducible technique to analyze samples with different degrees of hydration, and cystine was found in the same samples left in the open air without any fixative for 6 h.

RS appears to be a precise tool to assess material accumulation in *ex vivo* samples and has also been recently adapted for *in vivo* applications,[20 22] but it still has several limitations, namely the need to be handled by highly qualified personnel because the type and energy of the laser, pinhole size, width of the observed spectrum, and possible application of any filters may vary according to the samples to be analyzed, and the difficulty in locating the target point that has to be analyzed in a

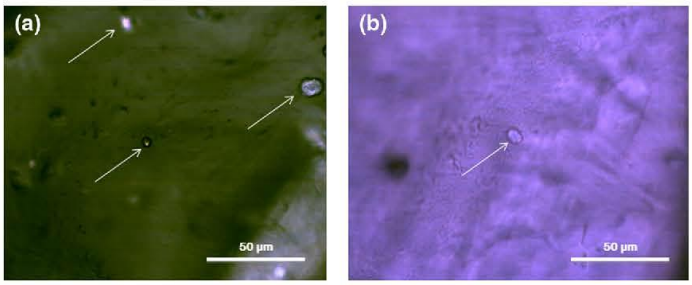

Fig. 4 Crystals' aspect under the optical microscope coupled to the Raman spectroscope (RS). (a) Skin and (b) cornea. The crystals are indicated by arrows.

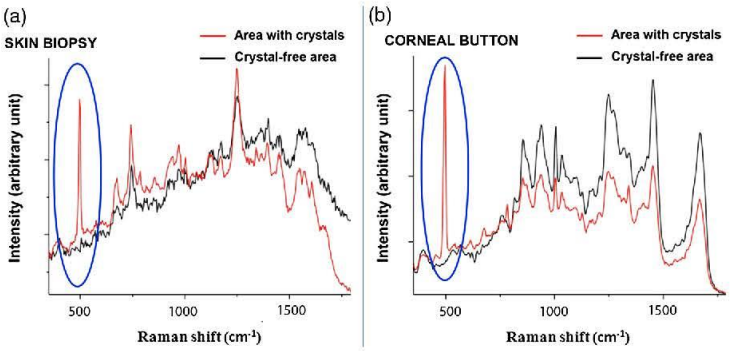

Fig. 5 *Ex vivo* Raman spectra of the cornea and of forearm skin. A spectrum was obtained in a crystal free zone (black) and compared with that of a zone containing crystals (light gray). The specific signature of cystine was clearly identified in both tissues thanks to the band at 499 cm^{-1} (circle).

heterogeneous sample. RS can be coupled with an optical microscope to scan the sample and target the area of interest; however, as tissue cannot be stained with the usual histological dyes because they would alter the Raman spectrum, it is sometimes difficult to distinguish the different structures under the microscope. In order to overcome these difficulties, Raman microspectroscopy has recently been combined with IVCM for both imaging and chemical analysis of the skin at cellular level.[23] Our data suggests that in the future, cystinosis could be diagnosed by means of a noninvasive technique that combines the use of IVCM to identify the crystals and *in vivo* RS to confirm their composition.

In conclusion, this is the first observation of a cutaneous and corneal cystine deposition made with a single IVCM suitable for both skin and eye, which will facilitate experience sharing between dermatologists and ophthalmologists, and it is the first RS characterization of these deposits previously identified by IVCM. Cystine is easily recognized by RS producing a characteristic Raman shift at 499 cm^{-1}. In the future, the diagnosis of NC could be based on a noninvasive skin and cornea examination by IVCM coupled with *in vivo* RS to identify cystine crystals with certainty. As it provides an optical signature of the chemical nature of the observed constituents, RS also opens promising new perspectives in other storage diseases.

Acknowledgments

We are very grateful to Gianfranca Gessa Shepheard and Luisa Galbusera for the English revision of the text.

References

1. M. J. Wilmer et al., "Cystinosis: practical tools for diagnosis and treatment," *Pediatr. Nephrol.* **26**(2), 205–215 (2011).
2. A. Labbé et al., "In vivo confocal microscopy and anterior segment optical coherence tomography analysis of the cornea in nephropathic cystinosis," *Ophthalmology* **116**(5), 870–876 (2009).
3. C. Chiavérini et al., "In vivo reflectance confocal microscopy of the skin: a noninvasive means of assessing body cystine accumulation in infantile cystinosis," *J. Am. Acad. Dermatol.* **68**(4), e111–e116 (2013).
4. R. Dohil, A. Carrigg, and R. Newbury, "A potential new method to estimate tissue cystine content in nephropathic cystinosis," *J. Pediatr.* **161**(3), 531–535 (2012).
5. J. J. Chui et al., "Bluebottle envenomation-induced crystalline keratopathy," *Cornea* **30**(7), 835–837 (2011).
6. G. Zhu et al., "Raman spectra of amino acids and their aqueous solutions," *Spectrochim. Acta A Mol. Biomol. Spectrosc.* **78**(3), 1187–1195 (2011).
7. M. Ulrich and S. Lange-Asschenfeldt, "In vivo confocal microscopy in dermatology: from research to clinical application," *J. Biomed. Opt.* **18**(6), 61212 (2013).
8. A. Nwaneshiudu et al., "Introduction to confocal microscopy," *J. Invest. Dermatol.* **132**(12), e3 (2012).
9. H. Y. Kang, P. Bahadoran, and J.-P. Ortonne, "Reflectance confocal microscopy for pigmentary disorders," *Exp. Dermatol.* **19**(3), 233–239 (2010).
10. S. González, "Confocal reflectance microscopy in dermatology: promise and reality of non-invasive diagnosis and monitoring," *Actas Dermosifiliogr.* **100**(Suppl. 2), 59–69 (2009).
11. R. L. Niederer and C. N. J. McGhee, "Clinical in vivo confocal microscopy of the human cornea in health and disease," *Prog. Retin. Eye Res.* **29**(1), 30–58 (2010).
12. C. N. Grupcheva, S. E. Ormonde, and C. McGhee, "In vivo confocal microscopy of the cornea in nephropathic cystinosis," *Arch. Ophthalmol.* **120**(12), 1742–1745 (2002).
13. J. E. Sutphin et al., "Evaluation of infectious crystalline keratitis with confocal microscopy in a case series," *Cornea* **16**(1), 21–26 (1997).
14. N. Houben and B. Foets, "Confocal microscopy in multiple myeloma associated crystalline keratopathy: case report," *Bull. Soc. Belge Ophtalmol.* (300), 13–17 (2006).
15. P.-P. Schauwvlieghe et al., "Confocal microscopy of corneal crystals in a patient with hereditary tyrosinemia type I, treated with NTBC," *Cornea* **32**(1), 91–94 (2013).
16. L. Toto et al., "Spectral domain optical coherence tomography and in vivo confocal microscopy imaging of a case of Bietti's crystalline dystrophy," *Clin. Exp. Optom.* **96**(1), 39–45 (2013).
17. C.-C. Lin, M.-T. Kuo, and H.-C. Chang, "Review: Raman spectroscopy—a novel tool for noninvasive analysis of ocular surface fluid," *J. Med. Biol. Eng.* **30**(6), 343–354 (2010).
18. M. Förster et al., "Confocal Raman microspectroscopy of the skin," *Eur. J. Dermatol.* **21**(6), 851–863 (2011).
19. M. Pudlas et al., "Raman spectroscopy: a noninvasive analysis tool for the discrimination of human skin cells," *Tissue Eng. Part C Meth.* **17**(10), 1027–1040 (2011).
20. N. J. Bauer, F. Hendrikse, and W. F. March, "In vivo confocal Raman spectroscopy of the human cornea," *Cornea* **18**(4), 483–488 (1999).
21. P. D. A. Pudney et al., "A new in vivo Raman probe for enhanced applicability to the body," *Appl. Spectrosc.* **66**(8), 882–891 (2012).
22. C. Brouillette et al., "Raman spectroscopy using 1550 nm (retina-safe) laser excitation," *Appl. Spectrosc.* **65**(5), 561–563 (2011).
23. C. A. Patil et al., "A handheld laser scanning confocal reflectance imaging-confocal Raman microspectroscopy system," *Biomed. Opt. Express* **3**(3), 488–502 (2012).

8.1.2 Identification of a soft tissue filler by ex vivo confocal microscopy and Raman spectroscopy in a case of adverse reaction to the filler

Background:

Soft tissue fillers are usually identified in the skin using the conventional histopathologic examination. *Ex vivo* RCM has been used in one case and Raman spectroscopy (RS), which has been recently applied for the identification of skin foreign bodies, has never been employed for fillers. We report the use of both these new techniques, *ex vivo* RCM and RS, to confirm the diagnosis of adverse reaction to a soft tissue filler and to identify its composition.

Methods:

We excised a skin nodule suspicious of adverse reaction to soft tissue filler, and we performed an *ex vivo* reflectance confocal microscopy (RCM) and an histopathologic examination, followed by a RS analysis.

Results:

Ex vivo RCM showed numerous hypo-reflective microspheres in the dermis that corresponded to rounded vacuoles at histopathologic examination, suggestive of polymethylmethacrylate (PMMA). RS showed a series of peaks at 600, 813, 970 1252, 1450, 1728, and 2951 cm^{-1} in correspondence to the microspheres, confirming the presence of PMMA. Conclusion: These results suggest that *ex vivo* RCM and RS are additional tools to conventional histopathologic examination to characterize soft tissue fillers in case of adverse reaction. RCM has the advantage compared with the histopathologic examination that can be extemporaneously performed on a fresh surgical specimen. RS allow a precise chemical identification of the filler.

Skin Research and Technology 2014; 0: 1–5
Printed in Singapore · All rights reserved
doi: 10.1111/srt.12166

Published by John Wiley & Sons Ltd
Skin Research and Technology

Identification of a soft tissue filler by *ex vivo* confocal microscopy and Raman spectroscopy in a case of adverse reaction to the filler

E. Cinotti[1], J. L. Perrot[1], B. Labeille[1], A. Boukenter[2], Y. Ouerdane[2], P. Cosmo[3], C. Douchet[3], D. Grivet[4] and F. Cambazard[1]

[1]*Department of Dermatology, University Hospital of Saint-Etienne, Saint-Etienne, France,*
[2]*Laboratoire Hubert Curien, CNRS UMR-5516 F, University of Saint-Etienne, Saint-Etienne, France,*
[3]*Department of Pathology, University Hospital of Saint-Etienne, Saint-Etienne, France and* [4]*Department of Ophthalmology, University Hospital of Saint-Etienne, Saint-Etienne, France*

Background: Soft tissue fillers are usually identified in the skin using the conventional histopathologic examination. *Ex vivo* RCM has been used in one case and Raman spectroscopy (RS), which has been recently applied for the identification of skin foreign bodies, has never been employed for fillers. We report the use of both these new techniques, *ex vivo* RCM and RS, to confirm the diagnosis of adverse reaction to a soft tissue filler and to identify its composition.
Methods: We excised a skin nodule suspicious of adverse reaction to soft tissue filler, and we performed an *ex vivo* reflectance confocal microscopy (RCM) and an histopathologic examination, followed by a RS analysis.
Results: *Ex vivo* RCM showed numerous hypo-reflective microspheres in the dermis that corresponded to rounded vacuoles at histopathologic examination, suggestive of polymethylmethacrylate (PMMA). RS showed a series of peaks at 600, 813, 970 1252, 1450, 1728, and 2951 cm ^{1} in correspondence to the microspheres, confirming the presence of PMMA.
Conclusion: These results suggest that *ex vivo* RCM and RS are additional tools to conventional histopathologic examination to characterize soft tissue fillers in case of adverse reaction. RCM has the advantage compared with the histopathologic examination that can be extemporaneously performed on a fresh surgical specimen. RS allow a precise chemical identification of the filler.

Key words: soft tissue filler – *ex vivo* – reflectance confocal microscopy – Raman spectroscopy – adverse reaction

Accepted for publication 8 March 2014

SOFT TISSUE fillers are usually identified in the skin by using the conventional histopathologic examination (1). *Ex vivo* reflectance confocal microscopy (RCM) has been used in one case of soft tissue filler adverse reaction to extemporaneously distinguish between the filler material and the surrounding tissue during the surgical excision of the filler (2). Raman spectroscopy (RS), that has been recently applied for the characterization of cutaneous foreign bodies (3) and of endogenous material accumulated in the skin in case of metabolic disorders (4), has never been employed for fillers. Here, we report the use of both *ex vivo* RCM and RS to confirm the diagnosis of adverse reaction to a soft tissue filler and to identify its composition.

Methods

Patient

A 46-year-old female presented with bilateral symmetrical nodules on her cheeks at the border of the lower eyelids for 1 year (Fig. 1). On examination, the nodules were painless, firm, and covered by intact flesh-colored skin. Personal history found that the patient had undergone an upper blepharoplasty 3 years earlier and had received one injection of hyaluronic acid filler into the nasolabial folds 1 year prior. The patient was in general good health and took no drugs. Suspecting the nodules to be a foreign body reaction to the hyaluronic acid injection, with an unusual displacement of the injected material from the nasolabial folds to

Fig. 1. Clinical presentation of the cutaneous nodules.

the lower eyelid, we performed a skin biopsy, passing from the lower eyelid (Fig. 2), for an *ex vivo* RCM, histopathologic, and RS analysis.

Ex vivo reflectance confocal microscopy
Ex vivo RCM was performed by the *ex vivo* reflectance confocal microscope dedicated to the skin VivaScope 2500 (Caliber, USA, distributed in Europe by Mavig, Germany) that allows to examine an entire fresh surgical specimen of up to 2 cm of diameter without any previous staining and without the need of cutting thin sections. For the reflectance mode, the VivaScope 2500 uses a diode laser at 830 nm wavelength that does not degrade the specimen and allow further conventional histopathologic examination. The specimen is fixed between two slides, to make horizontal its surface of observation. Images have a spatial resolution of <2.0 μm at the center of the field of view in the lateral dimension and <5.0 μm in the axial dimension.

Fig. 2. Biopsy of the skin nodules passing from the inferior tarsal mucosa.

An examination depth of 250–300 μm can usually be reached. Individual images of 750 × 750 μm field can be captured and saved. Adjacent fields can be imaged in sequence and then together yield a composite image of an area of 2 cm^2. Z-Stack can also be performed.

Histopathology
Histopathologic examination was performed using conventional hematoxylin and eosin stain.

Raman spectroscopy
RS was performed with the Horiba Jobin-Yvon confocal microspectrometer (LabRAM ARAMIS, Horiba Jobin-Yvon, Villeneuve d'Ascq, France) using a HeNe (633 nm) laser. The skin biopsy was cut in 100 μm thick horizontal slices to allow a better identification of the filler in this inhomogeneous tissue.

Results

Ex vivo RCM of the skin biopsy showed numerous hypo-reflective microspheres (Figs 3 and 4) in the dermis with a roundish hyper-reflective material in their central part (Fig. 4), markedly

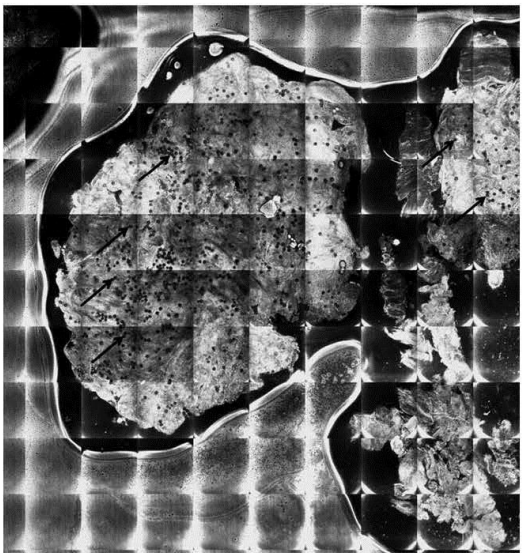

Fig. 3. Ex vivo confocal microscopy X-Y reconstruction (mosaic) of the entire bioptic skin specimen shows hypo-reflective roundish cavities (red arrow) distributed all over the specimen.

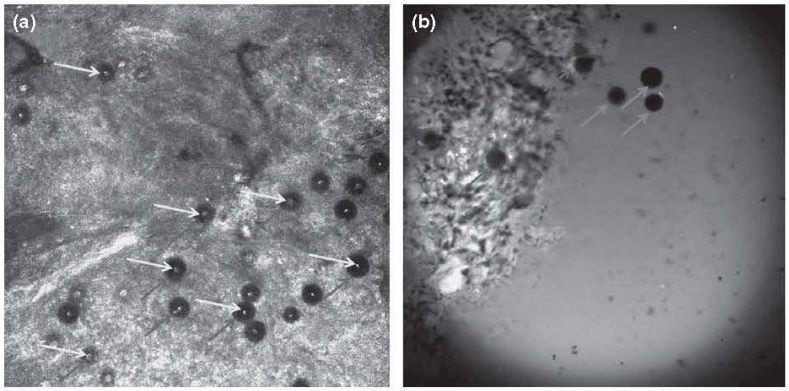

Fig. 4. Ex vivo confocal microscopy of areas of 750 μm of diameter shows numerous hypo-reflective roundish cavities (red arrow) in the dermis with hyper-reflective material in their central part (yellow arrow) (a). Some microspheres are out of the specimen (green arrow), at its borders (b). Probably they went out during the sample preparation, which consists of crushing the sample between two blades of glass, confirming that the microspheres are foreign material not connected to the skin tissue.

homogeneous in size (about 40 μm) and shape, evoking the histopathologic aspect of polymethylmethacrylate (PMMA). Curiously, some spheres were visible outside the specimen, probably went out during the sample preparation which includes crushing the specimen between two slides, indicating the presence of foreign material not connected to the skin tissue (Fig. 4).

The histopathologic examination confirmed the presence of rounded vacuoles of similar shape and size suggestive of PMMA, surrounded by a diffuse granulomatous infiltrate (Fig. 5). The vacuoles were sharply circumscribed, translucent, non-birefringent, and extracellular.

Raman spectroscopy showed a series of peaks located at around 600, 813, 970, 1252, 1450, 1728, and 2951 cm^{-1} (Table 1) characteristic of the spectrum of the PMMA (5, 6) in correspondence of randomly chosen microspheres present in the skin sample (Fig. 6). The control tissue, consisting of randomly chosen sites of microspheres-free skin, exhibits only a luminescence signal with no Raman signatures of PMMA particles presence.

Discussion

The precise identification of injectable soft tissue fillers is extremely important in case of adverse reaction for medico-legal issues. In our case, a precise identification of the filler was fundamental because we suspected a filler adverse reaction distant from the injection site. Moreover, *ex vivo* RCM and histopathologic examinations suggested that the filler was made of PMMA, in contrast to the clinical information.

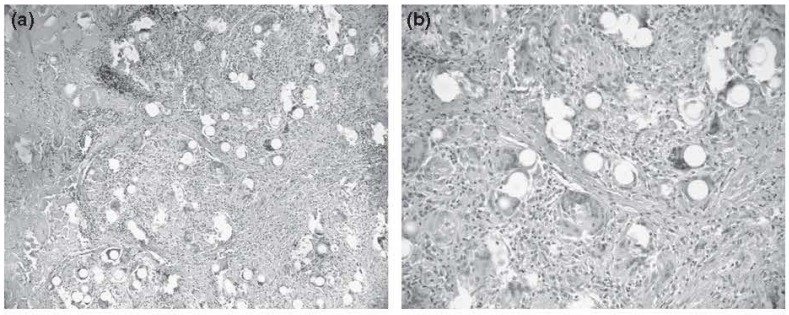

Fig. 5. Histopathologic examination shows rounded vacuoles of homogeneous shape and size, surrounded by a diffuse granulomatous infiltrate (hematoxylin and eosin stain, a ×20 and b ×40).

TABLE 1. Observed Raman bands in PMMA and their assignments

Raman band (cm^{-1})	Assignments (Corresponding chemical bond)
600	vs (C C O)
813	vs (C O C)
970	O CH3 rock
1252	ν(C O), ν(C COO)
1450	δa (C H) of α-CH_3, δa(C H) of O CH_3
1728	ν(C=O) of (C-COO)
2951	ν (C H)

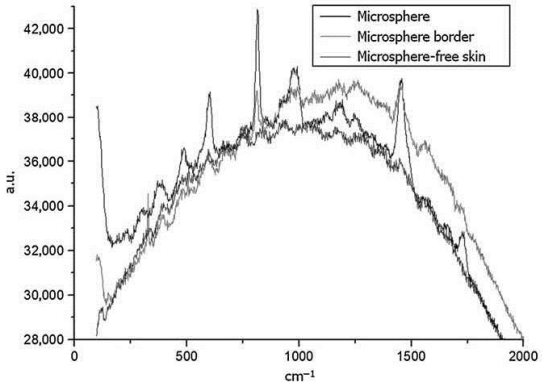

Fig. 6. Raman spectrum of the microspheres shows a series of peaks at 600, 813, 970, 1252, 1450 and 1728 cm^{-1} characteristic of polymethylmethacrylate; y-axis: intensity in arbitrary units (a.u.); peak at 2951 cm^{-1} is not shown in the present spectrum and a luminescence signal is also present in the graph; x-axis: wavenumber (cm^{-1}).

In fact, in our case both the surgeon who performed the blepharoplasty and the general practitioner who performed the hyaluronic acid injection denied to have injected PMMA. Furthermore, the general practitioner who performed the injections in the nasolabial folds declared to use needles and not cannulas that could have explained the displacement of foreign material far from the injection site. In addition, the patient declared to have only one filler injection in her life and denied any injection in the eyelid area. In this complicated case, RS allowed to corroborate the clinical diagnosis of filler adverse reaction, finding filler material in the skin, and confirmed the *ex vivo* RCM and histopathologic results, identifying PMMA in the skin biopsy.

PMMA based fillers are composed by microspheres that persist for years and induce a granulomatous foreign body reaction with a deposition of fibrous tissue, which is part of the wanted effect of the filler (1). This filler may cause excessive granuloma formation that generally appear from 6 to 24 months after the treatment (7), but that may also emerge several years after the injection. Histopathology can show the morphology of this filler and of other types of soft tissue fillers (1), but cannot provide the exact chemical composition.

Ex vivo RCM has been used in a case of adverse reaction to a filler during the surgical excision to distinguish between the filler material and the surrounding tissue (2). In this case, the filler was composed of hydroxyethylmethacrylate, ethylmethacrylate, and hyaluronic acid (DermaLive Dermatech, Paris, France) and presented under RCM with hypo-reflective polygonal pseudocystic structures of different sizes and shapes containing medium reflective material. The main advantage of *ex vivo* RCM is the opportunity to assess sections of freshly excised tissues in a resolution comparable to standard histopathology with a fast procedure. Our case confirmed the utility of *ex vivo* RCM for a rapid identification of filler on fresh excised tissue. We could find a good correlation with the histopathologic examination, finding microspheres of homogeneous size and shape suggestive of PMMA. However, differently from histopathology the microspheres were not optically empty but presented a roundish hyper-reflective material in their central part (Fig. 4).

Raman Spectroscopy, a technique that analyses materials by detecting their composition responses (8), confirmed the diagnosis of skin reaction to a foreign body through the chemical identification of the material itself, PMMA.

These results suggest that *ex vivo* RCM and RS are additional tools to conventional histopathologic examination to characterize soft tissue fillers in case of adverse reaction. RCM adds morphological information and has the advantage compared with the histopathologic examination that can be extemporaneously performed on a fresh surgical specimen. RS allows a precise chemical identification of the filler and is especially useful in difficult clinical cases like ours.

Conflict of interest

The authors declare not to have any conflicts of interest.

References

1. Requena L, Requena C, Christensen L et al. Adverse reactions to injectable soft tissue fillers. J Am Acad Dermatol 2011; 64: 1 34; quiz 35 36.
2. Horn M, Koller S, Gerger A et al. Surgery guided by confocal laser scanning microscopy for foreign filler granulomas. Dermatol Surg Off Publ Am Soc Dermatol Surg Al. 2008; 34: 1245 1247.
3. Cinotti E, Labeille B, Perrot JL et al. Characterization of cutaneous foreign bodies by Raman spectroscopy. Skin Res Technol 2013; 19: 508 509.
4. Cinotti E, Perrot JL, Labeille B et al. Optical diagnosis of a metabolic disease: cystinosis. J Biomed Opt 2013; 18: 046013.
5. Thomas K, Sheeba M, Nampoori V et al. Raman spectra of polymethyl methacrylate optical fibres excited by a 532 nm diode pumped solid state laser. J Opt A: Pure Appl Opt 2008; 10: 055303.
6. Willis H, Zichy V, Hendra P. The laser-Raman and infra-red spectra of polymethyl methacrylate Polymer. Polymer 1969; 10: 737 746.
7. Thioly-Bensoussan D. Non-hyaluronic acid fillers. Clin Dermatol 2008; 26: 160 176.
8. Schrader B. Infrared and Raman Spectroscopy. New York: VCH Publishers Inc.; 1995.

Address:
E. Cinotti
Hôpital Nord Saint-Etienne
42055 Saint Etienne Cedex 2
France
Tel: 00 33 (0)4 77 82 85 07
Fax: 00 33 (0)4 77 82 84 01
e-mail:elisacinotti@gmail.com

8.1.3. Unintended changes in the composition of a drug commonly used in dermatology caused by its container

Annales de dermatologie et de v n r ologie (2014) 141, 86—88

Disponible en ligne sur SciVerse ScienceDirect www.sciencedirect.com

Elsevier Masson France EM|consulte www.em-consulte.com

Formation médicale continue

NOTE DE PHARMACOVIGILANCE

Modification involontaire de la composition d'un m dicament couramment employ en dermatologie sous l'effet du r cipient utilis pour le transvaser

Unintended changes in the composition of a drug commonly used in dermatology caused by its container

E. Cinotti[a], J.-L. Perrot[a], I. Mar chal[a,b], A. Boukenter[c], Y. Ouerdane[c], A. Ranchon[d], M. Lef vre[e], C. Guy[f], C. Rigamonti[a], B. Labeille[a,*], F. Cambazard[a]

[a] *Service de dermatologie, h pital Nord, CHU, 42055 Saint- tienne cedex 2, France*
[b] *Service de pharmacie, h pital Nord, CHU, 42055 Saint- tienne cedex 2, France*
[c] *CNRS UMR-5516, laboratoire Hubert-Curien, university of St- tienne, 18, rue du Professeur-Benoît-Lauras, 42000 Saint- tienne, France*
[d] *Maison de retraite de la Loire, 11, route de Chambles, 42170 Saint-Just-Saint-Rambert, France*
[e] *Agence r gionale de sant de la Loire, 129, rue Servient, 69003 Lyon, France*
[f] *Service de pharmacovigilance, h pital Nord, CHU, 42055 Saint- tienne cedex 2, France*

Reçu le 18 avril 2013 ; accept le 28 juin 2013
Disponible sur Internet le 8 octobre 2013

La gale est une maladie parasitaire qui a actuellement une recrudescence en France. Le traitement topique le plus utilis est une lotion base de benzoate de benzyle, sulfirame, alcool thylique, polysorbate et eau (Ascabiol®, Zambon, France). Ce m dicament est contenu dans un flacon col troit et normalement, il est transvas dans un autre r cipient pour permettre l'utilisation d'un pinceau large pour une application sur presque toute la surface cutan e.

Mat riel et m thode

Pour transvaser ce m dicament, les infirmi res de notre service de sermatologie se servent d'un r cipient en plastique jetable. Nous avons pu observer que ce produit laiss dans un tel r cipient quelques heures entra ne une d gradation de celui-ci (Fig. 1).

Nous avons analys par spectroscopie Raman la composition chimique d'une coupelle en plastique habituellement utilis e pour mettre l'Ascabiol®, la composition de l'Ascabiol® laiss dans ce r cipient en plastique pendant 24 heures et la composition de l'Ascabiol® directement pr lev de son flacon. Nous avons constat des traces

* Auteur correspondant.
Adresse e-mail : bruno.labeille@chu-st-etienne.fr (B. Labeille).

0151-9638/$ — see front matter
http://dx.doi.org/10.1016/j.annder.2013.06.009

Figure 1. R cipient en polystyr ne d grad par l'Ascabiol®.

de la dissolution de la coupelle dans l'Ascabiol® laiss 24 heures dans cette derni re. Sur l'ensemble du spectre Raman, on observe trois bandes de vibrations dans la solution d'Ascabiol® provenant du spectre de la coupelle 2609, 3168 et 3205 cm, d montrant une interaction entre l'Ascabiol® et la coupelle (Fig. 2). Le r cipient en plastique utilis dans notre h pital tait en polystyr ne dur, ce qui est le cas de la majorit des r cipients plastiques jetables, tandis que le flacon o est contenu normalement le m dicament est d'une autre mati re plastique, le poly thyl ne haute densit . On envisage l'hypoth se que le benzoate de benzyle soit le composant de l'Ascabiol® qui interagit avec les mat riaux plastiques car c'est un produit tr s r actif. On ne sait pas si des composants toxiques peuvent tre lib r s dans ces r actions.

Ni sur l'emballage du produit, ni sur la notice jointe, ni dans le dictionnaire th rapeutique Vidal ne sont d taill es les pr cautions d'utilisation de la manipulation du produit. L'utilisation du pinceau est recommand e pour l'application cutan e mais le type de r cipient dans lequel le produit du flacon doit tre transvas n'est pas sp cifi . Ce m dicament est vendu dans plusieurs pays. Les notices anglaises sp cifient que la lotion peut ab mer le plastique et qu'il faut donc faire attention ne pas appliquer la lotion sur de telles surfaces.

Nous avons ensuite distribu des questionnaires 35 dermatologues de notre r gion l'occasion d'une r union de FMC pour leur demander s'ils donnaient des consignes pr cises aux patients concernant l'application du produit. Trente-trois ne donnaient aucune consigne pour son application, un pr cisait qu'il fallait le transvaser dans un r cipient usage unique et un autre pr cisait que ce r cipient devait tre en plastique. Une enqu te de pratique men e au moyen d'un questionnaire a t effectu e aupr s des infirmi res du service de dermatologie du CHU de Saint-tienne et de la Maison de retraite de la Loire, par leur cadre de sant , en demandant celles qui avaient appliqu le produit au moins une fois au cours du mois pr c dent de pr ciser dans quel type de r cipient elles mettaient le produit. Sur les 20 infirmi res r pondant aux crit res, toutes transvasaient le produit dans un r cipient qui pouvait tre en plastique (cit 15 fois), en verre (cit 4 fois) ou en m tal (cit 4 fois). Personne n'avait eu d'information concernant la nature du r cipient o recueillir le produit. La dur e moyenne pendant laquelle le produit tait gard dans le r cipient tait sup rieure 15 minutes pour 19 des infirmi res interrog es. Une seule infirmi re d clarait avoir aussi utilis le produit directement partir du

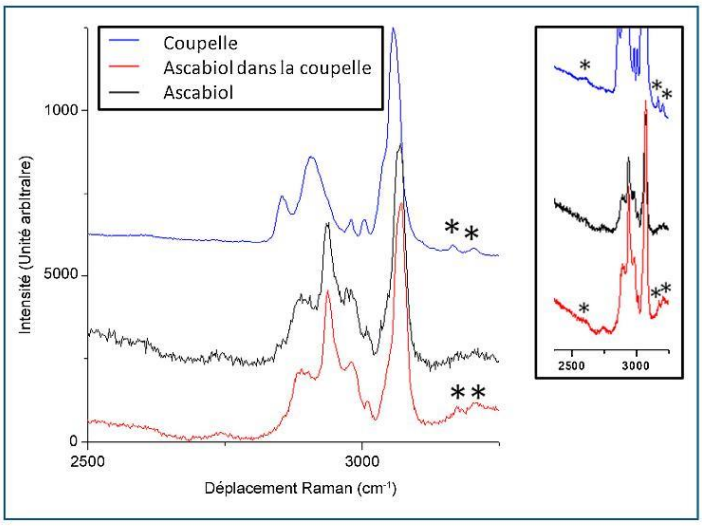

Figure 2. Spectre Raman de la solution d'Ascabiol® provenant du r cipient en poly til ne haute densit (rouge) compar avec le spectre de l'Ascabiol® pur (noir) et le spectre du r cipient (bleu). On observe trois bandes de vibrations dans la solution d'Ascabiol® provenant du spectre du r cipient 2609, 3168 et 3205 cm (toiles). Ces bandes ne sont pas pr sentes dans le spectre Raman de l'Ascabiol® directement pr lev de son r cipient en poly til ne haute densit et indiquent la pr sence de mat riel plastique dans la solution.

flacon gr ce un petit pinceau tremp directement dans le flacon.

Discussion

Dans notre pratique clinique, nous avons observ que l'Ascabiol® n cessite l'utilisation d'un deuxi me r cipient pour tre appliqu l'aide d'un pinceau large. Selon l'enqu te clinique que nous avons effectu e, les m decins ne donnent pas de consignes pr cises concernant l'application de ce produit aux patients. Les infirmi res utilisent, dans la majorit des cas, un r cipient en plastique car il est jetable. Par ailleurs, le produit d grade le r cipient en plastique. Une analyse Raman a t effectu e sur l'Ascabiol® mis en contact avec la coupelle en plastique pendant 24 heures. La spectroscopie Raman est une technique qui analyse la composition chimique des mat riaux et qui est bas e sur la d tection des vibrations mol culaires. Elle analyse le rayonnement diffus r sultant de l'interaction entre une source de lumi re monochromatique incidente et les mol cules du milieu tudier. L' change d' nergie entre le faisceau de lumi re incident et le milieu travers entra ne une modification de la longueur d'onde de la lumi re diffus e (effet Raman) qui est caract ristique et qui se traduit par un spectre du mat riel tudi [1]. L'analyse Raman a confirm l'interaction entre l'Ascabiol® et le plastique de type polystyr ne dur qui est le composant majoritaire des r cipients plastiques jetables. Le d lai d'apparition des produits lib r s par la d gradation du plastique en contact avec l'Ascabiol® est au maximum de 24 heures (d lai de r alisation de notre analyse), mais nous n'avons pas conduit des tudes de cin tique qui permettraient de pr ciser le d lai minimum de la premi re interaction d tectable, tudes lourdes de mise en œuvre. Toutefois on a constat un ramollissement du r cipient en plastique d s la sixi me heure de contact avec l'Ascabiol®. Nous ne savons pas si une interaction entre Ascabiol® et r cipient peut se produire en quelques minutes, d lai habituel avant l'application de l'Ascabiol® sur la peau du patient. Il est en effet peut- tre possible d' viter la d gradation du plastique en limitant la dur e de contact et des tudes sp cifiques pourraient pr ciser le d lai de d gradation du plastique. Avant de disposer de telles donn es, et comme nous n'avons pas d'informations sur la toxicit ventuelle des produits lib r s lors de la d gradation du r cipient, nous recommandons par pr caution l'utilisation d'un r cipient inerte comme le verre qui n'aura pas d'interactions avec cette lotion. Suite notre observation, une d claration de pharmacovigilance a t faite aupr s du centre r gional de pharmacovigilance de Saint- tienne (CRPV SE) le 22 octobre 2012 (d claration num ro SE 1200577). Un courrier a t envoy par le CRPV SE l'Agence nationale de s curit du m dicament et des produits de sant (ANSM), ce qui a motiv une discussion au comit technique de pharmacovigilance le 4 d cembre 2012. Ce dossier reste en cours de traitement par l'ANSM en date du 19 juin 2013. Le laboratoire Zambon commercialisant l'Ascabiol® a t averti par courrier et t l phone. Cette d marche de pharmacovigilance permettra que cette pr caution soit rajout e sur la notice du produit français comme il a d j t recommand dans d'autres pays. En attendant la modification de la notice, nous recommandons que les prescripteurs et les pharmaciens expliquent aux patients et aux infirmi res les modalit s d'utilisation d'Ascabiol® en pr cisant de plus qu'il est pr f rable d'utiliser rapidement, voire en extemporan , la lotion transvas e dans un r cipient inerte.

D claration d'int r ts

Les auteurs d clarent ne pas avoir de conflits d'int r ts en relation avec cet article.

R f rence

[1] Schrader B. Infrared and Raman spectroscopy. New York: VCH Publishers Inc.; 1995.

8.1.4 Characterization of coal tattoos by Raman spectroscopy

Skin Research and Technology 2015; 21: 511–512
Printed in Singapore · All rights reserved
doi: 10.1111/srt.12221

Published by John Wiley & Sons Ltd
Skin Research and Technology

Letter to the Editor

Characterization of coal tattoos by Raman spectroscopy

E. Cinotti[1], B. Labeille[1], A. Boukenter[2], Y. Ouerdane[2], F. Cambazard[1] and J. L. Perrot[1]

[1]Department of Dermatology, University Hospital of Saint Etienne, Saint-Etienne, France and [2]Laboratoire Hubert Curien, CNRS UMR-5516 F, University of St-Etienne, Saint-Etienne, France

THE IDENTIFICATION of tattoo pigments could be useful for dermatologists in case of allergic adverse reaction or for laser tattoo removal, but it is often difficult to identify them because ink manufacturers often do not disclose ingredients in their products. Moreover, the chemical composition of tattooing pigments continuously changes over time according to available technologies and materials (1). Natural colored metallic compounds and salts have been progressively substituted by synthetic organic pigments that possess superior light fastness, resistance to enzymatic digestion and are available in a wider range of hues (1).

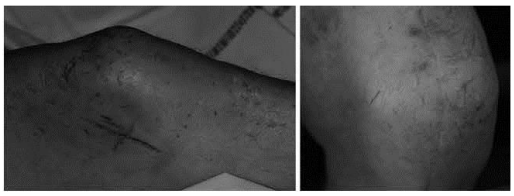

Fig. 1. Clinical appearance of the cutaneous pigmentations of the two minors.

Our group recently described the application of Raman micro-spectroscopy for the characterization of cutaneous foreign bodies (2, 3) and of endogenous material crystals accumulated in the skin in case of metabolic disorders (4). Poon et al. (1) demonstrated that it is possible to identify organic tattoo pigments using Raman micro-spectroscopy in cryo-sectioned pig skin samples.

We describe two cases where Raman Spectroscopy signatures identified the pigment of the tattoos of two coal-miners.

Two skin biopsies of 4 mm were taken from two dark lesions from two 77-year-old male subjects that had been presenting linear black

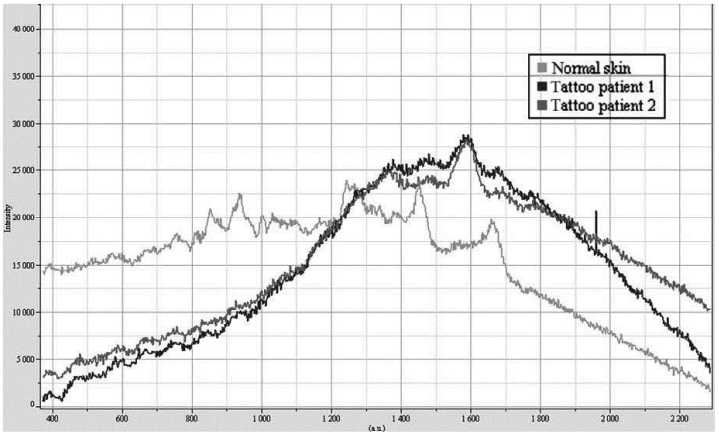

Fig. 2. The Raman spectrum of the cutaneous pigmentations showed two peaks at 1587 and 1364 cm $^{-1}$ characteristic of coal. y-axis: intensity in arbitrary units (a.u.); x-axis: wavenumber (cm $^{-1}$).

pigmentations on their knees for several years (Fig. 1). Both subjects had worked in the same coal mine of Saint-Etienne, France, and their lesions were clinically evocative for incidental coal tattoos.

The skin biopsies were immediately frozen at −20°C and analyzed 1 week later by the Horiba Jobin-Yvon confocal micro-spectrometer (LabRAM ARAMIS, Horiba Jobin-Yvon, Villeneuve d'Ascq, France) using a HeNe (633 nm) laser. Raman spectroscopy showed two peaks at 1587 and 1364 cm^{-1} (Fig. 2), characteristic of coal (5). It was therefore possible to confirm the diagnosis of coal tattoo by determining the chemical composition of the specimens. Interestingly the specimens of both patients showed exactly the same Raman peak signatures confirming that the pigment had the same origin corresponding to coal from the same workplace.

This anecdotal case shows that Raman spectroscopy, a powerful technique that analyses materials by detecting their composition responses (6), could be used for the chemical characterization and identification of tattoo pigments. Several future applications would be possible in the dermatological practice using in vivo Raman spectroscopy (7), for example to identify the composition of tattoo pigments to adjust laser treatments.

Conflict of interest

The authors declare not to have any conflicts of interest.

References

1. Poon KWC, Dadour IR, McKinley AJ. In situ chemical analysis of modern organic tattooing inks and pigments by micro-Raman spectroscopy. J Raman Spectrosc 2008; 39: 1227 1237.
2. Cinotti E, Perrot JL, Labeille B et al. Identification of a soft tissue filler by ex vivo confocal microscopy and Raman spectroscopy in a case of adverse reaction to the filler. Skin Res Technol 2015; 21: 114 118.
3. Cinotti E, Labeille B, Perrot JL et al. Characterization of cutaneous foreign bodies by Raman spectroscopy. Skin Res Technol 2013; 19: 508 509.
4. Cinotti E, Perrot JL, Labeille B et al. Optical diagnosis of a metabolic disease: cystinosis. J Biomed Opt 2013; 18: 046013.
5. Kostova I, Tormo L, Crespo-Feo E et al. Study of coal and graphite specimens by means of Raman and cathodoluminescence. Spectrochim Acta A Mol Biomol Spectrosc 2012; 91: 67 74.
6. Schrader B. Infrared and Raman spectroscopy. New York: VCH Publishers Inc., 1995.
7. Patil CA, Arrasmith CL, Mackanos MA et al. A handheld laser scanning confocal reflectance imaging-confocal Raman microspectroscopy system. Biomed Opt Express 2012; 3: 488 502.

Address:
E. Cinotti
Hôpital Nord Saint-Etienne
Saint Etienne Cedex 2 42055
France
Tel: 00 33 (0)4 77 82 84 21
Fax: 00 33 (0)4 77 82 84 01
e-mail: elisacinotti@gmail.com

8.1.5 Characterization of cutaneous foreign bodies by Raman spectroscopy.

Skin Research and Technology 2013; 19: 508–509
Printed in Singapore · All rights reserved
doi: 10.1111/srt.12065

Published by John Wiley & Sons Ltd
Skin Research and Technology

Letter to the Editor

Characterization of cutaneous foreign bodies by Raman spectroscopy

Elisa Cinotti[1], Bruno Labeille[1], Jean Luc Perrot[1], Aziz Boukenter[2], Youcef Ouerdane[2] and Frédéric Cambazard[1]

[1]*Department of Dermatology, University Hospital of Saint Etienne, Saint-Etienne, France and* [2]*Laboratoire Hubert Curien, CNRS UMR-5516 F, University of St-Etienne, Saint-Etienne, France*

THE CHARACTERIZATION of cutaneous foreign bodies is often a challenge for dermatologists. With technologic advancements, identification and characterization of exogenous material in human tissues are no longer limited to the histological morphologic study but takes advantage of emerging radiologic and ultrastructural techniques (1–3).

We describe the application of one of these emerging techniques (2), Raman Spectroscopy, to confirm the clinical diagnosis of the skin reaction to a foreign body through the identification of the material itself.

A 42-year-old female patient had been suffering from an erythematosus nodule on her right hand for 1 year. The examination revealed that the patient, who used to canoe, had been subject to a trauma produced by a paddle which had inflicted a wound on her hand.

Suspecting the nodule to be a foreign body reaction, probably due to a fragment of the paddle, we performed a skin biopsy for a histological examination.

The sample was first analysed by Raman spectroscopy using a Horiba confocal microspectrometer LabRAM ARAMIS which showed a spectrum characteristic of a resin usually used in composite materials. Indeed, the Raman spectrum showed a series of peaks at 826, 920, 1010, 1035, 1115, 1157 and 1188 cm ^{1} (Fig. 1) characteristic of a resin composed of diglicidyl ether of bisphenol-A and N′-(3-aminopropyl)-N, N-dimethyl-1,3-diamine (4, 5). In addition to this series of peaks, other peaks around 447 and 610 cm ^{1}, probably due to the reinforcing fibers used to produce the composite material, were observed.

It was therefore possible to confirm the diagnosis of foreign body reaction by determining the nature of the specimen. The diagnosis could be made thanks to the accurate determination of the foreign body and the following histological analysis was even superfluous.

Raman spectroscopy is a technique that analyses materials by detecting their molecular vibrations. It studies the scattered radiation arising from the interaction between a monochromatic light source and the molecules of the system to be studied. When a radiation passes through a medium, a fraction of its light is scattered. The energy exchange between the inci-

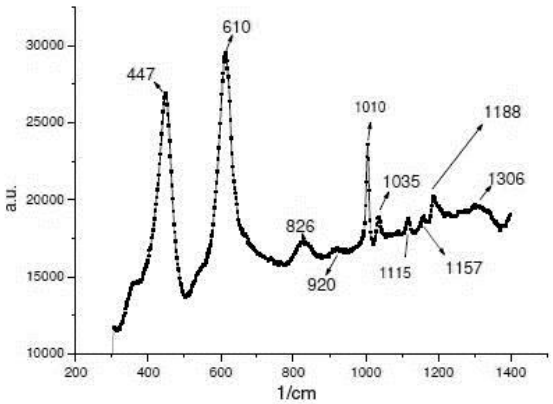

Fig. 1. The Raman spectrum of the skin biopsy showed a series of peaks at 826, 920, 1010, 1035, 1115, 1157 and 1188 cm^{-1} characteristic of an epoxy resin. y-axis: intensity in arbitrary units (a.u.); x-axis: wavenumber (cm^{-1}).

dent light beam and the medium results in a change of wavelength of the scattered light (Raman scattering) that is characteristic of the medium (6).

Raman spectroscopy is getting more and more applications in dermatology, having already been used to identify cancerous lesions such as basal cell carcinoma (7) and melanoma (7), to assess the amount of water in the dermis (8), to differentiate photoaging from chronoaging (9), and to follow the cutaneous penetration and metabolism of some drugs (10). It has also recently been employed for the chemical characterization of cutaneous foreign bodies to complete the histopathological examination of birefringent material in two skin biopsies, identifying two plastic materials used in previous surgical procedures in one case and an antibiotic (carbenicillin) in the other case (2).

This anecdotal case shows that Raman technique is applicable to the study of the composition of foreign material in the skin and can change the traditional way of making diagnosis. In fact, Raman spectroscopy technique can be used as an additional tool to complete the histopathological examination, currently based on morphology, thus adding information about the chemical composition of foreign bodies.

Several future applications would be possible in dermatology, such as identifying types of fillers injected in the case of side effects, analyzing components of implantable prostheses whenever there is a suspicion of contact allergy, identifying pigments of tattoos and following *in vivo* the cutaneous penetration of topical drugs or cosmetics. Raman spectroscopy is also more and more used in forensic medicine, for example in the identification of body fluid traces and latent fingerprints, and could apply to identify foreign inclusions in histological sections of biopsy or autopsy tissues for forensic purposes.

Moreover, a new system combining confocal reflectance microscopy with Raman spectroscopy in a handheld device has been recently developed (11). Such a device can open new perspectives for the *in vivo* study of foreign bodies; determining the composition of tattoo pigments to adjust the laser treatment could be one example.

In conclusion, the application of currently available and newly evolving analytic systems will expand our limits of detection and enhance our scientific knowledge.

Acknowledgement

Conflict of interest disclosure: The authors declare not to have any conflicts of interest.

References

1. Halaas GW. Management of foreign bodies in the skin. Am Fam Physician 2007; 76: 683 688.
2. Kalasinsky KS, Kalasinsky VF. Infrared and Raman microspectroscopy of foreign materials in tissue specimens. Spectrochim Acta A Mol Biomol Spectrosc 2005; 61: 1707 1713.
3. Murakata LA, Lewin-Smith MR, Specht CS et al. Characterization of acrylic polyamide plastic embolization particles in vitro and in human tissue sections by light microscopy, infrared microspectroscopy and scanning electron microscopy with energy dispersive X-ray analysis. Mod Pathol 2006; 19: 922 930.
4. Tait JKF, Edwards HGM, Farwell DW et al. Fourier transform Raman spectroscopic examination of two amine-based epoxy resin crosslinking agents. Spectrochimica Acta A 1995; 51: 2101 2106.
5. Vašková H, Kresalek V. Raman Spectroscopy of Epoxy Resin Crosslinking, 13th WSEAS International Conference on automatic control, modelling & simulation. Researches in Automatic Control (ACMOS'11) 2011; 357 361.
6. Schrader B. Infrared and Raman spectroscopy. New York: VCH Publishers Inc., 1995.
7. Bodanese B, Silveira FL, Zângaro RA et al. Discrimination of basal cell carcinoma and melanoma from normal skin biopsies in vitro through Raman spectroscopy and principal component analysis. Photomed Laser Surg 2012; 30: 381 387.
8. Nakagawa N, Matsumoto M, Sakai S. In vivo measurement of the water content in the dermis by confocal Raman spectroscopy. Skin Res Technol 2010; 16: 137 141.
9. González FJ, Castillo-Martínez C, Martínez-Escanamé M et al. Non-invasive estimation of chronological and photoinduced skin damage using Raman spectroscopy and principal component analysis. Skin Res Technol 2011; 18: 442 446.
10. Zhang G, Moore DJ, Sloan KB et al. Imaging the prodrug-to-drug transformation of a 5-fluorouracil derivative in skin by confocal Raman microscopy. J Invest Dermatol 2007; 127: 1205 1209.
11. Patil CA, Arrasmith CL, Mackanos MA et al. A handheld laser scanning confocal reflectance imaging-confocal Raman microspectroscopy system. Biomed Opt Express 2012; 3: 488 502.

Address:
Elisa Cinotti
Department of Dermatology
Hôpital Nord Saint-Etienne
42055 Saint Etienne Cedex 2
France
Tel: +33 (0) 477 828 421
Fax: +33 (0) 477 828 401
e-mail: elisacinotti@gmail.com

8.2-Microscopie confocale ex vivo

8.2.1 Rapid characterization of human brain aspergillosis by confocal microscopy on a thick squash preparation.

cytomegalovirus infection are easily differentiated from those of other viral infections by characteristic enlarged nuclei with large basophilic inclusions, surrounded by a conspicuous halo.[1] The recognition of the typical multinucleated epithelial cells with moulded ground-glass nuclei does not pose any diagnostic dilemma for herpes simplex virus infection.[1] However, cells in urine with non-typical viral inclusions of these two viruses, which may be identified as decoy cells, can cause difficulty in the differentiation from cells with other viral inclusions. Thus, cytological features seen in decoy cells are not specific to BKPyV. Therefore, the use of the term 'decoy cells' should be extended to similar atypical cells in urine caused by viral infection other than BKPyV. Other investigations for the identification of viral infections, such as immunostaining, electron microscopy and molecular studies, are advised in conjunction with the detection of decoy cells in urine cytology.

Acknowledgments

We thank Drs Harutaka Katano, Hideki Hasegawa and Tetsutaro Sata, Department of Pathology, National Institute of Infectious Diseases, Tokyo, Japan, for performing immunohistological staining for viruses.

M. Kimura* and T. Hayashi†
Department of Pathology, †Department of Urology, Kinki University Faculty of Medicine, Osaka-Sayama, Japan

References

1. Koss LG, Melamed MR. The lower urinary tract in the absence of cancer. In: *Koss Diagnostic Cytology and Its Histopathologic Bases*, 5th edn, vol. **1**. Koss LG, Melamed MR (eds). Philadelphia, PA: Lippincott Williams & Wilkins; 2006: pp. 738–76.
2. Buller RS. Human polyomaviruses. In: *Manual of Clinical Microbiology*, 10th edn, vol. **2**. Versalovic J, Carroll KC, Jorgensen JH, Funke G, Landry ML, Warnock DW (eds). Washington DC: ASM Press; 2011: pp. 1624–35.
3. De Las Casas LE, Hoerl HD, Bardales RH *et al.* Utility of urinary cytology for diagnosing human polyoma virus infection in transplant recipients: a study of 37 cases with electron microscopic analysis. *Diagn Cytopathol* 2001;**25**:376–81.
4. Funahashi Y, Iwata S, Ito Y *et al.* Multiplex real-time PCR assay for simultaneous quantification of BK polyomavirus, JC polyomavirus, and adenovirus DNA. *J Clin Microbiol* 2011;**48**:825–30.
5. Robinson C, Echavarria M. Adenoviruses. In: *Manual of Clinical Microbiology*, 10th edn, vol. **2**. Versalovic J, Carroll KC, Jorgensen JH, Funke G, Landry ML, Warnock DW (eds). Washington DC: ASM Press; 2011: pp. 1600–11.
6. Drachenberg CB, Beskow CO, Cangro CB *et al.* Human polyoma virus in renal allograft biopsies: morphological findings and correlation with urine cytology. *Hum Pathol* 1999;**30**:970–7.

Rapid characterization of human brain aspergillosis by confocal microscopy on a thick squash preparation

DOI:10.1111/cyt.12258

Dear Editor, Confocal *ex-vivo* microscopy is a new diagnostic tool with increasing applications in dermatology and dermatopathology. Recent studies suggest possible applications in the field of neurology on brain tumours. We illustrate a new possible application of confocal microscopy in neurosurgery and neuropathology.

A59 year-old patient was admitted to our hospital for recurrent falls. Clinical examination found a cerebellar syndrome. Magnetic resonance imaging examination showed a right parietal lobe ring-enhancing lesion with a mass effect on the cerebellum and the controlateral hemisphere. The patient was not immunocompromised and did not have any mycotic lung lesion. A diagnostic brain biopsy was performed.

We examined the brain biopsy extemporaneously with a smear technique (Figure 1a) and with confocal microscopy on thick squash preparations. Briefly, a 5 mm^3 freshly removed brain tissue sample was immersed in an acetic acid solution for 30 seconds, and then immersed in acridine orange for 30 seconds. Acridine orange binds to nucleic acids and highlight nuclei under fluorescence excitation light. Acetic acid highlights the contrast for a better morphological analysis. The sample was rinsed and mounted between two slides with a distance of 2 mm between the slides (Figure 1b) a 'thick squash preparation'. Confocal imaging was performed with Vivascope 2500® (CALIBER, distrib-

Correspondence:
Fabien Forest, Service d'anatomie et cytologie pathologiques. CHU de Saint Etienne, Hopital Nord, 42055 Saint Etienne, CEDEX 2, France
Tel.: +33(0)477127734; Fax: +33(0)47782829;
E-mail: fabien.forest@chu-st-etienne.fr

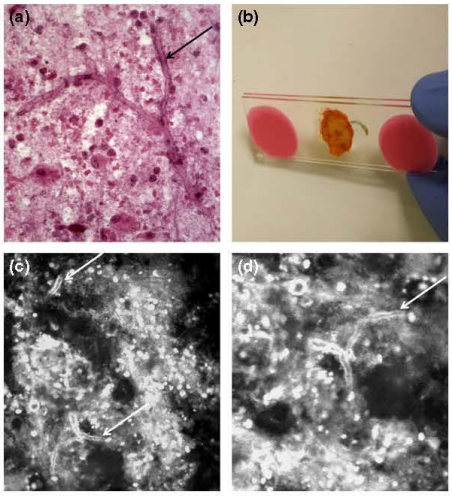

Figure 1. (a) Microphotography, brain tissue, smear, HE ×400 showing *Aspergillus fumigatus* hyphae (arrow). (b) Brain tissue on a thick squash preparation within two slides used for confocal microscopy imaging. (c) Confocal microscopy imaging showing numerous fungal elements (white arrows). (d) Confocal microscopy imaging showing *A. fumigatus* hyphae.

uted in Europe by MAVIG GmbH, Munich, Germany). This confocal microscope can realise optic sections on fresh tissue with a reflectance and fluorescence mode with a 3-D effect. After confocal imaging, the sample was fixed in formalin.

Confocal microscopy imaging revealed neural and necrotic tissue containing fungal hyphae, readily seen in the fluorescence mode (488 nm) (Figure 1c,d). The staining of the sample, acquisition and interpretation of the confocal images lasted less than 20 minutes, comparable to the time needed for a smear preparation. The fungal filaments were also seen on smears and tissue sections of the fragment used for confocal microscopy examination. Mycological culture showed *Aspergillus fumigatus*. The wall of the abscess was secondarily surgically completely excised, and the patient was treated with Voriconazole.

In vivo confocal microscopy is a new tool for the diagnosis of tumoural, inflammatory and infectious disease in the skin. Clinical applications of *ex vivo* confocal microscopy are increasing.[1] Few reports have used a confocal microscope for the diagnosis of brain lesions and mostly for tumoural lesions.[2,3] Thus far, the diagnosis of aspergillosis had been demonstrated to be feasible using *in-vivo* confocal microscopy on the human cornea and rat lung.[4–6] Although there are existing methods for the rapid detection of Aspergillus during an operation (mycological rapid direct examination, smears or frozen section, and/or rapid gomori-silver methamine stain), this report could suggest that *ex vivo* rapid diagnosis of brain aspergillosis could also be performed in daily routine practice. The main advantages of this procedure of imaging are that it can provide a rapid diagnosis, and it could represent a tissue-sparing method. Another advantage of confocal microscopy imaging compared with frozen sections is that it avoids freezing artefacts.[1] This report represents another application of confocal microscopy in the neuropathological and infectious diseases fields.

F. Forest*, E. Cinotti†, C. Habougit*, C. Ginguéné‡, J.-L. Perrot†, B. Labeille†, P. Flori§, E. Botelho-Nevers¶ and M. Péoch*
Department of Pathology, †Department of Dermatology, ‡Department of Neurosurgery, §Department of Mycology, ¶Department of Infectious Diseases, University Hospital of Saint Etienne, North Hospital, Saint Etienne CEDEX 2, France

References

1. Ragazzi M, Piana S, Longo C, *et al.* Fluorescence confocal microscopy for pathologists. *Mod Pathol* 2014;**27**:460–71.
2. Sanai N, Eschbacher J, Hattendorf G, *et al.* Intraoperative confocal microscopy for brain tumors: a feasibility analysis in humans. *Neurosurgery* 2011;**68**:282–90.
3. Peyre M, Clermont-Taranchon E, Stemmer-Rachamimov A, Kalamarides M. Miniaturized handheld confocal microscopy identifies focal brain invasion in a mouse model of aggressive meningioma. *Brain Pathol* 2013;**23**:371–7.
4. Morisse H, Heyman L, Salaün M, *et al. In vivo* molecular microimaging of pulmonary aspergillosis. *Med Mycol* 2013;**51**:352–60.
5. Morisse H, Heyman L, Salaün M, *et al. In vivo* and *in situ* imaging of experimental invasive pulmonary aspergillosis using fibered confocal fluorescence microscopy. *Med Mycol* 2012;**50**:386–95.
6. Winchester K, Mathers WD, Sutphin JE. Diagnosis of Aspergillus keratitis *in vivo* with confocal microscopy. *Cornea* 1997;**16**:27–31.

Skin Research and Technology 2016; 22: 203–207
Printed in Singapore. All rights reserved
doi: 10.1111/srt.12251

Published by John Wiley & Sons Ltd
Skin Research and Technology

Ex vivo confocal microscopy: a new diagnostic technique for mucormycosis

A. Leclercq, E. Cinotti, B. Labeille, J. L. Perrot and F. Cambazard
Department of Dermatology, University Hospital of Saint Etienne, Saint-Etienne, France

Background: Skin-dedicated *ex vivo* confocal microscopy (EVCM) has so far mainly been employed to identify cutaneous tumours on freshly excised samples. We present two cases where EVCM has been used to diagnose cutaneous mucormycosis.
Methods: The skin biopsies were evaluated by the skin-dedicated *ex vivo* confocal microscope VivaScope 2500® (MAVIG GmbH, Munich Germany) under both reflectance and fluorescence mode. Conventional direct optical examination on skin scraping and histological examination were later performed.
Results: *Mucormycetes* observed by EVCM presented as hyper-reflective elongated 20 μm in diameter structures with perpendicular ramifications. Fungi were found both under reflectance and fluorescence mode and were better visible with acridine orange under fluorescence EVCM. Conventional direct optical examination on skin scraping and histological examination found the same elongated and branching structures confirming the presence of *Mucormycetes*.
Conclusions: *Ex vivo* confocal microscopy has both the advantages of being fast as the direct optical examination, and to be able to show the localisation of the fungi in the tissue like the histological examination. In our cases, EVCM allowed to rapidly confirm the clinical diagnosis of mucormycosis, which is essential for the treatment of this fungal infection. Further studies are needed to compare the performance of EVCM with the findings of conventional histological and mycological examinations.

Key words: mucormycosis – Ex vivo confocal microscopy – histological examination – direct examination

Accepted for publication 17 May 2015

SKIN -DEDICATED *ex vivo* confocal microscopy (EVCM) is an emerging technique that provides high resolution images of the skin and that has so far mainly been employed to identify cutaneous tumours on freshly excised samples. *In vivo* confocal microscopy has recently been used for the diagnosis of onychomycosis (1) and hair dermatophytosis (2), but mucormycosis has never been diagnosed using EVCM. Mucormycosis is a life-threatening fungal infection that occurs in immunocompromised patients and has an increasing incidence due to the raise of allograft (3). We present the first two cases where EVCM has been used to diagnose cutaneous mucormycosis.

Case Report

Case 1

A 34-year-old man presented with a cutaneous lesion on his left thigh, 10 days after an allograft for an acute myeloid leukaemia. At the examination we could appreciate a roundish, three centimetres in diameter, regular, necrotic plaque with well-defined border (Fig. 1).

A complete excision of the plaque was performed, and the surgical specimen was evaluated by the skin-dedicated *ex vivo* confocal microscope VivaScope 2500® (CALIBER, NY, USA, distributed in Europe by MAVIG GmbH) finding elongated, 20 μm in diameter structures, with perpendicular ramifications (Fig. 2). Under reflectance EVCM, these structures were hyper-reflective, but they were better identified by fluorescence EVCM with acridine orange as highly fluorescence structures (Fig. 3). The latter staining was performed incubating the sample with acridine orange for 20 s and rinsing it with a saline solution for 5 s.

To confirm the EVCM analysis, the specimen was then analysed by conventional mycological examinations. Direct microscopy examination with saline solution and chlorazol black found broad, non-septate and irregularly branching hyphae. The histological sections from the same specimen observed under EVCM were stained

Fig. 1. Clinical aspect of the necrotic plaque of the left thigh of the first patient.

by Hematoxiline, Eosine and Safran (HES), Periodic Acid Schift (PAS) and Grocott stains (Fig. 4). These stains allowed to identify branching broad hyphae infiltrating the wall of arteries and forming thrombi. The culture on Sabouraud's medium at 25°C identified *Lichtheimia corymbifera*. The patient was promptly treated by amphotericin B (5 mg/kg/day) and due to an anaphylactic accident the treatment was changed into posaconazole (800 mg/day) and surgical debridement with a complete healing.

Case 2

A 54-year-old man with an untreated diabetes and depression was hospitalised for a septic shock with a fast progression to coma. He was treated by dobutamine and by an antibiotic and antimycotic therapy consisting of vancomycin, gentamicin, tazocillin, and ciprofloxacin. After a short improvement, his condition worsened. He presented bullous lesions that evolved into necrotic plaques on feet, hands, mouth and nose (Fig. 5). The diagnosis of mucormycosis was suspected.

A skin biopsy of a necrotic plaque from the face was evaluated by EVCM VivaScope 2500® and then by direct mycological examination (Fig. 6) and histological examination as for the previous patient, finding large elongated structures with irregular branching. Under EVCM these structures were hyper-reflective in the reflectance mode and highly fuorescence using acridine orange in the fluorescence mode (Fig 3).

The fungal culture on Sabouraud's medium at 25 and 37°C identified *Rhizopus sp.*

Unfortunately, the patient died one day after the introduction of amphotericin B (5mg/kg/day), before a surgical debridment.

Discussion

Mucormycosis is caused by ubiquitous mucoralean fungi, the so called *Mucormycetes*. It is an emerging fungal infection (3) that mostly involves the skin, the lung, and the rhino-cerebral tissues, and can also be disseminated. The mortality at 90 days is estimated to 22% in case of skin involvement, and can reach 79% in the disseminated forms (4). The filaments perforate the vessel walls, invade the vessels and form

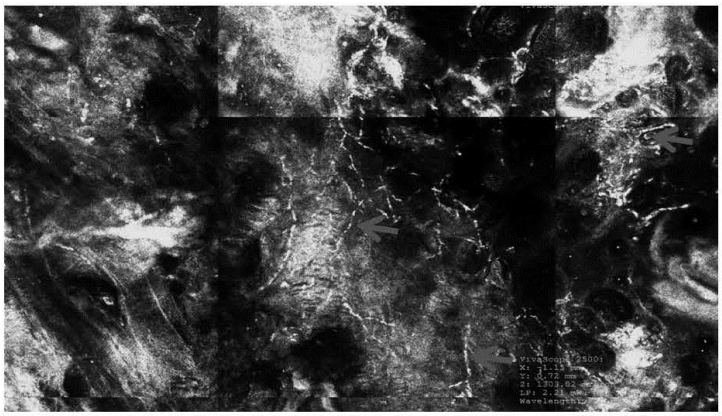

Fig. 2. Ex vivo reflectance confocal microscopy of the skin biopsy of the first patient shows hyper-reflective elongated structures, 20 µm in diameter crossing with perpendicular junctions, corresponding to fungal filaments (arrow).

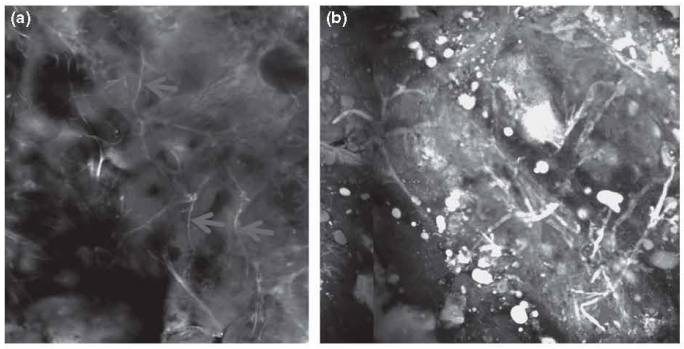

Fig. 3. Fluorescence ex vivo confocal microscopy after acridine orange staining of the skin biopsy of the first (a) and the second (b) patient enhances the fungal structures (arrow).

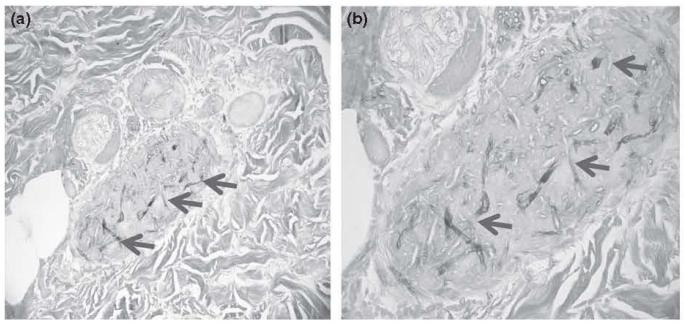

Fig. 4. Histological examination of the skin biopsy from the first patient shows 20 μm in diameter, non-septate, fungal filaments (arrow), invading the dermis and the wall vessels (Grocott; A, x20 and B, x40).

thrombi and emboli. The prognosis also depend on the immediate initiation of a systemic treatment and the addition of surgical debridement to antifungal treatment (4).

Three techniques are currently used for the diagnosis of mucormycosis: direct examination of a skin scraping under optical microscope, histological examination, and fungal culture. EVCM could be an additional technique.

In our cases, we used saline solution and Chlorazol black for the direct examination under optical microscope. Other stains frequently used in Europe are Blankophor and Calcofluor white (4). These stainings bind to cell walls of fungi and to celullose, so that fungi shine in ultra violet light (5). The sensibility of the direct optical examination is only 56% (4), mainly due to the small size of the sample that is observed because one part is used for the culture.

Differently from direct examination, EVCM allows to analyse the whole bioptical specimen that is made for the histological examination, without altering it, therefore possibly increasing the detection rate. Moreover, under direct examination the architecture of specimen is totally destroyed because the specimen consists of a skin scarping, whereas EVCM can show the fungal elements within the architecture of the tissue.

The sensitivity of the histological examination for the diagnosis of cutaneous mucormycosis is higher than direct examination and reaches 65% (4). However, histological examination is time consuming and only the slices that are cut are observed, and not the entire specimen. EVCM overcomes this problem because the preparation of the specimen is quick (no preparation is needed for the reflectance-mode examination and few minutes are necessary for the acridine

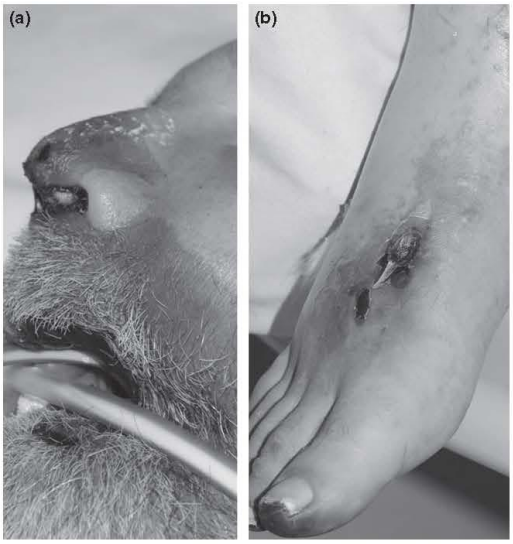

Fig. 5. Clinical aspect of the necrotic plaque of the face (a) and on the feet (b) of the second patient.

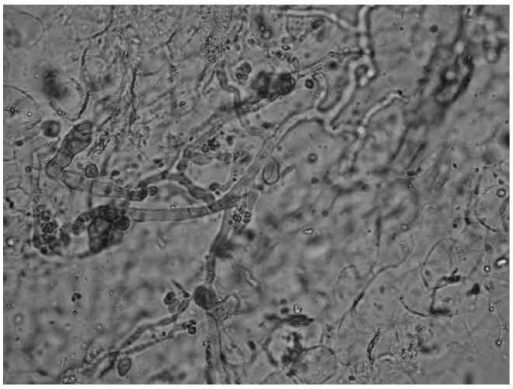

Fig. 6. Direct optical examination of a skin sample from the second patient shows elongated structures corresponding to fungal filaments.

orange staining) and images from the entire specimen can be easily taken by using the mosaic and stack mode to obtain horizontal and vertical sections.

Histological examination as well as EVCM and direct mycological examination have the limitation of not being able to identify fungal species (4).

The fungal culture is able to identify the species and has the additional advantage of having a sensitivity of up to 95% (6). However, culture has the drawback of giving a delayed response of some days (4). Moreover, a positive culture might be a false positive as these organisms are common in the environment (3). Therefore, cultures should be always evaluated together with the clinical aspect and other mycological analysis (7).

The use of molecular methods on both fresh material and paraffin slides for the diagnosis of mucormycosis is moderately supported (7) and these techniques are not available in daily practice. Polymerase chain reaction (PCR) that targets the 18S ribosomal DNA of mucorales seems to have a higher sensibility than culture (4), up to 100% (8). However, two studies showed a large variability in PCR performance in mucormycosis (4) and false positive are possible (9). The failure to amplify specific DNA might result from fungal DNA concentrations below detection limits, or the destruction of DNA during formalin fixation (7). Moreover, PCR is limited to some species like *Rhizopus microsporus* (10). EVCM could be used to increase the sensitivity of PCR amplification, being able to identify an area with high fungal concentration.

In our cases, EVCM with the reflectance mode allowed to easily identify the fungal hyphae since they appeared as hyper-reflective elongated structures. Moreover, acridine orange stained fungal elements simplifying their identification in the fluorescence mode.

The two main advantages of EVCM compared to conventional examinations are that an entire specimen of up 2 cm of diameter can be observed under the microscope without any special preparation (acridine orange staining takes few minutes and no cutting is needed) and that further histological examination is possible because this technique does not alter the specimen.

In our cases, EVCM gave similar information to the direct microscopy and histological examinations. However, it is likely that EVCM is more sensitive than conventional examinations because the entire bioptical specimen can be observed and because acridine orange facilitates the recognition of fungal walls.

Moreover, differently from fungal cultures, ECVM is fast and does not have the problem of false positive results due to environmental contamination, because the examination is made extemporaneously just after the specimen collection.

In conclusion, EVCM could be useful for an early diagnosis of cutaneous mucormycosis that is essential for a prompt treatment with a consequent better prognosis. Further studies are needed to define the EVCM features of mucormycosis and to compare the performance of EVCM with the findings of conventional histological and mycological examinations.

Acknowledgement

Conflict of interest disclosure: The authors declare not to have any conflicts of interest

References

1. Pharaon M, Gari-Toussaint M, Khemis A et al. Diagnosis and treatment monitoring of toenail onychomycosis by reflectance confocal microscopy: Prospective cohort study in 58 patients. J Am Acad Dermatol 2014; 71: 56 61.
2. Cinotti E, Perrot JL, Labeille B et al. Hair dermatophytosis diagnosed by reflectance confocal microscopy: six cases. J Eur Acad Dermatol Venereol 2014; doi:10. 1111/jdv.12557.
3. Bitar D, Che D. Epidemiology of mucormycosis in metropolitan France, 1997-2010. Med Sci 2013; 29: 7 12.
4. Cornely OA1, Arikan-Akdagli S, Dannaoui E et al. ESCMID and ECMM joint clinical guidelines for the diagnosis and management of mucormycosis 2013. Clin Microbiol Infect 2014; 20: 5 26.
5. Hamer EC, Moore CB, Denning DW. Comparison of two fluorescent whiteners, calcofluor andblakophor, for the detection of fungal elements in clinical specimensin the diagnosic of laboratory. Clin Microbiol Infect 2006; 12: 181 184.
6. Lanternier F, Dannaoui E, Morizot G et al. A global analysis of mucormycosis in France: the RetroZygo Study (2005-2007). Clin Infect Dis 2012; 54: 35 43.
7. Petrikkos G, Skiada A, Drogari-Apiranthitou M. Epidemiology of mucormycosis in Europe. Clin Microbiol Infect 2014; 20: 67 73.
8. Rickerts V, Mousset S, Lambrecht E et al. Comparison of histopathological analysis, culture, and polymerase chain reaction assays to detect invasive mold infectious from biopsy specimens. Clin Infect Dis 2007; 44: 1078 1083.
9. Lass-Florl C, Resch G, Nachbaur D et al. The value of computed tomography guided percutaneous lung biopsy for diagnosis of invasive fungal infection in immunocompromised patients. Clin Infect Dis 2007; 45: e101 e104.
10. Buitrago MJ, Aguado JM, Ballen A et al. Efficacy of DNA amplification in tissue biopsy samples to improve the fungal infection disease. Clin Microbiol Infect 2013; 19: e271 e277.

Address:
A. Leclercq
Hôpital Nord Saint-Etienne, 42055 Saint Etienne Cedex 2
France
Tel: +33 477828421
Fax: +33 477828401
e-mail: amaury.leclercq@hotmail.fr

8.2.3 Ex vivo confocal microscopy imaging to identify tumor tissue on freshly removed brain sample.

J Neurooncol (2015) 124:157–164
DOI 10.1007/s11060-015-1832-z

LABORATORY INVESTIGATION

Ex vivo confocal microscopy imaging to identify tumor tissue on freshly removed brain sample

Fabien Forest[1] · Elisa Cinotti[2] · Violaine Yvorel[1] · Cyril Habougit[1] · François Vassal[3] · Christophe Nuti[3] · Jean-Luc Perrot[2] · Bruno Labeille[2] · Michel Péoc'h[1]

Received: 29 September 2014 / Accepted: 27 May 2015 / Published online: 2 June 2015

Abstract Confocal microscopy is a technique able to realize "optic sections" of a tissue with increasing applications. We wondered if we could apply an ex vivo confocal microscope designed for dermatological purpose in a routine use for the most frequent brain tumors. The aim of this work was to identify tumor tissue and its histopathological hallmarks, and to assess grading criteria used in neuropathological practice without tissue loss on freshly removed brain tissue. Seven infiltrating gliomas, nine meningiomas and three metastases of carcinomas were included. We compared imaging results obtained with the confocal microscope to frozen sections, smears and tissue sections of formalin-fixed tissue. Our results show that ex vivo confocal microscopy imaging can be applied to brain tumors in order to quickly identify tumor tissue without tissue loss. It can differentiate tumors and can assess most of grading criteria. Confocal microscopy could represent a new tool to identify tumor tissue on freshly removed sample and could help in selecting areas for biobanking of tumor tissue.

Keywords Confocal reflectance microscopy · Meningioma · Glial neoplasms · Brain metastasis

✉ Fabien Forest
fabien.forest@chu-st-etienne.fr

[1] Service d'Anatomie et Cytologie Pathologiques - CHU de Saint Étienne, Hôpital Nord, 42055 Saint Étienne. Cedex2, France

[2] Service de Dermatologie - CHU de Saint Étienne, Hôpital Nord, 42055 Saint Étienne. Cedex2, France

[3] Service de Neurochirurgie - CHU de Saint Étienne, Hôpital Nord, 42055 Saint Étienne. Cedex2, France

Introduction

Confocal reflectance microscopy is a daily routine technique able to visualize tissues without fixation or staining used in classical histological technique. This technique represents a new approach for tissue imaging. In confocal microscopy, a laser-beam is focused on a point inside the object. The reflected light is gathered by a detector through a pinhole aperture. In reflectance mode, the light is naturally reflected because of differences in refraction within subcellular structures. The use of fluorochrome (fluorescence mode), allows the visualization of non-naturally reflected structures. This technique can be used in vivo and, i.e. allows skin tumor imaging since melanin is bright on reflectance mode. Available visualization modes are a so-called "reflectance mode" based on the refraction of the light within a tissue, and a "fluorescence mode" which can highlight fluorochrome-labeled elements. It can be applied either in vivo or ex vivo on freshly removed tissues. It has wide implications in daily dermatological practice for the diagnosis of skin tumors, the evaluation of resection margins, the follow-up after treatment and in other fields like infections, infestations and inflammatory diseases [1].

Brain tumors diagnosis and management of brain tissue are often difficult for pathologists, because they often have to deal with small surgical samples or biopsies. Biobanking of tumor tissue is often necessary for research or further diagnostic purposes, but tumor tissue in brain is often not distinguishable from normal tissue on naked eye for glial tumors.

The main objectives of our work are to assess if ex vivo confocal microscopy is capable of:- differentiating tumor tissue from normal brain;- identifying histopathologic criteria of brain tumors (metastasis, meningiomas, infiltrating

gliomas);- identifying World Health Organization (WHO) classification grading criteria [2].

Materials and methods

Patients and specimens handling

This study was conducted in the Dermatology, Neurosurgery and Pathology Units of the University Hospital center of Saint Etienne. All patients provided written informed consent and the design of this study was approved by local ethical board review. A total of 20 consecutive surgical brain biopsies or surgical excisions of brain tumor specimens from 19 patients were examined. The collected tumors consisted in seven infiltrating gliomas, nine meningiomas and three metastases. For each specimen, a sample was taken for confocal imaging and a contiguous sample was taken for intra-operative examination with a smear or frozen section technique. A normal control (brain sample given for scientific purpose) was obtained.

Confocal microscopy

Rapid imaging of fresh tissue was performed using VivaScope 2500® (CALIBER, distributed in Europe by MAVIG GmbH). VivaScope 2500 offers three wavelengths for excitation (488, 658, and 830 nm). 830 nm is used for the so-called "reflectance" mode, and 488 nm and 658 nm for fluorescence mode. The mode called fluorescence is not specific to the acridine orange label, other fluorechromes can be used with the same wavelength for excitation 488 nm and emission >500 nm. For reflectance mode the tissue is illuminated by a near-infrared laser beam. The laser beam passes through the superficial layers of the tissue and is partially backscattered due to natural refractive index of microanatomical structures. The reflectance mode it is not tissue autofluorescence. Reflectance imaging was performed either without any staining or after immersion in an acetic acid solution for 30 s. For fluorescence imaging, a 3 mm^3 freshly removed brain tissue sample was immersed in an acetic acid solution for 30 s, and then immersed in acridine orange for 30 s. The sample was rinsed in acetic acid, and directly mounted between two slides with a distance of 2 mm between the slides in order to avoid tissue crushing. The obtained images are a mosaic of several pictures, they were interpreted jointly with trained physicians and pathologists.

Histopathological examination

The samples used for imaging purpose on confocal microscopy were later formalin-fixed, paraffin-embedded with hematoxylin and eosin (HE) stain. All slides were reviewed by two pathologists with data collection about histopathological criteria used for pathological diagnosis and grading of each tumor. For each sample of glial tumor and metastasis, two smear slides were done. Briefly, 1–2 mm^3 of fresh tissue was crushed between two slides, immediately fixed in ethanol, then stained by HE and mounted. Frozen sections were performed for meningiomas.

Grading criteria

For each tumor, an analytical image analysis was performed. 2007 WHO classification grading criteria were used for infiltrating glial tumors and meningiomas [2]. For gliomas, the cellularity was appreciated and the "AMEN" criteria (Atypias, Mitosis, Endothelial/Vascular proliferation and Necrosis) were evaluated [2, 3]. For meningiomas, major criteria (brain invasion and mitosis count) and minor criteria (high cellularity, foci of small cells, necrosis, prominent nucleoli, and patternless architecture) were evaluated.

Results

For each case the whole confocal microscopy procedure (staining, image acquisition and interpretation) lasted less than 20 min which is similar to smears or frozen sections. There was no alteration of morphological or immunohistochemical quality on sections of formalin-fixed tissue previously used for confocal imaging except formalin fixation artefacts (Fig. 1). A normal control brain was imaged (Fig. 1).

Representative images were shown to junior (VY, CH) and senior pathologists (FF, MP) and complete concordance was obtained on the following criteria: tumor versus non-tumor, tumor type (glioma vs meningioma vs metastasis), low-grade versus high grade glioma.

Infiltrative glial tumors

Eight samples from seven patients with infiltrative glial tumors were included. The eight samples consisted of five high grade gliomas: three glioblastomas, one gliosarcoma and one anaplastic oligoastrocytoma; and of 2 low-grade gliomas: 2 grade II oligoastrocytomas and 1 peritumoral tissue.

Fibrillary background was identifiable in each tumor tissue on reflectance mode so as the identification of a glial tumor on smear or tissue section. Cellularity could be easily appreciated, especially on fluorescence mode in accordance with tissue section. Among the "AMEN" grading criteria, mitosis could not be evaluated on confocal

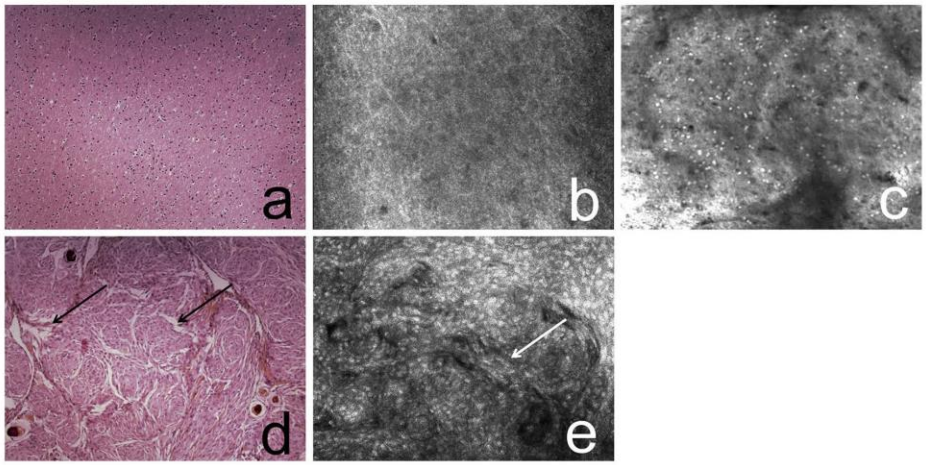

Fig. 1 Comparative aspect on sections of formalin-fixed paraffin-embedded tissue of normal white matter (**a–c**) and a meningioma (**d**, **e**). **a** Tissue section, HE × 100. **b** Confocal microscopy, reflectance mode (CMR). **c** Confocal microscopy, fluorescence mode after acridine orange staining (CMFA). **d** Tissue section, HE × 100, formalin fixation artefact: perivascular clefting (*arrows*). **e** CMR, lack of peri-vascular clefting around vessels (*arrow*)

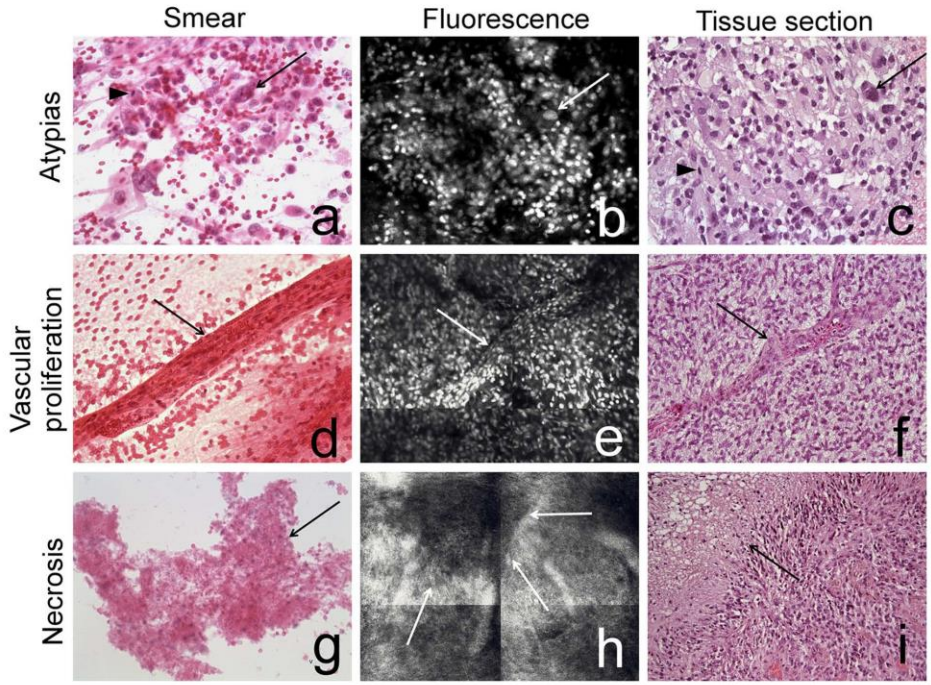

Fig. 2 Comparative aspect on smear, confocal microscopy and matched sections of formalin-fixed paraffin-embedded tissue of glioblastoma. **a** Smear, HE × 400, cytonuclear atypias (*arrow*) and mitosis (*arrowhead*). **b** CMFA, nuclear atypias (*arrow*). **c** Tissue section, HE × 400, cytonuclear atypias (*arrow*) and mitosis (*arrowhead*). **d** Smear, HE × 200, vascular endothelial proliferation (*arrow*). **e** CMFA, vascular endothelial proliferation (*arrow*). **f** Tissue section, HE × 200, vascular endothelial proliferation (*arrow*). **g** Smear, HE × 200, necrosis (*arrow*). **h** CMR, necrosis (*arrows*) within a fibrillary background. **i** Tissue section, HE × 200, palissading necrosis

microscopy whereas they were easily seen on tissue section or smears. Nevertheless, marked nuclear atypias were present (4/6), necrosis (2/6) and vascular proliferation (4/6) could be seen on confocal microscopy and was confirmed on the formalin-fixed tissue sample or smears (Fig. 2).

For the peritumoral tissue sample, the cellularity was low, without nuclear atypias, vascular proliferation or necrosis on confocal microscopy, so as on tissue sections. Peri-neuronal satellitosis, an aspecific feature seen in peritumoral tissue could be identified (Fig. 3).

Meningiomas

Reflectance and fluorescence confocal microscopy was performed on nine meningioma samples from nine patients. Histopathological subtypes were meningothelial (4), fibroblastic (1), transitional (1), microcystic (1) and 2 were classified as atypical meningiomas (1 because of 8 mitosis/10 HPF and 1 because of brain invasion). The histopathological features were strictly similar on frozen sections and tissue sections.

The architectural pattern, which is a component of meningiomas grading has been easily identified in reflectance and fluorescence confocal microscopy (Fig. 4). There was a concordance of architectural patterns on formalin-fixed tissue section counterpart (Fig. 4). Nuclear details such as nuclear pseudo-inclusions could be seen in fluorescence mode whereas they were not seen in reflectance mode (Fig. 4).

Among major grading criteria, mitosis could not be seen. Nevertheless, brain invasion, when present, was identified (Fig. 5). For the other meningiomas (8/9), brain tissue was absent. In one case, prominent nucleoli were seen in confocal microscopy and could be confirmed at histological level (Fig. 5). So as foci of necrosis, were present in one case on confocal microscopy and histological examination (Fig. 5). Cellularity could be evaluated, but in each meningioma it exhibited low cellularity.

Foci of small cells and patternless architecture were not present and could not be evaluated.

Metastasis

We applied our imaging procedure on three samples of metastatic carcinomas from three patients. 2 were undifferentiated non-neuroendocrine carcinomas despite extensive histological, immunohistochemical and molecular studies and 1 was a metastatic poorly differentiated lung adenocarcinoma.

Histopathological hallmarks of carcinomas were seen in reflectance and fluorescence mode with a concordance with the histological examination: cohesive or discohesive tumor cells without fibrillary background or typical

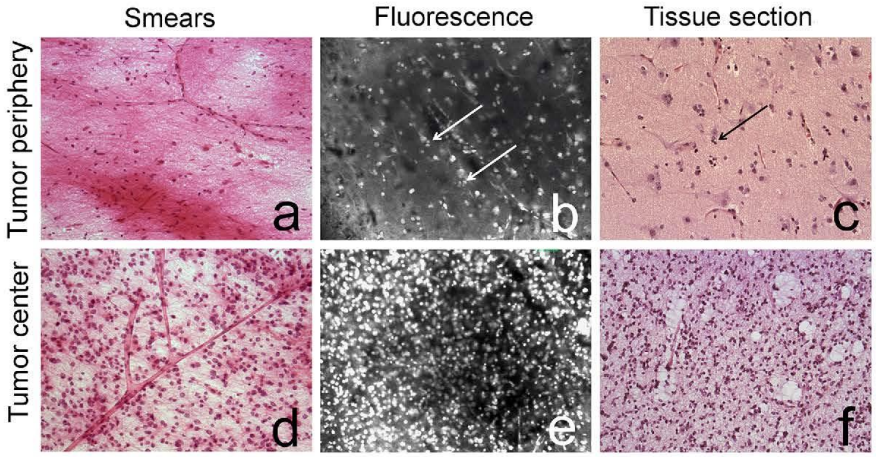

Fig. 3 Comparative aspect on smear, confocal microscopy and matched sections of formalin-fixed paraffin-embedded tissue of low grade glioma (grade II astrocytoma) in tumor tissue and peripheral tissue. **a** Smear, HE × 200, few glial cells with little cytonuclear atypias in a fibrillary background, without mitosis, necrosis or vascular proliferation. **b** CMFA, slight increase of cellularity, without nuclear atypias, with peri-neuronal satellitosis (*arrow*). **c** Tissue section, HE × 200, peri-neuronal satellitosis (*arrow*). **d** Smear, HE × 200, glial atypical cells within a fibrillary background, rare mitosis, no necrosis nor vascular proliferation. **e** CMFA, moderate nuclear atypias, no vascular proliferation. **f** Tissue section, HE × 200, increased cellularity, moderate cytonuclear atypias, rare mitosis, no necrosis nor vascular proliferation

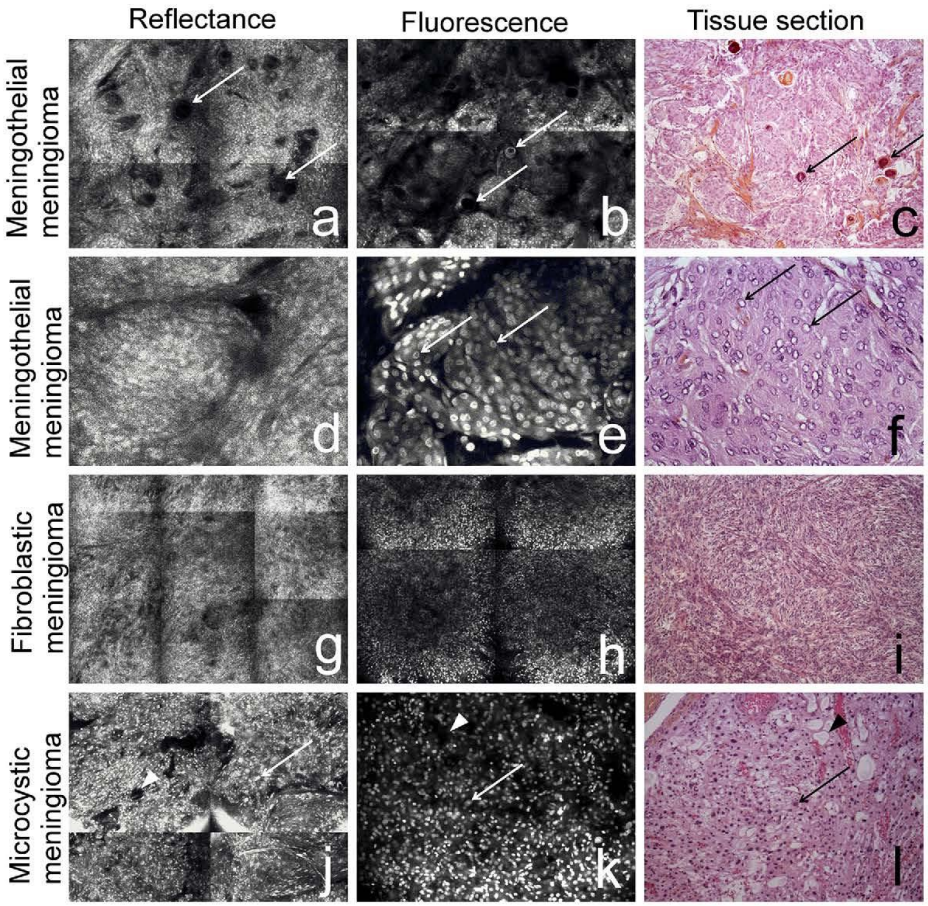

Fig. 4 Comparative subtypes and patterns on confocal microscopy and matched sections of formalin-fixed paraffin-embedded tissue of meningiomas. **a** CMR, meningothelial pattern with whorls and psammamatous bodies (*arrows*). **b** CMFA, meningothelial pattern with whorls and psammomatous bodies (*arrows*). **c** Tissue section, HE × 100, meningothelial WHO grade I meningioma with whorls and psammomatous bodies (*arrows*). **d** CMR, meningothelial pattern with whorl. **e** CMFA, meningothelial pattern with whorls and nuclear pseudo-inclusions (*arrows*). **f** Tissue section, HE × 400, meningothelial WHO grade I meningioma with nuclear pseudo-inclusions (*arrows*). **g** CMR, fibroblastic meningioma with fascicular pattern. **h** CMFA, spindle and elongated nuclei of a fibroblastic meningioma. **i** Tissue section, HE × 100, fibroblastic meningioma with fascicular pattern and spindle cells. **j** CMR, microcystic meningioma with microcysts (*arrowhead*) and scattered pleomorphic cells (*arrow*). **k** CMFA, microcystic meningioma with microcysts (*arrowhead*) and scattered pleomorphic cells (*arrow*). **l** Tissue section, HE × 200, microcystic meningioma with microcysts (*arrowhead*) and scattered pleomorphic cells (*arrow*)

architectural patterns of meningiomas, prominent nucleoli and highly pleomorphic cells were present (Fig. 6).

Discussion

Confocal microscopy is a technique which is able to realize "optic sections" of a tissue. It is widely used in research practice. Recent developments of optic and computer technology lead to the possibility of application of confocal microscopy in clinical practice. It permits imaging of several lesions without artifacts caused by fixation [4]. In the field of brain tumors, confocal microscopy has been used for imaging purpose of brain tumors in vivo on murine models [5, 6]. In studies involving humans in vivo and ex vivo confocal microscopy has been used [7]. The main difference with in vivo studies is the use of acridine orange instead of methylene blue staining [5, 6]. Our study

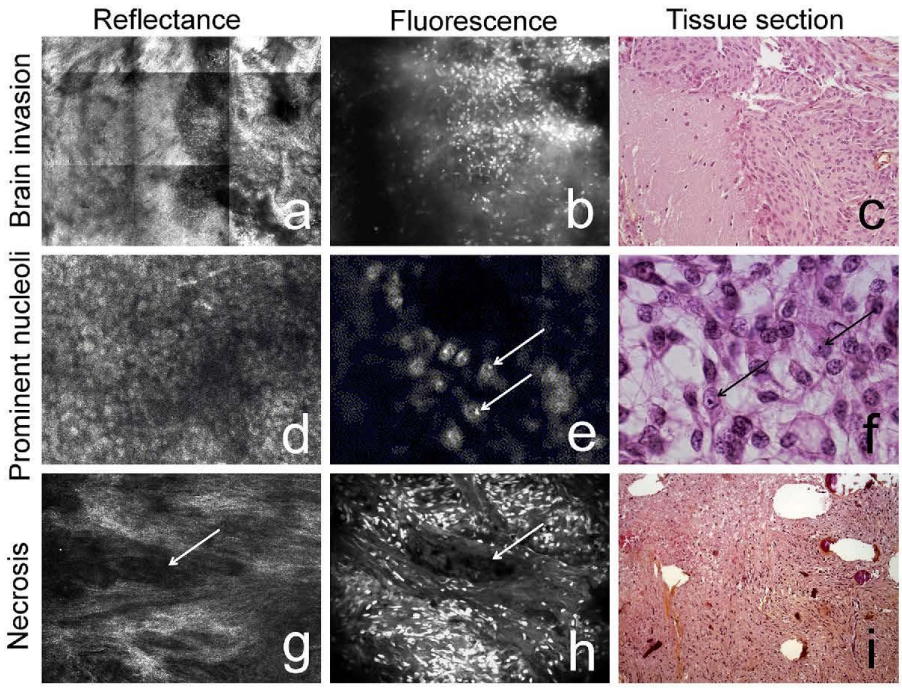

Fig. 5 Grading criteria of meningiomas: comparative imaging on confocal microscopy and matched sections of formalin-fixed paraffin-embedded tissue. **a** CMR, brain invasive meningioma. Typically fibrillary pattern of glial tissue on the left. **b** CMFA, brain invasive meningioma. Highly cellular meningioma on the right. **c** Tissue section, HE × 200, brain invasion in a grade II meningioma. **d** CMR, nuclear details of a meningioma with prominent nucleoli are not seen. **e** CMFA, prominent nucleoli can be seen (*arrows*). **f** Tissue section, HE × 400, prominent nucleoli in a meningioma. **g** CMR, focal area of necrosis. **h** CMFA, focal area of necrosis. **i** Tissue section, HE × 100, area of necrosis

uses a commercialy available confocal microscope and not of a microscope designed for research purpose [7].

On brain tissue, confocal microscopy is able to distinguish white from gray matter [5, 7]. It can identify tumor tissue and differentiate glial tumor tissue from normal tissue [5, 7, 8]. In our work, it was able to identify tumor-infiltrated brain from non-infiltrated brain. Within glial tumors, on few samples, the diagnostic accuracy of blinded study on confocal images seems to show that a correct in vivo diagnosis is often possible with a good sensitivity and specificity [7, 8]. For meningiomas, some diagnostic criteria such as typical meningothelial, fibroblastic or transitional architecture were identifiable. The features of brain metastasis on confocal microscopy are the same encountered on formalin-fixed tissue section: cohesive or discohesive large and pleomorphic cells [9]. Our work provides additional data showing that ex vivo confocal microscopy is capable of identifying diagnostic histopathologic hallmarks of brain tumors and for some of them histopathological subtype.

For glioma, among WHO grading criteria, cellularity, high nuclear pleomorphism and necrosis areas were identifiable [8]. They were not compared to other rapid diagnostic methods. For meningioma, among WHO grading criteria, it was possible to assess the cellularity [8], and brain invasion in a murine model [6]. Nevertheless, on in vivo study, prominent nucleoli and small cell foci were not seen on confocal images whereas they were evident on HE sections [8]. When prominent, nucleoli were easily seen in our study but the staining procedure is different with acridine orange use instead of fluorescein [8]. Nevertheless, mitosis which is a crucial parameter for most primitive brain tumors, cannot be identified neither by reflectance microscopy nor in fluorescence mode. In our best knowledge, no available fluorescent dye specific of mitotic cells with rapid staining procedure is available [10]. Ex vivo confocal microscopy is a recent technique, we think that technical improvement in future years will provide further nuclear details. Furthermore, since confocal microscopy images are numerised images, it might be

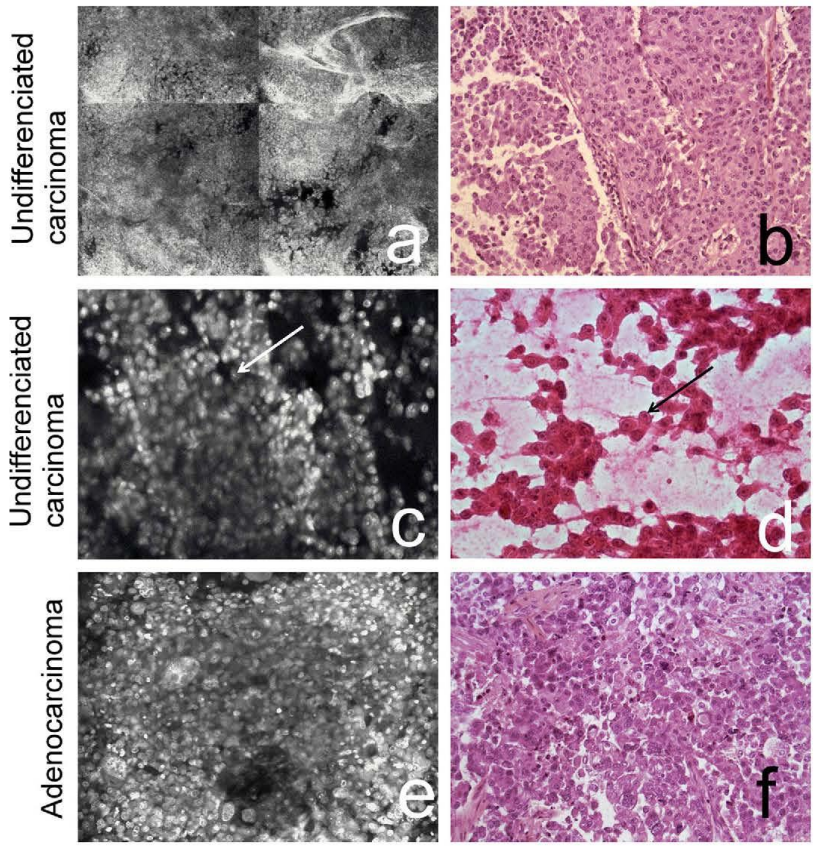

Fig. 6 Comparative aspect of brain metastasis of carcinoma on confocal microscopy, smears and matched sections of formalin-fixed paraffin-embedded tissue. **a** CMR, diffuse and discohesive pattern without fibrillary background of an undifferenciated carcinoma. **b** Tissue section, HE × 100, diffuse and discohesive pattern of an undifferenciated carcinoma. **c** CMFA, monomorphic cells with prominent nucleoli of an undifferenciated carcinoma (*arrow*). **d** Smear, HE × 400, monomorphic cells with prominent nucleoli of an undifferenciated carcinoma (*arrow*). **e** CMFA, highly pleomorphic cells of a metastatic adenocarcinoma. **f** Tissue section, HE × 200, metastasis of an adenocarcinoma with highly pleomorphic cells

possible to develop an image analysis program for mitosis detection.

Confocal microscopy could be used for the selection of areas of interest on fresh small samples for research purpose. It could be of interest in diagnosis because it is possible to identify rapidly tumor tissue without any tissue loss if compared to frozen section or smear technique. In addition, the confocal microscopy could ensure the quality and representativeness of frozen stored tissue in tumor banks [11].

Ex vivo confocal microscopy imaging is able to identify tumor tissue and histological hallmarks of most current brain tumors with a good concordance with matched formalin-fixed paraffin-embedded tissue section observed under optical microscope. Reflectance mode seems more accurate for tumor architecture while fluorescence mode allows imaging of cellular details. Combination of both methods seems the most informative for tumor identification. Confocal microscopy could represent a new tool for intraoperative diagnosis and spare tissue for further histological or molecular studies. Moreover, confocal microscopy may have an interest in the identification of area of interest on freshly removed brain tumor samples for

biobanking, per-operative diagnosis and research purposes without tissue loss.

Acknowledgments The authors declare no conflict of interest.

References

1. Debarbieux S, Perrot JL, Erfan N, Ronger-Savlé S, Labeille B, Cinotti E et al (2014) Reflectance confocal microscopy of mucosal pigmented macules: a review of 56 cases including 10 macular melanoma. Br J Dermatol 170:1276–1284. doi:10.1111/bjd.12803
2. Louis DN (ed) (2007) WHO classification of tumours of the central nervous system WHO Press. World Health Organization, IARC Lyon
3. Perry A (ed) (2010) Practical surgical neuropathology: a diagnostic approach. Churchill Livingstone/Elsevier, Philadelphia
4. Ulrich M, Roewert-Huber J, González S, Rius-Diaz F, Stockfleth E, Kanitakis J (2011) Peritumoral clefting in basal cell carcinoma: correlation of in vivo reflectance confocal microscopy and routine histology. J Cutan Pathol 38:190–195. doi:10.1111/j.1600-0560.2010.01632.x
5. Sankar T, Delaney PM, Ryan RW, Eschbacher J, Abdelwahab M, Nakaji P, Coons SW, Scheck AC, Smith KA, Spetzler RF, Preul MC (2010) Miniaturized handheld confocal microscopy for neurosurgery: results in an experimental glioblastoma model. Neurosurgery 66:410–417. doi:10.1227/01.NEU.0000365772.66324.6F
6. Peyre M, Clermont-Taranchon E, Stemmer-Rachamimov A, Kalamarides M (2013) Miniaturized handheld confocal microscopy identifies focal brain invasion in a mouse model of aggressive meningioma. Brain Pathol 23(4):371–377. doi:10.1111/bpa.12039
7. Snuderl M, Wirth D, Sheth SA, Bourne SK, Kwon CS, Ancukiewicz M, Curry WT, Frosch MP, Yaroslavsky AN (2013) Dye-enhanced multimodal confocal imaging as a novel approach to intraoperative diagnosis of brain tumors. Brain Pathol 23:73–81. doi:10.1111/j.1750-3639.2012.00626.x
8. Eschbacher J, Martirosyan NL, Nakaji P, Sanai N, Preul MC, Smith KA, Coons SW, Spetzler RF (2012) In vivo intraoperative confocal microscopy for real-time histopathological imaging of brain tumors. J Neurosurg 116:854–860. doi:10.3171/2011.12.JNS11696
9. Ragazzi M, Piana S, Longo C, Castagnetti F, Foroni M, Ferrari G, Gardini G, Pellacani G (2014) Fluorescence confocal microscopy for pathologists. Mod Pathol 27:460–471. doi:10.1038/modpathol.2013.158
10. Wang D, Chen Y, Leigh SY, Haeberle H, Contag CH, Liu JTC (2012) Microscopic delineation of medulloblastoma margins in a transgenic mouse model using a topically applied VEGFR-1 probe. Transl Oncol. 5:408–414
11. Bell WC, Sexton KC, Grizzle WE (2010) Organizational issues in providing high-quality human tissues and clinical information for the support of biomedical research. Methods Mol Biol 576:1–30. doi:10.1007/978-1-59745-545-9_1

9- Imagerie dermatologique de la répartition du tissu adipeux de l'obèse

Il s'agit d'une évaluation que l'on pourrait considérer comme à la fois très grossière de la peau et très éloignée du sujet de la thèse et pourtant nous restons parfaitement dans son sujet à savoir le caractère multi-échelle de l'imagerie de la peau.
En effet l'accumulation de graisse dans l'hypoderme des malades obèses en est, un des éléments caractéristiques, mais volontiers considéré comme sans grand intérêt en soit par le dermatologue qui est toutefois amené à en prendre en charge certaines conséquence de cette obésité : intertrigo des grands plis, phénomène de Koebner caractérisant l'exacerbation de certaines dermatoses dans les grands plis : psoriasis , folliculites, mycoses …..

Dans le cadre mon activité clinique et de recherche au sein de l'équipe du SNA Epis je suis amené à prendre en charge des malades atteints d'affections dermatologiques et obèses. Or la perte de poids de ces patients est caractérisée par une variation pondérale. Toutefois cette mesure n'est pas caractéristique d'une perte de tissus graisseux.

D'où l'idée de calculer la masse volumique du patient au cours du temps pour évaluer la perte de masse grasse en utilisant pour mesurer le volume du patient un système d'imagerie 3D : une caméra qui filme a totalité du corps

OBES SURG (2016) 26:1940–1941
DOI 10.1007/s11695-016-2230-0

LETTER TO THE EDITOR

Objective Non-irradiant Imaging of Fat Distribution: New Essential Tools for the Bariatric Surgery?

Claire Boutet[1] · Jean-Claude Barthelemy[2] · Olivier Tiffet[3] · Jean-Luc Perrot[4] · Radwan Kassir[2,3]

Published online: 2 June 2016

Evaluation of body fat is essential in the pre-surgical assessment of bariatric surgery This assessment can be done by using the body mass index (BMI) or better by using the body fat index (BFI) (total body fat/squared height), the obesity parameter most strongly associated with a decline in autonomic nervous system activity [1]. Visceral and subcutaneous fat can be distinguished with an automatic segmentation technique using preoperative computed tomography of the abdomen and pelvis [2] though bariatric surgery teams do not use this preoperative scan, whose principal disadvantage is to be irradiant.

The instantaneous full 3D raster stereography digitizer Orten, however old [3], makes it possible to obtain a three-dimensional (3D) image of the shape of the patient. Already used in the evaluations of scoliosis [4], this technique has an important potential in the field of the bariatric surgery. It is characterized by being non-irradiant because of the projection of structured light (fringes), as a result of light projectors coupled with cameras within the sensor 3D. Acquisition time is approximately 2 s, and the reconstructed 3D shape of the patient is obtained after 2 min of automated processing by the software. An example of an obtained image is presented in Fig. 1. Because of its extremely fast, non-invasive, non-irradiant and completely automatic technique, it is possible to objectively evaluate the fat distribution as either android, with a metabolic profile, or gynoïde, with an aesthetic profile.

We started a prospective study to evaluate the technique's role in the follow-up for the quantification of lost body volume, the evaluation of the homogeneity of lost volume, the determination of the zones having the most important variation and the evaluation of the kinetics of this variation, with repeated measurements. A heterogeneous distribution of body fat loss, which is not possible to objectively determine using only clinical examination, could explain the persistent painful symptomatology among some patients of bariatric surgery. The subjective measurement of waist circumference currently remains a limiting clinical factor given that this measurement is part of the criteria for metabolic syndrome. This technique, the instantaneous full 3D raster stereography digitizer Orten, would allow an objective measurement of the waist circumference and would thus also have a role in the diagnosis of metabolic syndrome, an essential component in the pre-surgical assessment of bariatric surgery.

Having these objective elements, the clinician would be less prone to making an incorrect surgical indication than if he were to make an indication using only waist circumference and BMI. The establishment of a new score, based on the combination of the BMI, the meta-

✉ Radwan Kassir
eRadwankassir42@hotmail.Fr

1 Department of Radiology, CHU Hospital, Jean Monnet University, Saint Étienne, France

2 Laboratory of Autonomic Nervous System Activity, EA407, CHU Hospital, Jean Monnet University, Saint Étienne, France

3 Department of General Surgery, CHU Hospital, Jean Monnet University, Saint Étienne, France

4 Department of Dermatology, CHU Hospital, Jean Monnet University, Saint Étienne, France

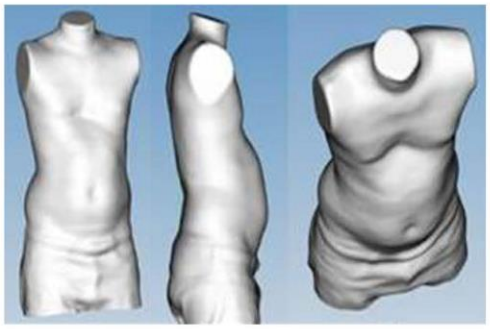

Fig. 1 Example of 3D shapes scanned by Orten 3D solution

bolic syndrome and the objective fat distribution, seems increasingly essential for an optimal evaluation of the obese patients.

Compliance with Ethical Standards

Conflict of interest The authors declare that they have no conflicts of interests.

A Statement of Informed Consent Informed consent was obtained from all individual participants included in the study.

A Statement of Human and Animal Rights Informed consent was obtained from all individual participants included in the study.

References

1. Assoumou HG, Bertholon F, Barthélémy JC, et al. Alteration of baroreflex sensitivity in the elderly: the relationship with metabolic syndrome components. Int J Cardiol. 2012;155(2):333–5.
2. Boutet C and Kassir R. Sleeve gastrectomy and Roux-en-Y gastric bypass lead to comparable changes in body composition after adjustment for initial body mass index. Obes Surg. Forthcoming 2016.
3. Sciandra J, de Mauroy JC, Rolet G, et al. Accurate and fast non-contact 3D acquisition of the whole trunk. In: D'Amico M, Merolli A, Santambrogio GC, editors. Three-dimensional analysis of spinal deformities. Amsterdam, Oxford, Washington DC: Ios Press; 1995. p. 81–5.
4. de Mauroy JC, Lecante C, Barral F, et al. Prospective study and new concepts based on scoliosis detorsion of the first 225 early in-brace radiological results with the new Lyon brace: ARTbrace. Scoliosis. 2014;9:19.

10. Varia
10.1 In vivo reflectance confocal microscopy in dermatology: a proposal concerning French terminology

Annales de dermatologie et de v n r ologie (2013) 140, 678–686

Disponible en ligne sur SciVerse ScienceDirect www.sciencedirect.com

Elsevier Masson France EM|consulte www.em-consulte.com

M MOIRE ORIGINAL

La microscopie confocale par r flectance *in vivo* en dermatologie : proposition de terminologie en langue française

In vivo reflectance confocal microscopy in dermatology: A proposal concerning French terminology

J. Kanitakis[a,*], P. Bahadoran[b], R. Braun[c], S. Debarbieux[d], B. Labeille[d], J.-L. Perrot[e], P. Vabres[f], au nom du Groupe d'Imagerie Cutan e Non Invasive de la Soci t française de dermatologie

[a] *Clinique dermatologique, groupement hospitalier Ed.-Herriot, CHU de Lyon, 5, place d'Arsonval, 69437 Lyon cedex 03, France*
[b] *Clinique dermatologique, centre de recherche clinique (CRC), h pital L'Archet, CHU de Nice, 151, route Saint-Antoine-Ginestiere, 06202 Nice cedex 3, France*
[c] *Clinique dermatologique, h pital universitaire de Zurich, R mistrasse 100, 8091 Zurich, Suisse*
[d] *Clinique dermatologique, centre hospitalier Lyon-Sud, CHU de Lyon, 165, chemin du Grand-Revoyet, 69495 Pierre-B nite, France*
[e] *Clinique dermatologique, h pital Nord, CHU de Saint- tienne, 42055 Saint- tienne cedex 2, France*
[f] *Clinique dermatologique, h pital du Bocage, CHU de Bourgogne, 2, boulevard Mal-de-Lattre-de-Tassigny, 21000 Dijon, France*

Reçu le 6 août 2012 ; accept le 1er juillet 2013
Disponible sur Internet le 26 septembre 2013

MOTS CL S
Microscopie confocale ;
Imagerie non invasive ;

R sum

Introduction. — La microscopie confocale par r flectance (« Reflectance Confocal Microscopy ») (MCR) est une technique r cente d'imagerie cutan e non invasive permettant d'examiner la peau *in vivo* en temps r el. Alors qu'il existe d j une litt rature abondante en langue anglaise concernant la MCR, il n'existe ce jour pas de terminologie officielle en langue française, malgr le nombre croissant de dermatologues francophones pratiquant cette nouvelle technique d'imagerie. Le but de ce travail tait de proposer une terminologie en langue française

* Auteur correspondant.
Adresses e-mail : jean.kanitakis@univ-lyon1.fr, jean.kanitakis@chu-lyon.fr (J. Kanitakis).

0151-9638/$ — see front matter
http://dx.doi.org/10.1016/j.annder.2013.07.020

Dermatologie ;
Terminologie ;
Français

adapt e la MCR, pour permettre aux dermatologues francophones pratiquant cette technique de communiquer dans un langage pr cis et homog ne.
M thodes. — Un groupe de dermatologues francophones ayant une bonne exp rience de la MCR, membres du groupe Imagerie Cutan e Non invasive (ICNI) de la Soci t fran aise de dermatologie (SFD), s'est attel proposer des termes fran ais applicables la MCR. Chaque membre du groupe a pris en charge un paragraphe particulier. Des changes par courrier lectronique ont eu lieu, puis la terminologie finalis e lors d'une r union des membres du groupe Paris en juin 2012.
R sultats. — Des termes d crivant des aspects de la peau normale et pathologique tudi e par MCR ont t propos s. Certains d'entre eux existaient d j car utilis s en histopathologie classique ; d'autres sp cifiques la MCR ont t cr s ou adapt s de l'anglais.
Conclusion. — Cette terminologie permettra aux dermatologues francophones pratiquant la MCR de communiquer leurs observations dans un langage homog ne. Elle pourra tre enrichie dans l'avenir par l'introduction de termes suppl mentaires d crivant de nouveaux aspects de la peau normale et surtout pathologique.

KEYWORDS
Reflectance confocal microscopy;
Non-invasive imaging;
Dermatology;
Terminology;
French

Summary
Background. — Reflectance confocal microscopy (RCM) is a recently introduced non-invasive imaging technique allowing real-time examination of the skin *in vivo*. Whereas a substantial literature concerning RCM exists in English, so far there is no official terminology in French, despite the fact that an ever-growing number of French-speaking dermatologists now use this new imaging technique. The aim of the present study is to propose a French terminology for RCM in order to allow French-speaking dermatologists to communicate in a precise and homogeneous language on this topic.
Methods. — A group of French-speaking dermatologists with solid experience of RCM, members of the Non-invasive Cutaneous Imaging group of the French Society of Dermatology, endeavored to suggest terms in French concerning RCM. Each group member dealt with a specific paragraph. The members exchanged comments via email and the terminology was finalized during a meeting of the group members in Paris in June 2012.
Results. — Descriptive terms referring to the RCM aspects of normal and diseased skin were proposed. Some of these already existed, being used in routine dermatopathology, while other specific terms were created or adapted from the English terminology.
Conclusion. — This terminology will allow French-speaking dermatologists using RCM to communicate their findings in a homogeneous language. It may be enriched in the future by the introduction of additional terms describing new aspects of both normal and, especially, diseased skin.

La microscopie confocale par r flectance (« Reflectance Confocal Microscopy » - MCR) est une technique relativement r cente d'imagerie tissulaire, permettant d'examiner des tissus, y compris la peau, *in vivo* en temps r el et de façon non invasive. Elle produit des coupes optiques d'une paisseur inf rieure 5 µm, parall les la surface du tissu (horizontales ou « en face »), avec un grossissement et une r solution (horizontale < 1,25 µm, verticale < 5 µm) proches de ceux obtenus par le microscope optique sur des coupes histologiques classiques. Elle fournit donc des informations sur des d tails architecturaux, cellulaires et nucl aires. Les images, qui apparaissent en niveaux de gris, sont obtenues gr ce la r flexion d'un rayon laser (d'une longueur d'onde de 830 nm pour l'appareil le plus couramment utilis) par les diff rentes mol cules contenues dans la peau — notamment m lanine, k ratine et collag ne (Fig. 1). Les images individuelles mesurent 0,5 × 0,5 mm et peuvent tre combin es entre elles sur un plan vertical ou horizontal, pour former des images en mosa que de plus grande taille (4 × 4 mm).

De par ses caract ristiques, la MCR se situe entre l'examen dermatoscopique et l'examen histologique classique. En effet, son caract re totalement non invasif, donc indolore, la possibilit de r p ter l'examen sur une m me zone cutan e de façon illimit e et l'orientation horizontale des images obtenues la rapprochent de la dermatoscopie ; en revanche, le grossissement et la r solution des images la rapprochent de l'examen histologique classique. Cependant, en raison de la dispersion des photons dans le tissu, l'examen en MCR n'est possible que pour la partie superficielle de la peau, jusqu' une profondeur d'environ 250 µm, correspondant l' piderme et au derme papillaire.

Le principe de la MCR a t initialement d velopp en 1955 par Marvin Minsky, de l'universit de Harvard (tats-Unis). Ce n'est toutefois qu' la fin des ann es 1990 que la peau a commenc tre examin e de façon syst matique avec des appareils plus perfectionn s utilisant ce principe. Des appareils de MCR commercialement

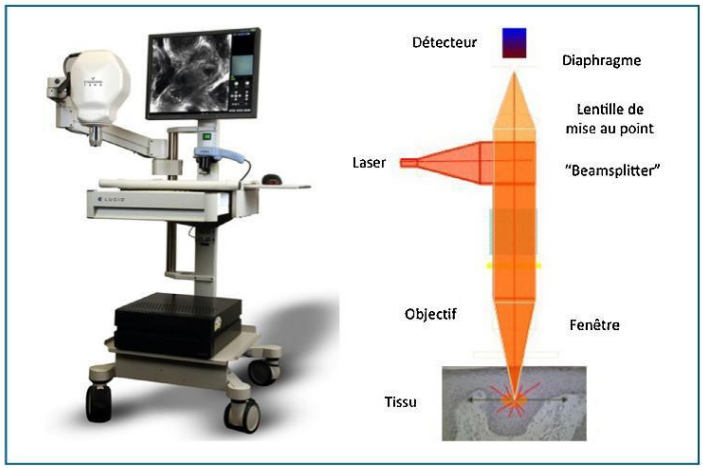

Figure 1. gauche : microscope confocal par r flectance : appareil couramment utilis pour l'examen *in vivo* de la peau. droite : vue sch matique et principe de fonctionnement du microscope confocal par r flectance.

disponibles quipent actuellement plusieurs tablissements dermatologiques, publics ou priv s, y compris en France et dans d'autres pays francophones. L'usage de la technique s' tant rapidement r pandu, la litt rature anglo-saxonne compte d j plusieurs dizaines d'articles originaux et revues g n rales consacr s aux applications diagnostiques de la MCR en dermatologie [1—8], ainsi que deux pr cis consacr s aux corr lations des aspects cliniques, histologiques et en MCR de plusieurs dermatoses inflammatoires et tumorales

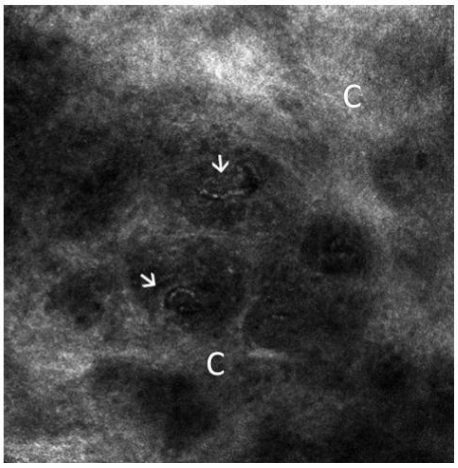

Figure 2. Trousseaux de collag ne (c) dans le derme papillaire. Les vaisseaux capillaires sanguins sont galement visibles sous forme de structures sombres allong es (canaliculaires) contenant des leucocytes (→).

[9,10]. Malgr un certain parall lisme avec l'examen histologique classique, les images de la peau obtenues par MCR ont des caract ristiques qui leurs sont propres. Il existe une terminologie sp cifique la MCR en langue anglaise, propos e par un groupe d'experts anglophones et ayant fait l'objet d'une publication [11]. Comme il n'existait pas de publication quivalente dans la litt rature française, le but du pr sent travail a t d' laborer une terminologie française adapt e la description des aspects de la peau normale et pathologique en MCR. En effet, l'utilisation de cette technique s' tendant progressivement, il est important d'utiliser une terminologie homog ne et consensuelle, dans le but de faciliter l'interpr tation des images et la communication entre les dermatologues.

Cet article est le fruit d'un travail collaboratif auquel ont particip plusieurs dermatologues francophones pratiquant la MCR, et est pr sent au nom d'un groupe th matique nouvellement constitu de la Soci t française de dermatologie, intitul « Imagerie Cutan e Non Invasive ». La terminologie propos e pourra tre enrichie dans l'avenir par la description de nouvelles alt rations qui seront observ es dans des dermatoses encore peu ou pas tudi es.

Termes d crivant les caract ristiques techniques des images

Niveau de l'image

C'est la profondeur anatomique du niveau horizontal (« en face ») de la peau visualis e par la MCR. Il peut tre galement d fini comme la profondeur (exprim e en microm tres) sous la couche corn e. Si des couches anatomiques diff rentes sont visibles sur la m me image, la coupe optique est qualifi e d'« oblique », repr sentant un plan

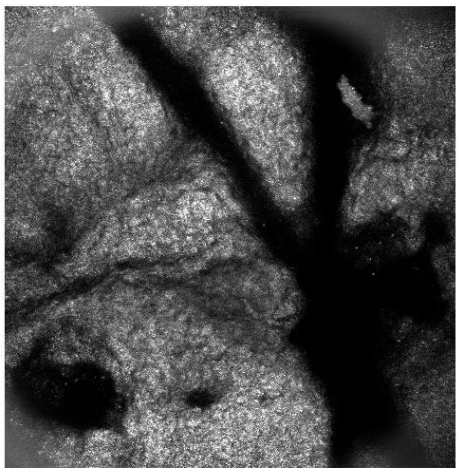

Figure 3. Couche corn e : la couche la plus superficielle de la peau appara t brillante (refl tante). Les corn ocytes sont agenc s en lots s par s par des d pressions sombres (dermatoglyphes).

non parall le la couche corn e. Des coupes obliques sont souvent produites lors de l'obtention d'une grande image mosa que d'une l sion en relief.

Qualit de l'image

La qualit de l'image est d termin e subjectivement par la quantit des d tails qu'elle contient. Elle peut tre bonne, moyenne ou faible.

Qualit bonne

Qualit bonne (bon contraste et bonne r solution) : les structures visualis es ont des contours nets et sont bien contrast es par rapport au tissu adjacent.

Qualit moyenne

Qualit moyenne (contraste et r solution moyens) : les contours des structures sont mal d finis (faible r solution) mais le contraste avec le tissu voisin est bon ou bien la structure est nette (haute r solution) mais peu contrast e.

Qualit faible

Qualit faible (contraste ou r solution faible, pr sence d'artefacts inacceptables) : les structures individuelles ne sont pas visibles dans l'image ; celle-ci peut tre trop sombre (ou claire), ou obscurcie par des artefacts (poils, bulles d'air, maquillage, cran solaire...).

Contraste de l'image

Il d pend :

- du niveau de l'image : la quantit de lumi re p n trant dans les niveaux les plus profonds de la peau est moindre, la r solution diminue et les structures apparaissent plus sombres et moins nettes ;
- de la saturation de l'image : le niveau de clart ou brillance (brightness) peut tre modifi en temps r el en ajustant l'intensit du rayon laser. Les images trop claires (sur- clair es ou satur es) apparaissent granuleuses et leur contraste est moindre. Les images trop sombres (sous- clair es) ont aussi un contraste faible ;
- de la nature de la l sion : les l sions pigment es sont g n ralement plus contrast es que les l sions non pigment es puisque la m lanine est fortement refl tante (reflective, refractile). Les autres mol cules refl tantes sont la k ratine et le collag ne.

R solution de l'image

C'est la distance minimale entre deux structures adjacentes que l'on peut distinguer dans une image. Les appareils actuels de MCR offrent une r solution horizontale de l'ordre de 1 µm (permettant de distinguer les noyaux).

Termes utilis s pour la description de la peau normale (par ordre alphab tique)

Collag ne

Structures ou faisceaux fibrillaires moyennement refl tants, allong s, d pourvus de structures cellulaires, de noyaux ou de mouvements visibles, dispos s c te- -c te dans tout le derme (Fig. 2). Le collag ne est habituellement r parti sous forme de spirales ou d'anneaux dans le derme papillaire, et sous forme de trousseaux parall les dans le derme r ticulaire. Les diam tres des fibres et des trousseaux de collag ne sont respectivement de 1 5 µm et de 5 25 µm.

Couches pidermiques

Couche corn e

La couche la plus superficielle de la peau pr sente une r flectance plus grande que les autres couches pidermiques cause de la r flexion de la lumi re par la surface cutan e (Fig. 3).

Couche granuleuse

Situ e 15 20 µm sous la surface, elle contient des k ratinocytes cytoplasme granuleux refl tant et noyaux ovalaires sombres ; leur cytoplasme contient des structures granuleuses de 0,5 1 µm.

Couche malpighienne (corps muqueux)

Situ e 20 100 µm sous la couche corn e, elle est compos e de k ratinocytes cytoplasme refl tant et noyau sombre, arrondi ou ovalaire.

Couche basale

Couche cellulaire unique situ e 50 100 µm sous la couche corn e, visible sous forme de cellules refl tantes group es en agr gats, ou dispos es selon un patron circulaire autour

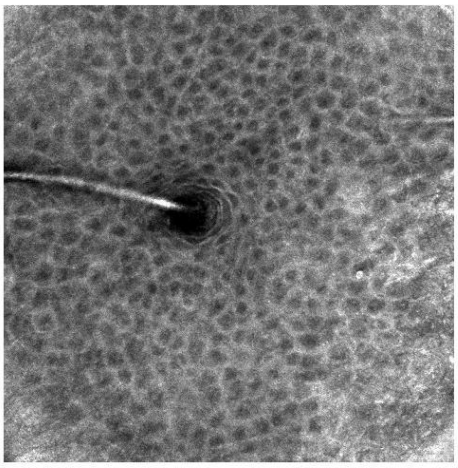

Figure 4. Aspect en nid d'abeilles de la couche malpighienne de l' piderme. Un ostium folliculaire et la tige pilaire qui en merge sont galement visibles.

des papilles dermiques sombres, formant les « anneaux papillaires dermiques » (dermal papillary rings).

Poil

Follicules pileux

Structure caract ris e par des cellules de taille variable selon un patron ordonn correspondant au degr de diff renciation cellulaire, allant de cellules basales petites (ovalaires ou polygonales) des cellules centrales plus volumineuses et aplaties. Le canal et la tige pilaire sont souvent visibles (Fig. 4).

Tige pilaire

Structure allong e cylindrique ou tubulaire, fortement et uniform ment refl tante, sans structure cellulaire centrale, bien que des structures cellulaires puissent tre observ es en p riph rie. Elle merge habituellement d'une zone circulaire sombre (ostium folliculaire) (Fig. 4).

Jonction dermo- pidermique (JDE)

Visible 55 65 µm sous la couche corn e, en fonction du site observ , elle est habituellement reconnue par la pr - sence de cavit s sombres dans l' piderme, correspondant l'ouverture de papilles dermiques, et galement par le flux capillaire sanguin lors de l'examen en temps r el. La JDE est moins bien visible lorsqu'elle est aplatie (par exemple : sur le visage d'une peau s nile).

Nid d'abeilles (aspect en) (honeycomb pattern)

Terme d crivant l'aspect de l' piderme normal au niveau des couches malpighienne et granuleuse, o les contours nets des cellules forment un maillage r gulier qui ressemble un « nid d'abeilles » (Fig. 4). Les cellules sont polygonales avec un diam tre d croissant vers la profondeur.

Plis cutan s (dermatoglyphes)

D pressions lin aires non refl tantes (sombres) s parant des lots de corn ocytes (Fig. 3).

Vaisseaux sanguins

Ils sont bien visualis s pendant l'examen en temps r el comme des structures dermiques plus sombres que le derme voisin, contenant des cellules en mouvement (leucocytes) (Fig. 2). Leur contour (outline) peut tre :

- canaliculaire (allong) : signifie que le vaisseau est orient « en face » (parall lement la surface cutan e). Les vaisseaux canaliculaires peuvent tre rectilignes ou sinueux ;
- rond : signifie que le vaisseau est orient perpendiculairement au plan de visualisation (par exemple, les segments ascendants ou descendants des anses capillaires dans les papilles dermiques).

Termes utilis s pour la description des caract res architecturaux et structurels des l sions m lanocytaires

Couches superficielles (suprabasales) de l' piderme

D limitation (demarcation) des cellules pidermiques (visible, peu ou pas visible)

Ce terme d crit la pr sence ou l'absence de l'aspect normal « en nid d'abeilles » de l' piderme suprabasal ; les limites cellulaires peuvent tre visibles, peu visibles ou invisibles (conservation ou perte partielle ou totale, respectivement, de l'aspect en nid d'abeilles).

Diss mination pag to de (pagetoid spread)

Pr sence de cellules rondes ou dendritiques noyau sombre et cytoplasme refl tant, souvent deux fois plus volumineux que les k ratinocytes normaux, dans les couches pidermiques sup rieures (Fig. 5).

Kystes corn s

Structures encapsul es refl tantes dans l' piderme superficiel.

Granules

Petites particules refl tantes non associ es un type cellulaire particulier.

Couche basale de l' piderme

Patron (pattern) des cellules basales

Terme d crivant le patron cr par les cellules refl tantes dans l'assise basale des l sions m lanocytaires.

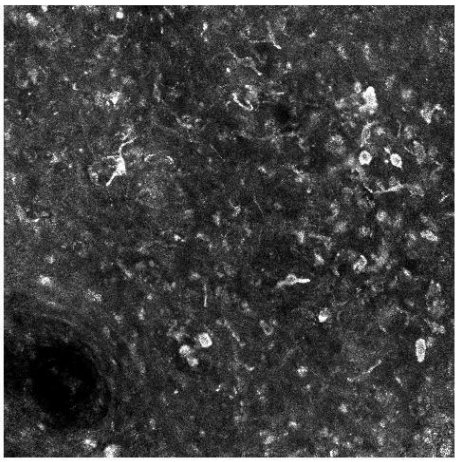

Figure 5. Cellules pag to des: cellules refl tantes, rondes ou dendritiques, observ es dans les couches sup rieures de l' piderme (m lanome).

Monomorphisme

Les cellules basales sont dites monomorphes lorsqu'il n'existe pas de variations individuelles de leur r flectance ni de leur contour. Les cellules basales monomorphes sont souvent dispos es selon un patron « pavimenteux » (Fig. 6) ou autour des papilles dermiques (« papilles margin es » — edged papillae) (Fig. 7).

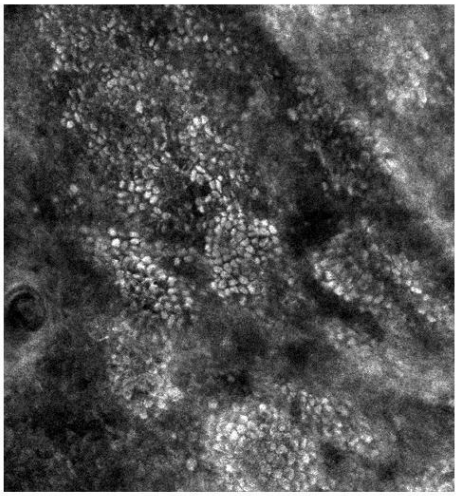

Figure 6. Cellules basales brillantes dispos es selon un patron pavimenteux.

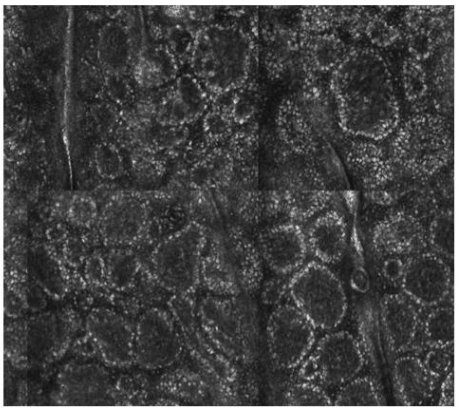

Figure 7. Papilles dermiques margin es: papilles arrondies ou ovalaires bien d limit es par des cellules basales refl tantes.

Patron pavimenteux (cobblestone pattern)

Patron constitu d'agr gats, dans l' piderme, de petites cellules polygonales cytoplasme clair (correspondant des k ratinocytes normalement pigment s) s par es par un contour moins refl tant (Fig. 6).

Disposition

D crite lorsque les cellules basales ne sont pas dispos es de mani re monomorphe:

- agr g e: ensemble de cellules basales refl tantes qui tendent se regrouper en amas;
- confluente: cellules basales refl tantes qui rendent confluer, formant une ligne continue entourant la papille dermique;
- dispers e: plusieurs cellules basales refl tantes isol es sans patron particulier.

Jonction dermo- pidermique et derme superficiel

Caract ristiques des papilles dermiques (PD)

Aspect (r gulier/irr gulier)

Terme utilis pour d crire le diam tre et la forme (allong e, circulaire, polygonale) des PD. Lorsque la taille et la forme des PD sont similaires, l'aspect est dit r gulier. La distribution des PD peut tre homog ne ou h t rog ne.

Contours (margin s/non margin s)

Les « papilles margin es » (edged papillae) pr sentent des contours bien limit s, habituellement constitu s de cellules basales refl tantes (Fig. 7); les papilles « non-margin es » (non-edged papillae) sont celles d pourvues de limites nettes.

Disposition (homog ne/h t rog ne)

La disposition est dite homog ne lorsque les PD sont dispos es de façon sym trique/uniforme.

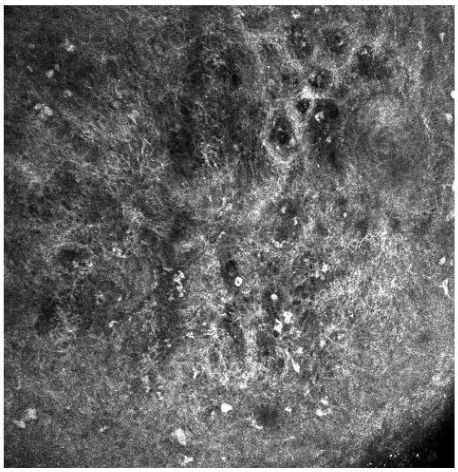

Figure 8. Jonction dermo- pidermique d sorganis e. Pr sence de cellules atypiques dans l' piderme (m lanome *in situ*).

Taille
Terme utilis pour d crire le diam tre des PD. La taille peut tre appr ci e par rapport la peau normale adjacente, ou bien exprim e en μm. Elle peut tre petite (< 100 μm), moyenne (100—200 μm) ou grande (> 200 μm).

D sorganisation (disarray) de la JDE

Elle peut tre :
- l g re : perte partielle de l'architecture normale de la JDE (en termes d'aspect, contours, distribution, taille des PD) ;
- mod r e : perte partielle ou totale, selon les endroits, de l'architecture normale de la JDE ;
- prononc e : perte totale de l'architecture normale de la JDE (Fig. 8).

Th ques (nests, clusters)

Formations arrondies ou ovalaires refl tantes (brillantes), bien limit es, constitu es d'amas de cellules qui sont souvent de grande taille, de r flectance variable.

Localisation

Th ques jonctionnelles
Th ques en contact avec la couche basale de l' piderme, p n trant dans les PD.

Th ques dermiques
Th ques situ es dans les PD/derme superficiel, sans connexion avec la couche basale de l' piderme (Fig. 9).

R partition

Focale en amas (aggregated)
Th ques (amas) pr sentes dans certaines r gions de la l sion seulement.

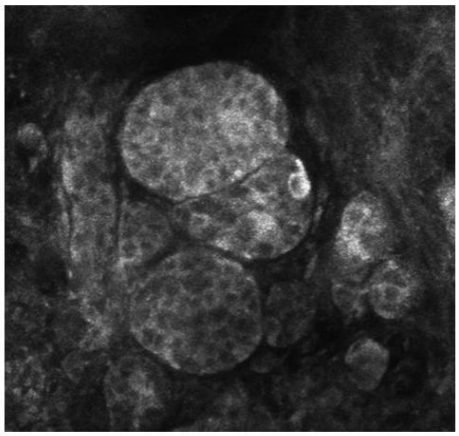

Figure 9. Th ques de cellules næviques dermiques monomorphes.

Diffuse
Nombreuses th ques au sein de la l sion.

Taille

Petite
Grand axe < 250 μm.

Moyenne
Grand axe entre 250 et 500 μm.

Grande
Grand axe > 500 μm.

Types

Th ques denses
Amas compacts form s de grandes cellules polygonales, noyau peu refl tant (sombre), cytoplasme finement granuleux, r alisant des structures poly driques.

Th ques l ches
Structures arrondies non refl tantes (sombres) bien limit es, contenant des cellules isol es, rondes ou ovales noyau sombre et cytoplasme refl tant, formant parfois une configuration polylob e.

Th ques c r briformes
Amas form s par des structures confluentes polygonales ou allong es, peu refl tantes (sombres), s par es par un halo peu refl tant, leur conf rant un aspect c r briforme.

Composant dermique

Terme g n ral d crivant toute structure refl tante (brillante) pr sente dans le derme.

Termes utilis s pour la description des aspects cytologiques en MCR

Atypies cellulaires

Pr sence de cellules dont l'aspect (noyau et/ou cytoplasme) diff re des cellules normales. Ce terme ne pr sage pas du caract re inflammatoire, r actionnel ou tumoral de ces anomalies (Fig. 8). Les atypies cellulaires peuvent tre distingu es en :

- l g res : le noyau et/ou le cytoplasme sont l g rement diff rents de ceux des cellules normales ;
- prononc es : le noyau et/ou le cytoplasme sont tr s diff rents des cellules normales. Les atypies sont dites prononc es lorsque les cellules sont volumineuses, ont une forme inhabituelle (par exemple triangulaire, toil e) ou lorsqu'elles ont un noyau volumineux et excentr . La densit des cellules atypiques devrait tre mentionn e (sporadiques/peu nombreuses, ou nombreuses).

Monomorphisme cellulaire

Terme utilis pour d crire des groupes de cellules dont la forme et la taille (y compris celle du noyau) sont similaires.

Pl omorphisme cellulaire

Variations morphologiques (taille, forme, r flectance) des cellules au sein d'une l sion ; elles peuvent varier de l g res prononc es.

R flectance (brillance) (reflectance, brightness)

Les diff rents types cellulaires ont des indices de r flectance (reflectance index) diff rents. Les cellules indice de r flectance lev apparaissent refl tantes (brillantes). La r flectance d'un type cellulaire peut varier en fonction de son activit m tabolique (par exemple, synth se accrue de m lanine par les m lanocytes) et du phototype.

R flectance lev e

Les cellules sont beaucoup plus brillantes que les cellules correspondantes normales.

R flectance faible

Les cellules apparaissent plus sombres que les cellules normales.

R flectance h t rog ne

Les cellules pr sentent une brillance variable, certaines tant plus brillantes, d'autres moins ou aussi brillantes que les cellules normales.

Forme cellulaire

Silhouette externe de la cellule (contour). Elle peut tre ronde, ovale, fusiforme (cellule allong e aux extr mit s effil es), allong e (terme plus g n ral d signant des cellules non ovales ou non fusiformes), toil e (pr sence de dendrites), triangulaire.

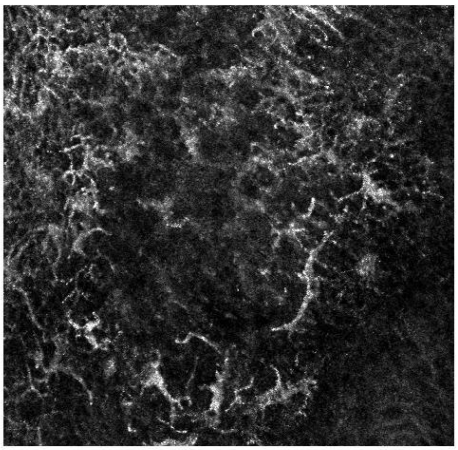

Figure 10. Cellules dendritiques refl tantes intra- pidermiques.

Taille cellulaire

Correspond au plus grand diam tre de la cellule ; elle peut tre qualifi e de sup rieure ou inf rieure par rapport la normale, ou tre exprim e en chiffre absolu (µm).

Taille des k ratinocytes

Couche corn e = 10—30 µm ; couche granuleuse : 25—35 µm ; couche malpighienne : 15—25 µm ; couche basale : 7—12 µm.

Taille des m lanocytes

La taille des m lanocytes normaux n'a pas t pr cis ment mesur e par MCR ; elle est estim e similaire celle des k ratinocytes basaux.

Dendrite

Structure allong e, ramifi e, manant du corps cellulaire, habituellement pr sente sur les m lanocytes et les cellules de Langerhans (Fig. 10). Les dimensions des dendrites (longueur, paisseur) peuvent tre compar es la taille du corps cellulaire.

Cellules dermiques

Cellule nucl e

Cellule brillante isol e, arrondie ou ovalaire, noyau sombre, pr sente dans le derme papillaire.

Dodue-brillante (plump-bright)

Cellule brillante (refl tante) de forme irr guli re, contours flous sans noyau visible, correspondant probablement un m lanophage (Fig. 11).

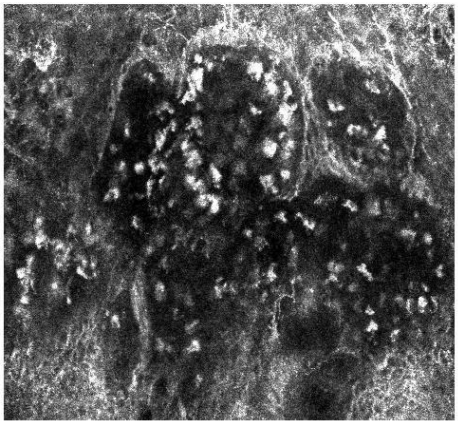

Figure 11. Cellules dodues-rondes refl tantes dermiques (m la-nophages).

Nucl ole

Structure peu apparente spiral e ou en m nisque parfois observ e dans le noyau des k ratinocytes comme un point refl tant au sein du noyau sombre.

Noyau

Zone sombre, g n ralement arrondie, au sein de la cellule.

Position

D finie par la pr sence d'une zone sombre dans la cellule ; peut tre centrale ou excentr e (cette derni re est associ e des cellules atypiques).

Pl omorphisme

Variation de la taille et de la forme du noyau au sein d'une m me population cellulaire.

Cellules pag to des

Cellules rondes ou ovalaires noyau sombre et cytoplasme brillant rond ou ovalaire, volontiers deux fois plus volumineuses que les k ratinocytes normaux, situ es dans les couches suprabasales de l' piderme (Fig. 5). La plupart des cellules pag to des visibles en MCR correspondent des m lanocytes suprabasaux.

Densit

Peut tre faible, moyenne ou lev e (1—3, 4—6 ou > 6 cellules par image de 0,5 × 0,5 mm).

Distribution

Peut tre focale ou diffuse.

Agr gats

Terme utilis pour d crire des cellules pag to des regroup es en amas.

D claration d'int r ts

Les auteurs d clarent ne pas avoir de conflits d'int r ts en relation avec cet article.

R f rences

[1] Ulrich M, Lange-Asschenfeldt S, Gonzalez S. Clinical applicability of in vivo reflectance confocal microscopy in dermatology. G Ital Dermatol Venereol 2012;147:171—8.
[2] Guitera P, Pellacani G, Crotty KA, Scolyer RA, Li LX, Bassoli S, et al. The impact of in vivo reflectance confocal microscopy on the diagnostic accuracy of lentigo maligna and equivocal pigmented and nonpigmented macules of the face. J Invest Dermatol 2010;130:2080—91.
[3] Kang HY, Bahadoran P, Ortonne JP. Reflectance confocal microscopy for pigmentary disorders. Exp Dermatol 2010;19:233—9.
[4] Hofmann-Wellenhof R, Wurm EM, Ahlgrimm-Siess V, Richtig E, Koller S, Smolle J, et al. Reflectance confocal microscopy — state-of-art and research overview. Semin Cutan Med Surg 2009;28:172—9.
[5] Koller S, Gerger A, Ahlgrimm-Siess V, Weger W, Smolle J, Hofmann-Wellenhof R. In vivo reflectance confocal microscopy of erythematosquamous skin diseases. Exp Dermatol 2009;18:536—40.
[6] Calzavara-Pinton P, Longo C, Venturini M, Sala R, Pellacani G. Reflectance confocal microscopy for in vivo skin imaging. Photochem Photobiol 2008;84:1421—30.
[7] Ahlgrimm-Siess V, Koller S, El Shabrawi-Caelen L, Hofmann-Wellenhof R, Kerl H. New diagnostic methods in dermatopathology: in vivo reflectance confocal microscopy. J Dtsch Dermatol Ges 2008;6:591—2.
[8] Gonz lez S, Gilaberte-Calzada Y. In vivo reflectance-mode confocal microscopy in clinical dermatology and cosmetology. Int J Cosmet Sci 2008;30:1—17.
[9] Gonzalez S, Gill M, Halpern A, editors. Reflectance confocal microscopy of cutaneous tumors. London: Informa Healthcare; 2008. p. 275.
[10] Hofmann-Wellenhof R, Pellacani G, Malvehy J, Soyer HP, editors. Reflectance confocal microscopy for skin diseases. Berlin: Springer; 2012. p. 500.
[11] Scope A, Benvenuto-Andrade C, Agero AL, Malvehy J, Puig S, Rajadhyaksha M, et al. In vivo reflectance confocal microscopy imaging of melanocytic skin lesions: consensus terminology glossary and illustrative images. J Am Acad Dermatol 2007;57:644—58.

10.2 Quantification of capillary blood cell flow using reflectance confocal microscopy.

purpose:

In vivo reflectance confocal microscopy (IVCM) is a new tool for skin microcirculation. However, the measure of quantitative blood cell flow (QBCF) has not been standardized. We studied the inter-investigator and the intra-capillary reproducibility of the manual measure of QBCF on IVCM videos and investigated if a software program might help measure QBCF and be sensitive to vascular occlusion tests.

Methods:

The inter-investigator reproducibility of the manual QBCF was evaluated on 107 videos. The intra-capillary reproducibility of QBCF measured manually and by 2 semi-automatic procedures based on Image J software analysis was evaluated on 19 capillaries. One of the semi-automatic methods (peaks of luminous intensity) was also used to measure the QBCF during vascular occlusion tests.

Results:

The manual measure did not show a good interinvestigator reproducibility (Pearson's coefficient <0.5). The 'peaks of luminous intensity' method was found to have a good intra-capillary reproducibility and to be sensitive to vascular occlusion.

Conclusion:

Differently from the manual count, the count of peaks of luminous intensity by Image J software seems to be promising to measure QBCF. The future is to create software allowing for real-time measure of the QBCF based on the peaks of luminous intensity inside the capillaries recorded by IVCM.

Skin Research and Technology 2014; 20: 373–378
Printed in Singapore · All rights reserved
doi: 10.1111/srt.12128

Published by John Wiley & Sons Ltd
Skin Research and Technology

Quantification of capillary blood cell flow using reflectance confocal microscopy

E. Cinotti[1], L. Gergelé[2], J. L. Perrot[1], A. Dominé[2], B. Labeille[1], P. Borelli[3] and F. Cambazard[1]

[1]Department of Dermatology, University Hospital of Saint Etienne, Saint-Etienne, France,
[2]Department of Anesthesia and Intensive Care, University Hospital of Saint Etienne, Saint-Etienne, France and [3]Unit of Statistics, Mathematics and Computer processing of data, University of Genoa, Genoa, Italy

Background/purpose: *In vivo* reflectance confocal microscopy (IVCM) is a new tool for skin microcirculation. However, the measure of quantitative blood cell flow (QBCF) has not been standardized. We studied the inter-investigator and the intra-capillary reproducibility of the manual measure of QBCF on IVCM videos and investigated if a software program might help measure QBCF and be sensitive to vascular occlusion tests.

Methods: The inter-investigator reproducibility of the manual QBCF was evaluated on 107 videos. The intra-capillary reproducibility of QBCF measured manually and by 2 semi-automatic procedures based on Image J software analysis was evaluated on 19 capillaries. One of the semi-automatic methods (peaks of luminous intensity) was also used to measure the QBCF during vascular occlusion tests.

Results: The manual measure did not show a good inter-investigator reproducibility (Pearson's coefficient <0.5). The 'peaks of luminous intensity' method was found to have a good intra-capillary reproducibility and to be sensitive to vascular occlusion.

Conclusion: Differently from the manual count, the count of peaks of luminous intensity by Image J software seems to be promising to measure QBCF. The future is to create software allowing for real-time measure of the QBCF based on the peaks of luminous intensity inside the capillaries recorded by IVCM.

Key words: *in vivo* reflectance confocal microscopy – reflectance – microcirculation – quantitative blood cell flow – Image J – blood cell – capillary – skin

Accepted for publication 4 January 2014

MICROCIRCULATION PLAYS a crucial role in the interaction between blood and tissues, both in physiological and in pathological states. It has a key role in numerous diseases including diabetes, systemic sclerosis, hypertension, sepsis, or multiple organ failure.

Its evaluation is therefore of great potential to obtain information about human physiology and to change treatment strategies (1). However, methods for direct visualization and quantitative assessment of human microcirculation at the bedside are limited.

The German group of Altintas et al. (2–8) has recently suggested evaluating skin microcirculation using *in vivo* reflectance confocal microscopy (IVCM), an emerging non-invasive skin imaging technique, with the advantage of associating quantitative data on blood flow with morphological data on the analyzed tissue. These authors measured the 'Quantitative blood cell flow' (QBCF) by counting blood cells passing through a given capillary recorded by IVCM. However, the team did not describe in detail how they could count the blood cells and if the count was done either manually or by using a dedicated software program.

Our study evaluated 3 methods to calculate the QBCF: (i) the manual count of the blood cells passing inside a capillary, (ii) the number of peaks of luminous intensity in the capillary area (corresponding to bright blood cells) calculated by Image J software, and (3) the average intensity of the capillary area calculated by Image J software.

The inter-investigator reproducibility of the manual count has been evaluated, as well as the intra-capillary reproducibility (reproducibility of the QBCF for different measures repeated on the same capillary) of the 3 methods. Vascular occlusion tests were also performed to evaluate whether a variation in QBCF was detectable by IVCM.

Materials and Methods

In vivo *reflectance confocal microscopy videos*
IVCM videos of the dermal capillaries were recorded by positioning the tip of the confocal microscope on the skin of interdigital spaces of the hand. We chose interdigital spaces because in this area, capillaries are more abundant and superficial than in the rest of the skin. To examine interdigital spaces, we used the *in vivo* confocal microscope with the handheld camera, VivaScope 3000 ® (CALIBER, New York, NY, USA, distributed in Europe by MAVIG GmbH, Monaco, Germany) that has a small tip that allows to reach this body area. To obtain stable videos, the camera had been fixed to a hinged support.

IVCM allows *in vivo* skin investigation up to 300 μm depth on cellular and subcellular levels with a lateral resolution <1.25 μm and a vertical resolution <5.0 μm in the center of the image field. The imaging rate is of 9 frames per second. The single frame field of view is 1000 × 1000 μm in diameter. The system uses 830 nm (near-infrared) laser, without any damage of the observed tissue.

Contrast in confocal imaging occurs by backscattering of a focused laser beam in varying degrees from different structures of the skin tissue. Dermal capillaries can be observed at a depth of about 200 μm as black holes inside dermal papillae that appear as dark areas surrounded by bright circles, corresponding to the epidermal spinous layer (Fig. 1). The capillaries appear in pairs, with an arterial and venous capillary next to another. For our study, we chose only the arterial capillaries, recognizable for their faster flow. Blood cells can be clearly observed in real time circulating through the lumina of dermal capillaries as bright roundish spots against a black background (Fig. 2).

Different blood cells are difficult to be distinguished by confocal microscopy as both red and white blood cells are refractive and have similar diameter of around 5–10 μm (Fig. 3). However, as red blood cells are more abundant with a ratio of about 1 white blood cell to every 600–700 red blood cells(9), vessel flow mainly corresponds to red blood cells.

We recorded 20 videos of 20 s in four different interdigital spaces (five videos per site registered one following the other) of a 28-year-old healthy non-smoker subject, and for each video,

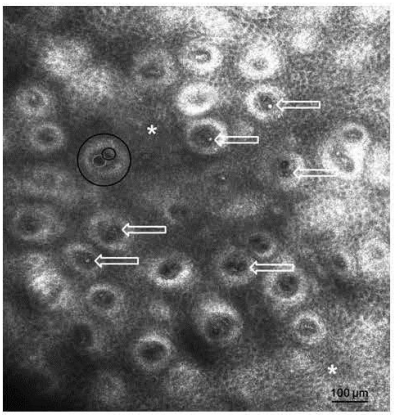

Fig. 1. In vivo confocal microscopy aspect of dermal capillaries. Dermal capillaries (blue and red circles) appear at a depth of 200 μm as black holes inside dermal papillae (black arrow). Blood cells can be clearly observed through the lumina of dermal capillaries as bright roundish spots against a black background (yellow arrows). Dermal papillae are interspersed within the epidermis (yellow asterisks).

we chose the 4–7 best-defined capillaries to be observed. Twenty-two capillaries and a total of 97 measures (being the same capillary analyzed in up to 5 different videos) were evaluated. Moreover, we recorded 10 videos of 10 capillaries from interdigital spaces of other 10 adult patients. The videos were recorded in basal condition, in a room at 23°C.

Blood cell count
QBCF was evaluated in all the measures performed in basal condition by three methods as (i) the manual count of the number of roundish white or light gray bodies (corresponding to blood cells) passing inside a capillary, performed in blind by four different doctors, (2) the number of peaks of luminous intensity in the capillary area (corresponding to bright blood cells) calculated by Image J software, and (3) the average intensity of the capillary area calculated by Image J software.

First blood cell count method: manual count of the blood cells
The quantification of QBCF was carried out manually and in blind by four doctors, who counted the number of circulating cells in the capillaries in the digitally recorded videos of 20 s. As it is impossible for the human eye to count the number of circulating cells directly

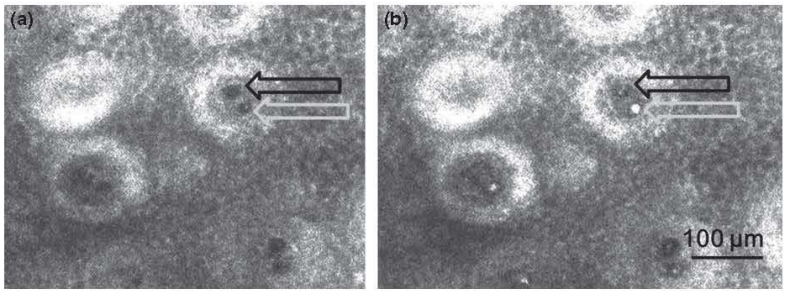

Fig. 2. In vivo confocal microscopy aspect of the blood cell flow inside dermal capillaries. The same arterial (red arrow) and venous (blue arrow) capillaries have been registered before (a) and during (b) the passage of blood cells in their lumina.

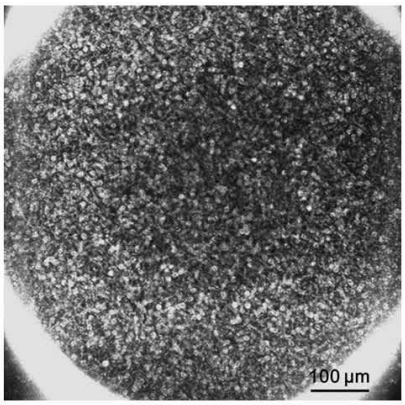

Fig. 3. Ex vivo confocal microscopy examination of a blood smear. Blood cells are refractive under reflectance confocal microscopy and have a diameter of around 5–10 µm.

from real-time videos, Image J software (freeware downloaded at http://rsbweb.nih.gov/ij/) was used to decompose the video into images (180 images for video) and to wind on these images at the speed of one per second.

All doctors used the same color monitor, with dimensions of 19" with 1280 × 1024 pixels. QBCF was counted as the number of roundish white or light gray body (corresponding to blood cells) inside the capillary alternated with dark images corresponding to the space between subsequent cells.

To standardize the count among the various operators, we established two conventions: (1) the first cell that was eventually present inside the vessel at the beginning of the video was not counted; (2) only blood cells preceded by a decrease in light intensity within the capillary, indicating the separation between two successive cells, were counted. Using the latter convention, a hyper-reflective image persisting over time inside a capillary was counted for only one blood cell, even if it could also correspond to a continuous flow of cells passing through the capillary without interruption.

Second blood cell count method: counts of the peaks of luminous intensity

As blood cells appear as bright objects on a dark background under IVCM, the analysis of the pixel intensity of the images corresponding to the capillary areas can measure blood cells as peaks of reflectance intensity.

Using the Image J software, we obtained the average intensity of each capillary area in each image composing the video by scanning the selection of a capillary through the Z Plot Profile command. These data were exported to Microsoft Excel Program, and the number of intensity peaks was calculated as the number of intensity values (x) that satisfied the conditions $x > x - 1$ and $x < x + 1$.

Third blood cell count method: average luminous intensity

Blood cells passing in the capillaries were measured as the average pixel intensity of the area of a single capillary in the video, each pixel representing a perfusion value. This average pixel intensity of a capillary in the video was calculated as average of the mean pixel intensity per image composing the video.

Vascular occlusion tests

A transient ischemia by arterial occlusion with a cuff placed around the arm for 2 min was induced and the QBCF was measured in basal condition before ischemia and after ischemia (6 min after removing the cuff) in 15 capillaries of one healthy subject. QBCF was measured as

counts of the peaks of luminous intensity in videos of 20 s.

Statistical analysis

We evaluated the inter-investigator correlation of the blood cell manual count on the 97 measures performed on the first subjects and on the 10 measures performed on the other 10 subjects using the Pearson's coefficient (ρ). The intra-capillary reproducibility of each of the three methods (manual count, counts of the peaks of luminous intensity, average luminous intensity) was assessed measuring the variance of the blood cell count in 93 videos of 19 capillaries (five videos for 17 capillaries and four videos for two capillaries). QBCF in basal condition before ischemia and 6 min after ischemia was compared by Student's *t*-test.

Results

On the 97 observations from the first 28-year-old subject, the four different operators counted an average of respectively 36.07 (standard deviation 8.15), 38.55 (standard deviation 7.70), 34.33 (standard deviation 9.68), and 29 (standard deviation 4.49) blood cells per capillary per video. The peaks of luminous intensity corresponding to blood cells were an average of 55.28 (standard deviation 4.23) per capillary per video. The average luminous intensity per capillary per video was 104.49 (standard deviation 25.89). On the 10 observations from the other 10 adult subjects, the four different operators counted an average of respectively 31.20 (standard deviation 5.98), 28.08 (standard deviation 8.78), 29.04 (standard deviation 7.17), and 27.12 (standard deviation 7.12) blood cells per capillary per video.

Each operator spent around 440 min (4 min per capillary) to perform the manual count of blood cells, whereas around 110 min (1 min per capillary) was needed to count the peaks and calculate the average of the reflectance intensity using Image J software.

There was no correlation among the manual counts of blood cells measured by the four different investigators on the 97 observations from the first subject and on the 10 observations from the other 10 subjects (Pearson's coefficient $\rho < 0.5$). There was no intra-capillary reproducibility of the blood cell for the manual count (variance range: 1–205) and for the average luminous intensity (variance range: 1–605), whereas the peak count showed a good intra-capillary reproducibility (variance range: 2–46). Moreover, the capillaries with less reproducibility of peak count corresponded to cases with blood flow variations among different measures that were also detectable by the manual count and the average luminous intensity.

Concerning vascular occlusion tests, there was a statistically significant difference ($P = 0.007$) among the count of the peak intensity of the capillary area in basal condition before ischemia (average 52.4, standard deviation 1.9) and after 6 min from ischemia (average 56.1, standard deviation 3.4).

Discussion

IVCM is a new *in vivo* transcutaneous imaging method to study cutaneous microcirculation. It is non-invasive and allows observing the capillary flow and imaging the tissue under observation, evaluating parameters like skin thickness, epidermal cell size, number of capillaries/mm^2, size, shape, and depth of the microvessels (2–4, 6–8, 10).

All other available techniques for the quantification of cutaneous microcirculation either are able to give morphological data of the microvessels, but not of the rest of the skin structures (optical microscopy-derived techniques such as intravital microscopy, nailfold videocapillaroscopy, orthogonal polarization spectral and later sidestream dark field), or cannot give any morphological data at all (laser Doppler flowmetry and indirect methods that use indices of tissue oxygenation) (1, 11–13). Other limitations of these techniques are either the need of the injection of fluorescent agents (intravital microscopy) and/or the restrictive area of observation (e.g. examination limited to the nailfold in case of nailfold videocapillaroscopy) or the impossibility of separating the capillary flow from that of the arterioles and venules.

IVCM has a high resolution and allows imaging the skin and the dermal capillaries and observing blood flow in real time. Several studies demonstrate its utility to evaluate the cutaneous microcirculation such as in flap donor sites (7), in flap follow-up after surgery (8), in burn shock patients (5), in human burn wound healing (4), in local superficial burns (7), and after temperature changes (2, 6, 7).

Our study compared the manual count of QBCF with two other semi-automatic methods to find the better technique to analyze QBCF from IVCM videos. We found that the manual count of QBCF per capillary on digitally recorded IVCM was time consuming and it is not an intra-capillary and inter-observers reproducible method because measures vary for different videos of the same capillary (variance range: 1–205) and according to the different observers (Pearson's coefficient $\rho < 0.5$). The difficulty of the manual count depends primarily on the fact that blood cells do not always present the same shape, size, and degree of reflectance under IVCM because they continue to change orientation during their course, altering these parameters. Moreover, the bodies passing in the capillaries may correspond to a single blood cell or to a group of cells that can determine irregular images. In addition, this method is time consuming as videos cannot be read at normal speed, but need to be slowed down.

The second method, the count of the peaks of luminous intensity obtained by the Image J software, has been found to have a good intra-capillary reproducibility and to be sensitive to reactive hyperemia after vascular occlusion tests. However, although less time consuming compared with the manual counting of the blood cells, it still needs time to analyze the videos and does not allow a real-time evaluation. We hope that this limitation will be overcome in the future with a software program that is able to perform a real-time reading of the videos, counting the peaks of intensity inside the capillary area. Another limitation of this method is that we do not know if each peak corresponds to a single blood cell or to a cell cluster.

The third method to measure the QBCF, the average luminous intensity, differs from the previous ones because it does not measure the passage of single cells in the vessels, but provides an index of capillary blood cell flux, quantified as medium intensity of the capillary lumen over time. The pixel intensity of the capillary area depends on the passage of bright cells in the vessel: more the intensity of the area, more cells pass over time. This method overcomes the problem of discerning single blood cells from group of cells that pass into the vessel because it does not measure the number of single blood cells per time, but provides an index of capillary flux. Although we had supposed that the mean intensity of the capillary could represent an index of skin perfusion, easy to obtain and proportional to the average blood cell concentration, this method did not show a good intra-capillary reproducibility. We suppose that this aspect might depend on some red blood cells that remain longer in the section of the vessel under observation and induce an increase in the average capillary lumen intensity.

Interestingly, in all the previous studies concerning the evaluation of QBCF by IVCM, the acquisition of the IVCM videos was performed with a camera (VivaScope 1500®) that needed fixation to the skin through a metal ring, procedure that is time consuming and is not applicable to injured skin. In our study, we first used the handheld camera (VivaScope 3000®) that does not need this procedure and it is therefore more suitable in clinical settings.

In conclusion, IVCM is a promising non-invasive new technique to evaluate human microcirculation and the morphology of the observed tissue simultaneously.

Our study shows that among the three selected methods to evaluate the QBCF, the count of intensity peaks is the most reliable one. The passage of bright blood cells in the vessels can be therefore assimilated to peaks of intensity of the capillary area and the count of these peaks revealed to be a good index of QBCF. Further studies should be performed to create a software program allowing for real-time quantification of the blood flow based on the peaks of reflectance intensity inside the capillaries recorded by IVCM.

Conflicts of Interest

The authors declare not to have any conflicts of interest.

References

1. Cerný V, Turek Z, Parízková R. Orthogonal polarization spectral imaging. Physiol Res 2007; 56: 141 147.
2. Altintas MA, Altintas AA, Guggenheim M et al. Insight in human skin microcirculation using in vivo reflectance-mode confocal laser scanning microscopy. J Digit Imaging 2010; 23: 475 481.

3. Altintas AA, Stasch T, Oezcelik A et al. In vivo comparison of microcirculation and histomorphology of two different flap donor sites. Microsc Res Tech 2011; 74: 308 313.
4. Altintas AA, Altintas MA, Ipaktchi K et al. Assessment of microcirculatory influence on cellular morphology in human burn wound healing using reflectance-mode-confocal microscopy. Wound Repair Regen 2009; 17: 498 504.
5. Altintas MA, Altintas AA, Guggenheim M et al. Insight in microcirculation and histomorphology during burn shock treatment using in vivo confocal-laser-scanning microscopy. J Crit Care 2010; 25: e1 e7.
6. Altintas MA, Meyer-Marcotty M, Altintas AA et al. In vivo reflectance-mode confocal microscopy provides insights in human skin microcirculation and histomorphology. Comput Med Imaging Graph 2009; 33: 532 536.
7. Altintas AA, Guggenheim M, Oezcelik A et al. Local burn versus local cold induced acute effects on in vivo microcirculation and histomorphology of the human skin. Microsc Res Tech 2011; 74: 963 969.
8. Altintas MA, Altintas AA, Guggenheim M et al. Monitoring of microcirculation in free transferred musculocutaneous latissimus dorsi flaps by confocal laser scanning microscopy a promising non-invasive methodical approach. J Plast Reconstr Aesthet Surg 2010; 63: 111 117.
9. Frenkel EP. The Merk Manual handbook, Components of Blood. Available at: http://www.merckmanuals.com/home/blood_disorders/biology_of_blood/components_of_blood.html. Accessed December 20, 2013.
10. Hegyi J, Hegyi V, Messer G et al. Confocal laser-scanning capillaroscopy: a novel approach to the analysis of skin capillaries in vivo. Skin Res Technol 2009; 15: 476 481.
11. De Backer D, Donadello K, Cortes DO. Monitoring the microcirculation. J Clin Monit Comput 2012; 26: 361 366.
12. Treu CM, Lupi O, Bottino DA et al. Sidestream dark field imaging: the evolution of real-time visualization of cutaneous microcirculation and its potential application in dermatology. Arch Dermatol Res 2011; 303: 69 78.
13. Roustit M, Cracowski J-L. Non-invasive assessment of skin microvascular function in humans: an insight into methods. Microcirculation 2012; 19: 47 64.

Address:
Elisa Cinotti
Hôpital Nord Saint-Etienne
42055 Saint Etienne Cedex 2
France
Tel: +00 33 (0)4 77 82 84 21
Fax: +00 33 (0)4 77 82 84 01
e-mail: elisacinotti@gmail.com

10.3 In vivo confocal microscopy for the diagnosis of lysosomal storage diseases

La microscopie confocale in vivo pour le diagnostic des maladies lysosomales de surcharge

In vivo confocal microscopy for the diagnosis of lysosomal storage diseases

Nous avons lu avec int r t l'article de Kluger et collaborateurs [1] r cemment paru dans les *Annales de Dermatologie* propos des indications de la biopsie de peaux « apparemment saines ». Nous souhaiterions partager notre exp rience de la microscopie confocale, m thode non invasive et rapide, dans le diagnostic des maladies lysosomales. En effet, il nous semble que l'apport de la microscopie confocale in vivo peut tre mis sur le m me plan que la biopsie de peau normale en ce qui concerne l'aide au diagnostic de certaines maladies m taboliques lysosomales de surcharge telles que la maladie de Fabry et la cystinose. Ainsi, il a t rapport dans la litt rature qu'il tait possible de mettre en vidence au sein de la corn e des inclusions intracellulaires hyper-refl tantes dans les cellules pith liales des patients atteints de maladie de Fabry (Fig. 1) [2] et dans les cellules pith liales et du stroma chez les patients atteints de cystinose (Fig. 2) [3]. Puis, Chiaverini et al. [4] ont mis en vidence la pr sence de cristaux de cystine dans la peau des patients atteints de cystinose, sous forme de structures hyper-refl tantes arrondies dans le derme superficiel. Enfin, nous avons pu montrer qu'avec l'utilisation du microscope confocal VivaScope 1500 (Caliber, tats-Unis, distribu en Europe par Mavig, Munich) [5], il tait possible de visualiser aussi bien dans la peau que dans la corn e (Fig. 2) les structures refl tantes caract ristiques de la cystinose. Une analyse par spectrom trie Raman d'un chantillon cutan et d'un chantillon de corn e nous a permis d'authentifier de mani re formelle que ces corps refl tants correspondaient la cystine [5].

La biopsie cutan e permet de r aliser le diagnostic d'un certain nombre de maladies syst miques de mani re fiable, peu co teuse, peu invasive et faible risque. L'examen en microscopie confocale in vivo, en tant totalement non invasif, correspond cet aboutissement ultime d'un examen cutan ou corn en simple pour diagnostiquer certaines maladies syst miques.

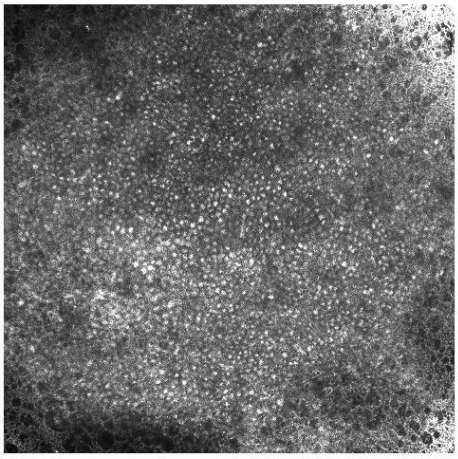

Figure 1. Image de microscopie confocale in vivo au moyen de la cam ra VivaScope 3000 : pith lium corn en avec cellule hyper-refl tantes en raison de d p t de sphingolipides chez un patient atteint de maladie de Fabry.

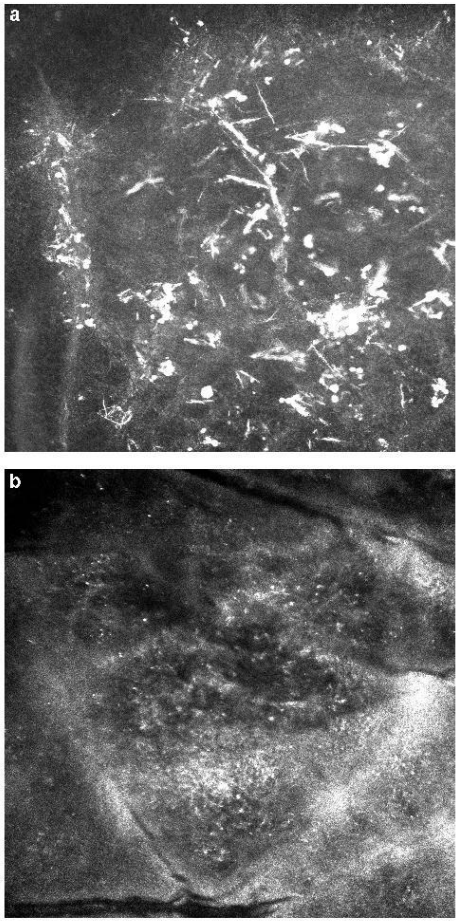

Figure 2. Image de microscopie confocale in vivo au moyen de la cam ra VivaScope 1500 : cristaux hyper-refl tants intra-corn ens en forme d'aiguilles (a) et intradermiques en forme de structures arrondies (b), li s des d p ts de cystine chez une patiente atteinte de cystinose.

D claration d'int r ts

Les auteurs d clarent ne pas avoir de conflits d'int r ts en relation avec cet article.

R f rences

[1] Kluger N, Fraitag S, Roguedas AM, Misery L. Indications extra-cutan es de la biopsie de peau normale. Ann Dermatol Venereol 2014;141:192—200.
[2] Wasielica-Poslednik J, Pfeiffer N, Reinke J, Pitz S. Confocal laser-scanning microscopy allows differentiation between Fabry disease and amiodarone-induced keratopathy. Graefes Arch Clin Exp Ophthalmol 2011;249:1689—96.
[3] Labb A, Niaudet P, Loirat C, Charbit M, Guest G, Baudouin C. In vivo confocal microscopy and anterior segment optical coherence tomography analysis of the cornea in nephropathic cystinosis. Ophthalmology 2009;116:870—6.
[4] Chiav rini C, Kang HY, Sillard L, Berard E, Niaudet P, Guest G, et al. In vivo reflectance confocal microscopy of the skin: a non-invasive means of assessing body cystine accumulation in infantile cystinosis. J Am Acad Dermatol 2013;68:e111—6.
[5] Cinotti E, Perrot JL, Labeille B, Espinasse M, Ouerdane Y, Boukenter A, et al. Optical diagnosis of a metabolic disease: cystinosis. J Biomed Opt 2013;18:046013.

J.-L. Perrot , E. Cinotti*, B. Labeille , F. Cambazard
Service de dermatologie, h pital Nord, CHU de Saint- tienne, 42055 Saint- tienne cedex 2, France

*Auteur correspondant.
Adresse e-mail : elisacinotti@gmail.com (E. Cinotti)

Reçu le 10 mai 2014 ;
accept le 1er septembre 2014
Disponible sur Internet le 25 octobre 2014

http://dx.doi.org/10.1016/j.annder.2014.09.008

10.4 Role of dermoscopy and reflectance confocal microscopy as an aid in the diagnosis of exogenous ochronosis

Annales de dermatologie et de vénéréologie (2016) 143, 318—320

Disponible en ligne sur ScienceDirect www.sciencedirect.com

Elsevier Masson France EM|consulte www.em-consulte.com

Formation médicale continue

FICHE THÉMATIQUE / MICROSCOPIE CONFOCALE PAR RÉFLECTANCE

Apport de la dermoscopie et de la microscopie confocale par réflectance dans le diagnostic d'ochronose exogène

Role of dermoscopy and reflectance confocal microscopy as an aid in the diagnosis of exogenous ochronosis

E. Cinotti[a,*], B. Labeille[a], C. Douchet[b], F. Cambazard[a], J.-L. Perrot[a], au nom du groupe imagerie cutanée non invasive de la Société française de dermatologie

[a] *Service de dermatologie, hôpital universitaire de Saint-Étienne, 42055 Saint-Étienne cedex 2, France*
[b] *Service d'anatomopathologie, hôpital universitaire de Saint-Étienne, 42055 Saint-Étienne cedex 2, France*

Reçu le 21 décembre 2015 ; accepté le 5 février 2016
Disponible sur Internet le 14 mars 2016

Observation

Une femme de 40 ans de phototype V se présentait pour une pigmentation grisâtre et symétrique, touchant les régions zygomatiques et temporales (Fig. 1), apparue depuis quelques années. La dermoscopie montrait des zones homogènes bleu-gris arrondies et confluentes dans des structures arciformes localisées autour des ouvertures folliculaires (Fig. 2).

Microscopie confocale par réflectance

Un examen en microscopie confocale (MC) (Vivascope 3000® ; Caliber Inc, Rochester, NY, États-Unis, distribué en France par Mavig, Munich) était réalisé pour orienter le diagnostic. Les structures bleu-gris vues en dermoscopie correspondaient à la présence de nombreux macrophages hyper-reflétants et de multiples zones hypo-reflétantes ovoïdes dans le derme papillaire (Fig. 3). L'examen histologique trouvait de multiples corps ocres ovoïdes et en forme de banane dans le derme papillaire et moyen (Fig. 4), caractéristiques d'ochronose.

Commentaires

L'aspect dermoscopique et en MC [1] était évocateur d'ochronose exogène. L'ochronose acquise de cause exogène est le plus souvent induite par l'application sur le visage de topiques à base d'hydroquinone pour blanchir la peau. Ceci était le cas de notre patiente qui, à l'interrogatoire, déclarait avoir utilisé une crème à base d'hydroquinone pendant plusieurs années dans un but

* Auteur correspondant.
Adresse e-mail : elisa.cinotti@gmail.com (E. Cinotti).

http://dx.doi.org/10.1016/j.annder.2016.02.012

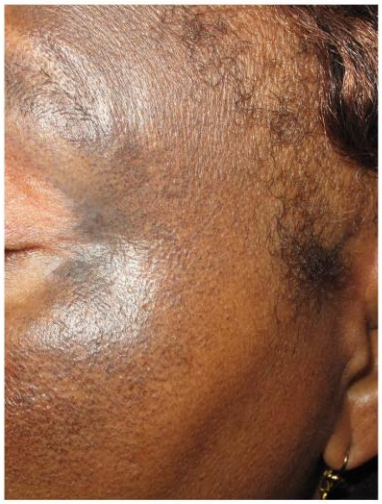

Figure 1. Aspect clinique.

cosmétique. Cliniquement, l'ochronose se manifeste par une hyperpigmentation grisâtre de la région malaire. Des structures arciformes gris-bleu homogènes autour des follicules pileux [1] ou l'oblitération complète des follicules par une pigmentation intense [2] sont caractéristiques de cette condition en dermoscopie. La couleur observée cliniquement et à l'aide de la dermoscopie est bleu-gris en raison de la localisation dermique du pigment. En revanche, chez les patients souffrant de mélasma, la pigmentation est plutôt brune en raison de la localisation plus superficielle du pigment. Il est à signaler qu'en en cas d'ochronose induite par le traitement à base d'hydroquinone du mélasma il est possible d'observer une pigmentation brune avec des zones grisâtres [1].

Des structures hypo-reflétantes dans le derme caractérisent l'ochronose exogène en MC. Elles peuvent être en forme de banane [1] ou ovoïdes. Dans notre cas, seules

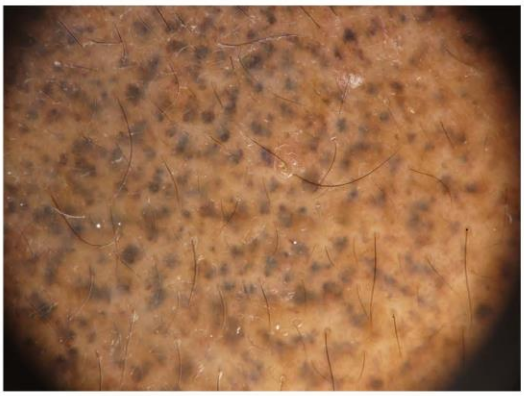

Figure 2. La dermoscopie montre des zones arrondies bleu-gris confluentes dans des structures arciformes situées autour des follicules pileux.

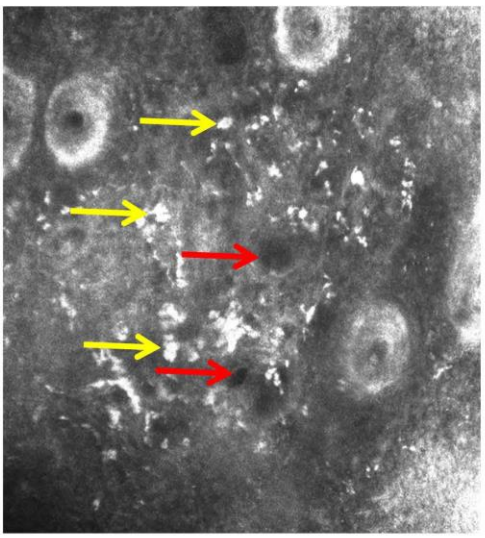

Figure 3. La microscopie confocale par réflectance (VivaScope 3000®; Caliber Inc, Rochester, New York, États-Unis, distribué en Europe par Mavig, Munich, Allemagne) montre des nombreux mélanophages pigmentés (flèche jaune) et de multiples espaces ovales noirs dans le derme papillaire (flèche rouge).

les sections ovoïdes étaient visibles. Ces structures sont l'équivalent histopathologique des corps couleur ocre et correspondent à des fibres collagènes altérées. Un indice en faveur d'ochronose exogène est la présence de macrophages chargés de mélanine (mélanophages) dans le derme papillaire indiquant une incontinence pigmentaire induite par l'application d'hydroquinone. Les mélanophages sont bien visibles en MC car la présence de mélanine augmente leur réflectance.

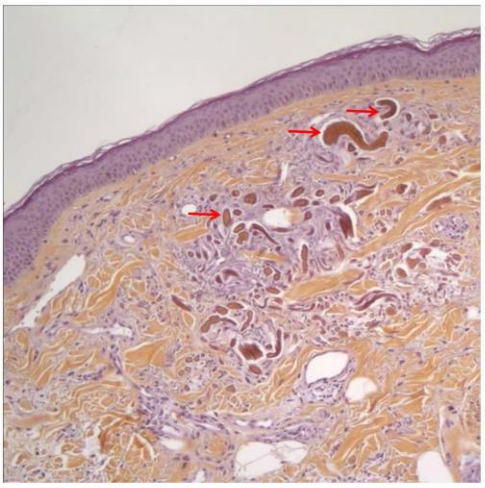

Figure 4. L'examen histopathologique montre du matériel exogène jaune-brun (corps « en forme de banane », flèche rouge) dans le derme papillaire et moyen (hématoxyline-éosine, × 10).

En conclusion, une pigmentation bleu-gris en dermoscopie et des structures hypo-reflétantes ovoïdes ou arciformes en MC accompagnées par des mélanophages pigmentés dans le derme peuvent aider le clinicien dans le diagnostic d'ochronose exogène.

Déclaration de liens d'intérêts

Les auteurs déclarent ne pas avoir de liens d'intérêts.

Références

[1] Gil I, Segura S, Martínez-Escala E, Lloreta J, Puig S, Vélez M, et al. Dermoscopic and reflectance confocal microscopic features of exogenous ochronosis. Arch Dermatol 2010;146:1021—5.

[2] Charlín R, Barcaui CB, Kac BK, Soares DB, Rabello-Fonseca R, Azulay-Abulafia L. Hydroquinone-induced exogenous ochronosis: a report of four cases and usefulness of dermoscopy. Int J Dermatol 2008;47:19—23.

10.5 The venous-arterial difference in CO2 should be interpreted with caution in case of respiratory alkalosis in healthy volunteer

The venous–arterial difference in CO_2 (ΔCO_2) has been proposed as an index of the adequacy of tissue perfusion in shock states. We hypothesized that the variation in $PaCO_2$ (hyper- or hypocapnia) could impact ΔCO_2, partly through microcirculation adaptations. Fifteen healthy males volunteered to participate. For hypocapnia condition (hCO_2), the subjects were asked to hyperventilate, while they were asked to breathe a gas mixture containing 8 % CO_2 for hypercapnia condition (HCO_2). The 2 conditions were randomly assigned. Blood gases were measured at baseline before each condition, and after 5–7 min of either hCO_2 or HCO_2 condition. Microcirculation was assessed by the muscle reoxygenation slope measured with near infrared spectroscopy following a vascular occlusion test and by skin circulation with in vivo reflectance confocal microscopy. ΔCO_2 was significantly increased with CO_2 while it tended to decrease with HCO_2 (non-significant). HCO_2 induced a moderate increase of the resaturation slope of NIRS oxygenation. Skin microcirculatory blood flow significantly dropped with hCO_2, while it remained unchanged with hypercapnia. Our results warrant cautious interpretation of ΔCO_2 as an indicator of tissue perfusion during respiratory alkalosis.

J Clin Monit Comput
DOI 10.1007/s10877-016-9897-6

ORIGINAL RESEARCH

The venous–arterial difference in CO_2 should be interpreted with caution in case of respiratory alkalosis in healthy volunteers

Jerome Morel[1] · Laurent Gergelé[1] · Alexandre Dominé[1] · Serge Molliex[1] · Jean-Luc Perrot[2] · Bruno Labeille[2] · Frederic Costes[3]

Received: 20 March 2016 / Accepted: 6 June 2016

Abstract The venous–arterial difference in CO_2 (ΔCO_2) has been proposed as an index of the adequacy of tissue perfusion in shock states. We hypothesized that the variation in $PaCO_2$ (hyper- or hypocapnia) could impact ΔCO_2, partly through microcirculation adaptations. Fifteen healthy males volunteered to participate. For hypocapnia condition (hCO_2), the subjects were asked to hyperventilate, while they were asked to breathe a gas mixture containing 8 % CO_2 for hypercapnia condition (HCO_2). The 2 conditions were randomly assigned. Blood gases were measured at baseline before each condition, and after 5–7 min of either hCO_2 or HCO_2 condition. Microcirculation was assessed by the muscle reoxygenation slope measured with near infrared spectroscopy following a vascular occlusion test and by skin circulation with in vivo reflectance confocal microscopy. ΔCO_2 was significantly increased with hCO_2 while it tended to decrease with HCO_2 (non-significant). HCO_2 induced a moderate increase of the resaturation slope of NIRS oxygenation. Skin microcirculatory blood flow significantly dropped with hCO_2, while it remained unchanged with hypercapnia. Our results warrant cautious interpretation of ΔCO_2 as an indicator of tissue perfusion during respiratory alkalosis.

✉ Jerome Morel
jerome.morel@chu-st-etienne.fr

[1] Département d'anesthésie Réanimation, Centre Hospitalier Universitaire de Saint Etienne, 42055 Saint Etienne, France

[2] Service de Dermatologie Clinique, Centre Hospitalier Universitaire de Saint Etienne, 42055 Saint Etienne, France

[3] Service de Physiologie Clinique et de l'Exercice, Centre Hospitalier Universitaire de Saint Etienne, 42055 Saint Etienne, France

Published online: 10 June 2016

Keywords Venous–arterial difference in CO_2 · Microcirculation · Hypocapnia · Hypercapnia · Healthy volunteers

1 Introduction

Adequate tissue perfusion, an important component of tissue oxygenation, is essential to bring oxygen and nutrients to cells and thus maintaining tissue homeostasis. Alteration of tissue perfusion is responsible of organ dysfunction and outcome in critical ill patients [1]. Several markers are available to its assessment, the venous oxygen saturation and the lactate being the most commonly used but their relations with tissue perfusion or tissue hypoxia are not straightforward and misinterpretation can occur [2, 3]. The venous–arterial difference in carbon dioxide tension (ΔCO_2) has been proposed as an index of the adequacy of tissue perfusion in shock states [4, 5]. ΔCO_2 reflects the capacity of venous blood flow to remove CO_2 produced by tissues [6]. Accordingly, ΔCO_2 is proportional to CO_2 production ($V'CO_2$) and inversely proportional to cardiac output [4]. Thus, ΔCO_2 increases with low cardiac output or with inadequate microcirculatory perfusion [7–9]. An understudied point is the consequences of arterial carbon dioxide partial pressure ($PaCO_2$) fluctuations on ΔCO_2. Artificial variation of $PaCO_2$ in ventilated hemodynamically stable postoperative patients can significantly influence ΔCO_2 [10]. Similarly, in healthy volunteers, Umeda et al. [11] showed that ΔCO_2 increased with hyperventilation in an intensity-dependent manner. An arterial vasoconstriction was claimed to explain this observation.

Few tools allow a non-invasive and easy assessment of the microcirculation in healthy subject or patient. Near infrared spectroscopy (NIRS) in the muscle and in vivo

reflectance confocal microscopy (IVCM) in the skin are two of them. NIRS is based on the differential absorption properties of oxygenated and deoxygenated haemoglobin to evaluate skeletal muscle oxygenation [12]. Reactive hyperaemia after a hypoxic challenge induced by a vascular occlusion test (VOT) [13] may be considered as a test of microcirculatory reactivity, evaluating the ability of tissues to adjust oxygen delivery to rapid changes in local demand. Reactive hyperaemia can be assessed with NIRS technology with the recovery slope, measured after the release of the vascular occlusion [14]. IVCM is an emerging imaging technique for the assessment of skin microcirculatory blood flow [15, 16]. Contrast in confocal imaging occurs by backscattering of a focused laser beam from different structures of the skin tissue and blood cells within dermal capillaries. Blood flow is measured in a selected dermal capillary.

We hypothesized that the variation in arterial partial pressure of carbon dioxide induced by changing the breathing condition would impact the venous–arterial difference in carbon dioxide tension. Moreover, we assessed the microcirculation at the muscle and skin levels and measured oxygen consumption to explain the potential effect of $PaCO_2$ and metabolism on ΔCO_2.

2 Methods

2.1 Subjects

The present study was approved by the Ethics Committee of Saint Etienne University Teaching Hospital (Comité de Protection des Personnes Sud Est-1, protocol number: 2013–10). Fifteen healthy males (age 19–46 years [min–max]) should be volunteered to participate in this study after obtaining their written informed consent. All were nonsmoker, non-diabetic and had no medical history of arterial hypertension. The experiment took place the same day for all the volunteers who were subjected to hypo and hypercapnia conditions. During the entire experiment, volunteers sat in an armchair with armrest. Room temperature was kept constant at 23 °C.

2.2 Study design

Four experimental time points were formed: baseline 1 (10 min of resting room air breathing), hypo- (hCO_2) or hypercapnia (HCO_2) condition, baseline 2, and hCO_2- or HCO_2 condition. The order of hCO_2 and HCO_2 condition was randomized.

Volunteers were breathing through a buccal piece connected to a pneumotachograph allowing the measurement of the minute ventilation (VE) and the respiratory rate (RR). Expired gases were analyzed breath-by-breath for O_2 and CO_2 concentrations (Medisoft Ergocard, Dinant, Belgium), allowing calculation of oxygen consumption ($V'O_2$), CO_2 production ($V'CO_2$), and end-tidal PCO_2 ($PetCO_2$). The respiratory exchange ratio (RER) was calculated as the ratio between $V'CO_2$ and $V'O_2$. The pneumotachograph and the gas analyzers were calibrated before every series of measurements on a subject.

2.2.1 Hypocapnia condition

The subjects breathed room air and were asked to hyperventilate in order to decrease $PetCO_2$ by >30 % of baseline values. When the target $PetCO_2$ was obtained, hyperventilation was maintained for 2 min (total 5–7 min of hyperventilation).

2.2.2 Hypercapnia condition

The subjects breathed a gas mixture containing 8 % CO_2, 21 % O_2 and the remaining N_2. The appropriate gas mixture was made up and controlled by an Altitrainer system (SMTEC, Nyon, Switzerland). Once $PetCO_2$ increased by >30 % of baseline value, hypercapnia condition was maintained for 2 min (total 5–7 min of CO_2 breathing).

2.3 Blood sampling and blood gas analysis

A humeral catheter was inserted for venous blood sampling. Arterialized blood was obtained from the earlobe after applying a vasodilation cream (Finalgon®, Boeringher Ingelheim company, Germany). Blood gases were immediately analyzed with a blood gas analyzer (ABL 800 Radiometer®, Copenhagen, Denmark). ΔCO_2 was calculated as the difference between $PvCO_2$ (venous blood) and $PaCO_2$ (arterialized blood). The extraction of oxygen (EO_2) was calculated as follows: $EO_2 = (CaO_2-CvO_2)/CaO_2$ (where CaO_2 and CvO_2 are the arterialized and venous oxygen content, respectively).

2.4 Microcirculation assessment

2.4.1 NIRS measurement of the forearm

Tissue oxygen saturation of the forearm (StO_2) was measured by Near InfraRed Spectroscopy (Oxymon Mk III, Artinis Medical Systems, Zetten, The Netherlands), at 2 Laser emitted wavelengths (775 and 850 nm) with a 25 mm optodes spacing. The probe was placed at the external surface of the forearm, facing the flexor digitoris muscle. Data acquisition was 1 Hz. In order to assess the muscle vascular reactivity, a vascular occlusion test (VOT) was performed at the end of each condition of the study

(baselines 1 and 2, hCO_2 and HCO_2). It consisted in inflating a sphygmomanometer cuff placed over the brachial artery up to 50 mmHg above the systolic blood pressure. The cuff was maintained during 3 min and then rapidly deflated [17]. Tissue Saturation Index (TSI %) was calculated from absorbance measured by the oxymeter. Data are expressed as basal condition, i.e. a 60-s averaged value before the vascular occlusion test, min and max as minimal and maximal values recorded at the nadir of desaturation and peak of reactive hyperemia, respectively.

2.4.2 In vivo confocal microscopy measurement

In vivo reflectance confocal microscopy videos (VivaScope 3000® Caliber, New York, USA) were recorded by positioning the tip of the confocal microscope on the skin of the second interdigital space (contralateral limb to the NIRS measurement). To obtain stable videos, the camera was fixed to a hinged support. Videos were recorded and analyzed offline. Dermal capillaries were observed at a depth of about 200 μm as black holes inside dermal papillae that appear as dark areas surrounded by bright circles. In a selected capillary, the number of peaks of luminous intensity in the capillary area (corresponding to bright blood cells) was calculated by Image J® software (freeware downloaded at http://rsbweb.nih.gov/ij/). A good intra observer reproducibility of the measurement has been previously reported [16]. Flow was measured on 2 different capillaries and average. Blood cells count was performed on 30 s period during the last minute of each experimental condition.

2.5 Haemodynamic measurements

Heart rate and mean arterial pressure were also recorded at the end of each experimental period. In a post hoc study in 10 healthy volunteers (4 were included in the initial study), we measured the cardiac output with a transthoracic echocardiography in hypocapnia condition.

2.6 Statistical analysis

On the basis of previous work [10], we anticipated a 3.5 ± 3 mmHg increase of ΔCO_2 in hypocapnia condition compared to baseline with α level of 0.05 and β level 0.9. The sample size was estimated to be 13 volunteers.

Data are expressed as mean ± standard deviation or absolute number and percentage. Values at different time points were compared with repeated measures ANOVA and Scheffe post hoc analysis. Statistical analysis was performed with SAS 9.3. Probability values <0.05 were considered statistically significant. The following parameters were measured or calculated offline using a dedicated EXCEL sheet: the StO_2 desaturation slope during the occlusion period, and the StO_2 recovery slope after release of the cuff inflation (arbitrary unit for both measurements).

3 Results

All the subjects reached the predetermined criteria for hypocapnia and hypercapnia conditions. Data are partially missing for 3 cases concerning IVCM or NIRS measurements.

Impact of experimental conditions on blood gas analysis and ΔCO_2 (Table 1; Fig. 1).

No significant difference was identified between both baseline conditions, meaning that the washout period allowed a full recovery of the induced ventilation variations. Blood lactate was moderately impacted by experimental conditions. Both $PaCO_2$ and $PvCO_2$ consistently decreased with hCO_2 and increased with HCO_2 (all $p < 0.05$). ΔCO_2 was significantly increased with hCO_2 (330 ± 44 %, $p < 0.05$) while it was trended to decrease with HCO_2 (−111 ± 19 %, $p = 0.06$). The substitution of partial pressure by the blood content in CO_2 brought similar results. Mean values of $\Delta CtCO_2$ were negative in both basal conditions and HCO_2 condition. We have no clear explanation concerning this point.

3.1 Impact of experimental conditions on cardiovascular system and oxygenation parameters (Table 2)

Compared to respective baseline condition, hypocapnia did not provoke any significant modification of mean arterial pressure (MAP) (85.6 ± 7.8 vs. 88.6 ± 8.6 mmHg), while hypercapnia induced a mild but significant elevation of MAP (94 ± 6 vs. 87 ± 7 mmHg, respectively $p = 0.0013$). Heart rate did not change significantly neither from baseline to hypocapnia condition (74 ± 12 and 77 ± 10 bpm, respectively) nor from baseline to hypercapnia condition (79 ± 9 and 83 ± 13 bpm, respectively, $p = 0.053$). In the post hoc study, $PaCO_2$ dropped from 36.4 ± 1.4 to 22.0 ± 4.1 mmHg ($p < 0.01$) and ΔCO_2 increased from 6.4 ± 3.1 to 13.1 ± 5.9 mmHg ($p = 0.005$). Cardiac output was similar between basal and hCO_2 condition (5.2 ± 0.9 to 5.3 ± 1.1 L/min, respectively $p = 0.83$).

$V'O_2$ trended to decrease with hCO2 but in the same time VE significantly increased. Hyperventilation in both experimental conditions leads to an increase of respiratory work to reach the targeted $PetCO_2$, and this could affect whole body $V'O_2$. Thus, we calculated $V'O_2$/VE ratio to compensate for this effect. We found that $V'O_2$/VE was nearly halved in HCO_2 condition compared to hCO_2 ($p < 0.05$). The respiratory exchange ratio was also significantly increased with hCO_2. SaO_2 was moderately but

Table 1 Results of blood gas analysis between both experimental conditions and their respective baselines

	Baseline hCO_2 condition	hCO_2 condition	Baseline HCO_2 condition	HCO_2 condition
pHa	7.42 ± 0.01	7.60 ± 0.05*	7.43 ± 0.02	7.32 ± 0.02*,§
pHv	7.37 ± 0.02	7.46 ± 0.06*	7.39 ± 0.03	7.32 ± 0.02*,§
Lactate v (mmol/L)	1.3 ± 0.5	1.6 ± 0.5	1.4 ± 0.4	1.3 ± 0.3§
PaO_2 (mmHg)	76.1 ± 9.7	91.1 ± 14*	81 ± 10.3	107.6 ± 9.6*,§
$PaCO_2$ (mmHg)	39.0 ± 2.6	20.9 ± 2.9*	37.6 ± 2.7	50.1 ± 6.4*,§
$PvCO_2$ (mmHg)	42.4 ± 5.9	34.5 ± 6.4*	39.8 ± 5.1	51.8 ± 2.7*,§
ΔCO_2 (mmHg)	3.4 ± 5.9	13.6 ± 5.3*	2.2 ± 5.0	−0.44 ± 1.9§
$CtaCO_2$ (mmol/L)	25.61 ± 1.73	21.48 ± 1.84*	25.45 ± 1.65	28.07 ± 1.39*,§
$CtvCO_2$ (mmol/L)	25.06 ± 2.44	25.30 ± 2.33	24.53 ± 2.86	27.49 ± 1.51*,§
$\Delta CtCO_2$ (mmol/L)	−1.28 ± 2.60	3.79 ± 1.46*	−0.57 ± 2.12	−0.41 ± 0.83§

Mean ± SD

hCO_2 Hypocapnia, *HCO_2* hypercapnia, *a* arterialized blood sample, *P* pressure, *Ct* content

* $p < 0.05$ versus corresponding baseline, § $p < 0.05$ between hCO_2 and HCO_2

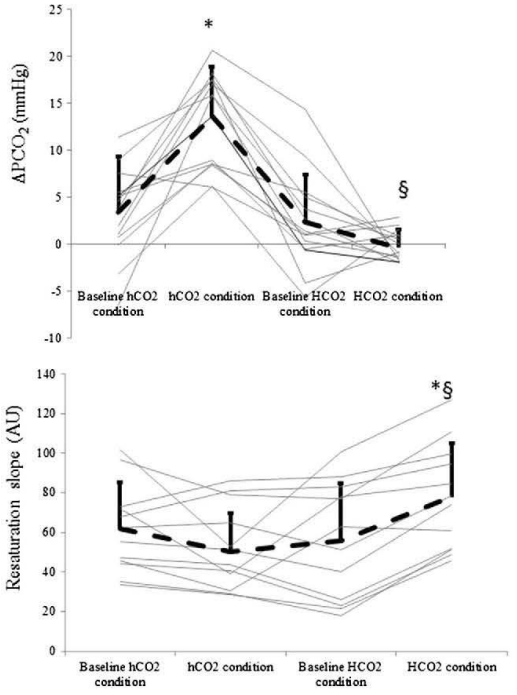

Fig. 1 Individual and mean (*dash line*) changes in ΔPCO_2 and StO_2 recovery slope during each experimental conditions. * $p < 0.05$ versus corresponding baseline, § $p < 0.05$ between hCO_2 and HCO_2

significantly increased in both experimental conditions ($p < 0.05$). We observed a non-significant decrease of forearm SvO_2 with hCO_2.

3.2 Impact of experimental conditions on microcirculation (Table 3, Fig. 1)

Muscle oxygen desaturation slope was not changed with experimental conditions suggesting no change in local VO_2. HCO_2 induced a moderate but significant increase of the resaturation slope ($p < 0.05$), indicating a higher local vasodilatory tone. Basal value of TSI did not differ before and after both conditions. Min and max TSI were similar (all non-significant), indicating a similar response to VOT. Skin microcirculatory blood flow accesses with IVCM significantly dropped with hCO_2 ($p < 0.05$), while it remained unchanged with hypercapnia. We obtained a good correlation between ΔPCO_2 and $PaCO_2$ ($r = -0.71$) but not between ΔPCO_2 and microvascular parameters (resaturation slope and IVCM).

4 Discussion

Venous-arterial difference in CO_2 (ΔCO_2) has been proposed as an index of the adequacy of tissue perfusion in shock states [4, 5]. ΔCO_2 has been beneficially evaluated, associated with other markers, to guide resuscitation in septic shock patients [9, 18]. We show here, in healthy volunteers, that ΔCO_2 should be interpreted with caution in case of respiratory alkalosis. Our results can be explained by a CO_2 effect on micro- and macrocirculation but also through potential metabolic properties.

Few studies have evaluated the impact of $PaCO_2$ variations on ΔCO_2. An increase of ΔCO_2 induced by a respiratory alkalosis has been reported in post cardiac surgery patients [10] or in healthy volunteers [11]. A parallel can

Table 2 Oxygenation parameters

	Baseline hCO_2 condition	hCO_2 condition	Baseline HCO_2 condition	HCO_2 condition
SaO_2 (%)	96.1 ± 1.2	99.2 ± 0.7*	96.6 ± 1.6	98.4 ± 0.6*
Forearm SvO_2 (%)	73.0 ± 14.7	66.3 ± 14.5	74.6 ± 13.8	72.2 ± 15.1
Forearm EO_2 (%)	24.1 ± 15.7	33.2 ± 14.4	22.7 ± 14.3	26.6 ± 15.4
VE (L min ^{1})	10.8 ± 2.04	21.2 ± 6.4*	10.4 ± 2.6	47.8 ± 8.8*,§
$V'O_2$ (L min ^{1})	0.32 ± 0.06	0.29 ± 0.06	0.34 ± 0.05	0.34 ± 0.07
$V'CO_2$ (L min ^{1})	0.28 ± 0.06	0.30 ± 0.06	0.28 ± 0.05	0.31 ± 0.08
RER	0.84 ± 0.07	1.04 ± 0.10*	0.84 ± 0.10	0.91 ± 0.10§
$V'O_2$/VE (×10 ^{4})	32.02 ± 7.41	14.45 ± 3.49*	33.35 ± 7.39	7.44 ± 1.88*,§

Mean ± SD

hCO_2 Hypocapnia, *HCO_2* hypercapnia, *VE* minute ventilation, *$V'O_2$* CO_2 production, *RER* respiratory exchange ratio

* $p < 0.05$ versus corresponding baseline, § $p < 0.05$ between hCO_2 and HCO_2

Table 3 Microcirculatory parameters obtained with NIRS and in vivo confocal microscopy (IVCM)

	Baseline hCO_2 condition	hCO_2 condition	Baseline HCO_2 condition	HCO_2 condition
NIRS derived parameters				
TSI (%) basal	61.0 ± 2.6	60.9 ± 2.5	60.5 ± 2.2	61.1 ± 2.0
TSI (%) min	45.6 ± 5.0	46.6 ± 3.8	45.5 ± 4.2	46.2 ± 4.8
TSI (%) max	66.9 ± 1.6	65.7 ± 2.6	66.3 ± 1.9	67.4 ± 1.5
Desaturation slope (AU)	−3.5 ± 0.6	−3.9 ± 0.8	−3.6 ± 0.8	−4.3 ± 1.2
Resaturation slope (AU)	61.8 ± 23.5	50.4 ± 20.9	55.9 ± 28.9	77.9 ± 26.9*,§
IVCM derived parameter				
Microcirculatory flow (cells/min)	60.5 ± 4.42	55.6 ± 6.1*	61.7 ± 3.0	62.4 ± 3.7§

Mean ± SD

hCO_2 Hypocapnia, *HCO_2* hypercapnia, *NIRS* near infrared spectroscopy, *TSI* tissue saturation index, *IVCM* in vivo confocal microscopy

* $p < 0.05$ versus corresponding baseline, § $p < 0.05$ between hCO_2 and HCO_2

be drawn between ΔCO_2 and the gradient between intramucosal and $PaCO_2$, a marker of gut perfusion, obtained with gastric tonometry. This gradient is also significantly increased after hyperventilation but remained essentially stable after hypercapnia in an experimental study [19]. Several factors can be considered to explain our results.

4.1 Systemic and microvascular regulatory effects of CO_2

Hypercapnia stimulates the sympathetic tone, thereby increases myocardial contractility and vascular tone. However this vasoconstriction is overcome by direct peripheral vasodilating effect of CO_2 so that, in total, peripheral resistance decreases [20]. Consequently, cardiac output is often reported to increase with HCO_2 [20–22]. We recorded a faster NIRS skin recovery slope associated with a moderate increase of microcirculatory flow which are in line with an increased tissue perfusion in HCO_2 condition. Conversely, hypocapnia induces vasoconstriction [11, 21] but no significant effect on cardiac output [23]. In a previous study, carried out in mechanically ventilated post cardiac surgery patients, artificial variations of $PaCO_2$ induced fluctuation of ΔCO_2 while cardiac output was unchanged [10]. Similarly, we did not record here any significant change of cardiac output with hCO_2 conditions in our post hoc study. In total, a vasoconstriction effect of hyperventilation induced hypocapnia is predominant [24–27]. We used two different techniques to evaluate the microcirculation. The decrease of skin blood flow observed with IVCM could be explained by an increase of the microvascular tone secondary to hCO_2. Indeed, Komori et al. [26] reported a decrease of microvascular diameter assessed by intravital microscopy of the rabbit ear microcirculation after a hypocapnia challenge. Another experimental study reported a decrease in microcirculatory blood flow with hypocapnia and a concomitant reduction in tissue oxygenation [28]. Although not significant, we found a

trend to a slower recovery rate of StO_2 after VOT, which is consistent with a reduced muscle O_2 delivery. In humans, we can obtain only indirect index of microcirculation, but the observed variations in tissue perfusion using NIRS or IVCM are in line with the CO_2 induced changes in vascular tone. Additionally, microcirculatory adaptations could react at different CO_2 thresholds in hypo- or hypercapnia. Thus the increase of ΔCO_2 could be explained by the development of a hypocapnia-mediated mismatch between perfusion and demand.

4.2 Metabolic effect of carbon dioxide

PaO_2 was significantly increased in both conditions due to the hyperventilation imposed by experimental conditions. More interesting, we report that for a same minute ventilation, a 2 folds increase of $V'O_2$ with hypocapnia condition compared to hypercapnia condition. Respiratory alkalosis has been shown to increase systemic $V'O_2$ and $V'CO_2$ independently of any significant cardiac output modification. Indeed, 2 h of hyperventilation in mechanical ventilated dogs increased $V'O_2$ and $V'CO_2$ by 25 and 20 %, respectively [23]. The mechanism involved is uncertain. This could be attributed to an increase of glycolysis as the phosphofructokinase, a key enzyme in the glycolytic cycle, has its activity markedly increased by alkalosis [29]. Conflicting results have been obtained with anesthetized patients showing either an increase in whole-body $V'O_2$ with hypocapnic alkalosis [30] or no significant modification [22]. In unstable condition (i.e. a few minutes of CO_2 flux variation), we obtained no change in $V'O_2$ or $V'CO_2$. However, we found a significant increase in RER only under hCO_2 condition, which suggests an increased flux of CO_2 compared to metabolic production. Of course, the hypocapnia-induced hyperventilation would thus further complicate the interpretation of the venous-arterial CO_2 difference. Conversely, under hypercapnic condition, a great amount of CO_2 could be stored in tissue which would decrease the CO_2 gradient (explaining some negative value). We cannot rule out the hypothesis that what we observed were only transient variations in CO_2 flux influencing the venous-arterial CO_2 difference. It was not possible to impose a longer hyperventilation state in our experimental condition to confirm that the changes in CO_2 persisted when a steady state of CO_2 was reached.

Other consequence of CO_2 variation has been shown on mitochondria oxidative phosphorylation. Acidosis and or supra physiological level of carbon dioxide can cause mitochondria dysfunction [31, 32]. Conversely, alkalosis and/or decrease of CO_2 effects on mitochondria have never been studied. Thus, a variation in $V'CO_2$ would impact ΔCO_2, independently of tissue perfusion changes.

4.3 Limits

Originally ΔCO_2 is the difference between mixed venous $PvCO_2$ and $PaCO_2$. It was previously showed that arterialized blood sampling accurately reflects arterial blood, especially for PCO_2 and pH, over a wide range of values [33]. It was ethically impossible to obtain mixed venous blood samples in volunteers. We do not think that the interpretation of our results can be ascribed to the localization of blood withdrawal (peripheral vein). Indeed, in cardiac surgery setting, we obtained similar results with mixed venous PCO_2 [10]. Consequently, similar experiment with patients with abnormal microcirculation could have brought different conclusion. We were unable to separate direct effect of change of pH or PCO_2, both have been shown to have consequences on the cardiovascular system [20]. Finally, the aim of the study was to detect consequences of hyperventilation on ΔCO_2. We cannot rule out that our study was underpowered to detect significant changes in tissue perfusion assessed with NIRS and IVCM. So we are unable to draw definite conclusions about the changes in local vascular tone and ΔCO_2.

5 Conclusion

In healthy volunteers, our results warrant cautious interpretation of ΔCO_2 as an indicator of tissue perfusion during respiratory alkalosis, in non-steady-state condition. CO_2 is an important modulator of vascular tone and its effect on oxygen consumption has to be investigated particularly in situation where aerobic metabolism is dependent of oxygen delivery.

Conflicts of interest None.

References

1. Shoemaker WC, Appel PL, Kram HB. Role of oxygen debt in the development of organ failure sepsis, and death in high-risk surgical patients. Chest. 1992;102(1):208–15.
2. Levy B, Gibot S, Franck P, Cravoisy A, Bollaert PE. Relation between muscle Na + K + ATPase activity and raised lactate concentrations in septic shock: a prospective study. Lancet. 2005;365(9462):871–5.
3. Perz S, Uhlig T, Kohl M, Bredle DL, Reinhart K, Bauer M, Kortgen A. Low and "supranormal" central venous oxygen saturation and markers of tissue hypoxia in cardiac surgery patients: a prospective observational study. Intensive Care Med. 2011;37(1):52–9.
4. Lamia B, Monnet X, Teboul JL. Meaning of arterio-venous PCO_2 difference in circulatory shock. Minerva Anestesiol. 2006;72(6):597–604.
5. Danin PE, Siegenthaler N, Levraut J, Bernardin G, Dellamonica J, Bendjelid K. Monitoring CO_2 in shock states. J Clin Monit Comput. 2015;29(5):591–600.

6. Vallet B, Teboul JL, Cain S, Curtis S. Venoarterial CO(2) difference during regional ischemic or hypoxic hypoxia. J Appl Physiol. 2000;89(4):1317–21.
7. Cuschieri J, Rivers EP, Donnino MW, Katilius M, Jacobsen G, Nguyen HB, Pamukov N, Horst HM. Central venous-arterial carbon dioxide difference as an indicator of cardiac index. Intensive Care Med. 2005;31(6):818–22.
8. Teboul JL, Mercat A, Lenique F, Berton C, Richard C. Value of the venous-arterial PCO_2 gradient to reflect the oxygen supply to demand in humans: effects of dobutamine. Crit Care Med. 1998;26(6):1007–10.
9. Vallee F, Vallet B, Mathe O, Parraguette J, Mari A, Silva S, Samii K, Fourcade O, Genestal M. Central venous-to-arterial carbon dioxide difference: an additional target for goal-directed therapy in septic shock? Intensive Care Med. 2008;34(12):2218–25.
10. Morel J, Gergele L, Verveche D, Costes F, Auboyer C, Molliex S. Do fluctuations of PaCO2 impact on the venous-arterial carbon dioxide gradient? Crit Care. 2011;15(6):456.
11. Umeda A, Kawasaki K, Abe T, Watanabe M, Ishizaka A, Okada Y. Hyperventilation and finger exercise increase venous-arterial PCO_2 and pH differences. Am J Emerg Med. 2008;26(9):975–80.
12. Myers DE, Anderson LD, Seifert RP, Ortner JP, Cooper CE, Beilman GJ, Mowlem JD. Noninvasive method for measuring local hemoglobin oxygen saturation in tissue using wide gap second derivative near-infrared spectroscopy. J Biomed Opt. 2005;10(3):340–57.
13. Cracowski JL, Minson CT, Salvat-Melis M, Halliwill JR. Methodological issues in the assessment of skin microvascular endothelial function in humans. Trends Pharmacol Sci. 2006;27(9):503–8.
14. Gomez H, Torres A, Polanco P, Kim HK, Zenker S, Puyana JC, Pinsky MR. Use of non-invasive NIRS during a vascular occlusion test to assess dynamic tissue O(2) saturation response. Intensive Care Med. 2008;34(9):1600–7.
15. Altintas MA, Altintas AA, Guggenheim M, Steiert AE, Aust MC, Niederbichler AD, Herold C, Vogt PM. Insight in human skin microcirculation using in vivo reflectance-mode confocal laser scanning microscopy. J Digit Imaging. 2010;23(4):475–81.
16. Cinotti E, Gergele L, Perrot JL, Domine A, Labeille B, Borelli P, Cambazard F. Quantification of capillary blood cell flow using reflectance confocal microscopy. Skin Res Technol. 2014;20(3):373–8.
17. Mayeur C, Campard S, Richard C, Teboul JL. Comparison of four different vascular occlusion tests for assessing reactive hyperemia using near-infrared spectroscopy. Crit Care Med. 2011;39(4):695–701.
18. Futier E, Robin E, Jabaudon M, Guerin R, Petit A, Bazin JE, Constantin JM, Vallet B. Central venous O(2) saturation and venous-to-arterial CO(2) difference as complementary tools for goal-directed therapy during high-risk surgery. Crit Care. 2010;14(5):R193.
19. Guzman JA, Kruse JA. Gut mucosal-arterial PCO_2 gradient as an indicator of splanchnic perfusion during systemic hypo- and hypercapnia. Crit Care Med. 1999;27(12):2760–5.
20. Richardson DW, Wasserman AJ, Patterson JL. General and regional circulatory responses to change in blood pH and carbon dioxide tension. J Clin Invest. 1961;40:31–43.
21. Cullen DJ, Eger EI 2nd. Cardiovascular effects of carbon dioxide in man. Anesthesiology. 1974;41(4):345–9.
22. Mas A, Saura P, Joseph D, Blanch L, Baigorri F, Artigas A, Fernandez R. Effect of acute moderate changes in $PaCO_2$ on global hemodynamics and gastric perfusion. Crit Care Med. 2000;28(2):360–5.
23. Khambatta HJ, Sullivan SF. Effects of respiratory alkalosis on oxygen consumption and oxygenation. Anesthesiology. 1973;38(1):53–8.
24. Curley G, Kavanagh BP, Laffey JG. Hypocapnia and the injured brain: more harm than benefit. Crit Care Med. 2010;38(5):1348–59.
25. Fujita Y, Sakai T, Ohsumi A, Takaori M. Effects of hypocapnia and hypercapnia on splanchnic circulation and hepatic function in the beagle. Anesth Analg. 1989;69(2):152–7.
26. Komori M, Takada K, Tomizawa Y, Nishiyama K, Kawamata M, Ozaki M. Permissive range of hypercapnia for improved peripheral microcirculation and cardiac output in rabbits. Crit Care Med. 2007;35(9):2171–5.
27. Winso O, Biber B, Martner J. Effects of hyperventilation and hypoventilation on stress-induced intestinal vasoconstriction. Acta Anaesthesiol Scand. 1985;29(7):726–32.
28. Gustafsson U, Sjoberg F, Lewis DH, Thorborg P. The effect of hypocapnia on skeletal muscle microcirculatory blood flow, oxygenation and pH. Int J Microcirc Clin Exp. 1993;12(2):131–41.
29. Dobson GP, Yamamoto E, Hochachka PW. Phosphofructokinase control in muscle: nature and reversal of pH-dependent ATP inhibition. Am J Physiol. 1986;250(2):71–6.
30. Slater RM, Symreng T, Ping ST, Starr J, Tatman D. The effect of respiratory alkalosis on oxygen consumption in anesthetized patients. J Clin Anesth. 1992;4(6):462–7.
31. Jubrias SA, Crowther GJ, Shankland EG, Gronka RK, Conley KE. Acidosis inhibits oxidative phosphorylation in contracting human skeletal muscle in vivo. J Physiol. 2003;553(2):589–99.
32. Vohwinkel CU, Lecuona E, Sun H, Sommer N, Vadasz I, Chandel NS, Sznajder JI. Elevated CO(2) levels cause mitochondrial dysfunction and impair cell proliferation. J Biol Chem. 2011;286(43):37067–76.
33. Zavorsky GS, Cao J, Mayo NE, Gabbay R, Murias JM. Arterial versus capillary blood gases: a meta-analysis. Respir Physiol Neurobiol. 2007;155(3):268–79.

G. PUBLICATIONS DE L’AUTEUR

1.1 Evolution de l'activité publicatoire de 1991 à 2016

Période : 1991 - 2016	
Année	**Nombre**
1991	0
1992	0
1993	0
1994	0
1995	2
1996	2
1997	2
1998	4
1999	7
2000	4
2001	3
2002	4
2003	1
2004	1
2005	1
2006	1
2007	0
2008	5
2009	5
2010	3
2011	4
2012	5
2013	9
2014	15
2015	22
2016	31
Total	**131**

Nombres de publications annuelles depuis 1991 en valeur ,données issus du Portail Système d'Information Recherche (logiciel SIGAPS)

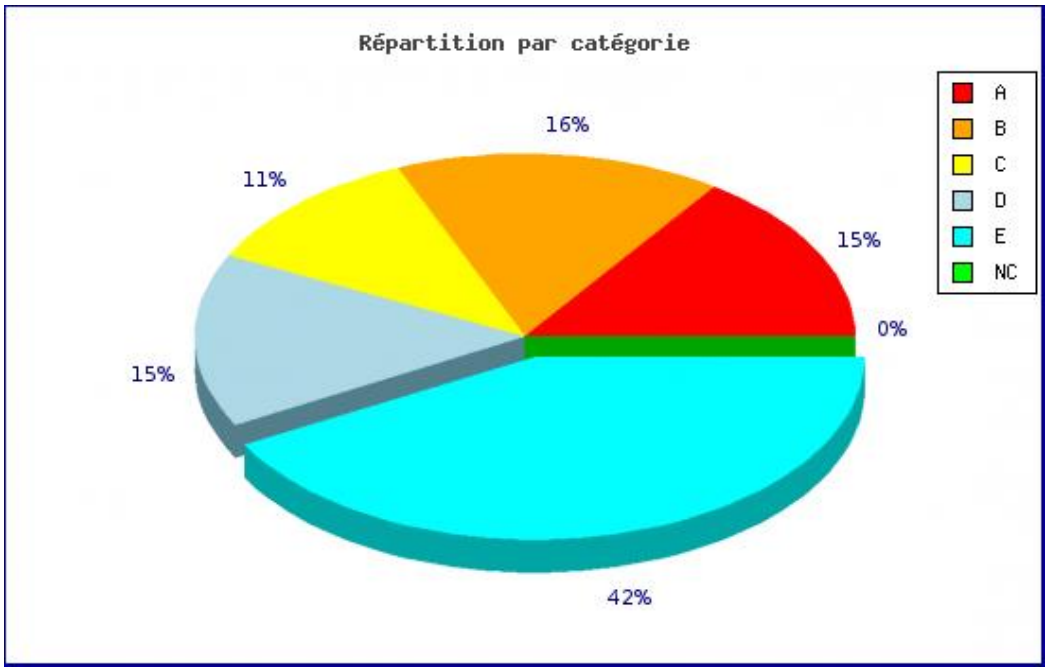

Répartition des publications annuelles depuis 1991 selon le rang des revues, données issues du Portail Système d'Information Recherche (logiciel SIGAPS)

Position de l'auteur en fonction du rang des revues depuis 1991 en valeur absolue (cf cidessus) et sous forme de diagramme cf ci-dessous) données issus du Portail Système d'Information Recherche (logiciel SIGAPS)

Période : 1991 - 2016							
Position	**Total**	**A**	**B**	**C**	**D**	**E**	**NC**
1	10	0	0	0	1	9	0
2	37	8	5	5	4	15	0
3	21	1	5	0	6	9	0
Inv	7	2	4	1	0	0	0
k	29	6	4	5	6	8	0
ADA	5	0	0	0	2	3	0
DA	22	3	3	4	1	11	0
Total	**131**	**20**	**21**	**15**	**20**	**55**	**0**

Nombres depoints SIGAPS annuels depuis 1991et cumul global, données issues du Portail Système d'Information Recherche (logiciel SIGAPS)

Période : 1991 - 2016								
Année	**Total**	**A**	**B**	**C**	**D**	**E**	**NC**	**Score**
1991	0	0	0	0	0	0	0	0
1992	0	0	0	0	0	0	0	0
1993	0	0	0	0	0	0	0	0
1994	0	0	0	0	0	0	0	0
1995	2	0	0	0	0	2	0	16
1996	2	0	0	0	1	1	0	9
1997	2	2	0	0	0	0	0	56
1998	4	0	0	0	2	2	0	23
1999	7	1	1	0	0	5	0	44
2000	4	1	0	0	1	2	0	23
2001	3	0	0	0	2	1	0	23
2002	4	1	0	0	2	1	0	46
2003	1	1	0	0	0	0	0	8
2004	1	1	0	0	0	0	0	24
2005	1	0	0	0	0	1	0	6
2006	1	0	0	0	0	1	0	4
2007	0	0	0	0	0	0	0	0
2008	5	1	1	0	0	3	0	28
2009	5	0	1	0	0	4	0	24
2010	3	0	0	0	2	1	0	11
2011	4	2	2	0	0	0	0	28
2012	5	1	0	2	0	2	0	34
2013	9	0	2	1	1	5	0	78
2014	15	2	1	2	5	5	0	143
2015	22	5	3	6	2	6	0	286
2016	31	2	10	4	2	13	0	324
Total	**131**	**20**	**21**	**15**	**20**	**55**	**0**	**1238**

1.2 – Publications soumises à comité de lecture (référencées dans la base PubMed) en date 31/12/2016 :

150. Espinasse M, Cinotti E, Grivet D, Labeille B, Prade V, Douchet C, Cambazard F, Thuret G, Gain P, Perrot JL. "En face" ex vivo reflectance confocal microscopy to help the surgery of basal cell carcinoma of the eyelid. Clin Exp Ophthalmol. 2016 Dec 19.

149. Ronin C, Grivet D, Kaspi M, Dumollard JM, Douchet C, Thuret G, Gain PLabeille B, Cinotti E, Perrot JL. [Contribution of reflectance confocal microscopy in the diagnosis of conjunctival melanoma]. Ann Dermatol Venereol. 2016 Dec 7. pii: S0151-9638(16)31153-X.

148. Cinotti E, Labeille B, Cambazard F, Perrot JL. [Dermoscopy and reflectance confocal microscopy examination of pigmented fungiform papillae of the tongue]. Ann Dermatol Venereol. 2016 Dec 7. pii: S0151-9638(16)31154-1

147. Couty E, Cinotti E, Labeille B, Schneider AB, Jaffelin C, Leclercq A, Cambazard F, Perrot JL; Groupe imagerie cutanée non invasive de la Société française de dermatologie.. [The role of reflectance confocal microscopy in diagnosis of pili migrans]. Ann Dermatol Venereol. 2016 Dec 2. pii: S0151-9638(16)31098-5

146. Cinotti E, Perrot JL, Labeille B, Biron AC, Vierkötter A, Heusèle C, Nizard C, Schnebert S, Barthelemy JC, Cambazard F. Skin tumours and skin aging in 209 French elderly people: the PROOF study. Eur J Dermatol. 2016 Oct 1;26(5):470-476.

145. Cinotti E, Labeille B, Cambazard F, Perrot JL. Confocal Microscopy for Special Sites and Special Uses. Dermatol Clin. 2016 Oct;34(4):477-485.

144. Cinotti E, Labeille B, Cambazard F, Perrot JL. Confocal Microscopy for Special Sites and Special Uses. Dermatol Clin. 2016 Oct;34(4):477-485.

143. Perrot JL, Julienne R, Kaspi M, Labeille B, Grivet D, Vercherin A, Cambazard F, Cinotti E ; au nom du groupe imagerie cutanée non invasive de la Société française de dermatologie. [The role of reflectance confocal microscopy in the diagnosis of ocular-cutaneous erucism or dermatitis and keratitis induced by pine processionary caterpillar hairs]. Ann Dermatol Venereol. 2016 Sep 19

142. Cinotti E, Espinasse M, Labeille B, Cambazard F, Perrot JL. Dermoscopy, confocal microscopy and optical coherence tomography for the diagnosis of bedbug infestation. J Eur Acad Dermatol Venereol. 2016 Aug 31

141. Cinotti E, Perrot JL, Labeille B, Heusèle C, Nizard C, Schnebert S, Pichot V, Bernois A, Rabillon C, Barthélémy JC, Cambazard F. Is there a relation between autonomic nervous system activity and skin aging? Evaluation of heart rate variability and skin aging in 209 elderly subjects. Exp Dermatol. 2016 Aug 30.

140. Leclercq A, Cinotti E, Labeille B, Cribier B, Biron AC, Vermersch C, Montlouis J, Cambazard F, Perrot JL; groupe imagerie cutanée non invasive de la Société française de

dermatologie. [The role of reflectance confocal microscopy in the diagnosis of secondary syphilis of the vulva and anus: A first case report]. Ann Dermatol Venereol. 2016 Aug 23

139. Debarbieux S, Perrot JL, Cinotti E, Labeille B, Fontaine J, Douchet C, Balme B, Thomas L. Reflectance confocal microscopy of Pigmented Bowen's disease: misleading dendritic cells. Skin Res Technol. 2016 Jul 19

138. Perrot JL, Labeille B, Habougit C, Douchet C, Tognetti L, Cambazard F, Cinotti E ; groupe d'imagerie cutanée non invasive (ICNI) de la Société française de dermatologie. [The role of reflectance confocal microscopy in the diagnosis of cutaneous melanoma metastasis]. Ann Dermatol Venereol. 2016 Jul 11

137. Kaspi M, Habougit C, Grivet D, Dumollard JM, Douchet C, Singer A, Thuret G, Gain P, Labeille B, Cinotti E, Perrot JL. [The role of reflectance confocal microscopy and optical coherence tomography in the diagnosis of epithelial-cystic conjunctival nevus]. Ann Dermatol Venereol. 2016 Jun 27.

136. Cinotti E, Perrot JL, Labeille B, Biron AC, Vierkötter A, Heusèle C, Nizard C, Schnebert S, Barthelemy JC, Cambazard F. Skin tumours and skin aging in 209 French elderly people: the PROOF study. Eur J Dermatol. 2016 Jun 28

135. Kassir R, Barthelemy JC, Roche F, Perrot JL, Tiffet O. Effect of Vagal Nerve Blockade on Moderate Obesity with an Obesity-Related Comorbid Condition: the ReCharge Study. Obes Surg. 2016 Jun 16. [Epub ahead of print] PubMed PMID:27307164.

134. Méry-Bossard L, Bagny K, Chaby G, Khemis A, Maccari F, Marotte H, Perrot JL, Reguiai Z, Sigal ML, Avenel-Audran M, Boyé T, Grasland A, Gillard J, Jullien D, Toussirot E. New-onset vitiligo and progression of pre-existing vitiligo during treatment with biological agents in chronic inflammatory diseases. J Eur Acad Dermatol Venereol. 2016 Jun 13.

133. Morel J, Gergelé L, Dominé A, Molliex S, Perrot JL, Labeille B, Costes F. The venous-arterial difference in CO(2) should be interpreted with caution in case of respiratory alkalosis in healthy volunteers. J Clin Monit Comput. 2016 Jun 10.

132. Cinotti E, Grivet D, Labeille B, Solazzi M, Bernard A, Forest F, Espinasse M, Cambazard F, Thuret G, Gain P, Perrot JL. The 'tissue press': a new device to flatten fresh tissue during ex vivo confocal microscopy examination. Skin Res Technol. 2016 Jun 5.

131. Boutet C, Barthelemy JC, Tiffet O, Perrot JL, Kassir R. Objective Non-irradiant Imaging of Fat Distribution: New Essential Tools for the Bariatric Surgery? Obes Surg. 2016 Jun 2

130. Couzan C, Cinotti E, Labeille B, Habougit C, Douchet C, Cambazard F, Perrot JL ; groupe imagerie cutanée non invasive de la Société française de dermatologie. [Role of reflectance confocal microscopy and optical coherence tomography as aids in the diagnosis of pemphigoid gestationis]. Ann Dermatol Venereol. 2016 Jun-Jul;143(6-7):483-5.

129. Cinotti E, Labeille B, Douchet C, Chovet M, Habougit C, Cambazard F, PerrotJL; Groupe imagerie cutanée noninvasive de la Société française de dermatologie.[Role of in vivo and ex vivo confocal microscopy and of optical coherence tomography as aids in the diagnosis of molluscum contagiosum]. Ann Dermatol Venereol. 2016 May 20

128. Cinotti E, Labeille B, Douchet C, Cambazard F, Perrot JL; groupe imagerie

cutanée non invasive de la Société française de dermatologie. [Role of dermoscopy and reflectance confocal microscopy as an aid in the diagnosis of exogenous ochronosis]. Ann Dermatol Venereol. 2016 Apr;143(4):318-20.

127. Phan C, Sigal ML, Lhafa M, Barthélémy H, Maccari F, Estève E, Reguiai Z, Perrot JL, Chaby G, Maillard H, Bégon E, Alexandre M, Toussaint P, Bastien-Jacquin M, Bravard P, Sauque E, de Quatrebarbes J, Pfister P, Beauchet A, Mahé E; GEM Resopso. Metabolic comorbidities and hypertension in psoriasis patients in France. Comparisons with French national databases. Ann Dermatol Venereol. 2016 Mar 8. pii: S0151-9638(16)00054-5.

126. Jalenques I, Rondepierre F, Massoubre C, Haffen E, Grand JP, Labeille B, Perrot JL, Aubin F, Skowron F; Lupus Group, Mulliez A, D'Incan M. High prevalence of psychiatric disorders in skin-restricted lupus patients: a case-controlled study. Br J Dermatol. 2016 Jan 8.

125. Leclercq A, Labeille B, Perrot JL, Vercherin P, Cambazard F. Skin graft secured by VAC (vacuum-assisted closure) therapy in chronic leg ulcers: A controlled randomized study. Ann Dermatol Venereol. 2015 Dec 21

124. Couzan C, Perrot JL, Habougit C, Labeille B, Douchet C, Cambazard F, Cinotti E ; Groupe d'imagerie cutanée non invasive de la Société française de dermatologie. [The role of reflectance confocal microscopy and of optical coherence tomography in the diagnosis of pemphigus]. Ann Dermatol Venereol. 2015

123. Bertolotto C, Lesueur F, Giuliano S, Strub T, de Lichy M, Bille K, Dessen P, d'Hayer B, Mohamdi H, Remenieras A, Maubec E, de la Fouchardière A, Molinié V, Vabres P, Dalle S, Poulalhon N, Martin-Denavit T, Thomas L, Andry-Benzaquen P, Dupin N, Boitier F, Rossi A, PERROT JL, Labeille B, Robert C, Escudier B, Caron O, Brugières L, Saule S, Gardie B, Gad S, Richard S, Couturier J, Teh BT, Ghiorzo P, Pastorino L, Puig S, Badenas C, Olsson H, Ingvar C, Rouleau E, Lidereau R, Bahadoran P, Vielh P, Corda E, Blanché H, Zelenika D, Galan P; French Familial Melanoma Study Group, Chaudru V, Lenoir GM, Lathrop M, Davidson I, Avril MF, Demenais F, Ballotti R, Bressac-de Paillerets B. Corrigendum: A SUMOylation-defective MITF germline mutation predisposes to melanoma and renal carcinoma. Nature. 2015 Dec 2

122. Cinotti E, Haouas M, Grivet D, PERROT JL. In Vivo and Ex Vivo Confocal Microscopy for the Management of a Melanoma of the Eyelid Margin. Dermatol Surg. 2015 Dec;41(12):1437-40.

121. Leclercq A, Cinotti E, Labeille B, PERROT JL, Cambazard F. Ex vivo confocal microscopy: a new diagnostic technique for mucormycosis. Skin Res Technol. 2015 Oct 27.

120. Cinotti E, Debarbieux S, PERROT JL, Labeille B, Long-Mira E, Habougit C, Douchet C, Depaepe L, Hammami-Ghorbel H, Lacour JP, Thomas L, Cambazard F, Bahadoran P ; Groupe Imagerie Cutanée Non Invasive de la Société Française de Dermatologie. Reflectance confocal microscopy features of acral lentiginous melanoma: a comparative study with acral nevi. J Eur Acad Dermatol Venereol. 2015 Oct 1

119. Cinotti E, Couzan C, PERROT JL, Habougit C, Labeille B, Cambazard F, Moscarella E, Kyrgidis A, Argenziano G, Pellacani G, Longo C. In vivo confocal microscopic substrate of grey colour in melanosis. J Eur Acad Dermatol Venereol. 2015 Sep 25.

118. Cinotti E, PERROT JL, Labeille B, Cambazard F. Reflectance confocal microscopy for cutaneous infections and infestations. J Eur Acad Dermatol Venereol. 2015 Sep 21.

117. Cinotti E, Labeille B, Cambazard F, Flori P, Raberin H, PERROT JL. Unusual reflectance confocal microscopy findings during the examination of a perianal nevus: pinworms. J Eur Acad Dermatol Venereol. 2015 Sep 15.

116. Rongioletti F, Kaiser F, Cinotti E, Metze D, Battistella M, Calzavara-Pinton PG, Damevska K, Girolomoni G, André J, PERROT JL, Kempf W, Cavelier-Balloy B. Scleredema. A multicentre study of characteristics, comorbidities, course and therapy in 44 patients. J Eur Acad Dermatol Venereol. 2015 Aug 24.

115. Cinotti E, Chevalier J, PERROT JL, Labeille B, Fouilloux B, Cambazard F. Outbreak of onychomadesis in a nursery: which diagnosis? G Ital Dermatol Venereol. 2015 Aug;150(4):475-6.

114. Cinotti E, Jaffelin C, Charriere V, Bajard P, Labeille B, Witkowski A, Cambazard F, PERROT JL. Sensitivity of handheld reflectance confocal microscopy for the diagnosis of basal cell carcinoma: A series of 344 histologically proven lesions. J Am Acad Dermatol. 2015 Aug;73(2):319-20.

113. Cinotti E, Labeille B, Cambazard F, PERROT JL. Reflectance confocal microscopy in infectious diseases. G Ital Dermatol Venereol. 2015 Oct;150(5):575-83.

112. Forest F, Cinotti E, Habougit C, Ginguéné C, PERROT JL, Labeille B, Flori P, Botelho-Nevers E, Péoćh M. Rapid characterization of human brain aspergillosis by confocal microscopy on a thick squash preparation. Cytopathology. 2015 Jun 30. doi: 10.1111/cyt.12258. [Epub ahead of print] PubMed PMID: 26126596.

111. Cinotti E, Labeille B, Cambazard F, Thuret G, Gain P, PERROT JL. Reflectance confocal microscopy for mucosal diseases. G Ital Dermatol Venereol. 2015 Oct;150(5):585-93.

110. Cinotti E, Labeille B, Bernigaud C, Fang F, Chol C, Chermette R, Guillot J, Cambazard F, PERROT JL. Dermoscopy and confocal microscopy for in vivo detection and characterization of Dermanyssus gallinae mite. J Am Acad Dermatol. 2015 Jul;73(1): e15-6.

109. Forest F, Cinotti E, Yvorel V, Habougit C, Vassal F, Nuti C, PERROT JL, Labeille B, Péoc'h M. Ex vivo confocal microscopy imaging to identify tumor tissue on freshly removed brain sample. J Neurooncol. 2015 Sep ;124(2):157-64.

108. Cinotti E, Labeille B, Habougit C, Douchet C, Cambazard F, PERROT JL ; Groupe imagerie cutanée non invasive de la Société française de dermatologie. [Contribution of reflectance confocal microscopy for the diagnosis of junctional naevus]. Ann Dermatol Venereol. 2015 Oct;142(10):595-7.

107. Cinotti E, PERROT JL, Campolmi N, Labeille B, Espinasse M, Grivet D, Thuret G, Gain P, Douchet C, Forest F, Haouas M, Cambazard F. The role of in vivo confocal microscopy in the diagnosis of eyelid margin tumors: reply from the authors. J Am Acad Dermatol. 2015 May;72(5): e123.

106. Kassir R, Barthelemy JC, Roche F, Blanc P, Zufferey P, Galusca B, PERROT JL, Garcin A, Charier D, Tiffet O. Bariatric surgery associated with percutaneous auricular vagal stimulation: A new prospective treatment on weight loss. Int J Surg. 2015 Jun; 18:55-6.

105. Cinotti E, Labeille B, Boukenter A, Ouerdane Y, Cambazard F, PERROT JL. Characterization of coal tattoos by Raman spectroscopy. Skin Res Technol. 2015 Nov; 21(4):511-2.

104. Cinotti E, PERROT JL, Labeille B, Grivet D, Habougit C, Douchet C, F; Groupe imagerie cutanée non invasive/ICNI de la SFD. [Contribution of reflectance confocal microscopy in the diagnosis of eyelid dermal nevus]. Ann Dermatol Venereol. 2015 Mar;142(3):226-8.

103. Cinotti E, PERROT JL, Labeille B, Thuret G, Espinasse M, Grivet D, Gain P, Douchet C, Campolmi N, Cambazard F. In vivo confocal microscopy for eyelids and ocular surface: a new horizon for dermatologists. G Ital Dermatol Venereol. 2015 Feb;150(1):127-9. PubMed PMID: 25686288.

102. Cinotti E, PERROT JL, Labeille B, Cambazard F. Dermatitis neglecta after airbag deployment. J Eur Acad Dermatol Venereol. 2015 Jan 30.

101. Jullienne R, He Z, Manoli P, Grivet D, Cinotti E, PERROT JL, Labeille B, Cambazard F, Gain P, Thuret G. In vivo confocal microscopy of pine processionary caterpillar hair-induced keratitis. Cornea. 2015 Mar;34(3):350-2.

100. Cinotti E, Couzan C, PERROT JL, Labeille B, Bahadoran P, Puig S, Wantz M, Vicente-Villa A, Habougit C, Butori C, Cambazard F. Reflectance confocal microscopy for the diagnosis of vulvar naevi: six cases. J Eur Acad Dermatol Venereol. 2014 Dec 29.

99. Cinotti E, PERROT JL, Labeille B, Campolmi N, Thuret G, Naigeon N, Bourlet T, Pillet S, Cambazard F. First identification of the herpes simplex virus by skin-dedicated ex vivo fluorescence confocal microscopy during herpetic skin infections. Clin Exp Dermatol. 2015 Jun;40(4):421-5

98. Cinotti E, PERROT JL, Labeille B, Cambazard F. A dermoscopic clue for scurvy. J Am Acad Dermatol. 2015 Jan;72(1 Suppl): S37-8.

97. Cinotti E, PERROT JL, Labeille B, Campolmi N, Espinasse M, Grivet D, Thuret G, Gain P, Douchet C, Andrea C, Haouas M, Cambazard F. Handheld reflectance confocal microscopy for the diagnosis of conjunctival tumors. Am J Ophthalmol. 2015 Feb;159(2):324-33.e1

96. PERROT JL, Cinotti E, Labeille B, Cambazard F. [In vivo confocal microscopy for the diagnosis of lysosomal storage diseases]. Ann Dermatol Venereol. 2014 Dec; 141(12):784-5.

95. PERROT JL, Labeille B, Douchet C, Cambazard F, Cinotti E ; Groupe imagerie cutanée non invasive de Société française de dermatologie. [Contribution of reflectance confocal microscopy to the diagnosis of fibroepithelioma of Pinkus]. Ann Dermatol Venereol. 2014 Oct;141(10):643-5.

94. Cinotti E, PERROT JL, Labeille B, Maguet H, Couzan C, Flori P, Cambazard F. Inefficacy of alcohol-based hand rub on mites in a patient with hyperkeratotic scabies. Clin Exp Dermatol. 2015 Mar;40(2):177-81.

93. Cinotti E, PERROT JL, Labeille B, Boukenter A, Ouerdane Y, Cosmo P, Douchet C, Grivet D, Cambazard F. Identification of a soft tissue filler by ex vivo confocal microscopy and Raman spectroscopy in a case of adverse reaction to the filler. Skin Res Technol. 2015 Feb;21(1):114-8.

92. Cinotti E, PERROT JL, Campolmi N, Labeille B, Espinasse M, Grivet D, Thuret G, Gain P, Douchet C, Forest F, Haouas M, Cambazard F. The role of in vivo confocal microscopy in

the diagnosis of eyelid margin tumors: 47 cases. J Am Acad Dermatol. 2014 Nov;71(5):912-918.e2.

91. Boudhraa Z, Rondepierre F, Ouchchane L, Kintossou R, Trzeciakiewicz A, Franck F, Kanitakis J, Labeille B, Joubert-Zakeyh J, Bouchon B, PERROT JL, Mansard S, Papon J, Dechelotte P, Chezal JM, Miot-Noirault E, Bonnet M, D'Incan M, Degoul F. Annexin A1 in primary tumors promotes melanoma dissemination. Clin Exp Metastasis. 2014 Oct;31(7):749-60.

90. Cinotti E, Labeille B, PERROT JL, Pallot-Prades B, Cambazard F. Certolizumab for the treatment of refractory disseminated pyoderma gangrenosum associated with rheumatoid arthritis. Clin Exp Dermatol. 2014 Aug;39(6):750-1.

89. Cinotti E, PERROT JL, Labeille B, Raberin H, Flori P, Cambazard F. Hair dermatophytosis diagnosed by reflectance confocal microscopy: six cases. J Eur Acad Dermatol Venereol. 2015 Nov; 29(11):2257-9.

88. Cinotti E, PERROT JL, Labeille B, Moragues A, Raberin H, Flori P, Cambazard F; groupe imagerie cutanée non invasive de la Société française de dermatologie. [Tinea corporis diagnosed by reflectance confocal microscopy]. Ann Dermatol Venereol. 2014 Feb;141(2):150-2.

87. Cinotti E, Gergelé L, PERROT JL, Dominé A, Labeille B, Borelli P, Cambazard F. Quantification of capillary blood cell flow using reflectance confocal microscopy. Skin Res Technol. 2014 Aug;20(3):373-8.

86. Cinotti E, PERROT JL, Maréchal I, Boukenter A, Ouerdane Y, Ranchon A, Lefèvre M, Guy C, Rigamonti C, Labeille B, Cambazard F. [Unintended changes in the composition of a drug commonly used in dermatology caused by its container]. Ann Dermatol Venereol. 2014 Jan; 141(1):86-8.

85. Cinotti E, PERROT JL, Labeille B, Douchet C, Cambazard F; au nom du groupe imagerie cutanée non invasive de la Société française de dermatologie. [Solar lentigo diagnosed by reflectance confocal microscopy]. Ann Dermatol Venereol. 2014 Jan;141(1):71-3.

84. Champin J, PERROT JL, Cinotti E, Labeille B, Douchet C, Parrau G, Cambazard F, Seguin P, Alix T. In vivo reflectance confocal microscopy to optimize the spaghetti technique for defining surgical margins of lentigo maligna. Dermatol Surg. 2014 Mar ; 40(3):247-56.

83. Debarbieux S, PERROT JL, Erfan N, Ronger-Savlé S, Labeille B, Cinotti E, Depaepe L, Cardot-Leccia N, Lacour JP, Thomas L, Bahadoran P ; Groupe d'Imagerie Cutanée Non Invasive de la Société Française de Dermatologie. Reflectance confocal microscopy of mucosal pigmented macules: a review of 56 cases including 10 macular melanomas. Br J Dermatol. 2014 Jun;170(6):1276-84.

82. Cinotti E, Fouilloux B, PERROT JL, Labeille B, Douchet C, Cambazard F. Confocal microscopy for healthy and pathological nail. J Eur Acad Dermatol Venereol. 2014 Jul; 28(7):853-8.

81. Cinotti E, PERROT JL, Labeille B, Cambazard F;Groupe imagerie cutanée non invasive de la Société française de dermatologie. [The contribution of reflectance confocal microscopy in the diagnosis of Paget's disease of the breast]. Ann Dermatol Venereol. 2013 Dec;140(12):829-32.

80. Cinotti E, Labeille B, PERROT JL, Douchet C, Cambazard F. Cells of Langerhans cell histiocytosis and epidermal Langerhans cells differ under reflectance confocal microscopy: first observation. Skin Res Technol. 2014 Aug;20(3):385-7.
79. Cinotti E, PERROT JL, Labeille B, Cambazard F. [Diagnosis of scabies by high-magnification dermoscopy: the "delta-wing jet" appearance of Sarcoptes scabiei]. Ann Dermatol Venereol. 2013 Nov; 140(11):722-3

78. Kanitakis J, Bahadoran P, Braun R, Debarbieux S, Labeille B, PERROT JL, Vabres P;Groupe d'Imagerie Cutanée Non Invasive de la Société française de dermatologie. [In vivo reflectance confocal microscopy in dermatology: a proposal concerning French terminology]. Ann Dermatol Venereol. 2013 Nov;140(11):678-86.

77. Cinotti E, PERROT JL, Labeille B, Douchet C, Thuret G, Cambazard F. Yellow globules in balloon cell naevus. Australas J Dermatol. 2013 Nov;54(4):268-70.

76. Cinotti E, Chol C, PERROT JL, Labeille B, Forest F, Cambazard F. Anal melanosis diagnosed by reflectance confocal microscopy. Australas J Dermatol. 2014 Nov;55(4):286-8.

75. Cinotti E, Douchet C, PERROT JL, Labeille B, Allombert-Blaise C, Cambazard F. Bullous pemphigoid in an infant with milk protein allergy. Br J Dermatol. 2013 Jul;169(1):191-2.

74. Cinotti E, PERROT JL, Labeille B, Douchet C, Mottet N, Cambazard F. Laser photodynamic treatment for in situ squamous cell carcinoma of the glans monitored by reflectance confocal microscopy. Australas J Dermatol. 2014 Feb;55(1):72-4

73. Cinotti E, PERROT JL, Labeille B, Espinasse M, Ouerdane Y, Boukenter A, Thuret G, Gain P, Campolmi N, Douchet C, Cambazard F. Optical diagnosis of a metabolic disease: cystinosis. J Biomed Opt. 2013 Apr;18(4):046013.

72. Cinotti E, Labeille B, PERROT JL, Boukenter A, Ouerdane Y, Cambazard F. Characterization of cutaneous foreign bodies by Raman spectroscopy. Skin Res Technol. 2013 Nov;19(4):508-9.

71. Cinotti E, PERROT JL, Labeille B, Cambazard F. [On the feasibility of confocal microscopy for the diagnosis of scabies]. Ann Dermatol Venereol. 2013 Mar;140(3):215-6.

70. Cinotti E, PERROT JL, Labeille B, Adegbidi H, Cambazard F. Reflectance confocal microscopy for the diagnosis of vulvar melanoma and melanosis: preliminary results. Dermatol Surg. 2012 Dec;38(12):1962-7.

69. Maubec E, Chaudru V, Mohamdi H, Blondel C, Margaritte-Jeannin P, Forget S, Corda E, Boitier F, Dalle S, Vabres P, PERROT JL, Lyonnet DS, Zattara H, Mansard S, Grange F, Leccia MT, Vincent-Fetita L, Martin L, Crickx B, Joly P, Thomas L; French Familial Melanoma Study Group, Bressac-de Paillerets B, Avril MF, Demenais F. Familial melanoma: clinical factors associated with germline CDKN2A mutations according to the number of patients affected by melanoma in a family. J Am Acad Dermatol. 2012 Dec;67(6):1257-64

68. PERROT JL, Cinotti E, Labeille B, Trau C, Rabérin H, Flori P, Cambazard F. [Rapid diagnosis of scabies by manual confocal reflectance microscopy]. Ann Dermatol Venereol. 2012 Jun;139(6-7):502-5.

67. Meaume S, Truchetet F, Cambazard F, Lok C, Debure C, Dalac S, Lazareth I, Sigal ML, Sauvadet A, Bohbot S, Dompmartin A; CHALLENGE Study Group. A randomized, controlled, double-blind prospective trial with a Lipido-Colloid Technology-Nano-OligoSaccharide Factor wound dressing in the local management of venous leg ulcers. Wound Repair Regen. 2012 Jul-Aug;20(4):500-11.

66. Cinotti E, PERROT JL, Labeille B, Vercherin P, Chol C, Besson E, Cambazard F. Reflectance confocal microscopy for quantification of Sarcoptes scabiei in Norwegian scabies. J Eur Acad Dermatol Venereol. 2013 Feb;27(2): e176-8.

65. Remy C, Barbaud A, Lebrun-Vignes B, PERROT JL, Beyens MN, Mounier G, Marsille F, Roy M, Mismetti P, Guy C. [Skin toxicity related to Percutalgine(®): analysis of the French pharmacovigilance database]. Ann Dermatol Venereol. 2012 May;139(5):350-4.

64. Schoof N, Iles MM, Bishop DT, Newton-Bishop JA, Barrett JH; Genomel Consortium. Pathway-based analysis of a melanoma genome-wide association study: analysis of genes related to tumour-immunosuppression. PLoS One. 2011;6(12): e29451.

63. Bertolotto C, Lesueur F, Giuliano S, Strub T, de Lichy M, Bille K, Dessen P, d'Hayer B, Mohamdi H, Remenieras A, Maubec E, de la Fouchardière A, Molinié V, Vabres P, Dalle S, Poulalhon N, Martin-Denavit T, Thomas L, Andry-Benzaquen P, Dupin N, Boitier F, Rossi A, PERROT JL, Labeille B, Robert C, Escudier B, Caron O, Brugières L, Saule S, Gardie B, Gad S, Richard S, Couturier J, Teh BT, Ghiorzo P, Pastorino L, Puig S, Badenas C, Olsson H, Ingvar C, Rouleau E, Lidereau R, Bahadoran P, Vielh P, Corda E, Blanché H, Zelenika D, Galan P; French Familial Melanoma Study Group, Aubin F, Bachollet B, Becuwe C, Berthet P, Bignon YJ, Bonadona V, Bonafe JL, Bonnet-Dupeyron MN, Cambazard F, Chevrant-Breton J, Coupier I, Dalac S, Demange L, d'Incan M, Dugast C, Faivre L, Vincent-Fétita L, Gauthier-Villars M, Gilbert B, Grange F, Grob JJ, Humbert P, Janin N, Joly P, Kerob D, Lasset C, Leroux D, Levang J, Limacher JM, Livideanu C, Longy M, Lortholary A, Stoppa-Lyonnet D, Mansard S, Mansuy L, Marrou K, Matéus C, Maugard C, Meyer N, Nogues C, Souteyrand P, Venat-Bouvet L, Zattara H, Chaudru V, Lenoir GM, Lathrop M, Davidson I, Avril MF, Demenais F, Ballotti R, Bressac-de Paillerets B. A SUMOylation-defective MITF germline mutation predisposes to melanoma and renal carcinoma. Nature. 2011 Oct 19;480(7375):94-8.

62. Amos CI, Wang LE, Lee JE, Gershenwald JE, Chen WV, Fang S, Kosoy R, Zhang M, Qureshi AA, Vattathil S, Schacherer CW, Gardner JM, Wang Y, Bishop DT, Barrett JH; GenoMEL Investigators, MacGregor S, Hayward NK, Martin NG, Duffy DL; Q-Mega Investigators, Mann GJ, Cust A, Hopper J; AMFS Investigators, Brown KM, Grimm EA, Xu Y, Han Y, Jing K, McHugh C, Laurie CC, Doheny KF, Pugh EW, Seldin MF, Han J, Wei Q. Genome-wide association study identifies novel loci predisposing to cutaneous melanoma. Hum Mol Genet. 2011 Dec 15;20(24):5012-23.

61. Stalder JF, Barbarot S, Wollenberg A, Holm EA, De Raeve L, Seidenari S, Oranje A, Deleuran M, Cambazard F, Svensson A, Simon D, Benfeldt E, Reunala T, Mazereeuv J, Boralevi F, Kunz B, Misery L, Mortz CG, Darsow U, Gelmetti C, Diepgen T, Ring J, Moehrenschlager M, Gieler U, Taïeb A; PO-SCORAD Investigators Group. Patient-Oriented SCORAD (PO-SCORAD): a new self-assessment scale in atopic dermatitis validated in Europe. Allergy. 2011 Aug;66(8):1114-21.

60. Biron-Schneider AC, Clemenson A, Tiffet O, PERROT JL, Peoc'h M, Gentil-Perret A. [Thoracic splenosis mimicking pleural and pulmonary metastasis]. Ann Pathol. 2010 Oct;30(5):382-5.

59. Koenig M, Bageacu S, Delorme MP, PERROT JL, Cambou M, Cuilleron M, Lambert M. [Asthenia, fever, jaundice in a 59-year-old man]. Rev Med Interne. 2010 Apr;31(4):318-20.

58. Ben Said B, Maitre S, PERROT JL, Labeille B, Cambazard F. [Hypercalcemia-hyperleukocytosis paraneoplastic syndrome complicating cutaneous squamous cell carcinoma. Report of two cases]. Rev Med Interne. 2010 Apr;31(4):309-11.

57. Duverger C, Tardy B, Richard A, Célarier T, Bayle S, Cambou M, PERROT JL, Cathebras P, Gonthier R; Fédération de Soins Palliatifs de Saint Etienne. [Prophylactic treatment of venous thromboembolic disease in palliative care. A survey about four different clinical cases]. Presse Med. 2009 Sep;38(9):1235-9.

56. Chraibi R, Gentil-Perret A, Clemenson A, Labeille B, PERROT JL, Cambazard F. [Infantile myofibromatosis with ulceration]. Ann Dermatol Venereol. 2009 Apr;136(4):366-7.

55. Magand F, PERROT JL, Cambazard F, Raberin MH, Labeille B. [Autochthonous cutaneous sporotrichosis in France]. Ann Dermatol Venereol. 2009 Mar;136(3):273-5.

54. Chraïbi R, Labeille B, PERROT JL, Cambazard F. [Congenital macroglossia (Wiedmann-Beckwith syndrome)]. Ann Dermatol Venereol. 2009 Jan;136(1):91-2.

53. de Benedictis FM, Franceschini F, Hill D, Naspitz C, Simons FE, Wahn U, Warner JO, de Longueville M; EPAAC Study Group. The allergic sensitization in infants with atopic eczema from different countries. Allergy. 2009 Feb;64(2):295-303.

52. Chraïbi R, Labeille B, PERROT JL, Cambazard F. [Porphyria cutanea tarda in a patient presenting hepatitis C treated with imatinib]. Ann Dermatol Venereol. 2008 Nov;135(11):775-6.

51. Grüber C, Warner J, Hill D, Bauchau V; EPAAC Study Group. Early atopic disease and early childhood immunization--is there a link? Allergy. 2008 Nov;63(11):1464-72.

50. Reitamo S, Rustin M, Harper J, Kalimo K, Rubins A, Cambazard F, Brenninkmeijer EE, Smith C, Berth-Jones J, Ruzicka T, Sharpe G, Taieb A; 0.1% Tacrolimus Ointment Long-term Follow-up Study Group. A 4-year follow-up study of atopic dermatitis therapy with 0.1% tacrolimus ointment in children and adult patients. Br J Dermatol. 2008 Sep;159(4):942-51

49. Lazareth I, Meaume S, Sigal-Grinberg ML, Combemale P, Guyadec TL, Zagnoli A, PERROT JL, Sauvadet A, Bohbot S. The Role of a Silver Releasing Lipido-colloid Contact Layer in Venous Leg Ulcers Presenting Inflammatory Signs Suggesting Heavy Bacterial Colonization: Results of a Randomized Controlled Study. Wounds. 2008 Jun;20(6):158-66.

48. PERROT JL, Labeille B, Denis Thely L, Maitre S, Blanchon MA, Cambazard F. [Patterns of skin diseases in the elderly]. Ann Dermatol Venereol. 2008 May;135(5):410-2. doi: 10.1016/j.annder.2007.12.015. French. PubMed PMID: 18457733.

47. Duport C, Tiffet O, PERROT JL, Prévot N, Rey Y, Cambazard F. [Sentinel node mapping in anorectal melanoma]. Ann Chir. 2006 Nov;131(9):550-2.

46. Perret AG, PERROT JL, Dutoit M, Fouilloux B, Peoc'h M, Cambazard F. [Superficial angiomyxoma: report of four cases, including two subungueal tumors]. Ann Pathol. 2005 Feb;25(1):54-7. French.

45. Tiffet O, PERROT JL, Gentil-Perret A, Prevot N, Dubois F, Alamartine E, Cambazard F. Sentinel lymph node detection in primary melanoma with preoperative dynamic lymphoscintigraphy and intraoperative gamma probe guidance. Br J Surg. 2004 Jul;91(7):886-92.

44. Misery L, Godard W, Hamzeh H, Lévigne V, Vincent C, PERROT JL, Gentil-Perret A, Schmitt D, Cambazard F. Malignant Langerhans cell tumor: a case with a favorable outcome associated with the absence of blood dendritic cell proliferation. J Am Acad Dermatol. 2003 Sep;49(3):527-9.

43. Misery L, Gregoire M, Prieur F, Froissart R, Guffon N, Maitre S, Fond L, Denis L, PERROT JL, Cambazard F. [Fabry's disease and hypoparathyroidism]. Ann Med Interne (Paris). 2002 Jun;153(4):283-5.

42. Misery L, Antoine JC, Touraine R, Wanders R, Maitre S, Has C, PERROT JL, Cambazard F. [Sjogren-Larsson syndrome: two cases with delayed diagnosis]. Ann Med Interne (Paris). 2002 Jun;153(4):280-2.

41. Maitre S, Jaber K, PERROT JL, Guy C, Cambazard F. [Increased serum and urinary levels of silver during treatment with topical silver sulfadiazine]. Ann Dermatol Venereol. 2002 Feb;129(2):217-9.

40. Misery L, PERROT JL, Gentil-Perret A, Pallot-Prades B, Cambazard F, Alexandre C. Dermatological complications of etanercept therapy for rheumatoid arthritis. Br J Dermatol. 2002 Feb;146(2):334-5.

39. Augusseau-Caillot A, Soler C, Teyssier F, PERROT JL, Tiffet O, Cambazard F, Cuilleret J, Dumollard JM. Interest of PS100 assay when (99m)Tc sestamibi scintigraphy failed to identify lymph node metastases of melanoma. Eur J Dermatol. 2001 Sep-Oct;11(5):432-5.

38. Cathébras P, PERROT JL. [What is a Caucasian? Race and ethnicity in the medical literature]. Presse Med. 2001 Jun 9;30(20):1012-4. French.

37. PERROT JL, PERROT S, Laporte Simitsidis S. [Is anticoagulant therapy useful when treating erysipelas?]. Ann Dermatol Venereol. 2001 Mar;128(3 Pt 2):352-7.

36. Puech-Plottova I, Michel JL, Rouchouse B, PERROT JL, Dzviga C, Cambazard F. [Solar urticaria: one case treated by intravenous immunoglobulin]. Ann Dermatol Venereol. 2000 Oct;127(10):831-5.

35. Reitamo S, Wollenberg A, Schöpf E, PERROT JL, Marks R, Ruzicka T, Christophers E, Kapp A, Lahfa M, Rubins A, Jablonska S, Rustin M. Safety and efficacy of 1 year of tacrolimus ointment monotherapy in adults with atopic dermatitis. The European Tacrolimus Ointment Study Group. Arch Dermatol. 2000 Aug;136(8):999-1006.

34. Tiffet O, PERROT JL, Soler C, Cambazard F, Dubois F, Seguin P, Cuilleret J. [Detection of lymphatic metastasis from malignant melanoma after identification of the sentinel node by preoperative lymphoscintigraphy and intraoperative radioisotopic detection]. Ann Chir. 2000 Jan;125(1):32-9.

33. Devidal R, Guy C, PERROT JL, Cathebras P, Ferron C, Ollagnier M. [Lyell's syndrome and phenobarbital: two cases]. Therapie. 2000 Jan-Feb;55(1):225-7.

32. Lê J, Dauchot P, PERROT JL, Cambazard F, Frey J, Chamson A. Quantitative zymography of matrix metalloproteinases by measuring hydroxyproline: application to gelatinases A and B. Electrophoresis. 1999 Oct;20(14):2824-9.

31. Fond L, Michel JL, Gentil-Perret A, Montelimard N, PERROT JL, Chalencon V, Cambazard F. [Granuloma annulare in the child]. Arch Pediatr. 1999 Sep;6(9):1017-21.

30. Fond L, Michel JL, PERROT JL, Montélimard N, Roy M, Seguin P, Cambazard F. [Bites by domestic animals]. Ann Dermatol Venereol. 1999 Jun-Jul;126(6-7):531-5.

29. Fond L, Godard W, PERROT JL, Michel JL, Misery L, Montelimard N, Boucheron S, Cambazard F. [Case for diagnosis. Pigmented foot lesion]. Ann Dermatol Venereol. 1999 Apr;126(4):341-2.

28. Misery L, Cambazard F, Rimokh R, Ghohestani R, Magaud JP, Gaudillere A, PERROT JL, Berard F, Claudy A, Guyotat D, Schmitt D, Vincent C. Bullous pemphigoid associated with chronic B-cell lymphatic leukaemia: the anti-230-kDa autoantibody is not synthesized by leukaemic cells. Br J Dermatol. 1999 Jul;141(1):155-7.

27. Fond L, Michel JL, Gentil-Perret A, Eve B, Montélimard N, PERROT JL, Cambazard F. [Psoriasis in childhood]. Arch Pediatr. 1999 Jun;6(6):669-74.

26. Michel JL, PERROT JL, Varlet MN, Fond L, Seffert P, Cambazard F. [Exanthematic pustulosis of pregnancy: favorable evolution using calcium and vitamin D2]. J Gynecol Obstet Biol Reprod (Paris). 1999 Feb;28(1):73-5.

25. Fond L, PERROT JL, Gentil-Perret A, Mosnier JF, Michel JL, Cambazard F. [Focal familial palmoplantar keratoderma with punctate hyperkeratosis of the palmar creases]. Ann Dermatol Venereol. 1998 Dec;125(12):898-901.

24. PERROT JL, Soler C, Tiffer O. Cutaneous malignant melanoma: scintigraphic detection of recurrent disease with Tc 99m MIBI. Eur J Dermatol. 1998 Mar;8(2):138.

23. Angel S, Boineau-Géniaux D, Salag P, Trepsat F, Chosidow O, PERROT JL, Will F, Grognard C. [Prevention of facial herpetic infections after chemical peel and dermabrasion: new treatment strategies in the prophylaxis of patients undergoing procedures of the perioral area]. Ann Dermatol Venereol. 1998 Jan;125(1):74-7.

22. Soler C, Beauchesne P, Moncet M, PERROT JL, Mosnier JF, Fotso MJ, Antoine JC, Brunon J, Dubois F. 99mTc-MIBI uptake in a primitive leptomeningeal melanoma. Eur J Dermatol. 1998 Apr-May;8(3):169-72.

21. Soler C, PERROT JL, Thiffet O, Beauchesne P, Lanthier K, Boucheron S, Dubois F, Cambazard F. The role of technetium-99m sestamibi single photon emission tomography in the follow-up of malignant melanoma and the detection of lymph node metastases. Eur J Nucl Med. 1997 Dec;24(12):1522-5.

20. Berthelot P, Guglielminotti C, Frésard A, Lucht F, PERROT JL. Dramatic cutaneous psoriasis improvement in a patient with the human immunodeficiency virus treated with 2',3'-dideoxy,3'-thyacytidine [correction of 2',3'-dideoxycytidine] and ritonavir. Arch Dermatol. 1997 Apr;133(4):531. Erratum in: Arch Dermatol 1998 Apr;134(4):452.

19. Deplaix P, Barthélémy C, Védrines P, PERROT JL, Lanthier K, Pignato F, Audigier JC. [Probable acute hemorrhagic colitis caused by isotretinoin with a test of repeated administration]. Gastroenterol Clin Biol. 1996 Feb;20(1):113-4. French.

18. Michel JL, PERROT JL, Mitanne D, Boucheron S, Fond L, Cambazard F. [Metastatic epidermoid carcinoma in idiopathic CD4+ T lymphocytopenia syndrome]. Ann Dermatol Venereol. 1996;123(8):478-82. Review. French.

17. PERROT JL, PERROT S, Poulard G, Soler C, Bour-Guichenez G, Lanthier K, Claudy AL, Cambazard F. [Bullous manifestations of Kaposi disease associated with AIDS]. Ann Dermatol Venereol. 1995;122(11-12):793-5. French.

16. PERROT JL, Lanthier K, Benoit F, Graille MC, Guy C, Bertheas MF, Cambazard F. [Acquired myelodysplastic syndromes after treatment of melanoma with fotemustine and dacarbazine]. Ann Dermatol Venereol. 1995;122(10):663-6.

15. PERROT JL, Cambazard F. [A case for diagnosis: Hydrea pseudo-dermatomyositis]. Ann Dermatol Venereol. 1994;121(6-7):499-500.

14. Misery L, Blanc L, PERROT JL, Boucheron S, Vasselon C, Guyotat D, Claudy A. [Sweet syndrome in agranulocytosis. A pathogenic hypothesis]. Ann Dermatol Venereol. 1994;121(5):414-5. French.

13. PERROT JL, Tardy B, Barthélémy C, Cambazard F. [Isolated burns after white-spirit ingestion in attempted suicide]. Ann Dermatol Venereol. 1994;121(5):396-8.

12. PERROT JL, Guy C, Bour Guichenez G, Amigues O, Servoz J, Cambazard F. [Porphyria cutanea tarda induced by HMG CoA reductase inhibitors: simvastatin, pravastatin]. Ann Dermatol Venereol. 1994;121(11):817-9.

11. Dacosta A, Guy JM, Cathebras P, PERROT JL, Decousus H, Tardy B, Gonthier R, Lamaud M, Rousset H, Verneyre H. [A rare cause of loss of consciousness: mastocytosis. Apropos of 3 cases]. Arch Mal Coeur Vaiss. 1993 Dec;86(12):1747-52.

10. Misery L, PERROT JL, Vergnon JM, Boucheron S, Emonot A, Claudy A. [Localized epidermal necrolysis after intravenous injection of vinorelbine]. Presse Med. 1992 Dec 19-26;21(44):2153.

9. Tchornobay AM, Claudy AL, PERROT JL, Lévigne V, Denis M. Fatal disseminated Mycobacterium marinum infection. Int J Dermatol. 1992 Apr;31(4):286-7. PubMed PMID: 1634297.

8. PERROT JL, Benoit F, Segault D, Jaubert J, Guyotat D, Claudy A. [Pyoderma gangrenosum aggravated by GM-CSF administration]. Ann Dermatol Venereol. 1992 ; 119(11): 846-8.

7. Lévigne V, PERROT JL, Gagnaire D, Teyssier G, Claudy AL. [Patch parapsoriasis simulating acanthosis nigricans in an adolescent girl]. Ann Dermatol Venereol. 1991 ; 118(1): 23-6.

6. Lévigne V, PERROT JL, Faisant M, Deville V, Claudy AL. [Fibroblastic rheumatism]. Ann Dermatol Venereol. 1990;117(3):199-202. French. PubMed PMID: 2360764.

5. Claudy AL, PERROT JL. Hyperpigmentation induced by UVB at the application site of estradiol. Dermatologica. 1990;181(2):154-5.

4. Euvrard S, Moulonguet-Michau I, Perillat Y, PERROT JL. [Proceedings of the 48th yearly meeting of the American Academy of Dermatology in San Francisco, 2-7 December 1989]. Ann Dermatol Venereol. 1990;117(6-7):496-500.

3. Lévigne V, Colomb M, Faisant M, Larbre B, PERROT JL, Mourier MC, Mazuy A, Claudy A. [Classical bullous Kaposi's disease]. Ann Dermatol Venereol. 1989;116(9):659-61.

2. PERROT JL, Colomb M, Mazuy A, Claudy A. [Urticaria with hypereosinophilia disclosing malignant T-cell lymphoma]. Ann Dermatol Venereol. 1989;116(6-7):467-9.

1. Lucht F, Guy C, PERROT JL, Ollagnier M. [Agranulocytosis caused by cefmenoxime]. Therapie. 1988 Oct-Dec; 43(6):505. French.

1 bis – Publication soumises à comité de lecture (Scopus) :

1. Jaffelin C, Cinotti E., Perrot J.-L., Labeille B, Cambazard F., Tognetti L., Rubegni P., Pittet J.-C. Practical interest of in vivo reflectance confocal microscopy quantification of cutaneous vascular flow during iloprost treatment (Conference Paper). 11th IEEE International Symposium on Medical Measurements and Applications, MeMeA 2016; University of SannioBenevento; Italy; 15 May 2016 through 18 May 2016. 4 August 2016, Article number 7533790.

2. Cinotti E, Perrot, J-L., Labeille B, Cambazard F, Vie R, Delalleau A, Tognetti L, Rubegni P. Season and anatomic site effect on skin color and xerosis quantified using an ultra-high definition videodermoscope (Conference Paper) 11th IEEE International Symposium on Medical Measurements and Applications, MeMeA 2016; University of SannioBenevento; Italy; 15 May 2016 through 18 May 2016; Category numberCFP16MEA-ART; Code 123196. 4 August 2016, Article number 7533791.

2 – Participation à des congrès
2.1) Journées Dermatologiques de Paris (JDP) :

mars 1990 :
. Facteur Von Willebrand et tumeur vasculaire : JL Perrot, J. Reynaud, S. Boucheron, A. Claudy.

mars 1992 :
. Pyoderma gangrenosum aggravé par l'administration de GMCSF : JL Perrot, F. Benoit, D. Segault, J. Jaubert, D. Guyotat, A. Claudy.

. Signes extra-cutanés associés à la sarcoïdose nasale : JL Perrot, L. Misery

mars 1993 :
. Nécrose linguale et scrotale induite par la Terlipressine : JL Perrot, G. Bour-Guichenez, K. Lanthier, F. Benoit, C. Jouffre, J.C Audigier, A. CLaudy.

. Neuroblastome congénital et métastases cutanées : JLPerrot, S. Boucheron, A. Dutour, G. Teyssier, F. Freycon, F. Cambazard.

décembre 1994 :
. Sarcome granulocytaire cutané (à propos de deux observations) : G. Bourg Guichenez, J.L.Perrot, G. Poulard, J. Jaubert, P. Guichenez, F. Cambazard.

décembre 1995 :
. Carcinome épidermoïde métastatique au cours d'une lymphopénie CD4 idiopathique. J.L. Michel, J.L.Perrot, F. Benoit Durafour, F Cambazard.

. Incidence des thromboses veineuse profondes des membres inférieurs au décours des érysipèles et cellulites de jambe. Etude prospective à propos de 86 malades. S.Perrot, J.L.Perrot, Ph Conchonnet. J.L. Michel, C. Bertrand, K. Lanthier, B. Tardy, A. Ros, F. Grattard, P. Lafond, F. F Cambazard.

. Métastases ganglionnaires médiastinales d'un carcinome basocellulaire compliquant la radiothérapie d'une teigne du cuir chevelu. J.L.Perrot, P. Fournel, J.F. JACQUIN, S.Perrot, K. Lanthier, F Cambazard.

novembre 1996 :
. Eruption vésiculeuse congénitale révélatrice d'une histiocytose langerhansienne d'évolution spontanément favorable F Cambazard, J.F. Blanc, J.L.Perrot, S. Boucheron.

. Complications cutanées de l'hydroxyurée : 17 cas. J.L. Michel, J.L.Perrot, L. Thomas, G. Moulin, B. Labeille, B. Fouilloux, D. Guyotat, J. Jaubert F Cambazard

décembre 1997 :

. Interactions Héparine - Ilomédine. L. Fond, S.Perrot, . J.L. Michel B. Tardy, J.L.Perrot, C. Guy, M. Roy, F Cambazard

. Pasteurelloses : une infection mordante. L. Fond, J.L.Perrot, . J.L. Michel, B. Eve, A. Ros, P. Laffont, P. Viallon, F Cambazard

. Lymphome à cellules NK. N. Rabeisin, J.L.Perrot, N. Montélimard, C. Vasselon, S. Boucheron, J. Jaubert, F Cambazard

. Toxidermies au NeuriplégeR : résultats de l'enquête nationale de Pharmacovigilance. C. Ferracin, C. Guy, M. Ollagnier, J.L.Perrot, F. Cambazard, Assocation Française des Centres Régionaux de Pharmacovigilance

décembre 1997 :

. Evaluation de la compréhension du risque solairechez 241 adolescentset de l'efficacité de linformation direct de proximité JL Michel, E Magant,JL Perrot,M Roy,L Fond ,F. Cambazard

.détection des métastases ganglionnaires de mélanome par scintigraphie au 99Tc m Sestamibi.Etude prospective36 observations avec contrôle histologique

.Incidence des thromboses veineuse profondes des membres inférieurs au cours des erysipèleset cellulites de jambes à propos de 161 observations :JL Perrot, S Perrot,PH Paruch,P Viallon , B Tardy,A Ros, P Lafond,F Cambazard

.Intérêt des prélèvements bactériologiques au cours des cellulites et érysipèles de jambeset coût économique à propos de 161 observations :JL Perrot, S Perrot,PH Paruch,P Viallon , B Tardy,A Ros, P Lafond,F Cambazard

.Lymphome à Cellules NK :N Rabeisin,JL Perrot,N Monthélimard,C Vasselon,S Boucheron, J Jaubert,F Cambazard

.Pasteurellose :une infection mordante :L Fond,JL Perrot,JL Michel,B Eve,A Ros,P Laffont,P Viallon,F Cambazard

.Interaction Héparine Ilomédine :L Fond,S Perrot,JL michel,B tardy,JL Perrot,C Guy,M Roy,F Cambazard

.Toxidermie au Neuriplègerésultat de l'enquête nationale de pharmacovigilance :C Ferracin, C Guy,M Ollagnier,JL Perrot,F Cambazard,association française des CRPV

décembre 1998 :

. Pronostic vital de la pemphigoïde bulleuse. Etude rétrospective de 62 observations. J.F. Bourdet, J.L.Perrot, . J.L. Michel, L. Fond, S. Boucheron, F. Cambazard

. Syndrome des paumes rouges secondaire à l'Oxeol : deux observations. J.L.Perrot, J.M. Vergnon, L Misery, D. P. Fournel, . J.L. Michel, M. Ollagnier, F. F Cambazard

. Pseudo-lymphome à l'Atrium à type de lymphome T pléomorphe à moyennes et grandes cellules. J.L.Perrot, S. Boucheron, F. Garcier, CH. Vasselon, P. Gaulard, C. Guy, M. Ollagnier, F. Billard. J.L. Michel, L Misery, F Cambazard

décembre 1999 :

. Ganglion sentinelle de mélanome :une localisation parfois inattendue.Résultats préliminires d'une étude prospective (42 observations). JL Perrot, G Tiffet ,C Soler ,N Prevot ,JM Dumollard , . J.L. Michel,L Misery, F Cambazard

. Vasculite leucocytoclasique au Biostim (comprimé) confirmée par exploration allergologique:premier cas rapporté: JLPerrot, C Dzviga, A Gentil Perret ,N Monthelimard, V Hansali , C Guy , F Cambazard

. Bandes de contention élastique et risque iatrogéne bactérien :quelle méthode de stérilisation proposer ?:JLPerrot, C Billon, S Perrot ,G Nuiry, L Anquetil, G Abeillon, MC Veyre , F Cambazard

. Evaluation de l'éfficassité de l'aspirateur de fumées vis à vis des fumées de laser CO2 lors du traitement de lésions à papillomavirus .JLPerrot, F Chord, . J.L. Michel,M Travasac, L Misery, B Pozetto, F Cambazard.

décembre 2000

. Résultats d'une exporation allergologique pour de spatients présantants des troubles trophique.Etudeprospective à propos de 130 cas

V. Hansali, J.L. Perrot, N. Montélimard, I. Puech ; F. Dechavanne-Badet, J.L. Michel, B. Rouchouse, C. Dzviga, F. Cambazard

. Détection du ganglion sentinelle du mélanome :A propos de 74 observations

J-L Perrot ,G Tiffet ,C Soler ,M Décousus ,N Prévot ,N Granjon ,J-M Dumollard ,A Gentil ,P Seguin ,L Misery ,F Cambazard ,et le groupe ligérien du mélanome

. Aspiration des fumées de laser Co2 et visualisation en infrarouge de leur flux.

Nécessité d'une nouvelle conception des systèmes d'aspiration et d'une protection individuelle fiable J-L Perrot°, F Chord°°, Ph Berthelot°°°, O Tiffet . J-L Michel° L Misery° ,F Cambazard°.

. PS 100 sérique et mélanome métastatique : étude prospective, suivi sur 3 ans, à propos de 46 observations.J-L Perrot , D Frêre , A Caillot , C Soler ,Y Lé , O Tiffet , J-L Michel ,L Misery , F Cambazard

. Hémorragie cataclysmique après exérèse d'un carcinome spinocellulaire : un facteur de risque hémorragique méconnu du dermatologue : le myélomeF Dechavanne-Badet, J-L Perrot, J Raynaud, M Dutoit, J-L Michel, L Misery, N Montélimard, F Cambazard

. Argyrisme à la Flammazine : premier cas français K Jaber, J-L Perrot, C Guy, N Montélimard, J-L Michel ,L Misery, F Cambazard

. Enquète sur l'utilisation de la Biafine au CHU de st - etienneF Grange°, J-L Perrot, F Cambazard, F Alquier, L Misery, R Colomb, V Dubois M-C Veyre

. Sébocystomatose vulvaire:aggravation et extension sous isotrétinoine,premier cas français.I Puech ,J-L Perrot ,C Guy ,L Misery ,J-L Michel ,F Cambazard.

Décembre 2003

. Mélanome de l'enfand'évolution fulgurante C Baudet,DTardieu, J. L. Perrot,JL Stephan, F. Cambazard

. Découverte fortuite d'un cancer du seintotalement asymptomatiqueau décours de la recherche d'un ganglion sentinellede mélanome du poignet.JL Perrot,O Tiffet,A Gentil Perret,N Prévot,F Cambazard

.Détection per-opératoire du ganglion sentinellede mélanome du tronc et des membrespar technique radio-isotopique exclusive JL Perrot,O Tiffet,A Gentil Perret,N Prévot,F Cambazard

.Mélanome du canal anal et ganglio sentinelle :1er cas rapporté JL Perrot,O Tiffet,A Gentil Perret,N Prévot,F Cambazard

.Valeurpronostique du dosage sérique de la PS100lors du diagnostic initial de mélanome (74malades) V Thollet,JL Perrot,D Frere,O Tiffet,P Vercherin,F Cambazard

.VigiPeaul :étude prospectivedescriptive des réactions cutanées médicamenteuses au cours de l'année 2002dans le département de la Loire.réflexion sur la sous notification médicamenteuse.JL Perrot , C Guy , F Cambazard

.Leishmaniose cutanée traitée avec succès par imiquimod5%créme.E Lanier,JL Perrot,H Rabeyrin,G Dimoux-Dime,F Cambazard

Les S Aureus Méthicilline Résistants(SAMR).Etude épidémiologiqueau cours de l'année 2001 dans un service de dermatologie d'un CHU français. J. L. Perrot, Berthelot P ,Ros A, F. Cambazard

Décembre 2004

. UV à usage récréatif :impact de la réglementationsur les pratiques professionnels de l'esthétique J. L. Perrot, S Maitre, F. Cambazard

Décembre 2005

. Miliaire sudorale pas toujours anodine L. Denis-Thely, S. Maitre, J. L. Perrot, B. Labeille, F. Cambazard

.Carcinomes basocellulaires dans le département de la Loire : identification des acteurs prenant en charge ces tumeurs. Données épidémiologiques préliminaires descriptives à propos de 551 carcinomes basocellulaires soit 488 malades. J. L. Perrot, B. Labeille, S. Maitre, B. Trombert, A. Gentil Perret, F. Cambazard

.Un carcinome hypoglycémiant. Annales de Dermatologie et de Vénéréologie C. Germain, J. L. Perrot, B. Labeille, S. Maitre, A. Gentil-Perret, F. Cambazard

.Un syndrome paranéoplasique original au cours d'un carcinome spinocellulaire. B. Bensaid, S. Maitre, B. Labeille, J. Perrot, F. Cambazard

.Le syndrome de Parsonage et Turner : une complication rare de l'immunothérapie par interféron alpha .S. Maitre, J. C. Antoine, J. L. Perrot, L. Denis-Thely, B. Labeille, F. Cambazard

.Exophtalmie alopéciante d'installation brutale. L. Denis-Thely, J. L. Perrot, F. G. Barral, A. Romier, S. Maitre, B. Labeille, F. Cambazard

.Expérience de la surveillance de la transmission de S auréus méthicilline résistant (SAMR) au sein d'un service de dermatologie (sur une période de 18 mois). J. L. Perrot, B. Labeille, A. Ross, S. Maitre, L. Denis, P. Berthelot, F. Cambazard

.Ganglion sentinelle et mélanome – Devenir de 206 malades après 31 mois de suivi moyen : rôle de la taille de la métastase initiale. JL Perrot, O. Tiffet, A. Gentil Perret, B. Labeille, N. Prevot, S. Maitre, F. Cambazard

.Mélanome dans le département de la Loire en 2004 – étude épidémiologique descriptive : données brutes. J. L. Perrot, B. B. Labeille, S. Maitre, B. B. Trombert, O. Tiffet, A. Gentil Perret, F. Cambazard

.Dress syndrome. Responsabilité de la vancomycine prouvée par test de réintroduction. B. Labeille, Jl. Perrot, C. Dzviga, M. Bouteloup, S. Maitre, C. Cazorla, F. Cambazard: P38 –

.Carcinomes basocellulaires dans le département de la Loire : étude des caractéristiques histologiques. Données épidémiologiques préliminaires du fichier carcinome basocellulaires du registre ligérien du mélanome à propos de 551 carcinomes basocellulaires. J. L. Perrot, B. Labeille, S. Maitre, B. Trombert, A. Gentil Perret, F. Cambazard Réseau ligérien du mélanome

.Analyse d'une relecture standardisée des coupes histologiques de mélanome primitif. A. Gentil Perret, J. Perrot, B. Labeille, F. Cambazard, M. Peoc'h

Décembre 2006

. Motifs de consultation des nourrissons en dermatologie : A propos de 3102 consultations, JL Perrot , B Labeille , S Maitre ,Dr L Denis Thely , F Cambazard

.Motifs de consultation d'une consultation de Dermato gériatrie :

.A propos de 6972 consultations du 01 janvier 2000 au 31 décembre 2005 JL Perrot , B Labeille S Maitre ,Dr L Denis Thely , F Cambazard

.Quelles sont les mesures d'hygiènes prise par les infirmières libérales pour les soins d'ulcères à domicile ? Enquête prospective JL Perrot , B Labeille , S Maitre ,Dr L Denis Thely , Pr Ph Berthelot F Cambazard

.Ultra-Violets à usage récréatif : étude comparative concernant les pratiques des professionnels de l'esthétique en institut, dans le département de la Loire en 2001 puis 2006 JL Perrot , B Labeille , S Maitre , Dr L Denis Thely ,B Trombert , F Cambazard et le Réseau Ligérien du Mélanome

.Existe t il une saisonnalité rythmant le diagnostic des Carcinomes baso cellulaires JL Perrot , B Labeille , S Maitre , Dr L Denis Thely ,B Trombert , F Cambazard et le Réseau Ligérien du Mélanome

.Marges d'exérèse des Carcinomes baso cellulaires Enquête prospective de pratique au sein d'un réseau de soinsA propos de 621 tumeurs JL Perrot , B Labeille , S Maitre , Dr L Denis Thely ,B Trombert , F Cambazard et le Réseau Ligérien du Mélanome

.Carcinomes baso cellulaires dans le département de la Loire au cours de l'année 2005 données épidémimiologiques JL Perrot , B Labeille , S Maitre , Dr L Denis Thely ,B Trombert , F Cambazard et le Réseau Ligérien du Mélanome :

Décembre 2007

.Description de la répartition pondérale chez des malades hospitalisés dans un service de dermatologie français en 2006 : à propos de 1870 admissions : JL Perrot , B Labeille ,Dr L Denis , F Cambazard

.Etude de l'exhaustivité des réunions de concertation de cancérologie dermatologique au sein d'un réseau en 2006 JL Perrot , B Labeille ,O Tiffet , O Collard , L Denis Thely ,Th Schmit¨¨ , F Cambazard et le Réseau Ligérien du Mélanome

.Existe t il une différence de motifs de consultation en fonction de l'age au sein d'une population gériatrique .A propos de 13765 consultations du 01 janvier 2000 au 31 décembre 2005 Jl Perrot, B Labeille, L Denis Thely ,MA Blanchon F Cambazard

.Carcinomes spino cellulaires dans le département de la Loire en 2006 :caractéristiques histologiques., et données épidémiologiques préliminaires à propos de 518 carcinomes spino cellulaire soit 496 malades JL Perrot , B Labeille , B Trombert , F Cambazard et le Réseau Ligérien du Mélanome

.A propos d'un cas de sporotrichose autochtone française F Magand , JL Perrot , B Labeille , H Raberin , F Cambazard

.Une grosse langue chez un nourisson R Chraibi, B Labeille JL Perrot F Cambazard

Décembre 2008

Types histologiques des Carcinomes Basocellulaires en fonction du sexe et de la topographie, dans le département de la Loire en 2005, à propos de 1489 tumeurs B Partrat Rouchouse , JL Perrot , B Trombert Paviot , B labeille , F Cambazard

Evaluation de la douleur au cours de la photothérapie dynamique par acide 5-aminolevulinique : à propos de 204 séances :E Cartier,C germain,JL Perrot , B Labeille, N Brunacci, AC Biron, F Magand, F Cambazard

Incidence pour les années 2005 à 2006 du carcinome baso cellulaire dans le département de la Loire JL Perrot , B Trombert Paviot , B Labeille , F Cambazard et les membres du réseau Ligérien du Mélanome

Incidence spécifique de l'âge pour les années 2004 à 2006 pour le mélanome dans le département de la Loire JL Perrot , B Trombert Paviot , B Labeille , F Cambazard et les membres du réseau Ligérien du Mélanome

Incidence spécifique de l'âge pour l'année 2006 des carcinomes spinocellulaires dans le département de la Loire JL Perrot , B Trombert Paviot , B Labeille , F Cambazard et les membres du réseau Ligérien du Mélanome

Premier cas d'hyperkératose filiforme généralisée induite par le Sorafenib E Cartier,JL Perrot, O Collard,B Labeille , C Guy , F Cambazard

Larves de Lucilia Sericata et traitement d'un Pyoderma gangrenosum S. Martelet1, JL. Perrot, B. Labeille, E. Cartier, C. Germain, C. Combe,MC. Veyre, F. Cambazard

Approche médico économique du traitement des ulcères de jambes par Larves de Lucilia sericata S. Martelet, JL. Perrot, B. Labeille, E. Cartier, C. Combe, MC.Veyre, F. Cambazard

Evaluation de la douleur dans le cas du traitement des ulcères par larves de Lucilia Sericata S. Martelet, JL. Perrot, B. Labeille,E Cartier, C. Combe, MC. Veyre, F. Cambazard

Suivi des carcinomes baso cellulaires dans le cadre de la pratique ambulatoire des dermatologues. Qu'en est il de l'application des recommandations de l'ANAES ? Etude à propos de 564 malades diagnostiqués en 2005JL Perrot , B labeille , F Cambazard et les membres du Réseau Ligérien du Mélanome

A propos d'un cas de maladie de Hailey-Hailey traité par photothérapie dynamique A.C Biron , J-L Perrot , B Labeille , F Cambazard

Décembre 2009

.Evaluation de la durée de réalisation des grands badigeons cortisonés dans un service de dermatologie en 2009 JL Perrot , M Alsahli , B Labeille , F Magand , AC Biron , MC Arnolin , N Brunacci , F Cambazard

.Anguillulose disséminée fatale au cours d'un lymphome de Sézary A Maudry ,JL Perrot ,P Flori ,B Labeille ,H Rabeyrin ,Ph Berthelot ,F Cambazard

.Evaluation de la durée de réalisation des pansements d'ulcère ou d'escarre dans un service de dermatologie en 2009 JL Perrot , M Alsahli , B Labeille , F Magand , AC Biron , MC Arnolin , N Brunacci , , F Cambazard

.Intérêt de la réalisation de pansement en pression négative lors de greffes cutanées dans 5 situations extrêmes JL Perrot , B Labeille ,O Tiffet ,F Magand , AC Biron , M Alsahli , N Brunacci , , F Cambazard

.Evaluation du poids des déchets de soins secondaire à la réalisation de pansements de trouble trophiques dans un service de dermatologie en 2009 JL Perrot , Alsahli , Maha , B Labeille ,B Paviot Thrombert ,N Brunacci , Ph Berthelot , F Cambazard

.Evaluation du poids des déchets de soins secondaire lors de la réalisation d'acte de chirurgie dermatologique de routine JL Perrot , Alsahli , Maha , B Labeille ,B Paviot Thrombert ,N Brunacci , Ph Berthelot , F Cambazard

.Incidence spécifique de l'âge pour l'année 2006 des carcinomes spinocellulaires dans le département de la Loire JL Perrot , B Trombert Paviot , B Labeille , F Cambazard et les membres du réseau Ligérien du Mélanome

.Incidence brute pour les années 2005 à 2008 du carcinome baso cellulaire dans le département de la Loire : une augmentation significative B Partrat Rouchouse , JL Perrot , B Trombert Paviot , B labeille , F Cambazard

.Evolution de l'incidence et des caractéristiques des mélanomes dans le département de la Loire de 2004 à 2008 B Partrat Rouchouse , JL Perrot , B Trombert Paviot , B labeille , F Cambazard

.Aspect dermoscopique de la papulose lymphomatoide : le patron volcanique ? JL Perrot B Labeille M D'Incan P Souteyrand F Cambazard

.Un cas de granulomatose lymphomatoïde sous Hydréa F Magand , JL Perrot , B labeille , J Servoz, A Gentil Perret , E Cartier, F Cambazard

.Evolution des marges latérales microscopiques d'exérèse des carcinomes basocellulaires dans la Loire et la Haute Loire de 2006 à 2008 JL Perrot, B Labeille, F Cambazard, W Godard, A Gentil Perret, G Chanoz Poulard, J Chanoz, I Laurent, C Bozon, F Billard, C Herve, C Douchet, A Vercherin et les membres du réseau Ligérien du Mélanome

.Un cas de dermohypodermite aigue à Campylobacter Jejuni F Magand , F Lucht , JL Perrot , B labeille , F Cambazard

Décembre 2010

Impact des recommandations Inca, HAS, SFD concernant les facteurs histo-pronostiques des carcinomes spinocellulaires sur la pratique des anatomopathologistes dans le département de la Loire JL Perrot , B Labeille , B Trombert Paviot , F Cambazard

Décembre 2011

J.-L. Perrot, B. Labeille, P. Flori, F. Cambazard: Aspect en microscopie confocale de la gale humaine. Annales de Dermatologie et de Vénéréologie 12/2011; 138(12):A258-A259.

E. Besson, J.-L. Perrot, B. Labeille, D. Frère, F. Cambazard: La protéine S100 bêta : un marqueur tumoral des mélanomes métastatiques ? À propos de 1299 dosages chez 225 patients. Annales de Dermatologie et de Vénéréologie 12/2011; 138(12):A288.

F. Cambazard, J.-L. Perrot, B. Labeille: Que doit faire évoquer l'apparition d'un angiome plan chez un enfant ?. Annales de Dermatologie et de Vénéréologie 12/2011; 138(12):A161-A162.

F. Cambazard, B. Labeille, J.-L. Perrot: Que faire en cas de d'apparition de poils sur le scrotum d'un nourrisson ?. Annales de Dermatologie et de Vénéréologie 12/2011; 138(12):A147.

J.-L. Perrot, B. Labeille, C. Douchet, T. Alix, G. Parraud, F. Cambazard: Repérage par microscopie confocale des marges d'exérèse de mélanomes in situ de type Dubreuilh : à propos de cinq observations. Annales de Dermatologie et de Vénéréologie 12/2011; 138(12):A282.

C. Chol, J.-L. Perrot, C. Guy, B. Labeille, F. Cambazard: Modalités de prise en charge des abcès après Vaccin BCG SSI : étude descriptive à partir de 1050 observations issues de l'enquête nationale de pharmacovigilance. Annales de Dermatologie et de Vénéréologie 12/2011; 138(12):A166.

J.-L. Perrot, B. Labeille, A.-C. Biron Schneider, E. Besson, C. Chol, E. Cartier, F. Cambazard: Traitement par photothérapie dynamique d'une maladie de Hailey-Hailey : comparaison rétrospective de la douleur selon deux modalités de délivrance de la lumière. Annales de Dermatologie et de Vénéréologie 12/2011; 138(12):A180-A181.

J.-L. Perrot, B. Labeille, C. Douchet, E. Cartier, A.-C. Biron, F. Cambazard: Diagnostic d'une métastase sous cutanée de mélanome par microscopie confocale à propos de quatre observations. Annales de Dermatologie et de Vénéréologie 12/2011; 138(12):A283.

J.-L. Perrot, B. Labeille, E. Cartier, A.-C. Biron, E. Besson, C. Chol, F. Cambazard: Résultats thérapeutiques de l'UVA1 thérapie chez 51 malades. Annales de Dermatologie et de Vénéréologie 12/2011; 138(12):A179.

C. Chol, J.-L. Perrot, C. Guy, B. Labeille, E. Cartier, F. Cambazard: Un cas de démence sous dacarbazine (Déticène®). Annales de Dermatologie et de Vénéréologie 12/2011; 138(12):A178.

E. Cartier, J.-L. Perrot, B. Labeille, F. Cambazard: Mélanome muqueux : caractéristiques cliniques et thérapeutiques dans la Loire. Annales de Dermatologie et de Vénéréologie 12/2011; 138(12):A217-A218.

J.-L. Perrot, B. Labeille, C. Douchet, A.C. Biron, F. Cambazard: Maladie de Paget du sein diagnostiquée en microscopie confocale, associée à un carcinome mammaire in situ. Annales de Dermatologie et de Vénéréologie 12/2011; 138(12):A213-A214.

J.-L. Perrot, B. Labeille, C. Douchet, F. Cambazard: Diagnostic en microscopie confocale d'un carcinome basocellulaire de type Pinkus. Annales de Dermatologie et de Vénéréologie 12/2011; 138(12):A209-A210.

J.-L. Perrot, B. Labeille, F. Cambazard: Visualisation de la nécrose cellulaire d'un carcinome basocellulaire traité par photothérapie dynamique en microscopie confocale. Annales de Dermatologie et de Vénéréologie 12/2011; 138(12):A211.

J.-L. Perrot, B. Trombert Paviot, B. Labeille, F. Cambazard: Étude de l'incidence standardisée française et mondiale du Mélanome in situ hors Dubreuilh dans le département de la Loire de 2004 à 2009. Annales de Dermatologie et de Vénéréologie 12/2011; 138(12):A285.

J.-L. Perrot, B. Trombert Paviot, B. Labeille, F. Cambazard: Étude de l'incidence standardisée française et mondiale des mélanomes de type Dubreuilh (Lentigo Malignant Melanoma) dans le département de la Loire de 2004 à 2009. Annales de Dermatologie et de Vénéréologie 12/2011; 138(12):A283-A284.

B. Labeille, J.-L. Perrot, F. Cambazard: Apport de la microscopie confocale par réflectance laser pour le diagnostic et le traitement par PDT des carcinomes basocellulaires du syndrome de Gorlin. Annales de Dermatologie et de Vénéréologie 12/2011; 138(12):A139-A140.

J.-L. Perrot, B. Labeille, P. Flori, F. Cambazard: Intérêt de la microscopie confocale pour le diagnostic de la gale humaine. Annales de Dermatologie et de Vénéréologie 12/2011; 138(12):A257-A258.

E. Cartier, J.-L. Perrot, B. Labeille, F. Cambazard: Épidémiologie du mélanome muqueux dans la Loire. Annales de Dermatologie et de Vénéréologie 12/2011; 138(12):A218.

J.-L. Perrot, B. Labeille, C. Schipkov, C. Douchet, F. Cambazard: Repérage par microscopie confocale des marges d'exérèse d'un carcinome basocellulaire infiltrant à propos d'une observation. Annales de Dermatologie et de Vénéréologie 12/2011; 138(12):A210.

Décembre 2012

J.-L. Perrot, B. Labeille, G. Thuret, P. Gain, D. Grivet, E. Cinotti, F. Cambazard: Faisabilité d'un examen de la conjonctive bulbaire au moyen d'un microscope confocal dédié originellement à la dermatologie. Annales de Dermatologie et de Vénéréologie 12/2012; 139(12):B217-B218.

S. Debarbieux, J.-L. Perrot, N. Erfan, B. Labeille, E. Cinotti, L. Depaepe, J.-P. Lacour, L. Thomas, P. Bahadoran: Étude par microscopie confocale in vivo des macules mélaniques muqueuses : 40 observations. Annales de Dermatologie et de Vénéréologie 12/2012; 139(12):B221.

J.-L. Perrot, B. Labeille, E. Cinotti, A.-C. Biron, C. Douchet, H. Adegbidi, F. Cambazard: Une étiologie inhabituelle de carcinome basocellulaire : le laminage des métaux. Annales de Dermatologie et de Vénéréologie 12/2012; 139(12):B276.

J.-L. Perrot, B. Labeille, A.-C. Biron, E. Cinotti, H. Adegbidi, B. Trombert, F. Cambazard: Aspects épidémiologique de 12 091 carcinomesbasocellulaires consécutifs pris en charge de 2005 à 2011 dansle département de la Loire. Annales de Dermatologie et de Vénéréologie 12/2012; 139(12):B246.

J.-L. Perrot, E. Cinotti, B. Labeille, Y. Ouerdane, A. Boukenter, P. Gain, G. Thuret, F. Cambazard: Diagnostic optique d'une affection métabolique, la cystinose : premier cas rapporté. Annales de Dermatologie et de Vénéréologie 12/2012; 139(12):B223.

J.-L. Perrot, B. Labeille, G. Thuret, D. Grivet, E. Cinotti, M. Espinasse, P. Gain, F. Cambazard: Examen en microscopie confocale de tumeurs du bord libre des paupières. Annales de Dermatologie et de Vénéréologie 12/2012; 139(12):B218. DOI:10.1016/j.annder.2012.10.375

F. Cambazard, J. Chevallier, E. Cinotti, B. Fouilloux, B. Labeille, J.-L. Perrot: Quel diagnostic envisager en cas de survenue d'une épidémie de chute des ongles chez les enfants d'une crèche ?. Annales de Dermatologie et de Vénéréologie 12/2012; 139(12):B154-B155. DOI:10.1016/j.annder.2012.10.234

B. Labeille, J.-L. Perrot, E. Cinotti, C. Douchet, H. Adegbidi, F. Cambazard: Microscopie confocale du mamelon : première observation de cancer canalaire du sein. Annales de Dermatologie et de Vénéréologie 12/2012; 139(12):B221-B222. DOI:10.1016/j.annder.2012.10.383

B. Labeille, J.-L. Perrot, N. Glas, E. Cinotti, H. Adegbidi, F. Cambazard: Sarcoïdose cutanée et pulmonaire induite par ipilimumab au cours d'un mélanome métastatique. Annales de Dermatologie et de Vénéréologie 12/2012; 139(12):B262-B263.

J.-L. Perrot, B. Labeille, E. Cinotti, A.-C. Biron, P. Flori, B. Tromber, F. Cambazard: Évolution du nombre des cas de gale vus au cours de 97 357 consultations successives dans un service de dermatologie de janvier 2001 à juin 2012. Annales de Dermatologie et de Vénéréologie 12/2012; 139(12):B192.

E. Maubec, V. Chaudru, H. Mohamdi, C. Blondel, P. Jeannin, S. Forget, E. Corda, F. Boitier, S. Dalle, P. Vabres, J.-L. Perrot, D. Stoppa-Lyonnet, H. Zattara, S. Mansard, F. Grange, M.-T. Leccia, L. Vincent-Fetita, L. Martin, B. Crickx, P. Joly, L. Thomas, B. Bressac-de-Paillerets, M.-F. Avril, F. Demenais: Mélanome familial : l'âge jeune au diagnostic du mélanome et la survenue de mélanomes primitifs multiples sont des facteurs prédictifs de mutations de CDKN2A dans les familles à deux cas. Annales de Dermatologie et de Vénéréologie 12/2012; 139(12):B111.

F. Cambazard, A. Phan, E. Cinotti, B. Labeille, H. Adegbidi, J.-L. Perrot: Manifestations cutanées atypiques du syndrome mains-pieds-bouche. Annales de Dermatologie et de Vénéréologie 12/2012; 139(12):B159-B160.

C. Guy, J.-L. Perrot, M. Beyens, G. Mounier, B. Labeille, F. Marsille, M. Roy, P. Mismetti, F. Cambazard: Enquête nationale de pharmacovigilance concernant le nicorandil. Annales de Dermatologie et de Vénéréologie 12/2012; 139(12):B294.

J.-L. Perrot, B. Labeille, J. Champin, E. Cinotti, C. Douchet, H. Adegbidi, F. Cambazard: Optimisation du traitement chirurgical du mélanome de Dubreuilh par l'identification des marges saines au moyen d'un microscope confocal à balayage laser in vivo. Annales de Dermatologie et de Vénéréologie 12/2012; 139(12):B217.

J.-L. Perrot, B. Labeille, E. Cinotti, A.-C. Biron, G. Thuret, C. Douchet, D. Grivet, F. Cambazard: Aspect en dermatoscopie et microscopie confocale d'un nævus à cellules ballonisantes de l'enfant : premier cas rapporté. Annales de Dermatologie et de Vénéréologie 12/2012; 139(12):B156-B157.

J.-L. Perrot, B. Labeille, O. Tiffet, C. Douchet, E. Cinotti, N. Mottet, F. Cambazard: Identification des marges d'exérèse d'une maladie de Paget extra-mammaire par microscopie confocale. Annales de Dermatologie et de Vénéréologie 12/2012; 139(12):B218-B219.

E. Cinotti, B. Labeille, J.-L. Perrot, A. Boukenter, Y. Ouerdane, M. Espinasse, F. Cambazard: Spectroscopie RAMAN pour identifier la nature des corps étrangers. Annales de Dermatologie et de Vénéréologie 12/2012; 139(12):B222-B223.

A.-C. Biron, J.-L. Perrot, B. Labeille, F. Cambazard: Prise en charge des plaies chroniques par électrostimulation. Annales de Dermatologie et de Vénéréologie 12/2012; 139(12):B279.

E. Cinotti, K. Billiemaz, C. Gay, J.-L. Perrot, B. Labeille, F. Cambazard: Première description des manifestations cutanées du syndrome tricho-hépato-entérique. Annales de Dermatologie et de Vénéréologie 12/2012; 139(12):B151.

Décembre 2013

J.-L. Perrot, N. Naigeon, B. Labeille, E. Cinotti, G. Thuret, N. Campolmi, T. Bourlet, C. Douchet, F. Cambazard: Première description de l'identification spécifique d'HSV1 au cours d'une infection cutanée au moyen d'un microscope confocal ex vivo en fluorescence. Annales de Dermatologie et de Vénéréologie 12/2013; 140(12):S578-S579.

J.-L. Perrot, N. Menant, B. Labeille, C. Elisa, F. Cambazard, A. Ros: Épidémiologie des SAMR dans un service de dermatologie de 2005 à 2011 : à propos de 266 malades. Annales de Dermatologie et de Vénéréologie 12/2013; 140(12):S472.

J.-L. Perrot, B. Labeille, E. Cinotti, D. Grivet, M. Espinasse, C. Douchet, G. Thuret, P. Gain, F. Cambazard: Diagnostic par microscopie confocale de mélanomes du bord libre des paupières : première série rapportée. Annales de Dermatologie et de Vénéréologie 12/2013; 140(12):S459.

J.-L. Perrot, E. Cinotti, B. Labeille, H. Raberin, P. Flori, C. Douchet, F. Cambazard: Intérêt de l'étude en microscopie confocale ex vivo pour le diagnostic de sycosis de la barbe. Première observation. Annales de Dermatologie et de Vénéréologie 12/2013; 140(12):S592.

C. Chol, J.-L. Perrot, A.-C. Biron-Schneider, B. Labeille, E. Cinotti, F. Cambazard: Suivi moyen en mois sur 336 patients opérés d'un mélanome entre 1998 et 2009. Annales de Dermatologie et de Vénéréologie 12/2013; 140(12):S499-S500.

J.-L. Perrot, E. Cinotti, B. Labeille, J. George, J.-M. Lagarde, A.-C. Biron, F. Cambazard: Analyse quantitative des images réalisées avec un dermatoscope HD : étude réalisée chez 79 femmes âgées de 77 à 78ans. Annales de Dermatologie et de Vénéréologie 12/2013; 140(12):S464-S465.

A.-C. Biron, C. Chol, J.-L. Perrot, B. Labeille, J. Chevalier, A. Leclercq, E. Besson, F. Cambazard: Greffe cutanée de plaies chroniques par ensemencement cellulaire autologue. Annales de Dermatologie et de Vénéréologie 12/2013; 140(12):S508.

J. Chevallier, E. Cinotti, J.-L. Perrot, B. Labeille, L. Thomas, F. Cambazard: Étude des mutations du gène c-kit de 43 mélanomes muqueux de la région Rhône Alpes. Annales de Dermatologie et de Vénéréologie 12/2013; 140(12):S496.

J.-L. Perrot, B. Labeille, E. Cinotti, D. Grivet, N. Campolmi, G. Thuret, C. Douchet, F. Forest, F. Cambazard: Microscopie confocale in vivo et ex vivo : application à la chirurgie micrographique de Mohs des tumeurs palpébrales : à propos de six carcinomes basocellulaires. Annales de Dermatologie et de Vénéréologie 12/2013; 140(12):S447.

S. Debarbieux, S. Ronger Savlé, E. Cinotti, P. Bahadoran, L. Depaepe, E. Long-Mira, J.-L. Perrot, B. Labeille, L. Thomas: Diagnostic non invasif en microscopie confocale in vivo de formes maculeuses de mélanomes muqueux. Annales de Dermatologie et de Vénéréologie 12/2013; 140(12):S460.

J.-L. Perrot, B. Labeille, E. Cinotti, F. Cambazard: Motifs d'envoi à propos de 1455 carcinomes basocellulaires consécutifs pris en charge en 2005 dans le département de la Loire. Annales de Dermatologie et de Vénéréologie 12/2013; 140(12):S448.

J.-L. Perrot, E. Cinotti, B. Labeille, C. Douchet, F. Cambazard: Essai de validation de la caméra Vivascope 3000 pour le diagnostic des carcinomes basocellulaires. Annales de Dermatologie et de Vénéréologie 12/2013; 140(12):S461.

J.-L. Perrot, B. Labeille, C. Elisa, O. Nuiry, J. Dietemann, F. Cambazard: Thérapie par pression négative des troubles trophiques : sept ans d'expérience dans un CHU. Annales de Dermatologie et de Vénéréologie 12/2013; 140(12):S508-S509.

E. Cinotti, J.-L. Perrot, B. Labeille, A. Biron, F. Cambazard: Reproductibilité inter-investigateur du score de vieillissement cutané SCINEXA. Annales de Dermatologie et de Vénéréologie 12/2013; 140(12):S475-S476. DOI:10.1016/j.annder.2013.09.261

J.-L. Perrot, E. Cinotti, A. Boukenter, B. Labeille, Y. Ouerdane, F. Cambazard: Dissolution de récipients en plastique au contact de l'Ascabiol® lors du traitement de la gale : un nouveau type de pharmacovigilance. Annales de Dermatologie et de Vénéréologie 12/2013; 140(12):S516.

M. D'Incan, F. Cachin, J.M. Chezal, J.-L. Perrot, B. Labeille, L. Machet, J.-P. Lacour, J.L. Schmutz, J.J. Grob, M.-T. Leccia, M.-C. Ferrier-Le Bouedec, J.-D. Grange, N. Meyer: L'123I-BZA2, nouveau traceur pour le diagnostic de métastases pigmentées de mélanome : résultats et perspectives d'une étude clinique de phase III. Annales de Dermatologie et de Vénéréologie 12/2013; 140(12):S405-S406.

J.-L. Perrot, B. Labeille, E. Cinotti, M. Espinasse, D. Grivet, N. Campolmi, G. Thuret, F. Cambazard: Intérêt diagnostic de l'examen en microscopie confocale in vivo des tumeurs des paupières à propos de 53 malades, 54 tumeurs. Annales de Dermatologie et de Vénéréologie 12/2013; 140(12):S459-S460.

B. Labeille, E. Cinotti, J.-L. Perrot, C. Douchet, F. Cambazard: Pyoderma gangrenosum disséminé associé à une polyarthrite rhumatoïde : évolution favorable sous-certolizumab. Annales de Dermatologie et de Vénéréologie 12/2013; 140(12):S556.

Décembre 2014

E. Cinotti, C. Couzan, J.L. Perrot, B. Labeille, P. Bahadoran, M. Wantz, C. Douchet, F. Cambazard: Premiers nævus vulvaires diagnostiqués par microscopie confocale. Annales de Dermatologie et de Vénéréologie 12/2014; 141(12):S326.

C. Couzan, E. Cinotti, J.L. Perrot, B. Labeille, F. Cambazard: Rôle de la microscopie confocale dans le diagnostic des lésions du mamelon. Annales de Dermatologie et de Vénéréologie 12/2014; 141(12):S326-S327.

B. Labeille, J.L. Perrot, E. Cinotti, C. Douchet, F. Cambazard: Carcinomes basocellulaires du syndrome de Gorlin régressant sous vismodegib : évaluation par microscopie confocale in vivo dans 20 cas. Annales de Dermatologie et de Vénéréologie 12/2014; 141(12):S326.

E. Cinotti, J.L. Perrot, B. Labeille, C. Chol, A.C. Biron, J.C. Barthelemy, C. Heusele, C. Nizard, S. Schnebert, F. Cambazard: Épidémiologie des kératoses actiniques chez une cohorte de 163 sujets âgés de 77ans. Annales de Dermatologie et de Vénéréologie 12/2014; 141(12):S316.

C. Chol, J.L. Perrot, A.C. Biron Schneider, B. Labeille, E. Cinotti, F. Cambazard: Première observation d'un herpès extensif du visage au cours d'un traitement par vémurafénib. Annales de Dermatologie et de Vénéréologie 12/2014; 141(12):S490.

J. Perrot, E. Cinotti, B. Labeille, F. Cambazard: Microscopie confocale et lésions vasculaires et analyse dynamique du débit vasculaire : un nouveau champ d'investigation de la microscopie confocale. Annales de Dermatologie et de Vénéréologie 12/2014; 141(12):S327-S328.

C. Chol, J.L. Perrot, A.C. Biron Schneider, B. Labeille, E. Cinotti, F. Cambazard: Données sur l'engaînement périnerveux et les emboles vasculaires des carcinomes spinocellulaires de la Loire entre 2011 et 2013 : à propos de 1761 cas. Annales de Dermatologie et de Vénéréologie 12/2014; 141(12):S314-S315.

J. Perrot, E. Cinotti, B. Labeille, F. Cambazard: Comparaison de l'efficacité imiquimod, 5FU, ingénol mébutate à propos d'un cas de porokératose actinique étendue ou comment proposer de manière objective et simple un traitement personnalisé. Annales de Dermatologie et de Vénéréologie 12/2014; 141(12):S489-S490.

J. Perrot, B. Labeille, E. Cinotti, D. Grivet, G. Thuret, C. Douchet, C. Chauleur, F. Cambazard: Premiers cas rapportés de contrôle de la qualité de l'exérèse d'un mélanome muqueux en microscopie confocale ex vivo : chirurgie de Mohs adaptée à la microscopie confocale. Annales de Dermatologie et de Vénéréologie 12/2014; 141(12):S328.

E. Cinotti, M. Le Cordroch, J.L. Perrot, B. Labeille, A.C. Biron, C. Chol, F. Cambazard: Dermatoscopie versus microscopie confocale pour le diagnostic de gale. Annales de Dermatologie et de Vénéréologie 12/2014; 141(12):S327.

J.-L. Perrot, E. Cinotti, B. Labeille, D. Charrier, J. Barthelemy, A. Biron, F. Cambazard: Quantification objective, par mesure de la variation du diamètre pupillaire, de la douleur induite lors de la réalisation d'une anesthésie locale cutanée par lidocaïne 2 %. Annales de Dermatologie et de Vénéréologie 12/2014; 141(12):S483.

J. Perrot, E. Cinotti, B. Labeille, D. Charier, A. Biron, C. Chol, J. Barthelemy, F. Cambazard: Comparaison de la douleur issue d'actes dermatologiques ambulatoires à la douleur de parturientes en travail et à celle de malades en salle de réveil post-opératoire. Annales de Dermatologie et de Vénéréologie 12/2014; 141(12):S482-S483.

J. Perrot, B. Labeille, E. Cinotti, A. Biron, F. Grattard, F. Cambazard: Données biométriques et biologiques des patients porteurs de SAMR dans un service de dermatologie de 2005 à 2011 : à propos de 266 malades. Annales de Dermatologie et de Vénéréologie 12/2014; 141(12):S454.

J. Perrot, E. Cinotti, B. Labeille, A. Biron, F. Cambazard, C. Chol: Étude de la variabilité inter-dermatologues du diagnostic de carcinome basocellulaire, spinocellulaire, mélanome et mélanome in situ chez 39 dermatologues d'un même département sur une période de 8ans. Annales de Dermatologie et de Vénéréologie 12/2014; 141(12):S362.

A.-C. Biron, C. Chol, J.-L. Perrot, B. Labeille, F. Cambazard: À propos de 1610 mélanomes dans le département de la Loire entre 2004 et 2013. Annales de Dermatologie et de Vénéréologie 12/2014; 141(12):S394-S395. DOI:10.1016/j.annder.2014.09.377

C. Chol, J.L. Perrot, A.C. Biron Schneider, B. Labeille, E. Cinotti, F. Cambazard: Épidémiologie des carcinomes basocellulaires de la Loire entre 2006 et 2013 : à propos de 160 001 cas. Annales de Dermatologie et de Vénéréologie 12/2014; 141(12):S360-S361.

C. Chol, J.L. Perrot, A.C. Biron Schneider, B. Labeille, E. Cinotti, F. Cambazard: Données histologiques et topographiques des carcinomes basocellulaires du département de la Loire entre 2006 et 2013 : à propos de 15 682 cas. Annales de Dermatologie et de Vénéréologie 12/2014; 141(12):S361.

C. Jaffelin, J.L. Perrot, B. Labeille, F. Cambazard: Gingivite pustuleuse immuno-allergique induit par le vémurafénib : nouvelle toxicité des inhibiteurs de BRAF. Annales de Dermatologie et de Vénéréologie 12/2014; 141(12):S403.

E. Cinotti, J.L. Perrot, B. Labeille, R. Touraine, J.C. Antoine, F. Cambazard: Explication génétique d'une ancienne entité clinique : angiokératome de Mibelli. Annales de Dermatologie et de Vénéréologie 12/2014; 141(12):S381.

A.-C. Biron, C. Chol, J.-L. Perrot, B. Labeille, F. Cambazard: Incidence du mélanome dans la Loire de 2004 à 2013 : une augmentation significative. Annales de Dermatologie et de Vénéréologie 12/2014; 141(12):S394.

C. Chol, J.L. Perrot, A.C. Biron Schneider, B. Labeille, E. Cinotti, F. Cambazard: Épidémiologie des carcinomes spinocellulaires du département de la Loire entre 2006 et 2013 : à propos de 4496 cas. Annales de Dermatologie et de Vénéréologie 12/2014; 141(12):S361-S362.

Décembre 2015

J. Perrot, E. Cinotti, B. Labeille, R. Julienne, A. Brehon, D. Grivet, G. Thuret, V. Prade, T. Alix, F. Cambazard: Place de la microscopie confocale pour la prise en charge des atteintes muqueuses la pemphigoïde cicatricielle à propos de 6 patients. Premiers cas rapportés de bulles conjonctivales. Annales de Dermatologie et de Vénéréologie 12/2015; 142(12):S515.

E. Cinotti, J. Perrot, B. Labeille, C. Jaffelin, A. Biron, A. Leclercq, F. Cambazard: Comparaison dermatoscopie et microscopie confocale pour le diagnostic de gale. Annales de Dermatologie et de Vénéréologie 12/2015; 142(12):S618-S619.

J. Perrot, B. Labeille, E. Cinotti, M. Bonne, F. Cambazard, J. Remy, A. Brehon, C. Schwab, G. Thuret: Apport de la microscopie confocale in vivo pour expliquer le la couleur bleuté de la sclère oculaire au cours de l'ostéogenèse imparfaite. Annales de Dermatologie et de Vénéréologie 12/2015; 142(12):S591.

L. Huppert, J.-L. Perrot, B. Labeille, A.-C. Biron, A. Leclercq, F. Cambazard: Épidémiologie des ulcères veineux et de l'indice de masse corporelle. Annales de Dermatologie et de Vénéréologie 12/2015; 142(12):S580-S581.

A.-C. Biron, J.-L. Perrot, B. Labeille, A. Leclercq, F. Cambazard: Incidence du mélanome de Dubreuilh dans la Loire de 2004 à 2014 : une nette augmentation chez l'homme. Annales de Dermatologie et de Vénéréologie 12/2015; 142(12):S578-S579.

E. Cinotti, J. Perrot, B. Labeille, A. Biron, A. Lelercq, A. Bernois, C. Chol, C. Nizard, S. Schnebert, C. Heusele, F. Cambazard, J. Barthelemy: Épidémiologie et description des tumeurs cutanées bénignes dans une population de personnes âgées considérée comme représentative de la population générale à propos de 209 sujets de la cohorte PROOF. Annales de Dermatologie et de Vénéréologie 12/2015; 142(12):S583-S584.

E. Begon, C. Droitcourt, C. Poiraud, C. Jacobzone, A. Vermersch, V. Descamps, J.L. Perrot, A. Khemis, V. Pallure, N. Beneton, A.C. Fougerousse, M. Sigal, Z. Reguiai: Tolérance et efficacité des biothérapies dans le psoriasis chez les patients cirrhotiques post-alcooliques : série rétrospective multicentrique de 19 cas. Annales de Dermatologie et de Vénéréologie 12/2015; 142(12):S477.

V. Prade, J. Perrot, E. Cinotti, B. Labeille, C. Douchet, F. Cambazard, T. Alix, Gicni: Examen extemporané en microscopie confocale ex vivo des marges chirurgicales du lentigo malin : étude prospective de 16 cas. Annales de Dermatologie et de Vénéréologie 12/2015; 142(12):S652-S653.

J. Perrot, E. Cinotti, B. Labeille, R. Julienne, A. Brehon, D. Grivet, G. Thuret, F. Cambazard: Nævus de la caroncule à propos de 6 cas examinés en microscopie confocale : premiers cas rapportés. Annales de Dermatologie et de Vénéréologie 12/2015; 142(12):S534.

J. Perrot, V. Prade, E. Cinotti, B. Labeille, C. Douchet, F. Cambazard, T. Alix: Évaluation par photogrammétrie 3D de la supériorité du repérage par microscopie confocale in vivo des marges chirurgicales du lentigo malin. Annales de Dermatologie et de Vénéréologie 12/2015; 142(12):S653.

J. Perrot, B. Labeille, E. Cinotti, A. Biron, A. Dellaleau, J. Lagarde, R. Vié, F. Cambazard: Correction des couleurs de photographies dermatologiques au moyen d'une mire standardisée et d'un logiciel de recalage des couleurs : application à la télémédecine. Annales de Dermatologie et de Vénéréologie 12/2015; 142(12):S530-S531.

L. Huppert, J.-L. Perrot, B. Labeille, A.-C. Biron, A. Leclercq, F. Cambazard: Épidémiologie des ulcères non veineux et de l'indice de masse corporelle. Annales de Dermatologie et de Vénéréologie 12/2015; 142(12):S584-S585.

E. Cinotti, B. Labeille, A. Biron, A. Lelercq, A. Bernois, C. Chol, C. Nizard, S. Schnebert, C. Heusele, F. Cambazard, J. Barthelemy, J. Perrot: Épidémiologie et description des tumeurs cutanées malignes dans une population de personnes âgées considérée représentative de la population générale à propos de 209 sujets de la cohorte PROOF. Annales de Dermatologie et de Vénéréologie 12/2015; 142(12):S583.

J. Perrot, E. Cinotti, B. Labeille, F. Cambazard, J. Barthelemy, D. Charier: Quantification objective, par mesure de la variation du diamètre pupillaire, de la douleur induite lors de la cryothérapie de kératoses actiniques et séborrhéiques et photothérapie dynamique. Annales de Dermatologie et de Vénéréologie 12/2015; 142(12):S683-S684.

J. Perrot, E. Cinotti, B. Labeille, A. Singer, D. Grivet, C. Douchet, M. Espinasse, G. Thuret, F. Cambazard: Amélioration du diagnostic des tumeurs du bord libre des paupières par microscopie confocale in vivo : à propos de 130 tumeurs. Annales de Dermatologie et de Vénéréologie 12/2015; 142(12):S518.

Décembre 2016

. L. Perrot 1, B. Labeille 1, C. Heusèle 2, C. Nizard 2, S. Schnebert 2, J.-C. Barthélémy 1, F. Cambazard 1Rapport entre le vieillissement cutané et la fonction du système nerveux E. Cinotti 1, □, J.-

. V. Mandel, S. Ciardo, E. Cinotti, B. Labeille, E. Benati, J.-L. Perrot, G. Pellacani, et ICNI Rôle de la microscopie confocale de réflectance et de tomographie par cohérence optique pour le diagnostic de la pemphigoïde bulleuse et du pemphigus

. J.-L. Perrot, B. Labeille, A. Biron Schneider, C. Douchet, F. Cambazard, E. Cinotti, et ICNI Lentigo malin et examen par OCT HD à propos d'une série de 29 malades : premiers cas rapportés

.Apport de la microscopie confocale in vivo pour le diagnostic de tumeurs conjonctivales bulbaires à propos de 129 tumeurs

. J.-L. Perrot, B. Labeille, A. Biron Schneider, M. Beyens, F. Cambazard, E. Cinotti Effets secondaires des radiations ionisantes administrées à but thérapeutique, qu'en est-il de la déclaration de ces effets secondaires en 2016 ?

. A. Singer, J.-L. Perrot, M. Kaspi, C. Ronin, B. Labeille, D. Grivet, C. Douchet, M.Espinasse,F. Cambazard, G. Thuret, E. Cinotti, et ICNI Apport de la microscopie confocale pour le diagnostic de 166 lésions tumorales du bord libredes paupières

B. Labeille, B. Fouilloux, J.-L. Perrot, E. Cinotti, C. Douchet, F. Cambazard, et Groupe ICNI Application de la microscopie confocale ex vivo aux tumeurs glomiques sous unguéales

J.L Perrot, E. Cinotti, B. Labeille, R. Julienne, A. Brehon, D. Grivet, G. Thuret, F. Cambazard, et BIIGC et GICNI Nævus de la caroncule à propos de 6 cas examinés en microscopie confocale : premier cas rapportés

A. Leclercq, J.-L. Perrot, B. Labeille, C. Douchet, B. Cribier, A. Biron,F.Cambazard, E. Cinotti, Icni Identification in vivo de Treponema Pallidum dans une syphillide secondaire génitale :1er casrapporté

J.L Perrot, E. Cinotti, B. Labeille, R. Julienne, A. Brehon, D. Grivet, G.Thuret, V. Prade, T. Alix, F. Cambazard, et BIIGC et GICNI Place de la microscopie confocale pour la prise en charge des atteintes muqueuses de lapemphigoïde cicatricielle à propos de 6 patients. Premiers cas rapportés de bulles conjonctivales

2.2) Autres congrès :

Journée Scientifique du Groupe ICNI 2014

Communication orale

.Microscopie conjonctivale des lésion oculopalpébralen JL Perrot B Labeille E Cinotti

.Cas clinique de spectrométrie Raman E Cinotti, Blaeille JL Perrot

SFIIC 2015 (Société française d'Imagerie et D'Ingiénérie Cutanée)

Communication orale

.Application d'un dermatoscope « clinique » à une étude du vieillissement cutanée Dr JL Perrot*, Dr E Cinotti, J Georges, C Heusele, C Nizard, S Schneber, A Bernois, Pr F Cambazard, Dr B Labeille

Journée Scientifique du Groupe ICNI 2015

Communication orale

Lentigo malin et examen par OCT HD à propos d'une série de 29 malades : premiers cas rapportés . J.-L. Perrot, B. Labeille, A. Biron Schneider, C. Douchet, F. Cambazard, E. Cinotti, et ICNI

19éme journée de dermatologie pédiatrique d'automne 2015.LYON

Orateur

.Imagerie de la gale . J.-L. Perrot

4th World Congress of Dermoscopy 16–18 April 2015 Vienna, Austria

Communications affichées

.Desmoplastic Melanoma : first case diagnosed by hight definition optical coherent tomography : Elisa Cinotti, Jean-Luc Perrot, Bruno Labeille, Frédéric Cambazard Dermatology, University Hospital of Saint-Etienne France

.Reflectance confocal microscopy and optical coherent tomography to differentiate gouty tophus from calcinosis : Elisa Cinotti, Jean-Luc Perrot, Bruno Labeille, Frédéric Cambazard Dermatology, University Hospital of Saint-Etienne France

.Quantification of skin necrosis an ultra hight definition videodermatoscope on a cohort of 149 healthy subjects :Elisa Cinotti, Jean-Luc Perrot, Bruno Labeille, Romain Vie,Jean-Michel Lagarde , Frédéric Cambazard

Reflectance confocal microscopy for the vascular flow analysis : a new field of exploration Elisa Cinotti, Jean-Luc Perrot, Bruno Labeille, Frédéric Cambazard

.Unconventional applications of reflectance and fluorescence confocal microscopy Elisa Cinotti, Jean-Luc Perrot, Bruno Labeille, Gilles Thuret, Damien Grivet, Philippe Gain, Alix Thomas, Frédéric Cambazard

.In and ex vivo reflectance confocal microscopy examination of xanthogranulomas from 5 patients Elisa Cinotti, Jean-Luc Perrot, Bruno Labeille, Frédéric Cambazard

Photonique et Pratiques Médiacles (Pole ORA) St-Etienne 2015

Communication orale

Correction des couleurs de photographies dermatologiques au moyen d'une mire standardisée et d'un logiciel de recalage des couleurs : application à la télémédecine Jean-Luc Perrot, Bruno Labeille, Romain Vie,Jean-Michel Lagarde , Frédéric Cambazard, Elisa Cinotti

SFIIC 2016 (Société française d'Imagerie et D'Ingiénérie Cutanée)

Communications orales

OCT HD – MCIV et colorants cosmétiques cutanéo-phanériens Dr JL Perrot*, Dr B Labeille, Dr AC Biro, Arielle Bertrou-Cantou,N Dalloz,Pr M Hebert, Pr R Clerc,Pr F Cambazard, Dr E Cinotti

Microscopie Confocale en dermatologie applications et sites non habituels JL Perrot*, B Labeille ,C Douchet, F Forest, G Thuret, D Grivet, Th Alix , V PradeR Clerc,M Ebert ,Y Ouerdane, F Cambazard, E Cinotti

MINALOGIC (MIcro NAnotechnologies et LOgiciel Grenoble-Isère Compétitivité) Grenoble 2016

Apport de la microscopie Confocale pour la médecine personnalisée en Dermatologie Dermato-gynécologie et Dermato-ophtalmologie JL Perrot, B Labeille ,C Douchet, F Forest , G Thuret, D Grivet, Ph Gain, Th Alix , V Prade ,F Cambazar, E Cinotti

J. CONCLUSIONS ET PERSPECTIVES

L'imagerie non invasive appliquée à la dermatologie est un ensemble de techniques en pleine évolution. A des contraintes techniques et physiques qui conditionnent les outils mis à la disposition des dermatologues, se joignent des considérations économiques qui contraignent les industriels qui fabriquent et distribuent ces instruments, mais aussi les dermatologues qui les achètent. Ceci rend particulièrement complexe et fragile cet ensemble scientifique et économique, ce qui explique en partie que des données théoriques physiques, déjà relativement anciennes, ne soient que souvent tardivement mises en application clinique.
Ensuit,e c'est aux dermatologues de valider ces dispositifs et d'établir, si ce n'est une hiérarchie, tout au moins, d'élaborer les critères permettant de positionner l'utilité et les contraintes relatives des techniques les unes par rapport aux autres, et de définir leur place dans la démarche diagnostique.
C'est pourquoi lorsque le dermatologue a la possibilité de participer à la création de nouveaux dispositifs d'imagerie il est nécessaire qu' il puisse collaborer d'emblée avec les industriels et les ingénieurs d'application. Ceci afin de participer à caractérisation des bénéfices qu'il espère tirer d'un nouveau dispositif mais aussi, dès l'initiation du projet de conception de ce dispositif, de son coût ultérieur, des contraintes ergonomiques, du temps d'apprentissage nécessaire pour d'une part manipuler l'instrument d'autre part interpréter les images, à'envisager les développements ultérieurs possibles et souhaitables. ….
Par ailleurs cela luis permet aussi de pouvoir participer àl'évaluation des contraintes, en terme d'hygiène , d'encombrement stéréotaxique du dispositif, d'évaluer le volume qu'il faudra prévoir pour l'archivage numérique des images….
Il s'agit en effet d'une somme de contraintes médicales non toujours perçue par les industriels, mais qui peuvent avoir des conséquences économiques fortes. Les échecs industriels sont nombreux dans ce domaine et ces différentes contraintes peuvent en partie en apporter des explications.

J'ai souhaité dans cette thèse témoigner de ma participation au développement de l'imagerie dermatologique actuelle pour permettre son application future dans le plus grand nombre de centres possibles au bénéfice des malades. Pour cela mes actions ont été multiples :

- La participation à l'élaboration d'un nouvel OCT projet validé par l'ANR , DOCT VCSEL
- La participation à validation d'un nouvel OCT HD avec la société DAMAE
- La participation à l'élaboration de 2 nouveaux projets ANR soumis en 2016 pour la création de nouveaux dispositifs d'imagerie : spectromètre Raman intégré dans un OCT HD in vivo, et nouveau dispositif d'analyse multi spectrale.
- La participation à la création du groupe d'Imagerie Non Invasive de la société Française de Dermatologie dont je suis depuis 2 ans le président.
- La participation à la création et l'animation de trois consultations multidisciplinaires de microscopie confocale : une dermato-ophtalmologique , une dermato-gynécologique et une d'allergo-ophtalmo-dermatologique pour apporter une réponse aux besoins de nos patients et réaliser de la recherche clinique.
- La participation à la publications d'articles nombreux notamment d'imagerie microscopique non invasive dans des revues à comité de lecture et indexés, la participation à la rédaction d'ouvrages (en cours) concernant la microscopie confocale mais aussi la participation à la publications d'articles dans des revues et journaux, sans comité de lecture, mais lus par de nombreux médecins ce qui participe néanmoins à la diffusion de ces techniques par un phénomène de capillarité.
- La réalisation de communications abondantes dans le domaine de l'imagerie lors de congrès nationaux ou internationaux ou d'EPU locales.
- La mise en place de collaborations dynamiques entre notre CHU et d'autres équipes dermatologiques universitaires françaises et européennes spécialisées en imagerie dermatologique mais aussi une collaboration avec des équipes de recherches non médicales des sciences dites dures : optique (Hubert Curien UMR CNRS 5516, Institut Supérieur d'Optique de St Etienne, CEA-LETI), mécanique (Laboratoire de Tribologie Dynamique des Système UMR 5513, ENMSE), traitement du signal (Le2i UMR CNRS 6306), micromécanique (FEMTO-ST UMR

CNRS 6174), Laser (LASS CNRS Toulouse),bio-ingénierie (BIIGC EA2521) ……..Mais aussi d'industriels impliqués dans l'imagerie de la peau : DAMAE (start up issue de l'Institut Supérieur d'optique de Palaiseau) LVMH, Dior, Chanel, Bioderma-Naos, Pierre Fabre dermocosmétique, Spikenet, Newtone, Mavig, Pixience, Orion, Kamax (start up issue de l'Institut XLIM , UMR CNRS 6172 - Institut Carnot , de Limoges)
Toutefois ceci n'est qu'une étape. En effet maintenant que notre socle technique et l'activité de recherche en imagerie non invasive ont pu être considérés par nos correspondant médicaux, industriels et scientifiques, français et étranger comme étant hautement significatif, de nouvelles ambitions vont pouvoir se concrétiser.

Premièrement, au travers d'objectifs d'acquisition de matériel.
- acquisition d'un échographe HD spécifique de la peau au printemps 2017
- acquisition d'un objectif pour appareil photo de polarisation croisée et parallèle, au printemps 2017
-utilisation de caméras d'analyse multi spectrale courant 2017 en collaboration avec la société Newtone et l'Institut Supérieur d'Optique de St Etienne (Pr M Hebert et Pr R Cler)
- l'intégration de la spectrométrie Raman, dans un service de soin, au moyen du couplage d'un spectromètre Raman au sein d'un OCT HD, ce qui sera l'un des prochains grands projets innovant du service.Un projet ANR en cours de soumission a ce sujet.
- un projet d'acquisition et déploiement d'un dispositif d'imagerie photo acoustique en collaboration avec le Laboratoire. H Curien (Pr Y Ouerdane)

Deuxièmement, au travers d'objectifs de partenariats industriels tout aussi variés que nos dispositifs d'imagerie :
- industrie dermato-cosmétique : des projets sont en cours : l'un visant au développement d'un dispositif totalement innovant en cours d'élaboration avec un industriel de ce secteur et un grand partenaire académique (confidentiel),les 2 autres applications étant purement cosmétique (confidentiel).
- industrie pharmaceutique : à titre d'exemple un projet de recherche associant protéomique, transcriptomique et différentes techniques d'imagerie non invasive de la peau va être déposé au CCPPRB au printemps 2017 financé par un industriel du médicament dans un but purement exploratoire et scientifique.
- acteurs de santé (mutuelles, industriels), réflexion déjà très avancée sur un système alliant imagerie 3D, reconnaissance de cibles, et divers systèmes d'intelligence artificielle en cours de discussion
- utilisation des données issues de l'imagerie dermatologique à des appplications de cyberprotection (travaux en cours avec des industriel majeurs du secteur)

Troisièmement, notre ambition est de participer à la création d'un regroupement et d'une mise en synergie à l'échelle de la région Rhône-Alpes Auvergne, d'un savoir-faire dispersé sur son territoire et qui regroupé et coordonné aura une valeur scientifique majeur du fait de sa rareté et de ses compétences. Ceci s'est récemment traduit par la mise en place d'un partenariat avec le Lyrec (Lyon Recherche Clinique) via Dermatec.
En effet, des acteurs performants existent en Rhône-Alpes : pour ce qui est des compétences optiques : le pôle optique Rhône-Alpes, le CEA LETI, la société Newtone …..des compétences concernant la mécanique des tissus vivant l'EMSE, EC Lyon (notamment avec le Laboratoire de Tribologie Dynamique des Système UMR 5513) des compétences en ingénierie des études cliniques avec le Lyrec, la DRCI de St Etienne …….des compétences en imagerie non invasive de la peau et ou de la physiologie de la peau : service de dermatologie St- Etienne, l'immuno-allergologie de la peau (notamment avec le Service d'Allergologie et Immunologie Clinique INSERM U851), la bioingiénérie (BIICG EA2521) …..
Enfin des industriels de dermato cosmétique sont présents dans notre région dont Bioderma Naos.

En conclusion

cette thèse est le témoin de ma participation aux premiers pas stéphanois en imagerie non invasive dermatologique, multi échelle multimodale, et parfois même dans certains domaines , Le premier pas, personne n'ayant jamais réalisé auparavant certaines de nos observations. Toutefois ce n'en est pas moins qu'un début.

De nombreux autres projets de recherche sont en maturation, à des stades divers, et dont l'ambition va croissante.Nous nous orientons plus particulièrement vers la combinaison de différentes techniques d'imageries non invasives entre elles, et l'utilisation de procédures d'intelligences artificielles, pour explorer de la peau saine, malade ou vieillissante.

Par ailleurs nous souhaitons appliquer ces différentes méthodes à l'évaluation d'autres organes ou processus fonctionnels et plus particulièrement le système Nerveux Autonome.

Enfin en plus de différentes modalité de la vision de la peau, actuelles et prochaines que nous appliqueront, nous souhaitons développer rapidement des travaux concernant sa perception palpatoire puis la combinaison de ces 2 approches,optique et mécanique.

L'ensemble de ces travaux ne pourra se concrétiser qu'au travers de multiples et durables collaborations tant avec des équipes médicales que de physiciens et ou d'industriels.

I. ANNEXES ET REFERENCES

Annexe 1

Principes et schémas succincts d'un microscope confocale

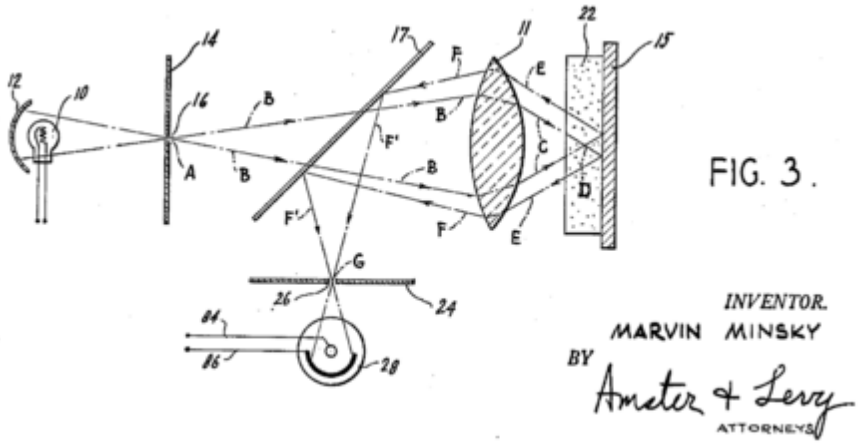

Figure 4.Schéma autographe de Marvin Minsky inventeur du principe

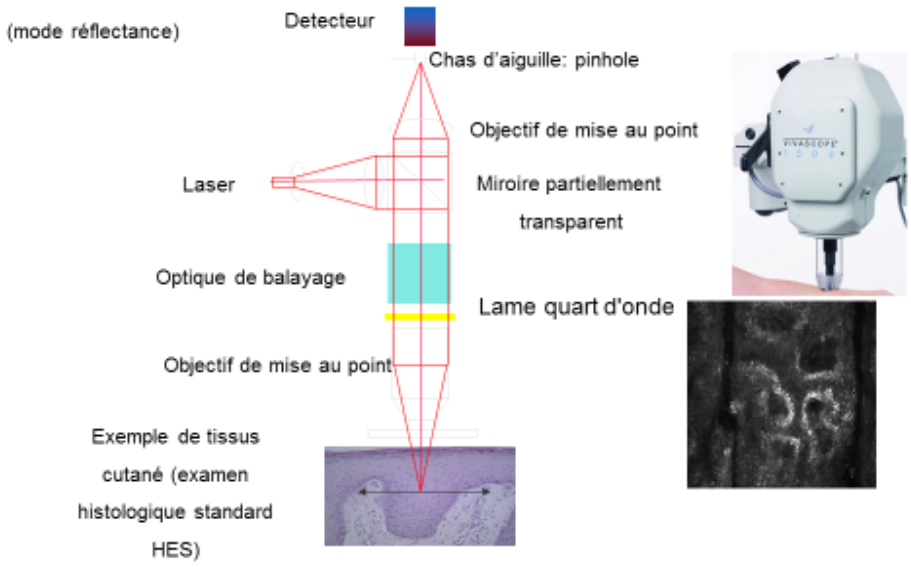

Figure 5. Description simplifiée de la caméra Vivascope 1500 et par analogie de la caméra Vivascope 3000 utilisé dans le service de dermatologie du CHU de St Etienne (Données Caliber Inc, Rochester, NY, Etats-Unis, distribué en France par Mavig, Munich)

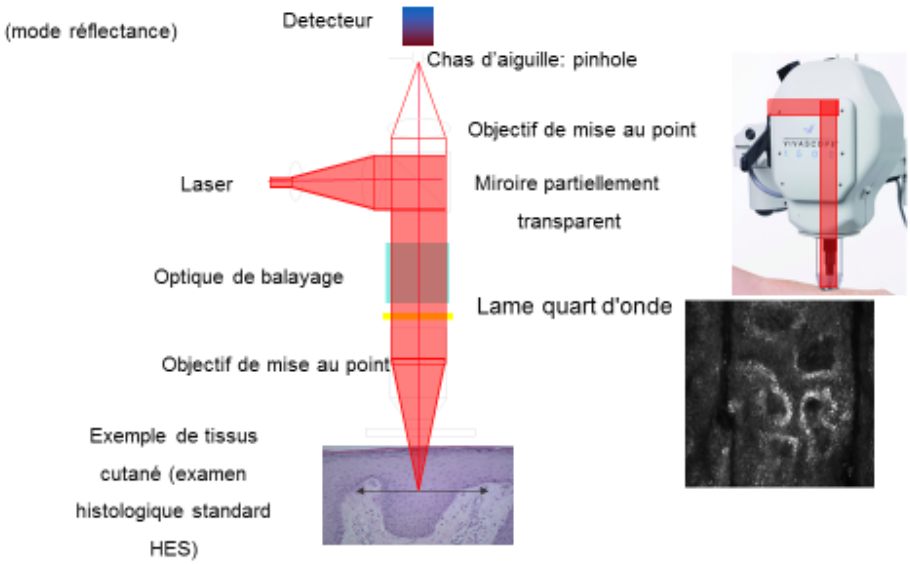

Figure 6. Emission du faisceau laser (rose) qui est dirigé via un miroir partiellement transparent après avoir été focalisé sur sa cible tissulaire en un plan focal (flèche noire horizontale)

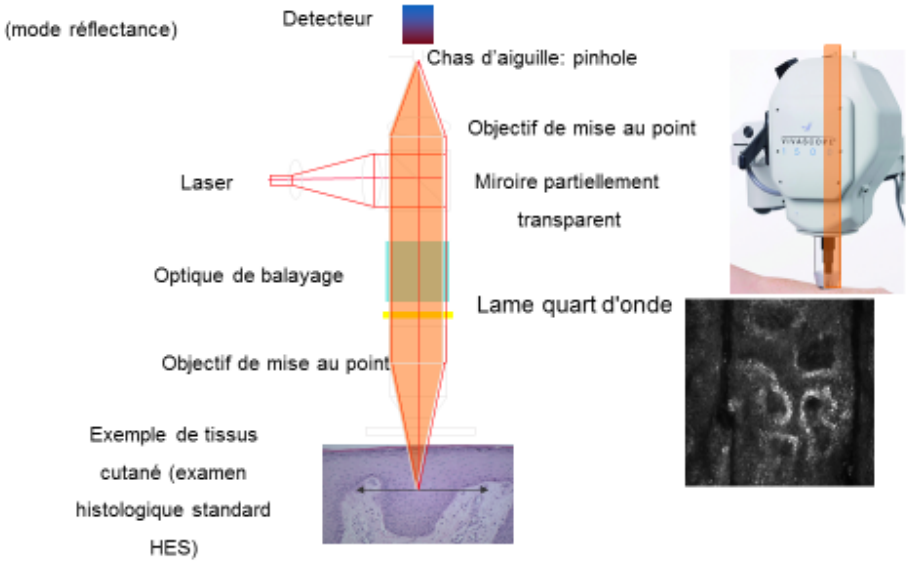

Figure 7. Réflexion du faisceau laser (orange) qui traverse le miroir partiellement transparent et est ensuite focalisé sur le détecteur en un 2éme plan focal

Annexe 2

Principes et schémas succincts d'un microscope OCT

Une lumière de large bande spectrale est projeté sur la cible via un miroir semi réfléchissant à 45° et qui sépare en 2 le faisceau lumineux : un des 2 faisceau éclaire une surface de référence tandis que l'autre éclaire la cible. La lumière réfléchie de ce dernier et dirigé vers la fente d'un spectroscope ainsi que le faisceau de référence ce qui va permettre d'obtenir des interférences qui par traitement mathématique (transformation de Fourier) permettent la formation d'image.

Figure 8 Exemple de montage d'un OCT

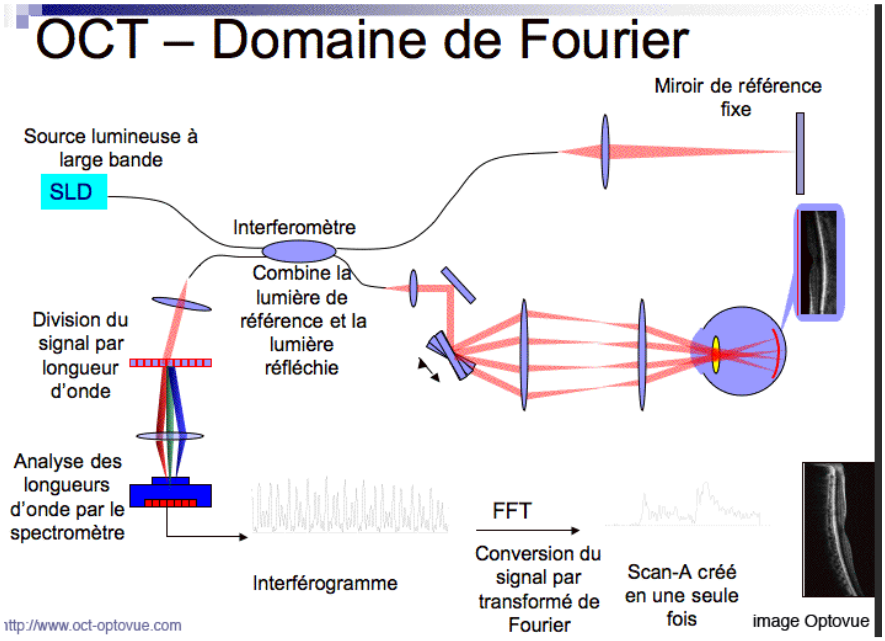

Figure 9. Schéma très simplifié de l'OCT Skintell acquis par le service

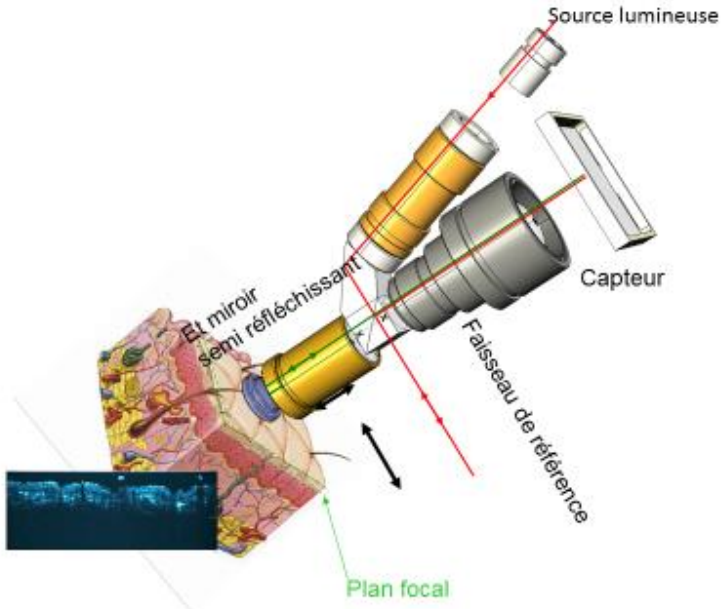

Annexe 3

Principes et schémas succincts d'un spectromètre Raman

La Spectroscopie Raman (SR) est une technique qui analyse la composition chimique des matériaux et qui est basée sur la détection des vibrations moléculaires.
La technique dérive d'un phénomène physique, découvert en 1928, par le physicien indien Raman, qui lui a valu le prix Nobel en 1931.
L'effet Raman, découle du fait, qu'une **fraction du rayonnement diffusé à partir de certaines molécules à une énergie autre que le rayonnement incident**. Cette différence d'énergie est liée à la structure chimique des molécules responsables de la propagation.
Quand un rayonnement monochromatique atteint la surface d'un objet, les photons incidents peuvent être:
Transmis : ils traversent l'objet sans subir des modifications
Absorbés : ils produisent une transition de l'objet à un niveau d'énergie plus élevé, en fonction de λ (par exemple UV-VIS et IR) et de la nature de l'objet éclairé
Reflétés : ils n'ont pas d'interaction avec la matière
Diffusés: ils provoquent une interaction mais sans causer de transitions énergétiques généralisées, ce phénomène concerne moins de 1 % du rayonnement.
C'est ce phénomène de diffusion qui est pris en compte dans l'effet Raman
Ainsi lors de la diffusion de la lumière :
-Soit elle s'effectue à la même fréquence v que la radiation incidente on parle d' **interaction élastique** (<1% de la lumière incidente) = diffusion de Rayleigh
-Soit avec un changement de fréquence on parle d' **interaction inélastique** (<1‰ de la lumière incidente), avec transfert d'énergie du photon incident à une particule de l'objet ou vice versa, le photon est diffusé avec une énergie inférieure ou supérieure à l'incidente: la différence en énergétique entre les photons incidents et ceux diffusé de manière inélastique corresponds aux niveaux vibrationnels de la molécule diffusante ce qui correspond à la **diffusion Raman ou effet Raman**
Ainsi lors de l'interaction inélastique :
soit le photon est diffusé avec une énergie inférieure à celle du photon incident: **raie de Stokes**
soit le photon est diffusé avec une énergie Supérieure à celle du photon incident: raie de anti-Stokes
La diffusion Stokes étant plus intense que la diffusion anti-Stokes, c'est celle-ci qui est plus souvent étudiée

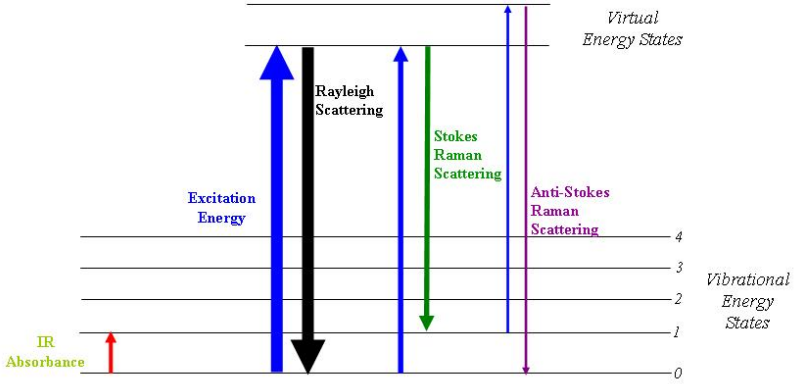

Un spectre Raman se carctérise en ordonnée par l'intensité de l'émission de lumière et en abscisse la fréquence absolue en cm-1 = Raman Shift (décalage Raman) = différence de longueur d'onde entre le rayonnement observé et le rayonnement incident. Mais on rappel que l'énergie associée à la vibration moléculaire est seulement la différence entre les 2 rayons, pas la λ absolue!

Schéma simplifié d'un spectromètre Raman.
Focalisation d'une lumière monochromatique issue d'un faisceau laser sur l'échantillon au moyen d'une lentille.
La lumière diffusée est ensuite recueillie grâce à une autre lentille qui tient lieu de filtre et est ensuite dirigée vers un monochromateur. L'intensité lumineuse est ensuite mesurée via un détecteur.

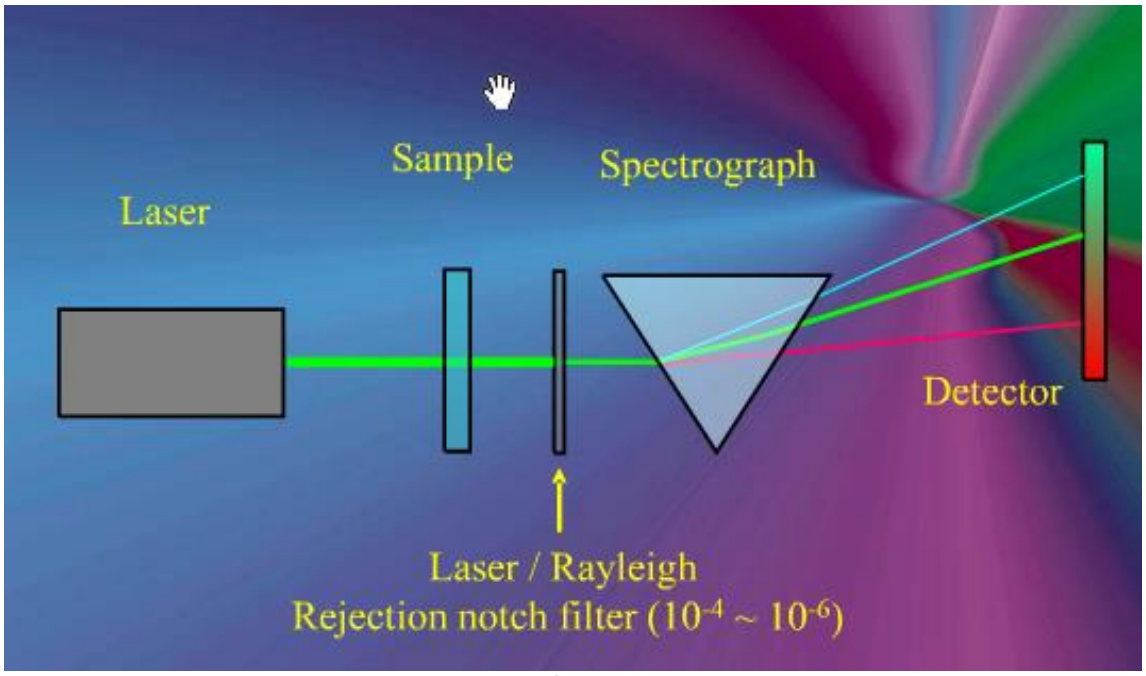

Figure 10 Schéma simplifié d'un spectromètre Raman.

Bibliographie

1. Goodall EW. Fracastor as an Epidemiologist: (Section of Epidemiology and State Medicine). Proc R Soc Med. févr 1937;30(4):341‑50.

2. Gilbert RO. Report of an outbreak of ringworm of the scalp due to M. audouini. Calif Med. mars 1949;70(3):194‑7.

3. Pfister R. [Practical possibilities of dermatoscopy for clinical and research purposes]. Hautarzt Z Für Dermatol Venerol Verwandte Geb. févr 1955;6(2):74‑7.

4. Stolz W, Bilek P, Merkle T, Landthaler M, Braun-Falco O. [Improving clinical diagnosis of pigmented skin changes in childhood with the dermatoscope]. Monatsschrift Kinderheilkd Organ Dtsch Ges Für Kinderheilkd. févr 1991;139(2):110‑3.

5. Tiffet O, Perrot JL, Gentil-Perret A, Prevot N, Dubois F, Alamartine E, et al. Sentinel lymph node detection in primary melanoma with preoperative dynamic lymphoscintigraphy and intraoperative gamma probe guidance. Br J Surg. juill 2004;91(7):886‑92.

6. Cinotti E, Perrot JL, Labeille B, Vercherin P, Chol C, Besson E, et al. Reflectance confocal microscopy for quantification of Sarcoptes scabiei in Norwegian scabies. J Eur Acad Dermatol Venereol JEADV. févr 2013;27(2):e176-178.

7. Le Sylphe (Victor Hugo) - Wikisource [Internet]. [cité 7 oct 2016]. Disponible sur: https://fr.wikisource.org/wiki/Le_Sylphe_(Victor_Hugo)

8. Cathébras P, Perrot JL. [What is a Caucasian? Race and ethnicity in the medical literature]. Presse Médicale Paris Fr 1983. 9 juin 2001;30(20):1012‑4.

9. Champin J, Perrot J-L, Cinotti E, Labeille B, Douchet C, Parrau G, et al. In vivo reflectance confocal microscopy to optimize the spaghetti technique for defining surgical margins of lentigo maligna. Dermatol Surg Off Publ Am Soc Dermatol Surg Al. mars 2014;40(3):247‑56.

J. TABLES ET FIGURES
ET
LISTES ET ABREVIATIONS

1 TABLE DES FIGURES

Figure 1. Cire anatomique d'une lépre nodulaire du visage (à droite) photographie sur plaque de verre (à gauche) d'une cire anatomique datant de la fin du XIXéme sciècle collection du service de dermatologie du CHU de St Etienne ancienne collection du Pr Gaté ……Page 17

Figure 2. 1er dermatoscope digital acquis par le service de dermatologie du CHU de St Etienne utilisée pour la première fois par la nouvelle génération de dermatologues stéphanoises spécialisées en imagerie non invasive dermatologique……..Page 19

Figure 3. La diaphane poudre de riz Sarah Bernhardt (Affiche J Cheret. Fond BNF Gallica) ……..Page 20

Figure 4.Schéma autographe de Marvin Minsky inventeur du principe …….Page 467

Figure 5. Description simplifiée de la caméra Vivascope 1500 et par analogie de la caméra Vivascope 3000 utilisé dans le service de dermatologie du CHU de St Etienne (Données Caliber Inc, Rochester, NY, Etats-Unis, distribué en France par Mavig, Munich)……..Page 467

Figure 6. Emission du faisceau laser (rose) qui est dirigé via un miroir partiellement transparent après avoir été focalisé sur sa cible tissulaire en un plan focal (flèche noire horizontale)……...Page 468

Figure 7. Réflexion du faisceau laser (orange) qui traverse le miroir partiellement transparent et est ensuite focalisé sur le détecteur en un 2éme plan focal……....Page 468

Figure 8 Exemple de montage d'un OCT……Page 469

Figure 9. Schéma très simplifié de l'OCT Skintell acquis par le service……Page 469

Figure 10 Schéma simplifié d'un spectromètre Raman. ……...Page 471

2 LISTES DES ABREVIATIONS

MCIV : Microscopie Confocale In Vivo

MCEV : Microscopie Confocale Ex Vivo

OCT : Optical Coherence Tomography

OCT HD : Optical Coherence Tomography Hight Definition

SNA : Système Nerveux Autonome

CCPPRB : Comité Consultatif pour la Protection des Personnes et la Recherche Biomédicale

DRCI :Direction de la Recherche Clinique et de l'Innovation

ANSM : Agence Nationale de Sécurité du Médicament

GICNI : Groupe d'Imagerie Cutanée Non Invasive

SFD : Socéié Française de Dermato-vénérérolgie

ICWG : International Confocal World Group

SFIIC : Société Française d'Ingiéniérie et d'imagerie Cutanée

GUS : Groupe Urticaire de la Société française de dermato-vénéréologie